Recrystallization in METALS and ALLOYS

S. S. GORELIK

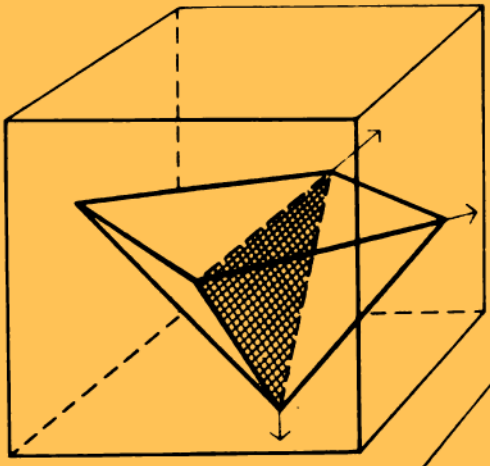

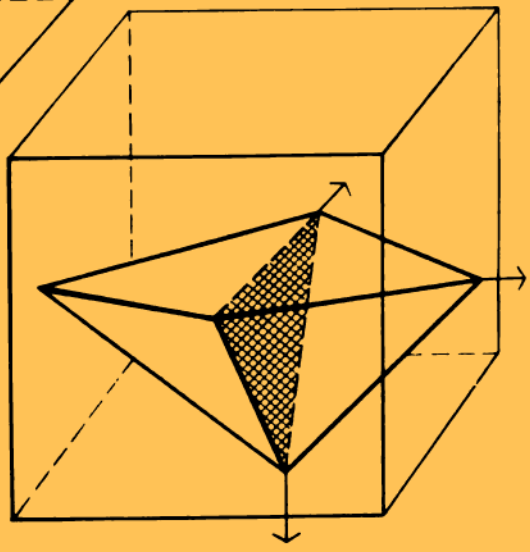

MIR Publishers · Moscow

The first Russian edition of this monograph was published in 1967 and immediately gained much recognition from specialists in physical metallurgy and metal science. It was awarded a prize established in honour of D. K. Chernov, a prominent Russian metallurgist.

The second edition was substantially revised to cover up-to-date theoretical and experimental data, in particular those concerning the influence of crystal lattice type, phase composition, and deformation on dislocation structures in deformed metals. The book was also supplemented with new chapters on recrystallization in compounds and in thin films. The book may be of value for research workers and technologists dealing with the problems of physical metallurgy, plastic working and heat treatment of metals, and may also be useful for senior students and post-graduates specializing in the field.

Recrystallization in METALS and ALLOYS

S.S.GORELIK

ИЗДАТЕЛЬСТВО
МИР

С. С. Горелик

РЕКРИСТАЛЛИЗАЦИЯ МЕТАЛЛОВ И СПЛАВОВ

Издательство «Металлургия»
Москва

S. S. GORELIK

Recrystallization in METALS and ALLOYS

Translated from the Russian
by
V. AFANASYEV

MIR Publishers · Moscow

First published 1981
Revised from the 1978 (2nd) Russian edition

The Russian Alphabet and Transliteration

А а	a	К к	k	Х х	kh
Б б	b	Л л	l	Ц ц	ts
В в	v	М м	m	Ч ч	ch
Г г	g	Н н	n	Ш ш	sh
Д д	d	О о	o	Щ щ	shch
Е е	e, ye	П п	p	ъ	″
Ё ё	e	Р р	r	ы	y
Ж ж	zh	С с	s	ь	′
З з	z	Т т	t	Э э	e
И и	i	У у	u	Ю ю	yu
Й й	y	Ф ф	f	Я я	ya

The Greek Alphabet

Α α	Alpha	Ι ι	Iota	Ρ ρ	Rho
Β β	Beta	Κ κ	Kappa	Σ σ	Sigma
Γ γ	Gamma	Λ λ	Lambda	Τ τ	Tau
Δ δ	Delta	Μ μ	Mu	Υ υ	Upsilon
Ε ε	Epsilon	Ν ν	Nu	Φ φ	Phi
Ζ ζ	Zeta	Ξ ξ	Xi	Χ χ	Chi
Η η	Eta	Ο ο	Omicron	Ψ ψ	Psi
Θ θ ϑ	Theta	Π π	Pi	Ω ω	Omega

На английском языке

© Издательство «Металлургия», 1978
© English translation, Mir Publishers, 1981

Contents

Preface 7

Chapter 1. Practical Significance of Recrystallization and the Role of Microstructure Parameters of Recrystallized Metal 9

1.1. The Evolution of Concepts on the Role and Significance of Recrystallization 10
1.2. Principal Parameters of Microstructure and their Effect on the Properties of Recrystallized Material 15

Chapter 2. Structural Changes in Deformed Metals and Alloys 18

2.1. Deformation in Single Crystals 19
2.1.1. Slip Deformation 19
2.1.2. Deformation by Twinning 38
2.1.3. Deformation by Irregular Rotation of the Crystal Lattice 44
2.2. Deformation in Polycrystalline Solids 49
2.2.1. Inhomogeneous Microstructure of Deformed Polycrystals 49
2.2.2. Deformation Textures 56
2.3. Other Effects of Macro- and Microinhomogeneity in Deformed Metals 61
2.4. Variations in Energy and Properties of Plastically Deformed Metals and Alloys 66

Chapter 3. Classification, and Driving Forces of Processes Occurring in Deformed Metals and Alloys on Heating 69

3.1. Recovery 71
3.1.1. Point-defect Annihilation 71
3.1.2. Polygonization 77
3.2. Recrystallization 90
3.2.1. Primary Recrystallization 92
3.2.2. Grain Growth 105
3.2.3. Secondary Recrystallization 113
3.3. Variations of Metal Properties During Recovery and Recrystallization 117

Chapter 4. Mechanism of Formation of Primary Recrystallization Nuclei 127

Chapter 5. Mechanism of Enlargement of Recrystallization Nuclei and Grains 165

5.1. The Structure of Grain Boundaries 165
5.2. The Rate of Boundary Migration 178
5.3. The Effect of Grain-boundary Tension 183
5.4. The Formation of Annealing Twins 193

Chapter 6. Recrystallization During Hot Deformation (Dynamic Recrystallization) 203

Chapter 7. Recrystallization on Critical Deformation 227

7.1. General Relationships 227
7.2. The Mechanism of Recrystallization after 'Critical' Deformation 233

7.3. Growing Single Crystals by Recrystallization after 'Critical' Deformation 252

Chapter 8. Inequigranular and Coarse Structures and Their Formation 258

8.1. Nickel and Iron Alloys with Disperse Phases 264
8.2. Aluminium Alloys 276

Chapter 9. Recrystallization Diagrams 289

Chapter 10. Recrystallization Textures 304

10.1. The Principal Theories of Formation of Recrystallization Textures 307
10.2. The Principal Types of Texture Changes in Recrystallization 310
10.2.1. Retention of Deformation Texture in Annealing 310
10.2.2. Texture Variations at Various Stages of Recrystallization 315
10.2.3. Weakening of Texture in Recrystallization 321
10.3. Texture Formation During Recrystallization in Electric Steel 322
10.3.1. Transformer Steel with {110} ⟨001⟩ Rib Texture 323
10.3.2. Transformer Steel with {100} ⟨001⟩ Cube Texture 335
10.3.3. Low-textured Dynamo Steel 338

Chapter 11. Effect of Alloying on the Temperature Level and Rate of Recrystallization in Metals and Single-phase Alloys 339

11.1. The Criteria for Estimating the Susceptibility of Metals and Alloys to Recrystallization 339
11.2. The Temperature Level of Recrystallization in Metals . . . 345
11.3. The Temperature Level of Recrystallization in Single-phase Alloys 347
11.3.1. Effect of Minor Concentrations of Impurities on t_r^s of Alloys 357
11.3.2. Effect of High Concentrations of Impurities on t_r^s in Single-phase Alloys 371

Chapter 12. Recrystallization in Supersaturated Solid Solutions and Heterophase Alloys 378

12.1. Mutual Effects of Primary Recrystallization and Decomposition of Supersaturated Solid Solutions 379
12.2. Recrystallization in Heterophase Alloys 397

Chapter 13. Recrystallization in Compounds 414

13.1. High-melting Compounds 414
13.2. Ferrites 418

Chapter 14. Recrystallization in Thin Films 426

Chapter 15. Methods for Studying Recrystallization 444

References 465

Index 476

Preface

Recrystallization is one of the most important processes that controls the formation of structures [1] and determines the structure-sensitive properties of materials. It attracts ever greater interest largely because the industry places increasing requirements on the main mechanical, physical, and technological characteristics of metals and alloys.

These requirements are satisfied in two ways: (1) by developing new technological processes and techniques of plastic working and heat treatment of metals and (2) by developing novel alloys and like materials. The list of materials whose use is associated with the problems of recrystallization noticeably extends.

Apart from the conventional materials, it includes alloys with special physical properties, superplastic alloys, semiconductor alloys (thermoelectric materials, ferrites, etc.), thin films of metals and semiconductors. Novel processes, such as thermomechanical treatment of metals or powder metallurgy, find expanding uses in the industry.

It is natural that a further improvement in the properties of materials requires a deeper insight into the mechanisms of structural changes and the ways for their controlling.

In recent years, a definite progress has been made in understanding the essence of recrystallization and the preceding or accompanying processes, specifically recovery and polygonization. Perhaps, this concerns most of all the analysis of the structure of deformed metals [2], the mechanism of nucleation, some laws of texture formation, etc., though many essential details of these processes still remain disputable or unclear.

In other countries, a number of review works on the related problems have been published recently, including the proceedings of symposia on some important problems of recrystallization, grain growth and texture formation [3, 4, 95]. In the USSR, a number of review works on individual problems of recrystallization have appeared [5, 6].

Unfortunately, this period has not seen a monograph that would thoroughly analyse, from a unique standpoint, the most essential effects of recrystallization and their interrelation. Such a monograph would be a good aid for specialists dealing with the problems of structure formation in metals and alloys and, in our view, for practical technologists in the fields of heat treatment and plastic working of metals. It would also be of use for senior students and postgraduates.

These considerations have impelled the author to revise his monograph *Recrystallization in Metals and Alloys*, first published in

1967, and supplement it with the newest data and the results of his own research. In view of the fact that a wealth of literature on dislocations has appeared in recent years and the basic theory of dislocations is now included in the curriculum of higher educational establishments training engineers in physical metallurgy and plastic working of metals, the author has thought it reasonable to exclude the chapters on dislocations in the new edition. The reader is assumed to be familiar with this literature on dislocations and also with the principles of structural crystallography, physical chemistry, and physical metallurgy.

The author has supplemented the chapters relating to dislocation structures in deformed materials with regard for the types of crystal lattice, phase composition, the degree of deformation, temperature of deformation, etc.

The modern concepts of deformation textures, recrystallization in hot-deformed metals, the effects of various parameters of recrystallized microstructure on metal properties are presented in more detail.

The author has also discussed in brief some features of recrystallization in semiconductors and thin films.

Chapter 1

Practical Significance of Recrystallization and the Role of Microstructure Parameters of Recrystallized Metal

Recrystallization involves a wide spectrum of structural changes which occur on heating of a metal or alloy and result in the replacement of grains of a phase by other grains of the same phase having a lower energy.

Recrystallization is the most common process which can form the structure of metals and alloys and hence determine their structure-sensitive mechanical and physical properties.

Some authors erroneously regard recrystallization only as the process that changes the microstructure of plastically deformed materials during heating. Actually, recrystallization is a much more common process and generally occurs when a metal or alloy is heated to a temperature at which migration of high-angle boundaries is possible.

The process of recrystallization almost always goes with polymorphous transformations and often with some other phase transformations that take place under heat. In real conditions, polymorphous transformations, for instance, the ferrite-austenitic ($Fe_\alpha \rightarrow \rightarrow Fe_\gamma$) transformation in iron, always proceed in two stages: the nucleation of a new phase of a different lattice than that of the matrix and the growth of grains (crystallites) of the new phase, first at the expense of the disappearing phase (stage 1) and later by consuming other grains of that new phase (stage 2).

Stage 1 is the process of phase transformation, whereas stage 2 is a purely recrystallizational process, more strictly, the process of grain growth.

In some cases where the polymorphous changes are accompanied by noticeable volume changes owing to a difference between the unit volumes of the initial and the new phase, grains of the matrix and of the new phase can undergo structural strain-hardening. This effect can result in primary recrystallization occurring immediately after or even parallel with phase transformation, following which only grain growth takes place. In very rare cases, primary recrystallization can take place on heating of a material in which phase strain-hardening has been caused not by polymorphous transformation, but by prior decomposition of the supersaturated solid solution or, more seldom, by prior eutectoid transformation.

Thus, in metals and alloys undergoing polymorphous (phase) transformations, structural changes can be induced both by these transformations and by recrystallization.

In materials where no phase transformation takes place, strain hardening and subsequent recrystallization are the sole means for effective alteration of the structure.

Grain growth on heating of precipitated polycrystalline films, which usually causes a change in texture, is also a process of recrystallization.

The structure of a deformed (strain-hardened) material can change on recrystallization within very wide limits: from a partially recrystallized structure that retains to a certain extent the original deformed structure to a fully recrystallized structure. Recrystallization is not, however, finished on disappearance of the deformed structure. Prolonged heating or especially heating at a higher temperature may lead to further structural changes associated with the growth of some grains at the expense of others. At the final stage of this process, which can only very rarely be attained in practice, the whole polycrystalline aggregate transforms into a single crystal.

In the majority of real cases we have to deal with materials whose condition is intermediate between the one in which the deformed structure disappears and the one in which the specimen becomes fully monocrystalline. Exactly this condition is of the highest practical importance.

For the same chemical and phase composition, the microstructure, which is sometimes called the grain structure, may feature a large diversity of parameters (see Sect. 1.2) and, accordingly, a large diversity of properties.

1.1. The Evolution of Concepts on the Role and Significance of Recrystallization

At an early stage, recrystallization attracted the interests of metallurgists as a process responsible for the formation of a microstructure in deformed metals and alloys on heating. For that reason, the main attention was paid to the analysis of grain size in metals upon deformation and heating [7, 8], though a few important works were concerned with the mechanism and driving forces of the process. The graphs relating the grain size of metal to the conditions of treatment are known as recrystallization diagrams.

The work on constructing recrystallization diagrams is being continued in view of the development of novel alloys, in particular heat-resisting ones, the increasing use of novel metals (such as rare

and rare-earth), introduction of new processes of deforming and heating, for instance, high-speed heating, etc.

The trend today is to use recrystallization diagrams not only for determining the absolute size of grains, but also for obtaining information on other parameters of the structure: equigranularity [9, 10], the existence of twins, texture [9, 11], the amount of strain-hardening of grains [12, 9].

On the other hand, metallurgists and specialists in plastic deformation have been always interested in recrystallization as a process that causes softening of a deformed metal and facilitates further deformation.

As has been established by the earliest studies, for metals there is a definite correlation between the absolute temperature of recrystallization (T_r, K) and melting point (T_m, K). It has also turned out that the temperature level of recrystallization, which is determined by the T_r/T_m ratio, may vary appreciably under the effect of various factors. It is then clear that softening of a deformed metal (as required for further deformation) can be obtained at a lower temperature of heating and, in general, more economically with a lower T_r/T_m ratio of that metal. This aspect of the problem has gained in importance with the growing demand on heat-resisting metals for power engineering, jet engines, and, later, for missile engineering.

As is known, these new engineering branches are characterized by ever increasing working temperatures. The change from piston to jet engines in post-war times was made possible due to the development of alloys capable of operating at 1000-1500°C. Still more heat-resisting materials (for temperatures of 2000°C and higher) are needed for rocket engineering, supersonic aviation, nuclear engineering, and magnetohydrodynamics.

To meet these requirements, it is essential to increase not only the melting point of an alloy, but also its relative temperature of recrystallization (T_r/T_m ratio) and, accordingly, the temperature of softening. The solution of these two contradicting problems—to lower T_r/T_m for one purpose and to raise it for another—requires a profound study into the mechanisms of recrystallization and the factors which can accelerate or decelerate the process. In that connection, many studies were conducted, mainly to determine the temperature level of recrystallization of metals and its dependence on alloying elements and conditions of treatment. Valuable results have been obtained in [1, 13-22, 300, 301].

An increasing practical importance of anisotropy of the physical and mechanical properties in components made of polycrystalline metals and alloys has resulted in ever growing number of research studies into recrystallization textures [5, 23-28]. Much work has been done to find methods for forming the desired type of texture

in metals and to analyse the effects of alloying, in particular with trace additions, on the type of texture. A remarkable example of persistent and successful work in that field is the scientific development of the processes of deformation and recrystallization annealing of transformer (silicon) iron to form a rib texture.

The study of the mechanism of texture formation, which is of high practical importance, has stimulated the use of fine methods of local structural analysis. This work has contributed much to understanding the mechanism of recrystallization in general and, in the first place, the mechanism of formation of recrystallization nuclei and the driving forces of grain growth.

The expanding requirements on the mechanical properties of alloys, heat-resisting alloys included, have raised some other urgent problems, such as polygonization and its relation to recrystallization [29-31], and inequigranularity which is quite diverse in its effects and can impair the mechanical properties [32, 33]. Among these problems are also the problems relating to the mechanism of structure 'coarsening' and the formation of coarse-grained structures during heating after light (critical) deformations, and, in some metals and alloys, after very heavy deformations. The increasing demand of modern technology for single crystals of most perfect structure has become an additional impetus for a deeper study into the mechanism of recrystallization after 'critical' deformation. The trend to utilize most fully the possibilities of additional hardening of alloys by thermomechanical treatment [34-36] has aroused interest among researchers in the problems of polygonization and recrystallization after 'hot' deformation (at elevated temperatures) and in the specific structures formed at the earliest stages of recrystallization.

Vigorous progress in powder metallurgy has given another stimulus to studies into the mechanism of grain growth, which is responsible for the kinetics of sintering, and into the role of surface tension, vacancies, pores, hard secondary-phase particles, texture, binder material, liquid phase and other factors in the process [37-39].

In recent time, powder metallurgy methods have found application in semiconductor technology for fabricating circuit elements and units from polycrystalline semiconductors. The mechanism of sintering and microstructure formation in these materials has a number of specifics owing to a lower symmetry of their crystal lattices compared to body-centred cubic (b.c.c) and face-centred cubic (f.c.c.) metals and because of the non-metallic nature of their chemical bonding. Research in this field is only in its initial stage and the problems will undoubtedly attract ever increasing attention, since these materials are very promising and their properties are very structure-sensitive.

Electronics and semiconductor technology increasingly use thin-film materials, whose structure and properties are also largely determined by recrystallization processes. The highly specific phenomena observed here are due to a very small film thickness which sharply increases the role of surface energy and thermal etch pits; they are also due to high concentration of point defects. In thin polycrystalline films obtained by sputtering, recrystallization usually takes place by the mechanism of grain growth; here, the initial size of grains is hundredths of a micrometer, i.e. one or two orders of magnitude smaller than it is in recrystallization on deformation. Besides, grain boundaries and boundary regions are noted for a very high concentration of vacancies and micropores. Because of this, the process has some specific features which have yet to be studied.

It should be recalled that a deeper insight into the mechanism of phase transformations has revealed that recrystallization also plays an important part in phase transformations involving phase strain hardening, particularly in martensitic transformations, $\alpha \rightarrow \gamma$-transformation in steels, the formation of coarse-grained fracture [40-42], and in decomposition of supersaturated solid solutions [43, 44].

This list of problems related to recrystallization is far from being exhaustive. All these problems can be divided into the main groups as follows:

1. The mechanism and driving forces of the formation and growth of recrystallization nuclei and, in general, the mechanism and driving forces of grain growth.
2. The effect of deformation pattern, the nature of material (lattice type, chemical and phase composition), thickness (of a film) and of other factors on the recrystallization mechanism.
3. The mechanism of formation of particular structures which will be called special-type structures: textured, inequigranular, coarse-grained, coarsened.
4. The mechanisms of influence of the chemical and phase composition of alloys on the temperature level and the rate of recrystallization and also on the shape of recrystallization diagrams.

Enormous factual material on the problems has been collected and many important relationships established, but many aspects of recrystallization still require explanation.

Among the problems to be studied more deeply are some radical aspects of the theory of recrystallization, such as the mechanism of redistribution and interaction of dislocations on the formation and growth of recrystallization nuclei; recrystallization following high-temperature deformation; the role of grain-boundary and surface energy at various stages of recrystallization; the mechanism and driving forces of formation of inequigranular and coarse structures;

the mechanism of formation of recrystallization textures; the reasons why trace additions raise the recrystallization temperature; possible ways of increasing the recrystallization temperature of alloys; recrystallization in thin films, two-phase alloys, materials with various types of bonding, etc.

The large diversity of the still unsolved problems in the theory of recrystallization is due to a number of reasons.

First, fine details of the dislocation structure of deformed metal, or in essence the initial conditions of recrystallization, are still unclear, as are the structures of various types of grain boundary [45-47]. Without full clarity in this aspect, it is impossible to understand the mechanism of texture formation, the role of trace impurities, etc.

Second, the process of recrystallization, seemingly quite simple, is actually extremely complicated for the mere reason that it is a structure-sensitive process that comes about owing to a nonequilibrium state of the system. Its course depends on the conditions of deformation and heating, the chemical and phase composition of alloy, the distribution and diffusion mobility of constituents, the interface energy, the structure in deformed state, and the amount of prior recovery and polygonization. In some alloys, phase and structural transformations (decomposition of solid solution, dissolution and coalescence of disperse phases, phase transformation, ordering, ascending diffusion, etc.) may go parallel with recrystallization.

Third, recrystallization nuclei differ from the deformed matrix only in lattice distortion, but have the same chemical composition and the type or spacing of lattice, as is the case with phase transformations. This complicates the use of many effective physical and structural methods for analysis of the early stages of the process.

In view of these difficulties, the experimental tools for studying recrystallization should be diversified and new indirect methods worked out to make appropriate conclusions.

In recent works on recrystallization, the attempts to describe in a purely mathematical form the rate of the process (R. F. Mehl, M. Avrami et al. [48]) have given way to the analysis of the atomic and dislocation mechanism, the physical essence and the driving forces of the process [1, 3, 4, 16]. Only this trend in research work can be fruitful in explaining and systematizing the vast factual material accumulated earlier and make it possible to control scientifically the process of recrystallization in existing and novel alloys, the type of the structure that forms in them, and thus their structure-sensitive properties. This exactly is one of the most important tasks of the physical metallurgy.

1.2. Principal Microstructure Parameters and Their Effect on the Properties of Recrystallized Material

The principal parameters of the microstructure formed on recrystallization have a substantial effect on the properties of the recrystallized material. These are: the average size of grains, $\bar{D}$, and subgrains, $\bar{d}$; the shape of grains, the size and misorientation of subgrains; the nature and degree of inequigranularity of the material; the existence and the type of texture, i.e. anisotropy of crystallographic orientation of grains in a specimen; the anisotropy of the external shape of grains.

Detailed discussion of the effects of these parameters on material properties seems to be unreasonable in the scope of this book, so that only a few typical examples will be analysed below.

The *average grain size* $\bar{D}$ practically affects all mechanical properties [41]. For instance, the elastic limit σ_{el} increases appreciably with an increase in grain size $\bar{D}$. There is a distinct correlation between $\bar{D}$, on the one hand, and the yield strength σ_y and ultimate strength σ_t, on the other. For many metals and alloys, the correlation between $\bar{D}$ and σ_y at conventional rates of deformation is described approximately by the Hall-Petch relationship [49]:

$$\sigma_y = \sigma_0 + k\bar{D}^{-n}$$

or, for metals with a distinct substructure

$$\sigma_y = \sigma_0 + k\bar{d}^{-n}$$

For b.c.c. metals and alloys, $n = 0.5$.

The yield strength σ_y increases with decreasing $\bar{D}$ more appreciably in metals having a lower number of operative slip systems (see Ch. 2).

Grain coarsening diminishes the work-hardening effect produced by deformation and lowers substantially ductile properties. In this connection, work-hardening due to grain refinement differs favourably from work-hardening caused by deformation in that it does not embrittle the metal but, on the contrary, increases its ductility.

The long-term strength versus grain size curve usually has a maximum. The curve describing the effect of $\bar{D}$ on fatigue resistance also has a maximum [52].

The effect of grain size on the yield limit under the conditions of superplastic flow (noted for a very low rate of deformation, elevated deformation temperature, and superfine grain) is opposite to the effect under common conditions of deformation, i.e. it is described by the relationship $\sigma_{y_{sp}} \approx D^a$ (where a is close to unity) rather than by the Hall-Petch relationship $\sigma_y \approx D^{-1/2}$.

In many high-melting metals, the ductile-to-brittle transition point rises with $\bar{D}$ [53].

$\bar{D}$ can also affect the magnetic properties and resistivity of metals. The coercive force H_c turns out to be especially structure-sensitive.

All the factors which impede the movement of domain boundaries and the rotation of the magnetic vector of the domain region increase H_c. Fine grains (10^{-4} to 10^{-5} cm) in ferromagnets and ferrites are usually single-domain owing to an increased energy of domain boundaries. On this ground, H_c diminishes with increasing grain size, but as $\bar{D}$ decreases to the size corresponding to the single-domain state of H_c, it reaches a maximum. The effect of grain size on H_c is most pronounced in the region of low values of $\bar{D}$. On the other hand, grain refinement increases H_c, but impairs the thermal stability of this characteristic which is a very important one in many magnetic materials, particularly in ferrites. This is because grain boundaries and grain volumes contribute differently to H_c, the contribution of boundaries being much more temperature-dependent.

The speed of response of ferrites decreases with grain coarsening.

The curves relating the total core losses in transformer steel to grain size show a maximum whose position depends on the method of steel making (more strictly, on the purity of steel) and may shift within a wide range from 0.3 mm to 1 mm [26, 54].

Grain size can also affect the resistivity of metals and alloys. With decreasing $\bar{D}$, the resistivity grows, though not sharply. For instance, with a decrease of $\bar{D}$ in commercial iron by a factor of three (from 150 μm to 50 μm), ρ rises roughly by 1%.

Inequigranularity (see Ch. 8) usually has an adverse effect on the mechanical properties at room temperature and elevated temperatures. The operating characteristics of gas-turbine blades made of nickel-base alloys are impaired appreciably at $D_{max}/\bar{D} > 3$ [52]. The short-term and the long-term strength of specimens having an inequigranular structure are 10-25% lower than those of specimens with uniform grain, and the rate of creep is respectively 3-5 times higher [32].

In ball-bearing chromium steel ШХ15, inequigranularity (lineage structure) lowers the impact toughness in as-hardened state, ultimate bending strength, contact resistance, and endurance of ball bearings [55]. Inequigranularity can greatly affect physical properties. For instance, it impairs the rectangularity of the hysteresis loop of square-loop ferrites [56] and increases the core loss in low-textured dynamo steel [57].

Imperfection of grains is associated with the presence of dislocation pile-ups (subboundaries) and with an irregular shape (waviness) of

grain boundaries. An increase in the misorientation angles between subgrains increases σ_y. The formation of a polygonal (subgranular) structure can raise the values of ultimate strength, heat resistance, and impact toughness and shift the ductile-to-brittle transition point towards lower temperatures.

The crystal texture in polycrystalline solids (see Ch. 10) has an especially strong effect on many of their properties.

The resistance of sheet materials to plastic deformation is characterized by the plastic anisotropy index, or rollability index R* [2]. In isotropic materials, $R = 1$ and in textured ones, $R \neq 1$. The capability of materials for deep drawing improves as R increases above unity.

In sheets of hexagonal metals, the (0001) $[10\bar{1}0]$ texture has the highest values of R. In cubic metals, particularly in steel sheets, drawability is the highest if the {111} planes are parallel to the plane of rolling, and the lowest if rolling is done in the {100} plane.

Sharp anisotropy of magnetic properties of ferromagnets, such as transformer steel, is utilized in the national economy. The problem will be dealt with in more detail in Ch. 10.

The anisotropy of thermal expansion may result in an oriented accumulation of defects and even change the dimensions of a specimen upon multiple heating-cooling cycles (thermocycling) [25]. This phenomenon has been examined most thoroughly on α-uranium rods [58].

The properties of textured materials can be influenced noticeably by the angle of misorientation between adjacent grains. For monotextured specimens, it is characterized by the angle of texture scatter. When the texture of a specimen consists of a number of components, the misorientation angle depends onto which components the nearest adjacent grains belong.

In metals and semiconductors with a lower symmetry than the cubic symmetry, the electric conductivity and thermal properties may be sharply anisotropic. This is more pronounced in materials of complicated structure. The phenomenon is utilized in thermoelectric materials.

Anisotropy of the external form of grains has a much less pronounced effect on the properties than the crystal texture. In some cases, however, the effect can be quite noticeable. For instance, magnetic steel sheets must have a favourable texture and shape of grains to minimize the demagnetization factor. This condition can be met easier at a greater linear size of grains in the direction of magnetization.

In steel sheets used for deep drawing, a flattened ('pancake') shape of grains improves drawability [59].

---

* R is the ratio between relative deformations across the width and thickness of a sheet.

Chapter 2

Structural Changes in Deformed Metals and Alloys

Primary recrystallization is the process that takes place during heating of cold-worked metals. In particular. it diminishes or eliminates fully the additional structural imperfections which have been caused by prior deformation.

It is then clear that the nature, density and distribution of these imperfections, i.e. the dislocation structure of the deformed material, should have the decisive effect on the course of recrystallization.

The structure of a deformed material in turn depends on the mechanism of deformation. The mechanisms of deformations and the involved structural changes have been discussed in a number of monographs and reviews [60-62].

The principal mechanism of plastic deformation in metals. and in all crystals in general, is the shear movement of some portions of a crystal (or crystallite) relative to other portions; it is effected through various dislocation movements. including movements along grain boundaries.

Under deformation at high temperatures, diffusion movement of dislocations (dislocation climb) also becomes possible; it contributes somewhat to the shear movement and changes its final result.

Finally, at low deformation rates and very high temperatures (above 0.5 T_m) these types of plastic deformation may be accompanied by a purely diffusion movement of some crystallites relative to others. The dislocation and diffusion mechanisms determine the development of intragranular and intergranular deformation.

Shear deformation can occur by a number of particular mechanisms, the principal ones being dislocation slip and cross-slip. twinning. kinking, etc.

In most cases, several mechanisms are operative at once, with one of them being predominant. The contribution of a particular mechanism is determined by many factors, among which are the pattern and conditions of deformation (deformation degree. temperature and rate), the type of crystal lattice and the stacking fault energy, the crystal orientation relative to the external stresses (in the case of single crystals or originally textured polycrystals), the size and shape of grains prior to deformation, the chemical and phase com-

position of the material, the size and plasticity of excess phase particles, etc.

Even this schematic description of the possible methods of deformation and of the principal affecting factors shows clearly that the phenomenon is quite complicated. This is why many of the problems associated with the changes in the structure and properties of plastically deformed metals have in the main been analysed only qualitatively.

A theory of plastic deformation should be based on the modern concepts of dislocations and their behaviour in metals and alloys and on the use of these concepts for the analysis of work-hardening of metals and alloys on deformation (analysis of stress-strain curves); the associated structural changes can be examined by fine methods of structural analysis.

2.1. Deformation in Single Crystals

2.1.1. Slip Deformation

Slip systems. Plastic deformation by slip is the displacement (shear) of individual dislocations on the crystal planes which are filled most densely with atoms (have the highest reticular density) and are respectively characterized by the largest interplane distances.

In some cases (in certain types of lattice at elevated temperatures and high deformation rates), dislocation slip is also possible on other planes whose reticular density is not at the maximum, but approaches this value.

On these planes, dislocations slip in the same directions i.e. along those dislocation lines which are most densely filled with atoms; this rule has almost no exceptions.

The shear strength possessed by the crystal lattice is the lowest in these planes and directions and the respective dislocations have the least Burgers vector. A slip plane and the direction of slip on that plane form what is called the *slip system.*

In f.c.c. metals and alloys, dislocation slip usually occurs on {111} planes in ⟨110⟩ directions. The four octahedral planes of the type {111} and the three directions of the type ⟨110⟩ form 12 possible slip systems in an f.c.c. lattice. Figure 1*a* shows a (111) plane and three ⟨110⟩ directions which form three slip systems on that plane. The slip systems in planes $(\bar{1}11)$, $(1\bar{1}1)$ and $(11\bar{1})$ could be illustrated in a similar manner.

In a number of metals and alloys with an f.c.c. lattice (such as aluminium or brass), slip on the planes of the cube can also occur along with slip on octahedral planes. In aluminium at elevated temperatures, around 40 per cent of slip lines belong to cube planes,

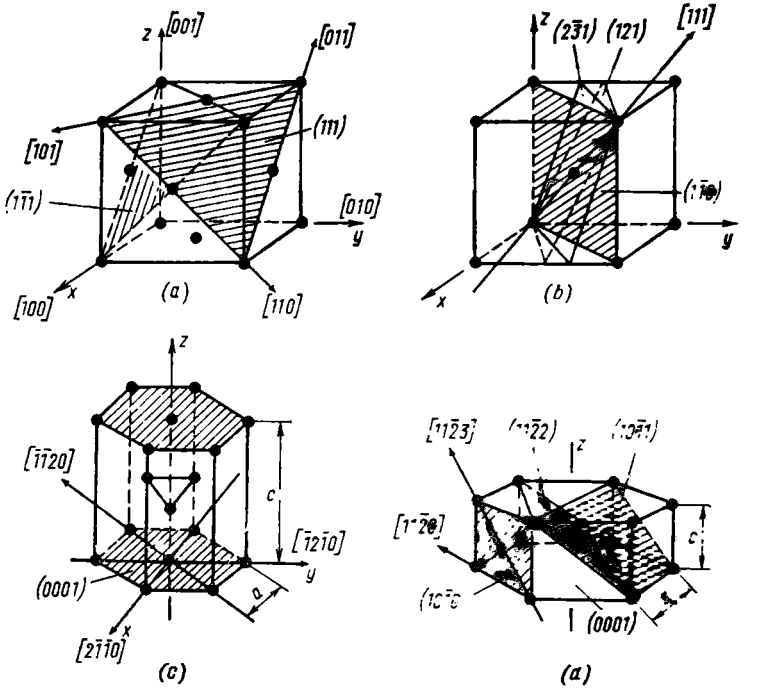

Fig. 1. Principal slip systems in various lattices
(*a*) f.c.c.; (*b*) b.c.c.; (*c*) c.p.h., $c/a = 1.633$; (*d*) c.p.h., $c/a < 1.633$; in the last picture, atoms located between the basal planes are not shown

In b.c.c. materials, planes of several sets, e.g. {110}, {112} and {123}, can serve as slip planes. These are planes with a relatively dense and high atomic packing, the {110} set showing a denser packing than the others, but neither of them has the closest packing. In all these cases, the ⟨111⟩ type is the direction of slip, as illustrated in Fig. 1*b*. The result is that the number of slip systems in b.c.c. materials may be as high as 48, as in iron where 12 planes belonging to the sets {110}, {112}, and {123} are located around each of the four ⟨111⟩ directions. In that case, the ⟨111⟩ directions form the common shear axis.

The large number of possible slip systems in iron and some other b.c.c. metals often results in that the slip in them occurs on a complicated surface (Fig. 2), which is the surface of a prism whose every face coincides with a particular slip plane and whose edges are the lines of intersection of these planes with the slip direction. The slip resembles here longitudinal shear in a bundle of pencils and for that reason has been called pencil glide. This type of slip becomes pos-

sible with a large number of slip systems having one and the same shear vector.

With metals and alloys possessing a close-packed hexagonal (c.p.h.) lattice, the type of operative slip systems depends in the first place on the c/a lattice ratio. As is known, in an ideal c.p.h. lattice built up of equal spheres, $c/a = 1.633$. Among real c.p.h. metals, however, only magnesium and cobalt have the c/a ratio close to that value, while for other metals it is either greater or lower than the ideal ratio. The greatest values have Zn (1.856) and Cd (1.886), and the lowest Ti (1.587) and Be (1.567).

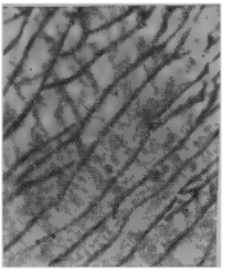

Fig. 2. Slip bands in α-iron, ×100

A change in c/a involves a change in the relative close packing in various planes. At large values of c/a (>1.633), the (0001) planes, i.e. the basal planes (Fig. 1*c*), are the closest packed, whereas at low values of c/a (<1.633), the closest packed planes are $\{10\bar{1}0\}$, which are called prism planes (see Fig. 1*d*).

An important factor which can affect the operative slip systems is the stacking fault energy γ_{sf}. As has been shown by A. Seeger, the dislocation energy in metals with a low value of γ_{sf} can be decreased by dissociation of dislocations into partial dislocations with the formation of stacking faults. In c.p.h. lattices, this dissociation is possible on the basal plane and impossible on prism planes. On the latter, the formation of dislocations is especially unfavourable energetically.

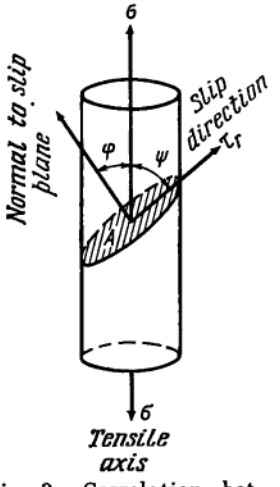

Fig. 3. Correlation between the applied stress σ and shear stress τ_r (schematic)
A is the slip plane

As a result, basal slip is predominant even in substances with a medium value of c/a (near 1.633). Further, there is also prismatic slip whose contribution increases as the c/a ratio becomes less than 1.633 (Table 1). It has been established experimentally that dislocations on the $\{10\bar{1}1\}$ and $\{11\bar{2}2\}$ pyramidal planes can also participate in slip. On these planes, dislocations can also dissociate into partial dislocations. The problem is discussed in more detail in [61].

The slip systems in selected materials are given in Table 1.

When analysing the process of slip under the action of an external stress (for instance, a tensile stress) σ, it should be remembered that shear is caused by a tangential stress operating on the slip plane in the

TABLE 1. Slip Systems

Metal or alloy	Slip systems at temperature	
	low	high
	f.c.c. lattice	
Al	$\left.\begin{matrix}\{111\}\\\{010\}\end{matrix}\right\}\langle\bar{1}01\rangle$	—
Cu, Ag, Au, Ni, α-brass	$\{111\}\langle\bar{1}01\rangle$	—
	b.c.c. lattice	
α-Fe	$\left.\begin{matrix}\{110\}\\\{211\}\end{matrix}\right\}\langle\bar{1}11\rangle$	$\left.\begin{matrix}\{110\}\\\{211\}\\\{321\}\end{matrix}\right\}\bar{1}11\rangle$
Mo	$\left.\begin{matrix}\{211\}\\\{110\}\end{matrix}\right\}\langle\bar{1}11\rangle$	$\left.\begin{matrix}\{110\}\\\{211\}\end{matrix}\right\}\langle\bar{1}11\rangle$
W	$\{211\}\ \langle\bar{1}11\rangle$	—
β-brass	$\left.\begin{matrix}\{110\}\\\{211\}\end{matrix}\right\}\langle\bar{1}11\rangle$	—
	c.p.h. lattice	
Cd ($c/a=1.886$)	$\left.\begin{matrix}\{0001\}\\\{1\bar{1}01\}\end{matrix}\right\}\langle11\bar{2}0\rangle$	$\left.\begin{matrix}\{0001\}\\\{1\bar{1}01\}\end{matrix}\right\}\langle11\bar{2}0\rangle$
Cd ($c/a=1.856$)	$\left.\begin{matrix}\{0001\}\\\{1122\}\end{matrix}\right\}\langle11\bar{2}0\rangle$	$\left.\begin{matrix}\{0001\}\\\{1\bar{1}00\}\\\{11\bar{2}2\}\end{matrix}\right\}\langle11\bar{2}0$
Mg ($c/a=1.624$)	$\left.\begin{matrix}\{0001\}\\\{1\bar{1}00\}\end{matrix}\right\}\langle11\bar{2}0\rangle$	$\left.\begin{matrix}\{0001\}\\\{1\bar{1}01\}\\\{1\bar{1}00\}\end{matrix}\right\}\langle11\bar{2}0\rangle$
Co ($c/a=1.621$)	$\left.\begin{matrix}\{0001\}\\\{11\bar{2}2\}\end{matrix}\right\}\langle11\bar{2}0\rangle$	—
Zr ($c/a=1.593$)	$\left.\begin{matrix}\{1100\}\\\{0001\}\end{matrix}\right\}\langle11\bar{2}0\rangle$	—
Ti ($c/a=1.587$)	$\left.\begin{matrix}\{1100\}\\\{0001\}\end{matrix}\right\}\langle11\bar{2}0\rangle$	—

slip direction. This is termed the resolved shear stress τ_r. The relationship between τ_r and σ is of the form

$$\tau_r = \sigma \cos\varphi \cos\psi \qquad (1)$$

which is called the Schmid law and can be explained by the scheme in Fig. 3*.

* The tensile stress σ' in the slip plane A is $\sigma' = \sigma\,(A/A_0)$, where A_0 is the cross-sectional area of the specimen and $A = A_0 \cos\varphi$. The shear stress in plane A is $\tau_r = \sigma' \cos\psi = \sigma \cos\varphi \cos\psi$.

Plastic deformation in a given slip system will appear when τ_r reaches the *critical shear stress* τ_{cr} (or the critical resolved shear stress), the latter being an important characteristic of the mechanical properties of a material.

It should be noted, however, that τ_{cr} is substantially higher in less pure metals, which fact should be taken into account when analysing the effects of other factors (temperature and rate of deformation, structure, etc.) on τ_{cr}.

It follows from equation (1) that τ_r depends heavily on the orientation of the slip system relative to the external stress. If the axis of tension is either normal or parallel to the slip plane, there will be no slip since $\tau_r = 0$. If the slip plane is at an angle of 45° to the axis of tension, τ_r will be at its maximum and equal to 0.5σ.

The stress causing a shear (deformation) can be better characterized by a shear stress, rather than by the tensile stress applied. Similarly, the actual deformation can be better characterized in terms of the relative displacement of the two nearest neighbouring slip planes (which is called the shear deformation), rather than by the total deformation, i.e. the total elongation of the specimen expressed as percentage. This is linked with the circumstance that the geometry of the specimen alters in the course of slip and, as a consequence, the direction of slip gradually rotates towards the axis of tension.

If we know, on the one hand, the original and the final orientation of the slip elements, i.e. the angles between the axis of tension and the directions of slip before and after deformation (λ_0 and λ_1), and, on the other, the angles between the slip plane before and after deformation ($\varkappa_0$ and $\varkappa_1$), we can find the shear deformation from the equation

$$\varepsilon = (\cos \lambda_1 / \sin \varkappa_1)\ (\cos \lambda_0 / \sin \varkappa_0)$$

If we know only the original orientation (λ_0 and λ_1) and l_0 and l_1, then

$$\varepsilon = (1/\sin \varkappa_0)\ [\sqrt{(l_1/l_0)^2 - \sin^2 \lambda_0} - \cos \lambda_0]$$

It should then be clear from the foregoing that if a crystal shows a few slip systems with different orientations relative to external forces, plastic deformation will occur first on the most favourably oriented system, namely, on the one in which the resolved shear stress reaches the critical value earlier than in the other systems. This slip system is called *primary*.

As the applied stress grows in magnitude, the slip spreads over other, less favourably oriented, slip systems (secondary systems).

It is practically important to represent graphically the orientations and slip systems of a crystal relative to an external stress (for instance, relative to the axis of tension). Stereographic projections are commonly used for the purpose.

These projections represent angular relationships between the families of planes and directions in a crystal and for that reason are identical for all crystals of the cubic system irrespective of the type of lattice (whether b.c.c. or f.c.c.) and the absolute value of the lattice spacing. With substances of hexagonal symmetry, the stereographic projections are identical for all crystals of a given *c/a* ratio.

To construct the stereographic projection of a crystal, the latter should be mentally replaced by a crystalline complex under which one understands the combination of planes and directions parallel to the planes and orientations of the crystal but displaced parallel to themselves until they intersect in a single point, the centre of the projection sphere (Fig. 4*a*).

The planes (or their normals) and directions of the crystalline complex are extended to intersect the upper half of the projection sphere. The intersection points are connected by straight lines with the lowermost point of the sphere (the point of intersection with the vertical diameter). The points of intersection of these straight lines with the projection circle — the larger horizontal circle of the projection sphere — represent the stereographic projection of the crystal for its given orientation (Fig. 4*b*).

Figure 4*b* shows the stereographic projection of the principal planes and directions of the types {100}, {110}, {111} and ⟨100⟩, ⟨110⟩, ⟨111⟩ in a crystal of the cubic system, which is oriented so that a direction of the type ⟨001⟩ (a normal to the cube plane) is vertical, and therefore its projection W_1 coincides with the centre of the projection circle. The [100] and [010] directions in the crystalline complex are disposed in the horizontal plane and are respectively represented by points W_2 and W_3 in the stereographic projection.

The projection is divided into 24 elementary stereographic triangles which are fully equivalent crystallographically. The apices of these triangles are the projections of the directions from the families ⟨100⟩, ⟨110⟩ and ⟨111⟩, or, respectively, the projections of the normals onto the planes {100}, {110} and {111}, and are denoted by symbols as shown in the figure.

Figure 4*c* shows the projection of a cubic crystal of the same orientation, with the crystal planes being replaced by their normals (gnomonic projection). It is called the standard projection of a corresponding orientation ([001] in the case considered).

The orientation of a crystal is usually characterized by a triangle with apexes [001], [011] and [111], which is located in the projection centre (triangle W_1AI in Fig. 4*b*). It is usually called the standard triangle. Having measured the angles between the crystal axis and the three directions indicated (it is sufficient to know two of the three angles), the position of that axis can be marked to a corresponding scale on the standard stereographic triangle.

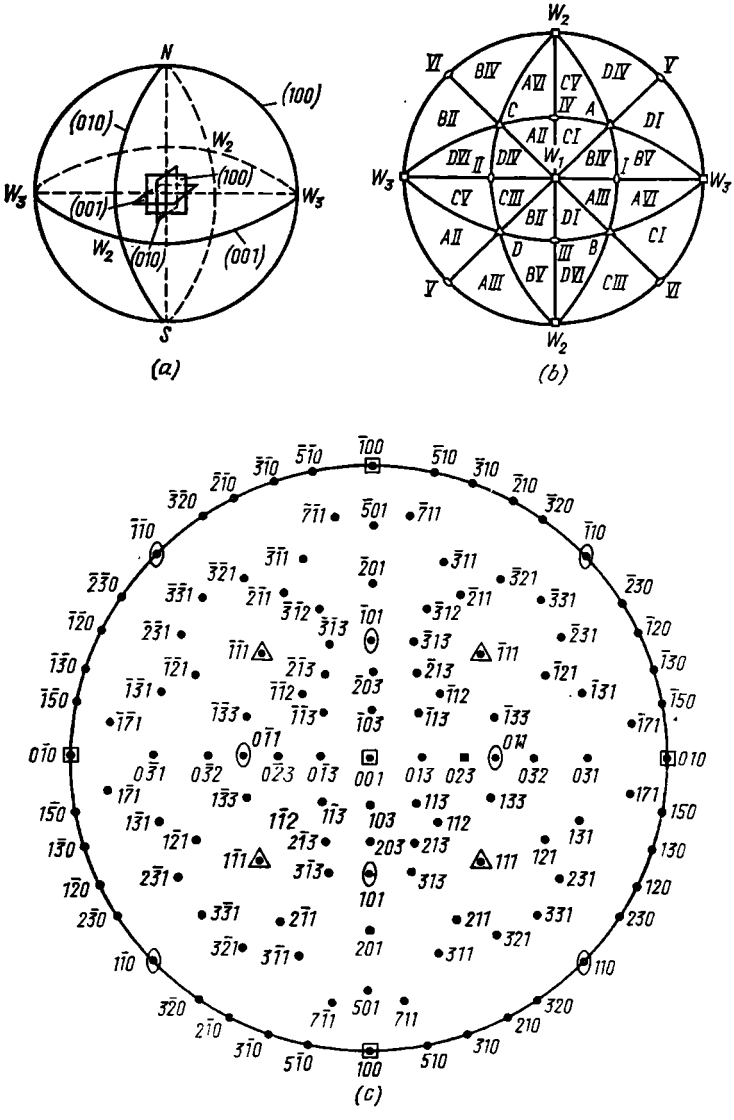

Fig. 4. Crystalline complex (*a*), stereographic projection (*b*) and gnomonic projection (*c*) of the principal planes of cubic lattice

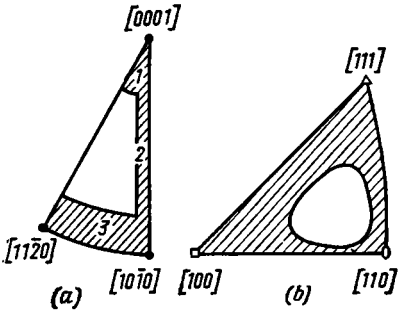

Fig. 5. Stereographic triangles for hexagonal crystals (*a*) and f.c.c. crystals (*b*). The orientation regions most favourable for easy slip (basal slip in case *a*) in tension are shown unhatched. The hatched regions in (*a*) *1*—twinning, for $(c/a) < \sqrt{3}$; *2*—double slip; *3*—slip, on prismatic and pyramidal planes and twinning, for $(c/a) > \sqrt{3}$

Let us consider the use of stereographic projections for analysis of slip deformations, for instance, in f.c.c. metals, which possess twelve possible slip systems of the type {111} ⟨110⟩. These systems are shown in the stereographic projection of Fig. 4*b*.

In that projection, the traces of the normals to the slip planes ($\bar{1}11$), (111), ($1\bar{1}1$) and ($11\bar{1}$) are denoted by letters *A*, *B*, *C*, and *D* [70], and the projections of the slip directions [0$\bar{1}$1], [0$1\bar{1}$], [$\bar{1}$01], [$1\bar{0}$1], [$\bar{1}$10] and [110] by digits *I*, *II*, *III*, *IV*, *V*, and *VI*, respectively.

Each elementary triangle in the projection represents a region in which only one slip system is operative. For the triangle W_1AI, this is the system (111) [$\bar{1}$01] denoted as *BIV*, etc.

Thus, for all crystals whose axis of tension lies inside the triangle $[W_1AI]$, deformation starts with the slip in the (111) [$\bar{1}$01] system, which is the primary slip system in this case.

For crystals whose axes of tension lie on the sides of the triangle, the slip usually proceeds in two systems at once. For instance, with crystals whose projections of the axes of tension lie on the side W_1I, the critical shear stress for the (111) [$\bar{1}$01] system is the same as that for the ($\bar{1}$11) [101] system, i.e. *BIV* and *AIII*, and the slip starts simultaneously in both systems.

The slip will be even more manifold in crystals whose projections of the axes of tension coincide with the apexes of the triangle. The [001] orientation is distinguished by the largest number of slip systems equally favourably oriented for slip (see Fig. 4*b*). Here, eight slip systems are possible (on four planes, with two directions in each); only four of these systems can be operative at once, since slip on a given plane is possible in one direction only.

Figure 5 (*a* and *b*) shows the standard triangles for c.p.h. and f.c.c. crystals with the regions of orientations most favourable for easy slip.

It is essential that in the course of deformation under usual conditions the slip is not limited to the primary slip systems. At a definite stage of deformation, whose magnitude is dependent on numerous factors, other slip systems become operative, which initially have been oriented less favourably. With single crystals, this is

mainly due to the fact that, as has been mentioned earlier, a crystal tends to rotate in the course of deformation.

Under tensile deformation, for example, the direction of slip turns towards the axis of tension. This means that the spherical triangle displaces relative to the point that represents the projection of the crystal axis. One can visualize this more easily as the displacement of the point in the immobile spherical triangle. The point may move from the inside of the triangle onto one of its sides, in which case it is not one but two slip systems that are equally operative. The slip system that begins to act together with the primary slip system is called the conjugate slip system.

In f.c.c. crystals deformed by tension, conjugate with the (111) [$\bar{1}$01] primary system is the ($\bar{1}\bar{1}$1) [001] system. In b.c.c. crystals, the system (011) [11$\bar{1}$] is conjugate with the primary (011) [$\bar{1}$11] slip system.

In c.p.h. crystals, slip at low temperatures usually occurs on the basal (0001) plane in one of the close-packed $\langle 11\bar{2}0 \rangle$ directions. With favourable orientations (where the angle between the axis of tension and the direction [0001] is 10-80°), the deformation in this primary system can be very high, 200 per cent or even more, before the conjugate slip systems become operative. If the orientation of the crystal is unfavourable (the basal plane is almost parallel to the axis of tension), non-basal slip is operative — prismatic or/and pyramidal—with an appreciably higher critical shear stress.

In c.p.h. crystals, double slip can be produced if their orientation is specially selected, i.e. when the orientation is such that the shear direction is the bisector of the two slip directions.

In polycrystals and in single crystals containing dislocation locks, additional slip systems become operative when dislocations in the primary system cannot move for some reason or other.

The other {111} planes in an f.c.c. lattice, which include the primary slip direction and on which, therefore, cross slip of screw dislocations of the primary system is possible, are called the cross-slip planes (plane *D* in Fig. 4*b*).

The significance of the problem on the nature and number of operative slip systems, which has just been discussed in detail, lies in that the number of simultaneously operating systems is decisive for the dislocation structure that forms on deformation and, hence, for the conditions of subsequent recrystallization.

Direct studies of dislocation structures in deformed metals and alloys are associated with appreciable difficulties. In the first place, the methods used should provide for a very high resolution. On the other hand, this results in ever greater localization of the volumes being investigated and, therefore, generates the need to resort to statistical analysis for higher reliability. In this connection, it is quite important to obtain data on the hardening effect produced by

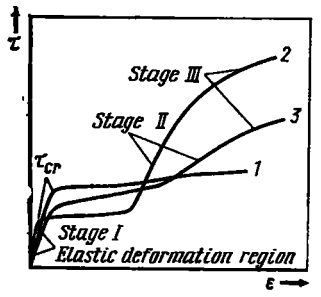

Fig. 6. Typical stress-strain curves for (*1*) hexagonal, (*2*) f.c.c. and (*3*) b.c.c. crystals favourably oriented for easy slip (schematic)

deformation. This remarkable peculiarity of metals is directly associated with the dislocation structure that forms on deformation and prevents further deformation of the metal. As a result, the critical shear stress τ_{cr} required for further deformation ε varies in the course of the process, and it does so more intensely when the dislocation structure formed by prior treatment offers an increased resistance to dislocation movement.

Stress-strain curves (hardening curves) actually show what amount of shear stress should be applied to cause further plastic deformation at a given dislocation density and dislocation distribution formed by prior treatment.

Plastic deformation is analysed in the following way. The initial data are the hardening curves obtained for various metals and alloys under various conditions of deformation. Proceeding from these data, dislocation models are constructed to explain the τ_r-ε relationships established. Finally, the validity of a proposed model is verified experimentally (by structural analysis).

Structural changes at various stages of hardening. Figure 6 shows typical stress-strain curves* for high purity f.c.c., c.p.h. ($c/a > > 1.633$), and b.c.c. crystals deformed by tension, the axes of tension at the initial moment being within the standard triangles.

The curve for an f.c.c. crystal is most typical. It shows more clearly than the other curves that hardening passes through three stages. Apart from the type of lattice, other factors can also affect the pattern of stress-strain curves and the relative contributions the three stages make to the total deformation. The principal among these factors are as follows:

(1) the stacking fault energy and the c/a ratio (for hexagonal metals);

(2) the purity of the material, the quantity and nature of impurities and alloying additions;

(3) the orientation of the crystal;

(4) the temperature and rate of deformation.

Let us now analyse the three stages of a stress-strain curve.

At the first stage, the curve has two linear portions: the initial portion of elastic (reversible) deformation and the portion of plastic (irreversible) deformation. The τ-ε curve has a bend as it passes

* These curves and the ones that follow are the plots of resolved shear stress against resolved strain.

from the first to the second portion. The bend is indicative of the beginning of plastic deformation.

According to Hooke's law, the work-hardening coefficient for the first portion is equal to the shear modulus G; in the linear portion of plastic deformation, the work-hardening coefficient θ_I is very low (of an order of 10^{-4} G for c.p.h. and f.c.c. metals and 10^{-3} G for b.c.c. metals). In view of the low value of θ_I, the first stage can be called the stage of easy slip. The critical shear stress τ_{cr} and the highest shear strain ε_I are also important parameters of this stage. As will be shown later, these characteristics can vary within very wide limits depending on the nature and purity of metals and the conditions of deformation.

For high-purity metals, τ_{cr} is very low (fractions of a kilogram per mm^2).

The second stage, which sets in as the deformation exceeds ε_{II}, is also characterized by a linear relationship $\tau = f(\varepsilon)$, but the work-hardening coefficient at this stage II is appreciably (by a factor of 30) higher than θ_I.

The second stage is less affected by various factors than the first. In particular, the coefficient θ_{II} is independent of temperature, though the moment at which the second stage passes to the third stage is variable. The portion of the curve corresponding to the third stage is typically parabolic rather than linear. The hardening effect in the third stage diminishes with increasing deformation; the phenomenon is called dynamic recovery. The onset of stage III is especially sensitive to the temperature of deformation, T_d. As this temperature rises, the onset of stage III shifts towards lower values of ε.

Now consider the specific structural changes at various stages of hardening.

At the first stage, in the case described by the τ-ε curves shown in Fig. 6, shear occurs through dislocation slip in a single primary slip system due to the sources that existed prior to deformation.

There are no substantial obstacles to dislocation movement, and therefore the free path of dislocation is as a rule long. Most dislocations reach the surface of the crystal and form jogs. Trails of a large number of dislocations which have moved on one and the same plane are revealed metallographically as slip lines. They can be detected on a polished surface of single crystals by optical microscopy. Electron microscopy reveals rather uniformly distributed long slip lines with jogs of a relatively low height (50-100 Å).

The hardening effect obtained in such an ideal case is associated with long-range interaction of dislocation loops in the primary slip system, which are spaced a distance R_0 apart.

According to Seeger, parallel dislocations of the same sign, which are located on parallel planes, produce a long-range stress field

whose maxima are separated by distances of an order of R_0' (the distance between dislocations). For a dislocation to move between two like dislocations, it should overcome the inverse long-range stress. To effect this, the stress applied to an edge dislocation must be

$$\tau_{edge} = \frac{G}{2\pi(1-\nu)} \frac{b}{R_0'}$$

and that to a screw dislocation,

$$\tau_{scr} = \frac{G}{2\pi} \frac{b}{R_0'}$$

With an increased number of dislocation loops, the inverse stress τ_{inv} that acts on dislocation sources grows. When τ_{inv} becomes equal to the increased shear stress, generation of dislocation loops ceases.

The work-hardening coefficient is

$$\theta_I = (8G/9\pi)/(R_0'/L)^{3/4}$$

where L is the length of dislocation.

All what has been said above is true for the cases where only one primary slip system is operative. This is realized most easily in hexagonal crystals (see p. 27).

Figure 5*a* shows the stereographic triangle for hexagonal crystals with the indication of crystal orientations responsible for a particular type of slip. As is seen, in a large region within the triangle, the slip occurs on a single family of basal planes, and there is no intersection of non-parallel slip planes. This also accounts for the fact that only in hexagonal crystals can the elongation (deformation) at stage I be as high as 200% or even more. Basal slip causes only small distortions, which is confirmed by the fact that reflections on Laue photographs of deformed crystals remain sharp up to deformations of 100% or more.

The extent (i.e. the interval) of the first stage decreases sharply if the crystal is oriented less favourably.

The crystal orientation has an even more pronounced effect on τ-ε curves for f.c.c. and b.c.c. crystals, where the extent of stage I and the hardening coefficient θ_I can vary within wide limits.

The extent of stage I for f.c.c. crystals (Cu, Ag, etc.) is at its maximum (up to 15%), where the orientation is close to [011] and at its minimum for crystals whose axis of tension is close to the [111]-[001] line or coincides with the [111] and [001] directions. As follows from the earlier discussion, respectively three or four slip systems must be operative in these cases. In the stereographic triangle for f.c.c. crystals (see Fig. 5*b*), the region of orientations for which stage I is the longest is shown unhatched. Even in this case stage I is much shorter than is the case for hexagonal crystals.

These data, along with direct structural investigations, give evidence that a small portion of slip occurs in secondary slip systems at the first stage, too, in f.c.c. crystals. This share of slip noticeably increases as the axis of a crystal turns in the direction of the [111]-[001] line. The fact that plastic slip indeed takes place in secondary systems at the first stage of deformation is also confirmed by the appearance of kink bands (see later in the book) which are sometimes detected at this stage. With b.c.c. crystals, the orientations which are favourable for slip on the primary system are located far from the [001]-[101] symmetry boundary.

I. I. Novikov and V. I. Tiraspol'sky [63] have established in experiments on tungsten single crystals that rolling in planes {001} and {011} with a reduction in thickness up to 5% gives a higher hardening effect than rolling in plane {123}.

Using another method of deformation (hydroextrusion), the authors have found that the stage of easy slip extends longer in the ⟨001⟩ directions than in the ⟨013⟩ or ⟨112⟩ directions. In the former case, the structure remains monocrystalline at a deformation up to 70%, and in the latter to 55-60%.

For the same purity, stage I for b.c.c. crystals is usually shorter than it is for f.c.c. crystals. The pattern of τ-ε curves for b.c.c. crystals depends on the content of impurities which, as is known, are difficult to remove.

The available data concerned with the effect of deformation temperature on stage I are not always definite, which is attributed to the fact that various researchers have dealt with different temperature intervals and with materials of different purity.

It seems reasonable to conclude that a reduction of test temperature prolongs stage I in f.c.c. and b.c.c. crystals (Fig. 7) and respectively reduces the rate of hardening θ_I. At lower temperatures, the critical shear stress τ_{cr}^{sec} in secondary systems increases, so that

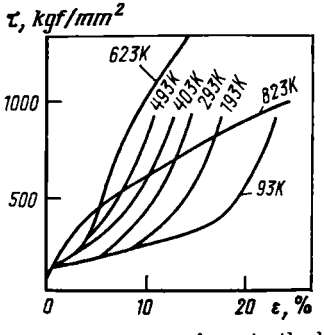

Fig. 7. τ-ε curves for similarly oriented copper crystals upon deformation at various temperatures

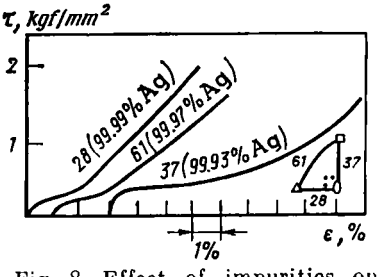

Fig. 8. Effect of impurities on τ-ε curves of silver crystals

heavier deformations are needed for the resolved shear stress τ_r to exceed τ_{cr}.

At relatively high temperatures ($T_d/T_m > 0.3$), the work-hardening coefficient begins to drop owing to recovery.

Irrespective of the type of lattice, impurities can affect drastically the first stage of hardening. Dissolved impurities prolong stage I, probably in the same way as does a reduction in temperature (Fig. 8) [2, 64]. In addition, dissolved impurities raise the critical shear stress τ_{cr} and make the yield point more pronounced. Furthermore τ-ε curves for b.c.c. crystals containing dissolved interstitial impurities exhibit a yield point and respectively the upper and the lower yield limit.

The appearance of the upper yield limit is due appreciably to locking of dislocations by impurity atmospheres. On the other hand, the strong effect of temperature on the resolved critical stress in b.c.c. crystals is convincing evidence that the appearance of the yield point is associated with temperature-dependent Peierls-Nabarro forces.

If impurities form a secondary phase, though in a small quantity, the first stage of hardening becomes shorter or even disappears fully. Disperse excess-phase particles serve as obstacles for dislocations of the primary slip system. As a result, slip in other slip systems is initiated in local regions near these particles already under light deformations.

As noted earlier, the second stage of hardening has an appreciably higher work-hardening coefficient θ_{II} (roughly by one order of magnitude) than the first stage.

An increase of the deformation temperature accelerates the onset of the third stage and thus shortens the second stage, without having any direct effect on the latter. The increased stacking fault energy γ_{sf} has a similar effect, i.e. it shortens the second stage without any change in θ_{II} and favours an earlier onset of the third stage (see later in this chapter). This suggests that the sharp rise in hardening at the second stage is due mainly to the contribution of temperature-independent processes.

Electron-microscopic studies have shown that slip lines at the second stage become appreciably shorter than at the first stage; besides, complex dislocation tangles are formed. These tangles are located along the operative slip planes and surround regions which are relatively free of dislocations. Thus, a cell structure begins to form already at the second stage (see below).

The onset of the second stage is also characterized by the appearance of dislocation dipoles (Fig. 9) which favour the formation of dislocation walls [65].

In the process, slip bands appear on the surface of deformed crystals which are essentially groups of closely located slip lines.

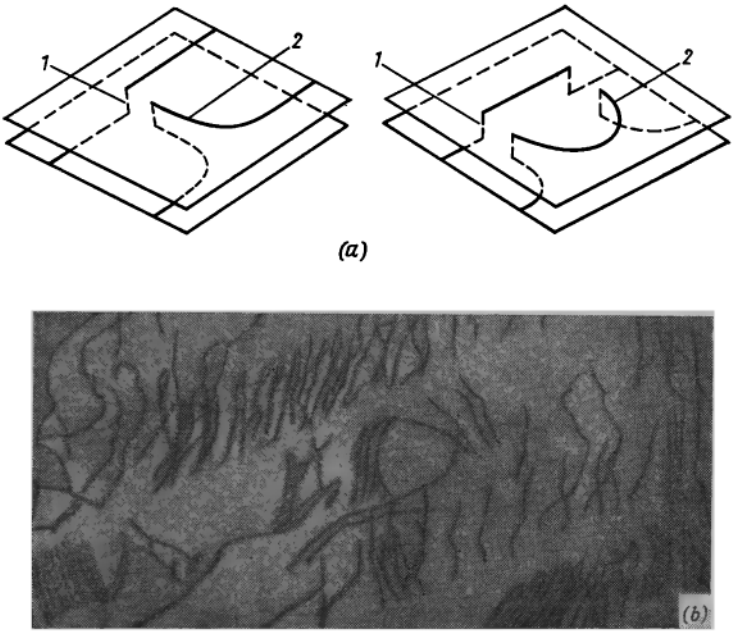

Fig. 9. Formation of dislocation dipoles in copper crystals at stage 2 hardening (*a*) schematic (*1*—jog, *2*—dipole); (*b*) electron micrograph copper-indium solid solution. ×40 000

Some fine details of the processes occurring at the second stage still remain disputable. There is no doubt, however, that slip in secondary systems plays an increasing part at the second stage.

Dislocations of primary and secondary systems can interact to form Lomer-Cottrell sessile dislocations which, according to Seeger, serve as locks on which small groups of dislocations of one sign form dislocation pile-ups. The average number of dislocations in such a pile-up, for instance in copper, is 20 to 25. Groups of opposite sign stabilize each other.

On the other hand, in Seeger's view, the interaction of primary and secondary slip systems can continuously form new dislocation sources of the Frank-Read type. These dislocation sources remain operative until the opposite long-range stress fields formed by dislocation pile-ups created by these sources will exceed the shear stress acting near that source. The same mechanism can also explain why dislocation pile-ups have roughly the same number of dislocations.

The distances through which dislocations can move diminish with increasing deformation.

According to Kuhlmann-Wilsdorf [66], dislocation pile-ups probably tend to shorten the length of dislocation portions, which serve as Frank-Read sources. This in turn must cause an increase in the shear stress since the sources of a shorter length become active at a higher stress.

According to N. F. Mott and P. B. Hirsch, jogs on primary system dislocations, which result from the intersection of these dislocations with the dislocations of secondary systems, can also serve as dislocation barriers.

Non-conservative movement of a jog on screw dislocations is unfavourable in terms of energy, since the process must also entail the formation of vacancies or interstitial atoms. In metals of low stacking fault energy, a jog may additionally dissociate into partial dislocations with a stacking fault formed between them. As they follow dislocations, such jogs certainly form dipoles, sometimes already at the first hardening stage. Therefore, stage 2 hardening must be more intensive in crystals of a lower stacking fault energy; this has been observed experimentally.

In all the assumptions considered, it is taken that the number of obstacles to dislocation movement, N, increases in the second stage, whereas the distance l between the obstacles diminishes, and, since the stress is inversely proportional to distance l and $N \approx 1/l^3$, $\tau_{cr} \approx N^3$.

Analysis of the behaviour of various types of crystals at stage 2 allows us to conclude that f.c.c. crystals harden much stronger than c.p.h. crystals or even b.c.c. crystals, though the relation between hardening and the number of slip systems is not linear. In crystals of high stacking fault energy γ_{sf}, such as aluminium, the second stage is less pronounced.

The second stage of hardening is less influenced by orientation than the first stage.

The third stage of hardening (in which the stress-strain relationship is parabolic) is characterized by a reduced intensity of hardening. At this stage, θ_{III} is a variable that diminishes with increased strain. This stage is much less sensitive to most of the factors that are essential at stages 1 and 2, such as crystal orientation, impurities, and the type of lattice. Exceptions are the temperature of deformation and the stacking fault energy; these two factors have a substantial effect on the onset of stage 3 hardening and on its contribution to the total deformation.

As the temperature of deformation rises, the third stage begins to act at lower strains and its contribution to the total deformation becomes more and more predominant. This is illustrated for copper in Fig. 7 [67].

The stress τ_{III} for the onset of the third stage diminishes with increasing temperature by a logarithmic law:

$$\ln (\tau_{III}/G) = \ln (\tau_{III(0)}/G_{(0)}) - BT$$

where B is a coefficient, and $\tau_{III(0)}$ and $G_{(0)}$ are respectively the stress and the shear modulus at 0 K. This relationship has been verified experimentally for many f.c.c. metals.

The stacking fault energy γ_{sf} has a similar effect. In substances with high values of γ_{sf} (Ni, Al, Cr, etc.), the transition to the third stage occurs at lower temperatures than in substances with low values of γ_{sf}, such as Cu, Ag, Au, etc. (see Table 2).

TABLE 2. Averaged Values of Stacking Fault Energy γ_{sf}, erg cm^{-2}, for Selected Metals [68]

Metal	Lattice type	γ_{sf}, erg/cm^2	Metal	Lattice type	γ_{sf}, erg/cm^2	Metal	Lattice type	γ_{sf}, erg/cm^2
Ni	f.c.c.	120	Ag	f.c.c.	20	W	b.c.c.	300
Al	f.c.c.	200	Mg	c.p.h.	150	Fe	b.c.c.	140
Pt	f.c.c.	120	Zn	c.p.h.	250	Ta	b.c.c.	110
Cu	f.c.c.	60	Cr	b.c.c.	300	V	b.c.c.	140
Au	f.c.c.	50	Mo	b.c.c.	300	Nb	b.c.c.	30

As is known, the stacking fault energy is largely responsible for the ability of a material to develop thermally activated cross-slip. At higher values of γ_{sf}, a screw dislocation (stacking fault) has a lower dissociation width, and therefore a lower stress is needed to compress the dissociated dislocation and transfer it from the slip plane where its movement is locked to another slip plane of the same family, which has the same shear direction as the primary slip system, so that the dislocation could continue its movement in this new plane.

These facts have suggested a conclusion to the effect that the third stage begins when dislocations have the possibility to bow (by cross slip) around the dislocation locks they have formed on their paths at the second stage, in the first place, Lomer-Cottrell locks.

Seeger [60] has derived the following expression for the shear stress τ_{III} required to compress dissociated leading dislocations of a dislocation pile-up:

$$\tau_{III} = (\sqrt{2}G/4\pi - 2\gamma/b)/n$$

where n is the number of dislocations in a pile-up. Using this expression and experimental values of τ_{III} for lead and aluminium at 4 K, it has been found that $n \approx 25$.

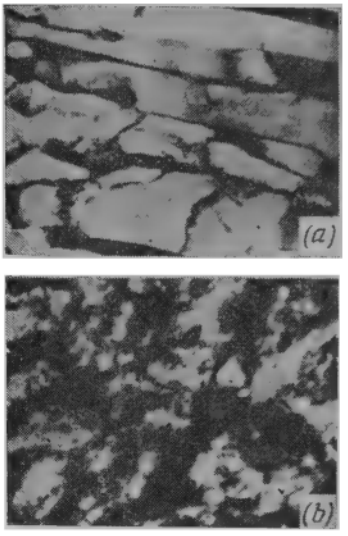

Fig. 10. Effect of stacking fault energy on the formation of dislocation cell structure. Cold deformation $\varepsilon = 60\%$, $\times 20\,000$; (*a*) aluminium; (*b*) copper

Dislocation cross slip results in partial stress relaxation and grouping of dislocations into spatial networks (cells) within which less distorted regions of the lattice are located, i.e. in the formation of what is called the cell structure.

Thus, a cell structure forms more easily at higher values of γ_{sf} (Fig. 10). Cross slip also allows for annihilation of individual dislocations of unlike sign. This in turn diminishes both elastic stresses and the work-hardening coefficient.

The size of cells is of the order of a micrometre (from a few tenths of a micrometre to a few micrometres). The thickness of cell walls is a few tenths of the cell size and decreases as the deformation temperature and γ_{sf} increase.

These conclusions have been confirmed experimentally. In aluminium, for instance, three distinct stages are observed only when deformation takes place at the temperature of liquid nitrogen (78 K); at room temperature, work hardening begins almost immediately from the third stage. Metals of lower stacking fault energy (copper, silver, gold, etc.) behave in deformation at room temperature as aluminium does at 78 K, i.e. they have a distinct stage 2; in deformation at elevated temperatures, they behave as aluminium at room temperature, i.e. the second stage is weak or absent.

A typical feature of stage 3 is the appearance of coarse slip bands, which are groups of closely located slip lines. Slip bands are relatively short and are connected with one another by means of cross slip. The formation of slip bands also involves partial annihilation of dislocations [60]. In the further deformation, slip is concentrated on slip bands, with no shear occurring in interband spaces.

Let us recall that in single crystals oriented favourably for easy slip, dislocation pile-ups and cell structure do not appear until very heavy strains come into play; at the same amount of deformation, the formation of a cell structure is facilitated by way of increased deformation temperature.

In ⟨110⟩ oriented molybdenum single crystals, drawing deformation can form a cell structure much more easily than in ⟨100⟩ oriented crystals.

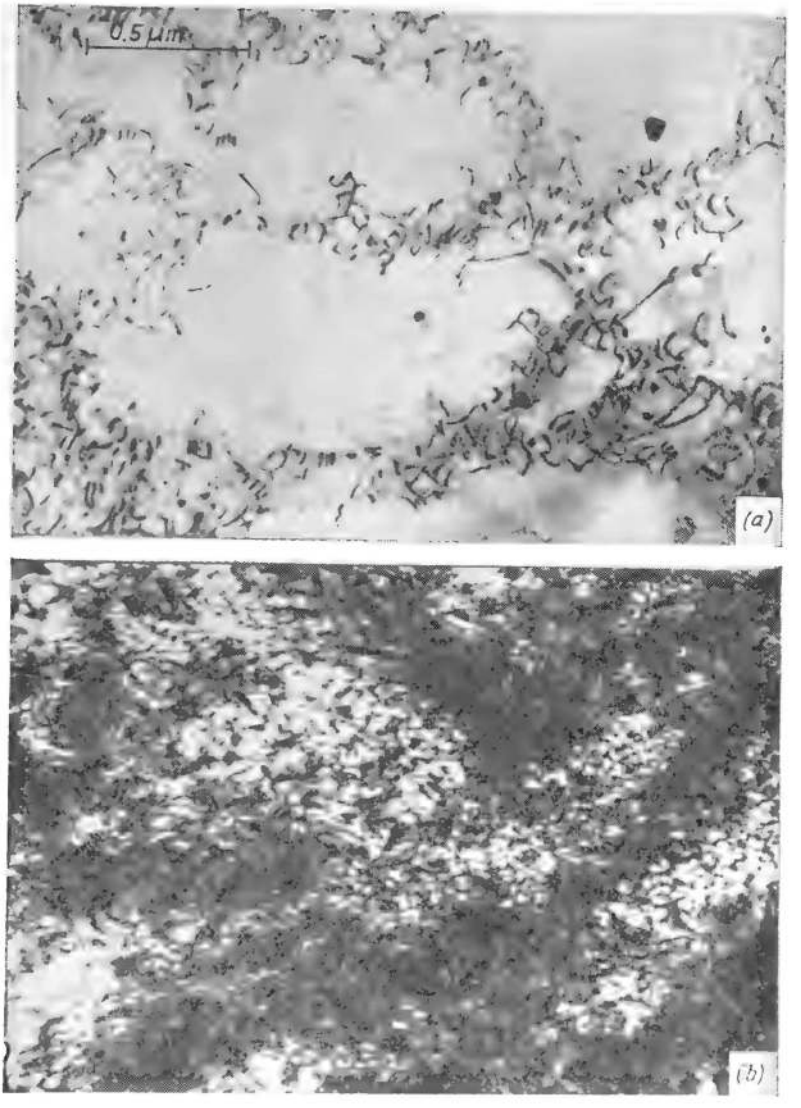

Fig. 11. Effect of orientation on the formation of cell structure in rolled copper [83]. ×40 000

(*a*) {100} ⟨010⟩, $\varepsilon = 35\%$; (*b*) {110} ⟨112⟩, $\varepsilon = 75\%$

Figure 11 shows the structure of copper single crystals rolled along {100} ⟨010⟩ and {110} ⟨112⟩ systems, respectively. As seen, a distinct cell structure has formed in the former, and a structure with a relatively uniform distribution of dislocations in the latter. This can be understood easily, since, as follows from the data given on the stereographic triangles for f.c.c. and b.c.c. crystals, only the second orientations out of the indicated ones are favourable for easy slip.

2.1.2. Deformation by Twinning

Under special conditions of deformation of a number of hexagonal metals (zinc, cadmium) and b.c.c. metals (iron), crystals (crystallites) develop metallographically revealed localized regions which etch differently than the surrounding matrix crystal. A typical feature of such regions is the rectilinearity and clear strict crystallographic orientation of their two parallel boundaries (Fig. 12*a*). In some cases, only one straight boundary is revealed. This occurs when the reoriented region is either very narrow (and the two boundaries merge into one on etching) or is located at the periphery of the crystal and is bounded on one side by the straight boundary and on the other by the external boundary of the crystal. A similar metallographic picture is often detected in annealing of certain hexagonal and f.c.c. metals and alloys, such as copper, brass, nickel, Ni-Cr (see Fig. 12*b*).

As has been established by diffraction analysis, these regions principally differ in orientation from the matrix. Atoms within such regions are mirror-images of the atoms in the matrix crystal. The straight boundary is the trace of intersection of the surface of crystal (microsection) with an atomic plane which serves as the mirror image plane. Such reoriented regions in crystals are called respectively deformation twins and annealing twins, the process of their formation is called twinning, and the mirror image planes are twin habit planes, or twinning planes.

In contrast to common boundaries, twinning planes are coherent. The meaning of this term lies in that there is a regular correlation in the arrangement of atoms on both sides of the boundary. Atoms in a twinning plane occupy the sites which are common for the crystal portions on both sides of that plane (Fig. 13). X-ray or other radiation scattered by atoms of the two crystal portions is regularly phase-shifted, i.e. coherent. The two other (edge) boundaries of a twin are usually incoherent.

Deformation twinning is one of the mechanisms of plastic shear deformation. Twinning is usually a fast process and is often accompanied by energy release in the form of sound. On stress-strain curves,

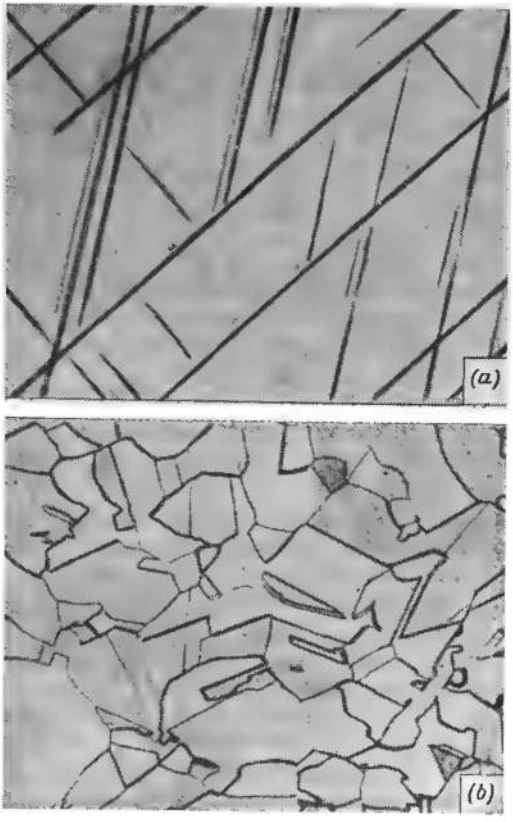

Fig. 12. Deformation and annealing twins
(*a*) iron, as deformed; (*b*) nickel, as annealed

the portion corresponding to twinning has a toothed or saw-like shape [69].

Twinning can start at a definite shear stress $\tau_{cr(tw)}$ (see later), similarly to the critical shear stress which is required for deformation slip.

The onset of twinning should evidently be preceded by slip which forms dislocation pile-ups acting as local stress concentrators. On the other hand, $\tau_{cr(tw)}$ remains appreciably lower than the stress corresponding to the theoretical strength. On that ground, twinning cannot be associated with simultaneous movement of all atoms in a twin and is probably realized through successive displacements of atoms, i.e. as in dislocation movement.

In modern views, twinning is associated with movement of partial dislocations, resulting in that the sites occupied by atoms on both

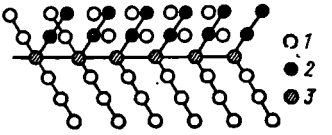

Fig. 13. Twinning (schematic)

1—positions of atoms prior to twinning; *2*—twinned positions of atoms; *3*—atoms in coincident positions

sides of slip planes cease to be equivalent. To illustrate the point, let us examine an f.c.c. lattice typical of which is the fact that its close-packed {111} layers are arranged successively one above another in positions *ABCABCABC*... (Fig. 14).

Let a dislocation be in a plane above plane *A* (the plane of the drawing). On movement of perfect dislocations with vector b_1, the sequence *ABCABCABC* will remain unchanged. If, however, a partial dislocation with vector b_2 moves, the packing sequence will change and atoms in the slip plane will pass from *B* to *C*. If such partial dislocations will pass on certain planes of a family of planes {111}, as shown in Fig. 15, the orientation of this volume of the crystal will change to a twinning orientation [64].

Partial dislocations move by the following mechanism. If a twin includes *n* planes across its thickness, it is difficult to assume that its formation has been associated with movement of *n* partial dislocations (one dislocation in each of these *n* planes). The existence of dislocations arranged in such a manner is practically improbable. The formation and growth of a twin seems to be most probable owing to the movement of a single partial dislocation (twinning dislocation) by what is called the polar mechanism whose meaning is explained in Fig. 16. The partial dislocation meets on its path a forest dislocation of a screw orientation. Atomic planes are arranged around that forest screw dislocation as if around an axis, in the form of helical planes.

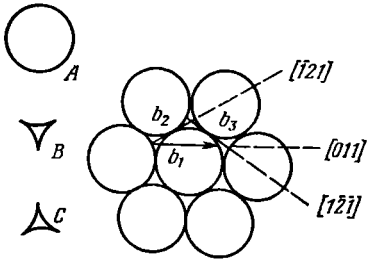

Fig. 14. Arrangement of atoms in close-packed {111} layers of f.c.c. lattice and {0001} layers of c.p.h. lattice. The figure shows also the Burgers vectors of perfect (b_1) and partial (b_2 and b_3) dislocations

When the partial dislocation reaches the screw (polar) dislocation, it will move by one of its portions on the lower plane of the helix and by the other portion, on the upper plane. Further, owing to its rotation around the screw (polar) dislocation, this partial dislocation can successively pass on each of the parallel planes and form a twin. This mechanism explains the rate

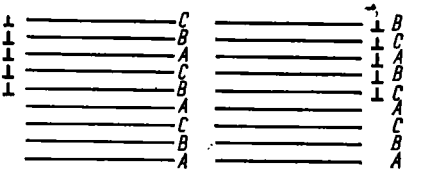

Fig. 15. Twinning in an f.c.c. crystal due to movement of partial dislocations on slip planes

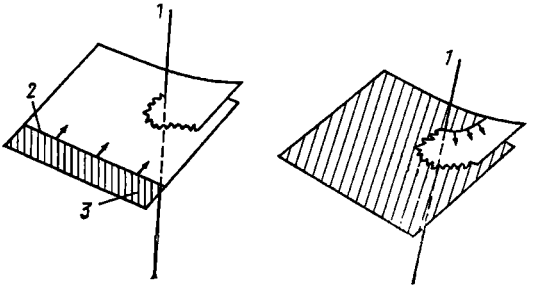

Fig. 16. Polar mechanism of twinning

On the left: a partial dislocation approaching a polar dislocation. On the right: two branches of a partial dislocation starting to form a helix around the pole; *1*—polar dislocation; *2*—partial dislocation; *3*—region of stacking fault associated with partial dislocation

of formation of deformation twins observed in experiments. Also, it evidences the fact that the growth of a twin occurs by displacement of its incoherent boundary in a direction parallel to the coherent boundary. A reverse process eliminates twins upon annealing.

The process of elimination of twins in high-temperature annealing of nichrome was observed experimentally in [70]. It was found that a twin disappears owing to the movement of an edge boundary, more precisely, as a result of successive movement of its individual steps (Fig. 17). Such a mobile step often forms in the middle portion of a twin and the latter is cut, as it were, into separate bands (Fig. 17*c*). It may be taken that the width of a step is determined by the length of the screw (polar) dislocation. With this mechanism of the formation and elimination of twins, it is then clear that each atom is displaced through a smaller distance than the interatomic spacing.

The energy of an incoherent boundary is appreciably (5 to 10 times) higher than that of a coherent boundary. The latter can be judged of by the stacking fault energy of the metal (alloy). Indeed, a stacking fault represents, as it were, a twinned interlayer of one atom in thickness. The energy of a coherent twin boundary must then be one half that of the stacking fault. This means, however, that the probability of twinning must be inversely proportional to the stacking fault energy.

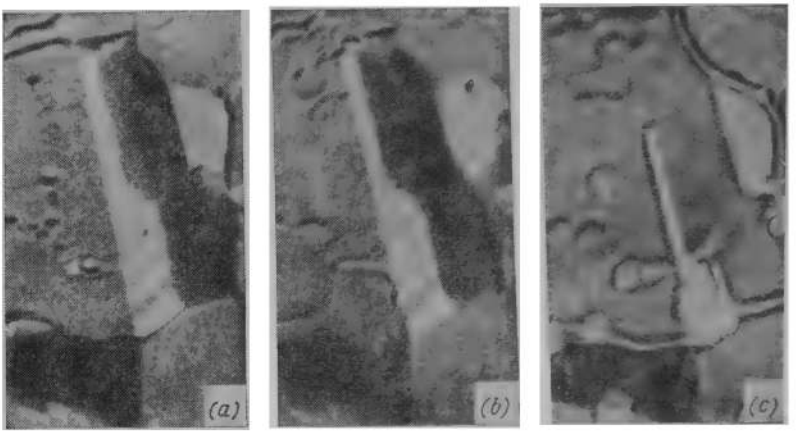

Fig. 17. Annihilation of a twin on high-temperature annealing of Ni-Cr. ×640
(a) original state; (b) 1000°C, 180 s; (c) 1150°C, 600 s

The quantitative relationship between the twinning shear stress $\tau_{cr(tw)}$ and stacking fault energy, as proposed in [370], is of the form

$$\tau_{cr(tw)} = \gamma_{sf}/b + Gb_1/2a$$

where b is the Burgers vector of the twinning dislocation, G is the shear modulus, and a is the radius of a half-loop of the twinning dislocation.

With a high value of γ_{sf}, $\tau_{cr(tw)}$ can be greater than the critical shear stress from common slip, and slip is realized on non-twinning planes.

Twinning is realized when γ_{sf} is low and $\tau_{cr(tw)}$ is smaller than $\tau_{cr(sl)}$. This agrees well with the results of experimental observations. For instance, twins (and especially annealing twins) are observed very frequently in copper ($\gamma_{sf} \leqslant 60$ erg/cm^2) and in copper alloys, but are very rare in aluminium ($\gamma_{sf} > 200$ erg/cm^2). With a high-rate deformation, twinning in copper begins at a pressure of 3×10^{-4} at, compared to 3×10^5 at in nickel.

Owing to their low energy, coherent boundaries are immobile and the twins are quite stable. A coherent boundary practically never migrates, and therefore twins grow in width only due to the migration of incoherent boundaries (jogs). Thus, rather high temperatures of annealing are needed to eliminate twins.

In addition to the low stacking fault energy, twinning can be favoured by particular conditions of deformation, which are unfavourable for common dislocation slip, for instance, when the number of slip systems is small. Thus in hexagonal crystals, where twinning is most common, the basal slip, as has been noted earlier, becomes

impossible if deformation occurs in a direction parallel to the basal plane or deviates from the plane by 5-10%. Under such conditions, the deformation is realized by twinning, though the resolved twinning stress is, on the average, by an order of magnitude higher than the slip stress (for cadmium, respectively 100-700 gf/mm^2 and 20-30 gf/mm^2). In hexagonal crystals with $c/a > 1.633$, twinning is initiated by tensile deformation and in those with $c/a < 1.633$ by compressive deformation.

In b.c.c. crystals the factors that aid in the formation of twins are an increased rate of deformation and a decreased temperature of deformation. In b.c.c. metals, twins in the form of very thin regularly oriented platelets, known as Neumann bands (see Fig. 12*a*), were first detected in impact-stressed specimens.

Heavy deformations (>60%) produce more intricate shapes of Neumann bands. The orientation of Neumann bands depends on the degree of deformation and the orientation of the matrix. According to [71], rolling of (Fe + 3% Si) single crystals with {100} ⟨001⟩ orientation produces bands oriented in {100} ⟨011⟩ + {114} ⟨221⟩.

Alloying with certain substitutional impurities, for instance, adding silicon to iron, facilitates twinning (probably owing to a decrease in γ_{sf}). In silicon-alloyed iron (Fe + 3% Si), Neumann bands appear on relatively light deformations (≈10%). Interstitial impurities give an opposite effect.

In deformed f.c.c. crystals (copper, gold, silver and some other metals and alloys), twins can form if the deformation is carried out at a rather low temperature (<77 K). Twinning in these metals occurs at very high shear stresses (15 kgf/mm^2 for copper, 30 kgf/mm^2 for nickel), which are much higher than they are in b.c.c. metals. Alloying with substitutional impurities noticeably facilitates twinning in f.c.c. metals, especially if an impurity heavily decreases the stacking fault energy. A number of workers [2] have found that

TABLE 3. **Crystallographic Characteristics of Twinning**

Lattice type	Metal	Twinning plane	Twinning direction
F.c.c.	Cu, Ni, Ag, Au, α-brass	{111}	⟨112⟩
B.c.c.	Fe, Mo, W, Nb, Ta, Cr, β-brass	{112}	⟨111⟩
C.p.h.	Mg, Be, Zn, Cd, Zr, Mg, Ti	{10$\bar{1}$2}; {10$\bar{1}$1}; {11$\bar{2}$2}	⟨10$\bar{1}$1⟩ ⟨10$\bar{1}\bar{2}$⟩ ⟨11$\bar{2}\bar{3}$⟩
Rhombohedral	Bi	{110}	⟨001⟩

the stacking fault energy decreases more readily, and thereby twinning begins more easily, in alloys having a larger number of valence electrons per impurity atom.

Annealing twins are found very often in f.c.c. metals and alloys having a low stacking fault energy (copper, nickel, silver, gold, and their alloys).

Like slip, twinning occurs on certain preferable slip planes and in particular twinning directions. These are given in Table 3 for the three principal types of crystal lattice.

The twinning boundaries that have formed at the earlier stages of deformation, serve as dislocation locks in the course of further deformation and cause the formation of appreciable distortions near the dislocations. The result is that in heating the regions around twin bands often become preferable sites for the formation of recrystallization nuclei, though much less frequently than grain boundaries.

2.1.3. Deformation by Irregular Rotation of the Crystal Lattice

A special case of slip is the deformation of a crystal that forms regions tilted relative to the remaining crystal through angles that do not comply with the laws of twinning (and the laws of symmetry in general). The magnitude of these angles depends on the degree of deformation, the initial orientation of the crystal relative to deforming forces, the type of lattice, etc.

Deformation by irregular rotation of the lattice evidently plays an important part in the formation of deformation textures and probably of recrystallization textures, and also in the formation of recrystallization nuclei in general.

Deformation of this type has not been studied thoroughly. A review of the most interesting works in the field has been done by A. A. Urusovskaya [72].

The effects of deformation due to irregular orientation of the lattice are very diverse. Deformation of this kind was first discovered in compressed minerals and later in rock salt crystals. In 1952, E. Orowan observed the formation of a knee-shaped kink in a cadmium rod on its compression in a direction almost parallel to the slip plane. The region in the knee was much similar to the tilt region in minerals and was called the kink band in the literature.

Kink bands were later observed in zinc on compression, and also in single crystals of a number of metals (aluminium, zinc, bismuth, magnesium) on tension.

In f.c.c. crystals, kink bands form perpendicular to the planes and direction of slip (Fig. 18*a*). The crystal lattice is rotated in them relative to the remaining lattice around an axis in the slip plane and perpendicular to the slip direction. These bands contain local regions

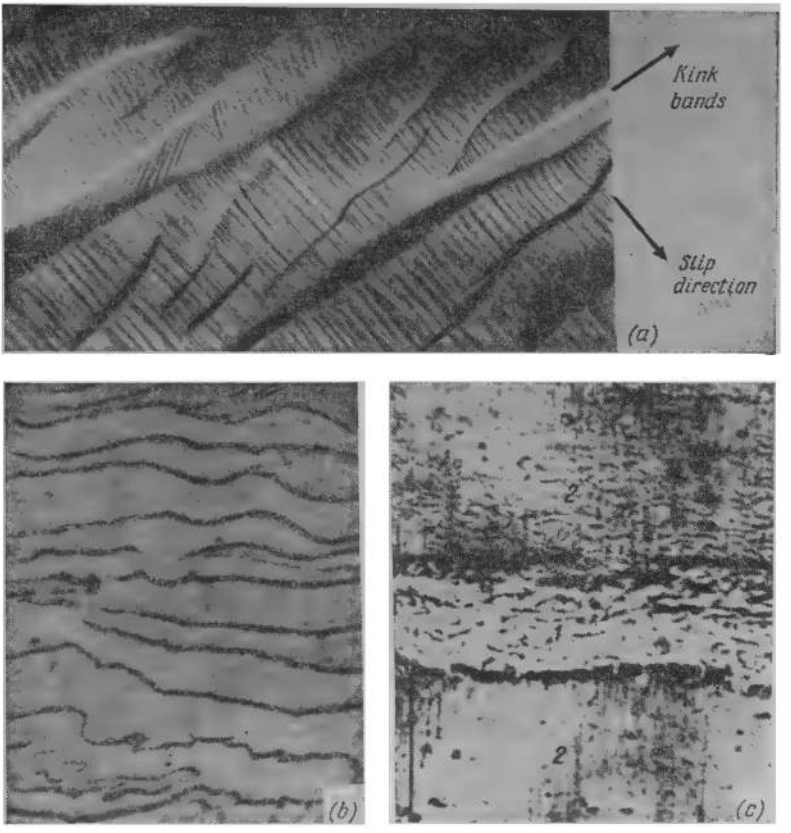

Fig. 18. Deformation due to irregular reorientation of the lattice

(a) kink bands in an aluminium single crystal; (b) deformation bands in α-iron, ×200; (c) deformation bands (2) and microband (1) in chromium bronze. ×900

of curved lattice (Fig. 19), consisting of two zones of opposite curvature. On heavy deformations, kink bands become locks for dislocation movement [2]. Regions of large curvature are sites where the formation of recrystallization nuclei occurs at the highest rate.

Another and probably more frequent type of deformation associated with irregular orientation of the lattice in metals is deformation bands and microbands (Fig. 20). They have been detected in α-iron, Fe-Si alloys, α-brass, chromium bronze, and other metals. According to C. S. Barrett, they can appear in all f.c.c. metals [100].

Upon compression of a crystal (or crystallite), bands with irregular wavy boundaries appear on its surface; these bands do not look

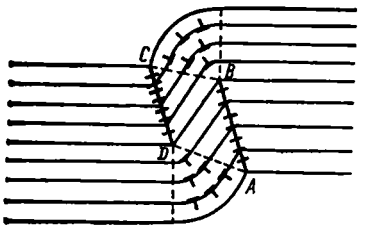

Fig. 19. A kink band (schematic)

like slip trails and etch in a different way than the surrounding material. The difference in etchability of these bands becomes more pronounced with heavier deformations (see Fig. 18, *b* and *c*) [73].

As has been found by X-ray analysis, the lattice in a band is tilted relative to the remaining portion of a crystal through an angle of a few degrees or a few tens of degrees, which probably causes different etchability.

It has also been found that the tendency to form deformation bands depends on the orientation of a crystal relative to the direction of deformation. Deformation bands did not form in iron crystals with the [100] or [111] axis oriented parallel to the axis of compression.

Hu [74] has established that single crystals of silicon iron with the (001) [100] orientation are divided, as it were, on rolling into two groups of deformation bands tilted through 30-40° relative to each other. Adjacent deformation bands are separated by narrow microbands of a thickness of a few micrometres, each of which consists of 12-15 cells (or subgrains) across the width. The large misorientation of adjacent deformation bands is realized at the expense of microbands in which neighbouring cells are tilted through 3-4° relative to one another. Single crystals with the (001) [110] orientation do not form any deformation bands on rolling. On subsequent heating, (001) [100] crystals readily recrystallize, with recrystallization nuclei forming in microbands. In (001) [110] crystals, only in-situ recrystallization takes place. These results have been confirmed in [71, 73, 75].

V. Yu. Novikov and L. V. Roshchina [71] have studied in detail the orientations and the pattern of arrangement of deformation bands, microbands and deformation twins (Neumann bands) which form on rolling of Fe-Si single crystals with the {110} ⟨001⟩ initial

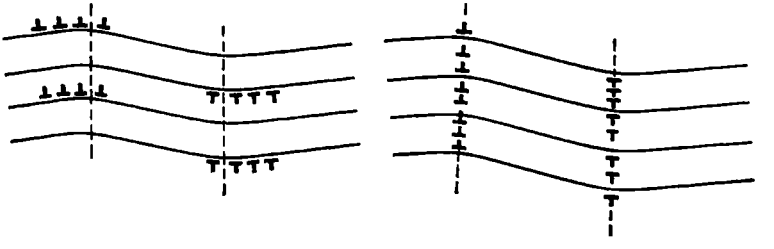

Fig. 20. Dislocation schemes of the formation of deformation bands (after Indenbom)

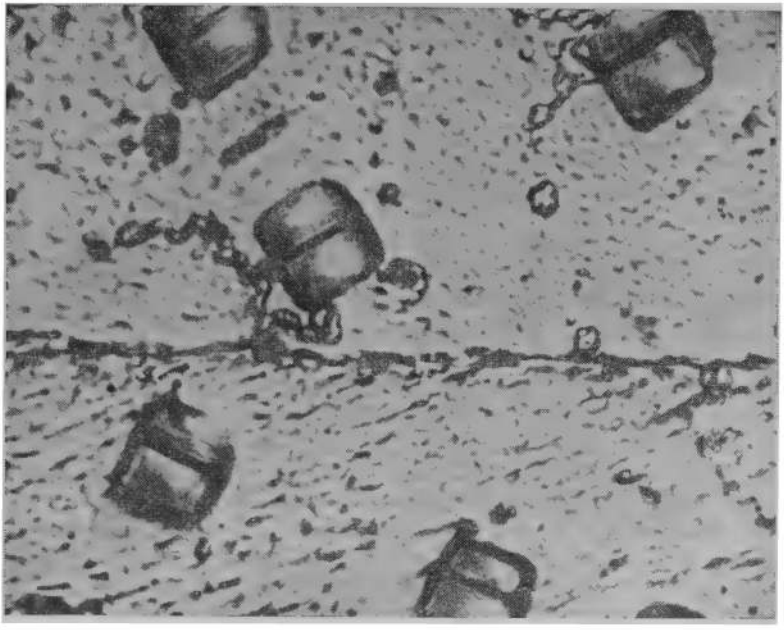

Fig. 21. Sudden change from (111) $[\bar{1}1\bar{2}]$ to (111) $[11\bar{2}]$ orientation in adjacent deformation bands of Fe-3.5% Si crystallites. Etch pits are bounded by {100} planes (V. Yu. Novikov)

orientation. The deformation texture of the crystals consists of two strong symmetrical components of the type {111} ⟨112⟩. This is because adjacent regions of the crystal rotate during deformation in opposite directions around $[1\bar{1}0]$. This rotation takes place in various layers of the crystal, which are parallel to the rolling plane. The result is a lineage structure formed by deformation bands interlaced with thin microbands. These deformation bands have the orientation of the matrix structure.

The orientations of adjacent deformation bands separated by a microband have been examined by successive etching of metal layers and X-ray photographing of pole figures. It has turned out that on transition from one deformation band to another the main structural component of the texture changes suddenly from $(11\bar{1})$ [112] to (111) $[11\bar{2}]$. This has also been verified by the location of etch pits on microsections cut from the side surface of a specimen (Fig. 21). Deformation bands extend alternately across and along a specimen as well as across its thickness. Judging by the pattern of etch pits, the maximum misorientations within a deformation band are not large and differ from one another by not more than $\pm 5°$.

The crystallographic link between adjacent deformation bands is effected through a thin microband (3-4 μm thick); in Fig. 21, it is seen as a linear boundary between adjacent deformation bands.

Reorientation in a microband can be imagined as the rotation around a [1$\bar{1}$0] axis in the rolling plane [71]. The result is that a set of discrete orientations appears in the microband starting from (110) [001], which corresponds to the initial crystal orientation and evidently falls on the middle portion of the microband, up to {111} [112], which corresponds to the orientation of the adjacent deformation band. The misorientation 'pitch' is equal to the misorientation angle between neighbouring cells (subgrains) in the microband and constitutes 3-4°. The number of cells (subgrains) in the microband is 10 to 20. Thus, the reorientation from one deformation band to the other is effected in the microband by 10 to 20 successive discrete rotations from one subgrain to another.

An important fact for understanding some specifics of texture formation in silicon-alloyed iron is that the nature and arrangement of deformation bands depend on the state of the material, for instance, on whether its crystals have been annealed or hardened prior to rolling [83], i.e. whether the solid solution has decomposed before rolling or has solved the impurities.

Misorientations in hardened crystals within deformation bands are several times greater than in annealed crystals (10 to 20° against 5°) [83]. Alloying of the solid solution obviously affects the stacking fault energy γ_{sf} and varies the number of operative slip systems.

In addition to the effects mentioned above, other effects of nonuniform deformation can also occur, such as accommodation zones or secondary shear bands.

From the standpoint of the theory of dislocations [76], the formation of reoriented regions should be attributed to the interaction of dislocation groups. V. L. Indenbom [76] regards the formation of kink bands and deformation bands as the result of interaction of unlike edge dislocations in parallel slip planes. If the external stress does not exceed τ_{cr}, two unlike dislocations moving towards each other on parallel slip planes will stop at a definite distance from each other in accordance with the scheme in Fig. 20. They will then retain other dislocations which move after them. The dislocation pile-ups thus formed will inhibit dislocation slip in adjacent planes and promote the appearance of ever new pile-ups, as a result of which a deformation band will form gradually, with positive dislocations positioned on its one side and negative ones on the other.

The principal difference between deformation bands and kink bands is that dislocation movement in the former case occurs outside the band and the lattice in the band retains the original orientation, whereas in the latter case the plastic deformation and lattice reorientation occur within the band. This is shown schematically in Figs. 19

and 20. The former figure illustrates the structure of a kink band in a compressed hexagonal crystal. The two regions of strongly distorted lattice are separated from each other and from the undistorted crystal by kink planes AB and CD, which are arrays of edge dislocations. Each of the curved regions has an excess of like dislocations. In these regions the rate of formation of recrystallization nuclei is at its maximum.

Secondary shear bands form by a somewhat different mechanism. They can appear in crystals having several slip systems. In that case, lattice rotation is effected owing to the fact that slip in bands occurs on a different plane system than it does in the remaining portions of the crystal.

Deformation due to irregular rotations of the lattice, being first detected in single crystals, is quite significant under plastic deformation of polycrystalline solids. Because of the interaction between crystallites, here the probability of non-uniform deformation and appearance of bending moments in individual crystallites is especially high.

2.2. Deformation in Polycrystalline Solids

2.2.1. Inhomogeneous Microstructure of Deformed Polycrystals

In polycrystals, which are encountered most often in practice, the nature of structural changes with deformation and the shape of τ-ε curve, especially at the initial stage of hardening, greatly differ from those in single crystals.

On the other hand, the principal features of the changes in single crystals in the second and the third stage of work-hardening are essentially the same as in polycrystals.

The main changes result from the fact that every crystallite in a polycrystal is oriented in space, and therefore relative to external forces, in a different manner than are the surrounding adjacent crystallites from which the crystallite in question is separated by grain boundaries.

Therefore, even when a polycrystal is subjected to external stresses of the simplest anisotropic nature, for instance, to uniaxial tension, slip begins in individual crystallites not at the same time and proceeds along differently oriented slip systems. Consequently, dimensional changes (elongation) of various crystallites will be different in various directions. For that reason, apart from external forces, every crystallite experiences the action of neighbouring crystallites which may have a different orientation.

In order to ensure the integrity and continuity of the material on passage through grain boundaries in crystallites, multiple slip should be realized already at the earlier stages of deformation.

The nature and the result of the influence of adjacent crystallites on a given crystallite depend appreciably on the type of grain boundaries and their ability to impede the movement of dislocations.

In cases of cold deformation, grain boundaries are always stronger than the internal volumes of grains. At high temperatures, when the contribution of diffusion processes becomes tangible, boundaries turn out to be less strong than grains proper*.

In cold deformation, the strength of boundaries depends on the angle of misorientation, i.e. on the dislocation density at a boundary**. Chalmers and Clark [77] have demonstrated on bicrystals of tin and aluminium that the elastic limit and the yield limit increase appreciably (1.5 and 4 times) with an increase in the angle of misorientation up to approximately 60°. This implies that grain boundaries grow in importance as barriers for dislocation movement and cause dislocations to pile up. This does not mean, however, that the deformation ceases as it reaches a grain boundary. The latter may be and usually is the site of a sharp deformation gradient.

Usikov and Utevsky [78] observed the excitation of dislocation sources on grain boundaries in nickel and Ni-Cr under the effect of stresses that induce in a given grain the dislocations of an adjacent grain, which come to the boundary and stand arrested by it. The authors called this phenomenon the 'relay-race' (grain-to-grain) transmission of strain. In some cases where adjacent grains possess a coincident slip direction, the slip line can cross the boundary without altering its direction. In the general case, however, slip systems on the two sides of a boundary are different.

Grain boundaries are responsible for a highly inhomogeneous deformation of grains that results, for example, in dislocation pile-ups on grain boundaries. Multiple slip, which forms regions of the highest misorientation relative to the surroundings, starts in these regions earlier than in the bulk of grains.

Slip systems at grain boundaries and in the bulk of grains often differ from one another because they experience the effect of neighbouring grains; as a result, strains near grain boundaries and in the bulk of grains differ too. This difference grows with the size of original grains, especially when strains are low or moderate.

In fine-grain materials, regions of multiple slip propagate from grain boundaries and extend into the bulk of crystallites. Furthermore, the interaction of dislocations moving from various boundaries of a grain can occur within the grain in such a material.

* The temperature at which boundaries and grain volumes have the same strength is called equicohesive temperature.

** For more detail on the structure of grain boundaries see Ch. 5.

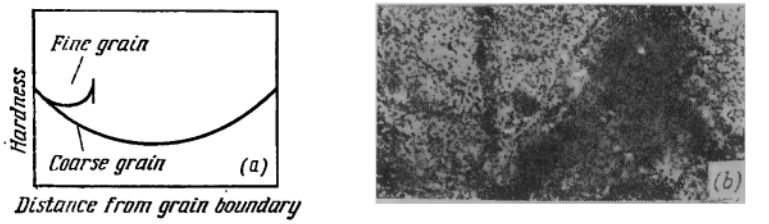

Fig. 22. Effect of size of grains on microinhomogeneity of their deformation
(*a*) schematic; (*b*) microstructure of Cr-Ni alloy upon upsetting deformation, hardening and ageing; defects are decorated by γ-phase precipitates. ×200

The result is that fine-grained materials undergo a more intensive work-hardening than coarse-grained ones (Fig. 22*a*). Besides, core volumes of grains in coarse-grained materials become work-hardened to a smaller degree than boundary regions [79]. These phenomena are important for understanding recrystallization.

Figure 22*b* shows the arrangement of dislocations revealed by internal decoration (due to ageing) in a relatively coarse-grained Cr-Ni alloy after upsetting by 20% [80]. The dislocation arrangement near the triple joint, where the opposite boundaries of grains lie close to each other, is similar to that which must be observed in the bulk of a fine-grained material. It may be seen clearly that the dislocation density near the triple joint is much higher than in the bulk of a large grain and that the slip proper is of a multiple nature.

A complex nature of stressed state in some grains of a polycrystal explains why some workers have discovered in polycrystals a greater number of operative slip systems than are usually observed in single crystals of the same materials. For instance, Boas and Ogilvie [79] examined polycrystals of aluminium and α-brass upon relatively light deformations and detected trails of six slip systems in some grains, including on {111}, {100} and {110} planes.

Since different slip systems may be operative in various volumes of a grain, polycrystals exhibit (much more often than single crystals) a non-uniform deformation in various volumes, which causes bending and various local rotations of the lattice, such as twinning, kink bands, strain bands, microbands, etc., whose formation mechanism has been discussed earlier when considering single crystals. These specifics of the structure of deformed polycrystals are of prime importance for understanding the mechanism of recrystallization.

Goldstein and Gorelik [75] examined by means of electron microscopy and electron microdiffraction the nature of substructure and local misorientations in transformer steel crystallites deformed by cold rolling. The results obtained are evidently typical of polycrystals.

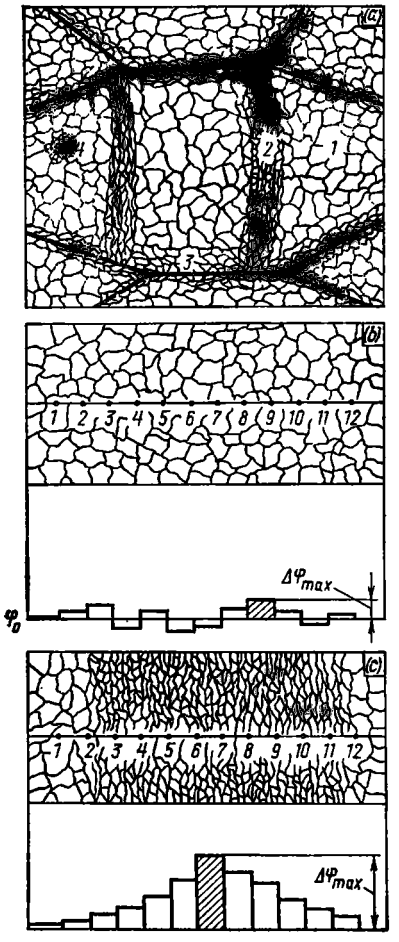

Fig. 23. Substructure and local misorientations, $\Delta\varphi$, of adjacent subgrains in deformed transformer steel (schematic)

$\Delta\varphi_{max}$ = maximal misorientation within a band; (*a*) typical regions in deformed crystallites (*1*—deformation bands, *2*—microbands; *3*—boundary regions, *4*—regions at inclusions); (*b*) and (*c*) misorientation of cells (subgrains) in deformation bands and in microbands respectively

The authors found that five typical microregions can be separated in crystallites, four of them are shown schematically in Fig. 23: *1* strain bands; *2* microbands; *3* boundary regions (regions adjoining large-angle boundaries of the original grains); *4* regions around nonmetallic inclusions (disperse phase particles in general); and *5* deformation twins (often called Neumann bands) in transformer steel).

The features of the structure and misorientations after deformation and, in particular, microbands in polycrystals are similar to those established for single crystals. They can be described by using for analysis a typical example of crystallites which have the (111) [11$\bar{2}$] orientation upon rolling (the picture is principally the same for most of the other orientations).

The microbands that separated strain bands of the orientation (111) [11$\bar{2}$] were regions stretched normal to the rolling direction (see Fig. 23*a* and *c*)*. They were a few micrometres thick and consisted of 15-20 cells (segments). Cells along a microband were oriented in the direction [110], but differed from one another in the orientation of the (111) plane. This plane rotated from cell to cell discretely and regularly through 3-4° around the [110] direction, so that the misorientation in the middle of the microband relative to neigh-

* A similar result was obtained for chromium bronze [73] (see Fig. 18*b*).

bouring strain bands was at its maximum and reached 30-40°.

In strain bands, which had the size of tens of micrometres, misorientations between neighbouring cells were also approximately 3°. In contrast to microbands, however, misorientations of strain bands were of a random nature and were not accumulated on passage from one cell to another. As a result, the tensor dislocation density averaged for a whole strain band (excess of like-sign dislocations) was practically zero (see Fig. 23*b*).

Boundary regions are distinguished by the fact that misorientations are accumulated in them from cell to cell, i.e. as in microbands, but less regularly. The nature and the extent of misorientations depend essentially on the orientations of adjacent crystallites relative to one another and on external deforming forces. Neumann bands are detected only in relatively large grains and have a more perfect substructure than strain bands. Regions near inclusions have a typical strong local misorientation (see later).

Cahn [74] detected microbands roughly 3 μm thick in iron, with the total misorientation over that stretch being near 30°.

In polycrystalline aluminium deformed 40% by pressing, the total misorientation within individual grains roughly 700 μm in size reached 52°, including 35° for a microband 33 μm in size. At 50-% deformation, each grain had at least one microband.

Owing to sharp misorientations, microbands, like grain boundaries, become the preferable sites of formation of recrystallization nuclei (see Ch. 4). Further studies into the mechanism of formation of intragranular regions with an irregular reorientation of the lattice in polycrystals and into the role of these regions in the formation of recrystallization nuclei are very important, but are associated with appreciable experimental difficulties. These regions are very small in size, especially in fine-grained materials, so that their misorientation and dislocation structures can only be detected by local methods of very high resolution with the use of narrow beams of X-rays and electrons.

In addition to intragranular inhomogeneity, deformed polycrystals are characterized by an appreciable intergranular inhomogeneity, i.e. by non-uniform deformation of adjacent grains. This feature makes itself felt heavily at relatively low strains and substantially influences the nature of subsequent recrystallization. For instance, as has been found in recent work [2] with the use of reference marks, the elongation in some grains of coarse-grained aluminium may vary from 2 to 14% or even more, with average elongation of a specimen of 5%. Similar variations are established for the values of microhardness in local regions. Additional data on the non-homogeneous nature of deformation of individual grains, as obtained by X-ray diffraction analysis, are given in Ch. 7.

The above features of deformation in polycrystals enable us to understand quite readily the characteristic features of stress-strain curves of polycrystalline materials. The principal feature—almost complete absence of the first stage—is due to the fact that multiple slip begins in crystallites upon relatively light deformations, in the first place, in boundary regions. According to Jaoul [81], for instance, ε_I in aluminium at the first stage of deformation does not exceed 2%. In many, if not in most cases, ε_I is still lower.

The second stage is more pronounced than the first. As in single crystals, it proceeds in a linear fashion, and its extent and the onset of the third stage obey the same laws. A decrease in the temperature of deformation and in the stacking fault energy extends the second stage to higher degrees of deformation and increases the absolute value and intensity of work-hardening.

It is then clear why in high-purity aluminium, which has a high value of γ_{sf} and a relatively low melting point, the second stage is not detected at all on deformation at room temperature.

The third stage is described by a parabolic curve (as with single crystals) and depends in a similar manner on the temperature of deformation and stacking fault energy.

The influence of the type of lattice is in accordance with the above described data on single crystals. Other conditions being the same, b.c.c. polycrystals are hardened to a lesser degree than f.c.c. polycrystals. Stress-strain curves of b.c.c. metals, such as iron and high-melting transition metals of groups V and VI, have a typical yield point, which is more pronounced with finer grain. The upper yield limit, which is associated with the movement of locked dislocations, increases intensively. This effect cannot be explained solely by the influence of Cottrell atmospheres and interstitial impurities; the specific structure of dislocation pile-ups and the length of dislocation sources possibly play a certain part.

Direct electron-microscopic examinations confirm that the strains at which dislocation arrays and cell structure form in polycrystals are appreciably lower than is the case with single crystals. For instance, the formation of dislocation arrays in iron [82, 83] begins already at a tensile strain of 2%, while at ε = 13-15% most dislocations are locked into tridimensional arrays with cells 0.5-2 μm in diameter. Adjacent fragments separated by an array are misoriented by 1.5-2° at ε = 13% and by 2-3° at ε = 95.5% [83].

In pure aluminium [84], the cell structure begins to form on rolling at a 5-% deformation. At a 30-% deformation, cells become surrounded by a clear network of dislocation boundaries. In nickel, the cell structure forms at a strain of 5-10% [85].

In polycrystals, other conditions being the same, a lower value of γ_{sf} implies a higher temperature of deformation at which the cell structure starts to form, a smaller size of cells at the given tempera-

ture, and a greater thickness of cell walls. A higher degree of deformation and a lower deformation temperature are also favourable for the formation of smaller cells.

At heavy deformations (70% or more), the dislocation density grows sharply, individual dislocations in cell walls usually cannot be resolved, but dislocation pile-ups in the walls are retained. Weissmann [84] has demonstrated that small-angle boundaries of cells (walls) in heavily deformed aluminium become more asymmetrical and 'twisted' and that the dislocation density in walls (but not in cells) increases.

In addition to the total dislocation density N_d, an important characteristic of the dislocation structure for recrystallization is the excess of like-sign dislocations, which causes bending and misorientation of various regions of a crystal. It can be described by a dislocation density tensor [86]. Therefore, with any transformations in an array (its flattening or redistribution of dislocations which can involve partial annihilation of unlike-sign dislocations), the original misorientation of fragments remains practically unchanged, since the excess of like-sign dislocations which cannot dissociate remains the same. Misorientation can only be changed on attachment of dislocations from the outside or if part of the dislocations move from the array.

An excess of like-sign dislocations is determined not only by the deformation pattern, but also by the temperature at which deformation occurs and by the composition of the alloy (more particularly, by its susceptibility to cross slip).

It should be emphasized that an increase of deformation temperature not only facilitates cross slip and the onset of the third hardening stage, but also favours the formation of a cell structure with more perfect and narrow arrays, though less regular than those formed on cold deformation and polygonization. On the other hand, the total density of defects diminishes owing to partial annihilation of dislocations in cross slip and to annihilation of point defects. The excess of like-sign dislocations decreases and their distribution becomes more uniform.

In contrast to it, a deformation at room temperature occurs under the conditions where cross slip of dislocations is hampered, the mobility of point defects is low and the number of operative slip systems diminishes. The total density of defects and the excess of like-sign dislocations then increase; dislocations are distributed less uniformly and the texture changes to a different type. These peculiarities have an appreciable effect on the kinetics of recovery and recrystallization processes occurring during heating of deformed metals and alloys.

2.2.2. Deformation Textures

One of the most important consequences of plastic deformation in polycrystals is that their properties become anisotropic to some extent or other, i.e. grains which have been randomly oriented prior to deformation acquire a preferable crystallographic orientation which is called the texture*.

During deformation of a metal specimen, its crystallites also change their shape and tend to orientate themselves definitely according to the external deforming forces.

As noted earlier, the direction of shear in single crystals subjected to tensile stresses rotates until it coincides with the axis of tension, and in the single crystals in compression, the direction of shear tends to coincide with the plane normal to the direction of compression. A stable final orientation thus established is not changed on further deformation.

In polycrystals, such rotations, though of a more complicated nature, occur in individual crystallites. The orientation changes gradually as the deformation increases.

Practically, it is never possible to cause all crystallites in a body to line up on deformation strictly in the direction they tend to. Some subgrains and grains always remain more or less misoriented relative to the ideal direction, in which case a scatter of texture is said to take place. In heavily deformed metals, deformation textures are most pronounced, with texture scatter of 5 to 10 degrees. It should also be remembered that owing to a complicated interaction with adjacent grains texture scatter may be appreciable not only between grains, but also within them.

A slight texture can be detected by special X-ray methods even upon a slight deformation of a few per cent.

The nature of a texture is determined by many factors associated with the particular properties of the material and the conditions of strain. A well-grounded theory of deformation textures based on the concepts of dislocations has yet to be developed. The existing hypotheses proceed from the decisive role of the deformation scheme (the scheme of stressed state) and the number and nature of the operative slip systems. Each slip system leads to a definite rotation of a grain in the course of deformation, and the superposition of the rotations resulting from various slip systems gives the final orientation.

---

* Crystallographic texture should not be confused with a fibrous structure which is sometimes observed metallographically. A fibrous structure, i.e. extension of grains in a particular direction, may form no texture, but may be due to a particular pattern of arrangement of secondary phase particles and nonmetallic inclusions.

Drawing (or, in general, any uniaxial deformation) produces what is called an axial texture in which all crystallites show a definite crystal direction [*uvw*] along the axis of drawing, but occupy random positions around the [*uvw*] axis. For instance, drawing of b.c.c. metals (iron, molybdenum, tungsten, niobium, etc.) results in that the direction of the type ⟨110⟩ is established parallel to the drawing direction (the axis of wire, see Table 4).

TABLE 4. Deformation Textures [87]

Metal	Lattice	Texture characteristics
	Wire drawing and pressing	
Fe, Mo, W	b.c.c.	⟨110⟩*
	Uniaxial compression	
Al	f.c.c.	⟨111⟩ — 100%
Ni, Cu, α-brass	f.c.c.	60% ⟨111⟩+40% ⟨100⟩
Pb	f.c.c.	⟨111⟩ — 100%
Fe	b.c.c.	⟨111⟩ and ⟨100⟩ parallel to the compression axis
	Rolling	
Fe, Fe + Si	b.c.c.	{001} ⟨110⟩+{112} ⟨110⟩+{111} ⟨112⟩
Ag, α-brass	f.c.c.	{110} ⟨112⟩
Al, Ni, Cu, Fe-Ni, Cu-Zn, Cu-Sn, Cu-Ni	f.c.c.	{110} ⟨112⟩+{112} ⟨111⟩
	Tube drawing	
Steel 10	b.c.c.	{112} ⟨110⟩+{110} ⟨110⟩+{110} ⟨112⟩

* Additions to the solid solution do not change the texture.

In b.c.c. metals, the principal slip system is {110} ⟨111⟩. In the (110) plane, however, there are two equivalent directions of the family ⟨111⟩ (Fig. 24). These two directions, for instance $[1\bar{1}1]$ and $[11\bar{1}]$ in Fig. 24, should in the final result be symmetrical to the wire axis. This is possible with two crystallographic directions of the axis: ⟨100⟩ and ⟨110⟩ or, for the case shown in Fig. 23, [001] and $[1\bar{1}0]$. Practically, the direction ⟨110⟩ is realized, since the angle $\varphi_1/2$ between ⟨110⟩ and ⟨111⟩ is smaller than the angle $\varphi_2/2$ between ⟨100⟩ and ⟨111⟩.

In f.c.c. metals and alloys, a fibrous texture may include two orientations: ⟨111⟩ and ⟨100⟩. This means that two groups of grains may be in a drawn wire, one group being oriented in the ⟨111⟩ direc-

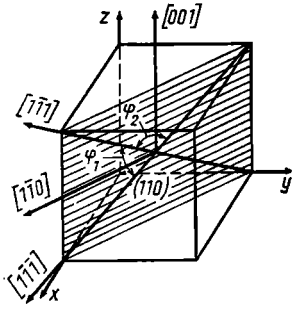

Fig. 24. A scheme to explain how the ⟨110⟩ type direction becomes the texture axis in drawn b.c.c. metals

tion along the wire axis and the other group in the ⟨100⟩ direction. The probability and contribution of either of these two orientations depend on the stacking fault energy γ_{sf} and, consequently, on the susceptibility to cross slip. A decrease in the stacking fault energy favours the formation of a texture with the ⟨100⟩ orientation. In aluminium, for instance, only the ⟨111⟩ orientation can form, whereas in silver and α-brass (where the stacking fault energy is low), both orientations are possible (see Table 4).

In c.p.h. metals with basal slip, a fibrous ⟨10$\bar{1}$0⟩ texture forms, i.e. a direction in the basal plane appears, which goes parallel to the axis of drawing. If, in addition to the basal planes, other slip planes are also operative, a more complicated fibrous texture forms.

Rolling produces more intricate textures and fixes not only a direction [*uvw*] parallel to the rolling direction, but also a crystal plane {*hkl*} parallel to the plane of rolling. Such a texture is designated by a pair of symbols {*hkl*} ⟨*uvw*⟩ composed of the indices relating to the corresponding crystal plane and the direction.

The mechanism of formation of a rolling texture, e.g. {001} ⟨110⟩, in b.c.c. metals has been discussed in [23, 24].

The complex deformation on rolling can be conditionally represented as the result of tension along the rolling axis and of compression in a direction normal to the surface of specimen In accordance with what has been said of b.c.c. metals drawing, the direction ⟨110⟩ must be ensured along the axis of tension in rolling, i.e. parallel to the rolling direction. This means that one of the crystal planes with the ⟨110⟩ direction must be set up perpendicular to the direction of compression in rolling.

Owing to the symmetry of a cubic lattice, pairs of equivalent mutually perpendicular planes of the family {110}—one of the principal families in slip systems of b.c.c. metals—participate in the slip during compression. Slip occurs in directions of the type ⟨111⟩, the resulting direction being ⟨100⟩. For another pair of planes of the type {110}, slip also occurs in a direction of the type ⟨100⟩, which is perpendicular to the former direction.

This implies, however, that slip should occur in a plane which includes two directions of the family ⟨100⟩ and one of the type ⟨110⟩. This condition is met by a plane of the type {100}, which thus must be positioned normal to the compression axis. This gives a stable

{100} ⟨110⟩ texture, which is usually found in b.c.c. metals. As has been noted earlier, however, the number of possible slip systems is large, especially in b.c.c. metals (see Table 2), so that more than one orientation usually forms on rolling, i.e. all crystallites are divided in a few groups, each of a particular orientation. One of these orientations may occur more often than others and thus the corresponding group may include a larger quantity of crystallites. Such a texture is designated by several pairs of symbols $\{hkl\}$ $\langle uvw \rangle$, the pair of symbols for the most frequently occurring orientation being written first.

For instance, the texture of iron after 98-% cold rolling deformation [83] is characterized by the following orientations written in the decreasing order of their probable occurrence: $(1\bar{1}2)$ [110] + + (001) [110] + (111) [11$\bar{2}$]. These three orientations are as a rule typical of all b.c.c. metals and alloys, though the order in which they occur is somewhat different since the (001) [110] orientation is usually the principal one.

A rolling texture can be controlled by rolling the metal alternately lengthwise and crosswise. This method of rolling enhances the {001} ⟨110⟩ texture component of b.c.c. crystals.

The formation of rolling textures in f.c.c. metals and alloys, which has been studied most thoroughly, is definitely dependent on the stacking fault energy, more exactly, on cross slip. If cross slip is impeded, a simple single-component {110} ⟨112⟩ texture forms. As cross slip becomes easier, the {112} ⟨111⟩ orientation appears and its contribution becomes more and more important. This is why the {110} ⟨112⟩ texture, which is often called 'alloy texture' or 'brass texture', usually forms in f.c.c. metals and alloys with a low stacking fault energy γ_{sf} (silver, α-brass and many solid solutions based on f.c.c. metals).

Metals of a higher stacking fault energy γ_{sf} (aluminium, copper) give a {110} ⟨112⟩ + {112} ⟨111⟩ texture, which is called 'metal texture' or 'copper texture', though high-purity copper develops even a more intricate texture.

The term 'alloy texture' can be explained as follows. The formation of substitutional solid solutions usually lowers γ_{sf}, especially at a higher valency of the alloying impurity. For that reason, even if a pure original metal gives a copper texture, its alloys, more strictly, high-concentration solid solutions on its basis, make for a simple {110} ⟨112⟩ texture.

This explains well the phenomenon of what is called texture transition [89], which consists essentially in that, as the deformation temperature increases and thus facilitates cross slip, the texture maxima are shifted from the position corresponding to an 'alloy texture' towards that of a 'metal texture'.

Texture transition has been found to occur in many alloys. In Cu + 2% Ge and Cu + 32% Zn alloys it is observed on raising the deformation temperature from −196° to +20°C [102, 103]; in Cu + 15% (at.) Al alloys, from −196° to +270°C [104]; and in Co + 30% Ni alloys, from 20° to 600°C [105]. Only materials of a very low stacking fault energy γ_{sf} can retain a brass texture up to rather high temperatures of rolling ($0.5T_m$).

In c.p.h. metals, the {0001} ⟨1120⟩ orientation is the principal component of the rolling texture. The texture is more complicated in metals with the *c/a* ratio deviating more from the regular value (1.633).

The results of studies of texture formation in rolled single crystals are of large importance for establishing the structural peculiarities of a deformed state which can affect essentially the process of recrystallization. These results are also important in themselves in association with the growth of single crystals of various size and cross section.

In the studies discussed, the role of orientation of slip systems relative to deforming forces has been established especially clearly. A texture developed in rolled single crystals is determined by the original orientation of the single crystal relative to the direction and plane of rolling. For instance, on Fe + 3.5% Si single crystal of an orientation (001) [110], i.e. the orientation imparted to b.c.c. polycrystals upon heavy rolling, retains that orientation unchanged on rolling up to very high degrees of deformation. This is the only orientation which meets completely the conditions of stability. The (100) [001] orientation of a crystal breaks up into two orientations upon rolling. Rolling of a (110) [001] crystal is realized through slip and twinning in the {112} ⟨111⟩ system and rotation of the lattice on the ⟨110⟩ axis which is normal to the rolling direction; the result is that the texture changes to a (111) [11$\bar{2}$] texture.

In rolling of a polycrystalline steel of a texture (110) [001] and of a large grain size (approx. 10 mm), the changes in orientation are analogous to those in a single crystal of the same orientation when subjected to the same range of deformations. On a deformation of 70-87 per cent, the original (110) [001] orientation changes to (111) [11$\bar{2}$]. With heavier deformations, this orientation changes partially to (112) [110] and further transforms into (001) [110]. The resulting texture is typical of b.c.c. metals (see Table 4).

The {111} ⟨112⟩ orientation is probably unstable also in single crystals on heavy deformations.

With a decrease of the original grain size, the above texture transition {110} ⟨001⟩ → {111} ⟨112⟩ → {112} ⟨110⟩ → {100} ⟨011⟩ occurs at lower deformations.

A summary of the results obtained by B. V. Molotilov [25] and many other workers shows that b.c.c. single crystals change their orienta-

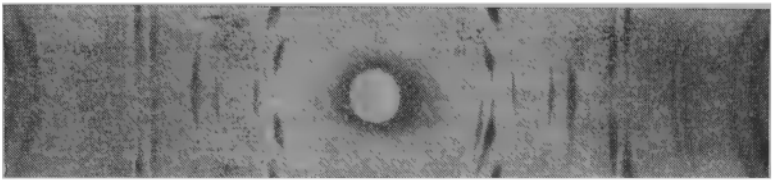

Fig. 25. X-ray photograph showing a distinct texture in pressed aluminium alloy

tion on cold rolling to a stabler orientation by the following scheme:

$$\{110\}\ \langle uvw\rangle \rightarrow \{111\}\ \langle 112\rangle;$$

$$\{110\}\ \langle 001\rangle \rightarrow \{111\}\ \langle 112\rangle;$$

$$\{110\}\ \langle 112\rangle \rightarrow \{121\}\ \langle 517\rangle \rightarrow \{121\}\ \langle 101\rangle;$$

$$\{110\}\ \langle 111\rangle \rightarrow \{121\}\ \langle 101\rangle;$$

$$\{210\}\ \langle 001\rangle \rightarrow \{211\}\ \langle 113\rangle \rightarrow \{211\}\ \langle 011\rangle;$$

$$\{310\}\ \langle 001\rangle \rightarrow \{311\}\ \langle 114\rangle \rightarrow \{311\}\ \langle 011\rangle;$$

$$\{100\}\ \langle 001\rangle \rightarrow \{100\}\ \langle 011\rangle;$$

$$\{100\}\ \langle 011\rangle \rightarrow \{100\}\ \langle 011\rangle;$$

$$\{100\}\ \langle 0vw\rangle \rightarrow \{100\}\ \langle 011\rangle;$$

$$\{hkl\}\ \langle 011\rangle \rightarrow \{100\}\ \langle 011\rangle \rightarrow \{211\}\ \langle 011\rangle$$

As seen, the {100} ⟨011⟩ orientation is the sole stable initial orientation which is not changed by deformation. Many crystals of a different original orientation develop this orientation when deformed.

The principal method for examination and analysis of deformation textures is radiography. When there is no texture in a specimen, lines (or rings) on a radiogram are uniformly dark. In the presence of a texture, radiographic lines have regular interference maxima of blackening (Fig. 25). Analysis of X-ray photographs will be described briefly in Ch. 15.

2.3. Other Effects of Macro- and Microinhomogeneity in Deformed Metals

Inhomogeneities due to friction forces. Under friction forces acting between a deforming tool and the metal being deformed, the rate of plastic deformation and other parameters of metal flow may vary over the workpiece cross section. This involves differences in the dislocation structure and texture over the cross section and the appearance of internal stresses between the surface and core layers of

the metal. These macrostresses (also called zonal stresses, or first-order stresses) are counterbalanced in macrovolumes of the metal.

Friction forces depend on the conditions of rolling, including the diameter and temperature of rolls, the temperature of the metal, the rate of deformation, the presence of scale or lubricant on metal surface, etc.

In f.c.c. metals, cold rolling forms the {001} ⟨110⟩ texture in surface layers of the metal, though no such texture appears in deeper layers. The depth to which this orientation penetrates increases with increasing coefficient of friction, μ, and the amount of deformation per pass. At very high values of μ, a weak component of the {111} ⟨011⟩ texture appears on the surface.

In sheets of low-carbon steel, the surface layers of ferrite differ from the deeper ones by a strong scatter of the {001} ⟨110⟩ and {112} ⟨110⟩ orientations I. P. Kudryavtsev [23] discovered an asymmetrical distribution of textures over the cross section and the appearance of an intermediate subsurface layer with an axial texture between the surface and core layers.

The existence of three zones (core, subsurface and surface) with different textures has also been established in cold-rolled sheets of transformer steel [90]. Figure 26 shows curves of distribution of various texture components over the cross section of a strip on using various process lubricants. As is seen, there are three zones. It is also clear that the textures are asymmetrical, the texture in the lower surface being somewhat different from that in the upper surface. As has been found, this difference is associated with the different thickness of scale on the upper and lower surface of a slab, and also with the conditions of cooling of the surface layers by cold rolls during prior hot rolling. A subsurface layer of a different texture than the surface layer can form when the lubricant used (e.g. rosin) increases the coefficient of friction. In such cases, even the surface layer shows orientations not typical of the deformation textures of b.c.c. metals. A lubricant which reduces friction (e.g. castor oil) favours the formation of the principal texture components in the surface. These factors have an appreciable effect on subsequent recrystallization.

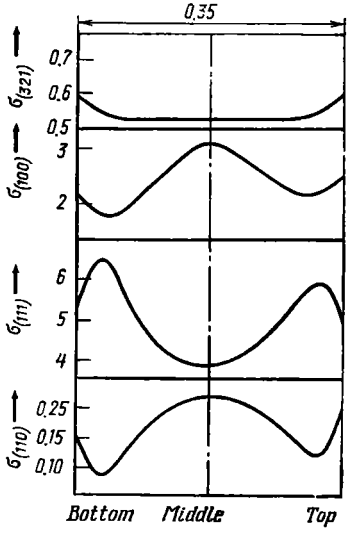

Fig. 26. Relative distribution of various components of a deformation texture over the cross-section of rolled transformer steel strip [90]

Other methods of deformation, e.g. drawing, extrusion, etc., can also produce texture inhomogeneity over the cross section. As has been noted, nonuniform conditions of metal flow can cause the apperance of zonal stresses apart from the formation of textures. The zone where the flow of metal during deformation has been more intensive (surface layers in rolling and core layers in extrusion) is subjected to residual compressive stresses, and the zone with a lower rate of metal flow experiences residual tensile stresses.

These stresses can be quite high, up to 70 kgf/mm^2 in steel; they can result in warpage, cracking, etc., but sometimes can be useful. Under certain conditions of deformation of supersaturated solid solutions, macrostresses may have an accelerating or decelerating effect on decomposition. If the decomposition of a solid solution occurs with an increase in the unit volume, it will be facilitated by tensile stresses and impeded by compressive ones, and vice versa. Decomposition of a solid solution, especially if it is inhomogeneous, and the subsequent dissolution of excess phases play the most important part in recrystallization processes.

The thermal stability of macrostresses has been studied insufficiently because of certain experimental difficulties. The main nondestructive method for analysing these stresses is X-ray structural analysis. Under the effect of zonal stresses, the interplane spacings in all the planes of the same orientation relative to the acting forces vary uniformly, which causes displacement of lines on X-ray photographs in a direction corresponding to the sign of stress. This displacement is slight and cannot be measured accurately due to blurring of the lines caused by the associated structural changes.

Inhomogeneities due to excess phases. The appearance of a secondary phase in an alloy may have an appreciable effect on the nature of the dislocation structure that forms on deformation. This effect is especially high if particles of the secondary phase are very hard and their number is large.

Figure 27 shows the dislocation structure revealed by M. P. Usikov and L. M. Utevsky [85] in an overaged XH80T2IO alloy (10 h, 850°C), deformed 8 per cent. Thick pile-ups of bent dislocations and dislocation loops are seen around particles, which have precipitated in ageing, and near them. This attests to a more turbulent character of plastic flow near the particles that impede the movement of dislocations.

Having analysed the dislocation structures of the specimens aged at 700°C for 16 h prior to deformation, in which high-disperse inclusions were present, the authors [85] have come to a conclusion that both disperse particles proper and the stress fields that surround them offer resistance to dislocation movement.

Ashby [91] detected prismatic dislocation loops around oxide particles in internally oxidized copper alloys. He explained their forma-

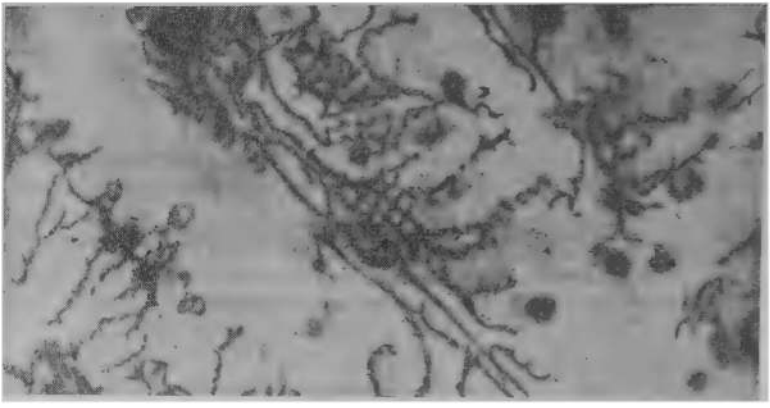

Fig. 27. Dislocation structure in XH80T2IO alloy (ageing at 850°C, 10 s) deformed 8%

tion due to local cross slip of dislocations to bow around obstacles.

All these data are convincing evidence that the dislocation density increases more quickly in alloys which contain excess phase particles. As mentioned earlier, the appearance of strongly misoriented regions around non-metallic inclusions has been detected in cold-rolled transformer steel [75]. It should also be noted that excess phase particles can serve not only as barriers for moving dislocations but also generate dislocations in heat treatment processes (heating, cooling, thermocycling) owing to the differences in thermal expansion and unit volume between these particles and the matrix.

The formation of point defects in deformation. The above-mentioned structural changes occurring in deformation are only associated with changes in the density and distribution of dislocations. The picture will be incomplete if we disregard the problem of how deformation affects the concentration and distribution of point defects, in the first place, of vacancies which play an important part in subsequent processes of recovery and recrystallization.

Plastic deformation is accompanied by the formation of two types of point defect — vacancies and interstitial atoms — to concentrations a few orders of magnitude greater than the equilibrium concentration. The mobility of interstitial atoms in metals is quite high, and their flow to dislocations and boundaries occurs at rather low temperatures (<0.1 of T_m). For that reason, the effect of interstitial atoms on recrystallization can evidently be neglected, which is not the case with vacancies.

Though a major portion (about 70%) of vacancies formed in deformation run off on heating to a temperature below the recrystallization point, a certain fraction (20-30%) probably remains in the metal

until the onset of recrystallization and affects the conditions and the rate of the processes of dislocation climb and dislocation redistribution.

In commercially pure metals and alloys, the thermal stability of vacancies and their actual concentration at the beginning of recrystallization are higher than in perfectly pure metals and largely depend on the presence and type of impurities. The low-mobile impurity-vacancy complexes which are thus formed are favourable for preserving the increased concentration of vacancies up to higher temperatures.

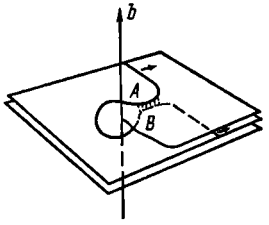

Fig. 28. Formation of vacancies and interstitial atoms as an edge dislocation bows around a screw dislocation

Further, vacancies, like impurity atoms, can form atmospheres around dislocations and thus lock them. This has been confirmed by the results of comparative mechanical tests of metals with various concentrations of vacancies. For instance, the critical shear stress in hardened aluminium (having an elevated concentration of vacancies) has turned out to be five times that in aluminium slowly cooled down from a high temperature.

The particular mechanisms of the formation of point defects in the course of deformation are yet little studied in view of certain experimental difficulties. Some, most probable, of them can be specified, however, from the geometrical analysis of interaction of dislocations. One of the principal mechanism [92] is obviously associated with non-conservative movement of dislocation jogs whose Burgers vector has a different orientation to that of the main dislocations.

If a stress is applied to a screw dislocation with jogs (which cannot slip), the dislocation will be bent between the locking jogs. Vacancies will form on the jogs owing to thermal activation, and this will enable the dislocation to slip forward. The vacancy so formed will diffuse into the volume of the crystallite.

The probability of dissociation of a dislocation jog is high in metals having a low stacking fault energy. A dissociated jog can move along the dislocation only non-conservatively and will cause the formation of point defects.

N. F. Mott [93] has proposed a model to explain the formation of vacancies and interstitial atoms in cases where a glissile edge dislocation bows around a screw dislocation (Fig. 28). As soon as the edge dislocation has bowed around the screw one, the two portions, A and B, of its loop move opposite to each other and dissociate. Since, however, the screw dislocation has caused a displacement with a pitch equal to the interplane spacing, an interval AB, one interatomic distance wide, will form between the annihilating loops. This interval is essentially a row of vacancies.

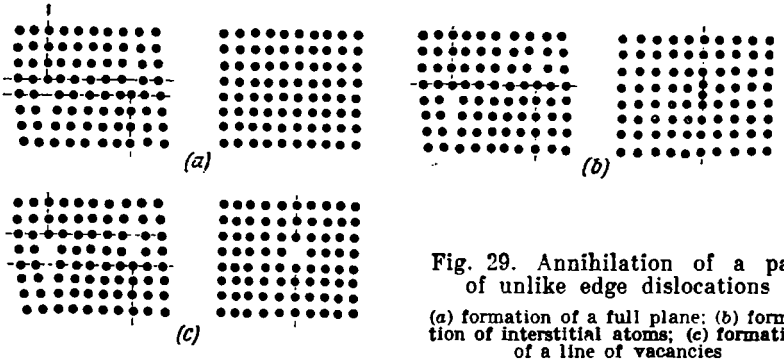

Fig. 29. Annihilation of a pair of unlike edge dislocations

(a) formation of a full plane; (b) formation of interstitial atoms; (c) formation of a line of vacancies

One-dimensional lines of point defects can also form on interaction (annihilation) of a pair of unlike edge dislocations. If the slip planes on which the dislocations move are spaced one interplane spacing apart, the corresponding half-planes will combine into a full plane (Fig. 29*a*). If two dislocations move on the same slip plane, they form a row of interstitial atoms upon annihilation (Fig. 29*b*). If the two slip planes are spaced two or more interatomic distances apart a line of vacancies forms on annihilation (Fig. 29*c*).

2.4. Variations in Energy and Properties of Plastically Deformed Metals and Alloys

Plastic deformation increases the internal energy of metals and alloys. Quantitatively, this energy is a portion of the total mechanical energy of deformation, E_d, that is stored in the material and remains in it upon removal of external forces; it is respectively called the stored energy of cold work, E_s.

Measurements of E_s and its variations on heating, with parallel analysis of the structure and physical properties of the material, can give valuable information on the nature of cold work and on the essence and mechanism of restoration of the structure in recovery and recrystallization.

The stored energy of cold work is distributed non-uniformly in a work-hardened metal. Its principal carriers are most distorted portions, i.e. crystal lattice defects. Each type of defect has a corresponding excess energy depending on the composition of alloy. Quantitative assessment of this energy involves much difficulty and the data obtained are not always reliable; for many materials there are no data at all. A review of the available information is given in [94]. One can judge of the energy of various lattice defects from the following values obtained for copper. The energy of formation of a vacancy is approximately 1 eV. The energy of a unit length of dislocation

is roughly 5 eV per atomic plane intercepted by the dislocation axis. The energy of a stacking fault is approximately 40-60 erg/cm², that of a twin boundary, 20-30 erg/cm², and that of a low-angle dislocation boundary, approximately 300 erg/cm².

The absolute unit value of the stored energy of cold work may vary within wide limits, from a few hundredths of a calorie to a few tens of calories per g-atom. In view of the nonidentical conditions of experiments, it is difficult to analyse the results obtained by various researchers and establish general relationships. Certain generalizations can be made by analysing a large volume of data given in [2, 94].

The stored energy of cold work, E_s, increases with the amount of cold work, first intensively and then more and more slowly as it approaches the saturation limit. In deformation of copper, the stored energy E_s and its ratio to the total energy spent in deformation, E_d, are 2-4 times as high as they are for aluminium. For instance, in drawing of copper wire at a rate of 0.42 m/min, $E_s = 15$ cal/g-atom and $E_s/E_d = 9\%$, whereas the corresponding values for aluminium are 4 cal/g-atom and 2% [95].

This difference can obviously be explained by the different structure of these two metals in deformed state. The matter is that they differ in susceptibility to cross slip and in mobility of defects at room temperature, so that a fraction of defects in aluminium can disappear either in the course of deformation itself or in the time interval between the deformation and calorimetric tests.

The stored energy of cold work, E_s, increases on addition of impurities to pure metals and also with a decrease in the temperature of deformation.

According to McQueen and Jonas [95], the stored energy of materials deformed at the temperature of liquid nitrogen is approximately four times that at room temperature. After a 20-% deformation of copper at 78 K, its resistivity and hardness (measured at room temperature) grow respectively by 25% and 10% over the corresponding values after deformation at 298 K.

The structural changes caused by deformation and the associated stored energy E_s lead to drastic changes in the structure-sensitive mechanical and physical properties of the material; in particular, they cause a heavy increase in strength parameters and a corresponding decrease in plastic parameters (Table 5).

Work hardening greatly depends on the type of crystal lattice. Thus, the hardening effect in f.c.c. alloys is several times that in b.c.c. alloys (see Table 5).

The effect of the stacking fault energy is evident from the changes in the properties of alloys based on aluminium ($\gamma_{sf} > 200$ erg/cm²), nickel ($\gamma_{sf} \approx 120$ erg/cm²), and copper ($\gamma_{sf} \approx 60$ erg/cm²). On a 90-% deformation, the ultimate strength in an aluminium-base alloy increases three times, whereas in nickel and copper-base alloys, where

TABLE 5. Changes in Mechanical Properties of Steels on Cold Drawing

Steel type	ε, %	σ_t, kgf/mm²	σ_y, kgf/mm²	δ, %	ψ, %
Low-carbon (0.08% C)	0	41.8	30	31	73
	70	83.5	65	6	31
	95	108.0	90	5	25
Austenitic (18% Cr, 8% Ni)	0	61.9	24.6	80	71.8
	40	112.5	105.4	—	—
	90	182.8	182	5	43

dynamic recovery is impeded, it grows by a factor of more than 7.

The yield strength σ_y increases in deformation more sharply than the ultimate strength σ_t (see Table 5), so that the difference $\sigma_t - \sigma_y$ decreases with increasing deformation and therefore the capability of a material for further plastic deformation also decreases.

The work-hardening effect increases with an increase in the content of disperse hard particles, which can be explained by a more turbulent and non-uniform pattern of deformation.

Work hardening also increases electric resistivity due to a greater scatter of conduction electrons on lattice defects. The gain in resistivity ($\Delta\rho$) depends on the composition and state of the material; $\Delta\rho$ is low (2-6%) in pure metals, in solid solutions it amounts to 10-20%, and, finally, reaches 100% or more in ordered solid solutions.

Work hardening also affects the structure-sensitive magnetic properties. The coercive force H_c increases monotonically, permeability μ decreases, and remanent induction B_r drops sharply on light deformations (5-8%) and more slowly on heavier deformations.

Deformation can also affect the density of materials. With increasing deformation, the density can decrease by a few tenths of a per cent. For instance, the unit volume of the metal in cold-rolled tubes of steel ШХ15 is 0.16% higher than that in hot-rolled tubes. Very heavy deformations often diminish the density less intensively than lighter deformations.

Of large importance is the anisotropy of properties which appears owing to the formation of textures on heavy deformations.

Chapter 3

Classification and Driving Forces of Processes Occurring in Deformed Metals and Alloys on Heating

Though the structural changes occurring in deformed metals and alloys on heating have been studied for a long time, there is a lack of consistency in their classification and the terminology used.

A number of terms and designations were proposed at a stage when the resolution of structural analysis methods was low and the essence of structural changes remained unclear.

In the last two decades, the situation has changed drastically, and the mechanisms of these processes have been under extensive study. But the scientific information on these mechanisms is growing so vast every year that the wide circles of metallurgists are hardly able to cope with the abundance of newest data. Furthermore, some textbooks contain certain definitions which are incorrect from the modern standpoint. For instance, a number of authors of textbooks do not distinguish between secondary recrystallization and grain growth [366]. Usually, no distinction is made between point defect annihilation and recovery, or between a cell and a subgrain. Some authors allege that there is no relation between the orientation of the centres of primary recrystallization and the surrounding deformed medium.

In recent years, some authors have come to deny the existence of grain boundary migration in general and as a process by which grain enlargement is realized. They claim that grain enlargement proceeds through coalescence of grains separated by large-angle boundaries which disappear without migration, leaving the initial misorientations intact (which is utterly impossible).

There is confusion of the concepts concerning the interrelation between polygonization and recrystallization. The fact that some authors recommend polygonization as a means for preventing recrystallization, irrespective of prior deformation, is one of the examples which points to a confused notion of polygonization.

The present state of physical metallurgy makes it possible to suggest a more consistent classification of the processes which remove the effects of cold work in heating. Such a general classification will undoubtedly be of great value for correct estimation of the effectiveness of various processes of metal treatment and also for better understanding between metallurgists.

The state of cold-worked metal is thermodynamically unstable at any temperature. The free energy of such a metal is higher than it is in as-annealed metal due to the distortion energy brought about by the dislocations and point defects formed by deformation. So, unlike common phase transformations, the transition of a deformed metal to a stabler state of lower free energy is not strictly associated with a particular temperature.

On the other hand, the deformed state is quite stable ('frozen') at reduced temperatures, and for the transition to occur it is necessary that thermal activation (activation energy Q) be enough to overcome the potential energy barrier.

The time τ this process takes to set in shortens with increased temperature T by an exponential law $\tau = \tau_0 \exp(Q/RT)$, where τ_0 and Q have different values in various temperature intervals.

As has been given in Ch. 2, the types and mechanisms of distribution of crystal structure defects produced by deformation are quite diverse. These defects are eliminated on heating by way of various elementary processes which occur with different rates, in various temperature intervals, and with a different activation energy. If a number of elementary processes are superimposed on one another, Q usually increases and becomes the 'effective', rather than the actual activation energy of the process (for more detail see Ch. 11).

The elementary processes which can occur on heating of a deformed metal and decrease the activation energy are as follows (in the order of the development of each during heating):

(1) diffusion of point defects and their disappearance in dislocations and boundaries, accompanied by partial annihilation of vacancies with interstitial atoms and by the formation of complexes and groups of point defects;

(2) redistribution of dislocations by simple and cross slip, accompanied by partial dissociation of unlike dislocations and by narrowing of dislocation loops;

(3) redistribution of dislocations by climb, which, in combination with dislocation slip, results in 'flattening' or, sometimes, on the contrary, in unraveling of dislocation arrays and their crystallographic reorientation;

(4) formation of low-angle boundaries associated with the processes indicated under (2) and (3);

(5) migration of low-angle boundaries and large-angle boundaries into the deformed matrix accompanied by annihilation (sweeping-out) of defects;

(6) migration of grain boundaries between recrystallized grains and coarsening of these grains.

It should be emphasized that the above classification is only conditional and many of these elementary processes are not yet studied thoroughly.

The above-mentioned elementary processes can occur either successively or superpose on one another, depending on the amount and nature of deformation, the rate and time of heating, the nature and purity of the material and some other factors. As a result, the effects of cold work on the structure and properties of a metal (alloy) can be eliminated in different ways and to a different extent.

The following stages are distinguished in the process of elimination of cold work on heating (in order of increasing activation energy):

1. Recovery:
   (a) point defect annihilation;
   (b) polygonization.
2. Recrystallization:
   (a) primary recrystallization;
   (b) grain growth (uniform);
   (c) secondary recrystallization (often called 'exaggerated grain growth').

3.1. Recovery

Recovery is a multistage process that includes all the elementary processes which take place prior to recrystallization.

Recovery should be understood as the process of structural perfection of a work-hardened metal by redistribution and annihilation of point defects and, besides, by redistribution and partial annihilation of dislocations either without the formation of new boundaries (point defect annihilation proper) or with the formation and migration of low-angle boundaries only (polygonization).

3.1.1. Point-defect Annihilation

In this process, point defects are redistributed and their concentration is diminished due to their annihilation and dislocations are redistributed by conservative movement without forming new boundaries.

The detailed list of the elementary processes which should be related to point defect annihilation is not generally adopted. This is because the available experimental data are still insufficient for reliable generalization and interpretation of the processes at each particular stage, which depend appreciably on the material and method of study.

The difficulty is that direct detection of most defects annihilated in this process, in the first place, point defects, is linked with certain complications, while indirect detection does not always give unambiguous results.

A partial way out from the situation has been found by using certain methods (particle irradiation or, less frequently, hardening from a high temperature) which produce only point defects in a material. By analysing the changes in the physical properties of these materials (mainly the electric resistivity and density) on heating, it is possible to establish the temperature intervals, kinetics and activation energy for annihilation of these defects. The results obtained are then applied to deformed materials.

When studying recovery in deformed materials, a useful information on the course of a particular elementary process can be obtained by analysing in parallel the changes in resistivity, hardness, yield and elastic limit, and the pattern of lines on X-ray photographs of polycrystals (or of individual reflections on those of single crystals).

This approach has been used in [98, 99] for studying recovery and recrystallization in copper, aluminium and their alloys deformed at the temperature of liquid nitrogen (78 K) and at room temperature (293 K).

Valuable information can be obtained by calorimetric analysis of the release of the stored energy in deformed metals on heating [94], analysis of density changes [99, 100] and internal friction [101, 102].

When analysing the results obtained by various methods, the effect of a particular type of defect on a given property should be considered. For instance, the concentration of point defects has the highest influence on resistivity; the density and distribution of dislocations on the yield limit and the pattern of X-ray lines; the type of dislocation locking on the elastic limit and internal friction; and the concentration of vacancies and interstitial atoms on the density.

These methods have revealed that some elementary processes of point defect annihilation require a very low activation energy and can occur at quite low temperatures, hundredths of the melting temperature (T_m). For instance, Molenaar and Aarts [103] studied recovery in wire specimens of copper, silver and aluminium deformed at 90 K. Annealing at 293 K diminished the deformation-induced gain in resistivity roughly by 30%, but had practically no effect on yield strength. Consequently, the whole loss in resistivity was due mainly to a reduction in point defect concentration. Thus it is natural that studies of recovery should be done on specimens deformed at the lowest possible temperature (preferably at liquid helium temperature, 4.2 K) and then heated gradually. Otherwise, there is a risk to miss the part of the stored energy of cold work that is released in recovery already at the stage of deformation or after it but before measurements. Therefore, the experimenter will record a fewer number of stages.

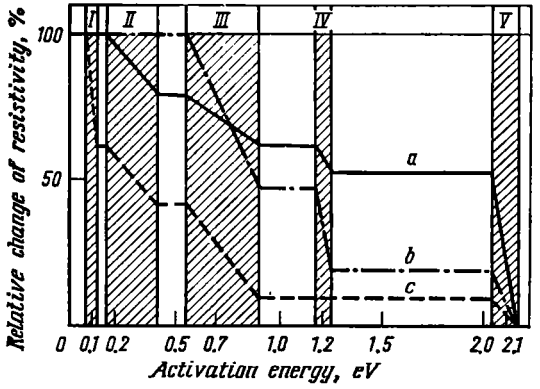

Fig. 30. Stages (I-V) of restoration of resistivity in copper and gold during heating [97]

(a) after strain-hardening; (b) after hardening; (c) after irradiation

Van Bueren [97] has generalized a number of studies on irradiated, hardened and deformed copper and gold and proposed a classification of the processes of restoration of electric resistivity. This classification is shown in Fig. 30 and partially (with slight modifications) in Table 6.

Though van Bueren's classification is not fully unique and exhaustive, it still has not lost its significance. A large number of studies made on recovery in recent years [6] have not given principally new results, but an enormous factual material was collected. The number of established recovery stages which differ from one another in activation energy according to measurements of resistivity varies from two [104] to six [105]. It has been shown that the conditions of deformation, the purity of metal and the nature of impurities, and the stacking fault energy have an appreciable effect on the number of stages, their intensity and the temperature at which they occur. Some results and conclusions made are undoubtful, such as a relation between the first three elementary processes and point defects, high influence of these defects on the restoration of resistivity in irradiated materials, particularly in deformed materials (up to 30%, see Fig. 30); increased dependence of the mechanical properties on the density and distribution of dislocations, etc.

Among the processes indicated in Table 6, the processes at stages II and III seem to be most disputable and least probable. It is still unclear what particular type of point defects influences, by migration, a given stage and how this migration affects dislocation movement. Some workers consider the division of recovery into stages to be purely conditional and associate the restoration of resistivity, especially at temperatures above room temperature, with a combi-

TABLE 6. Elementary Processes of Restoration of Electric Resistivity in Copper and Gold [97]

Restoration stage	Elementary process	Temperature range, K	Activation energy, eV	Supposed mechanism of elementary processes
Recovery: point defect annihilation	I	30-40 (0.03 T_m)	0.1	Recombination of interstitial atom-vacancy pairs
	II	90-200 (0.1-0.15 T_m)	0.2-0.5	Migration of interstitial atoms
	III	210-320 (0.16-0.20 T_m)	0.7	Migration of vacancies to traps. Migration of bivacancies
polygonization	IV	350-400 (0.27-0.35 T_m)	1.2	Migration of vacancies to dislocations, resulting in their redistribution (with the formation of low-angle boundaries) and partial annihilation
Primary recrystallization	V	400-500 (0.35-0.4 T_m)	2.1	Climb and thermally activated slip of dislocations causing their partial annihilation and formation of large-angle boundaries

Notes: 1. A change in metal purity can change the temperature range of a process. 2. 1 eV = $1.6 \cdot 10^{-19}$ J = 23 kcal/g-atom.

nation of processes that have a continuous spectrum of activation energies [97].

Evidence in favour of this conclusion is the data on the release of stored energy at the recovery stage in cold-worked nickel of various purity [106, 107]. In a less pure nickel, there are two distinct maxima at temperatures above room temperature, whereas in a purer nickel these maxima merge into a single blurred maximum. Consequently, impurities can interact with point defects and affect (usually diminish) point defect mobility. The existence of a few maxima can be explained by the different mobility of impurities or complexes in which they participate.

This explanation agrees well with the results of studies on recovery in oxygen-containing niobium [108]. At the stage associated with migration of interstitial atoms, the authors have detected two substages with approximately equal values of activation energy. They have supposed that migration of interstitial niobium atoms occurs at the first substage and that of oxygen atoms at the second.

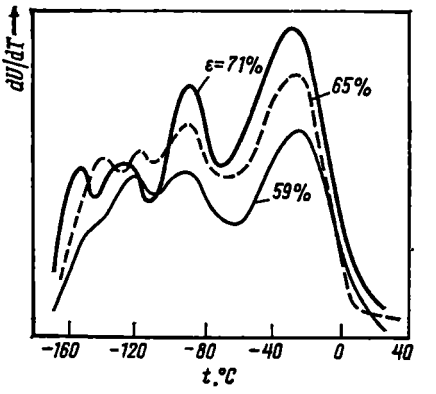

Fig. 31. Release of stored energy in specimens of copper (99.999% pure) deformed to various degrees at 88 K as a function of temperature

As has been established in a number of works [6], impurities can affect stage III recovery, which is associated with the diffusion of vacancies. Impurities with the atomic radius substantially different to that of the matrix retard the diffusion of vacancies to sinks and shift the process to higher temperatures.

As regards stage I recovery, most workers agree that impurities have practically no effect on the kinetics of annihilation of interstitial atom-vacancy pairs.

It is not yet established for certain that recovery of point defects has no effect on mechanical properties. G. Goedeme *et al.* [104], for instance, have discovered that the concentration of vacancies has a substantial effect on the recovery of the yield strength in gold. Lihl *et al.* [109] have found that annealing of deformed aluminium at 22°C is associated with a slight increase in σ_y, a more appreciable increase in density than on recrystallization, and a slower rate of subsequent recovery. The authors [109] explain these facts by the formation of vacancy clusters. The interesting problem of the role of these clusters in recovery is not yet studied thoroughly.

The stages of recovery must also be influenced by the conditions of deformation, which are responsible for the type, concentration and distribution of defects. As has been shown in [104, 109], the time and temperature at which a particular stage sets in depend on the concentration of defects and the sites of their annihilation. For instance, the temperature of the maximum at stage III recovery in molybdenum decreases with increasing concentration of deformation-produced dislocations that serve as sinks for interstitial atoms and vacancies.

Figure 31 shows the effect of temperature on the release of stored energy of deformation in high-purity (99.999%) copper deformed to various degrees. As seen, heavier deformations increase the energy

released at the recovery stage and shift the temperature intervals of recovery, each of the two maxima being shifted in a somewhat different way to the other.

Van Bueren's classification, however, disregards a number of important processes, in particular, the process of dislocation-displacement type associated with thermal activation, which was suggested by D. Kuhlmann-Wilsdorf and confirmed by Hibbard and Dunn [111] in metallographic studies of recovery on bent single crystals of silicon-alloyed iron. During heating at 400°C ($0.37\ T_m$)*, the authors observed the displacement of dislocations on their slip planes in a direction opposite to that of their motion on deformation, which resulted in their more uniform distribution. The authors attribute this phenomenon to a reduction of internal stresses in the elastically distorted region due to thermally activated shear when the yield strength at an elevated temperature becomes lower than the elastic strain produced by dislocations.

This is in accord with the results of investigations into the effect of recovery at room temperature on the dislocation structure in an aluminium foil (1-2.5 μm) deformed directly in an electron microscope column. At a voltage of 500 kV, it has been found that during two days recovery causes no noticeable changes in the dislocation density, the size and shape of dislocation cells, but entails appreciable changes in the dislocation configurations. In particular, many dislocation segments and the contrast at tangled dislocations disappear. Dislocations move through small distances and some of them form pile-ups. Some of the dislocation lines become broken. This stage of recovery must apparently precede polygonization, i.e. lie in a temperature range between stages III and IV.

As found in [111], the process of annihilation of dislocations associated with climb also took place, though it did not form new boundaries.

A large number of research papers, as reviewed in [16], were concerned with mathematical description of the rate of recovery. Most of them are of only formal nature and their authors do not proceed from the particular concepts of the mechanism of recovery, since this is impossible at present.

But the authors reliably established a typical and characteristic feature of recovery, which shows up in that the process has no incubation period. Its rate is at a maximum at the initial moment ($\tau = 0$) and then decreases exponentially (Fig. 32). This principle can be expressed through a relation which satisfactorily describes a low-temperature restoration of resistivity and yield limit in copper:

$$X = 1 - \exp\left[-k'\tau \exp\left(-Q/RT\right)\right]$$

* Polygonization occurred only at 600°C.

where X is the restored fraction of a given property, T and τ are the absolute temperature and time of heating, Q is the activation energy, R is the gas constant, and k' is a coefficient.

For an isothermal process, $X = 1 - \exp[-k'\tau]$; $dv/d\tau = k/\tau$, i.e. the rate of variation of a property that is restored by recovery is inversely proportional to time and has a maximum at the beginning of the process ($\tau = 0$).

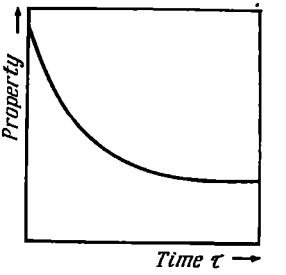

Fig. 32. Variation in the rate of property restoration during isothermal heating. Ordinates show how a property in terms of relative units decreases during recovery

It should be noted in conclusion that complete restoration of properties at the stage of point defect annihilation to the properties of as-annealed metal can only occur when the deformation is limited to easy slip in a single slip system. This can be realized in hexagonal crystals with a favourable orientation for basal slip or in specially oriented f.c.c. and b.c.c. crystals at light deformations (see Ch. 2). If more than one slip system participates in slip, the properties can be restored only partially at the point-defect annihilation stage, even if slip in secondary systems is relatively slight.

3.1.2. Polygonization

Among the processes which can noticeably change the structure of a deformed material on heating, polygonization is the most low-temperature one*. The term polygonization was first introduced by E. Orowan [111] and was later used by R. Cahn [112] to describe a particular type of structural changes, which were observed by a number of workers, during prerecrystallization heating of certain metals and alloys.

The first mention of these changes was made in a work of S. T. Konobeevsky and I. I. Mirer (1932) who found that radially extended spots (asterism streaks) in Laue photographs of rock salt crystals deformed in bending were separated into single reflections on annealing (Fig. 33). Each reflection is a trace of an interference beam 'reflected' from an individual block. This effect can be explained by assuming that a bent crystal disintegrates on annealing into a series of structurally perfect blocks which are discretely tilted thro-

* It is naturally assumed that the amount of deformation is the same in all cases. Otherwise, recrystallization in a heavily deformed material would occur at a lower temperature than polygonization in a lightly deformed material.

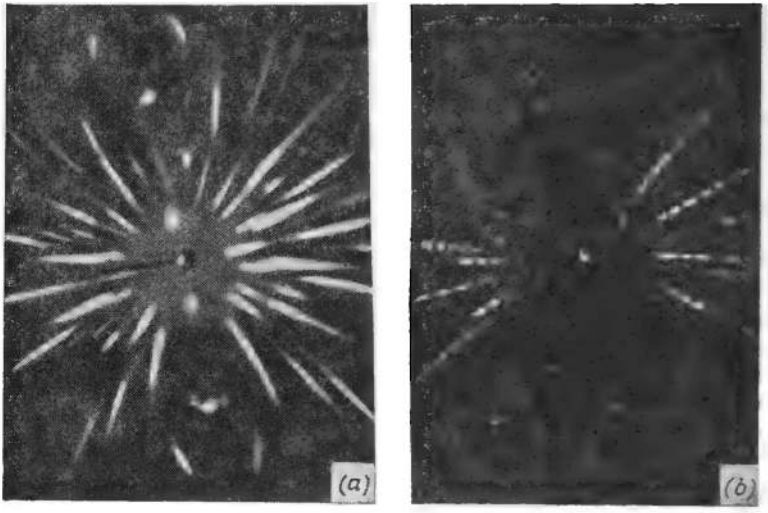

Fig. 33. Asterism of a rock salt single crystal
(*a*) as bent, (*b*) polygonized

ugh small angles relative to one another, with the total misorientation of the bent crystals remaining unchanged.

Similar X-ray effects were later revealed in single crystals of a number of metals and in coarse-grained polycrystals.

According to the concepts existed before the development of the dislocation theory, the Konobeevsky-Mirer effect could be explained by the release of second-order stresses (microstresses) in a bent crystal owing to plastic shear on particular atomic planes, which separate the crystal into individual blocks. With increasing temperature, the critical shear stress decreases, so that plastic shear occurs in portions where this stress turns out to be less than the residual stress.

With advances in the theory of dislocations, new crystallographic concepts of the mechanism of polygonization were proposed by R. Cahn [113], N. F. Mott [114], and A. Cottrell [115].

The dislocation mechanism of polygonization can most clearly be described by considering a single crystal deformed by bending (i.e. by easy slip corresponding to stage I work-hardening), which has an excess of like-sign edge dislocations (see Fig. 34*a*). The increased energy of the crystal includes the energy of dislocations proper and an additional energy of mutual repulsion of like dislocations located in common slip planes. On annealing, dislocations are re-grouped and partially annihilated. Excess edge dislocations of one sign, which are driven by elastic interaction, slip on the planes and then climb to form new (not existed before heating) tilt boundaries nor-

mal to the slip plane (Fig. 34*b*) and possessing no long-range stress fields. A typical feature of the dislocation subboundaries formed in this way is their low curvature and therefore low mobility (see later).

The regions of the crystals separated by these low-angle boundaries are free of dislocations and represent blocks or polygons.

Later, convincing evidence of the fact that dislocations arrange themselves into flat subboundaries has been obtained metallographically by many workers. In these experiments, dislocations are revealed as rows of etch pits on surfaces normal to the slip direction [116, 117].

Thus, polygonization was initially understood as the process of redistribution of dislocations by slip and climb in heating of

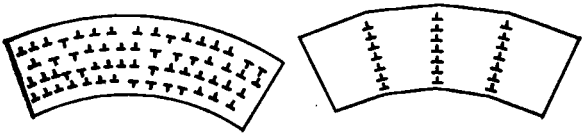

Fig. 34. Distribution of dislocations in a crystal deformed by bending; on the left: before polygonization; on the right: after polygonization

a crystal deformed by easy glide; the process breaks the crystal into polygons, i.e. dislocation-free regions separated from one another by dislocation (low-angle) boundaries normal to the primary slip planes. In the course of polygonization, the boundaries of polygons are formed anew; these boundaries (or their contours) do not exist in the as-deformed metal.

Later, the concept of polygonization has been given a broader meaning. It is described as a process of redistribution of dislocations resulting in the formation of subgrains in single crystals and polycrystals deformed to any degree (including deformation by multiple slip); the boundaries of these subgrains consist of networks including screw and edge dislocations, with adjacent polygons having a complex type of misorientation.

On heating of a deformed material with a cell structure (the most common case in practice), polygonization involves flattening of spatial dislocation pile-ups, or cell walls, and transformation of dislocation pile-ups (Fig. 35*a*) into flat subboundaries (Fig. 35*b*) consisting of dislocation arrays (Fig. 35*c*). In this process, cells are transformed into subgrains [118].

A typical feature of the process is that flattening of cell walls occurs through redistribution of dislocations, but in contrast to redistribution of dislocations in a bent crystal, screw dislocations move by cross slip and also by conservative slip and climb.

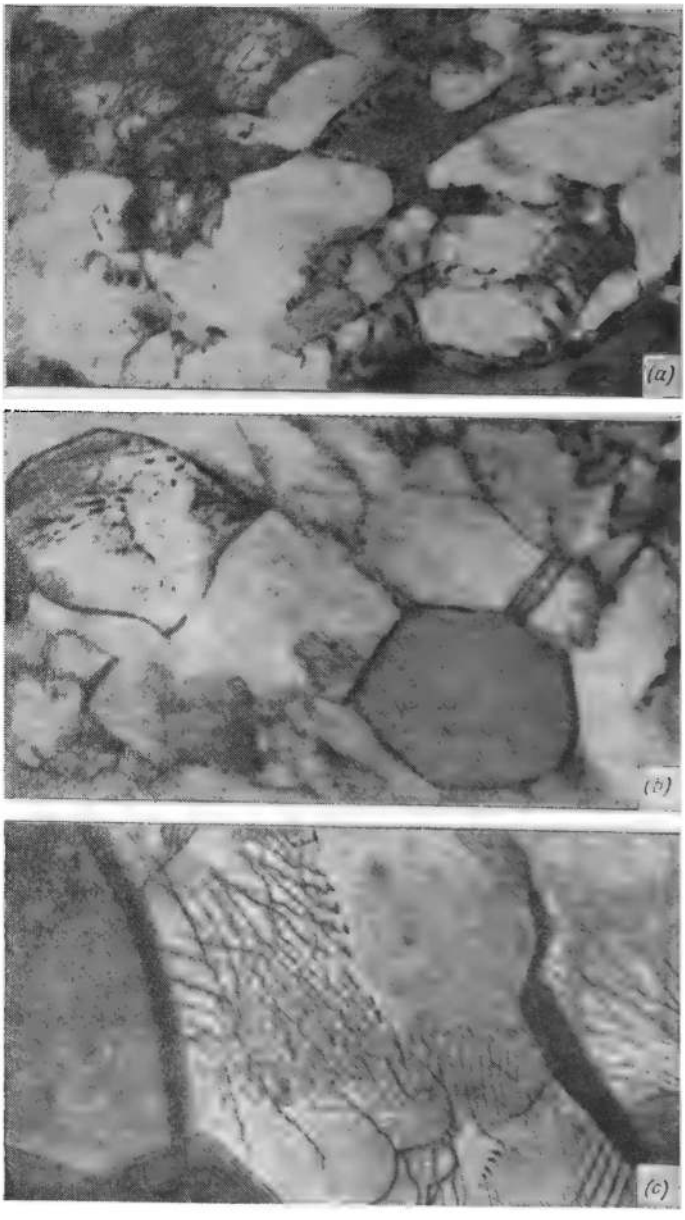

Fig. 35. Substructures in aluminium after cold rolling and prerecrystallization heating (*a*) deformed 70% at —50°C, ×12 000; (*b*), (*c*) heated in saltpetre at 270°C, ×12 000 and ×25 000, respectively

Another feature of polygonization in a heavily deformed metal is that the polygon boundaries being formed are outlined already in the as-deformed state by spatial dislocation arrays (networks)*.

One more feature of importance is that the boundaries formed by flattening have a large curvature and respectively a relatively high mobility.

The final feature is that the temperature of heating has practically no effect on polygonization of heavily deformed crystals (with a cell structure) and on the structure being formed. With increasing temperature, the process is only accelerated, but the paths of redistribution of dislocations vary only weakly with temperature. Lightly deformed crystals, however, behave in a different way.

By varying the temperature of heating, it is possible to vary the paths of redistribution of dislocations, and therefore the type of polygonal structure. At lower temperatures, dislocations move preferably by slip (simple or cross slip) and form stable boundaries of a low curvature. At higher temperatures, the role of diffusion climb increases, so that polygonal boundaries have a greater curvature and larger mobility.

The above-mentioned specifics of polygonization in deformed crystals (with or without a cell structure) have a number of consequences of practical importance. In the first place, there is a relation between polygonization and recrystallization. There has been a great deal of discussion on the problem of whether polygonization is a process competing with recrystallization or simply the initial stage of the latter, in other words, whether recrystallization nuclei form from subgrains produced by polygonization or in a different way. This problem is of practical and scientific importance, since (assuming that the two processes are competing) polygonization can be utilized in certain cases to prevent unwanted recrystallization.

If the ways of redistribution of dislocations in polygonization are the same as they are at the initial stages of recrystallization, then polygonization is apparently only an initial stage of recrystallization; otherwise, the two processes can be competing.

It follows from this approach that, if a cell structure has formed in a deformed material, then its cells will transform on heating into subgrains with a large curvature and polygonization

* In the specialist literature, there is a lot of confusion in the use of the term 'cell', 'subgrain', 'block', 'polygon', 'cell walls', and 'subboundaries'. For instance, Cahn [64] denotes polygons as cells, etc. Because of these ambiguities, it is sometimes difficult to analyse and interprete the results obtained by various authors. In this connection, it seems rational to classify these concepts on the basis of the structure of dislocation boundaries. The regions separated by spatial dislocation pile-ups (networks) should therefore be called cells and the networks that separate them, cell boundaries, or cell walls. The regions separated by flat boundaries should be called subgrains (or polygons, or blocks) and their flat boundaries, subboundaries.

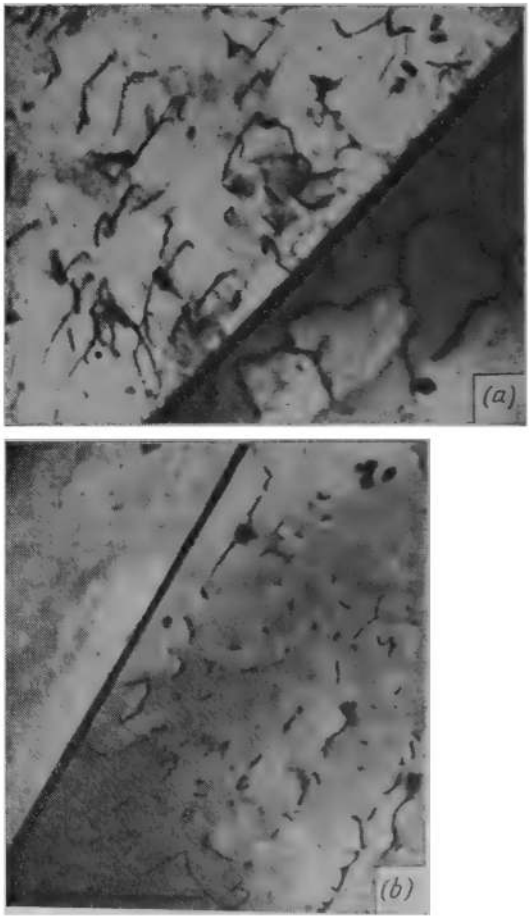

Fig. 36. Dislocation structure of
(*a*) after heating at 900°C; (*b*) stabilizing polygonization

will essentially be an initial stage of recrystallization. If, however, the material has been deformed within stage I work-hardening or at the beginning of stage II, i.e. before the formation of a cell structure, the result may be different depending on the temperature of heating. On heating to a relatively low temperature, dislocations are redistributed by climb and cross slip and the subgrains formed will have low-mobile boundaries of low curvature. This structure is unfavourable for the formation of recrystallization nuclei, and polygonization will compete with recrystallization. At higher temperatures of heating, conservative slip begins to play an important part and

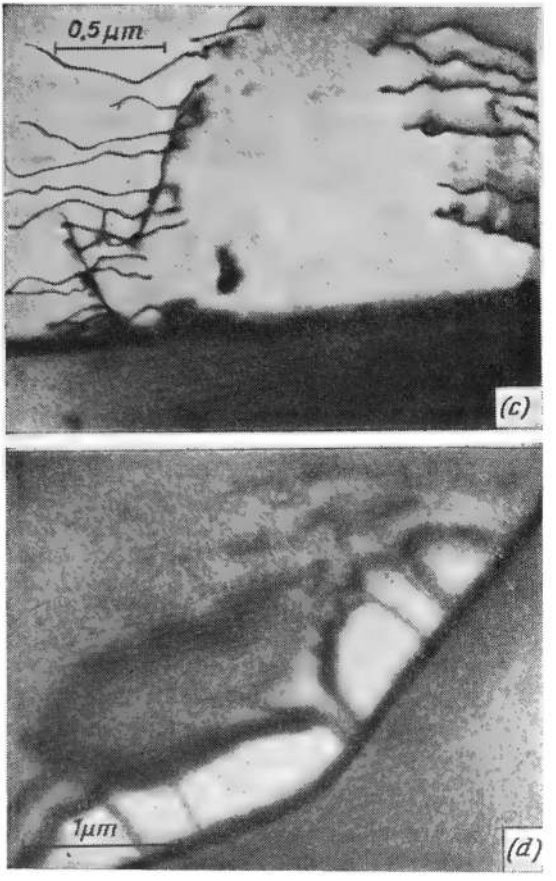

polycrystalline Ni-Cr alloy deformed 5%
at 1100°C; (c, d) formation of recrystallization nuclei

dislocations will be redistributed in a different manner. The formation of subboundaries will be preceded by the formation of spatial dislocation networks and their subsequent flattening. The new subboundaries formed in this way will not be strictly normal to the slip planes and will have a greater curvature and higher mobility. Migration of these boundaries will result in that some of the subgrains formed will become recrystallization nuclei. The validity of this assumption is confirmed by some published experimental data.

In his early work, J. Talbot [119] has shown that polygonization is a competing process to recrystallization. Heating of lightly deformed high-purity polycrystalline iron caused polygonization which

did not result in recrystallization even on prolonged annealing. In all later studies, the competing effect of polygonization was found to show up only in relatively lightly deformed materials.

In the earlier edition of this book [1, pp. 109-111] it was shown that heating of polycrystalline Ni-Cr at 900°C after 5-% deformation induced simple polygonization: dislocation subboundaries formed in planes normal to the slip planes and turned out to be very stable (Fig. 36*a* and *b*). Additional heating to 1050°C caused no recrystallization. On the other hand, direct heating after similar deformation, but immediately to 1100°C produced a different redistribution of dislocations. Initially, spatial networks formed and then subgrains of a large curvature (Fig. 36*c* and *d*). Part of these subgrains transformed into recrystallization nuclei through boundary migration.

In other portions, heating at 1100°C caused primary recrystallization of the type of strain-induced migration (see p. 148) which was due to non-uniform deformation of adjacent grains, and was realized by migration of local portions of the initial large-angle boundaries towards more heavily work-hardened grains (see Fig. 56).

A distinct cell structure was formed in specimens of the same nichrome on a heavier cold deformation. Recrystallization took place on heating to 700°C. Prior heating to a temperature below 700°C only slowed down somewhat the recrystallization that occurred at 700°C, probably owing to point-defect annihilation which always competes with recrystallization.

In view of the foregoing, it seems reasonable to differentiate polygonization depending on the structure forming on polygonization and introduce the concept of two types of polygonization: stabilizing polygonization and prerecrystallization polygonization, the two terms implying the following.

Stabilizing polygonization is a process of redistribution of dislocations on heating of a deformed material with a homogeneous dislocation structure formed through operation of a few number of slip systems; the process results in annihilation of unlike dislocations and formation of new stable subboundaries of a low curvature and low misorientation angles. The process is a competing one to recrystallization.

Prerecrystallizational polygonization is a process of redistribution of dislocations on heating of a deformed material with a cell structure, which results in partial annihilation of dislocations in dislocation pile-ups that form cell walls and in flattening of these pile-ups into flat subboundaries of a relatively high curvature and mobility. In this process, cells are transformed into subgrains with different misorientation relative to one another. The process is essentially an initial stage of recrystallization.

A practical conclusion is that polygonization, as a process that prevents or impedes recrystallization, can be effective only on

relatively light cold deformations. In cases of hot deformation, this is also valid for higher degrees of deformation, especially at lower deformation rates. In particular, stabilizing polygonization can sharply inhibit grain coarsening on heating after critical deformation, i.e. lower the first maximum of grain size in recrystallization diagrams.

Polygonization, however, fails to prevent the appearance of grain-size maxima on heavier deformations, which are associated with the processes of secondary recrystallization; the problem will be dealt with more thoroughly in Chs. 4 and 7.

If the redistribution of dislocations in polygonization occurs by different mechanisms, such as simple slip, cross slip and climb, the rate of the whole process is apparently limited by the slowest mechanism, dislocation climb, i.e. by the flow of vacancies to dislocations or appearance of new vacancies on dislocations. Vacancies can be attached most easily to dislocations on dislocation jogs. Therefore, polygonization is likely to occur more easily and quickly when there are more jogs on dislocations.

The thermodynamically equilibrium number of jogs per unit length of dislocation, n_j, and the density of vacancies, n_v, depend exponentially on temperature:

$$n_j = n_0 \exp(-Q_j/kT); \quad n_v = n_0 \exp(-Q_v/kT)$$

where n_0 is the number of atoms per unit length of dislocation or per unit volume, and Q_j and Q_v are the activation energies for the formation of a jog and a vacancy respectively.

The total activation energy of dislocation climb is

$$Q_t = Q_j + Q_v + Q_m$$

where Q_m is the activation energy of vacancy migration, and the sum $Q_m + Q_v$ is equal to the activation energy of self-diffusion.

The rate and activation energy of polygonization may vary appreciably depending on the initial state of the material and the conditions of the process. Let us explain this by the following examples.

1. Let polygonization occur under the conditions such that the concentration of jogs and vacancies is high, for instance, in heating of a plastically deformed metal with high internal stresses or in heating of a metal with simultaneous stressing (as in creep and fatigue tests). In the course of recovery, dislocations move under the action of these stresses across a dislocation 'forest'. This forms additionally a large number of jogs and vacancies, so that the rate of polygonization is only limited by the rate of vacancy migration. Practically, $Q_t = Q_m$. According to Mott [114], the rate of diffusion ascent of dislocations in this case is

$$v = \nu b (b^2F/kT) \exp(-Q_m/kT) = (D'/kT) Fb$$

where ν is the characteristic frequency of atomic oscillations, b is the Burgers vector, and D' is the effective coefficient of vacancy diffusion.

The process should occur very easily. Indeed, as has been shown in a number of works [120, 121], polygonization in specimens during creep and fatigue tests proceeds at lower temperatures than in heating after cold deformation.

2. Let polygonization take place at an elevated concentration of jogs. This is the case where heating of a deformed metal of high stacking fault energy γ_{sf}, i.e. low energy of formation of dislocation jogs, occurs under the conditions of low stresses in the metal and in the absence of vacancy supersaturation.

Here the rate of polygonization is limited by the rate of formation and migration of vacancies, i.e. by the rate of self-diffusion, and Q_t is practically equal to the sum $Q_v + Q_m$, so that polygonization begins at a higher temperature, when the equilibrium concentration of dislocation jogs on which vacancies can form is sufficiently high.

Gilman [122] has found that the activation energy of polygonization in bent single crystals of zinc greatly varies with the temperature interval. Above 525 K it turns out to be close to the activation energy of self-diffusion, but below 525 K it is almost three times as high, obviously due to the contribution of Q_j. Then the rate of climb in the upper temperature interval is

$$v = \nu b\,(b^2F/kT)\exp\{-[(Q_v+Q_m)/kT]\} = (D'b/kT)\,Fb$$

and in the lower interval

$$v = \nu b\,(b^2F/kT)\exp\{-[(Q_j + Q_v + Q_m)/kT]\} = (D/kT)\exp[-Q_j/kT)\,Fb]$$

where D is the coefficient of diffusion of vacancies.

3. Let polygonization take place in a lightly deformed metal having a low stacking fault energy. In this case the energy of jog formation increases and the equilibrium concentration of jogs decreases [97]. The result is that the rate of polygonization is determined by the amount of energy needed for the formation of jogs and vacancies and migration of the latter. The rate of the process will then be described by the last of the equations given above.

In addition to climb, the process of polygonization necessarily involves slip, including cross slip, which occurs more easily at higher γ_{sf}. Since cross slip is also a thermally activated process, it contributes somewhat to the dependence of polygonization rate on temperature.

The stacking fault energy is evidently responsible for the difference in susceptibility to polygonization in copper and in aluminium. Polygonization occurs very easily in aluminium and is hardly observed in copper.

Apart from the movement of individual dislocations, polygonization also includes the migration of dislocation groups (at the stage of formation of subboundaries) and migration of low-angle dislocation boundaries (at the stage of growth of subgrains). Details of these processes, especially of the migration of dislocation groups, are still not clear.

Hibbard and Dunn [111] investigated the mechanism of polygonization in Fe-Si single crystals from the initial stages to completion of the process. Single crystals were deformed by bending which raised the dislocation density from 2×10^6 cm^{-2} to 10^8 cm^{-2}. By the observations of the authors, in the first stage of polygonization due to shear and to subsequent climb of individual dislocations, short boundaries formed, which contained a few dislocations. These closely located boundaries then merged together through conjugate shear and climb of the whole dislocation complex and formed triple Y-junctions (Fig. 37). The free ends of boundaries surrounded by the elastic distortion field turned out to be most mobile. The Y-junction then moved parallel to a merging boundary until the other of the two

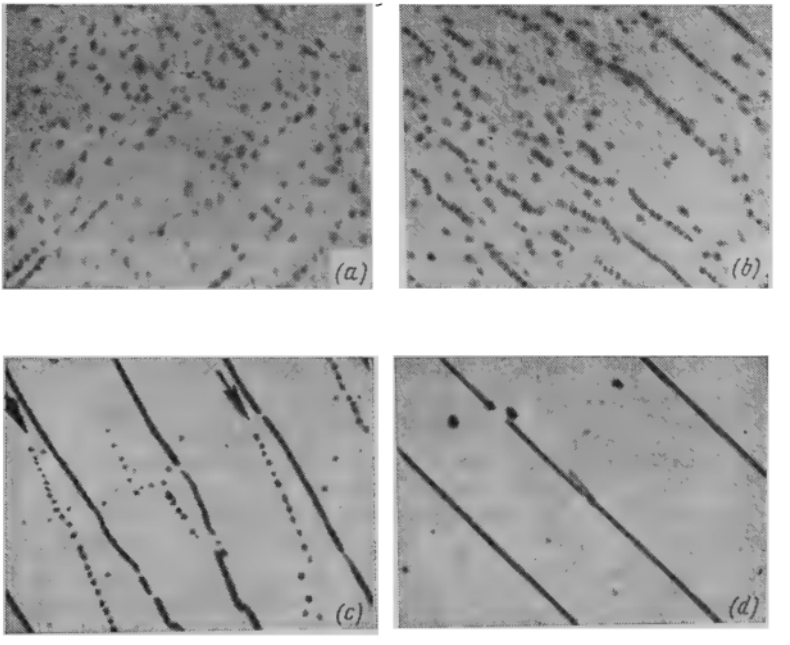

Fig. 37. Variations in the distribution of dislocations in the (211) plane of a bent Fe + Si single crystal during polygonizing annealing at various temperatures ($\tau = 1$ h), $\times 100$ [111]

(*a*) 700°C; (*b*) 750°C; (*c*) 925°C; (*d*) 1060°C

boundaries disappeared (see the arrows in Fig. 37). The process may occur in a few stages. The boundaries with a misorientation angle greater than the initial angle first have a very broken shape but then straighten owing to climb of individual dislocations within a boundary.

Further growth of the subgrains formed at the first stage of polygonization occurs under the effect of boundary tension and due to the difference in the volume energy of adjacent polygons. The boundaries of polygons migrate and take up new dislocations. The misorientation angles between subgrains usually increase, but the rate of misorientation growth may be quite different.

Crussard [123] observed subboundary migration during annealing of a deformed aluminium single crystal. In the course of migration, subgrains grew to an appreciable size (a few micrometres) without any noticeable change in their orientation relative to that of the original single crystal and of other subgrains. Crussard called this process in-situ recrystallization. Later studies have shown that the process occurs very often in metals.

In high-purity aluminium heated after deformation at room temperature, in-situ recrystallization was revealed when polygonization and primary recrystallization got separated by a large temperature interval. The first sharp reflections from large subgrains appeared on X-ray photographs after heating to 350°C. No changes occurred in X-ray photographs, however, up to 510°C, and only beginning from 520°C the number of reflections in X-ray photographs increased rapidly, indicating the actual start of primary recrystallization.

No such temperature interval was observed when the same aluminium was deformed at the temperature of liquid nitrogen. Redistribution of dislocations resulted directly in the formation of regions separated from the matrix by mobile large-angle boundaries.

The analysis of broadening of X-ray interference lines showed that the dislocation structures in aluminium deformed at room temperature were substantially different to those obtained at the liquid-nitrogen temperature. The metal passed through the stage of dynamic recovery in the former case and did not in the latter, which resulted in a more non-uniform deformation, a greater excess of like-sign dislocations in dislocation pile-ups (i.e., a greater misorientation), and a higher density of defects as a whole.

As has been noted in Ch. 2, deformed single crystals and large crystallites of polycrystalline silicon iron show deformation bands and microbands [71, 75] with different misorientation of adjacent cells. In deformation bands, the orientation of cells varies statistically from cell to cell, so that there is no accumulation of misorientation, whereas in microbands the misorientation of cells increases continuously relative to the original misorientation (see Fig. 23). It is clear that in the former case the growth of a subgrain by migrati-

on of its boundaries will cause no noticeable increase in misorientation, i.e. will be realized by in-situ recrystallization. In the latter case, however, the misorientation of a growing subgrain relative to the matrix will increase continuously and its boundaries will quickly transform into large-angle boundaries.

Evidently, in-situ recrystallization must generally occur where prior deformation gives no excess of like-sign dislocations. At a lower excess of like-sign dislocations, a polygon can grow to a larger size and remain within low-angle boundaries.

What are the conditions for obtaining a low excess of like-sign dislocations, or, in other words, what conditions are favourable for in-situ recrystallization? It can be concluded from the material in Ch. 2 that the required conditions are preferably easy slip and the absence of barriers for dislocation slip. In the first place, light degrees of deformation ensure these conditions. The degree of deformation should be lower in materials with more impeded cross slip. An increase in deformation temperature must also aid in in-situ recrystallization.

Polygonization slows down whenever in action are the factors that retard the diffusion of vacancies, diminish the number of active dislocation jogs, encourage the formation of Cottrell or Suzuki atmospheres around dislocations, decrease γ_{sf} and thus impede cross slip.

J. Talbot [119] and J. Montuelle [124] have shown that polygonization in iron and aluminium of various purity can be retarded very strongly by elastic interaction of impurity atoms and dislocations with the formation of Cottrell 'clouds'. According to their results given below, the temperature of the beginning of polygonization in these metals increases abruptly on increasing the content of impurities:

Iron:	
zone-melted [10×10^{-4}% C (by mass)]	200°C
electrolytic [150×10^{-4}% C (by mass)]	650°C
Armco iron (500×10^{-4}% C)	850°C
Aluminium:	
(99.999%)	450°C
(99.992%)	570°C
(99.95%)	620°C

Important information about the inhibiting effect of dislocation locking by impurities on polygonization and the upper temperature limit of this locking has been obtained by analysing the effect of temperature on the elastic limit σ_{el} of deformed materials [125]. The value of σ_{el} characterizes the shear resistance of mobile dislocations existed in a specimen before tests.

3.2. Recrystallization

Among the processes which can change the structure of deformed metals and alloys, primary recrystallization is a stage that immediately follows polygonization. Primary recrystallization reduces most radically the volume energy of deformed crystallites, principally by diminishing the number of structure defects caused by prior deformation, and restores the structure and properties the metal had before deformation.

The reduction of the volume energy of deformed material is the main driving force of primary recrystallization.

The essence of the process is that recrystallization nuclei form in the deformed matrix and grow at the expense of the matrix. These nuclei are matrix portions having an undistorted lattice; they are separated from the deformed matrix by large-angle boundaries. Primary recrystallization comes to an end as soon as the deformed matrix disappears.

On its further heating, the material in which primary recrystallization has taken place can go through the stages of grain growth and/or (under particular conditions) of secondary recrystallization. In these processes, the grains which have grown from primary recrystallization nuclei increase in size by consuming adjacent grains through the migration of their large-angle boundaries; the free energy of crystallites diminishes still further, though its rate of decrease is not so as in primary recrystallization.

The difference between grain growth and secondary recrystallization consists in that the former process occurs uniformly whereas the latter does not so since there are some grains which can grow exaggeratedly, i.e. at an appreciably higher speed than the others and thus serve as secondary 'nuclei'. This difference is clearly seen from the curves of grain size scatter, given in Fig. 38. The principal driving force of grain growth is the tendency to diminish the grain boundary energy by shortening the length of grain boundaries. This driving force can be active under the conditions of unbalanced tension of adjoining grain boundaries. Depending on the existing conditions, secondary recrystallization can be stimulated by various factors and correspondingly result in a gain in the grain-boundary, the volume or the surface energy.

Many authors define recrystallization as the process which begins with noticeable changes in the microstructure of a deformed metal during annealing. This definition cannot be generally applicable and relates only to primary recrystallization. Furthermore, it makes the essence of the process dependent on the method of observation. Indeed, it is well known now that the structural changes occurring in deformed metals and alloys can be quite different, depending on the driving force and the nature and mechanism of these changes.

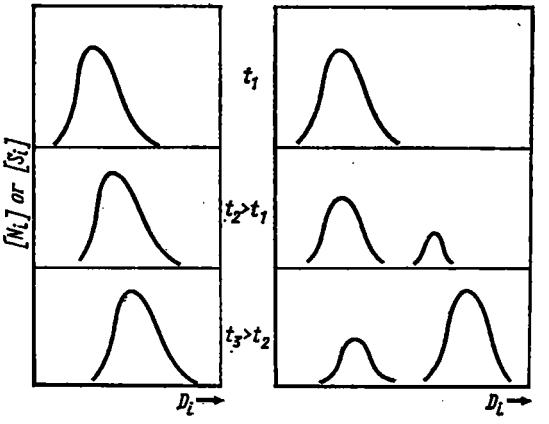

Fig. 38. Variations in grain size distribution during grain growth (on the left) and secondary recrystallization (on the right). N_i is the number of grains of a given size; S_i is the area occupied by grains of a given size

Therefore, the start of these changes may be detected at various stages of the process, depending on the resolution of the method applied.

The most important and specific feature of recrystallization at all its stages, which distinguishes it from other processes occurring in heated metals, is that this process is associated with the formation and motion of large-angle boundaries.

This allows us to define recrystallization as the process in which some grains of a given phase are replaced by the same-phase grains of a higher structural perfection and lower energy. The process occurs through the appearance and motion of large-angle boundaries (primary recrystallization) or only through the motion of these boundaries (grain growth and secondary recrystallization).

An advantage of this definition is that the phenomenon is independent of the method of observation. This definition also makes a distinct boundary between recrystallization and polygonization which is associated with the formation and motion of low-angle boundaries.

The rate of recrystallization at any of its stages is primarily determined by a gain in free energy ΔF. This gain serves as the driving force of the process. The gain in free energy related per mole is usually denoted as P_{dr}.

As has been noted earlier, a gain in volume energy, P_v, in grain-boundary energy, P_b, in surface energy, P_s, may serve as the driving force at various stages of the process, so that in the general case $P_{dr} = \Sigma P_i = P_v + P_b + P_s$.

Under real conditions, one should regard the factors which can lower the driving force of growth of nuclei (crystallites) and thus retard recrystallization. These include, in the first place, solute impurities and excess-phase particles. The force that retards boundary migration is denoted as P_{ret}.

All the stages of recrystallization except for the formation of recrystallization nuclei are realized through the migration of large-angle boundaries. The rate of boundary migration depends on P, which determines the direction of motion of a boundary, and also on the mobility M of the boundary proper, which is determined by the structure of the boundary.

Thus, the rate of boundary motion and therefore the rate of recrystallization can be written in the general form as $v = M\Sigma P_i$. For primary recrystallization, $v_{pr} = MP_v$; for grain growth. $v_{gr} = MP_b$; and for secondary recrystallization, $v_{sec} = MP_b$ or $v_{sec} = MP_v$, or $v_{sec} = MP_s$, depending on the particular conditions.

Regarding the retarding forces, the rate of boundary migration may be found as $v = M(P_{dr} - P_{ret})$.

3.2.1. Primary Recrystallization

Primary recrystallization is the process of formation and growth in a deformed matrix of new grains which are distortion-free and appreciably more perfect than the matrix proper and are separated from the latter by large-angle boundaries.

The driving force of primary recrystallization is the excess volume energy that has been accumulated during prior plastic deformation. This energy is almost fully localized in the stress fields which surround the dislocations formed by deformation.

In a rough approximation, this energy can be estimated as follows: the energy of a dislocation per unit length is Gb^2, where G is the shear modulus and b is the Burgers vector.

If ΔN_d is the difference of dislocation densities in the deformed material and in a recrystallization nucleus, the driving force is

$$P_{dr}^{pr} \approx k\Delta N_d G b^2$$

where k is a factor that takes account of the nature of distribution of dislocations (these may be singular, in pile-ups, in polygonal subboundaries, etc.); the value of k may range from 0.1 to 1.

Assuming* that $N_d = 10^{10}$ cm^{-2}, $G = 10^{12}$ dyne cm^{-1}, and $b = 3 \cdot 10^{-8}$ cm, we obtain $P_{dr}^{pr} \approx 10^7$ dyne cm^{-1}.

* The dislocation density in as-deformed metal sufficient to initiate recrystallization is $N_d \approx 10^{12}$ cm^{-2}. But recrystallization nuclei are in general not ideally perfect and can contain dislocations, which fact is confirmed by the existence of a substructure (subgrains) in recrystallized grains. For that reason, ΔN_d, which provides the driving force for primary recrystallization, is always less than 10^{12} cm^{-2}.

The mechanism of the process will be discussed in the next chapter. Here we shall only consider the principal effects of the process, which can be observed microscopically, and the laws which describe the rate of its development according to external factors (conditions of deformation and heating) and metal composition.

Primary recrystallization occurs during heating of a metal deformed to a certain degree. This amount of deformation, often called critical depends on the conditions of deformation and heating.

Recrystallization nuclei which appear during heating of a material deformed above the critical deformation are formed first of all in

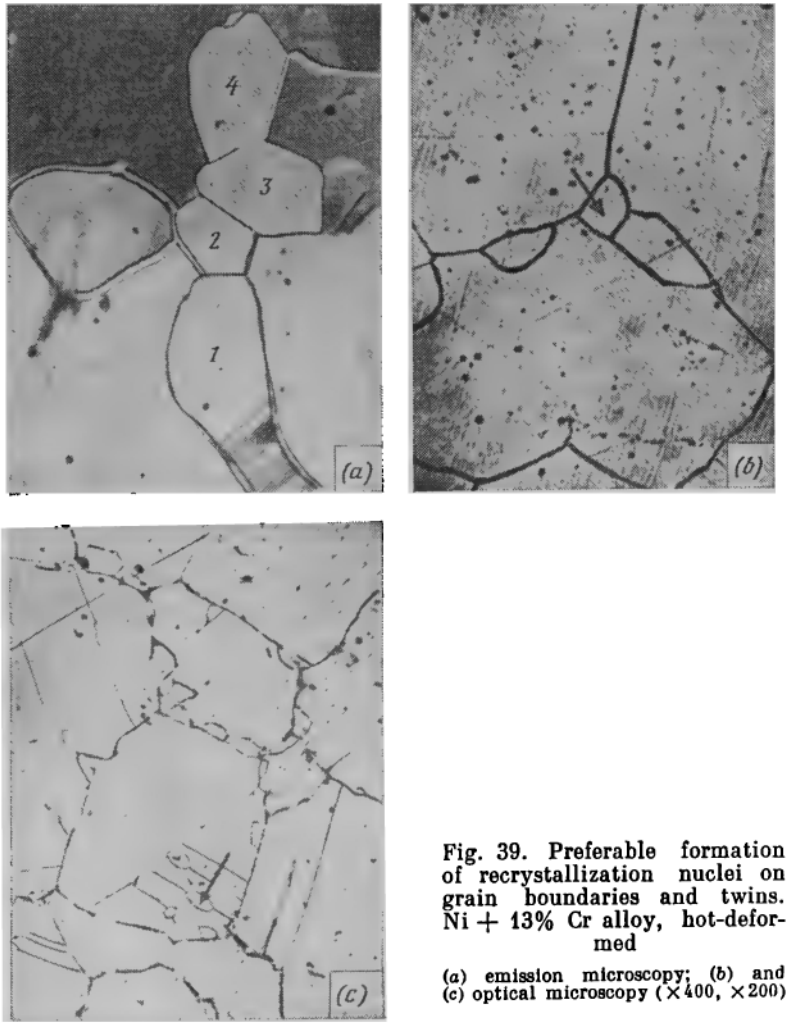

Fig. 39. Preferable formation of recrystallization nuclei on grain boundaries and twins. Ni + 13% Cr alloy, hot-deformed

(*a*) emission microscopy; (*b*) and (*c*) optical microscopy (×400, ×200)

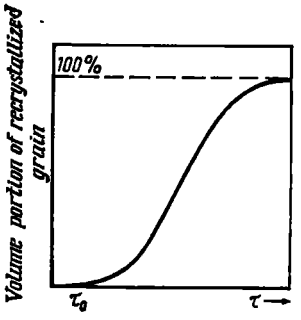

Fig. 40. Variation of primary recrystallization rate during isothermal heating (annealing)

portions of the crystal lattice that have been misoriented most severely and distorted by cold work (see Ch. 4), i.e. at grain boundaries (*1-4* in Fig. 39*a*) and their joints (Fig. 39*b*), in microbands (see Fig. 54); at twin boundaries (Fig. 39*c*), etc. New grains appear and grow after a definite incubation period τ_0 which is shorter at a higher temperature t of annealing and at a heavier prior deformation ε. The rate of primary recrystallization is characterized by the variation of the relative amount of recrystallized volume in the deformed matrix with the time of annealing τ. This relationship is described by a sygmoidal curve (Fig. 40) which is typical of primary (and also of secondary) recrystallization. Thus, in contrast to recovery, the rate of primary recrystallization is zero at the initial moment and then increases and passes through a maximum.

The recrystallized volume in the material increases during annealing owing to two processes: the nucleation and the growth of nuclei. The rate of these processes is described by two parameters: the rate of nucleation, N (the number of nuclei formed per unit time, $\Delta n/\Delta\tau$), and the rate of growth, G (an increase in the linear size of a nucleus per unit time, $\Delta D/\Delta\tau$).

The type of the structure that forms at the end of primary recrystallization is determined by the ratio of these two rates, N and G. The final size of grains is smaller at higher values of N and lower values of G. Both parameters and their ratio depend on a great number of factors. For an alloy of a particular composition, they primarily depend on the amount of cold deformation (and to a lesser degree, on the temperature of heating); in hot deformation, they depend both on the amount and rate of deformation.

The formal theory of the kinetics of recrystallization [48] is based on the analogy of this process to crystallization and on the fluctuation concepts of the mechanism of nucleation (see pp. 129-130).

The principal concepts and final conclusions of this theory agree with those proposed earlier by I. L. Mirkin and A. N. Kolmogorov [126] for the description of the rate of crystallization (recrystallization). They used the following assumptions:

1. The rate of nucleation is constant in time; nucleation sites are distributed statistically over the volume.
2. The rate of nucleation is time-independent and isotropic.
3. The rate of growth of nuclei diminishes in sites of their collision and remains invariable elsewhere.

Using these assumptions, the linear size D of a recrystallization nucleus in the period between its nucleation τ_0 and collision with other nuclei varies with the time τ of isothermal annealing by the equation $D = G(\tau - \tau_0)$.

Accordingly, for a specimen whose linear dimensions are appreciably greater in all three directions than the size of a recrystallized grain, the volume V of an individual recrystallized grain at moment τ will be $V = fG^3(\tau - \tau_0)^3$; for a sheet specimen whose thickness δ is smaller than the lateral size of new grains, $V = fG^2\delta(\tau - \tau_0)^2$; for a thin (unidimensional) wire specimen, $V = fG\delta^2(\tau - \tau_0)$, where f is the shape factor of a nucleus.

The volume of the recrystallized portion of a specimen (we shall further consider only the first case) with no collisions of nuclei in isothermal annealing will be

$$X' = fG^3 \int_0^\tau (\tau - \tau_0)^3 N \, d\tau \tag{2}$$

In the course of the process, the volume in which new recrystallization nuclei can appear diminishes continuously. In this connection, the ratio between X and X', i.e. between the recrystallized portion of a material in the general case and the portion in the absence of collisions can be written under certain assumptions as follows:

$$(dX/dX') = 1 - X \text{ or } dX' = dX/(1 - X)$$

Substitution into (2) gives

$$\int_0^X \frac{dX}{1-X} = -\ln(1-X) = fG^3 \cdot \int_0^\tau (\tau - \tau_0)^3 N \, d\tau$$

whence

$$X = 1 - \exp\left[-fG^3 \int_0^\tau (\tau - \tau_0)^3 N \, d\tau\right] \tag{3}$$

The final expression depends on the form of the relation between the rate of nucleation and the time of annealing, $N = f(\tau)$.

Assuming N to be time-independent, as has been done by W. A. Johnson and R. F. Mehl [48], expression (3) will take the form

$$X = 1 - \exp(1 - 0.25\, fG^3 N\tau^4) \tag{4}$$

which coincides with the expression proposed by A. N. Kolmogorov for structural recrystallization [126].

Later research has shown however that expression (4) gives unreliable results. A few other assumptions on the nature of the relationship $N = f(\tau)$ have then been proposed. Using statistical methods, J. K. Stanley and R. F. Mehl [48] have found that N increases shar-

ply with time τ and is connected with the latter by the relationship $N = a \exp(b\tau)$. The authors have concluded that the relationship can be determined most reliably only by experiments.

In contrast to this, M. Avrami [127] proceeded from the assumption that N should diminish with time in the course of isothermal annealing and found the following expression to describe the kinetics of isothermal recrystallization:

$$X = 1 - \exp(-B\tau^k) \tag{5}$$

where the coefficients B and k depend respectively on temperature and the nature of nucleation and growth. For tridimensional recrystallization, k should lie within $3 \leqslant k \leqslant 4$, for twodimensional cases, within $2 \leqslant k \leqslant 3$, and for unidimensional cases, within $2 \leqslant k \leqslant 1$*.

The above relationships have been verified experimentally by metallographic methods for pure aluminium, copper and silver under light deformations [48].

As has been found, the process is well described by the parameters N and G, though the relationship $N = f(\tau)$ may be quantitatively different.

Direct metallographic verification of N and G in strongly deformed materials is rather difficult to make. In a number of works (M. Cook and T. L. Richards and others), the kinetics of recrystallization in high-purity copper was analysed indirectly through the time variations in hardness at various temperatures (see Ch. 15).

Deeker and Harker [128] studied the kinetics of recrystallization in copper from variations in the intensity of X-ray reflections. Their results are described fairly by Avrami's formula. They also found that k depends on temperature and on the form of specimens.

The effect of the form of specimens on k seems to be very important. X-ray studies of the temperatures of the beginning and end of recrystallization in many nickel alloys have shown (Fig. 41) that there is a temperature interval within which recrystallization cannot be finished during a rather long time of annealing. This fact has been confirmed for a copper alloy (Cu + 10% Al) by the method of photoemission microscopy [129] which can reveal the structure at rather low temperatures and makes it possible to distinguish between recrystallized and deformed grains.

As has been found, at certain annealing temperatures recrystallization is arrested and does not develop further notwithstanding the fact that the deformed surrounding medium is partially retained.

---

* Avrami's relationship is now used most widely and applied not only to recrystallization and recovery, but also to decomposition of solid solutions. In the last case X is the part of the volume in which decomposition has come to its end (heterogeneous decomposition).

Therefore, Avrami's relationship is inapplicable for these temperatures.

These results as well as the known results of observations on the parallel occurrence of recovery and recrystallization, the orientational dependence of G (see Ch. 5), the role of collisions of nuclei, and the effect of dissolved and undissolved impurities on the kinetics of the process suggest that there is a principal difference between the kinetics of phase transformations and recrystallization. Thus, the assumptions underlying the relationships (2) and (4) are not generally applicable and can only be used in particular cases. In view of the large complexity of the phenomenon, universal relationships that would be applicable for proper description of the kinetics of recrystallization are yet not available. Further progress in the study of the kinetics of recrystallization is evidently improbable without more reliable concepts of the mechanism of the process that would take into account the diverse factors affecting the process.

Let us consider the available data on the effect of various factors on N and G.

The *amount of deformation* ε. Beginning from a critical deformation ε_{cr}, an increase in ε causes N and G and therefore the rate of recrystallization to grow [48]. For silicon ferrite, N rises more quickly than G; for aluminium, G increases noticeably with ε only in the range of light deformations. On increasing ε above 15%, G rises only feebly. This explains well the fact that the size of grains

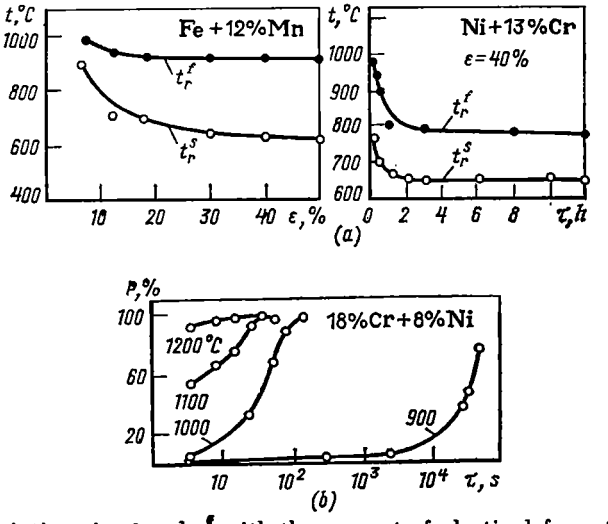

Fig. 41. Variations in t_r^s and t_r^f with the amount of plastic deformation and the time of annealing (*a*) and proportion of recrystallized volume versus the temperature of deformation (ε = 25%) and time of annealing (*b*) [366]

at the end of primary recrystallization is smaller with greater prior deformations. There are however some exceptions from this rule. In real alloys, coarse grain can sometimes form after moderate or heavy deformations. Such cases are usually associated with secondary recrystallization caused by superposition of the processes of precipitation and dissolution of disperse phases on recrystallization proper. It seems probable that, with heavy deformations, deformation texture can play an important part in certain cases.

If deformations are below the critical value (see later in the book), only polygonization takes place during heating. It diminishes the gradient of distortion between adjacent crystallites and thus impedes recrystallization. An elevated temperature of heating and also all the factors which increase the non-uniformity of deformation facilitate 'critical' recrystallization and enable the process to occur on lower strains.

Slower heating shifts ε_{cr} towards greater values, as also does prior point defect annihilation. The reverse is true at higher rates of heating. The causes and the mechanism of this phenomenon will be discussed in more detail in Ch. 7.

Heating temperature. The kinetics of primary recrystallization is markedly temperature dependent. For a given strain, the effect of annealing temperature on G is described by an exponential formula of the type of Arrhenius' equation:

$$G = G_0 \exp(-Q_G/RT)$$

This expression is valid for a temperature range in which G_0 and Q_G are constant. However, Q_G diminishes with increasing temperature [48], which additionally raises the rate of growth. The temperature dependence for N is similar to that for G given above. At the same temperatures, the values of Q_N and Q_G turn out to be equal to each other, except for the region of light deformations ($\varepsilon \approx 3\text{-}5\%$) where $Q_N > Q_G$. For that reason, the grain that forms at the end of primary recrystallization at conventional heating rates (furnace heating) becomes noticeably coarser with a further increase in temperature. The size of grain is more dependent on the amount of deformation. The effect of heating temperature is often masked in practice by the fact that heating is done relatively slowly. An increase in heating temperature involves a longer time during which the metal is held at high temperature. The laws are different (see later) in heating at very high rates (hundreds of degrees per second).

In most practical cases, recrystallization annealing lasts rather long, so that grain growth has time to occur all the same, at least partially. This is why the size of grain formed on recrystallization is larger at higher temperatures of annealing (see Fig. 136).

This is only valid for cases where no structural recrystallization occurs in an alloy with an increasse in temperature. If, however, an

increased temperature causes structural recrystallization, this results in grain refinement. The case may be illustrated by the recrystallization diagram for a low-carbon steel (see Fig. 137*a*). As can be seen from the diagram, the $\alpha \rightarrow \gamma$-transformation is associated with grain refinement.

When analysing the effect of annealing temperature on N and G and on the type of final structure under real conditions, one should consider the probable effect of accompanying processes, such as dissolution of disperse phases or, on the contrary, decomposition of the solid solution, formation of segregates, etc., since all these factors can affect N and G (see later).

The *time of annealing*. According to most researchers, the average rate of growth G, in contrast to N, is independent of annealing time until the growing recrystallization nuclei begin to collide. On the other hand, it has been established by direct observations on the growth of grains that the actual rate of growth does vary in time. The growth proceeds jumpwise, with maximal rates being roughly one order of magnitude greater than the average value. The causes are still unclear.

At relatively low supercritical deformations [48], the value of N increases sharply from 0 at $\tau = 0$ to N and then drops to zero. At heavier deformations the relation is more complicated.

When deformations slightly exceed the critical value, one should keep in mind the fact that two processes can occur in parallel, i.e. the growth of some of the initial grains and the formation and growth of recrystallization nuclei. The result is that the dependence of the average grain size on annealing time at various strains turns out to be rather complicated.

Prior recovery. The available results on the effect of recovery are controversial. Most workers are of the opinion that prior recovery increases somewhat the incubation period τ_0, diminishes N, and has only an insignificant effect on G. As a consequence, the size of grain after recrystallization becomes somewhat greater if prior recovery has previously taken place. On light deformations equal to or slightly above the critical value, prior recovery (more strictly, polygonization) gives an inverse effect, i.e. produces a finer recrystallized grain.

The effect of recovery, which is associated with polygonization, depends appreciably on the purity of metal, i.e. the presence of impurities. For instance, zone-refined iron deformed 10% undergoes polygonization at 250°C and does not recrystallize, whereas in iron with 0.03% C polygonization has no time to come to an end and gives way to recrystallization.

An explanation to this can evidently be found not only in the fact that interstitial impurities directly retard polygonization by impeding dislocation redistribution during heating, but also in

that they influence the type of the structure that forms on deformation by accelerating the onset of Stage 2 or 3 work-hardening. The problem will be analysed more thoroughly in the next chapter.

The effect of recovery not associated with polygonization (i.e. the effect of point defect annihilation) is probably due largely to a reduction in the concentration of vacancies. The following two cases can be conceived.

1. The excess vacancies formed by deformation disappear easily on heating owing to their high mobility and/or to a large number of sinks, so that the effect of recovery at common heating rates is not detected since the metal actually always undergoes recovery, even in cases where special low-temperature annealing is not employed.

2. The lifetime of vacancies is quite long, so that if no prior recovery has taken place, the vacancies participate in the formation of recrystallization nuclei for they facilitate dislocation climb and redistribution of dislocations. Where prior recovery is the case, excess vacancies have enough time to move to sinks and will not participate in the formation of recrystallization nuclei.

It is known that certain factors can prolong the lifetime of vacancies. For instance, a lower amount of deformation decreases the number of sinks and the number of excess vacancies proper. This factor is evidently responsible for the marked effect of recovery on recrystallization in bent silver crystals, as has been reported in [130]. Certain impurity atoms can also lock vacancies and retard their motion.

The controversial data on the effect of prior recovery may, in particular, result from neglect of the above considerations.

Rate of heating. A higher rate of heating increases N and therefore favours the formation of a finer structure by the end of primary recrystallization.

According to some authors [131, 132], during high-speed induction heating the recovery process has no time to take place before the onset of recrystallization. This facilitates the nucleation and growth of new grains. The result is that the effective activation energies Q_N and Q_G are appreciably lower than at common heating rates (for low-carbon steel, 12-17 kcal/g-atom against 50-55 kcal g-atom). The rate of nucleation, N_{ind}, and the rate of growth, G_{ind}, in induction heating attain their maxima already at the initial period of heating and largely exceed the respective values in common salt-bath heating and even more so the values typical of furnace heating, N_{fur} and G_{fur}; the N_{ind}/N_{fur} ratio is much greater than the G_{ind}/G_{fur} ratio, as is seen from the following data:

Heating temperature, °C	570	600	630	650
N_{ind}/N_{fur}	380	300	240	200
G_{ind}/G_{fu}	90	80	30	28

This fact explains why induction heating produces a finer recrystallized grain.

Recrystallization during induction heating (or any high-speed heating in general) is evidently accelerated by the vacancies which form at the initial recrystallization stage. The phenomenon is of a large interest and will be discussed in more detail in the next chapter.

Induction heating, which is usually employed without isothermal holding after reaching the heating temperature, also raises sharply the temperature of the beginning of recrystallization (t_r^s).

For instance, the temperature of the beginning of recrystallization in Armco iron deformed 60% is found to be (without isothermal holding at the specified temperature):

Furnace heating	500
Heating at a rate of 500°C/s	700
Heating at a rate of 650°C/s	900

Of significance here is the time during which the metal is held in the temperature region where the processes of recovery and recrystallization proceed most intensively.

The effect of heating rate can be utilized for grain refinement. For this, a short-time high-temperature high-speed heating which produces a large number of nuclei is combined with subsequent isothermal holding at a lower temperature. High-speed heating is especially effective with metals subjected to light and moderate deformations provided that the strain is non-uniform over the volume and the time of incubation period of the formation of recrystallization nuclei, τ_0, is sharply different in various portions. During slow heating, recrystallization nuclei will form much earlier in portions with the lowest values of τ_0 than elsewhere. In portions where τ_0 is the highest, recrystallization nuclei will not be realized at all, since the corresponding portions are consumed by the growing nuclei of low τ_0, or, if realized, will be much smaller in size. During high-speed heating, the metal is heated up to a high temperature before the realization of recrystallization nuclei of low τ_0, when the difference in τ_0 between various portions is still small. The result is that an appreciably larger number of potential nuclei are realized and the final structure is much finer and more uniform than on slow heating.

Deformation rate. This factor has a decisive effect in hot deformation. An increase in the rate of deformation has the same effect as an increase in the amount of deformation. In the case of cold deformation, the rate of deformation has a noticeable effect on the type of recrystallized structure only at low near-critical deformations. An increase in the deformation rate shifts ε_{cr} in the region of lower values.

In steels and Ni-Cr alloys, a higher rate of cold deformation results in a quicker completion of recrystallization and a coarser structure. The value of G increases, evidently owing to the fact that the deformation is less uniform.

In high-speed deformation (explosion forming), recrystallization occurs in a special manner.

The *size of original grain.* A finer original grain accelerates the process of primary recrystallization.

According to C. S. Barrett, aluminium with a fine original grain recrystallizes fully on annealing at 350°C 6.6 times as fast as coarse-grained aluminium. The size of original grain probably has a heavy effect on the rate of nucleation, N, since boundaries of initial grains are the sites where recrystallization nuclei form most early. This effect is especially pronounced in hot deformation.

Recent investigations have revealed that refinement of original grain accelerates recrystallization in a heavily deformed material also because it has an effect on the dislocation structure and on hardening produced by deformation. As given in Ch. 2, a decrease in grain size makes it possible to produce a stronger work-hardening effect (see Fig. 22) since multiple slip begins earlier and the dislocation structure in the volume of crystallites becomes more complicated.

Solute impurities. Solute impurities and alloying additions strongly influence the rate of primary recrystallization. The effect is especially marked in high-purity metals on addition of only thousandths or hundredths of an atomic per cent of impurities. In less pure metals, the effect of impurities is weaker and becomes negligible at concentrations of an order of one atomic per cent. Accordingly, the effect of impurities on recrystallization in high-alloyed solid solutions is not large.

For instance, addition of a few per cent of manganese, phosphorus and sulphur to carbonyl iron raises the temperature of recrystallization from 350° to 500°C. Aluminium of 99.99% purity recrystallizes roughly at 100°C, whereas high-purity aluminium (99.999%) recrystallizes at room temperature and that additionally refined by zone melting and deformed at the liquid-nitrogen temperature begins to recrystallize already at 223 K. Tellurium, if dissolved in copper in an amount of 10^{-5} atomic per cent, lowers the rate of recrystallization by a factor of 10^6.

Unfortunately, the available data on the separate effect of solute impurities and alloying elements on N and G are very scarce and mainly relate to the rate of growth of G.

An analysis of the kinetics of growth of recrystallization nuclei in pure nickel and in nickel alloyed with soluble elements such as aluminium, titanium, chromium, molybdenum, and niobium (1 atomic per cent) shows that minor additions can appreciably increase (almost two times) the activation energy of grain growth Q_G

(from 50 to 80-90 kcal/g-atom). Though the preexponential changes here too (from 10^{10} to 10^{15}-10^{17}), the retarding effect on grain growth is very large.

Lucke [22], Larikov [16] and other workers are inclined to explain the total effect of minor additions on the rate of recrystallization by their retarding effect on the growth of recrystallization nuclei. It is obvious, however, that the sharp increase of the incubation period is also associated with the retarded redistribution of dislocations during the formation of recrystallization nuclei, but not only with their growth to a visible size.

This is well confirmed by the results of separate determination of the activation energies of nucleation and grain growth in zone-refined aluminium [133]. The activation energies turned out to be different and equal respectively to 19.0 and 13.5 kcal/g-atom. Minor additions of copper ($3 \cdot 10^{-5}$ %) only slightly changed the rate of growth and sharply decreased the rate of nucleation.

The effect of various additions grows with an increase in the difference ΔR between the atomic radii of an addition and matrix and with a decrease in solubility of the addition in the base metal. These problems will be discussed in greater detail in Ch. 11.

Undissolved inclusions and heterogeneity of an alloy. The effect of undissolved particles present in a metal (alloy) may be different. On the one hand, these particles may serve as barriers on which dislocations are accumulated on deformation. This enhances the inhomogeneity of dislocation slip and distribution of dislocations, which in turn shortens the incubation period of the formation of recrystallization nuclei and increases N. On the other hand, these particles can inhibit boundary migration (of both low- and large-angle boundaries) and thus retard the growth of recrystallization nuclei, i.e. diminish G.

As particles grow in size and become less 'penetrable' to dislocations, N increases in magnitude. The value of G decreases with increased dispersion of particles and decreased distances between them. Particles of Al_2O_3 a few fractions of a micrometer in size, if present in a SAP alloy (Al + Al_2O_3) in an amount of 6-8% (by volume), retard primary recrystallization practically up to matrix fusion. The fact that age-hardening alloys possess the highest temperature level of recrystallization can also be attributed to the retarding effect of disperse particles on recrystallization. Disperse-phase particles precipitated from the solution during heating after deformation can lower sharply both N and G (see Ch. 12).

On the other hand, a relatively low content of carbide particles of the Fe_3C type in low-carbon steel lowers the temperature of the beginning of recrystallization by 50°C compared to that in Armco iron. Besides, non-uniform distribution of disperse particles, which dissolve on recrystallization annealing, can enhance sharply the

growth of individual grains and cause inequigranularity at the end of primary recrystallization and coarsening of the structure upon subsequent secondary recrystallization.

Undissolved impurities diminish grain size in recrystallization after critical deformation and also diminish the effect of deformation rate on grain size.

For instance, an increased rate of deformation in the region of ε_{cr} of killed steel containing Al_2O_3 particles had almost no effect on the grain size after annealing. In rimming steels of the same composition, this caused a sharp rise in grain size [134].

If heating upon deformation to ε_{cr} is attended with partial dissolution of disperse particles, the size of grains can greatly increase (see Ch. 9).

The temperature of the beginning of primary recrystallization, t_r^s (the temperature of appearance of recrystallization nuclei) is an important characteristic for many practical applications. It depends on the composition and purity of a metal and, as shown in Fig. 41, also on the strain ε and the time of annealing, τ.

With an increase in ε and τ, the temperature t_r^s diminishes first sharply and then more and more slowly and approaches asymptotically a threshold value (t_{th}^s).

The dependence of t_r^s on ε and τ can be expressed by functions of the type $t_r^s = a\varepsilon^{-b} + t_{th(\varepsilon)}^s$ and $t_r^s = c\tau^{-d} - t_{th(\tau)}^s$, where a, b, c, and d are constants whose values depend on the composition of a metal and the conditions of deformation and heating.

This is also true for the temperature of the end of primary recrystallization t_r^f, which as a rule diminishes less intensively with increasing ε and τ, especially in heavily alloyed metals and supersaturated solid solutions.

The above considerations are illustrated by the data given in Table 7 and Fig. 41.

TABLE 7. Values of t_r^s (Numerators) and t_r^f (Denominators) Depending on Deformation (During Annealing for 1 h)

Metal (alloy)	t_r^s and t_r^f, °C, at ε, %:					
	10	25	40	55	70	80
Fe *	700/850	600/660	580/630	560/580	540/570	520/560
Ni + Cr	720/825	675/800	650/800	640/740	—	—
XH77TIOP	950/1000	875/975	850/975	840/970	—	—

* 0.064 % Si, 0.46 % Mn, 0.02 % P, and 0.034 % S.

The minimal temperature of recrystallization (upon heavy deformation and long annealing) is usually taken as the temperature threshold of recrystallization, respectively t^s_{th} and t^f_{th}. The deformation ε_{th} above which t^s_r diminishes only insignificantly is usually 60 to 70%.

Similarly, the longest time of annealing, i.e. that after which there is almost no effect on t^s_r, is usually 1 to 3 hours.

It follows from the above that a slightly deformed metal may fail to recrystallize at all at any temperature up to the melting point.

The curves in Fig. 41 suggest another conclusion of importance. It turns out that for any material there is a temperature interval between t^s_r and t^f_r within which isothermal annealing, even if it lasts for a very long time (in the case considered, above 12 h at 700-800°C for H5Г12 alloy and at 700°C for Ni + 13% Cr alloy), does not result in complete primary recrystallization. After 2 or 3 hours of isothermal holding, when still not the whole volume is recrystallized, further development of recrystallization practically ceases.

Primary recrystallization involves certain texture changes. Primary recrystallization nuclei and the grains which grow from them are usually oriented regularly relative to the initial grains in the deformed matrix. The result is that a deformation texture changes to a recrystallization texture which either repeats the former or differs from it in a regular manner.

In some cases, however, the initial texture can disappear and change upon recrystallization to a texture with randomly oriented crystallites.

Undissolved particles present in a material before deformation can influence the texture in a material during its recrystallization heating. In metals and alloys undergoing phase transformations, heating of the deformed material above the temperature of phase transformation can also affect or even eliminate fully the texture. For illustration, refer to the data on elimination of deformation texture in uranium upon the $\alpha \rightarrow \beta$-transformation, see Ch. 1.

3.2.2. Grain Growth

This stage sets in after primary recrystallization, more strictly, as the growing recrystallization nuclei begin to collide with one another. Grain growth is defined as the growth of some new grains at the expense of other (also new) grains under the conditions at which individual grains cannot grow preferably and exaggeratedly; in this respect it differs from secondary recrystallization which is also called exaggerated grain growth. In the course of grain growth, the curve of grain size distribution does not change its form, but is shifted towards larger grain sizes (Fig. 38*c* and *d*)*.

* The curves of grain size distribution in plane sections of grains, even for grains of the same size, are always asymmetric, as in Fig. 38.

It is generally adopted that the principal thermodynamic driving force of grain growth is the trend to diminish the grain-boundary ('surface') energy and counterbalance the grain-boundary ('surface') tension of adjoining boundaries, which is realized through shortening of the boundaries as they migrate until an equilibrium configuration of grain boundaries is established. This is confirmed by the results of numerous studies related in particular to the specifics of grain boundary migration in grain growth.

The following facts have been established:

1. Boundaries move to the centres of their curvature.
2. Boundaries tend to move so as to have the angles at grain joints close to 120°. This occurs through preferable consumption of those grains which form sharper corners in triple joints. Boundaries migrate

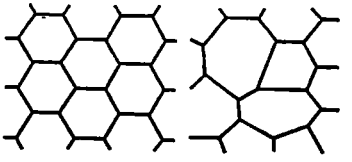

Fig. 42. A stable (on the left) and unstable (on the right) microstructure (schematic)

faster with an increased deviation of the angles from 120°. In a single-phase alloy, grain growth slows down sharply or practically ceases when most triple-joint angles become equal to 120° and any grain has six ribs in its section*, despite the fact that the absolute size of grains may be quite small. In the presence of disperse inclusions, grain growth can terminate even before the equilibrium angles have formed.

3. As the grains diminish in size the rate of their consumption by neighbours grows.

Thus, a stable structure is determined by the angles in triple joints and by the number of sides in grain sections, rather than by the absolute size of grains (Fig. 42).

Neglecting the deviation of the boundary configuration from the equilibrium, the driving force of grain growth should be equal to the grain boundary energy per unit volume.

Its maximum value can be estimated approximately as follows.

Let us assume that grains have the shape of a cube with the edge of length D. Then the grain boundary energy for a grain is $\gamma =$

* This rule (that equilibrium angles are equal to 120 and the number of ribs is six) relates only to substances possessing a weak anisotropy of grain-boundary energy (f.c.c., b.c.c. and c.p.h. substances) and does not apply to substances with a sharp anisotropy of grain-boundary energy (see Ch. 5).

$= (6D^2/2)\gamma_b = 3D^2\gamma_b$. The energy per unit volume, i.e. the unit grain-boundary energy is $\gamma_{b.u} = (3D^2/D^3)\gamma_b = 3\gamma_b/D$.

This quantity, however, represents only the potential driving force of grain growth, which can be realized if the following conditions are observed: adjacent grains differ from one another in size and the boundary tension in triple joints is not balanced (see Ch. 5).

If grains of a polycrystal are of the same size and the triple joints are balanced, the system will be in a quasistable state which can exist so long as it remains undisturbed and does not collapse due to fluctuations.

If adjacent grains are not equal in size, the difference in unit energies of grain boundaries will represent the driving force of the process of either grain growth proper or secondary recrystallization:

$$P_{dr}^{gg} = \Delta\gamma_{b.u} = 3\gamma_b (1/D_1 - 1/D_2) = 3\gamma_b \Delta D/D_1 D_2 \qquad (6)$$

So, the driving force grows with the difference in grain size (it should be emphasized that the product D_1D_2 decreases with an increased value of ΔD). This is also the case with a decrease in the absolute size of grains.

Let us now determine how P_{dr}^{gg} varies with grain size. We assume that the adjacent grains differ in size at most by a factor of three (otherwise, we have to deal with secondary recrystallization). Taking $\gamma_b = 500$ erg cm^{-2}, we can calculate the driving force of grain growth against the absolute grain size (Table 8).

TABLE 8. **Effect of Different Size of Adjacent Grains on P_{dr}^{gg}**

D_1, cm	D_2, cm	ΔD, cm	D_1D_2, cm^2	P_{dr}^{gg}, dyne cm^{-1}
$1\cdot10^{-4}$	$3\cdot10^{-4}$	$2\cdot10^{-4}$	$3\cdot10^{-8}$	10^7
$10\cdot10^{-4}$	$30\cdot10^{-4}$	$20\cdot10^{-4}$	$3\cdot10^{-6}$	10^6
$100\cdot10^{-4}$	$300\cdot10^{-4}$	$200\cdot10^{-4}$	$3\cdot10^{-4}$	10^5

Thus, only at a very small size of grains (of about one micrometre), which is commensurable with the size of primary recrystallization nuclei, the driving force of grain growth is of the same order of magnitude as it is in primary recrystallization.

With larger grains, such as they are at the end of grain growth, the driving force of the process is one or two orders of magnitude smaller than would be the case for primary recrystallization, even if the grains differ in size by a factor of three. If, however, the structure is more uniform, P_{dr}^{gg} is three or four orders of magnitude smaller with primary recrystallization.

Formula (6) is applicable also for determining the driving force of growth of subgrains during polygonization and in-situ recrystallization. Since the energy of low-angle boundaries γ_b^{la} is only a fraction (one-fourth to one-eighth) of the large-angle boundary energy, the driving force of the enlargement of subgrains during in-situ recrystallization must be substantially lower than the driving force of grain growth proper and still lower than that of primary recrystallization. The elementary act by which grain boundary migration is realized in the general case of grain growth is evidently similar to that which occurs in boundary self-diffusion, though it has some features of its own (see Ch. 5). Based on the energy needed to move an atom through the boundary from one grain to another, an analysis [48] of the rate of grain boundary motion, G, at the grain-boundary energy γ_b, gives a simplified relationship:

$$G = k\,(\gamma_b V/D)\,\exp\,(-Q_G/RT)$$

where V is the volume of 1 g-atom, D is the average size of grains, and k is a constant.

Substituting $dD/d\tau$ for G and integrating, we obtain

$$D^2 - D_0^2 = k \exp(-Q_G/RT)\,\gamma_b V \tau$$

where D_0 is the size of grains at the initial moment $\tau = 0$.

If $D_0 \ll D$, the dependence of grain size on temperature and time τ of heating is of the form

$$D = [k \exp(-Q_G/RT)\,\gamma_b V \tau]^{1/2}$$

The dependence of the average grain size $\bar{D}$ on the time of annealing is described quite fairly by an empiric equation $\bar{D} = c\tau^n$, where c and n are time-independent parameters; c strongly depends on temperature; the value of n is close to 0.5 for pure metals, but in most cases is less than 0.5 and may vary appreciably. The equation above is valid only for the values of D in the range $D_f \gg D \gg D_0$, where D_f is the final ultimate size of grains attainable at a given temperature and dependent on the number of insoluble inclusions. As noted above, grain growth in isothermal annealing often terminates soon after grains have reached a definite size which is characteristic of a given temperature. This size is larger at a higher temperature and in more pure metals (i.e. with a low content of inclusions).

Temperature. As with primary recrystallization, the dependence of the rate of grain growth on temperature is described by an analytical expression of the form

$$G = G_0 \exp(-Q_G/RT)$$

The activation energy of grain growth, Q_G, depends strongly on the purity of metal (alloy) and in some cases on the temperature interval of annealing [48]. For commercial-purity brass, for instan-

ce, $Q_G = 63$ kcal/g-atom in the interval from 500 to 750°C. At higher temperatures, G increases more quickly than would be expected for the indicated activation energy, i.e. the effective Q_G diminishes. For a brass of the same composition but of higher purity, $Q_G = 43$ kcal/g-atom and does not depend on the temperature interval.

These effects can be explained by the presence of disperse phases at grain boundaries and by their dissolution in certain temperature intervals. For this and other reasons and despite the apparent diffusion mechanism of grain boundary migration during grain growth, the effective value of Q_G often turns out to be different to the activation energy of boundary self-diffusion.

Solute impurities. Impurity atoms in a solid solution decrease the rate of boundary migration during grain growth much more sharply than they do in primary recrystallization. This is explained by the fact that, for the same resisting force, the driving force of grain growth is lower than that of primary recrystallization. An example of the effect of tellurium additions on the growth of nuclei in copper has been given earlier. An addition of 0.01% Mn to highest-purity aluminium decreases the boundary mobility by a factor of 10^{11} [22]. Minor additions of magnesium sharply diminish the rate of grain growth in aluminium, as also do additions of molybdenum and tantalum in nickel [135].

Disperse inclusions. Disperse particles of excess phases can sharply retard or even stop further grain growth. The parameters c and n in the expression $D = c\tau^n$ then diminish; at a definite concentration and dispersity of particles, n may even approach zero.

This effect is widely utilized in practice. It is well known, for instance, that thorium is added to tungsten to prevent unwanted grain growth; transformer steel is alloyed with nitride, sulphide and other particles to obtain a stable (110) [001] rib texture on annealing; in structural steels, the size of grains is stabilized by AlN nitride particles, etc.

The retarding effect of disperse particles on grain growth (migration of grain boundaries) is explained by the fact that their appearance on grain boundaries reduces the energy of the system.

Indeed, the surface area of an interface boundary (between a particle and matrix) is practically independent of whether the particles are positioned on grain boundaries or in the bulk of grains, whereas this affects appreciably the surface area of the intergranular boundaries of the matrix.

Assuming for simplicity that all particles are spherical and of the same radius r_0, we can find that they diminish the surface area of a boundary at a maximum by a value of πr_0^2 (see Fig. 43) [136]. The energy of the boundary will then diminish by $\pi r_0^2 \gamma_b$, where γ_b is the unit grain-boundary energy. It is clear that if the boundary

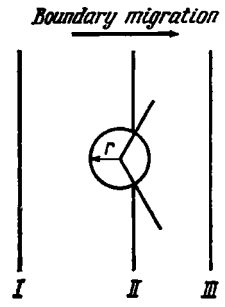

Fig. 43. Retardation of grain growth by disperse particles. A scheme of interaction of a boundary with particles (*I-III* are stages of the process)

moves through a distance r_0, its energy will be increased by that value.

Figure 43 shows the relative positions of a particle and a migrating boundary at three stages of the process. It is clear from the figure that the movement of the boundary from *I* to *II* will diminish the surface area of the boundary and therefore the boundary energy. The effect is greater at a higher unit energy of the boundary.

The detachment of the boundary from the particle (the passage from *II* to *III*) is energetically unfavourable, since it is equivalent to the return to position *I*. Therefore, the particle will impede boundary migration.

Given a particle concentration N_V per unit volume, the unit braking force per unit boundary area is $P_{br} = 2\pi r_0^2 \gamma_b N_V$, or, expressing it through the volume concentration of particles $f = 4\pi r_0^3 N_V/3$,

$$P_{br} = 3f\gamma_b/d \qquad (7)$$

where d is the particle diameter. The formula was first proposed by C. Zener [48].

It follows from Zener's formula that the retarding effect is greater at a higher volume concentration of inclusions, smaller size of particles and higher values of γ_b. P. A. Beck [153] notes that submicroscopic particles can retard boundary migration more effectively than larger particles which can be observed microscopically.

Taking into account the retarding effect of particles, the expression for boundary migration takes the form

$$v = M(P_{dr} - P_{br})$$

where P_{dr} is the driving force of boundary migration. This suggests a conclusion of high importance: the effect of disperse particles is greater at a lower driving force of the process.

It is clear that boundary migration is possible only when $P_{dr} > P_{br}$. Since P_{dr} is different at various stages of recrystallization (primary recrystallization and grain growth) and $P_{dr}^{pr} > P_{dr}^{gg}$, the values of P_{br} and therefore of f and d should be different at various stages of recrystallization for effective braking of boundary migration by particles.

To retard the enlargement of nuclei in primary recrystallization, which is stimulated by the different density of defects at a nucleus and in the deformed matrix, the volume concentration of undissolved particles should be greater and the particle size should be smal-

ler than when it is required to retard grain growth by boundary migration, which is stimulated only by the trend of the system to diminish its boundary energy.

For instance, 1% of particles 0.5 μm in diameter can form a braking force equal to 10^5 dyne cm^{-1} at a grain boundary of an energy of 500 erg/cm^2.

It follows from what has been stated earlier in this chapter that such particles cannot retard the enlargement of primary recrystallization nuclei, since the driving force of this process exceeds 10^7 dyne cm^{-1}, but can impede grain growth if the particle size is 10 μm or larger.

In the course of grain growth, as the size of grains increases and the difference in grain-boundary tension at grain joints decreases, the effect of disperse particles becomes more and more pronounced, with the result that grain growth ceases.

Proceeding from the above, Zener and Smith found that the maximum grain size in the matrix, D_{max}, which can be obtained if the matrix has disperse particles, is related to an average size d_{av} and volume concentration f through the expression

$$D_{max} \approx d/f$$

In Zener-Smith expression, the two parameters f and d, which determine the effectiveness of boundary migration, can be reduced to a generalized parameter, the distance between particles λ. The average values of $\bar{\lambda}$ and $\bar{d}$ and the volume concentration of particles, f, are related by the expression

$$\bar{\lambda} = (\bar{d}/2)\,(4\pi/3f)^{1/3} \qquad (8)$$

It has been shown in a number of recent research works (see Ch. 12) that there is a good correlation between $\bar{\lambda}$ and the conditions of recrystallization in heterophase alloys.

To retard grain growth, particles thus need not form a continuous barrier; it suffices to have the distances between them equal to about 50-100 interatomic spacings. In alloys where disperse particles can coagulate, this makes it possible to control the final grain size by prior treatment which can provide a desired degree of dispersity.

Note also that Zener-Smith's relation is based on the assumption that particles are distributed uniformly in the volume of matrix. For that reason, to initiate recrystallization in supersaturated solid solutions, where particles precipitate preferably on grain boundaries, the volume concentration of disperse particles should be smaller than would be found from equation (8).

The effect of disperse particles is encountered very often in practice: in heterophase alloys, in supersaturated solid solutions (if the temperature of annealing corresponds to the two-phase region), in al-

loys and steels deoxidized by aluminium, in open-air melted alloys, if these contain elements which can react readily with atmospheric gases and form stable compounds, in thin films, etc.

Disperse particles play an important part in the formation of recrystallization textures and in secondary recrystallization (see later in the book). Note finally that disperse particles can be partially responsible for retention of dislocations in recrystallized materials (see Ch. 4 and Fig. 64).

The *thickness of a specimen.* In specimens (thin wires, sheets, thin films) in which one or more dimensions are small, grain growth can be retarded or stopped altogether even in the absence of disperse

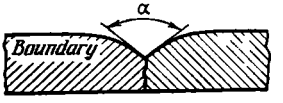

Fig. 44. Formation of a thermal etch pit at a grain boundary on the surface of a specimen (schematic)

inclusions as soon as grains grow to a size slightly exceeding the minimal dimension of a specimen. The phenomenon is called the 'thickness effect'.

P. Beck et al. [137, 138] were first to observe it in aluminium sheets (99.997% pure) of a thickness of 0.508 mm. In annealing below 600°C, the growth of grains obeyed well the equation $D = c\tau^n$ until D remained less than 0.35 mm. Further growth was retarded and stopped at $D = 0.60$ mm. Annealing at 650°C for 250 h did not increase the grain size above that value.

Mullins [139] proposed a sound explanation for the effect of thickness. During annealing, grooves are formed on the surface of a specimen along grain boundaries (Fig. 44) because of thermal evaporation which is facilitated by an increased boundary energy. The expansion angle of a groove, α, is equal to $(180 - 2\varphi)$, where φ is related to the grain boundary energy γ_b and surface energy σ_s (for the crystallographic planes parallel to the sheet surface) by an expression

$$\tan \varphi \approx (\gamma_b/2\sigma_s)$$

A groove fixes the boundary portion under the surface, since any movement of the boundary would increase the surface area of the groove and this in turn would form a braking force $P_{br}^{gr} = 2\gamma_b \times \tan \varphi/H = \gamma_b^2/H\delta_s$, where H is the thickness of sheet. Calculation gives that $P_{br}^{gr} \approx 10^4$ dyne cm^{-1} (at $\gamma_b = 0.5\sigma_s$ and $H \approx 0.1$ mm).

The relative maximum grain size at which the thickness effect appears can be found by equating P_{dr}^{gg} and P_{br}^{gr} 1. This gives $D_{max} \approx \approx$ (3 to 4) H for sheets and $D_{max} \approx 2H$ for wire, though actually

these values are somewhat lower in practice. The migration of a boundary in the depth of a specimen forms at a definite moment the conditions under which the detachment of the boundary from the groove is favourable energetically. This phenomenon can partially explain the jump-wise migration of grain boundaries, which is often observed on the surface of specimens. Based on work [138], we may suppose that the braking effect of thermal-etch grooves on grain growth diminishes with an increased size of grains. If the linear dimensions of grains in the surface of a sheet exceed 4-5 times the sheet thickness, grooves cease to retard grain growth, i.e. the thickness effect is not observed. Grain growth occurs due to a gain in the surface energy which now becomes sufficient to compensate for the enlarged surface area of a groove.

3.2.3. Secondary Recrystallization

Like grain growth, secondary recrystallization takes place when a material, in which primary recrystallization has occurred, is heated to higher temperature t_{sr}, but differs from the former in that the grains grow not uniformly, but exaggeratedly, i.e. a portion of grains which have preferable conditions for growth increase in their size at the expense of the main portion of grains whose growth is impeded for some reason or other.

The process is similar to primary recrystallization in that the growth of secondary 'nuclei' also begins after a definite incubation period and that the size of the growing grains (before collisions begin) is linearly dependent on the time of heating. For that reason the time relationship for the portion of the volume that has undergone secondary recrystallizaton is also described by a sygmoidal curve (see Fig. 40).

A feature typical of secondary recrystallization only is a peculiar pattern of grain size distribution and its variation in the process. This peculiarity shows up clearer if, instead of a curve describing the dependence of the number of grains of a given size, N_i, on their size D_i, we construct a curve relating the area S_i occupied by grains to their size D_i. Distribution curves $S_i = f(D_i)$ and their variations in the course of secondary recrystallization are shown in Fig. 38. The curves are characterized by two maxima spaced widely apart, i.e. by the existence of two groups of grains of sharply different dimensions. In the course of the process, this difference increases since the size of the growing grains and the area occupied by them increase continuously, whereas the size of the other grains remains unchanged and the area occupied by them diminishes owing to that they are consumed by the growing ones.

It follows from the diagram that secondary recrystallization inevitably involves inequigranularity which can disappear only on completion of the process. In view of this, local inequigranularity can be regarded as a typical feature of unfinished secondary recrystallization.

In the inequigranular structure, the largest grains (not numerous) are those which have formed in primary recrystallization; for some reason or another they have had the advantage in growth over the main mass of grains and thus have become centres of secondary recrystallization. This can occur for the following reasons:

(1) if some grains have a lower volume energy (lower concentration of defects) than other grains;

(2) if their size is larger than that of the remaining mass of grains;

(3) if their crystal orientation is different to that of the main mass of grains;

(4) if the crystal faces of these grains on the surface of a sheet or wire have a lower surface energy (at the metal-atmosphere boundary).

Accordingly, the driving force of secondary recrystallization is a change in the free (volume, grain-boundary or surface) energy.

At the end of primary recrystallization, grains may have different volume energy for a number of reasons. For instance, primary recrystallization nuclei formed through coalescence of subgrains may be less perfect than those formed through sub-boundary migration. Grains containing more disperse particles may have a higher dislocation density. If a material after primary recrystallization is subjected to light deformation or weak structural work-hardening, its various grains will usually be deformed unevenly. In heating, less strongly deformed grains will grow at the expense of those which have been distorted more heavily, resulting in coarsening of the structure (the first maximum of grain size, see Ch.7). Recrystallization after a critical amount of deformation can therefore be regarded conditionally as a particular case of secondary recrystallization due to a difference in the volume energy of various original grains.

The difference in grain size and thus in grain-boundary energy may be due to various causes. One of the probable causes is a non-uniform distribution and therefore a non-uniform dissolution of disperse particles. Owing to the latter fact, grain boundaries are freed and can migrate more quickly, so that the grain-boundary energy diminishes. Naturally, larger grains appear in less contaminated portions (Fig. 45). In this process, the texture of primary recrystallization usually disappears.

Another probable cause is a favourable crystal orientation of a growing grain relative to the surrounding grains of the textured matrix. In that case, the grain boundary mobility becomes non-monotonic and dependent on the angle of boundary misorientation

(see Chs. 5 and 10). It is then clear that, if a textured matrix has 'inclusions' of a certain number of differently oriented grains, the grains with most mobile boundaries will grow at the highest rate and will soon attain a size appreciably greater than that of the grains with a different orientation.

Secondary recrystallization caused by the dependence of boundary mobility on orientation can in some cases result in the formation of more distinct textures than are the textures of primary recrystallization.

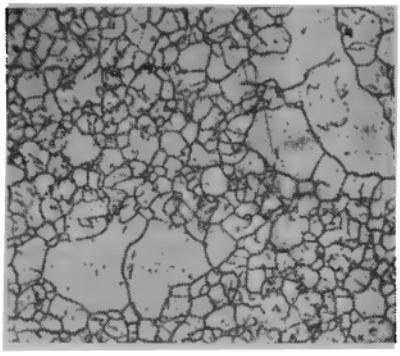

Fig. 45. Secondary recrystallization nuclei formed as a result of non-uniform distribution and dissolution of disperse carbonitride particles. A nickel-chrome alloy with an elevated content of carbon and nitrogen

The presence of sharply differing grains in the recrystallized matrix determines some essential peculiarities of their growth. With all grains being approximately of the same size (in grain growth), the direction of migration is determined only by the disbalance of grain-boundary energy at grain joints. Less balanced joints migrate more quickly.

If grains are sharply different in size (in secondary recrystallization), the direction of migration is determined by the difference ΔP or $\Delta\gamma_b$. The rate of migration of a boundary will be greater in the direction of smaller grains. This explains well the above-mentioned fact that the rate of consumption of small grains increases as the anomalously large centres of secondary recrystallization grow in size.

Calculation of the driving force of secondary recrystallization (assuming that secondary recrystallization centres are 10 times the size of other grains and $\gamma_b = 500$ erg cm^{-2}) gives values close to the driving force of primary recrystallization:

D_1, cm	D_2, cm	ΔD, cm	$D_1 D_2$, cm^2	P_{dr}^{sr}
$1 \cdot 10^{-4}$	$10 \cdot 10^{-4}$	$9 \cdot 10^{-4}$	$1 \cdot 10^{-7}$	$1.4 \cdot 10^{7}$
$10 \cdot 10^{-4}$	$100 \cdot 10^{-4}$	$9 \cdot 10^{-3}$	$1 \cdot 10^{-5}$	$1.4 \cdot 10^{6}$

Thus, at least two conditions are needed for secondary recrystallization to occur: (1) the enlargement of the main mass of grains formed at the end of either primary recrystallization or the grain growth process must be impeded (to obtain the so-called stable matrix) at temperatures below t_{sr} and (2), at temperatures above t_{sr}, some grains must grow at an appreciably higher rate than the remaining mass.

Secondary recrystallization textures in thin sheets can also form due to a difference in surface energy of the grain faces parallel to the sheet surface.

Under particular conditions the surface energy can play a greater part in the process of growth than the grain-boundary energy. It is clear that the role of the surface energy is more prevailing at a smaller thickness of the metal.

The driving force of secondary recrystallization, P_{dr}^{sr}, due to the surface energy must be determined by the difference in the surface energies of adjacent grains, $\Delta\sigma_s$. If large grains have grown to the thickness H of a sheet, they come to the surface of sheet on its both sides and then $P_s = 2\Delta\sigma_s/H$.

TABLE 9. Theoretical Values of σ_s (*hkl*) for Selected Metals [134]

Metal	Lattice type	σ_s, erg cm^{-2}, for planes			Metal	Lattice type	σ_s, erg cm^{-2}, for planes		
		(100)	(110)	(111)			(100)	(110)	(111)
Cr	b.c.c.	1770	1550	1650	Ag	f.c.c.	800	980	690
Fe	b.c.c.	1600	1300	1540	Co	f.c.c.	1500	1700	1300
Cu	f.c.c.	1350	1600	1200	Ni	f.c.c.	1600	1800	1450

Table 9 gives calculated values of σ_s for various atomic planes of a number of metals. Taking $\Delta\sigma_s = 150$ erg cm^2 and the sheet thickness 100 and 1000 μm, the value of P_s is respectively equal to $3 \cdot 10^4$ and $3 \cdot 10^3$ dyne cm^{-1}.

As follows from the table, the general relationship reduces qualitatively to that the atomic planes spaced the largest distance apart possess the least values of surface energy. These are planes of the maximum interplane spacing [(110) in b.c.c. lattices and (111) in f.c.c. ones].

The surface energy apparently plays the decisive part in the formation of cubic textures (see Ch. 10).

It has been found recently that exaggerated growth of individual grains under the effect of the surface energy begins not immediately after primary recrystallization, but after secondary recrystallization that has been stimulated by some other factors. Walter and Dunn [140] and Coulomb and Lacomb [141] proposed to call this phenomenon '*ternary recrystallization*'. The term ternary recrystallization is sometimes used erroneously to describe all cases of grain growth stimulated by surface energy.

3.3. Variations of Metal Properties During Recovery and Recrystallization

A deformed material changes its structure on heating so that it acquires the structure it had in the undeformed state and thereby regains its original properties. This by no means sets the limits on changes in the properties of the deformed material. Even at the end of primary recrystallization, and what is more, on completion of secondary recrystallization, it is possible to form a structure substantially different to the original one as regards the size of grains and texture. Accordingly, the properties of a recrystallized material will differ substantially from those the material had prior to deformation.

The properties and structure of a material can be restored in a number of stages. In some cases, a particular property can be brought to its original state long before the full restoration of the structure, i.e. at the stage of recovery or incomplete primary recrystallization.

Firstly, this is associated with the fact that various defects can affect differently a particular property. Secondly, the mobility of these defects may be different. For instance, the mobility of vacancies is much greater than that of dislocations. The slip mobility of dislocations in a material that has been subjected only to slight slip is appreciably higher than in a material where multiple turbulent slip has taken place. Cross slip occurs more easily in materials of a high stacking fault energy, etc.

The higher is the mechanical and thermal stability of dislocations and dislocation pile-ups formed by deformation, the less easily they are redistributed at the recovery stage.

Let us discuss some laws governing the restoration and variations of the properties of cold-worked materials during annealing.

Single crystals exhibit an especially marked dependence of the original dislocation structure on the structural changes in heating and softening. In cases where the deformation is uniform and is effected by easy slip, recovery takes place in a crystal and its properties are restored completely without the onset of recrystallization. This occurs during heating of deformed hexagonal single crystals (Zn, Cd), in which the stage of easy slip (on basal planes) is strongly extended over the deformation stages.

A similar result was obtained by H. Hu [74] who analysed the variations of structure and properties in differently oriented silicon-iron single crystals. The metal was rolled parallel to the (001) plane, but some crystals became oriented parallel to the rolling directions with their [110] direction, and others with their [100] direction. With the (001) [110] orientation, the deformation was uniform, while the (001) [100] orientation gave sharply misoriented deformation bands (see Ch. 2).

The density of metal proved to be most sensitive to heating. Its intensive rise was noticed already on heating to 100-150°C. The density continued to rise, though less intensively, up to 800°C. The rise in density up to 150-200°C was evidently due to the disappearance of point defects, since narrowing of X-ray lines and redistribution of dislocations began approximately from 200°C. In (001) [110] crystals, subgrains began to form at 500-600°C and their growth continued up to 800°C. The hardness began to drop from 400°C and was restored fully (without recrystallization) at 800°C.

In (001) [100] crystals, recrystallization started at 600°C, in the course of which the hardness dropped (on heating up to 800°C) to the values found in (001) [110] crystals.

Of special interest are some works in which the evolution of the latent energy of cold work was studied by various calorimetric methods [94, 142, 143, etc.]. The first quantitative analysis of the thermal effect during heating of various torsion-deformed metals and alloys was reported by S. Sato [158].

All the metals (copper, silver, iron, low-carbon steel), with the sole exception of aluminium, showed only one peak on the heating temperature-energy curves. The author attributed this peak to the onset of recrystallization.

In aluminium, the evolution of energy occurs in a wide range from room temperature to 550°C, i.e. during recovery and recrystallization.

L. M. Clarebrough et al. [74] tested copper specimens of various purity (from 99.999 to 99.6%) deformed by tension and torsion at room temperature to various degrees and obtained the results which confirm Sato's conclusion. According to their results, the predominant portion of the energy is liberated within a temperature range characteristic of the beginning of recrystallization only in heavily deformed and in less pure materials. In this temperature interval, the dislocation density diminishes sharply, which is confirmed by direct electron-microscopic observations, and the hardness, density and other physical properties are restored. In lightly deformed and in less pure metals (where the beginning of recrystallization is shifted to higher temperatures), a small portion of the energy (which grows with a decrease in deformation) is evolved before recrystallization.

Given below are the data on the total latent energy of cold work (E_{cw}) and the share of its energy (E_r/E_{cw}) evolved on recovery of copper deformed to various degrees [74]:

Elongation, %	10.8	17.5	30.5	39.5
E_{cw}, cal/g-atom	2.52	3.62	5.00	6.21
E_r/E_{cw}	0.10	0.05	0.05	0.03

The kinetics of energy evolution at these two stages is different and has specific features typical respectively of recovery and recrystallization. The rate of energy evolution at the recovery stage is

first at its maximum and then decreases in time. In recrystallization, the rate is initially low, then rises to its maximum, following which it begins to drop. However, no reliable data on the essence of the processes in this prerecrystallization temperature interval have been obtained by direct structural methods.

As is shown for copper and nickel (Fig. 46), the part of the energy evolved at the recovery stage increases sharply with decreasing purity of a metal. For instance, the E_r/E_{cw} ratio is equal to 0.05 for 99.988%-pure copper, 0.3 for 99.967% copper, and even 0.6 for copper with 0.35% As, i.e. in the last case the energy evolved in recovery is greater than that in recrystallization.

Impurities in copper raise substantially the temperature of the beginning of recrystallization. It might be supposed that the impurities are responsible for a rise in E_r/E_{cw} ratio because they extend the temperature interval of recovery. However, the evolution of energy in recovery of less pure metals is often observed at temperatures below the temperature of the beginning of recrystallization of a purer metal.

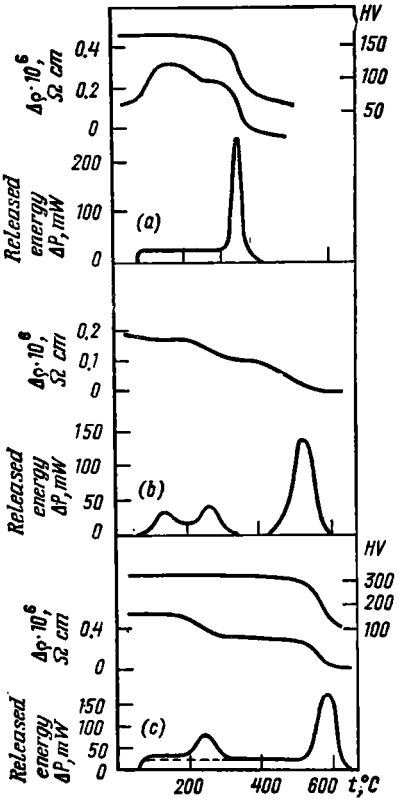

Fig. 46. Resistivity, hardness, and thermal effect versus the temperature of heating of various metals deformed by torsion

(*a*) copper; (*b*) iron; (*c*) aluminium

Clarebrough et al. explain these interesting facts as follows. Deformation of metal forms small groups (flat pile-ups) of high-energy dislocations, as well as complex dislocation aggregates. The possible existence of such groups of 3-4 dislocations in spatial aggregates that form sub-boundaries is noted by J. E. Bailey and P. B. Hirsch. In pure metals, such groups relax at room temperature immediately after deformation or in a very short time interval. In less pure metals, dislocations are locked by impurity atoms and relaxation takes place only in heating. If locking is not very firm, small high-energy dislocation pile-ups are redistributed before recrystallization, i.e. at the recovery stage.

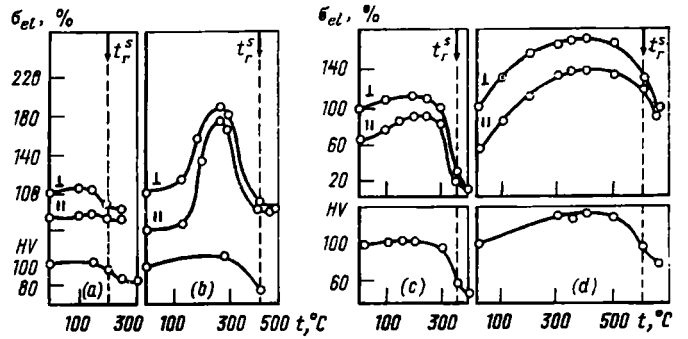

Fig. 47. Effect of annealing temperature on σ_{el} and HV of cold-rolled alloys of f.c.c. metals: (*a*) copper, (*b*) bronze, (*c*) nickel, (*d*) nichrome. Specimens were cut across ($\perp$) and along ($\parallel$) rolling direction. 100% of σ_{el} for (*a*), (*b*), (*c*) and (*d*) is respectively 260, 320, 430 and 710 mm/m². 100% of Vickers hardness is respectively 740, 2600, 2110 and 3230 mm/m²

Direct electron-microscopic results in support of relaxation of dislocation groups are still unavailable, but certain indirect data confirm this supposition.

Hibbard and Dunn [111] observed redistribution of dislocations at the recovery stage in silicon iron and interpreted the phenomenon as the movement of dislocations on their slip planes. They assume that this redistribution is one of the probable causes for an increase in hardness which is sometimes observed upon prerecrystallization annealing.

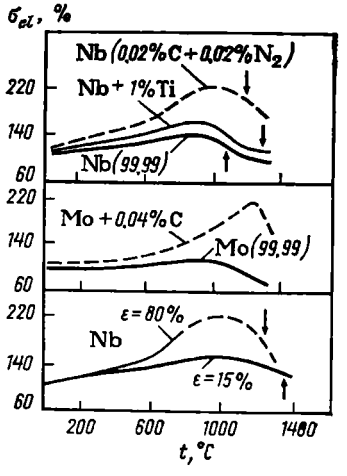

Fig. 48. Effect of annealing temperature on σ_{el} of cold-rolled b.c.c. metals. Arrows indicate temperatures of the beginning of recrystallization

As found in a number of works [125, 143], heating of certain deformed metals and alloys at temperatures below the recrystallization temperature results in a noticeable rise of the elastic limit (resistance to light plastic deformations) and in a lower anisotropy of this characteristic.

Some workers studied the effect of the temperature of preliminary heating on the elastic limit σ_{el} of a number of metals (Al, Cu, Ni, Fe, Nb, Mo, Zr, and Ti) and alloys (Ni + 20% Cr, Cu + 15% Al) of various purity. The results are given in Figs. 47 and 48. As is seen, the gain in σ_{el} is 5 to 25% in copper and nickel (98.99% pure) and up to 200-300% in bronze, brass and nichrome.

In all the materials tested, except for aluminium, σ_{el} first rises to a maximum at a definite temperature (see Fig. 47) which is always lower than the recrystallization temperature, and then decreases and returns to the initial value at t_r^s.

The gain in σ_{el} is greater in less pure metals and grows with the degree of deformation. The width of X-ray lines diminishes only insignificantly. The intensity of texture maxima and the texture scatter change somewhat.

In b.c.c. metals with a low solubility interstitial impurities (Nb, Mo), the gain in σ_{el} is especially large on addition of carbon (Fig. 48). At 0.02-0.04% C, σ_{el} reaches a maximum, which is roughly twice as high as in pure metals. Addition of another impurity inhibiting carbon diffusion (such as titanium or niobium) suppresses the rise in σ_{el}, but raises the temperature at which σ_{el} attains its maximum.

The elastic limit σ_{el} increases even more in Ni + 20% Cr and Cu + 15% Al alloys in which short-range ordering occurs on heating. This phenomenon is undoubtedly of large practical importance.

By modern views, this effect arises from resistance to dislocation movement (due to the friction force of the lattice); this resistance grows with the difference in the atomic diameters, valencies and elastic properties between the impurity and the solvent and depends on the degree of ordering.

An increase in σ_{el} on prerecrystallization heating and a decrease in its anisotropy in pure copper and nickel are apparently due to nothing else than redistribution and partial annihilation of mobile dislocations and locking of the remaining dislocations in more stable configurations (i.e. due to polygonization).

The rise of σ_{el} in alloys is evidently determined mainly by the formation of segregates on dislocations, so that the effectiveness of dislocation locking turns out to be even higher than in the above case.

J. Talbot describes the effect of polygonization on the form of the stress-strain curve for pure electrolytic iron containing $6 \cdot 10^{-4}$ to 10×10^{-4} per cent carbon (by mass). Unpolygonized specimens show a short horizontal portion between the regions of elastic and plastic deformation. Specimens subjected to polygonization before tension give a very smooth stress-strain curve (Fig. 49). Talbot explains this difference as follows. In unpolygonized iron, small amounts of carbon atoms surround dislocations (Cottrell atmospheres) and cause the appearance of a horizontal portion on the stress-strain curve. In polygonized metal, dislocations are concentrated on boundaries and are

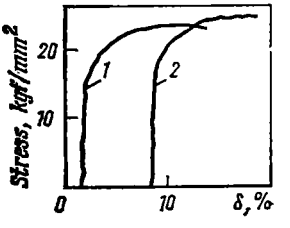

Fig. 49. Stress-strain curves for electrolytic iron
1—unpolygonized; *2*—polygonized

locked by carbon atoms. The distribution of carbon becomes non-uniform, with most carbon being concentrated in low-angle boundaries. On extension of such a specimen, fresh dislocations are not locked by carbon atoms, so that the stress-strain curve has no kink at the elastic limit.

In copper deformed at room temperature, the decrease in resistivity gained in deformation is small at the recovery stage (see Fig. 50), which is evidently associated with a reduction in the number of point defects. A sharp decrease in resistivity begins only during recrystallization, i.e. at the stage of mass redistribution and annihilation of dislocations. The hardness is observed to drop noticeably only at the start of recrystallization (see Fig. 50).

Figure 51 shows the variations in some properties of deformed iron and nickel on heating. The curves closely resemble in form the curves for copper. Electric resistance is the first to recover. The recovery of resistivity ρ reaches 70-80% at the beginning of recrystallization. The rate of dissolution decreases partially at the recovery stage. The hardness remains almost unchanged up to the beginning of recrystallization.

In aluminium, recovery occurs in a different manner. It is accompanied by the evolution of a large amount of latent energy of cold work (see Fig. 46) and by a more intensive (than in copper) restoration of the properties, including strength characteristics.

As seen from Fig. 50, in aluminium rolled 28% at 20°C, the strain-induced gain in hardness drops 30% by the beginning of recrystallization.

Perrimen observed a still more intensive softening at the recovery stage in cold-rolled Al + 2.87% Mg alloy (annealed at 250°C). Its hardness was restored fully before the start of recrystallization.

This peculiarity of aluminium and its alloys should evidently be attributed to the fact that cross slip and dislocation redistribution can easily occur in them. For the same reason, probably, intensive softening takes place in molybdenum at the recovery stage.

Deformation at the temperature of liquid nitrogen changes noticeably the latent energy of cold work and the conditions for its relaxation. According to McQueen and Jonas [95], the stored energy in this case is approximately four times its value on deformation at room temperature. This is due largely, but not exceptionally, to a higher concentration of point defects. As is seen from the curves in Fig. 50, the values of both resistivity and room-temperature hardness for specimens deformed at −193°C are higher than those for specimens deformed at 20°C.

The density and distribution of dislocations on deformation at −193°C are different to those on deformation at +20°C, which is confirmed indirectly by the different type of texture and higher stacking fault concentration.

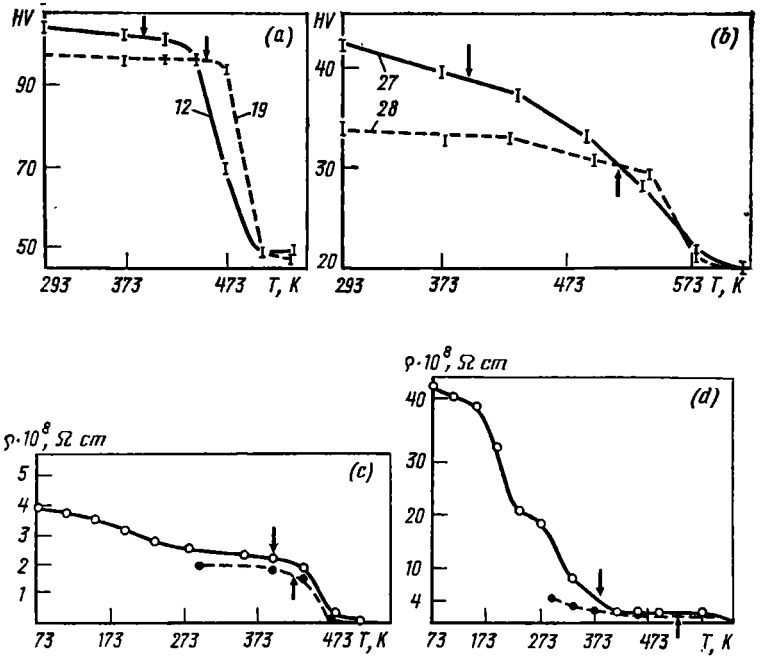

Fig. 50. Changes in hardness (*a*, *b*) and resistivity (*c*, *d*) during heating of copper (*a*, *c*) and aluminium (*b*, *d*) deformed at 78 K (solid lines) and 293 K (dotted lines). Arrows indicate the beginning of recrystallization

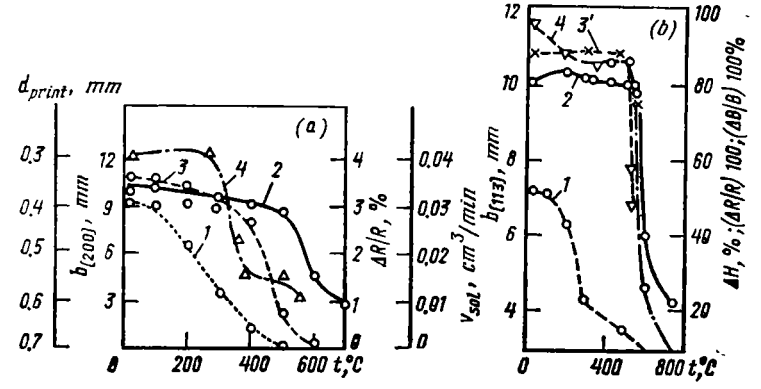

Fig. 51. Variations in the properties of deformed iron (*a*) and nickel (*b*) during heating

1—resistivity; *2*—hardness; *3*—dissolution rate; *3'*—magnetic induction; *4*—line width

The energy liberated at the recovery stage in copper (99.999% pure) deformed at —193°C is also quite large and constitutes 0.7 of the total energy stored, against 0.1 upon deformation at —20°C. The liberation of energy begins already at quite low temperatures, approximately —160°C, and is accompanied by a partial restoration of the resistivity and density, but without variations in the mechanical properties.

The main portion of the energy liberated below room temperature is evidently associated with the annihilation of point defects. Redistribution of dislocations probably contributes somewhat to this effect [95].

It should be emphasized that the restoration of the properties on light deformations at room and lower temperatures has a slightly different nature. Not only the resistivity, but also the mechanical properties are restored appreciably or sometimes almost completely at the recovery stage, i.e. before the onset of recrystallization.

The general features of variations in the properties on recovery and primary recrystallization are as follows:

1. At the early stages of recovery which are associated only with redistribution and annihilation of point defects, the resistivity and density are restored partially, while the mechanical properties remain almost unchanged.

2. Recovery, which is due to redistribution and annihilation of dislocations, changes the mechanical properties too. If the deformation has been restricted to easy slip, the mechanical properties can be restored almost fully on recovery.

In a particular case, recovery due to the redistribution of dislocations and the formation of more stable dislocation aggregates can cause a slight increase in σ_t and hardness and raise substantially the resistance to light plastic deformations (elastic limit).

In commercially pure metals and especially in alloys, this effect is appreciably enhanced, since dislocations are locked by impurities.

3. Under common conditions of deformation of single crystals and especially of polycrystalline cubic-lattice metals, the properties are restored on recovery only partially and their full restoration to the properties typical of metals in the undeformed state takes place only on recrystallization.

4. In metals and alloys of high stacking fault energy, where a distinct cell substructure forms immediately in deformation, subgrain boundaries are flattened and migrate during annealing (a process of the type of in-situ recrystallization), which causes softening of the metal. In such cases, work hardening can be eliminated substantially and sometimes completely without recrystallization.

5. In metals and alloys of low stacking fault energy no intensive

redistribution of dislocations in dislocation pile-ups takes place up to the stage of recrystallization. Especially stable dislocation pile-ups form on heavy deformations. In such materials, noticeable softening can only take place at the onset of recrystallization.

6. Primary recrystallization usually involves a rise in ductility, though there are some exceptions. In certain high-melting b.c.c. metals (tungsten, molybdenum, etc.) having a low solubility for interstitial impurities, the ductility drops appreciably at the early stages of recrystallization (the phenomenon is called recrystallization embrittlement). The probable causes of this phenomenon will be discussed in Ch. 4.

Grain growth and/or secondary recrystallization, which follow primary recrystallization, produce further, though less substantial, changes in the metal properties. The result is that the final properties may be different to those the material had prior to deformation.

The final properties depend on the uniformity of grain size and the absolute size of grains, on the nature and perfection of the texture, etc.

The effect of grain size is associated with some peculiarities in the variations of the mechanical properties during recrystallization after high-speed heating.

With an increase in the rate of heating of a deformed metal to a few hundred °C/s, the rate of formation of recrystallization nuclei begins to surpass noticeably the rate of their growth, resulting in grain refinement at the end of primary recrystallization. The effect is stronger with a higher heating rate.

In addition, it should be noted that in high-speed heating the metal is subjected to the action of high temperature only for a short time which is commensurable with the time the metal is subjected to high temperature during cooling. Therefore, the mechanical properties can be affected substantially both by the rate of subsequent cooling and by the rate of electric heating. It should also be taken into account that special conditions should be observed when heating alloys with disperse phases. Using high heating rates, it is possible to initiate recrystallization in the matrix without noticeable dissolution of the disperse phases [132]. If, however, the rate of heating is lowered or the temperature of heating raised, disperse particles will be dissolved during recrystallization, resulting in a different hardening effect in the solid solution.

The effect of recrystallization textures on metal properties will be discussed briefly in Ch. 10. The reader may refer to special monographs [23, 24, 87] for more detail.

It should be noted that the above-discussed features are only true for cases where no other processes, such as solid solution decom-

position, dissolution and coagulation of disperse phase or phase transformation, are superposed on the processes of recovery and recrystallization. Otherwise, the total effect on metal properties may be quite different.

The variations of metal properties at the early stages of recrystallization after hot deformation have certain peculiarities which will be partially discussed in Ch. 6. These peculiarities determine the properties obtained after what is called high-temperature thermomechanical treatment [34].

Chapter 4

Mechanism of Formation of Primary Recrystallization Nuclei

The mechanism of formation of recrystallization nuclei is the key problem in the theory of recrystallization. Since nuclei are very small at the early stage of formation and appear in microvolumes of the highest dislocation density, methods of optical microscopy are inapplicable for examining early stages of nucleation.

Valuable results can be obtained by analysing the relation between the orientations of a deformed and a recrystallized matrix by means of pole figures. The method, however, gives an averaged picture and fails to determine the orientation of a given nucleus and of its surroundings.

Much progress has been made with the appearance of thin-foil transmission electron microscopy which has a resolution of a fraction of a micrometre and makes it possible to determine the orientations of nuclei and the surrounding matrix by means of microdiffraction. But because the areas under examination are small, there is little probability that a nucleus will be detected and a typical picture will be observed. A vast statistical material is needed to obtain reliable results.

It is even more difficult to examine the structure of dislocation pile-ups and the dislocation reactions associated with the transformation of cell walls into sub-boundaries and with the migration of the latter. The study of these problems depends on the progress in the theory of structure defect diffraction and the theory of contrast.

The attempts to overcome the difficulties in the analysis of early stages of recrystallization caused the appearance of a number of works in 1930's and 1940's, which aimed to clarify the mechanism of recrystallization by analysing the kinetics of the process and the affecting factors. These works have constituted the basis of what is called the fluctuation theory whose essence will be discussed later in the book. Though many assumptions were not confirmed in later studies, they made it possible to postulate and express mathematically many important relationships.

Modern dislocation concepts of the nucleation mechanism were formulated in 1950's. The subsequent works were based on these dislocation concepts and mainly dealt with some specific details of the individual stages of the process.

Before discussing the essence of these concepts, it is reasonable to emphasize the principally important experimental facts and laws of the process, which must be explained within the framework of any theory. The following observations are the most essential for understanding the mechanism of nucleation.

1. Recrystallization nuclei form in sites of the highest distortion of a crystal lattice due to plastic deformation, mainly in local regions of a substantial misorientation relative to the surroundings. Since lattice misorientations are produced by the excess of like-sign dislocations, this means that the formation of such dislocations is indispensable to nucleation. Kidin and Shtremel [86] were among the first researchers who stressed the importance of this fact.

It has been well known for long that what is needed to initiate recrystallization is not just a high degree of prior deformation but necessarily a deformation by multiple slip.

In single crystals of hexagonal metals (zinc, cadmium) oriented with the [0001] direction parallel to the tension axis or with the (0001) plane parallel to the rolling plane, no recrystallization takes place in heating even at deformations of 100% or more. The effects of deformation are eliminated during heating by recovery and stabilizing polygonization (see Ch. 2).

Zakharova and Kuznetsov [143] analysed in detail the effect of plastic deformation on polygonization and recrystallization in 99.99-% pure aluminium single crystals of various orientations.

Single crystals were strain-tensioned to various degrees at two temperatures: room temperature and that of liquid nitrogen. The specimens were then annealed and subjected to metallographic and X-ray structural analysis. The least deformations enough to initiate recrystallization at 450°C in single crystals were found to be 10%, 15%, 20%, and 30%, for the respective orientations ⟨111⟩, ⟨110⟩, ⟨100⟩ and ⟨135⟩. Of importance is the fact that in all cases the degree of deformation lay within stage III of the hardening curve and far from the beginning of that curve. In other cases, when the deformation was within stages I and II, only stabilizing polygonization took place on heating.

Similar results were obtained by many authors on deformation of differently oriented single crystals of an Fe + (3.0-3.5)% Si alloy, molybdenum, and other metals.

Using special methods of X-ray structural analysis of local misorientations (Kossel's method), it has been found [144] in annealing of deformed aluminium that only regions with a misorientation of at least 15-20° relative to the surrounding deformed matrix can form recrystallization nuclei.

When deformation is sufficient to initiate recrystallization, new grains nucleate not uniformly over the whole volume but only in some preferable places, mainly on grain boundaries and triple

joints and, less frequently, on twin boundaries (see Fig. 39). Particles of other phases, if any, can also serve as sites of preferable nucleation. This may be illustrated by the microstructure photographs given in Fig. 54.

2. The least size of a recrystallization nucleus formed during heating of a deformed metal, i.e. the size of a region separated from the deformed matrix by large-angle boundaries, is of an order of 1 to 3 micrometers.

3. Minor quantities of solute impurities and high-disperse undissolved inclusions always inhibit nucleation and growth of nuclei. In some cases this raises the temperature of recrystallization by a few hundred degrees.

4. In all cases there is a complicated but regular relationship between the textures of recrystallization and deformation. In rare cases these textures may be identical, but most often they differ in a definite manner.

To discuss the mechanism of nucleation in recrystallization, let us start with the fluctuation theory which was very popular at one time. In our opinion, the theory is now of only historical interest, though some researchers still adhere to it. For instance, Cahn [64] concludes that it can be competitive with other theories.

For primary recrystallization, there is no critical temperature t_{cr} regarding it in the sense which is commonly accepted for phase transformations. Among the solid-state processes, however, allotropic transformations are the closest to recrystallization. They also pass through the stages of nucleation and growth of nuclei, do not involve changes in metal composition, and require no atom diffusion through distances greater than interatomic spacings. It is natural to compare the mechanism, rate and driving forces of recrystallization with those of allotropic transformations.

First attempts to establish the laws of recrystallization by analogy with phase transformations were made by H. Alterthum and coworkers. They suggested the fluctuation theory of nucleation in recrystallization [48], according to which nuclei of a size close to the atomic size appear in crystal-lattice portions having the highest distortion. The followers of the fluctuation theory [16] regard these portions as amorphized regions in crystals, whose energy state is similar to that of supercooled liquids. The appearance and further growth of nuclei to the critical size occur owing to a series of thermal fluctuations.

Becker proceeded from the assumption that, as in common phase transformations, the formation of recrystallization nuclei is associated with the appearance of a new interface or an increase of the existing one, i.e. the large-angle boundary of a nucleus. The energy for the formation of new boundaries is taken from the decreasing residual volume energy of plastic deformation, W, and the external energy

of thermal fluctuations. A critical nucleus is an undistorted region of such a size as that for which the unit (per volume) boundary energy is lower than the unit residual energy W liberated in recrystallization.

Hence, for a cubic nucleus, the inequality $6\gamma_b/l \leqslant W$ must be true, where γ_b is the energy of the boundary between the deformed matrix and recrystallized grains, and l is the linear size of the nucleus.

Using the concepts of the general theory of phase transformations, the fluctuation theory gives the following expression for the rate of nucleation [48]:

$$N_\varepsilon = n\,(kT/h)\exp(-\Delta F/RT)\exp[(-K\gamma_b^3)/(z_\varepsilon^2 kT)] \qquad (9)$$

where n is the number of atoms per unit volume of deformed matrix, ε is the deformation, z_ε is the elastic energy of the lattice due to deformation, ΔF is a change in the free energy on the transition of an atom from the deformed to the recrystallized region, and K, k, k, and R are constants.

It follows from formula (9) that N_ε increases drastically with an increase in deformation. The fluctuation theory thus explains the preferable nucleation in the regions of the highest deformation and the necessity of an incubation period for fluctuational formation of nuclei. In all other aspects, this theory contradicts the available experimental facts.

According to the fluctuation theory, recrystallization nuclei are separated from the deformed matrix by large-angle boundaries at the very beginning of their nucleation, i.e. starting at the moment when their size is close to the atomic size. But, as noted earlier, no one has ever observed nuclei of a size less than a few tenths of a micrometre, which would be separated from the matrix by large-angle boundaries. The fluctuational formation of nuclei of such a size is utterly improbable. According to that theory, the growth of nuclei, beginning from the atomic size (since these nuclei are already separated by large-angle boundaries) should be imagined as a process occurring through random diffusion motions of individual atoms. It then follows that the elementary processes of nucleation and and growth in recrystallization and, therefore, the process as a whole, should be of a purely diffusional nature.

These concepts are based on the assumption that the rate of recrystallization depends exponentially on temperature; in many cases the effective activation energies, more strictly, the temperature-rate relationships for self-diffusion and for recrystallization turn out to be rather similar.

However, the attempts to use this similarity to state that the mechanisms of diffusion and recrystallization have much in common fail to be convincing. As will be shown later (Ch. 11), the effective activation energy of recrystallization often has no physical sense

and may have quite different values depending on the conditions of experiment.

Pines [145] assumed that recrystallization was effected completely through directed diffusion of vacancies under the action of grain-boundary tension. But he also revealed, using the X-ray microbundle technique [146], that the early stage of recrystallization in pure metals was associated with a 'jumpwise' increase in the size of blocks. In iron, blocks increase 'jumpwise' from 0.4 μm to 4 μm, i.e. ten times, and in copper roughly four times. Subsequent growth of these blocks proceeds slowly and obeys the regularities corresponding to the diffusion mechanism of growth. These data indicate that at least the early stage of recrystallization does not occur diffusionally.

One can recall a number of processes which undoubtedly differ in their mechanism from common diffusion, but whose rate has the temperature dependence close to that of self-diffusion. As has been shown by J. E. Dorn et al., for instance, the activation energies of volume diffusion and creep practically coincide, though the two mechanisms undoubtedly differ substantially from each other. Diffusion controls the rate of creep, but is not the main mechanism by which creep occurs.

Anderson, Mehl, Mott, Burgers and Lücke [48] paid attention to the fact that the preexponential for recrystallization is 10^6-10^{14} times that for diffusion when the activation energies of recrystallization and diffusion are close in value. The authors explain this regarding recrystallization as a process which occurs by attachment of large atomic groups, rather than of single atoms, to a growing nucleus in the activation process.

The peculiarity of the diffusion mechanism of recrystallization was also noted by Delinger [147] who assumed that nuclei most probably formed by the movement of dislocations, similar to that taking place in polygonization, i.e. by a combination of a diffusional and a diffusionless process. McLean [45] holds that diffusion can only control the rate of boundary migration.

The fluctuation theory is at variance with the experimental facts concerning the effect of minor additions on recrystallization rate. By equation (9), the nucleation rate in recrystallization must sharply depend on the grain-boundary tension (must increase with a decrease in the latter). In that case one would expect that recrystallization should be accelerated by surface-active additions. Actually, however, and as has been noted earlier, all impurities retard recrystallization. It has been shown in Ch. 2 that impurities usually intensify strain-hardening, accelerate the onset of stage III work-hardening and increase the stored energy of deformation, especially at higher values of $\Delta R/R_0$. From this standpoint, one would expect the effect to be quite opposite to that observed actually, i.e. recrys-

tallization would be retarded more at higher values of $\Delta R/R_0$.

Finally, the fluctuation theory fails to explain the actually observed orientation relationships between a deformed matrix and recrystallization nuclei. It follows from this theory that the lattice of a nucleus must have an orientation very close to that of the surrounding deformed matrix. The latter must play the part of a 'wall' on which the formation of a nucleus is energetically favourable (as in heterogeneous crystallization). In that case, the recrystallization textures must correspond to the orientation of the least deformed regions in the initial (prior to annealing) state of a specimen. Experimental data do not provide support for this view.

A convincing objection to the fluctuation theory was raised by M. O. Kornfeld in 1936. Taking an average time interval between fluctuations as θ, and noting that the place in which a fluctuation has formed 'drops out' from the process, the probability of the formation of a nucleus during the annealing time τ will be $W = 1 - \exp(-\tau/\theta)$.

The dependence of the number N of nuclei formed in a unit volume on the annealing time τ will be determined by the equation

$$N = N_0 \int_0^\infty \varphi(\theta)\,[1 - \exp(-\tau/\theta)]\,d\theta$$

Since the derivative of N is negative, $d^2N/dt^2 \leqslant 0$, the curve $N = f(\tau)$ should be convex upwards. Experimentally found curves of this type are however usually convex downwards, i.e. towards the time axis.

A detailed analysis of the fluctuation concepts of the nucleation mechanism in recrystallization has been done by L. N. Larikov [16].

Since the fluctuation theory could not explain the experimental facts and was contradictive to many of them, there appeared new hypotheses and theories, according to which recrystallization is not associated with the formation of nuclei similar to those of a new phase in phase transformations. Recrystallization 'nuclei' are simply certain regions of the crystal lattice which can exist stably in the deformed metal. In phase transformations, the initial material has no stably existing regions with the lattice of the new phase.

In allotropic transformations, the surface energy of a nucleus is the main inhibiting force for nucleation, so that new-phase nuclei of a size less than the critical size are thermodynamically unstable. In recrystallization, on the contrary, any nucleus, however small, is stable and can grow irreversibly, first slowly, until it reaches the critical size (or critical misorientation), after which its growth accelerates jumpwise (this will take place provided that the nucleus in question is not devoured by a larger one).

One of the earliest hypotheses of the formation of nuclei in certain regions of deformed metal was advanced in 1933 by E. F. Bakhmetyev, A. A. Bochvar, G. S. Zhdanov, and Ya. S. Umansky.

Later, two different theories of nucleation in recrystallization were formulated, one based on the concept of low-energy blocks and the other of high-energy blocks [48].

The former proceeds from the assumption that blocks which have undergone the least deformation become recrystallization nuclei. These blocks are more stable than the more strained surroundings and can grow at the expense of the latter. An increase in the boundary energy is the main cause for the existence of an incubation period and of slow growth of blocks during that period.

The high-energy block hypothesis assumes that future nuclei are just the most distorted regions in a deformed material. During heating, the redistribution and relaxation of the distortion energy begin most early in these blocks. The stored strain energy is so high that its disappearance in heating is fully compensated for by the increase in the energy associated with the increase of the surface area of a growing nucleus. According to this hypothesis, the incubation period is determined by the time of relaxation of the distortion energy in blocks.

The weakest point of this hypothesis is that there are no definite concepts of the atomic mechanism of nucleation.

Substantial progress in the evolution of the theory of recrystallization nucleation has been made in the last two decades due to the achievements in the theory of dislocations and development of experimental methods for observation of dislocations. The results obtained by these methods are especially valuable due to the fact that they make it possible to formulate certain concepts of the atomic mechanism of the process and, in many cases, to predict the course and the results of the process, which the fluctuation theory was unable to do.

Beck [148] and Cahn [64] were among the first workers to suppose that the formation of recrystallization nuclei is associated with dislocation regrouping, resulting in polygonization. In this process, undistorted or slightly distorted regions tilted through certain angles to one another are formed in the lattice. Among them there are some regions large in size and distorted less than others; these can serve as nuclei. In this case the incubation period includes the time required both for polygonization to be completed and for low-angle boundaries thus formed which in their motion absorb new dislocations, to be transformed into large-angle mobile boundaries. Hence, according to Cahn, the length of the incubation period τ_0 is proportional to the local curvature radius ρ of a block.

Cahn's concepts were later developed and supplemented by a number of workers.

All these studies in combination made it possible to clarify some details of the atomic mechanism of the process, though many aspects still remain unclear. Cottrell [115] has pointed out that nuclei must form preferably in regions of the greatest curvature, i.e. in those containing the highest number of like-sign excess dislocations.

According to Burgers [149], an indispensable condition for intensive growth of selected polygonized regions, i.e. for their transformation into nuclei, is a 'contrast' in the size of blocks and in their orientation relative to the surrounding matrix. Burgers explains the experimental fact established by Talbot [119] and Montuelle [124] that as-deformed high-purity zone-melted iron and aluminium cannot recrystallize on annealing by the absence of this 'contrast'. A small addition of an impurity, for instance, a few hundredths of a per cent of carbon to iron, provides the required conditions for recrystallization. Probably, deformation in very pure metals produces a more uniform dislocation structure, so that polygonization in them is of the type of stabilizing polygonization with the formation of a relatively uniform and balanced polygonized structure. Impurity atoms make the dislocation structure that forms in deformation more complicated, accelerate the onset of stage III strain-hardening and thus facilitate the formation of a 'size and orientation contrast' during polygonization.

On the other hand, the results of works [119, 124] and some other works have later provoked Cahn to conclude that polygonization is a process competing with recrystallization, rather than the initial stage of the latter. This unclear understanding of the role of polygonization remained in Cahn's later works [64].

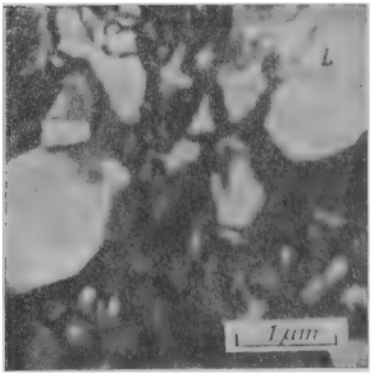

Fig. 52. A recrystallization nucleus *L* separated from the deformed matrix by a large-angle boundary in one portion and by a low-angle boundary in another

Of certain interest are some conclusions made by Bollman [150] who was one of the first to analyse recrystallization in nickel by thin-foil transmission electron microscopy.

Bollman observed nuclei which were separated from the deformed matrix by large-angle boundaries in some portions and by low-angle ones in others, i.e. nuclei at the stage of their unfinished formation (Fig. 52.) The author reasonably regarded this fact as evidence that the nucleus grew from a subgrain. Similar observations were later made by many workers.

Bollman emphasized further that for a nucleus to grow at the ex-

pense of the deformed matrix, it need not be separated from that matrix by large-angle boundaries on all sides. The critical radius of a nucleus should be regarded as a local curvature radius which may vary from one point to another and increase to a definite limit in the course of growth.

According to Bollman, F_S is the grain-boundary free energy per unit area, which is determined by the density of dislocations forming the boundary; ΔF_V is a change in the free energy per unit volume, determined by the volume density of dislocations in local volumes of the matrix adjacent to a given portion of the nucleus. It then follows from the equation $R_{cr} = 2F_S/\Delta F_V$ that F_S and R_{cr} increase with an increase of the misorientation of a growing nucleus. R_{cr} ceases to rise when the boundary becomes large-angle, with its individual dislocations undiscernible. At that moment, the rate of growth reaches its maximum and becomes constant. Further growth does not increase the unit grain-boundary energy.

Thus, if an individual, even very small, portion of a recrystallization nucleus differs substantially in its orientation from the surrounding deformed matrix, the curvature radius of the portion is greater than the critical value, since the growth of the nucleus in that portion causes no increase in the grain-boundary energy. The result is that the nucleus grows preferably in that direction. This conclusion is a good explanation of the phenomenon of recrystallization by strain-induced migration of the initial boundaries, which will be discussed later.

Bollman found also that recrystallization in most preferable portions begins before the completion of polygonization in the whole volume. Thus, polygonization can proceed in parallel with recrystallization in adjacent microvolumes of a specimen. If polygonization is accompanied by a decrease in the density of dislocations due to their partial dissociation or it represents stabilizing polygonization in character, then the rate of growth of nuclei must decrease and, in the general, primary recrystallization must slow down somewhat. With an increase in prior deformation, the incubation period of the formation of recrystallization nuclei shortens, i.e. the conditions for stabilizing polygonization become less and less favourable.

An analysis of the mechanism of formation of a large-angle boundary shows that it can be realized in various ways. Cahn and Cottrell proceeded from the assumption that the large-angle boundaries of nuclei are formed from the low-angle boundaries of polygons produced by polygonization as these boundaries migrate and take up dislocations from the deformed matrix. Bollman confirmed this by experiments on nickel [150].

Fujita [151] and Weissmann [152], who carried out electron-microscopic studies of aluminium foils, came to a somewhat different conclusion. According to their results, large-angle boundaries of

nuclei form directly during deformation. They surround lattice regions consisting of a few subgrains. In Fujita's view, the incubation period is associated with the growth of subgrains due to the migration of their boundaries within these regions. This growth is essential for decreasing the volume energy of a region bounded by large-angle boundaries of a nucleus, but inessential for the formation of the boundary proper.

Fujita's concept is close to the hypothesis proposed earlier by B. Ya. Pines [145], who regarded recrystallization as the "process of growth of blocks into which crystal grains have been broken by plastic deformation". The process is not associated with lattice distortions. According to Pines, the elimination of distortions and complete differentiation in the orientation of blocks occur in the course of recovery.

A system consisting of such blocks should be susceptible to grain growth under the effect of the block boundary energy γ_{bl}. The low value of γ_{bl} (due to low misorientation of blocks) is compensated for by the small size of blocks proper, since $dl/d\tau$ (the rate of change of a linear dimension l of blocks) is proportional to γ_{bl}/l. As the blocks grow, the difference in their orientation increases and, therefore, γ increases too. But since l also increases, the rate of growth remains practically unchanged.

A heavier deformation accelerates recrystallization by increasing the dispersity of blocks and their misorientation angles.

This mechanism of primary recrystallization can hardly be accepted, however, at least as the general one. It disagrees with many experimentally established facts. For instance, if we assume that the volume distortions of the lattice are eliminated fully in recovery, it will be unclear why heating of deformed metals produces two distinct thermal effects which coincide respectively with the temperature intervals of recovery and primary recrystallization. These effects were discovered by Sato [142].

As found by Fujita and Weissmann, recrystallization nuclei in aluminium are essentially certain regions (blocks) of the lattice, which have formed on deformation and are free of dislocations. This fact should evidently be attributed to the high stacking fault energy γ_{sf} of aluminium, which is much higher compared to other metals, and thus to a distinct cell structure with thin cell walls in as-deformed state.

In metals and alloys of low γ_{sf}, the formation of such walls in cold deformation is impossible.

Li [153] and H. Hu [74] suggested a different mechanism of coarsening of subgrains formed through dislocation redistribution at an early stage of heating. Hu studied the formation of recrystallization nuclei from subgrains in a Fe + 3.0% Si single crystal rolled along (001) [100] and concluded that the principal mechanism of this pro-

cess was the coalescence of subgrains, which showed up in a disappearance (unravelling) of their subboundaries.

The most important feature of the coalescence mechanism proposed by Li and observed by Hu is, in their view, that the coalesced subgrains become reoriented and a large-angle boundary is formed around them. The most probable atomic mechanism of this coalescence is the motion of dislocations from a disappearing low-angle boundary to the boundaries which surround a group of coalescing subgrains. The process is induced by the stress field of the boundaries and inevitably includes climb of a portion of the dislocations of the disappearing boundary; this climb can occur through volume diffusion and dislocation slip.

In that case the incubation period includes the time of coalescence required to form a large-angle boundary and to allow the subgrain to grow to the required size.

Thus, by all the modern concepts, the formation of recrystallization nuclei is associated with redistribution of dislocations and prerecrystallization polygonization.

On flattening, spatial cell walls form flat subboundaries on which dislocations from the bulk of cells dissociate. Subgrains thus formed have a lower dislocation density than the surrounding deformed matrix. Coarsening of these subgrains increases their angles of misorientation relative to the matrix. The moment at which low-angle boundaries transform into large-angle ones points to completion of the formation of recrystallization nuclei.

The particular details of the process, such as flattening of cell walls, coarsening of subgrains and increasing misorientation, are quite important in themselves (see later) and are rather different in various materials. These differences are due to variations in the dislocation structure formed by deformation and in the nature of materials, first of all, in the value of stacking fault energy γ_{sf}.

The role of dislocation structure and γ_{sf} can be illustrated by analysing the early stages of recrystallization [98] in high-pure aluminium (99.992%) and copper (99.995%), which differ sharply in γ_{sf} and in the susceptibility to cross slip in deformation and heating.

Specimens of both metals were deformed at room temperature and at the temperature of liquid nitrogen (78 K) at which dynamic recovery is impeded; this increased even more the above-mentioned differences in dislocation structure.

After treatment under different conditions, the distribution of microstrains $\left(\sqrt{\overline{\varepsilon^2}}\right)$ in the lattices and the size of coherent scatter regions (D_{cs}) were examined by methods of harmonic analysis of (200) and (400) X-ray lines.

The analysis of the shape of X-ray lines gave qualitative information on changes in the excess of like-sign edge dislocations, the contribution of edge and screw components to dislocation redistribution,

and the evenness of this redistribution. It was assumed that the lattice distortion was associated mainly with edge dislocation components and the excess of like-sign dislocations.

The formation of undistorted lattice regions, roughly 1 μm in size, was determined by the appearance of point reflections in Debye rings on radiograms. The changes in hardness and resistivity were also analysed. Figure 50 shows variations in the hardness and resistivity of copper and aluminium deformed at 78 K and 293 K during heating. Arrows indicate values of t_r^s (see also Table 10).

TABLE 10. Effect of Deformation Temperature on t_r^s and Changes in the Properties of Copper and Aluminium During Heating [98]

Metal	Deformation temperature, K	t_r^s, K (± 10°)	Δt_r^s, K	Hardness at 293 K after deformation, HV	ΔHV, %	Softening at the start of recrystallization, %	Loss of resistivity at the start of post-recrystallization, %
Cu	78	415	35	105	8	4	45
	293	450		97		0	25
Al	78	390	130	42	25	14	88
	293	520		34		28	80

At first signs of recrystallization, the scatter in the values of hardness in copper and aluminium differs in character. The hardness distribution curve for copper has two maxima: one is representative of the original hardness before heating and the other, of the hardness in recrystallized portions. Thus, unrecrystallized portions in copper show practically no change in hardness.

The hardness in aluminium dropped over the whole volume, but most intensively in recrystallized portions. This was indicative of quite appreciable softening also in the regions where recovery took place. In copper and aluminium specimens deformed at room temperature, the number of reflections on radiograms differed with the heating temperature. In copper, first reflections were detected at 180°C. A further slight increase in the annealing temperature caused a sharp rise in the number of reflections. In aluminium, a few weak reflections were revealed at 80°C, but their number remained almost unchanged up to 240°C and began to rise vigorously only after heating to 250°C (Fig. 53).

This was not the case with specimens deformed at the temperature of liquid nitrogen. The dependence of the number of reflections on heating temperature was roughly the same both in copper and in aluminium.

The results of X-ray analysis and resistivity measurements made it possible to conclude that the structure of copper deformed at 78 K differs somewhat from that deformed at 293 K. Though the density of defects was high in both, the former had a less uniform distribution of dislocations, a higher excess of like-sign dislocations in individual portions, higher stresses, greater concentration of vacancies, and evidently more dislocation locks.

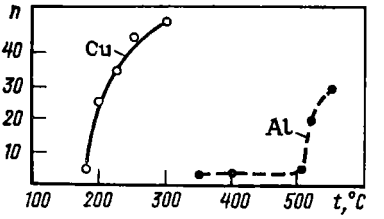

Fig. 53. Effect of heating temperature on the number of X-ray reflections n for copper and aluminium deformed at 20°C. The beginning of actual recrystallization in aluminium is preceded by in-situ recrystallization

These differences are most probably attributed to the different number of operative slip systems and to the different type of slip in copper at the two temperatures. This is confirmed indirectly by the fact that the textures in copper deformed at 78 K and 293 K are different.

In copper deformed at 78 K, slight dislocation redistribution by conservative slip takes place even within the temperature interval 78-293 K and the concentration of defects decreases noticeably. Further heating to 373 K and then to 408 K results in a greater partial redistribution of dislocations by diffusion climb of edge components and a weak enlargement of subgrains. This can be judged from the sharper drop in resistivity. The metal, however, still retains an excess of vacancies (as follows from its resistivity) and a less uniform distribution of dislocations compared to copper deformed at 273 K. An additional temperature rise only by 7 K, i.e. up to 415 K, causes vigorous jumpwise growth of subgrains (up to 1-3 μm, i.e. by a factor of a few tens) and the appearance of first point reflections on radiograms.

Evidently, diffusion climb of dislocations disturbs the equilibrium of dislocation arrays and clears the way for mass redistribution of dislocations by conservative slip and cross slip.

In copper specimens deformed at room temperature, the structure is much more stable. The enlargement of subgrains and the reduction of concentration of defects occur much less intensively up to 445 K. Heating to 450 K, i.e. 5 K higher, also causes a jumpwise change in the structure and the beginning of recrystallization. The size of a recrystallization nucleus in copper at the end of its formation is approximately 1 μm.

In aluminium, the differences between the structures on deformation at different temperatures are substantially greater than in copper.

The structure of aluminium deformed at 293 K is characterized by large-size cells with a low excess of like-sign dislocations and a low curvature. The cells are thus very similar to subgrains.

This structure is a natural consequence of the fact that dynamic recovery easily occurs in aluminium. On heating up to 350-370°C, the strain-induced gain in resistivity diminishes somewhat, the total dislocation density decreases, and the regions of coherent scatter become larger; first reflections appear on radiograms and their number then remains almost constant up to 510°C. A vigorous increase in the number of reflections, which is typical of primary recrystallization, begins only on heating up to 520°C. At the same time, resistivity drops abruptly. Hardness remains almost unchanged during heating to 370°C, then decreases gradually in the interval from 370° to 510°C, and drops steeply beginning from 520-530°C.

The structure of aluminium deformed at 78 K is closer to that of deformed copper. The total density of defects is relatively high, dislocations are distributed unevenly, evidently because there is a noticeable excess of like-sign dislocations in cell walls, which is responsible for lattice curvature. Coherent scatter regions are small (approx. 600 Å).

On heating up to 293 K, the size of these regions increases somewhat, but the dislocation density and microstrains remain at a higher level than in specimens deformed at 293 K. This difference is retained up to 373 K.

At 410 K, numerous reflections from recrystallized grains appear on radiograms and their number increases with a further rise in temperature. At the same time, hardness drops abruptly (see Fig. 50). In this case, there is no interval of sluggish rise of the number of reflections. The size of recrystallization nuclei at the end of their formation is evidently even greater than that in copper.

All these results enabled the authors [98] to conclude that the dislocation structure can influence substantially the process of recrystallization.

In cases where the excess of like-sign dislocations is high, large-angle boundaries are likely to form as a result of flattening of spatial dislocation arrays during intensive redistribution of dislocations.

This is evidently the mechanism of the onset of recrystallization in heavily deformed copper.

With a low excess of like-sign dislocations, only low-angle boundaries can form on flattening of dislocation arrays. Subgrains must increase in their size to form a large-angle boundary, i.e. to initiate recrystallization.

In the other case considered, recrystallization thus includes a few stages: (1) the formation of low-angle boundaries, (2) migration of these boundaries, which involves an increase in misorientation angles, and (3) the final period of formation of large-angle bounda-

ries and quick migration of these boundaries; the last stage is recrystallization proper.

This mechanism of the beginning of recrystallization is evidently realized in aluminium deformed at room temperature.

If dynamic recovery takes place easily, it impedes or, on heavy deformations, precludes the formation of a structure with a large excess of like-sign dislocations, i.e. with a high tensor density of dislocations. In this case, the second stage takes much time and the third stage may be absent at all. Subgrains may grow large, to a size of a few micrometres, yet left surrounded by low-angle boundaries. This is essentially the case of in-situ recrystallization.

It should be noted also that, because of a small width of dissociated dislocations, cross slip easily occurs in aluminium during heating too, which manifests itself in a marked softening at the recovery stage.

Recrystallization in aluminium deformed at the temperature of liquid nitrogen (in which case dynamic recovery is impeded) is of an intermediate nature, but by its mechanism it more resembles recrystallization in copper. The stage of in-situ recrystallization is quite feeble here.

These conclusions make it possible to predict the cases in which in-situ recrystallization may be a noticeable stage and to understand the effect of alloying additions on the temperature level of recrystallization.

The experiments described above give an averaged pattern of structural changes in primary recrystallization and show its dependence on the averaged structure in as-deformed state.

Since, however, deformation is non-uniform in various microvolumes (see Ch. 2), it should be expected that the formation of primary recrystallization nuclei will also be non-uniform both in conditions and in character. For the theory and practice of recrystallization, it is very important to understand what structural features of microvolumes can be responsible for making them preferable sites of nucleation.

Figure 54 [75] shows the sites of preferable nucleation during primary recrystallization in cold-rolled polycrystalline transformer steel. These

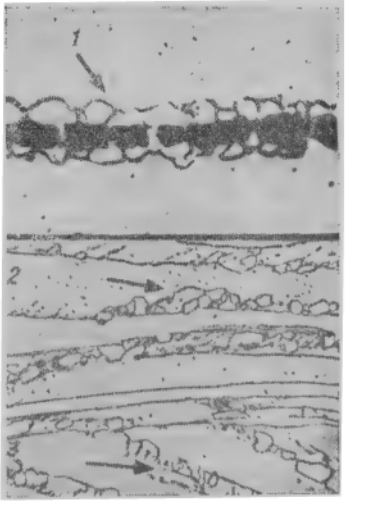

Fig. 54. Sites of preferable nucleation during primary recrystallization in cold-rolled polycrystalline transformer steel

1—on an inclusion; *2*—on grain boundaries; *3*—in microbands. ×200

are microbands, regions near the boundaries of the original grains, and regions near non-metallic inclusions. As regards strain bands and twin bands, nuclei can form only near their boundaries, as a rule on the outside of these bands and do so much less frequently than in regions of the three types mentioned above.

This can be explained by the results of an experimental study of recrystallization in aluminium [144]. It has been found that only the nuclei in transition bands whose boundaries are misorientated more than 15-20° relative to the matrix are capable of growing quickly. Boundaries within strain bands have a lower misorientation (not more than 10-12°), grow very slowly and are rapidly devoured by the more quickly growing nuclei of adjacent microbands.

As given in Ch. 2, microbands are characterized by a regular and discrete misorientation of their subgrains relative to one another. In the middle of a microband, the misorientation reaches 30-40°. Microbands are a few micrometres in thickness and usually contain 15 to 20 subgrains across their width.

It follows that for a subgrain in a microband to become a primary recrystallization nucleus, i.e. for its boundaries to become highly mobile (misoriented by more than 15-20° relative to the matrix), the size of this subgrain should increase up to 1 μm, i.e. become equal to the size of a few (5 to 8) subgrains. This is also true of the regions adjoining the large-angle boundaries of original grains and the interphase boundaries.

In contrast to this, the growth of subgrains in strain bands cannot increase the misorientation angles (owing to the specifics of misorientation, see p. 53) and, therefore, is not accelerated with an increase in subgrain size. The process is thus limited to the stage of in-situ recrystallization.

What is the essence of the incubation period of nucleation? To initiate mass redistribution of dislocations in dislocation pile-ups and their migration by slip, it is obviously necessary to disturb the elastic equilibrium in dislocation arrays, which can be effected by cross slip and/or climb. Both processes can be thermally activated and constitute the essence of the incubation period.

If the initial dislocation density and the excess of like-sign dislocations are relatively low, the incubation period also includes the stage of migration of low-angle boundaries which take up new dislocations and gradually transform into large-angle boundaries.

If deformation is effected at elevated temperatures, low-angle boundaries can form just in deformation. This is especially true of materials with a high value of γ_{sf}. Such was obviously the case described by Fujita and Weissmann [151, 152].

The above conclusions are valid for high degrees of deformation. If a material is subjected to a light or moderate deformation (within

stage II hardening or at the beginning of stage III), the results of heating may be different depending on heating temperature. A change in temperature must not only change the quantity of defects which simultaneously participate in redistribution of dislocations, but also change the relative contributions of the various mechanisms of dislocation movement to this redistribution. As a consequence, this must vary the paths (trajectories) of dislocation movement and thereby produce a qualitatively different result. For explanation, consider a simple example.

Let a pile-up of edge dislocations be formed at an obstacle. On heating to a temperature t_1, the stresses are insufficient to overcome this obstacle, but there are favourable conditions for diffusion climb of dislocations to other slip planes. With a sufficiently long time of heating, climb is realized and the nature of the stress field will be changed.

At a higher temperature t_2, the stresses may prove to be high enough to overcome the shear resistance offered by the obstacle, so that a dislocation can move by conservative (or cross) slip and climb. Since the rate of slip is now much higher, shear will be realized, i.e. the result will be qualitatively different than that in the former case.

It is clear that the results will be even more different if many dislocations of various types are redistributed simultaneously. In this case, unlike-sign dislocations can dissociate, new stable configurations can form, some dislocations can be intercepted or locked by other dislocations, etc. This increases the probability for the formation of polygons with boundaries of a large curvature.

This can be illustrated by the results of electron-microscopic analysis of the dislocation structure in a Ni-Cr film deformed 5% and heated to 1100°C in one case and to 900°C in the other (see in Ch. 3 and Fig. 36).

The temperature curves in Fig. 55 show how the line (420) narrows, the microstresses $\Delta a/a$ diminish, the size D of blocks (regions of coherent scatter) increases, and the hardness (HV) decreases during heating of copper alloys with 0.01% Ti on a rolling deformation of 20 and 70%. The temperatures of the beginning of recrystallization in the alloys are indicated by arrows.

With a light deformation (20%), the above effects become noticeable at a temperature which is 30-50°C below the temperature of recrystallization. The microstresses (revealed by X-ray analysis) are relieved markedly by the beginning of recrystallization.

In specimens deformed 70%, no recovery can be practically revealed up to the temperature of the beginning of recrystallization. First signs of recovery, i.e. a slight narrowing of the lines, a reduction in microstresses and an insignificant increase in the size of coherent scatter regions, appear but together with the first signs of the begin-

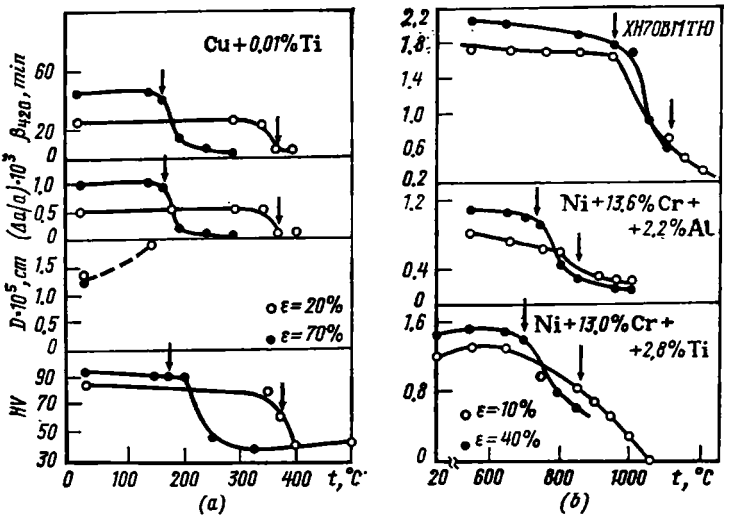

Fig. 55. Effect of heating temperature on the width of lines. β, size of coherent scatter regions, D, microstresses $\Delta a/a$ and hardness (HV) in deformed alloys based on copper (*a*) and nickel (*b*)

ning of recrystallization. With a further rise in temperature, strain-induced distortions are eliminated very vigorously.

A similar relation has been earlier found for a large group of nickel alloys [1]. As shown in [95], the fraction of energy released at the recovery stage grows with a decrease in the degree of deformation.

Taking into account the results discussed earlier, this relation can be explained by the fact that a thermally activated process of cross slip of a portion of dislocations takes place at relatively low temperatures of heating a lightly deformed material. This causes a slight disturbance in the elastic equilibrium of dislocation pile-ups. But since the absolute dislocation density and the stresses are low, there occurs no mass redistribution of dislocations by cross slip and climb. These processes can only begin at higher temperatures.

In heating heavily deformed materials, in which case the dislocation density and the associated elastic energy are high, even a slight diffusion disturbance of the elastic equilibrium of dislocation pile-ups is sufficient to initiate an intensive process of dislocation redistribution. This process results in the formation of boundaries of recrystallization nuclei, which either have large misorientation angles from the very beginning or transform into large-angle boundaries over a certain interval of time. This redistribution proceeds at a rate that highly exceeds the rate of diffusion of vacancies and

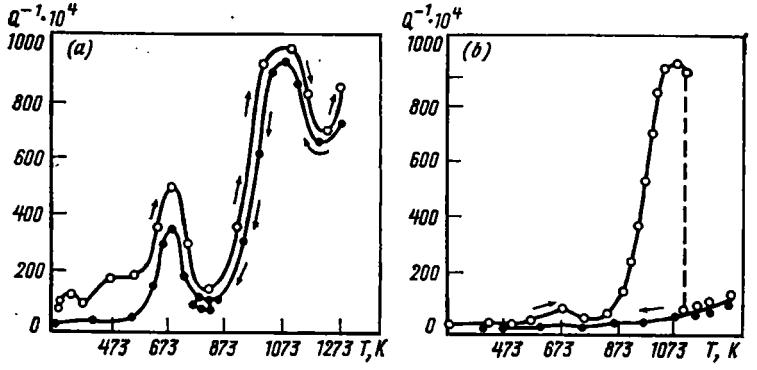

Fig. 56. Effect of temperature on internal friction in thread-like copper crystals [102]

(*a*) $\varepsilon < \varepsilon_{cr}$; (*b*) $\varepsilon > \varepsilon_{cr}$

dislocated atoms and thus outstrips stabilizing polygonization, which depends mainly on dislocation climb.

This conclusion is readily confirmed by the results of analysis of the kinetics of nucleation during primary recrystallization in thread-shaped crystals of copper. The results are obtained from the data on the variations in the internal friction [102] and relaxation of stresses. Deformation was effected by torsion. The diameter of crystals was 10-20 μm. The size of recrystallization nuclei at the moment of their formation was commensurable with the diameter of specimens. The number of nuclei at the beginning of recrystallization was only a few units.

Figure 56 shows the effect of temperature on internal friction under the conditions of continuous heating and cooling for specimens subjected to a subcritical (Fig. 56*a*) and a supercritical (Fig. 56*b*) degree of deformation.

As is seen, the internal friction Q^{-1} in the second case varies jumpwise at a definite temperature. A parallel X-ray structural analysis has shown that this temperature is exactly the temperature at which recrystallization begins. The abrupt change in internal friction has always occurred within a time interval between two measurements (1 to 2 minutes).

The kinetics of the process was also studied by analysing the stress relaxation during isothermal annealing in a special plant. A specimen was preliminarily plastic-deformed by torsion after which a minimum twisting stress was applied; the relaxation of this stress was recorded at various temperatures during isothermal annealing.

Figure 57 shows the typical curves for specimens subjected to a subcritical (curves *1* and 3) and a supercritical (curve *2*) degree of plastic deformation. As seen, a jumpwise stress relaxation τ takes place in the second case. This moment corresponds to the appearance of detectable recrystallization nuclei. The time of their formation proved far less than 1 s, i.e. not enough for marked development of diffusion processes.

The kinetics of stress relaxation during isothermal holding at room temperature was also studied [102] on thread-shaped copper crystals deformed by compression at the temperature of liquid helium.

Recrystallization was examined by the X-ray express photography technique with an exposure of 6-10 min. First traces of recrystallization were revealed after a holding time of 15-24 h. The whole process of primary recrystallization took a few days, but every recrystallization nucleus appeared in a shorter time than the time of exposure.

Thus, at least the initial stage of recrystallization — nucleation—is associated with collective, including shear, displacements of atoms. Diffusion of single atoms (vacancies) plays only a subordinate part; it forms favourable conditions for mass redistribution of dislocations.

As mentioned earlier, many workers have found that stabilizing polygonization does not facilitate, but on the contrary, impedes or even precludes subsequent recrystallization [119, 124, 154]. Talbot [119], who thoroughly analysed polygonization and recrystallization in iron of various purity, concludes that polygonization is not an intermediate stage between the as-deformed and the recrystallized state of a metal. According to his results, it is impossible to form large crystals in zone-melted iron with $1 \cdot 10^{-3}$% carbon (by mass) by deformation to the critical strain and subsequent recrystallization. When this iron deformed by elongation up to 20% was heated, redistribution of dislocations occurred easily and resulted in a very stable regular polygonal structure (i.e. stabilizing polygonization was realized). Despite long annealing at 850-880°C, not a single polygon could transform into a recrystallization nucleus. Similar results were obtained by P. Lacombe and L. Beaujard, and later by J. Montuelle for aluminium (99.99 and 99.999% pure).

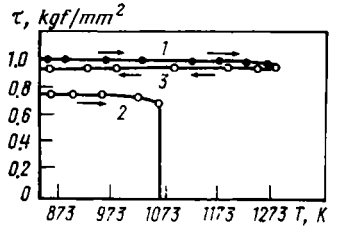

Fig. 57. Stress relaxation curves for thread-like copper crystals deformed to a subcritical (*1*, *3*) and critical degree (*2*) [102]

Talbot carried out a very illustrative experiment on specially prepared specimens with carbon concentration varying along their length. In zones of an elevated concentration of carbon — above $4 \cdot 10^{-2}$% (by

mass)— recrystallization took place and new large grains that formed had no traces of polygonization. In zones of a reduced carbon content, the structure included fine original grains in which polygonization was realized. At boundaries between these regions large grains were found to incorporate fine polygonized grains which were left undevoured by the large grains in the process of growth. Therefore, uniform stabilizing polygonization can stabilize even grain boundaries and diminish their mobility.

Well known are the structural features of aluminium alloys of the Avial type after hot pressing. The structure is characterized by high thermal stability. Notwithstanding an appreciable amount of prior deformation and a distinct deformation texture, the alloy is not recrystallized up to rather high temperatures of heating, which exceed by 100-150°C the normal recrystallization temperature of alloys of this type. This exactly is one of the peculiarities of what is called the 'extrusion effect' [155].

X-ray analysis of the structure of pressed specimens shows that the matrix is in a polygonized state. This can be explained easily if we recall that the process of dislocation climb and, therefore, polygonization are sharply accelerated under the combined effect of stresses and temperature.

A feature common of both stabilizing and prerecrystallizational polygonization is that the two processes take place through redistribution of dislocations, though the nature of this redistribution is quite different.

An essential point is that the rate of each of these processes depends differently on deformation. On heavier deformations, recrystallization is facilitated. During slow heating after light deformation, stabilizing polygonization has time to occur before prerecrystallizational polygonization, while after heavy deformation recrystallization always begins earlier and stabilizing polygonization cannot be practically realized (Fig. 58). Experimental determination of the differences in the mechanisms of dislocation movement in stabilizing and prerecrystallizational polygonization is an important and interesting problem.

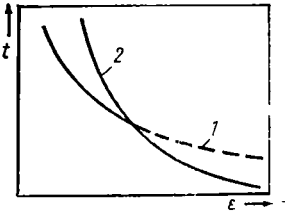

Fig. 58. Effect of deformation on the rate of stabilizing polygonization (*1*) and the rate of prerecrystallization polygonization (*2*)

Thus, the formation of recrystallization nuclei is not associated with the appearance of new interfaces. Nuclei and their interfaces are formed only through redistribution of the dislocations available in the deformed material. The result is that the energy of large-angle boundaries being formed is always lower than the energy of their dislocations (before redistribution). Therefore, the

formation of a recrystallization nucleus is always accompanied by a gain in the volume energy, which exceeds the boundary energy of the nucleus.

In this case the incubation period of nucleation is associated with the time needed for completion of the thermally activated processes which disturb the elastic equilibrium of dislocations and make their redistribution possible. In that connection, the conventional concept of the critical nucleus is inapplicable to recrystallization. A nucleus which can serve as a 'critical' one differs from other regions of a deformed crystal by its higher structural perfection and the presence of large-angle boundaries (or their portions) which can migrate at least in one direction into the deformed matrix at an appreciably higher rate than boundaries of a lower misorientation angle.

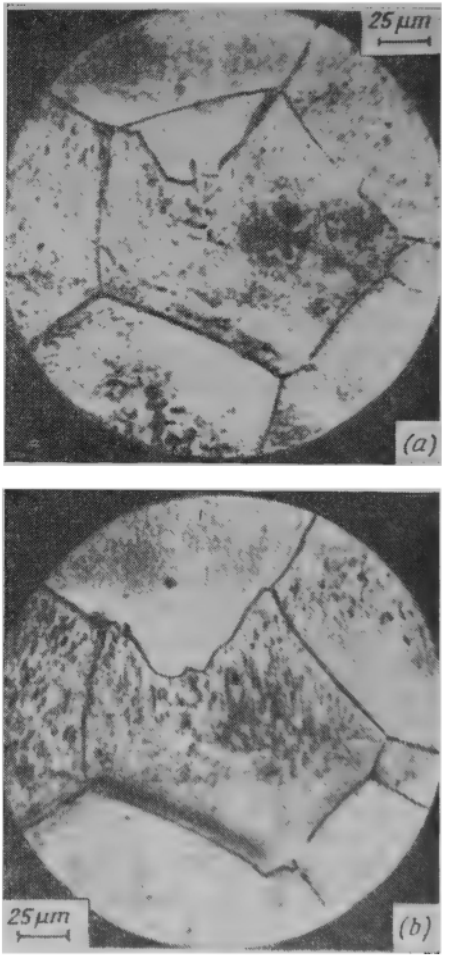

Fig. 59. Recrystallization by the formation of tongues on a large-angle boundary between deformed grains of electrolytic iron before (*a*) and after (*b*) repolishing. Deformation 40%, annealing at 450°C for 15 h (After Hilger)

A particular illustration of this concept of nucleation is the common phenomenon of primary recrystallization due to *strain-induced migration.*

This phenomenon, first discovered by Beck and Sperry [156] and then observed by many researchers in various materials [6], consists in the following. In heating after a relatively light deformation, some of the original grains grow at the expense of their neighbours by the migration of local portions of their large-angle boundaries. The result is that protrusions, or 'tongues', form on a migrating boundary (Fig. 59).

The driving force of the process is the local difference in

volume energies (the difference in dislocation densities) on the two sides of a boundary, which is produced by non-uniform deformation. A portion where this difference is at a maximum migrates from the region of a relatively low dislocation density into the adjacent region of another grain with a higher dislocation density. The migrating boundary 'sweeps out', as it were, all defects on its path. Regions with different dislocation density are etched differently and thus can be revealed easily (see Fig. 59).

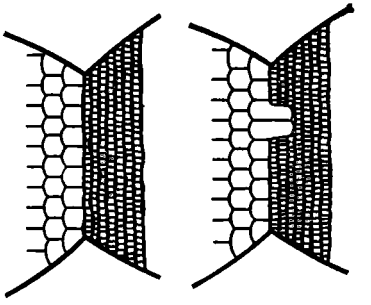

Fig. 60. Migration of a portion of a boundary between original grains due to strain-hardening. On the left, the structure before migration; on the right, after the start of migration

According to Bailey and Hirsch [157], local migration of a boundary can occur when the drop in the volume energy due to sweeping out of defects is greater than the gain in the grain-boundary energy associated with an increase in the length of a boundary on the formation of a tongue. This condition can be written as

$$P^{pr}_{dr\,(m)} = [\Delta E_{def} - \gamma_b\, dS/dV] > 0$$

where ΔE_{def} is the difference in the stored strain energy on both sides of the boundary, γ_b is the unit grain-boundary energy, and dS/dV is the rate with which the area of the boundary increases as the tongue grows in volume.

The critical (minimum) length of a boundary portion on which the formation of a tongue is energetically favourable at moderate deformations (10-30%) is estimated to be approximately 10^{-4} cm.

Figure 60 shows the scheme of migration of a local portion of grain boundary due to strain-hardening. The scheme has been proposed by Beck.

The length of cell boundaries characterizes the volume energy (dislocation density) of grains. The smaller the size of cells, the greater is this energy. As seen from Fig. 60, the direction of migration of a tongue is associated with the size of cells in neighbouring grains.

It should not be thought, however, that the volume energy gradient required to form a tongue is inevitably associated with a difference in the size of cells on both sides of a boundary in as-deformed state. The required volume energy gradient can also be obtained with a low difference in the size of cell structure (dislocation density) on both sides of a boundary. For instance, if the cells are of the same size, but the stability of cell walls and thus the coalescing ability on both sides of a large-angle boundary are different,

the necessary difference in the volume energy can be obtained in the course of heating owing to the coalescence of a group of cells on one side of the boundary. The scheme of such a process, as proposed by Ryum [158], is shown in Fig. 61.

Recrystallization by the formation of tongues was observed in lead, aluminium, electrolytic iron, Zn + 0.01% Fe, Ni-Cr, Al-Zn-Mg alloys, etc. [5]. Tongues disturb the balance of grain-boundary energy in joints, so that the migration, which is initially of a local nature, may in the course of further heating cause a serious rearrangement of the whole system of grain boundaries (due to a trend to equalize that energy) and, under favourable conditions, produce a sharp grain enlargement.

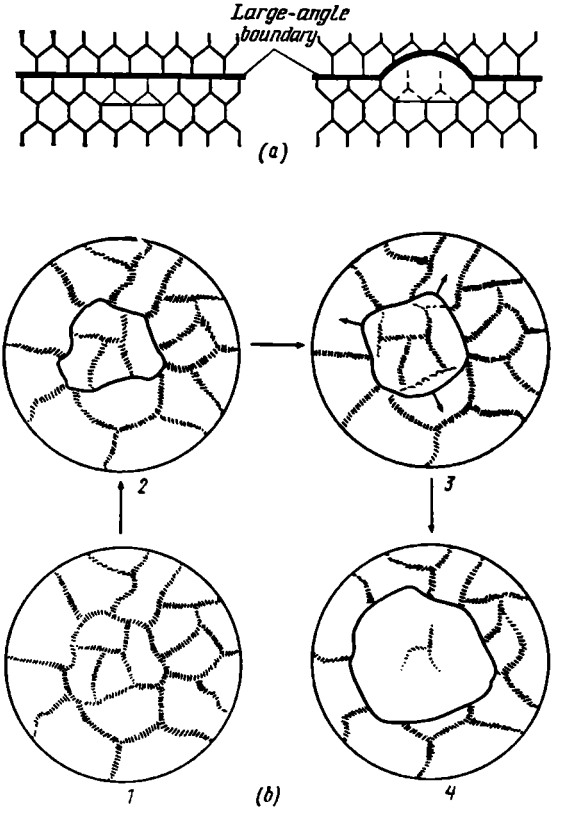

Fig. 61. Various cases of subgrain coalescence resulting in the formation of primary recrystallization nuclei

(*a*) coalescence of a group of subgrains adjacent to the original large-angle boundary, which produces the driving force for recrystallization through the formation of a tongue (on the left, prior to coalescence) [158]; (*b*) unraveling of dislocation arrays in a coalescing group of cells after the start of migration of the subboundary that surrounds this group and the detachment of the subboundary from adjacent arrays

The role of recrystallization by the migration of boundaries of the original grains decreases with increased deformation. If the deformation process forms a distinct cell structure, these cells gain in importance as future recrystallization nuclei. As has been noted earlier, the transformation of some of these cells into nuclei involves two stages: (1) the formation of subgrains bounded by flat boundaries, and (2) a decrease in the dislocation density in the bulk of subgrains due to their migration to subboundaries and a parallel increase in the size of subgrains.

The last process deserves a more detailed discussion. It can be realized either through migration of low-angle boundaries by the mechanism similar to the migration of large-angle boundaries or through coalescence of neighbouring subgrains with the disappearance of the subboundaries which separate them.

The studies into this problem can be divided into two groups. The first includes those in which the authors attempted to determine the mechanism of enlargement of subgrains by analysing the effect of the time of isothermal annealing, τ, on the average size $\bar{D}'_{sg}$ of subgrains and by comparing these results with the calculated data for two probable mechanisms of subgrain enlargement: by migration of triple joints and by coalescence of neighbouring pairs of subgrains.

Another group includes numerous experimental works in which attempts were made to observe directly the structural changes occurring at the early stages of recrystallization. These experiments were mainly made by the methods of transmission electron microscopy, with the use of local microdiffraction in some cases.

Most authors in the first group have obtained the results which suggest that the experimentally observed subgrain enlargement is more intensive than would be expected on the basis of the model of pairwise coalescence. The authors conclude from this that migration of subgrain boundaries plays a predominant part. This process seems actually to occur more frequently. It was observed directly in studies of recrystallization in aluminium and nickel [159], in Cr-Ni alloys [160], in Fe-C-Cr alloys [161], etc.

On the other hand, a large number of researchers of the second group [74, 162] observed directly the formation of recrystallization nuclei by coalescence of subgrains. Coalescence was observed in molybdenum [163], aluminium [162], tungsten [164], vanadium [165], nickel [166], Fe-Si alloys [74], Al-Zn-Mg alloys [158], etc.

An important observation is that coalescence involves, as a rule, not a pair of subgrains, but a group of a few subgrains (3 to 5) as seen from Figs. 61-63. The probability of group coalescence evidently eliminates any objections to coalescence, which follow from the lack of correlation between the statistical results of measurements of $\bar{D}'_{sg} = f(\tau)$ and the analytical calculations based on the pairwise coalescence model.

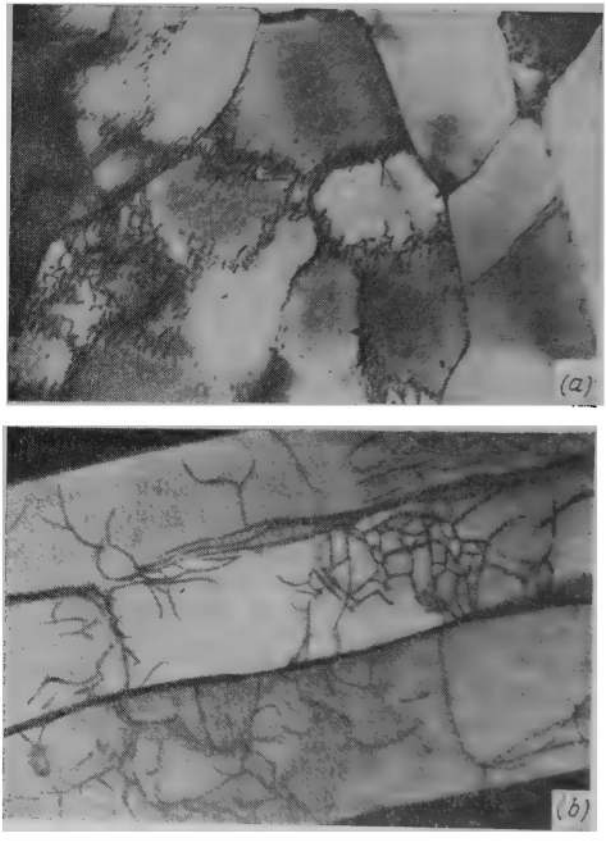

Fig. 62. Coalescence by dissociation of spatial cell walls and plane subboundaries. ×15 000

(*a*) aluminium, dissociation of spatial walls; (*b*) austenitic steel, dissociation of flat subboundaries (After Kaputkina)

A continuous observation of structural changes during annealing of aluminium, which has been carried out by means of a high-voltage microscope [162], has shown that coalescence, which is determined by the thermal instability of subboundaries, depends on what dislocation density they have. Subboundaries of low dislocation density disappear, while those of high density migrate and quickly transform into large-angle boundaries. Similar results were obtained for vanadium [165].

In most cases the dislocation pile-ups dissociating in coalescence are spatial walls (Fig. 62*a*); less frequently, they are two-dimensional subboundaries (Fig. 62*b*).

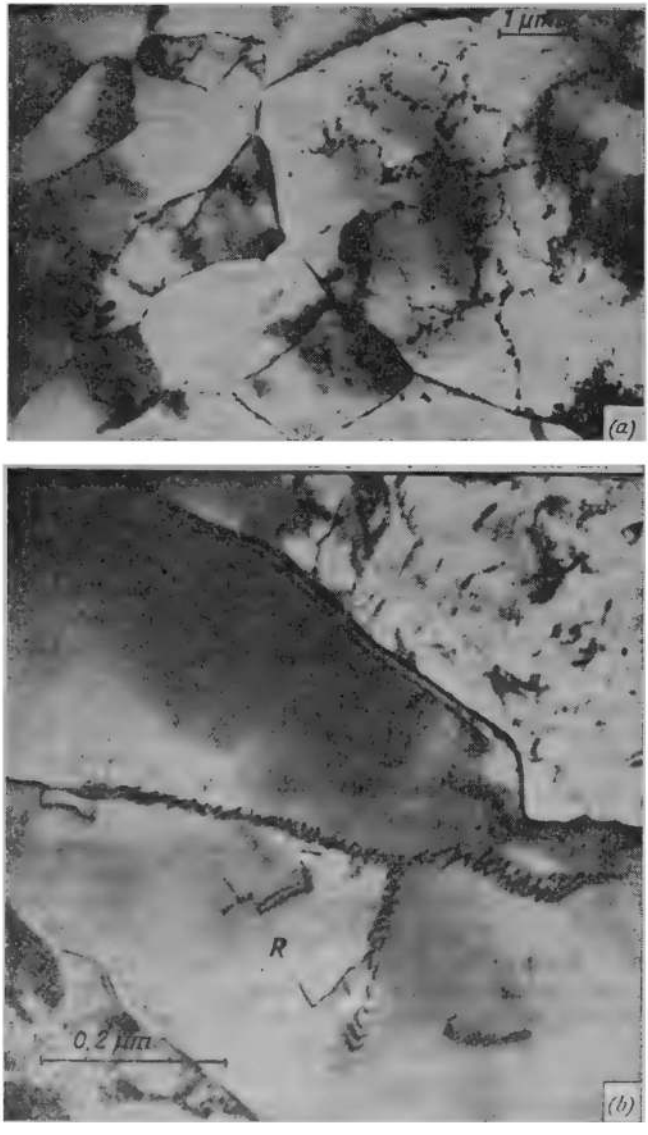

Fig. 63. Coalescence which begins with the dissociation of peripheral portions of subboundaries (cell walls)

(*a*) aluminium (After Sagalova); (*b*) transformer steel (After Goldstein)

Dissociation of walls most often begins from the peripheral portions adjoining the subboundary that surrounds a whole group of coalescing cells (Fig. 63).

The mechanism of coalescence may probably be quite different in its details. Various mechanisms can be realized in one and the same specimen depending on the local features of the dislocation structure. The following cases, in particular, are possible.

1. Coalescence takes place within a certain region whose external boundary is immobile. The migration of that boundary can only start when the volume energy of that region becomes lower than that in the surrounding material (due to coalescence).

Since the conditions of deformation are non-uniform, the flattening of cell walls must evidently occur non-uniformly too. Walls possessing the highest stress field should flatten first. These may be the walls surrounding the groups of subgrains. The subboundaries that have formed earlier than the others in flattening can attract dislocations from neighbouring unstable cell walls in which flattening has not yet taken place.

When the dislocation density in the bulk of a large subgrain becomes lower than that in the surrounding matrix, the subgrain boundary begins to migrate towards the strain-hardened matrix.

2. The migration of a subboundary initially takes place in its region surrounding a group of cells (subgrains) or in one of its portions; this results in the detachment of the subboundary from adjacent cell walls. Coalescence of cells (subgrains) within that region begins after the balance of stresses in walls has been disturbed by the boundary detachment. This forms favourable conditions for unraveling of cell walls and migration of dislocations to the subboundary of that region. The process is shown schematically in Fig. 61*b*.

The probability of detachment depends on a number of factors, first of all on the mutual arrangement of dislocations in unraveling walls and in the subboundary being detached from the walls. The detachment is realized most easily if dislocations in walls are parallel to the subboundary plane. Besides, the discussed mechanism seems to be more probable with a low misorientation of coalescing cells (subgrains).

3. Coalescence of cells (subgrains) within a region and migration of the external boundary of that region or of its local portion take place simultaneously. This case obviously is the most common in practice.

For thorough analysis of the mechanism of nucleation in recrystallization, it is necessary to accumulate more experimental facts and formulate theoretical generalizations relating to the conditions for the formation of dislocation arrays, cells and subboundaries of different thermal stability and, therefore, of different susceptibility

to coalescence. It is clear that coalescence can occur only if the cell walls formed by prior deformation are unstable and the interaction (attraction) between the dislocations of a given wall is weaker than that between these dislocations and the stress fields external relative to that wall.

These external stresses may obviously be due to various causes. In some cases, these are long-range stress fields of certain dislocation pile-ups (boundaries) closest to a given unstable wall, and in other cases, it is the stress fields that act on particles of secondary phases (inclusions) and appear in heating due to a difference in thermal expansion between these phases and the matrix.

On this basis, it is possible to explain the fact that nucleation by coalescence in transformer steel is most often observed in microregions near grain boundaries and near particles of non-metallic inclusions. Nuclei formed in microbands are mainly enlarged by migration of subboundaries.

The mechanism of coalescence of subgrains can be realized more probably at a higher stacking fault energy of a material, i.e. at a greater susceptibility to cross slip.

Coalescence is more often observed during heating after deformations at elevated temperatures than after cold deformation [167, 168]. It is also more common in local portions where the slip has been more complicated in character. The process is favoured by a higher stacking fault energy.

The problem of how coalescence can influence the angle of misorientation between the region of coalescence and the matrix still remains unclear. In contrast to H. Hu [74], for instance, Guttmann [165] regards this influence to be scarcely probable. Indeed, one can hardly imagine a mechanism by which the orientation of closely oriented subgrains could be changed substantially by coalescence. The role of coalescence obviously reduces to the formation of a region which is relatively free from defects and exceeds appreciably the surrounding grains in size.

Coalescence seems to be responsible for the fact that recrystallized grains retain partially their defects. Boundary migration, as a rule, makes a material free from defects. Exceptions are only possible in the presence of disperse phase particles which can partially lock dislocations (Fig. 64).

On the other hand, it is well known that grains are never ideally perfect even in fully recrystallized materials. They are also composed of subgrains separated by low-angle boundaries. It is still unclear how such a substructure is formed. No special studies were devoted to this problem.

It is possible to make the following assumptions. If an alloy contains inclusions of other phases, heat treatment must (as noted earlier) produce elastic stresses due to a difference in thermal expan-

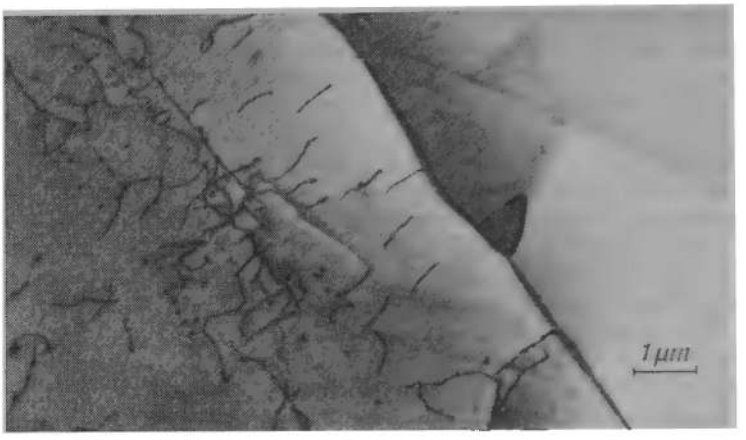

Fig. 64. Dislocations arrested by disperse phase particles during boundary migration

sion coefficients and in some cases, due to a difference in unit volumes. The higher these differences, the higher the stresses and the greater the probability that they will exceed the critical stresses at elevated temperatures and cause plastic deformation. Thus, the stresses initiated by inclusions will generate dislocations whose redistribution and interaction can result in subboundaries. Thermal stresses appearing during cooling after recrystallization annealing and in subsequent heat-treatment procedures can also be sources of dislocations and subboundaries.

The most important source of dislocations in recrystallized grains are obviously remainders of sub-boundaries which have not disappeared fully in coalescence. If nucleation is realized by the mechanisms given under 2 and 3 on p. 154, the large-angle boundary of a nucleus can be formed and begin to migrate intensively even when the nucleus retains partially the dislocations belonging to cell walls (Fig. 65).

The concepts of the dislocation mechanism of nucleation in recrystallization can be used to explain the processes of texture formation in recrystallization (see Ch. 10) and some other important phenomena. Among these phenomena, only poorly described in the literature, is, in our view, the formation of point defects at the stage of primary recrystallization.

If nucleation is realized by redistribution and partial dissociation of dislocations, it is natural to expect that the concentration of point defects (vacancies and their groups) will increase temporarily in the course of the process, which should influence many important phenomena associated with diffusion.

This, however, is in contradiction to the concepts of recrystallization-diffusion relations, which existed in the specialist literature (B. Ya. Pines, S. Weissmann) [145, 152]. According to their concepts concerning the collective nature of primary recrystallization, the stage of recovery must be associated with an increase in diffusion rate. This acceleration must diminish in further heating. The beginning of recrystallization must cause no new increase in the diffusion rate.

Experimental verification of which of the two suppositions is true is difficult to make, since it is difficult to compare the rate of diffusion in deformed specimens where recovery and recrystallization have not yet set in with that in specimens where these processes

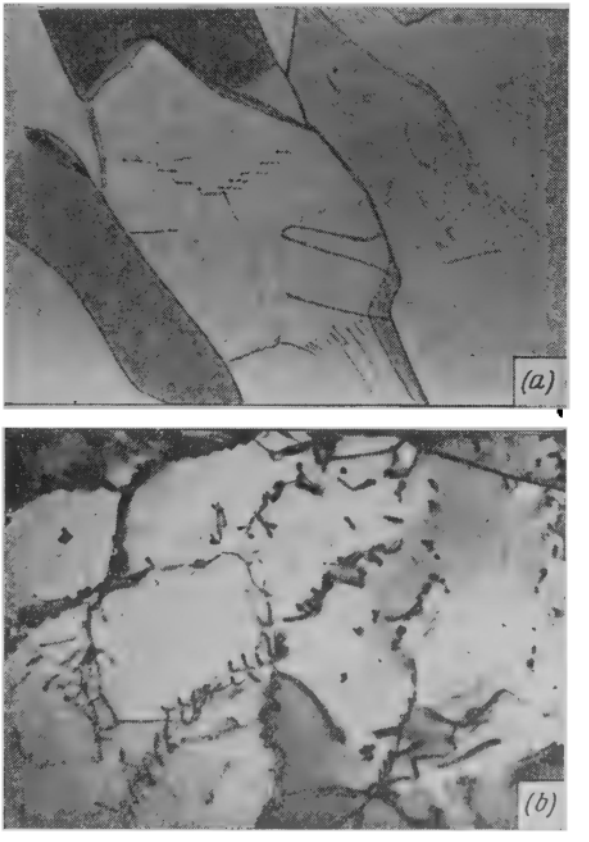

Fig. 65. Dislocations preserved in the bulk of nuclei formed by subgrain coalescence

(*a*) aluminium, ×12 000; (*b*) transformer steel, ×30 000

occur parallel with diffusion. The point is that common methods for studying diffusion require a long time of holding at elevated temperatures, with the result that recrystallization and especially recovery have enough time for completion before diffusion becomes noticeable. These common methods were used in a number of works [169] for an analysis of the effect of prior deformation on diffusion rate, but diffusion was studied essentially in the recrystallized state of specimens. A detected rise in diffusion rate might be associated with refinement of the structure due to recrystallization (compared with the structure of undeformed metal), i.e. with a greater contribution of boundary diffusion.

An analysis of the separate effects of recovery and recrystallization on diffusion rate was made possible by using special radioactive isotope techniques. These methods can measure very low rates of diffusion ($D = 10^{-12}$ to 10^{-15} cm/s) and require an appreciably shorter time of diffusion annealing. These are the 'thick layer' method and the 'print' method proposed respectively by A. A. Zhukhovitsky and V. A. Geodakyan [170]. Both methods were used in [171] for analysis of a nickel alloy with 13% Cr. Specimens were deformed 20% by upsetting. The temperature of recrystallization was sufficiently high and the interval of recrystallization sufficiently long, so that the size of recrystallized grains was roughly the same as in the original state.

The 'print' method made it possible to measure diffusion rates beginning from a temperature of 700°C. The method essentially consists in the following: a radioactive isotope whose diffusion rate is to be measured is applied in a thin layer onto the surface of specimens. In the course of annealing, the surface concentration C of the isotope diminishes by the well-known equation $C = q \mid \sqrt{\pi D \tau}$, where D is the diffusion coefficient and τ is the time of annealing.

To determine the concentration of the diffusion component in the surface of a specimen, a 'print' is made on a piece of filter-paper by the method of microanode dissolution after each annealing operation. The activity of the print, which is proportional to the surface concentration of the isotope, is measured by a radiation counter.

In order to determine the difference in diffusion rates, the experiments were carried out on pairs of specimens. In each pair of specimens hardened from 1150°C, one was deformed 20% by upsetting and the other left undeformed.

Apart from the activity of the print, the total γ-radiation activity of a specimen, characteristic of the total quantity of the diffusing substance, was measured after each annealing operation. After that, the I_{print}/I_{ysp} ratio was calculated.

To find the relative rate of diffusion in the pair of specimens (1 and 2) after each annealing operation time τ long, the ratio

$(I_{print}/I_\gamma)_2$: $(I_{print}/I_\gamma)_1 = k$ was determined and the k-τ curve was plotted.

The rate of diffusion was studied on ^{60}Co. The experimental technique was described in detail in [171]. The time it took recrystallization to set in, as determined radiographically, was 14 h in isothermal annealing at 700°C, 45-50 min at 800°C, and 16-20 min at 850°C. The time taken for recrystallization to come to completion was respectively 16, 10 and 4 hours.

Before recrystallization, recovery that took place in the alloy was very intensive judging by a sharp narrowing of interference lines.

In order to determine the separate effects of recovery and recrystallization, a pair of specimens were held at 700°C for 100 min, 2 h or 3 h and then annealed (for a time length from 15 to 405 min) at 850°C. After each annealing operation, prints were made and radiation counted. The results are given in Fig. 66.

At the beginning of annealing at 700°C, the rate of diffusion rose, but then began to drop and returned almost to the initial value on the completion of recovery. But after the specimen was heated to a higher temperature (850°C) and started to recrystallize the rate of diffusion again rose noticeably. It should be emphasized that this gain in diffusion rate was sensible even some time after the completion of primary recrystallization.

Thus, the rise in diffusion rate due only to recovery is most intensive in the initial moments of annealing. The rise in diffusion rate due to recrystallization makes itself felt gradually in the course of isothermal annealing and, on passing through a maximum, begins to decline. This difference agrees with the fact that recrystallization requires an incubation period and recovery does not (see Fig. 32).

The acceleration of diffusion in the course of primary recrystallization disproves the earlier assumption that primary recrystallization is essentially the growth of blocks formed in recovery.

What specific features of primary recrystallization can accelerate diffusion?

What makes this acceleration different to that observed in recovery?

In the general case, diffusion can be accelerated due either to the formation of an additional number of free vacancies or to an increase in the number of large-angle boundaries and dislocations on which diffusion is known to occur at the highest rate. Large-angle boundaries formed in recrystallization cannot exert a substantial

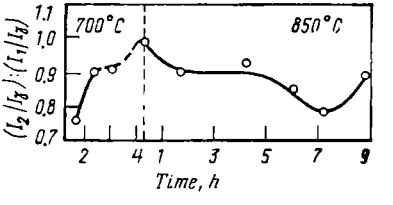

Fig. 66. Relative intensities of ^{60}Co prints taken from the surface of specimens of deformed Ni + 13% Cr alloy versus time of annealing at 700° and 850°C (successively)

influence on the difference in diffusion rates in the case considered. The size of grains after primary recrystallization was roughly equal to that of the original grains. Therefore, the length of large-angle boundaries should also be roughly the same as in the undeformed metal. Naturally, the dislocation density could not increase on recovery. Consequently, the acceleration of diffusion at the onset of recrystallization should mainly be attributed to an increased number of mobile vacancies. It seems probable that the process of redistribution and dissociation of dislocations in primary recrystallization is accompanied by the formation of vacancies.

The theory of dislocations [92, 115] suggests a number of probable mechanisms for the formation of vacancies during movement and dissociation of dislocations. Some of these mechanisms were described in Ch. 2 (p. 65).

To explain the causes of the high rate of migration of boundaries of recrystallization nuclei, Lücke [22] made a proposal that primary recrystallization is accompanied by an increase in the concentration of vacancies. According to Lücke, this high rate is due to an elevated concentration of vacancies on boundaries of nuclei that results from the dissociation of dislocations on a moving boundary. This must lead to a higher rate of boundary diffusion.

However, all the effects of primary recrystallization cannot be explained only by an acceleration in boundary diffusion.

A higher rate of diffusion during recovery in a predeformed material, as compared to that in undeformed state, is obviously attributed to a higher mobility of vacancies that are already present in the undeformed specimen. This is why this acceleration is at a maximum in the initial period of annealing, i.e. when the number of these vacancies is the highest. As the concentration of vacancies approaches the equilibrium value at the given temperature of annealing, the rate of diffusion decreases.

In recrystallization, the number of mobile vacancies is minimum at the beginning of the process and then rises with the number of dislocations that participate in redistribution and dissociation. After that, the above-mentioned mechanism of movement and annihilation of vacancies becomes operative. The number of vacancies reaches a maximum and then decreases.

These concepts explain well why, as has been noted earlier, the rates of diffusion in recovery and recrystallization are different and depend on the time of heating.

If excess vacancies appear in primary recrystallization, they should influence other properties of the material, in particular, electric resistance and density, apart from diffusion.

Under the conditions of slow heating in furnaces, the density D of a deformed metal increases monotonically and its resistivity

decreases, though the vacancies being formed should be expected to lower D and increase ρ or at least to retard the recovery of these parameters to the initial values.

In experiments with brass foils (Grade Л68) 0.11 mm thick recrystallized by quick heating (at a rate of 500°C/s) and air cooling, the resistivity was found to increase compared with the value obtained on furnace heating.

These facts indicate that if excess vacancies indeed form in primary recrystallization, they have enough time to dissociate during heating or relatively slow cooling.

To reveal excess vacancies, recrystallization is carried out under the conditions of fast heating and cooling. On this basis, the author and co-workers [100] carried out experiments on determining the changes in the density and resistivity during primary recrystallization of grade Л68 brass (69.0% Cu, 0.07% P, and 0.008% Fe) deformed 50%. Brass specimens were heated fast (500°C/s) in air by passing electric current through them (the heating time was approximately 0.3 s) and then quenched in water.

Density was determined by hydrostatic weighing in tetrabromoethane kept at a constant temperature accurate within $\pm$ 0.02°C. The error did not exceed 0.01% for a single specimen, but was slightly higher for a pair of specimens.

Resistivity was measured by the twin bridge method.

The error for a single specimen was roughly 0.2%, but the measured values varied noticeably in various specimens.

The measured results for density and resistivity are shown graphically in Fig. 67. As found by metallographic analysis, recrystallization does not yet start in heating up to 400°C; at 450°C it is about half way through; at 500°C, specimens contain only individual unrecrystallized portions; and at 550°C and 600°C recrystallization becomes complete. As seen from the figure, density diminishes during primary recrystallization (450° and 500°C), while resistivity either increases (at 450° against 400°C) or remains the same as for recovered metal (500°C against 400°C).

These results show convincingly that excess vacancies of their small complexes appear on primary recrystallization. Taking the volume of a vacancy to be approximately 0.5 of the atomic volume, a drop in D by 0.065% corresponds to approximately 0.1% (at.) of the concentration of vacancies

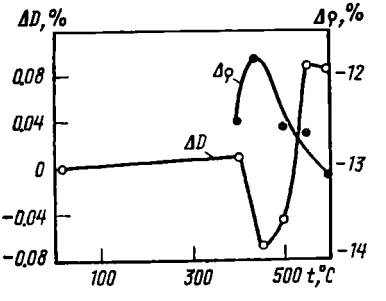

Fig. 67. Variations of density and resistivity of 50-% deformed brass Л68 during primary recrystallization

(disregarding the change in density due to the decrease in the number of vacancies). The result (0.1%) is quite high, though does not exceed substantially the known estimations of the ultimate concentration of vacancies in metals at the melting point.

It is important that excess vacancies in α-brass, when fixed by fast cooling from the temperature of primary recrystallization, remain stable at room temperature. Some specimens were held for about a month, after which their density was measured. Repeated measurements of D, made two months after the first measurements, gave results within the accuracy of the experiment. This may be evidence of the fact that vacancies form stable complexes. Thus, the results of density measurement confirm the results obtained in studies of diffusion (i.e. that vacancies formed in primary recrystallization possess a relative thermal stability). There are no data at present, however, for a substantiated judgement of the state of these excess vacancies.

An astonishing result, on the face of it, is that the unit volume increases in primary recrystallization. This means that the effect of decreasing the density due to the formation of vacancies is stronger than the effect of increasing the density due to dissociation of dislocations, which causes the appearance of these vacancies.

Bernstein [36] revealed an increase in volume at the initial stage of recrystallization in steel grade 50ХГА in the course of isothermal holding at 900°C. The results obtained in [172] are, in our view, another confirmation of the fact that the volume of metal increases in primary recrystallization. The authors studied the effect of uniform pressure on the kinetics of recrystallization in copper. Cold-rolled copper (deformed over 90%) was annealed under a pressure of 1 to $15 \cdot 10^3$ kgf/cm^2. It turned out that uniform pressure slowed down the process of primary recrystallization; the effect was especially strong on the rate of nucleation, but somewhat weaker on the rate of growth.

The results are in full conformity with the well-known Le Chatelier principle.

The fact of the formation of vacancies in primary recrystallization (which may be called the internal 'injection' of vacancies) has not yet found wide recognition. Nonetheless, it enables us to explain a whole series of practically important phenomena. Some of them will be briefly discussed below.

1. A number of workers, who studied the susceptibility of high-melting b.c.c. metals (tungsten etc.) to brittle fracture, have found that an annealing operation, if associated with primary recrystallization, increases the brittleness of tungsten and some other metals. This phenomenon, called 'recrystallization embrittlement' has still found no explanation.

In our view, this phenomenon is associated with the formation of vacancies in primary recrystallization. These vacancies must facilitate the diffusion processes of decomposition of a supersaturated solid solution, the formation of segregates or the precipitation of carbide phases on grain boundaries in the metals mentioned above, which possess a typically low solubility for interstitial impurities.

2. Creep is mainly effected by shear, but its rate is controlled by the rate of diffusion [173]. For further steps of shear to occur stress relaxation by diffusion is needed. Prior strain-hardening increases the resistance to creep, but only to a temperature level below the recrystallization temperature. If tests are carried out so that creep and recrystallization take place simultaneously, the rate of creep increases sharply and turns out to be substantially greater than would be found for undeformed specimens.

This effect may largely be associated with the formation of vacancies in recrystallization, which facilitate diffusion processes and thus accelerate creep.

3. As was noticed long ago by metallurgists experimenting in high-speed heating, high-rate recrystallization-heating facilitates recrystallization and heavily decreases the effective activation energy of the process [132].

Most workers claim this effect to be due to the suppression of recovery by fast heating, with the result that a large part of the energy stored in deformation is preserved by the beginning of recrystallization. This factor seems to be operative. Besides, the role of vacancies formed in primary recrystallization should also be important. Under the conditions of fast heating, the concentration of vacancies must be especially high since many nuclei appear per unit time. In addition, there is not enough time for annihilation of vacancies. For these reasons, vacancies should markedly facilitate recrystallization.

The contribution of each of these two factors can be verified experimentally by making a comparative study of the kinetics of recrystallization during high-speed heating of specimens immediately after their deformation and after preliminary recovery.

4. Preliminary strain hardening of powder materials greatly increases their sinterability, despite the fact that the time they take to recrystallize is tenths of the time period required for sintering.

B. Ya. Pines [145], who was one of the first to notice this effect, attributes it to the formation of vacancies, but holds that they form in recovery, rather than in recrystallization.

5. As has been found by Babich *et al.* [174] who studied the recrystallization in carbon steels with various contents of carbon and with various shapes of cementite particles, recrystallization in cold-rolled steels with the structure of lamellar pearlite always involves an intensive spheroidization of Fe_3C carbide lamellae. A

heating operation, even for a very long time, at a temperature slightly below the temperature of the beginning of recrystallization, cannot influence the shape of lamellar carbide particles.

Babich explains this interesting and practically important effect by the role of vacancies which form in primary recrystallization and accelerate the diffusion process of spheroidization of cementite platelets.

The effect of accelerated coagulation of disperse phases at the beginning of recrystallization has been observed by a number of workers in many alloys, but nobody has attempted to explain it from the above-mentioned positions.

Chapter 5

Mechanism of Enlargement of Recrystallization Nuclei and Grains

The enlargement of recrystallization nuclei and grains is one of the fundamental elementary processes in recrystallization and the sole elementary process at the stages of grain growth and secondary recrystallization.

The growth of nuclei or new grains can be effected only by boundary migration. Adjacent grains can grow in size directly by confluence (coalescence) only in a very rare and hardly probable case when two grains are by chance oriented identically in space and are separated by a certain self-dissociating dislocation configuration*. If two grains are misoriented, even slightly, relative to each other, one of them can acquire the orientation of its neighbour only by migration of the boundary that separates them.

Let us initially discuss the problems relating to the structure of boundaries, the rate and direction of their migration, and the factors which can stimulate migration.

5.1. The Structure of Grain Boundaries

Under grain boundaries of polycrystals one understands the regions of contact (conjunction) of adjacent crystallites with different orientation in space.

At relatively low temperatures, the boundaries of grains are somewhat stronger than the grains proper. At high temperatures, the reverse is true. The temperature at which grains have the same strength as their boundaries, called the equicohesive temperature, is approximately 0.4 T_m. It follows that the interatomic forces in boundaries and, hence, interatomic spacings, must be of the same order of magnitude as in the bulk of grains. On the other hand, grain boundaries have a higher energy compared with the bulk of grains owing to a higher concentration of defects in their atomic structure and a certain difference in bonds on both sides of a boundary.

As is known, atoms in the surface layers of a material have an elevated energy due to the disbalance of atomic bonds; this energy

* In this case, however, we have to deal with a subboundary, rather than with a common large-angle boundary.

is called the surface energy. For that reason, a certain amount of work must be done to form a new surface. This work per unit surface area represents surface tension γ_s.

By analogy, an excess energy of atoms at grain boundaries causes the appearance of grain-boundary energy and grain-boundary tension γ_b.

The magnitude of γ_b has yet to be determined. There are some methods for determining the relative values of γ_b by the angles in triple joints of grains in a quasi-balanced state. The calculation proposed by Smith [175] is given in Sec. 5.3. Further, for a known angle φ in a groove formed by thermal etching (see Fig. 44), it is possible to find the ratio of the grain-boundary energy to the surface energy:

$$\gamma_b/\gamma_s = 2\cos(\varphi/2)$$

Hence, the absolute value of γ_b can be determined from a known value of γ_s.

The values of γ_s, γ_b and γ_b/γ_s for selected metals, as found by this method, are given in Table 11. The table also gives values of

TABLE 11. Average Values of Various Types of Boundary Energy (γ_{tw}, γ_b). Surface Energy γ_s (erg cm^{-2}) and Temperature Coefficient T_K for Selected Metals

Metal	γ_{tw}	γ_b	γ_s	γ_b/γ_s	$T_K = (\delta\gamma_b/\delta T)$
Al	120	625	—	—	—
Cu	40	645	1700	0.38	—
Ag	—	790	1140	0.24	—0.4±1.0
Au	20	365	1400	0.27	—3.2±1.3
Pt	—	1000	2500	0.4	—
Ni	—	750	1750	0.38	—1.1±0.8
Fe_γ	—	550	2100	0.25	—
Fe_α	—	700	1950	0.35	—
Nb	—	800	2100	0.38	—
W	—	—	2900	—	—
Sn	—	160	685	0.28	—

the energy of a coherent twin boundary, γ_{tw}, and the temperature coefficients of grain-boundary energy, $\delta\gamma_b/\delta T$ (which are negative and low in magnitude). Noting these coefficients, we have: $\gamma_b = \gamma_0 + T(\delta\gamma_b/\delta T)$.

Metallophysicists have for long paid attention to the development of appropriate models of the atomic structure of boundaries. Significant achievements have been made in this field in the last

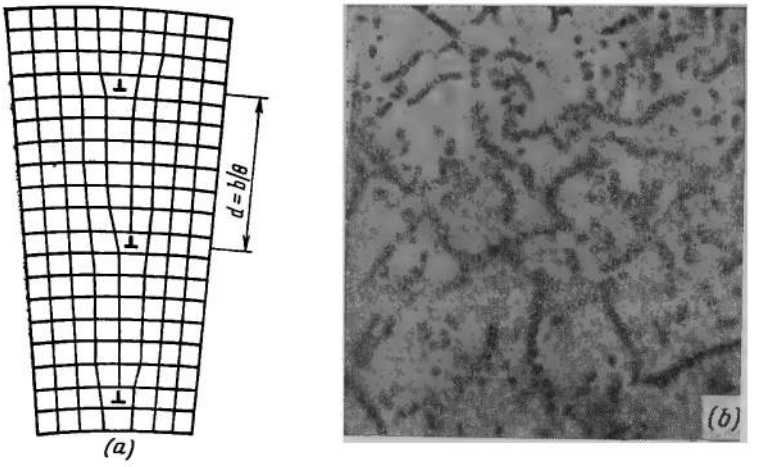

Fig. 68. A low-angle dislocation boundary
(a) tilt boundary (schematic); (b) dislocation trails along low-angle boundaries in nickel

two decades owing to the progress in the theory of dislocations and in experimental methods of high resolution [167]. Nevertheless, some of the concepts in this field still remain hypothetical.

In the general case, a grain boundary possesses five degrees of freedom, three of them being associated with the rotation of the crystallites separated by the boundary about the three axes of coordinates and the remaining two, with the spatial orientation of the boundary proper.

Analysis of randomly oriented boundaries possessing all the five degrees of freedom is practically unfeasible. Particular cases with a low number of degrees of freedom are less complicated. The simplest among them are the two types of boundary of a distinct dislocation structure having only one degree of freedom; these are respectively a tilt boundary and a twist boundary.

The structure of a tilt boundary can be easily understood from the scheme shown in Fig. 68*a*. The axis of rotation of crystallites relative to each other is perpendicular to the normal drawn to the boundary plane.

The angle of rotation about axis $\bar{u}$ is arbitrary and represents a single degree of freedom. With such rotation, a boundary is found to be formed by parallel edge dislocations arranged in a vertical row one above the other. If a boundary is symmetrical, the dislocations in it are equidistant and the misorientation angle of the boundary can be found from the formula

$$\sin(\theta/2) = 0.5\ b/h$$

where b is the Burgers vector and h is the distance between the nearest dislocations; for low-angle boundaries, $\theta = b/h$.

If adjacent crystallites are turned relative to each other by an angle θ about the $\bar{u}$ axis, which is perpendicular to the boundary plane (i.e. the axis of rotation and the normal to the boundary are parallel to each other), the boundary consists of a network of screw dislocations and is called a twist boundary. In the general case, boundaries may have both tilt and twist components.

Figure 68*b* shows grain boundaries formed by creep in a nickel single crystal. The rows of etch pits are trails of dislocations on the surface of the crystal. If the dislocation density in a boundary is low and the misorientation angle is small (θ = 10 to 15′), then dislocation trails are separated by distances that greatly exceed the interatomic spacings, therefore they are readily revealed as separate trails. If the misorientation angle θ is large (a few tens of minutes or a few degrees), dislocation trails are spaced so closely that they cannot be revealed by etching (etch pits merge into a continuous line).

A typical feature of symmetrical tilt and twist dislocation boundaries is that they have no long-range stress fields (stresses decrease drastically with an increase in the distance from the boundary).

As found by Read and Shockley [176], the curves relating γ_b to θ are of the form as shown in Fig. 69. Initially, γ increases linearly with the misorientation angle, then the growth in γ slows down, the curve reaches a maximum and begins to decline. The angle θ_m is different for various materials and depends on the type of energy in dislocation pile-ups. For tin, lead and Fe-Si alloy, it is respectively 12.2°, 25.0°, and 26.0°. The Read-Shockley relationship is written as $\gamma_b/\gamma_m = (\theta/\theta_m)\ [1 - (\theta/\theta_m)]$.

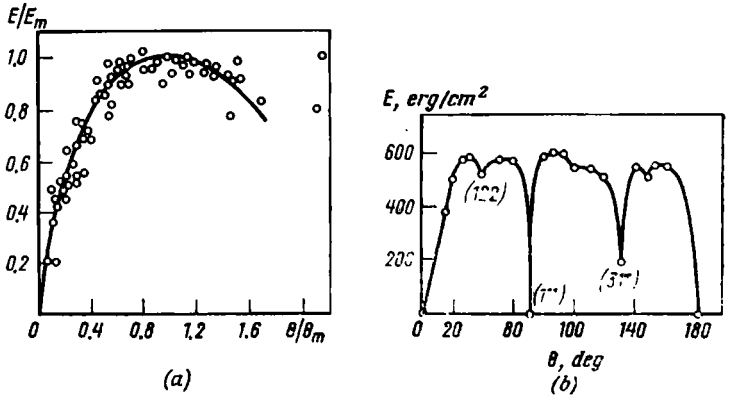

Fig. 69. Boundary energy as a function of misorientation angle
(*a*) average angle [176]; (*b*) angle of rotation about ⟨011⟩ in aluminium [364]

As has been shown experimentally, the values of $\gamma_b = f(\theta)$ for a number of f.c.c. metals agree well with a single curve $\gamma_b/\gamma_m = f(\theta/\theta_m)$ (Fig. 69). As seen from the figure, with large angles θ, i.e. with $(\theta/\theta_m) > 1$, the experimental points fall outside the Read-Shockley theoretical curve. This is obviously associated with an increased contribution of the distortion energy in a dislocation pile-up, which cannot yet be calculated.

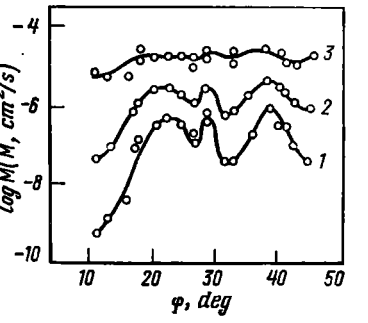

Fig. 70. Orientational relationship for the mobility of tilt boundaries in aluminium [178]
1—394°C; *2*—496°C; *3*—638°C

In later studies, many new peculiarities in the behaviour and structure of large-angle boundaries have been clarified.

One of the most important features of these boundaries is that some of their properties, such as mobility (Fig. 70) and diffusion rate (Fig. 71) depend non-monotonically on orientation. With twin-type misorientations, the properties change drastically (see the minima on the curves in Figs. 71 and 69*b*); with some other types of orientation, they change rather insignificantly.

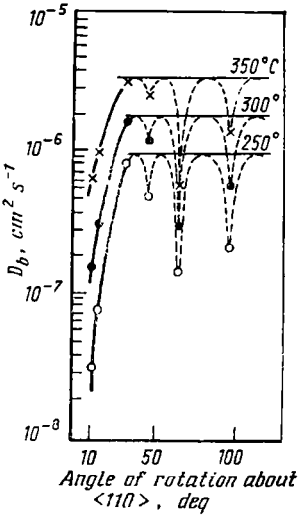

Fig. 71. Orientational relationship for the rate of boundary diffusion D_b of zinc in aluminium; tilt boundaries ⟨110⟩ [183]

Let us refer to the following experimental results. A lightly deformed aluminium single crystal was subjected to a strong local deformation (needle scratching) and annealing [177]. Recrystallization nuclei of different orientation formed around the scratch and then began to grow into the depth of the crystal. Grains turned by an angle of 40° about the ⟨111⟩ direction relative to the matrix crystal grew most quickly. In copper, rotation through an angle of 30° corresponds to the highest mobility.

On the other hand, Burgers and Lacombe have found that the boundaries of two closely oriented grains are the least mobile, as also is a twin boundary.

A systematic examination of boundary mobility in zone-melted aluminium (99.9992%-pure) versus grain orientation has been made by Schwindlerman *et al.*

[178], who studied the migration of tilt boundaries formed by rotation through various angles from 10° to 45° about the ⟨100⟩ direction.

The controlled driving force of the process was kept constant by properly selecting the size of subgrains on the two sides of a migrating boundary.

For all the specimens tested, the boundary mobility M plotted in the log M-$(1/T)$ coordinates showed a fairly linear dependence on temperature (Fig. 72). Here, $M = dV/dP$ and $V = v_0 \exp(-Q/RT)$

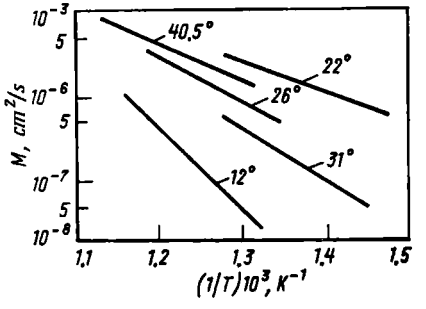

Fig. 72. Effect of temperature on the mobility of tilt boundaries in aluminium for various angles of rotation about ⟨100⟩ [178]

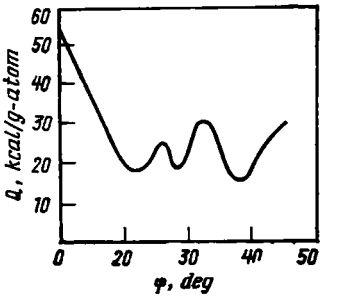

Fig. 73. Orientational relationship for the activation energy of migration of ⟨100⟩ tilt boundaries in aluminium [178]

(with v being the rate and Q, the activation energy of the process), which indicates the activation character of the process.

The dependence of Q and M on orientation is shown graphically in Figs. 72 and 73. It is seen to be non-monotonic.

As regards various lattices, the rate of migration is found to be maximum for the following orientation relationships between adjacent grains: f.c.c. lattices—rotation by 20° and 30-40° about ⟨111⟩; b.c.c. lattices—rotation by 25-30° about ⟨110⟩; c.p.h. lattices—rotation by 30° about ⟨0001⟩.

In f.c.c. lattices, the grain boundaries of least mobility are those whose mutual orientation corresponds to rotation by 60° (or 0°) about the ⟨111⟩ axis which is parallel to them. On the other hand, small deviations from 'singular' orientations cause only slight changes in properties (Figs. 70-73).

Kronberg and Wilson [179] and later V. I. Arkharov [180] have shown that if the lattices of two identical crystals are made coincident and one of them is then rotated relative to the other about a particular crystallographic direction, then at definite discrete values of the angles of rotation part of the atoms in both lattices will occupy

common positions which are called coincidence sites. These common sites form, as it were, a tridimensional 'superlattice'.

For instance, if two f.c.c. lattices are brought into coincidence and one of them is rotated about the common ⟨111⟩ direction by 38.2°, the position of every seventh atom in the new orientation will coincide with its position before rotation, as shown in Fig. 74. Accordingly, if two crystallites are found to be in the positions corresponding to this rotation, every seventh atom on the boundary between the crystallites will belong to both lattices. So that other atoms at the boundary (in an immobile lattice) will occupy the positions answering to the new orientation, it is sufficient that they move through distances smaller than the interatomic spacings, as shown in Fig. 74. Such boundaries (or orientations) are also called *coincidence boundaries.*

A 'superlattice' is also termed a coincidence-site lattice. It is characterized by the ratio of the sites in the main lattice per site in the coincidence lattice. In the example shown in Fig. 74, this ratio is $\Sigma = 7$. The lowest value of Σ is three.

It is clear that the number of coincidence sites grows and the boundary energy diminishes with a decrease in Σ. McLean [181] has found that for high-purity copper the energy of coincidence boundaries is 0.2-0.26 and that of randomly oriented boundaries is 0.32 of the surface energy of the {100} plane. Twin boundaries also belong to boundaries of low ratio Σ. Table 12 gives the values of

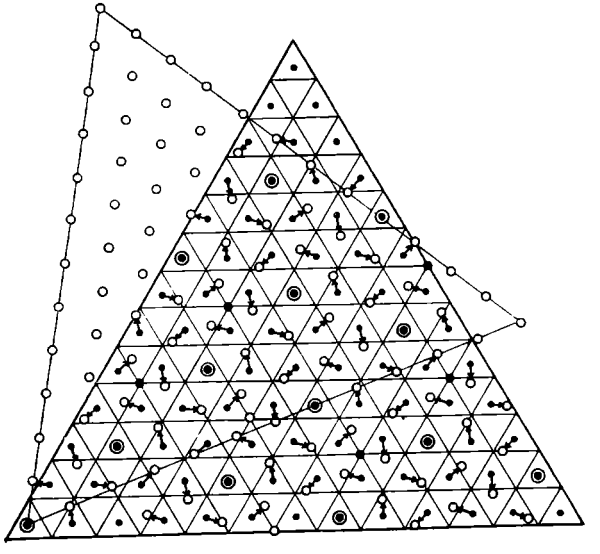

Fig. 74. Arrangement of the atoms in (111) planes that belong to two f.c.c. lattices rotated 38.2° one relative to the other about ⟨111⟩ [179]

TABLE 12. The Degree of Coincidence of Lattice Sites, Σ, and the Corresponding Orientation Relationships [46] in F.C.C. and B.C.C. Lattices

Rotation axis	Minimum angle of rotation, degrees	Σ	Rotation axis	Minimum angle of rotation, degrees	Σ
⟨100⟩	36.9	5	⟨211⟩	180	3
	28.1	5		101.6	5
	22.6	5		135.6	7
⟨110⟩	70.5	3	⟨311⟩	146.4	3
	38.9	9		154.2	5
	50.5	11		67.1	9
⟨111⟩	60.0	3	⟨411⟩	180.0	9
	38.2	7		129.6	11

Σ for certain coincidence boundaries and the corresponding directions and angles of rotation.

It was only over ten years later that the conception of Kronberg and Wilson received proper recognition. At the end of 1950's, Aust and Rutter [182] utilized it to explain the different rate of migration of differently oriented boundaries in lead crystals with a controlled content of impurities (tin). Boundaries with misorientation angles close to 23° or 36-42° relative to the ⟨111⟩ axis and also those with misorientations close to 23°, 28° or 37° relative to the ⟨100⟩ axis (i.e. corresponding to the angles given in Table 12) were found to migrate in the presence of impurities much more quickly than randomly oriented boundaries. The difference in migration rates grew with an increased content of tin (Fig. 75) and with a decrease in temperature.

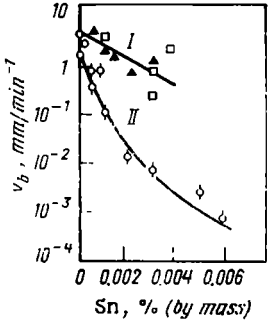

Fig. 75. Effect of tin concentration on the rate of boundary migration, v_b, in lead [182]

I—partially coherent (singular) boundaries; *II*—arbitrary boundaries

In zone-refined lead, the mobility of coincidence boundaries at 175°C is higher than that of common boundaries, but the rates of migration are equalized at 300°C.

From the observations of Aust and Rutter, coincidence boundaries in very pure metals migrate no quicker than common boundaries (see Fig. 75).

One may infer from this fact that coincidence boundaries are less receptive to impurities than common boundaries. They have a higher migration rate not because they are more mobile by their structure. The matter is that impurities retard the

migration of the former boundaries more heavily than the migration of the latter. In a direct experiment on a lead tricrystal containing two 'random' boundaries and one coincidence boundary Gleiter [183] has shown that an addition of copper lowers the energy of the random boundaries more strongly than that of the coincidence boundary.

According to McQueen and Jonas [201], the effect of segregation of impurity atoms must be more pronounced on boundaries with a stronger long-range stress field. In turn, the extent to which stress fields exert their effect depends mainly on the structure of boundaries (see later).

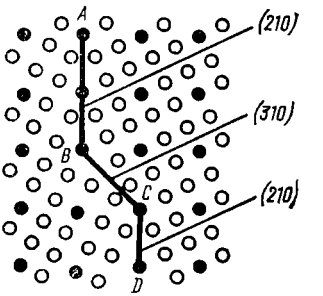

Fig. 76. The shape of a large-angle boundary with a slight deviation from a coincidence plane with a low value of Σ

On the other hand, as seen from Fig. 75, the effect of retarding the migration of random boundaries comes to a 'saturation' point at relatively high concentrations of an impurity, and, therefore, the difference in the mobility of various types of boundary should evidently disappear. There are no systematic data in the literature on how large is this difference when the concentration of an impurity is above the solubility limit. It may be supposed that in the general case the effect of segregates on the mobility of random boundaries will again be stronger than on the mobility of coincidence boundaries. Thus, the problem of the effect of impurities on the mobility of various boundaries in a wide range of impurity concentrations still requires a more detailed examination.

In the above-mentioned cases, we have made a clear distinction between singular and random boundaries, taking into account only the lattice misorientation for adjacent atoms, i.e. only three degrees of freedom out of the five. Under real conditions, the orientation of the boundary plane relative to the close-packed planes S_{cl} in the coincidence lattice is also essential. A boundary may be oriented so that its plane forms a definite angle with the plane S_{cl}. In that case, according to Brendon's model [46, 47], the boundary will have a stepwise form.

In Fig. 76, the plane of the boundary passes along the line $ABCD$ whose sections AB and CD lie within S_{cl}, while the length of section BC, which does not belong to that plane and whose structure cannot be described by means of partial dislocations, depends on the distance between neighbouring S_{cl} planes. Therefore, such a boundary consists of portions of good and poor coincidence and in that respect is similar to a boundary described by Mott's islet model [45, 46].

An advantage of Brendon's model is that it admits the appearance of slight deviations from the ideal arrangement of a boundary in the plane of coincidence sites compensated by dislocations, without any sharp change in the properties of the boundary. These dislocations are commonly called grain-boundary dislocations. It is clear that such compensating dislocations introduce local disturbance in the atom arrangement and therefore produce local elastic distortions.

Twin boundaries are another type of boundaries often found in recrystallized materials. The boundaries of twins are evidently formed here not only by the planes belonging to a system of deformation twins (see Table 3), but also by some other planes with a high density of coincidence sites, i.e. with a low value of Σ.

If a boundary plane between grains coincides with a twin boundary, the boundary is coherent. Its energy is very low (3-10% of the energy of random large-angle boundaries). The boundary is virtually sessile and makes no place for easy diffusion. Nor is it usually decorated by disperse phase particles and therefore is seldom revealed by common etching.

Twins always have both coherent and incoherent boundaries. The latter are boundaries whose plane is tilted by a certain angle φ from the twinning plane. The result is that protrusions (similar to those in Brendon's model) are formed on the boundary. They are essentially partial dislocations (called twinning dislocations) the Burgers vector of which depends on the distance between neighbouring twinning planes (see Fig. 76).

Because of the low energy of twin boundaries, random large-angle boundaries can under favourable conditions change to twin boundaries in the course of grain growth or secondary recrystallization. Such cases will be discussed later.

Annealing twins are found most often in recrystallized f.c.c. metals. The sole exception is obviously aluminium due to its high stacking fault energy γ_{sf}. Since the energy of a twin boundary is equal to approximately one half the stacking fault energy, the probability of twin formation decreases with increased values of γ_{sf}.

The coincidence site model was later improved and developed by Bishop, Chalmers and Gleiter [184, 183, 47].

The improved model, called initially by Gleiter the structural unit model [184, 183] and later the repetition segment model [47] is an important contribution to understanding the atomic structure of boundaries. Its essence is as follows.

As noted earlier, the strength of interatomic bonds at a boundary is of the same order of magnitude as in the crystal bulk. It follows that atoms in boundary layers should be arranged in such a manner and at such distances from one another as to enable the boundaries to have the least energy and the highest strength.

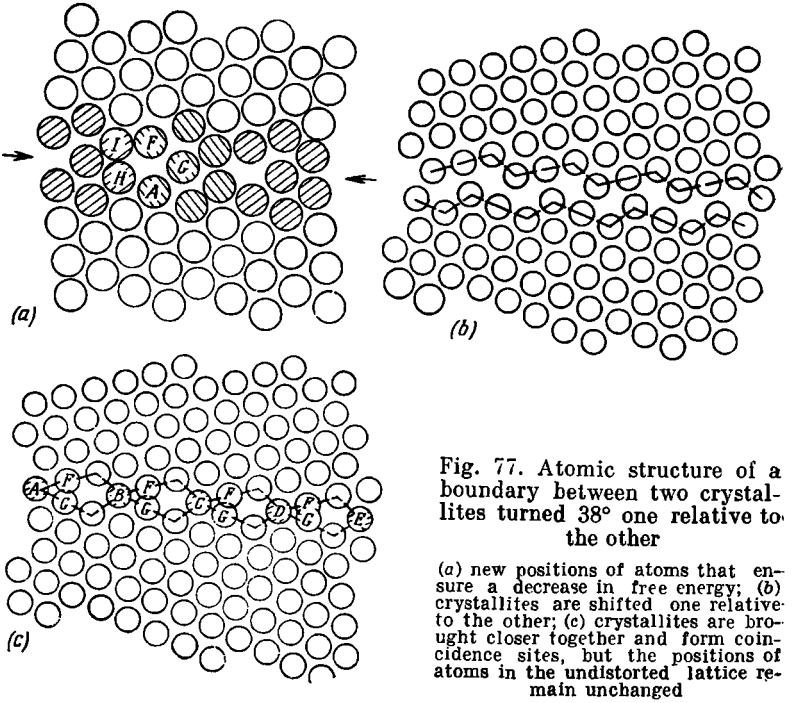

Fig. 77. Atomic structure of a boundary between two crystallites turned 38° one relative to the other

(*a*) new positions of atoms that ensure a decrease in free energy; (*b*) crystallites are shifted one relative to the other; (c) crystallites are brought closer together and form coincidence sites, but the positions of atoms in the undistorted lattice remain unchanged

Gleiter [183] has calculated by means of an electronic computer the energy of the system for various arrangements of atoms. The structure of a boundary with the least calculated free energy is shown in Fig. 77*a*. It has a typical periodicity in the arrangement of atomic groups. This structure can be obtained from an original structure (Fig. 77*b* and *c*) by slight displacement of the crystallites relative to one another and by subsequent slight relaxation displacement of individual atoms in the boundary proper.

Thus, the coincidence-site model in its virgin form cannot ensure a minimum of the energy of a boundary and therefore the sole fact of appearance of coincidence sites cannot be characteristic of coincidence boundaries. According to Gleiter [183], coincidence groups can exist if there is a definite periodicity in the arrangement of atomic groups in a boundary. The author has emphasized that these groups must contain a small number of atoms and the arrangement of these atoms in a group should closely resemble that in the bulk of a crystallite. Such a group of atoms, which is periodically repeated in a boundary, has been initially called a structural unit and later a repetition segment.

In rare cases, when a boundary is perfectly symmetrical, it is formed of repetition segments of the same type. With an orientation

relationship corresponding to a different discrete number of coincidence sites, a boundary will be formed by repetition segments of another type (Fig. 78).

With a definite deviation from the ideal orientation, a boundary will be constructed of a mixture of segments (taken in a certain proportion) whose orientations repeat the nearest ideal orientations. This fact explains well why the properties of a boundary vary gradually rather than jumpwise when its orientation deviates from the ideal one.

This mechanism of formation of random boundaries causes distortions (strains) and the appearance of long-range stress fields in the lattice of crystallites, which play an important part in the interaction between random boundaries and impurities.

The model discussed can be applied quite widely.

The model represents a boundary as a region with an elevated concentration of vacancies. Indeed, as seen from Fig. 77*c*, the region surrounded by atoms *A*, *G*, *F*, *I*, and *H* (Fig. 77*a*) has a higher unit volume than the perfect crystal.

The model enables us to regard a boundary as a system of stepon atomic planes. The stepwise shape of boundaries (which has attracts ed the attention of metallurgists only quite recently) must undoubtedly exist and exert influence on the growth of crystallites roughly in the same way as it affects the growth of crystallites from the vapour and liquid phases.

The concept of stepwise shape of boundaries provides a good explanation of a number of important phenomena.

The principal mechanism of growth of crystallites is the movement of individual atoms across the boundary to a growing crystallite. The high value of the activation entropy says in favour of the

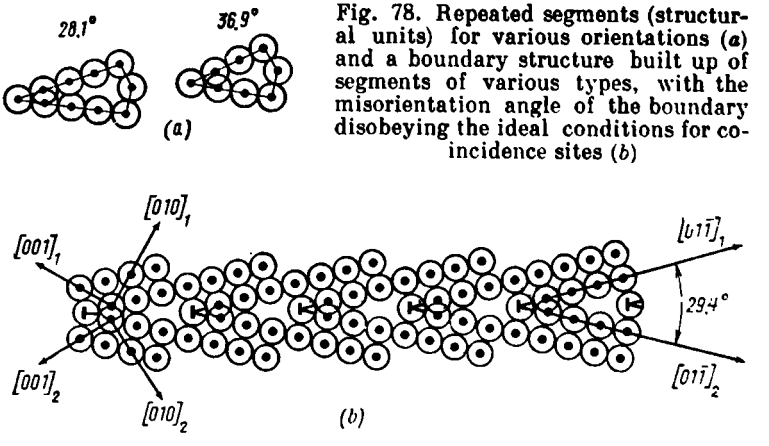

Fig. 78. Repeated segments (structural units) for various orientations (*a*) and a boundary structure built up of segments of various types, with the misorientation angle of the boundary disobeying the ideal conditions for coincidence sites (*b*)

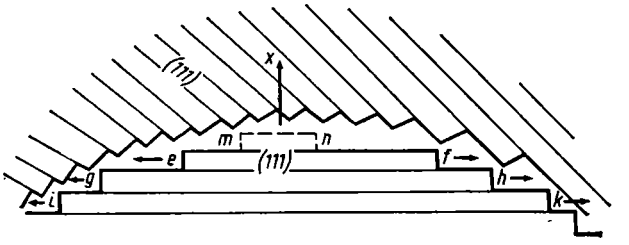

Fig. 79. The growth of a twin through the formation of two-dimensional nuclei and movement of a jog [183]

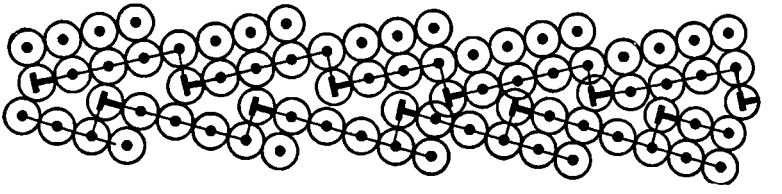

Fig. 80. Grain-boundary dislocations (schematic)

existence of cooperative movements of atoms at the stage of growth, but so far no researcher has managed to demonstrate this directly.

Having analysed the results of electron-microscopic observations of boundary migration in an Al + 0.46% (by mass) Cu alloy, Gleiter [183] concludes that grain boundary migration is realized by the transfer of atoms from steps of one crystallite onto the steps of another. From this standpoint, the author explains why coherent twin boundaries do not migrate, while incoherent boundaries migrate at a high rate.

In f.c.c. metals, coherent boundaries are parallel to the close-packed (111) planes which contain no steps. The mechanism which controls the transfer of atoms from steps of one grain to the steps of another grain is still unclear. Gleiter considered this mechanism by examining a twin boundary (111), but, as follows from the above discussion, a similar mechanism can also be realized when applied to other twins.

Let a portion of boundary be parallel to the (111) planes of a crystallite (the lower one in Fig. 79). For the boundary to migrate upwards, a two-dimensional nucleus (mn) must form on the (111) planes. The nucleus will then grow parallel to (111) through attachment of new atoms to the step thus formed. This cycle of atom transfer must then be repeated many times.

If a nucleus occupies positions which do not correspond to the f.c.c. packing (for instance, if atoms of the nucleus are in positions *C*,

instead of B, on the substrate whose atoms are in A positions), a twin boundary will form.

Thus, the growth of a twin, which externally appears as the migration of a boundary, actually occurs by way of the formation of a two-dimensional nucleus that grows parallel to a coherent boundary (or through migration of an incoherent boundary if we assume that the step is essentially an incoherent boundary).

With the further progress of the theory of grain boundary structure, it has been established that grain boundaries (including large-angle ones) can contain, apart from steps, also grain-boundary dislocations (see Fig. 80).

In this case, grain boundaries are regarded as if consisting of portions of coincidence sites and grain-boundary dislocations.

Grain-boundary dislocations may be either mobile or sessile, depending on their Burgers vector. The former can move along a boundary and play an important part in the process of grain slip on boundaries. The rate of slip usually increases with an increase in the density of grain-boundary dislocations.

The concepts of grain-boundary dislocations have recently been supported experimentally through electron-microscopic examination of boundaries in specially grown bicrystals.

5.2. The Rate of Boundary Migration

A principal problem which has not yet found a clear experimental solution is the problem of whether the migration of boundaries is effected by single non-associated atomic movements across a boundary between adjacent grains (i.e. by diffusion) or by a coordinated interrelated movement of atomic groups (chains). The former view is more popular, though there are certain reasons to suppose that the process may be of a cooperative nature, at least in some particular cases.

Since the frequency of jumps of atoms from one side of a boundary to the other (and vice versa) is different due to a number of factors that go under the general name 'driving force', a flow of atoms appears which results in a directed migration of the boundary.

By analogy with diffusion, the rate of migration in that case is $v = (D_m/RT)\,(\Delta F/d)$, where ΔF is variation in free energy of the system (the driving force of migration); d is the length of a single jump, equal roughly to the interatomic spacing; D_m is the effective coefficient of diffusion in migration; $D_m = Zd^2\nu \exp(-Q_m/RT)$. Here ν is the vibration frequency of atoms; Q_m is the potential barrier an atom overcomes as it moves from the lattice of one grain to that of another grain (the activation energy of the process); and Z is a geometrical factor.

Denoting ΔF referred to one mole by P (driving force) and $(D_m/RT)(1/d)$ by M (boundary mobility), we obtain $v = MP$, i.e. the expression given earlier in Ch. 3.

Thus, the boundary mobility is determined by a parameter having the physical sense of diffusion coefficient. Since atoms jump across a grain boundary, it might be assumed that the magnitude of D_m should be close to that of boundary diffusion coefficient. It should be noted, however, that atomic jumps in common grain-boundary diffusion occur along a boundary, whereas in boundary migration, atoms jump across a boundary. Of importance are also the structure of a boundary, its misorientation, the presence of steps, impurity atoms, vacancies, etc. For that reason, D_m and D_b (boundary self-diffusion coefficient) may differ greatly in value.

The effect of the driving forces which produce a directed and accelerated movement of atoms is also worth mentioning. An analogy with heterodiffusion, which occurs more quickly than self-diffusion, seems to be appropriate here.

According to Einstein, an increased coefficient of heterodiffusion, D, compared to the self-diffusion coefficient D^* is attributed to the effect of a field of forces due to a difference in concentrations. This field can be characterized by a thermodynamic factor $[1 + (d \ln f_1/d \ln \gamma)]$, where f is activity coefficient, and γ is the molar concentration of a diffusing component I.

In that case $D = D^* [1 + (d \ln f_1/d \ln \gamma)]$.

Similarly, the thermodynamic factor for the case of recrystallization is the driving force P of the process, so that the relationship between D_m and D^* should be of the form $D_m = D^*P$.

Experimental determination of migration rates in various materials and under various conditions and, besides, comparison of these rates with the characteristics of diffusion mobility can be useful for better understanding of the mechanism of migration, the structure of boundaries, etc. Some of these problems will be discussed below.

Table 13 gives boundary migration rates determined by various workers at the stages of primary recrystallization and secondary recrystallization (or grain growth). The migration rates were principally determined from the difference in grain size on isothermal annealing; measurements were made at relatively long time intervals since the non-uniformity and sometimes jumpwise variations in migration rate with time were disregarded, the tabulated data are in most cases lower than the actual ones.

In order to obtain migration rates more conformable to the actual values, a series of experiments were carried out on iron, aluminium and Ni + 13% Cr alloy. The results are given in Table 14. As follows from the table, the rate of migration is in most cases one to three orders of magnitude greater than the respective values in Table 13.

TABLE 13. Boundary Migration Rates

Metal	Test temperature, °C	Migration rate observed, cm/s	Source
	Primary Recrystallization		
Al	400	$4.9 \cdot 10^{-4}$	[182]
Al	400	10^{-4}	[224]
Fe_γ	700	$1 \cdot 10^{-3}$	[94]
	Secondary Recrystallization		
Al	500	$2.5 \cdot 10^{-5}$	[185]
Al	500	$5 \cdot 10^{-2}$	
Al	400	$1 \cdot 10^{-3}$	[94]
Fe_γ	900	$8.4 \cdot 10^{-5}$	[186]
Fe_γ	800	$6 \cdot 10^{-4}$	[94]

To compare these results with diffusion characteristics, we have to pass from the boundary migration rates to the corresponding diffusion coefficients.

It is possible to use for the purpose the formula that relates the coefficient of diffusion, D, to an average displacement of an atom, x, in migration during time τ: $D = \bar{x}^2/2\tau$.

TABLE 14. Comparison of Effective Diffusion Coefficients Determined From Grain-boundary Migration Rates with Coefficients of Volume and Boundary Self-diffusion

Metal (alloy)	t, °C	x*, cm	τ_m, s	D_m, cm²/s	D_v, cm²/s	D_b, cm²/s	D_m/D_v	D_m/D_b	Method for determining the grain growth rate
Fe	700	10^{-4}	0.1	$5 \cdot 10^{-8}$	10^{-13}	10^{-10}	10^{5}	10^{2}	Induction heating **
Fe	800	$2.5 \cdot 10^{-2}$	60	$5 \cdot 10^{-6}$	10^{-11}	—	10^{5}	—	High-frequency heating after critical deformation ***
Ni + 13% Cr	1050	$5 \cdot 10^{-2}$	60	$2 \cdot 10^{-5}$	10^{-10}	—	10^{5}	—	Emission microscopy
Al	450	10^{-3}	1	10^{-8}	10^{-12}	—	10^{4}	—	Polarized-light observation

* x = boundary migration length.
** By the time of appearance of first recrystallization nuclei.
*** By enlargement of grain size.

In common diffusion, x is the average depth of penetration of a diffusing substance. In grain boundary migration, x may be taken as the length of boundary migration in time τ. The diffusion coefficient so calculated and denoted D_m should be regarded as a conditional diffusion coefficient, i.e. the one that would have to be if the growth of recrystallization nuclei and the migration of grain boundaries should occur by common diffusion.

The calculated values of diffusion coefficients D_m are given in Table 14. Besides, the table gives the coefficients of common volume diffusion, D_v, and of boundary diffusion, D_b, for the same metals and temperatures, and also the ratios D_m/D_v and D_m/D_b. The coefficient D_m is five or six orders of magnitude greater than the volume diffusion coefficient and two or three orders of magnitude higher than the boundary diffusion coefficient. The tabulated rates of grain growth are closer to the actual values at the moment of migration, but nonetheless they are on the conservative side, too, and hence the actual discrepancy between D_m and D_v (or D_b) is even greater.

The high values of D_m point to the high driving forces that add to atom mobility in recrystallization.

It is clear that changes in the driving force P and in the mobility D^* proper, which result from the conditions of deformation and heating, the nature of alloying, the type of lattice and other factors, may disturb the strict correlation between D_m and D^* in undeformed metal.

In addition to the absolute rate of migration, the activation energy of the process, Q_m, and the preexponential V_0 are also important parameters of the boundary migration process.

The values of Q_m are given in many research works. The scatter of these values may be quite large depending on metal purity, conditions of deformation, etc. (for more detail see Ch. 11). We will only note here that Q_m is lower in more pure metals, where it approaches the value of the activation energy of boundary self-diffusion. In the general case, the diffusion of single atoms is obviously the actual elementary act that controls the process of migration.

On the other hand, the values of the preexponential do not agree with the assumption that diffusion of single atoms is the principal mechanism of the process. In all cases the preexponential is excessively high.

The values of V_0 are especially high (a few orders of magnitude greater than would be expected theoretically) at enhanced driving force of migration (at the stage of primary recrystallization). But even at low values of P, the calculated value of V_0 exceeds the theoretical limit (Table 15).

As follows from Gleiter's theoretical analysis [187], such high values of V_0 can be justified if the principal elementary process of boundary migration is coordinated by atomic movements.

TABLE 15. Boundary Migration Parameters of Pure Metals

Metal	Characteristic of specimens. Recrystallization stage	P, dyne/cm^2	Q_m, kcal/g-at.	V_0, cm·s^{-1}	
				experimental	calculated (max.)
Al	Polycrystal. Primary recrystallization	$1.7 \cdot 10^7$	15.0	$2 \cdot 10^6$	$4.3 \cdot 10^3$
Al	Single boundary. Polygonized substructure	$8.4 \cdot 10^3$	13.0	1.6	2.1
Ni	Polycrystal. Primary recrystallization	$6 \cdot 10^7$	30.1	$6 \cdot 10^6$	$5.4 \cdot 10^3$
Pb	Polycrystal. Grain growth	$6 \cdot 10^3$	6.0	0.4	0.2

The concentration of vacancies is usually named among the factors which influence boundary mobility, though there are no convincing experimental results in support of this view. Lücke et al. are disposed to believe that vacancies are indeed responsible for a sharp decrease in the temperature of recrystallization of a material after its deformation at the temperature of liquid nitrogen rather than at room temperature. Other workers explain the decreased rate of migration during isothermal annealing by the removal of vacancies. This is not, however, the sole probable explanation.

In all the cases relating to the effect of vacancies, it is emphasized that what is actually meant is the effect of vacancies on boundary mobility. It is thus implied that vacancies have no noticeable effect on the driving force of the process and on the direction of movement (except for the case of growth of nuclei at the stage of primary recrystallization).

What are actual driving forces of boundary migration at various stages of recrystallization?

In the case of primary recrystallization, the principal stimulus for the growth of nuclei, as has been given in Chs. 3 and 4, is the difference between the volume density of structure defects (both linear and point defects) in the nuclei and in the surrounding deformed matrix. A boundary moves towards a higher density of defects, absorbs these defects and leaves behind a relatively pure material. The direction of movement of the boundary of a nucleus in primary recrystallization, at least until mutual collisions begin, is not related directly with the position of the centre of curvature of that boundary.

In our view, the elevated rate of growth in primary recrystallization is also due to an increase in the concentration of vacancies, which takes place at the early stages of this process (see Ch. 4), and thus to an increase in the mobility of boundaries, i.e. the value of D^*.

5.3. The Effect of Grain-Boundary Tension

Most workers hold that the effect of grain-boundary tension in primary recrystallization may be neglected. By McLean [45], this effect is negligible compared with the effect of volume elastic energy. Mehl, Avrami [127], and some other researchers [48] also neglected this energy in developing the formal theory of recrystallization rate (see Ch. 4). But these authors gave no experimental evidence in support of this view and, in their reasoning likened the process to phase transformations.

Smith, McLean *et al.* have shown that grain-boundary tension has a decisive role in grain growth. As a rule, it is assumed that the driving force of the process in this case is the trend of the system to decrease the total grain-boundary energy, i.e. to shorten the total length of boundaries.

Proceeding from this standpoint, we have to admit that grain growth must culminate in the disappearance of grain boundaries and the transformation of a specimen into a single crystal.

Experience shows however that even in the absence of disperse phase particles on grain boundaries grain growth practically comes to an end when a specimen still remains polycrystalline. The structure proves to be quasi-equilibrium, though its energy is not at the minimum.

As has been shown by Smith [175] and some other workers, the nature of equilibrium microstructure of a metal (the shape of grains) can be explained by using the concept of the balanced grain-boundary (surface) tension γ_b (unit free grain-boundary energy) of adjoining boundaries.

As is known, the effect of surface tension on the equilibrium shape of particles in a given volume manifests itself in that the sum of products $\sigma_i S_i$ (where σ_i is the surface tension for a certain face of a particle and S_i is the area of that face) acquires the lowest value at a constant volume of the particle: $\sigma_{tot} = \Sigma \sigma_i S_i \rightarrow \min$.

This explains well why a droplet of a liquid at the boundary between the other two immiscible liquids has a lenticular shape.

For polycrystals, the condition of an equilibrium shape of crystallites is met when the vector sum of the grain-boundary tension coefficients laid in a plane normal to the common edge of three intercepting prismatic grains is equal to zero.

Let two of the three adjoining grains (Fig. 81) belong to phase α and one to phase β. Let the grain-boundary tension at a boundary between differently oriented α-crystallites be denoted as $\gamma^1_{\alpha_1\alpha_2}$ and the interphase tension at the boundaries between α- and β-crystallites as $\gamma_{\alpha_1\beta}$ and $\gamma_{\alpha_2\beta}$.

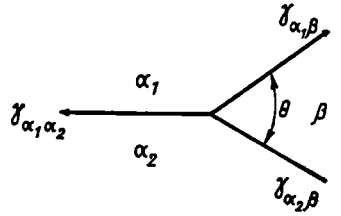

Fig. 81. Vector representation of grain-boundary tension on boundaries in a triple joint

Based on the equilibrium conditions, we project all the coefficients onto the $\gamma_{\alpha_1\alpha_2}$ direction and equate to zero their vector sum:

$$\gamma_{\alpha_1\alpha_2} - \gamma_{\alpha_1\beta}\cos(\theta/2) - \gamma_{\alpha_2\beta}\cos(\theta/2) = 0$$

Since $\gamma_{\alpha_1\beta} = \gamma_{\alpha_2\beta}$, $\gamma_{\alpha_1\alpha_2} = 2\gamma_{\alpha\beta}\cos(\theta/2)$, we have

$$\gamma_{\alpha\beta}/\gamma_{\alpha\alpha} = 1/[2\cos(\theta/2)] \qquad (10)$$

i.e. the interfacial angle θ characterizes under the equilibrium conditions the ratio between surface tensions at the boundaries of grains belonging to the same phase and at the boundaries of grains of various phases.

Substituting various actual values of θ into formula (10), we can determine the ratio of the coefficients $\gamma_{\alpha\alpha}$ and $\gamma_{\alpha\beta}$ corresponding to a given angle θ.

In recrystallization, adjoining grains belong to a single phase, say α. Neglecting the anisotropy of grain-boundary energy, which is admissible when dealing, for instance, with cubic-lattice metals and alloys, we find that $\gamma_{\alpha\alpha} = \gamma_{\alpha\beta}$. The equilibrium angle θ can then be found from the equality $\cos(\theta/2) = 0.5$, whence $\theta = 120°$. Thus, the surface planes of equilibrium grains in a single-phase isotropic alloys must join at angles of 120°.

Therefore, in a single-phase alloy having practically an isotropic grain-boundary energy and straight boundaries, the only grains that can be in equilibrium are the grains in which the number of sides in a section is equal to six ($n = 6$). Grains with the number of sides less than six must have convex boundaries in order to form angles of 120° in triple joints, and grains where the number of sides is more than six must have concave boundaries (see Fig. 82).

Since the position of atoms on the concave side of a boundary is more stable than on the convex one, the frequency of atomic jumps onto the concave side is greater than otherwise; the result is that the boundaries between grains of a single phase usually migrate towards their centres of curvature as they tend to equilibrium. This is why grains with the number of sides more than six must grow during boundary migration toward the outside and those with the number of sides less than six must disappear as the boundary migrates inside the crystallite (see Fig. 82). It also follows from the above that joints of more than three boundaries are unstable.

The angles θ are practically measured in plane sections (microsections), which results in a certain scatter of the found values. The actual angle θ is equal to the angle which is found most often in microsections [188]. This makes it possible to find actual angles θ on the

curve of statistical distribution of the measured values of θ_i.

The rate of variation of an angle towards the equilibrium is at a maximum at the beginning of annealing, then decreases. A migrating non-equilibrium joint exerts a drag on a boundary. Apart from angular conditions, the magnitude of γ_b can also influence the rate of growth; the rate of migration grows with increased values of γ_b.

Up to this point, we neglected the anisotropy of γ_b. It should be emphasized in this connection that the above-mentioned conditions for an equilibrium structure ($\theta = 120°$ and $n = 6$) are only true for substances in which the anisotropy of grain-boundary tension may be neglected. As a rule, these are cubic-lattice materials. For materials of a lower symmetry, the anisotropy of γ_b may be substantial and cannot be neglected. As has been checked experimentally, the equilibrium values of angle θ, the shape of grains, and the number of their faces differ appreciably from those observed in isotropic structures.

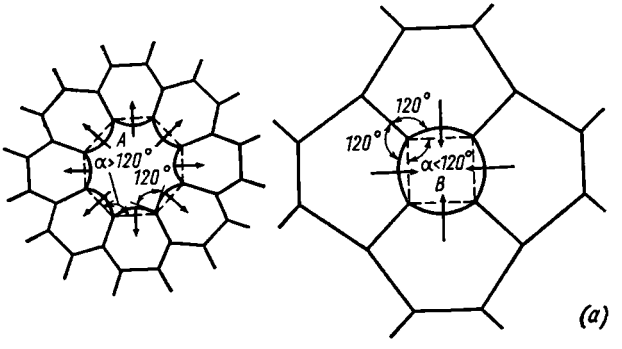

Fig. 82. Concave boundaries of grain *A* (more than six faces) and convex boundaries of grain *B* (less than six faces)

(*a*) scheme (arrows indicate the direction of boundary migration); (*b*) microstructure of nickel alloy, ×300

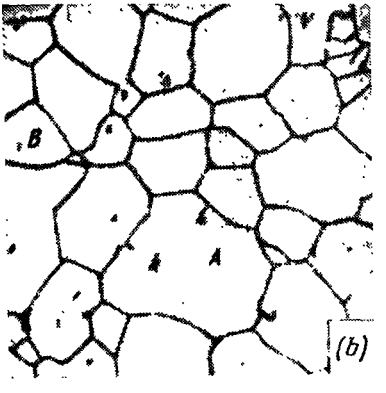

An important problem of the atomic mechanism by which grain-boundary tension forces come to an equilibrium still remains unclarified. Some authors [189] hold that equilibrium is established owing to a different mobility of atoms on surfaces of various curvature; others attribute it to boundary 'creep' of atoms; and still others to plastic deformation arising due to grain-boundary tension. None of these assumptions has been verified experimentally.

In our view, the vacancy mechanism of boundary migration under the action of unbalanced forces of grain-boundary tension, as proposed by B. Ya. Pines [145], seems to be most convincing. According to that concept, the convex portions of adjacent crystallites on a boundary are compressed and the concave ones are tensioned. Accordingly, there is a deficiency of vacancies in the former and an excess in the latter, so that a flow of vacancies exists from the latter to the former and a flow of atoms in the reverse direction. In that case, boundary migration can be regarded as a directed movement of atoms whose driving force is the resultant of the grain-boundary tension of adjoining boundaries.

It is difficult to make a quantitative estimation of the effect of grain-boundary tension in boundary migration, compare it with other influences, and show how this effect changes in alloying, since there are no reliable data on the magnitude of γ_b for metals in solid state and particularly for alloys.

By the end of primary recrystallization, not all grains (and not all simultaneously) come to a state in which their angles θ are equal to 120° and the number of their sides to six. This occurs gradually in the course of subsequent grain growth. If a grain collides with a growing adjacent grain, the equilibrium of its grain-boundary tension is often disturbed, which provides a new impulse for accelerated local migration of boundaries adjacent to the unbalanced joint. Boundaries are less stable and migrate faster with a greater deviation of their angles from 120°.

Figure 83 gives a typical example which illustrates the nature of boundary movement during grain growth in aluminium. The figure shows the successive positions of the boundaries which have been revealed owing to alternate operations of annealing and electrolytic etching with the application of anodic films (polarized-light photographs).

In the original state, grains A and C are in intimate contact along the common boundary 1-2, while grains B and D have no common boundary. The angles α and β are respectively 90° and 80°. In the course of annealing, grains B and D grow towards each other and the angles α and β approach 120°. The rate of boundary migration at a joint with a less equilibrium angle β is higher than with angle α. As grains B and D come in contact, the boundary 1-2 between grains A and C disappears and the number of faces of these grains according-

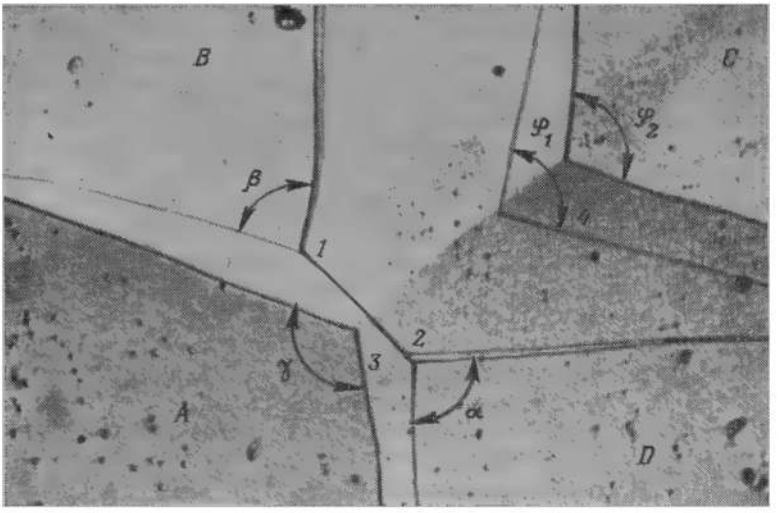

Fig. 83. Grain boundary migration during grain growth in aluminium, stimulated by the tendency to balance out the grain-boundary tension in grain joints. Polarized-light microphotograph showing intermediate positions of boundaries, ×400

ly diminishes by one. Now, four boundaries intersect in one point of the microsection plane. Two new angles have formed, γ and φ, with γ being close to 120°. This quadruple joint is unstable, so that the movement of joints and boundaries continues. There appears a new boundary 3-4 between grains *B* and *D*. The angles α and β become equal to 120° and φ approaches this value. As may be seen from Fig. 83, the angle φ_1, equal to 100°, has changed to $\varphi_2 = 110°$.

The rates of boundary migration at the two new joints with the angles γ and φ turn out to be sharply different. The boundaries at the joint with angle γ, which is close to 120°, have moved very little, roughly by 50 μm, whereas the rate of migration at the joint with angle φ, which is far from equilibrium ($\varphi \ll 120°$), is 15-18 times higher and the boundaries have moved roughly through 750 μm.

This example shows that the rate of boundary migration in grain growth can vary in various directions by a factor of a few tens due to unbalanced grain-boundary tension.

Thus, *unbalanced grain-boundary tension is one of the most important conditions for realizing the effect of the driving force of the process that tends to shorten the length of boundaries.* Vacancies and the gradient of their concentrations on both sides of a migrating boundary undoubtedly accelerate boundary migration. This gradient, however,

is due to an unbalanced grain-boundary tension which determines the direction of migration.

Consider the nature of boundary migration in primary recrystallization. Figures 39 and 54 show the structures of respectively nichrome and transformer steel with recrystallization nuclei in such a state that they have time to grow to a size of a few micrometres.

As may be seen, there is a sharp anisotropy of the rate of growth of nuclei. In many cases, the rate of growth is at a maximum along a boundary and at a minimum crosswise. The rates in these two directions differ by a factor of 3 to 4, so that isolated nuclei formed at a boundary between two grains have a lenticular shape (see Fig. 39) and nuclei formed in triple joints, the shape of convex tetrahedrons. These forms satisfy the conditions of the least surface energy.

Volume energy is the principal driving force of growth of nuclei at the stage in question. This is confirmed by the fact that all boundaries of nuclei migrate away from their centres of curvature. Anisotropy of the rate of growth is obviously due, in the first place, to a non-uniform distribution of the volume energy, which is caused by a difference in the density of defects along the boundary and in various directions in the bulk of the original grains. A regular lens-like shape of nuclei may be due partially to the effect of grain-boundary energy. At an early moment of formation, nuclei cannot have such a regular shape.

As noted earlier, the effect of grain-boundary energy on the rate of primary recrystallization is usually neglected. This neglect seems however to be unfounded in the light of the experimental results that will be discussed below.

Figures 84 and 85 show the successive positions of recrystallization nuclei on a boundary between two original grains before, at the moment of, and after collision. Upon collision of nuclei *3* and *4*, further migration along the original boundary is stopped. No nuclei can grow at the expense of others as long as the deformed state exists. The direction of the highest rate of growth becomes normal to the original boundary, i.e. rotates by 90°. A new boundary then forms between nuclei *3* and *4*, which is usually straight at that stage. This fact is typical of the process and confirms the conclusion that all nuclei have the same volume energy; this also points to the trend of the system to minimize the grain-boundary energy and equalize the grain-boundary tension.

That boundary migration is indeed accelerated somewhat at points of collision can be confirmed by considering the fact that new angles (such as in grains *1* and *2*, Fig. 85*a* and *b*), being initially equal to 130-140° at the moment of collision, increase in further boundary migration up to 150-170°.

The fact that an angle increases and differs more and more from 120° can obviously be explained as follows. Since the volume ener-

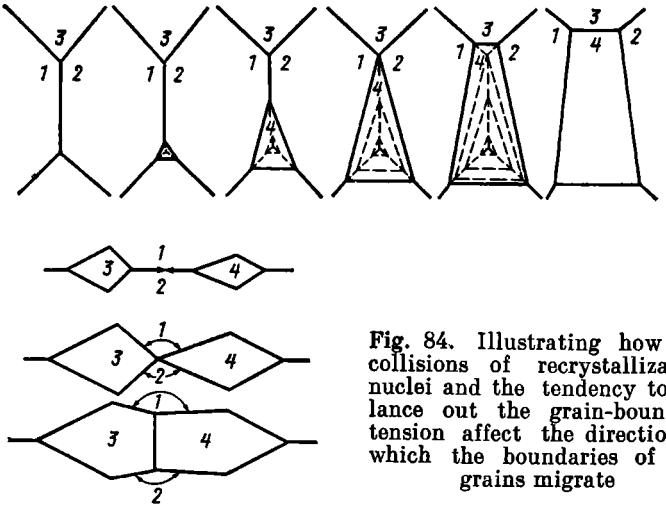

Fig. 84. Illustrating how the collisions of recrystallization nuclei and the tendency to balance out the grain-boundary tension affect the direction in which the boundaries of new grains migrate

gies of growing nuclei and the deformed matrix are different, the two media can be regarded thermodynamically as two different phases. As follows from equation (10), however, γ_b at the boundary between different phases is greater than that at a boundary between two grains of the same phase. In that case, the $\gamma_{\alpha\beta}/\gamma_{\alpha\alpha}$ ratio should be greater than unity and the corresponding angle θ should be greater than 120°.

Because of multiple collisions, nuclei change their initial shape to a polygonal (in cross section). Thus, collisions of nuclei can result in a local acceleration of boundary migration and formation of new boundaries under the effect of unbalanced grain-boundary tension. This factor may be quite essential, since the frequency of collisions of nuclei at the stage of primary recrystallization is especially high.

Consequently, the rate of boundary migration during annealing after primary recrystallization (and therefore the rate of grain growth) should be higher when the grain-boundary tension in grain joints is more unbalanced. This is confirmed by the results of analysis of the rate of grain growth in Fe-W and Fe-Si alloys given below.

Specimens of an age-hardening Fe-W alloy deformed 10% and 50% were heated for 3 min at 1300°C. According to the data of X-ray structural analysis, this temperature corresponded to the end of primary recrystallization. The structure upon 10% deformation was less balanced. The most probable number of faces per grain in specimens was 4.75 for 10-% deformation and 5.45 for 50-% deformation. Accordingly, grain angles in the former deviated more from the equilibrium value (Fig. 86).

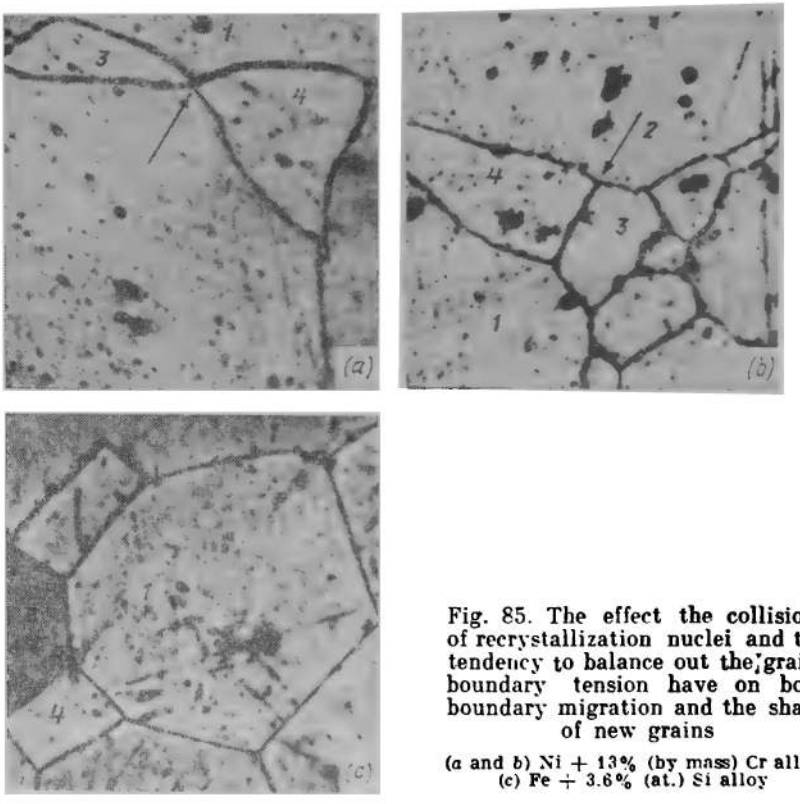

Fig. 85. The effect the collisions of recrystallization nuclei and the tendency to balance out the grain-boundary tension have on both boundary migration and the shape of new grains

(*a* and *b*) Ni + 13% (by mass) Cr alloy; (c) Fe + 3.6% (at.) Si alloy

Specimens were then heated at 1300°C for a longer time and the rate of growth was determined by the maximal grain size obtained after various periods of holding. Though after a 3-minute heating the absolute grain size was greater in 10-% deformed specimens, the rate of further growth also proved greater in the same specimens (0.051 mm/min against 0.042 mm/min for 50-% deformed specimens). Thus, with a lower absolute grain-boundary energy (smaller length of boundaries), the rate of grain growth turned out to be higher in the structure with a less balanced grain-boundary tension.

The results of the analysis of grain growth rate in Fe-W and Fe-Si alloys at 1300°C have shown that the grain-boundary tension and its disbalance may under certain conditions have a greater effect on the process rate than diffusion mobility. The coefficient of diffusion of silicon in iron at 1300°C exceeds by more than one order of magnitude that of tungsten in iron. The rate of self-diffusion of iron in Fe-Si alloy is also substantially higher than in Fe-W alloy. It might be expected, therefore, that the rate of grain growth in Fe-Si

alloy would be noticeably higher than in Fe-W alloy. An opposite result was however obtained in the experiments. At 1300°C (Fig. 87), the average size of grains by the beginning of grain growth was approximately the same in both alloys, but the grain size distribution and the balance of grain-boundary tension in joints were different. The structure in Fe-W alloy was less balanced than that in Fe-Si alloy, since growth of grains at the early stages of recrystallization was retarded by unevenly distributed Fe_2W particles which later dissolved fully at 1300°C. For that reason, isothermal annealing at 1300°C produced a relatively balanced structure in Fe-Si alloy much quicker than in Fe-W alloy. Therefore, the rate of growth in the former was correspondingly lower. In the time interval of 3 to 22 minutes the rate of growth in Fe-W alloy was found to be four times that in Fe-Si alloy (0.042 mm/min against 0.009 mm/min).

As noted in Ch. 3, many workers have observed a peculiar and still unclear phenomenon: the rate of growth in the course of primary recrystallization often remains actually constant during isothermal annealing. This phenomenon was first described by R. Karnop and G. Sachs and later confirmed in a number of studies. The rate of growth was found to decrease with time only in tin. It is also known that prior recovery, which increases the incubation period, has practically no effect on the rate of growth of nuclei in primary recrystallization. This has been demonstrated by M. O. Kornfeld, V. A. Pavlov, J. K. Stanley, R. F. Mehl, etc. The nature of this phenomenon is still unclear. Proceeding from the assumption that the volume strain energy is the driving force of this growth, one would expect that the rate of growth during primary recrystallization should gradually diminish as a result of the process of recovery that simultaneously takes place in the still unrecrystallized mate-

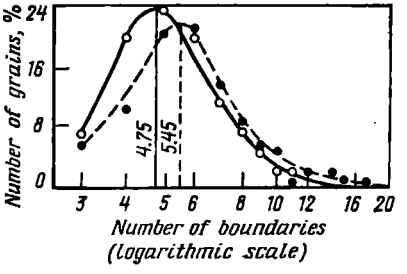

Fig. 86. Grain distribution according to the number of boundaries by the end of primary recrystallization in Fe-W alloy deformed 10% (white circles) and 50% (black circles)

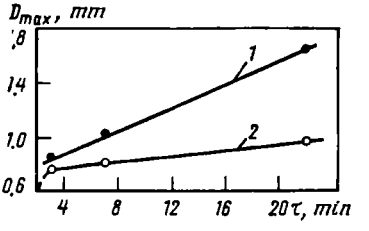

Fig. 87. Effect of heating time (at 1300°C) on the maximum size of grains in Fe-W (*1*) and Fe-Si alloy (*2*) of the same concentration (3.6 atomic per cent) of the second element. The rate of grain growth is 0.042 mm/min and 0.009 mm/min respectively

rial. Since this is not the case, the constant rate of growth can partially be attributed to the generation of vacancies in primary recrystallization. A constant rate must facilitate boundary migration of nuclei.

On the other hand, the effect of unbalanced grain-boundary tension, which continuously acquires new stimulating pulses in the course of primary recrystallization (due to random collisions), cannot be neglected. From this standpoint, the growth of recrystallization nuclei can be regarded as a process which compensates by itself a loss in its rate. This self-compensating effect should be greater at higher values of γ_b. This fact can probably explain the results obtained for tin where the rate of grain growth decreases with time (in contrast to other metals, say, aluminium). The available data indicate that $\gamma_{Sn} \ll \gamma_{Al}$ (160 and 625 erg/cm^2 respectively).

The data on the grain growth rate in Fe-W and Fe-Si alloys also agree well with this conclusion.

That the absolute rate of growth in primary recrystallization is higher than in the grain growth process can be explained well if we recall that the driving force due to a difference in volume energies is higher than that due to grain-boundary energy. Besides, in primary recrystallization, the effect of grain-boundary tension is added to the effect of volume distortions, whereas in grain growth the grain-boundary tension is actually the sole driving force of the process.

These results indicate also that the recrystallization rate relationships derived by Mehl and Avrami [48] on the basis that the process is similar to phase transformations, do not reflect properly the specifics of the recrystallization mechanism since they proceed from the conditions not found in recrystallization. Sites of formation of nuclei have a sharply expressed selective rather than a statistical character, and the rate of growth of nuclei is anisotropic and varies in a complicated manner with time. In view of the high complexity of these phenomena and the multitude of the affecting factors, it is as yet impossible to give a universal quantitative description of the rate of recrystallization.

The effect of grain-boundary tension is responsible for another frequently encountered phenomenon of high practical importance: the interaction of grain boundaries with undissolved impurities (inclusions) which retard their migration (see Chs. 3 and 4). The retarding force P_{br} (see p. 92) attenuates the effect of the driving force of migration, P_{dr}. With $P_{br} > P_{dr}$, migration is stopped. With $P_{br} < P_{dr}$, however, a boundary migrates in a peculiar jumpwise manner; migration of the boundary is retarded locally when it encounters a particle of inclusion and then is accelerated sharply as the boundary bows around that obstacle. Examples of such type of migration in aluminium and nichrome are shown in Figs. 88 and 89.

With aluminium (Fig. 88), a boundary approaches an undissolved particle (obviously Al_2O_3), bows around this particle and takes a strongly curved shape, with the inclusion left in the concavity. Only after the boundary has locally increased much in length, does it overcome that obstacle jumpwise. The boundary then straightens under the effect of grain-boundary tension: the portion left behind begins to move at a higher rate than the other portions. Similar phenomena have also been observed in nichrome (Fig. 89).

Fig. 88. Retardation of grain boundary migration in aluminium by undissolved impurities. Polarized light photograph showing intermediate positions of boundaries

The conclusions given earlier [145] can explain well the retarding effect of inclusions on boundaries and the mechanism of subsequent 'bowing around'.

In the course of grain growth, a boundary migrates towards its centre of curvature. When the boundary starts bowing around an obstacle, its length and curvature increase, therefore the resultant force of grain-boundary tension, which is directed towards the centre of curvature, increases too, as also does the concentration of

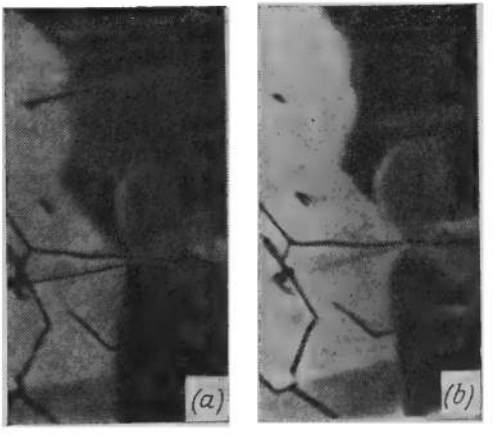

Fig. 89. Retardation of grain boundary migration in Ni + 13% Cr alloy by undissolved impurities. Emission microscopy. The photos show successive positions of boundaries

vacancies in front of the inclusion. As the concentration of vacancies reaches a definite level, the boundary bows around the inclusion. Since no retarding forces act now on the boundary, its curved middle portion moves faster under the added effect of the high concentration of vacancies, so that the boundary quickly straightens.

5.4. The Formation of Annealing Twins

The problem of the formation of annealing twins is important in many aspects. In this field, the concepts developed by Feltham [190] are used most widely. Briefly, they state that under favourable conditions of migration some large-angle boundaries split, as it were, into two boundaries one of which is coherent and lies in one of {111} planes. This splitting lowers the grain-boundary energy of the system and thus serves as the driving force of the process.

Burgers [48] has suggested another model, according to which the formation of twins is attributed to the collisions of two growing grains which are in a twinning orientation relative to each other. By that model, the probability of the formation of twins must increase as the primary recrystallization texture in a material becomes more pronounced. Khayutin [191] carried out experiments to verify these models for Л68 brass rolled 96% and annealed at 400°C for 15 minutes. The mutual orientation of twins and matrix was determined on diffraction electron micrographs.

The texture determined by X-ray analysis contained the following orientations: (311) $[\bar{1}12]$—30%; (110) $[1\bar{1}2]$—30%; and (110) $[\bar{1}10]$—10%.

According to Feltham's model, twinning should be uniform in all {111} planes; i.e. the (110) planes of one half of twins and the (11$\bar{4}$) planes of the other half should be parallel to the rolling plane. By the other model, all twins should have their (110) planes parallel to the rolling plane.

In actual fact, of the total number of 80 grains, 80% proved oriented with their (110) plane parallel to the foil surface. This means that direct collisions of two grains with the mutual twinning orientation are the main cause of the formation of annealing twins.

Khayutin's model [191] disregards both the role of the orientation of a large-angle boundary, which has separated two grains before the formation of a twin, and the mechanism by which that boundary is transformed into a twin boundary.

Further, this model does not explain the mechanism of formation of a few twins (especially with different orientations) within a single grain.

In a number of materials, twins do not often intersect all grains, but are interrupted inside a grain (these are called 'intragranular

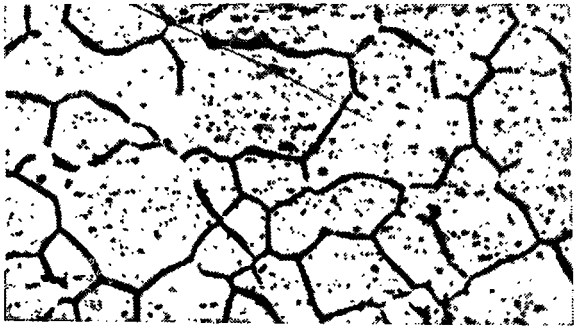

Fig. 90. Dangled boundaries in XH70BM0T nickel-base alloy revealed by common metallographic analysis, ×300

twins'). According to Hu and Smith [192], they are formed by detachment of a growing twin from a large-angle boundary which had 'dragged' the twin during the growth of the grain. If a twin intersects the whole grain, the energy of coherent boundaries in that grain is $E_c = \pi r^2 \gamma_c$ and that of incoherent boundaries, $E_{in} \approx 2\pi r \gamma_{in}$. The ratio $(E_c/E_{in}) \approx r\,(\gamma_c/\gamma_{in})$ increases with grain size, i.e., if the length of a twin is equal to grain diameter, the energy of the twin boundary increases in annealing faster than the energy of grain boundaries. Therefore, the detachment of a twin from a boundary becomes energetically favourable as the grain attains a definite size. A new portion of an incoherent large-angle boundary then forms at the end of the twin. The probability of detachment is higher at higher values of the γ_c/γ_{in} ratio.

Intragranular twins can also form by another mechanism, i.e. by the transformation of some portions of a large-angle boundary into a step consisting of a coherent and an incoherent portion, after which the latter migrates. This mechanism, which is similar to that proposed by Feltham [190] is obviously operative at the stage of secondary recrystallization, i.e. when normal migration of large-angle boundaries is retarded by disperse particles.

This process can result in structure coarsening, which is found under definite conditions in alloys containing disperse phase particles. The effect of coarsening is observed on heating to a high temperature at which slow dissolution of these particles begins.

Let us consider as an example a nickel-base XH70BM0T (ЭИ765) alloy which has a f.c.c. lattice [80].

Until quite recently, it was generally accepted that a very coarse structure results from migration of large-angle grain boundaries.

In a number of recent publications [41, 193, 194, 195, 366, etc.], it is claimed, however, that anomalously large grains form by coalescence of adjacent grains with disappearance (without migration)

of the separating large-angle boundary, rather than by boundary migration.

The authors state that the process takes place by 'unraveling' of some large-angle boundaries into low-angle dislocation boundaries under the effect of thermal activation.

The coalescence mechanism has been proposed to explain the effect of grain coarsening in complex-alloyed steels and alloys with a high content of disperse particles, and also in transformer and carbon steels and in tungsten, where the content of disperse particles is relatively low.

The authors of the above publications hold that the following data obtained by metallographic analysis at room and elevated temperatures are convincing evidence in favour of coalescence:

1. Some boundaries between grains disappear, which is accompanied at the early stages of the process by the formation of 'open' or 'interrupted' boundaries. An example of such a structure is shown in Fig. 90.

2. There are no intermediate positions of a large-angle boundary in which it would pass through the bulk of the original grains; this is, however, typical of boundary migration. In the course of structure coarsening, the boundaries of an anomalous grain always pass along the boundaries of the original grains.

3. Coarse grains retain the substructure in which the size and shape of subgrains repeat the size and shape of the original grains formed in prior primary recrystallization.

Some workers proceed from these observations to make far going conclusions on the mechanism of secondary recrystallization and claim this to be mainly due to grain coalescence.

A drawback of the publications mentioned is that they contain no data on direct measurements of mutual misorientations of coalescing grains and of their variations in the course of coarsening. In addition, grain coalescence, if any, is obviously possible only when neighbouring grains are closely oriented, i.e. are separated by low-angle boundaries and the migration of these boundaries cannot proceed easily owing to the 'barrier' effect of disperse particles and excess phases. F. K. Tkachenko, M. I. Vinograd *et al.* observed the formation of 'dangled boundaries' in steels only within a definite interval of heating temperatures. In heating to a higher temperature at which disperse particles can be dissolved intensively, the structure was coarsened by boundary migration. At intermediate temperatures, both mechanisms were operative. Inequigranularity was also at an intermediate level.

The mechanism of grain coarsening in a nickel-base alloy (15% Cr, 1.2% Ti, 2.1% Al, 3.8% Mo, 5.0% W, 0.8% Fe, and 0.14% C) was analysed thoroughly in [80]. In addition to the common metallographic techniques, the following methods were applied:

(1) thermal etching in vacuum during annealing at 1210-1250°C, which made it possible to observe the positions of boundaries before and after annealing;

(2) formation of an oxide film on the surface of specimens by using Sadovsky's reagent to produce a high polarizing contrast so as to estimate misorientations and reveal fine details of the microstructure;

(3) X-ray topographic technique (Schultz's method) for analysing the perfection and the structure of anomalously large grains.

Prior to final annealing, which was made at 1210-1250°C (τ from 5 minutes to 10 hours), specimens were tension-deformed 1.0 to 1.2%.

Figure 91*a* is an optical micrograph of a large recrystallized grain formed in a fine-grain matrix on annealing at 1230°C and etched in vacuum. An oxide film was then deposited on the specimen without intermediate polishing, and the specimen was examined in polarized light (Fig. 91*b*).

Polarized light revealed quite a different structural pattern of the grain. The large bright area in Fig. 91*b* is a single grain with the (111) orientation, as was determined on a reflected-light Laue photograph. The internal structure of the anomalous grain (on the right side) turned out to be associated with the decoration of the original grain boundaries by excess phase particles. Upon repolishing and repeated slight etching, the old boundaries in the grain disappeared.

Subsequent etching by Sadovsky's reagent (Fig. 91*c*) revealed more clearly the boundaries of the growing grain and its internal structure. An important feature of the structure, as seen in polarized light, is a large number of coherent twin boundaries. They cannot be detected by common metallographic techniques, probably because of their low energy and, therefore, poor etchability compared with large-angle boundaries (see *1-5* in Fig. 91*a*).

The polarized light technique has made it possible to determine the fact that there are no 'interrupted' boundaries in the volume of the grain. The point of interruption of a boundary, as seen in an optical microscope, is actually always a joint of two or three boundaries, e.g. an interrupted large-angle boundary and twin boundaries (Fig. 91*b*, *d*); these are not revealed by common etching since they are not decorated by disperse particles (see earlier).

At higher temperatures and longer time of annealing, common optical microscopy indeed gives a picture in which grain boundaries are dissolved, as it were, and a boundary becomes interrupted and disappears (see Fig. 90). This 'dissolution' is however only imaginary. Actually, the excess phase particles which have precipitated on grain boundaries and decorated the latter are dissolved unevenly. Etch pits are oriented differently, which is evidence that the earlier misorientation between grains remains unchanged.

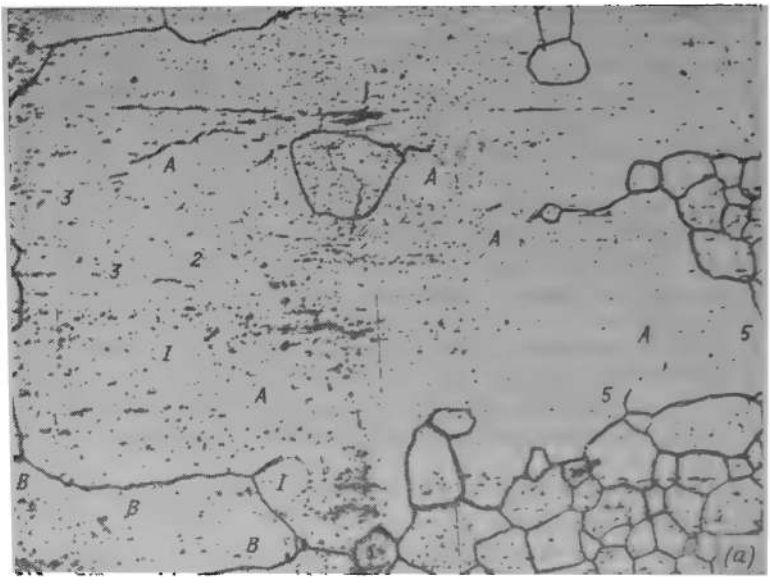
A
A
A
3
3
2
I
A
A
5
5
B
B
B
I
(a)

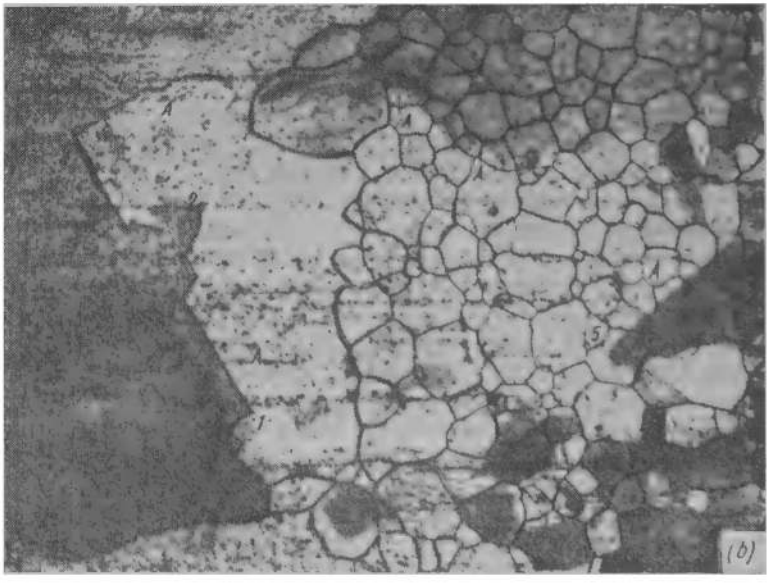
A
A
A
5
I
(b)

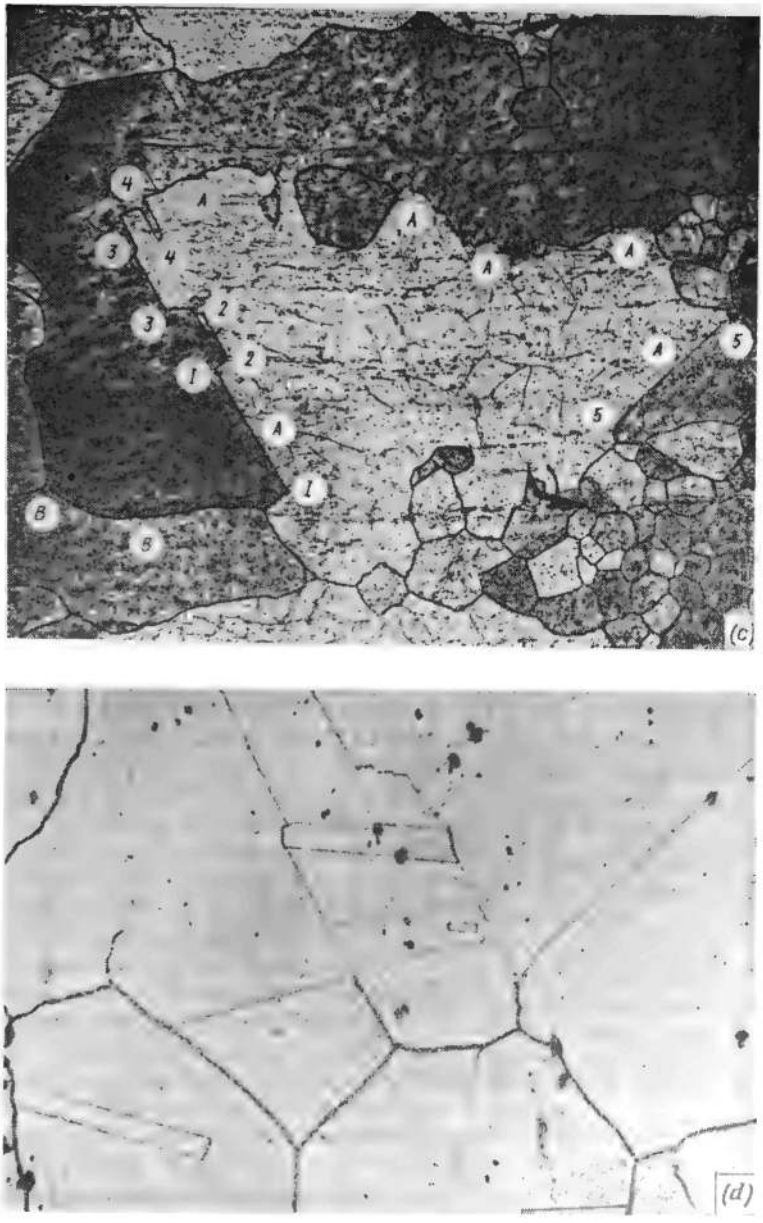

Fig. 91. Formation and growth of annealing twins in ХН70ВМюТ alloy and 12Х18Н9Т steel (letters and numerals indicate the same portions in various figures), ×200

(*a*) alloy, optical microscopy, common etching; (*b*) alloy, polarized light, before repolishing; (*c*) alloy, polarized light, after repolishing and etching by Sadovsky's reagent; (*d*) steel, optical microscopy (Zhak)

A substructure which repeats the contours of original grains (see Fig. 91*a*) is associated with the decorating effect of excess phase particles. During annealing at 1210-1250°C a most part of the disperse carbides and carbonitrides is dissolved intensively, but the composition in the volume of a whole grain is not equalized fully. The solution near grain boundaries is supersaturated and part of undissolved particles remains in places of the former grain boundaries, so that during cooling the disperse phases precipitate preferably in these places and decorate the original position of a boundary. Traces of old grain boundaries can be eliminated by repolishing and slight etching.

X-ray analysis by Schultz's method shows that the grown grains contain large subgrains whose boundaries have a different composition and an elevated dislocation density.

Thus, the formation of anomalously large grains in recrystallization of XH70BM0T alloy upon critical deformation is actually realized by migration of grain boundaries and, what is most important and typical in this case, preferably by migration of 'twin boundaries' which form in the course of the process (see Fig. 91).

This peculiarity can obviously be explained by the fact that the process of recrystallization occurs under the conditions at which, notwithstanding a high temperature of heating, the normal migration of grain boundaries is impossible because of the barrier effect of a large quantity of poorly soluble disperse phase particles.

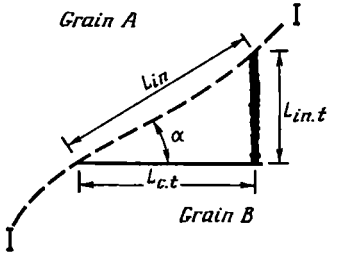

Fig. 92. Transformation of a portion of original large-angle boundary into a jog comprising a coherent and incoherent twin boundary (schematic)

Under such conditions, the boundary energy can be partially decreased by a mechanism similar to that proposed by Feltham [190]. Boundaries of individual favourably oriented grains (see below) assume a stepwise shape instead of being curvilinear. In a plane microsection, the steps may be likened to the catheti of a rectangular triangle whose hypothenuse is the section of the disappearing original boundary (*I-I* in Fig. 92).

One of the catheti of the triangle represents a coherent twin boundary $L_{c.t}$ (this may probably hold for any of the boundaries with a large number of coincidence sites, which are characterized by weak long-range stress fields). The other cathetus is an incoherent large-angle boundary, $L_{in.t}$. The vertex angle of the triangle is the angle between the direction of the original boundary and that of the coherent boundary. In a rough approximation, the energy conditions for this rearrangement of boundaries can be estimated as follows.

Suppose that the unit energy of an original large-angle boundary γ_{in} is about equal in value to that of an incoherent twin boundary, $\gamma_{in.t}$, and substantially greater than the energy of the coherent twin boundary $\gamma_{c.t}$, i.e. $\gamma_{in} = \gamma_{in.t}$ and $\gamma_{in.t} > \gamma_{c.t}$.

Since a step increases the total length of the boundary ($L_{in} < L_{in.t} + L_{c.t}$), its formation is energetically favourable only if

$$L_{in}/\gamma_{in} > L_{in.t}\gamma_{in.t} + L_{c.t}\gamma_{c.t}$$

or

$$(L_{in} - L_{in.t})\gamma_{in} > L_{c.t}\gamma_{c.t}$$

Since $L_{in.t} = L_{in} \sin \alpha$ or $L_{c.t} = L_{in} \cos \alpha$,

$$\gamma_{in}(1 - \sin \alpha) > \gamma_{c.t} \cos \alpha$$

whence

$$(1 - \sin \alpha)/\cos \alpha > \gamma_{c.t}/\gamma_{in} \qquad (11)$$

It follows from expression (11) that the rearrangement of a large-angle boundary between two grains in a twinning orientation is energetically favourable if the energy of that boundary is at least three or four times that of a twin boundary. The reaction is more probable at a lower energy of a coherent twin boundary, and, therefore, at a lower stacking fault energy in a given material.

The probability for two grains of a material to be in a twinning orientation is determined in the first place by the texture of the material and the size of grains. Steps on boundaries are obviously formed mainly in places where local dissolution of disperse phases begins. As the dissolution proceeds, the driving force, even if it is small, becomes at a certain moment sufficient to move an incoherent boundary. The subsequent growth of an adjacent step will increase the width of a twin, i.e. will produce the same effect as would occur in migration of the coherent boundary.

This type of migration is shown schematically in Fig. 92, and a metallographically revealed stepwise boundary (2*A*) is shown in Fig. 91*b* and *c*. The process described obviously begins first in triple joints of original grain boundaries, resulting in the formation of 'interrupted' boundaries (see Fig. 90). Owing to a difference in the grain-boundary tension of coherent twin boundaries and a large-angle boundary, the equilibrium angles between the boundaries in a triple joint should differ from 120°. Therefore, the triple joint will be acted upon by a force tending to change its angles. This driving force will tend to move the joint until the large-angle boundary disappears. Disperse particles which lock the large-angle boundary retard this movement and their dissolution accelerates the disappearance of the boundary.

To estimate quantitatively the contribution of twin boundaries to grain growth in isochronous annealing at 1100-1250°C, measure-

ments were made of the average length of twin boundaries and of the average number of these boundaries per unit area, n/S. The results were correlated with the average number and diameter of grains.

It turned out that immediately after hot deformation (t_d = = 1100°C), twin boundaries were present in every sixth grain. Upon annealing at 1210°C for 2.5 h, twin boundaries were found in every third grain, and after annealing at 1230°C (before the stage of anomalous growth) in more than every second grain. Thus, twin boundaries seem to play an important part in the formation and growth of anomalous grains at a definite stage of the process.

On completion of structure coarsening and the formation of equally anomalous large grains, twin boundaries begin to disappear, which lowers further the internal energy of grains. The mechanism of this disappearance is the same as that described in [196]. The mechanism of the formation of twins in annealing is of high importance and, in our view, deserves a more detailed examination.

Thus, the principal mechanism of the formation and growth of anomalously large grains in XH70BM0T (ЭИ765 alloy) (which appears as grain 'coalescence') is migration of incoherent boundaries of the twins formed in the process and of large-angle boundaries of original grains.

With a long time of annealing under the conditions in which disperse particles retard large-angle boundary migration and are dissolved unevenly in individual grains, a large-angle boundary can transform into a stepwise boundary consisting of coherent and incoherent twin sections. All other conditions being the same, the probability of this rearrangement is higher at a lower stacking fault energy and finer grain of a material.

Chapter 6

Recrystallization During Hot Deformation (Dynamic Recrystallization)

Hot plastic deformation of metals and alloys includes processes occurring in a wide range of temperatures and deformation rates, from slow deformation under the conditions of superplasticity up to high-speed operations of rolling, pressing, die-forging, stamping, extrusion, etc.

Hot deformation differs from cold deformation principally in that it takes place at an enhanced plasticity of a material, including its diffusion plasticity. In the course of hot deformation of a metal, two competing processes occur in parallel, i.e. strain-hardening and softening.

The strain-hardening effect is due to an increase in the dislocation density under the action of external forces and to the interaction of dislocations which form dislocation pile-ups of various degrees of stability and mobility.

The processes of softening consist in a decrease of the dislocation density and in redistribution of dislocations into energetically more stable configurations.

In distinction to cold deformation, hot deformation may involve the process of dislocation redistribution due to vacancy climb, the formation of recrystallization nuclei and their growth by migration of large-angle boundaries under appropriate conditions (temperature, amount and rate of deformation). By analogy with dynamic recovery, where the word 'dynamic' implies that the partial softening (due to cross slip of screw dislocations) occurs during the deformation proper, the process described is often called '*dynamic recrystallization*' to emphasize the fact that it occurs during deformation.

Accordingly, the process of recrystallization which takes place after cold or hot deformation in subsequent heating or cooling (after hot deformation only) may be called '*static recrystallization*'.

The mechanism of dynamic recrystallization is discussed in a number of Soviet works published recently. Reviews of some foreign publications have been made in [95, 197-199]. An analysis of the process is associated with some additional difficulties. The processes of strain-hardening and softening are time-dependent. Their rates heavily depend on a number of factors, such as the temperature, amount and rate of deformation, the stacking fault energy, the initial structural state and phase composition of a material.

Since strain-hardening and softening occur in parallel, their realization and the contributions to the final structure depend sharply and in a complicated manner on the factors mentioned above.

As will be shown later, slight variations in these factors during hot deformation can influence the nature of structural changes more appreciably than in cold deformation. In addition, in a hot-deformed material it is sometimes difficult to distinguish between original and recrystallized grains, since the processes of deformation and recrystallization occur in parallel and some recrystallized grains may again be deformed. This difficulty can be eliminated to a certain extent by using single crystals as test specimens.

In hot deformation, it is not always possible to distinguish between the structural changes taking place directly during deformation and those which occur in subsequent cooling. Holding a material only for a few fractions of a second at high temperature after deformation is sufficient to cause serious structural changes.

It should be noted also that the course of recrystallization during hot deformation and subsequent cooling in many steels and alloys can be complicated by the processes of precipitation from the solid solution and by ascending diffusion; these factors introduce additional difficulties in the study of the process. In that connection, it is advisable to cool sharply the specimens immediately after hot deformation in order to analyse the structural changes, especially those associated directly with dynamic recrystallization.

In experiments on polycrystalline specimens, the presence of a deformed substructure (stretched subgrains, distorted annealing twins, an elevated dislocation density) in equiaxial grains is evidence of the completed dynamic recrystallization. Such a substructure forms in recrystallized grains which have nucleated at earlier stages of deformation.

For a long time, it was generally accepted that dynamic recrystallization can only occur at high rates of hot deformation, whereas at low rates, which are typical of creep, the softening effect is due completely to recovery (polygonization). More and more experimental results show that the deformation rate is not the only factor, though it undoubtedly plays a decisive role.

As has been shown in a study made in 1930's, lead recrystallizes in the process of creep. On the other hand, some metals and, in particular, aluminium [199] most often do not recrystallize at all even at the common practical rates of hot deformation.

Analysis shows that the different behaviour of these two metals is mainly associated with the difference in their stacking fault energies, γ_{sf}. This explains well why silver, copper, γ-iron and nickel, which have a low value of γ_{sf}, behave like lead, while α-iron and some ferritic steels, i.e. metals with a high stacking fault energy, behave like aluminium.

The correlation between the stacking fault energy γ_{sf} and the behaviour of metals in hot deformation over various temperature intervals can be illustrated by the results given in Fig. 93 [197], which shows the effect of temperature (related to the melting temperature) on the shear stress-to-G modulus ratio in single crystals of selected f.c.c. metals with various values of γ_{sf}. The curves are representative of the moment at which a uniform elongation of specimens comes to an end, i.e. before 'necking' takes place.

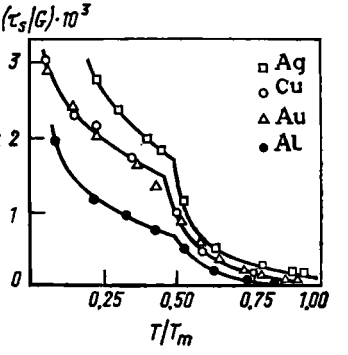

Fig. 93. Flow stress in single crystals of aluminium, gold, copper and silver as a function of homologous temperature [197]

As seen from the pattern of the curves, there are two distinct temperature intervals, one up to $0.5T_m$ and the other, above that temperature. Accordingly, the behaviour of the metals tested is also different, especially within the lower temperature interval. The ratio τ_{cr}/G is higher at a lower stacking fault energy γ_{sf}, i.e. when dissociated dislocations are wider in which case the processes of cross slip that control dynamic recovery can occur less easily.

This correlation suggests that the first temperature interval should be associated with dynamic recovery. Mecking and Kirch [197] have proved the validity of this assumption. At temperatures above $0.5T_m$ the contribution of diffusion climb of dislocations becomes noticeable and favours the onset of dynamic recrystallization.

It can be concluded from the shape of the curves that the deformation processes in which dynamic softening is controlled by cross slip should be related to cold deformation. The processes in which dynamic softening is controlled by diffusion dislocation climb and by dynamic recrystallization should be regarded as hot deformation.

A deeper insight into the processes occurring in deformation at elevated temperatures can be gained by analysing simultaneously the stress-strain curves (strain diagrams, or strain-hardening curves) and the structural changes at various stages of deformation and at various deformation rates and temperatures. It is essential in the analysis to maintain a constant rate of deformation, ε.

In common tests for tension or upsetting, the speed of movement of a tool is usually constant. Therefore, as the length of a specimen changes, the actual rate of deformation either decreases (in tension) or increases (in upsetting). Special testing machines are needed to ensure a constant rate of deformation. The actual rate of deformation,

ε, is found by the equation

$$\dot{\varepsilon} = \frac{d\varepsilon}{d\tau} = \left[d\left(\ln\frac{L}{L_0}\right)\Big/dL\right]\frac{dL}{d\tau} = \frac{v}{L}\ [s^{-1}]$$

where L_0 and L is the initial and the current length (height) of a specimen, $\varepsilon = \ln(L/L_0)$ is actual deformation, and v is the speed of tool.

In the most common processes of plastic working of metals, the rate of deformation $[s^{-1}]$ can vary within the following limits:

Rolling	1 to 10^2
Pressing	10^{-2} to 10
Hydraulic stamping	10^{-2} to 10^2
Hammer forging	10 to 10^3

The σ-ε curves (where ε is the actual deformation) for plastic working at elevated temperatures differ in shape from the curves for cold deformation (see Ch. 2 and Fig. 6).

Typical σ-ε curves for hot deformation are shown in Fig. 94 [200].

As may be seen, stage I is absent in these curves. The hardening effect typical of stage II is observed at the earliest stages of deformation. In the course of the process, the initial hardening changes to slight softening, after which a stage of stable deformation begins (at which the stress remains constant). This stable stage can be regarded as the principal feature of hot deformation in contrast to cold deformation.

This can be illustrated well by comparing the σ-ε curves for an aluminium alloy at 20° and 300-400°C (see Fig. 94).

The flow stress typical of the stable stage depends on a number of factors, in the first place, on the temperature and rate of deformation. The higher the temperature of deformation and the lower its rate, the smaller this stress.

The initial ascending portion of the curve (stage II) is associated with an increase in dislocation density and the beginning of the formation of a cell structure. Dislocation loops move from Frank-Read sources which have formed within cells. These loops intersect other dislocations and form jogs which in turn, in the further movement of dislocations, generate point defects. These facilitate the climb of edge dislocations. The stress diminishes owing to the dissociation of unlike-sign dislocations on cell walls.

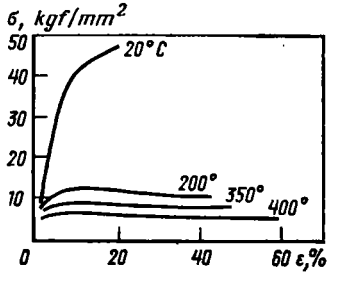

Fig. 94. Stress-strain curves for cold and hot deformation of aluminium alloys [200]

At the stable stage of deformation, dynamic equilibrium sets in between the forming and dissociating dislocations.

What is most important at this stage is that subgrains are equiaxial and unvarying. Also, the angles of misorientation between the subgrains are constant.

Using electron microscopy, McQueen and Jonas [201, 202] studied the structure of aluminium pressed at a rate of about 1 s^{-1} in the temperature range of 250-500°C. A higher temperature of pressing increased the size of subgrains and decreased the thickness of their walls and the dislocation density in subgrains.

It should be noted that the elementary processes of structure changes in high-temperature deformation are largely thermally activated processes.

The effect of the temperature and rate of deformation on the shape of σ-ε curves is primarily associated with the influence of these factors on the structure which forms in deformation due to the thermally activated processes of dislocation movement. These processes include the processes of overcoming the obstacles formed by close-range stress fields, such as 'dislocation forests', jogs on screw dislocations, Lomer-Cottrell locks or Peierls-Nabarro locks**.

To describe the prerecrystallization stage of the process in a wide range of deformation temperatures and rates, the following relationship has been proposed:

$$\dot{\varepsilon} = A(\sinh \alpha\sigma)^n \exp(-Q_d/RT) \qquad (12)$$

where A, α and n are constants independent of temperature and stress; Q_d is a quantity close to the activation energy of self-diffusion, but depends on temperature and on ε or σ. In addition, it has been established experimentally that Q_d increases on addition of soluble or insoluble minor impurities to a metal**.

Cross slip of dislocations as well as dislocation climb is among the most important thermally activated processes by which dislocation structures are formed. Both processes are facilitated with a decrease in the width of dissociated dislocations. This is why the stacking fault energy γ_{sf} influences the rate of deformation at elevated temperatures. In this connection, it is interesting to refer to the following relationship which includes the stacking fault energy as a pro-

---

* Locks that form long-range stress fields are athermic, since the energy required to overcome them is much greater than the energy of probable thermal fluctuations.

** Relationship (12) was used to analyse the processes of dynamic recovery and recrystallization in f.c.c. metals with various values of γ_{sf} in a wide range of deformation rates [199]. At low rates, when only dynamic recovery took place, Q turned out to be close to the activation energy of self-diffusion. At high diffusion rates (above $4 \cdot 10^{-3}$ s^{-1}), dynamic recrystallization was realized and Q was much greater than the activation energy of self-diffusion. The cause of this phenomenon still remains unclear.

cess parameter [197]:

$$\dot{\varepsilon} = A' D \gamma_{sf}^{3.5} (\sigma/E)^5 \qquad (13)$$

where $D = D_0 \exp(-Q_s/RT)$, A' is a constant, D is the coefficient of self-diffusion, and E is Young's modulus.

It follows from equation (13) that the hardening effect due to hot deformation is stronger in metals and alloys having a low coefficient of diffusion, high modulus of elasticity, and low stacking fault energy.

Let us consider the particular features of hot deformation accompanied by dynamic recrystallization.

Figure 95 shows the typical curves obtained by Richardson [203] in creep tests of copper at two various values of the stress. As seen, the stable creep stage changes at definite values of deformation to a stage in which the rate of creep increases sharply. This is due to dynamic recrystallization. A peculiar feature of this process is that the cycles of hardening and softening follow each other alternately. For each of the stresses in Fig. 95, dynamic recrystallization begins twice.

This periodicity has also been observed on stress-strain curves taken under certain conditions. It has been established for copper, nickel, iron and their alloys in hot tensile and upsetting tests conducted at deformation rates exceeding the typical values for creep.

As an example, Fig. 96*a* shows the curves obtained for steel with 0.25% C, tension-deformed in austenitic state (at 1375 K) at four various deformation rates [204]. As may be seen, the periodicity depends appreciably on deformation rate. At a high rate, there is only one peak immediately after the stable stage (the uppermost curve in Fig. 96*a*). The same cyclicity is clearly seen in Fig. 95 which gives the curve for a copper single crystal. At lower deformation rates, more peaks may appear (the lower three curves in Fig. 96*a*).

Before going into the causes and conditions of cyclic hardening and softening, it should be proved that the sharp hardening effect is actually associated with recrystallization. To do this, it is required, in the tests, to interrupt quickly the deformation at various stages of the process, quench the deformed material, and analyse its structure. As noted earlier, single crystals or coarse-grained polycrystals are more suitable for these tests, since nuclei of new grains can be easily revealed in them.

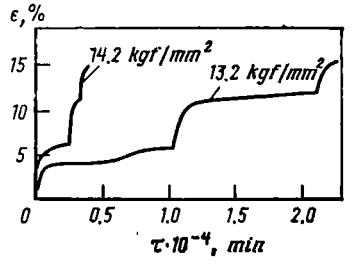

Fig. 95. Creep curves for copper at 935 K and two stresses: 14.2 kgf/mm² and 13.2 kgf/mm² [203]

In addition, it is important to determine whether the process of recrystallization takes place during defor-

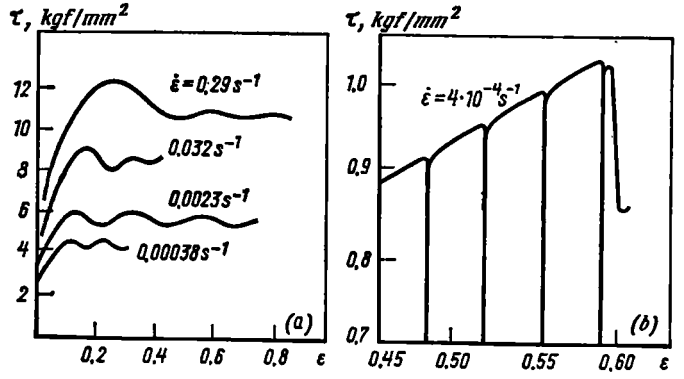

Fig. 96. Stress-strain curves for steel with 0.25% C (*a*) and a copper single crystal (*b*) at various deformation rates [204]

mation or afterwards, i.e. in subsequent curing or cooling. Some researchers deny the possibility of recrystallization in the course of deformation. But the experimental results obtained by Rossard and Blain [204] on copper single crystals ($\dot{\varepsilon} = 4 \cdot 10^{-4} s^{-1}$, 975 K) have shown that primary recrystallization can actually take place during deformation. The authors note that recrystallization was always observed in specimens deformed beyond the point at which the flow stress drops off and was never found in those specimens where this point was not reached.

Figure 96*b* shows a portion of the stress-strain curve for a copper single crystal deformed in a process of cyclic stressing and unstressing for 5 minutes. At the beginning of each deformation cycle, the flow stress was somewhat lower than immediately before unstressing. Consequently, partial recovery took place during 5-minute intervals.

After the last unstressing procedure, the plastic flow stress increased quite insignificantly and then dropped abruptly due to recrystallization. It should be emphasized that simultaneous deformation enhances recrystallization to a greater extent than does a longer time of holding at the given deformation temperature. A holding time of 5 minutes during the last unstressing cycle was insufficient to initiate recrystallization, whereas an appreciable volume of the crystal was involved in recrystallization in a time less than 1 s when deformation was renewed and increased slightly against the previous value.

Thus, dynamic recrystallization can start at a definite 'critical' deformation which in turn depends on the plastic flow stress. To explain this, we may assume that a particular dislocation structure should be formed to initiate dynamic recrystallization. This can

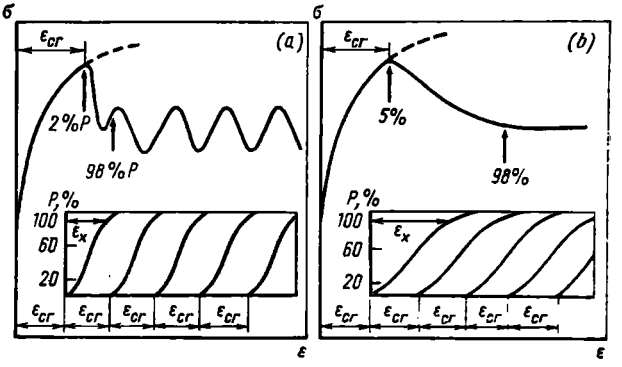

Fig. 97. Stress-strain curves for copper in the case of dynamic recrystallization at $\varepsilon_x < \varepsilon_c$ (*a*) and $\varepsilon_x > \varepsilon_c$ (*b*)
P is recrystallized volume, % [205]

also explain the fact that dynamic recrystallization during hot deformation ($T_d > 0.5T_m$) is mainly observed in metals of low stacking fault energy (silver and copper) and very rarely in aluminium.

In gold, which has a moderate value of $\gamma_{s.f.}$, dynamic recrystallization can take place too, but only in high-speed deformation ($\varepsilon > 10^{-3}$ s^{-1}). All these data imply that dynamic recovery can compete with recrystallization and preclude the formation of a favourable dislocation structure for the onset of recrystallization.

What is the cause of cyclic hardening and softening? Luton and Sellars [205] hold that this is associated with a particular relation between the 'critical' deformation ε_{cr} required to initiate recrystallization and the deformation ε_x which occurs in the course of recrystallization. They assume in their reasoning that the processes of softening and hardening can occur simultaneously during recrystallization, the former in the microregions where the deformation has been most intensive and the latter in neighbouring less distorted microregions.

This explains well why at $\varepsilon_x < \varepsilon_{cr}$ recrystallization proceeds not continuously but periodically, with softening and hardening cycles appearing on the σ-ε curve (Fig. 97*a*). When $\varepsilon_x > \varepsilon_{cr}$, a given recrystallization cycle begins before completion of the previous cycle and the macroscopic stress remains constant, since the processes of softening and hardening occur in parallel, but in different microregions (Fig. 97*b*). A stable stage can appear in this process, as in dynamic recovery, but the preceding softening cycle is sharper.

The positions of the first maxima on the four σ-ε curves for a steel with 0.25% C deformed at four different rates (see Fig. 96*a*) suggest that with a lower deformation rate recrystallization (softening) be-

gins at a greater amount of deformation. For a given deformation rate, ε_{cr} increases with deformation temperature.

Using these relationships, it is possible to control ε_{cr} and ε_x and thus the formation of structure in hot deformation, by varying the temperature and rate of deformation. Some examples will be given later in this chapter.

Let us first analyse the structures of hot-deformed materials and in particular those formed at the stable stage that precedes dynamic recrystallization.

The problem has been studied most thoroughly for f.c.c. metals [199] and especially for aluminium and its alloys [206].

In a stage close to the stable stage, a cell structure forms owing to intensive dynamic recovery. The walls of these cells are appreciably thinner than those formed on cold deformation. With an increase in temperature, cell boundaries become more distinct and their structure becomes similar to that of subgrain boundaries, i.e. two-dimensional boundaries. In this process, cells (subgrains) grow in size. The dislocation density in cells is low and diminishes with an increase in deformation temperature. Misorientation angles between subgrains (cells) first increase to a definite limit. The misorientations angles between adjacent subgrains do not exceed 1-3 degrees, i.e. they are only one-half to one-fourth of those in cold deformation.

Yu. M. Weinblat and S. S. Khayurov [206] have analysed the effect of deformation temperature on the substructure of aluminium (the average size d of subgrains and their misorientation angle φ). Specimens were deformed by various methods (pressing, upsetting, rolling) to an actual amount of deformation of 2.2, which corresponded to the stable stage.

As seen from Fig. 98, the average size of subgrains depends almost linearly on the deformation temperature and the latter has only a slight effect (within the studied interval) on misorientation angles. The relationships obtained in various deformation processes turned out to be almost identical, which makes the results very convincing. In further deformation on attaining the stable stage, the structure remained statistically invariable, i.e. the processes of formation and dissociation of dislocations were in dynamic equilibrium.

As noted in [198], with the average misorientation angle kept unchanged,

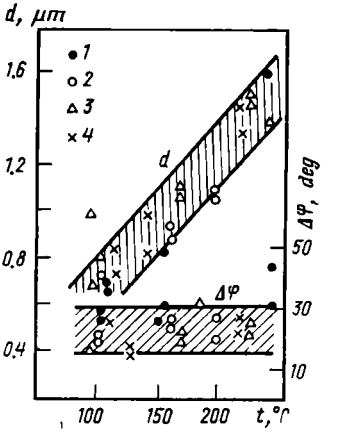

Fig. 98. Effect of deformation temperature on substructure parameters in aluminium (actual deformation approx. 2.2)

1—pressed rod; *2*—pressed strip; *3* -upsetting; *4*—rolling

the scatter of real values from that angle increases with deformation.

The amount of deformation at which a cell structure begins to form is lower at a lower deformation rate. For creep, it is roughly from 1 to 10%.

The shape of subgrains at the stable stage is determined by the applied stress and temperature. At high stresses and at deformation temperatures (less than 0.6 or 0.7 of T_m), subgrains are stretched in the direction of deformation.

At higher temperatures, they become equiaxed even in very heavy deformations (up to 4000%).

The mechanism by which grains remain equiaxed in intensive and directed plastic deformation is still unclear. Experiments on creep [197] suggest a conclusion that the climb of edge dislocations or of edge dislocation jogs on screw dislocations may play an important part at that stage. The process of slip and annihilation of dislocations seems to depend on climb. Since the rate of dislocation climb depends on the rate of diffusion of vacancies through the volume of a crystal (towards dislocations or away from them), the process as a whole must depend appreciably on the conditions and rate of self-diffusion.

Climb is obviously not the sole process operative during hot deformation at common rates, since it would require an enormous quantity of vacancies. By Honeycomb [199], 'repolygonization' is very likely to occur at the stable stage, i.e. the process of continuous destruction and rearrangement of subboundaries.

In that case, a structure should contain a certain amount of unstable subboundaries at every given moment in the course of deformation. This circumstance seems to be very important. It explains why a substructure formed in hot deformation is less stable than that formed by cold deformation and subsequent heating. It also helps us to understand why coalescence of subgrains, for which the existence of unstable easily annihilating subboundaries is essential, plays a very important part in the formation of recrystallization nuclei on hot deformation.

The results obtained by Pluhař *et al.* [369] and by Ya. I. Spektor, N. V. Tikhy and R. V. Yatsenko [368] have shown that the dislocation pile-ups formed during hot deformation have a low stability and the primarily recrystallized grains have an elevated dislocation density. The authors [368] have made separate measurements of the microhardness of unrecrystallized and recrystallized grains and of its variations in subsequent operations of isothermal annealing.

The microhardness of recrystallized grains (on hot deformation) turns out to be higher than that of annealed metal, but lower than that of unrecrystallized hot-deformed grains. Unrecrystallized grains, however, soften intensively at the recovery stage, so that at the end of that process their hardness differs only slightly from that of recrystallized grains (Fig. 99*a*).

These results have been confirmed by electron-microscopic analysis. In unrecrystallized grains immediately after hot deformation, the cell structure is in the form of flattened cells extended in the direction of rolling, but their dislocation structure is non-uniform. The thickness of cell walls is not large, but the scatter of dislocation density within the volume of a cell is substantial. In specimens annealed even for a very short time after deformation, some walls are flattened and some unraveled (see Fig. 99*d*).

The dislocation density in recrystallized grains is also quite non-uniform. In many grains (Fig. 99*e*), the dislocation density is much higher than in as-annealed metal and ranges into 10^9-10^{10} cm^{-2}.

It is interesting to note that the average size of grains varies anomalously during isothermal annealing after hot deformation carried out within a definite range of rates, degrees, and temperatures of deformation.

Upon the initial grain refinement due to primary recrystallization, grains increase in size during the stage of grain growth, after which they intensively refine anew and then begin to grow slowly (Fig. 99*a* and *b*).

As has been found experimentally, the repeated grain refinement is accompanied by the appearance of numerous annealing twins in the structure (Fig. 99*c*). These twins can be detected at an early stage of their formation by electron microscopy.

Similar relationships were earlier found by Pluhař *et al.* [369] for austenitic nickel and chrome-nickel steels; they called the phenomenon 'repeated recrystallization'.

The anomalous repeated grain refinement takes place however, only at particular temperatures of annealing. In austenitic steel 45Г17103, for instance, the effect was observed in annealing at 900° and 1000°C and was not at 1100°C. The effect was less pronounced or even disappeared fully with an increase in the amount and rate of deformation. The particular mechanism of 'repeated recrystallization' remained unclear up to quite recently.

Jonas *et al.* [95] later observed a similar phenomenon and gave the following explanation. When hot deformation comes to an end and dynamic recrystallization proceeds, the material already has a definite quantity of dynamic recrystallization nuclei which play the same part as the boundaries of original grains that have started to migrate towards grains with an elevated dislocation density. In subsequent isothermal holding, these nuclei can grow further and their boundaries can migrate without any incubation period, which is so essential in static recrystallization.

Jonas *et al.* suggested the term 'metadynamic' (or post-dynamic) recrystallization for the softening effect resulting from this growth and migration. Since this type of recrystallization requires no incubation period, it begins at the earliest stages of annealing. This stage

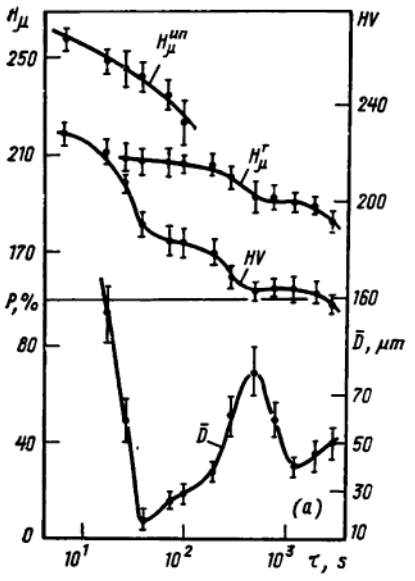

Fig. 99. Effect of the time of isothermal holding at 1000°C of austenite deformed by rolling at the same temperature on

(*a*) microhardness of unrecrystallized (H_μ^{un}) and recrystallized (H_μ^{r}) grains, Vickers hardness (HV), and average grain diameter $\bar{D}$; (*b*, *c*) microstructure, ×200 (*b* — $5 \cdot 10^2$ s; *c* — $1.2 \cdot 10^3$ s); (*d*, *e*) dislocation structures, ×17 000 (*d*—unrecrystallized grains, 5 s; *e*—recrystallized grains, 5 s) [366, 368]

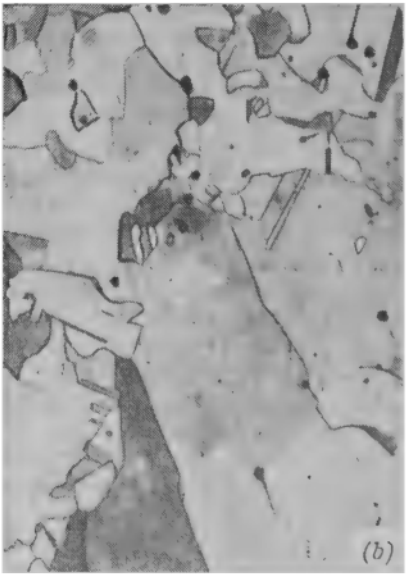

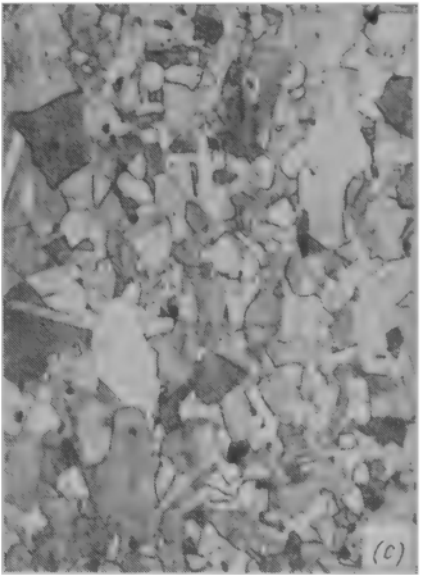

corresponds to the first decrease in the average grain size observed by Pluhař and N. V. Tikhy.

In parallel to this process, the processes of static recovery (without incubation period) and static recrystallization (with an incubation period) take place in other, less deformed, portions of crystallites during isothermal holding. The incubation period of static recrystallization can be rather long if disperse phases precipitate in the alloy. The beginning of delayed static recrystallization underlies the essence of the phenomenon that has been called 'repeated rectystallization'.

On the one hand, an increase in the amount of deformation (or deformation rate) shortens the incubation period of static recrystallization and, on the other, increases the volume in which dynamic recrystallization has taken place and in which metadynamic recrystallization is realized during heating of deformed material. Thus, the effect of grain refinement associated with delayed static recrystallization disappears.

This can be illustrated by the curves given in Fig. 100*a* and *b*. As may be seen, a change in the amount of deformation changes the number of processes responsible for softening, the contribution of each of these processes to the softening effect, and the sequence in which these processes take place.

On low deformations, dynamic recovery takes place. With an increase in the amount of deformation, static recovery and static

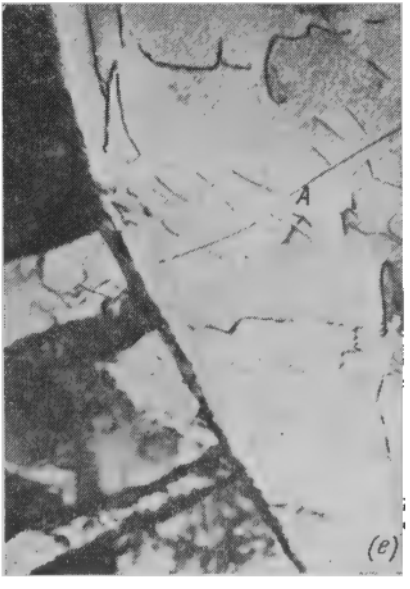

recrystallization are operative, and on heavier deformations, these are static recovery, metadynamic recrystallization and static recrystallization. Finally, on very heavy deformations, only static recovery and metadynamic recrystallization are operative.

In hot-deformed metals and alloys, large-angle boundaries of original grains are places of the greatest inhomogeneity. That is why during dynamic recrystallization nuclei preferably form on these boundaries. This is the case for a large number of metals and alloys. Nucleation in the bulk of grains, which is common in cold-deformed materials, is almost never observed during hot deformation (except at very high deformation rates).

Yu. M. Weinblat, T. B. Sagalova and I. G. Rodina [208, 209] have found that nucleation on grain boundaries in dynamic recry-

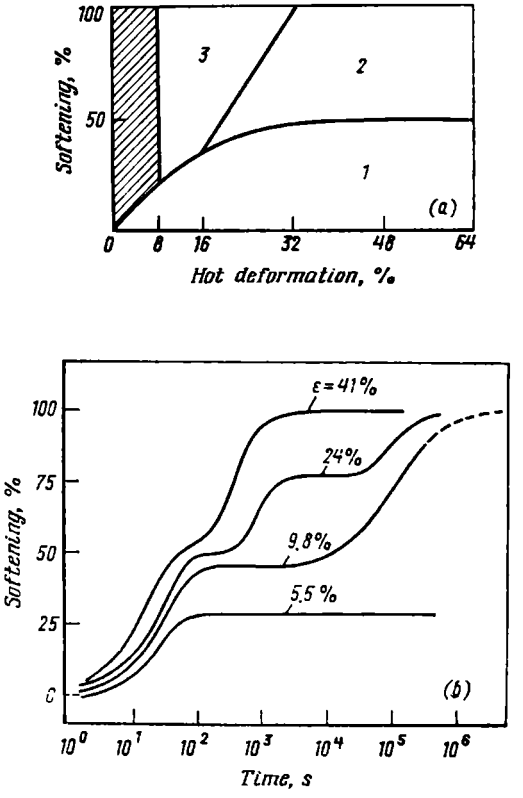

Fig. 100. Effect of degree of hot deformation (*a*) and time of isothermal post-deformation annealing (*b*) on the contribution of the processes of static recovery (*1*), metadynamic recrystallization (*2*) and static recrystallization (*3*) to softening of austenite [95]

stallization results from local migration of an original large-angle boundary that is similar to strain-induced migration in appearance. The result is that protrusions form on the boundary, which becomes tooth-shaped (Fig. 101).

A similar conclusion has later been made by the authors of work [207], who observed tooth-shaped boundaries in a group of hot-deformed structural ferritic and austenitic steels. They explain the effect by local inhomogeneity of deformation in boundary volumes and, as a result, by a difference in the density of defects in local volumes on both sides of the original boundary; this difference stimulates the migration of small portions of the boundary towards a volume having a higher density of defects.

E. N. Sokolkov, V. D. Sadovsky and M. G. Lozinsky [207, 210] were among the first to observe the formation of tooth-shaped boundaries during high-temperature thermomechanical treatment of some heat-resisting alloys. At that time, however, they failed to explain properly the cause of the phenomenon they discovered.

A recrystallization nucleus most often forms on an original boundary by coalescence of adjacent subgrains (see Fig. 61) whose subboundaries disappear completely or partially. The result is that the subgrains formed on one side of a large-angle boundary have an appreciably larger average size than those formed on the other side. If the degree of deformation has been high and a deformation texture has formed in the material, the above-described mechanism is most often realized at the boundaries which separate the deformed grains belonging to different components of the deformation texture. For instance, recrystallization nuclei in hot-deformed aluminium appear at a boundary of the components ⟨100⟩ and ⟨111⟩, on the ⟨100⟩ side. The nuclei ('protrusions') thus formed grow at the expense of ⟨111⟩.

The critical size of such a nucleus is determined by the ratio of grain-boundary tensions of large-angle and low-angle boundaries of

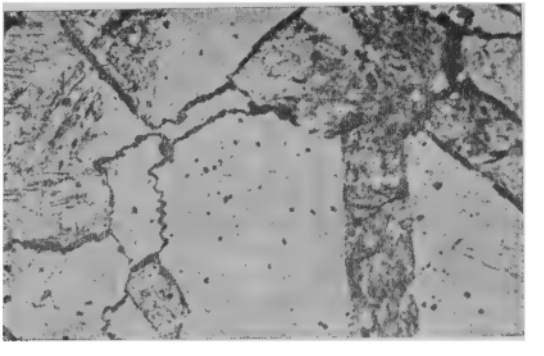

Fig. 101. Tooth-shaped grain boundary formed by dynamic recrystallization in steel ШХ15СГ in austenitic state, ×270

subgrains. By Bailey and Hirsch, the critical size of nucleus is $L_{cr} \geqslant 2\gamma_{la}/E$, where γ_{la} is the unit grain-boundary energy of a large-angle boundary and E is the volume energy.

Neglecting the energy of the dislocations retained in the nucleus upon coalescence and assuming that all the energy stored in deformation is concentrated in subboundaries, we have $E = 2\gamma_{sa}\, d$, where γ_{sa} is the unit energy of a small-angle (low-angle) boundary and d is the size of subgrain. Then, $L_{cr} \geqslant (\gamma_{la}/\gamma_{sa})\, d$. i.e. the critical size of a nucleus must exceed the size of surrounding subgrains as many times as the unit grain-boundary energy of the large-angle boundary exceeds that of the low-angle one.

If we assume, on the basis of literature data, that $\gamma_{la}/\gamma_{sa} = 4$ to 5, then a subgrain formed by coalescence can become a nucleus provided it has at least 4 or 5 times the average size of subgrains to be consumed.

This is but true for cases where a boundary has no additional locking points, such as disperse phase particles on grain boundaries. This circumstance should be considered properly, since boundary locking by disperse phases that precipitate from the solid solution directly during hot deformation or in subsequent isothermal holding occurs more frequently and proves more effective than that observed in the course of recrystallization after cold deformation. The high effectiveness of locking is due, on the one hand, to a lower driving force of recrystallization (lower perfection of nuclei and therefore a lower difference in dislocation densities between the nucleus and deformed matrix) and, on the other, to a higher dispersity of particles.

Honeycomb and Pethan [199] examined the effect of disperse sulphide particles on dynamic recrystallization in Cr-Ni steel (20% Cr, 25% Ni) containing 0.06% S (by mass). A special technique, overheating by 5 degrees above the solidus point and slow cooling, was used to ensure fusion of sulphides and their precipitation on grain boundaries. On subsequent hot deformation by approximately 20% at 1375 K, recrystallized grains were found in non-overheated specimens and no traces of recrystallization in overheated ones.

N. V. Tikhy *et al.* have studied the kinetics of recrystallization in hot deformation of austenite with various degrees of alloying. As has been found, recrystallization and softening are retarded sharply when the deformation temperature is lowered to a level at which excess carbides and other phases can precipitate. Stronger carbide-formers produce a stronger retarding effect with increased temperature. Besides, it should be kept in mind that hot deformation itself accelerates markedly the decomposition of supersaturated austenite.

When a large-angle boundary is rigidly locked by disperse particles and the growth of a nucleus into an adjacent grain is impossible, recrystallization proceeds by the growth of the nucleus into a matrix

grain. Since, however, the mobility of the boundary is low (due to small misorientation), the boundary migrates slowly and the process reduces to in-situ recrystallization. Recrystallization in internal volumes of grains is effected in the same manner.

These specifics of dynamic recrystallization suggest a number of important conclusions.

As compared to cold deformation, the size of recrystallized grains after hot deformation is more closely associated with their size prior to deformation. This should obviously be attributed mainly to the preferable nucleation on boundaries of original grains.

Oriented nucleation and its role in the formation of recrystallization textures are more noticeable in dynamic recrystallization than in recrystallization after cold deformation. As a rule, a texture formed in dynamic recrystallization or in recrystallization during heating of hot-deformed metal repeats the deformation texture.

In hot deformation, the rate of deformation and the rate of cooling after high-speed deformation are of special importance. By varying these two characteristics, it is possible to change substantially the structure, homogeneity and thermal stability of metals and alloys and thereby to control their properties.

The principal basis for this is that the critical degree of deformation required to initiate dynamic recrystallization increases with a decrease in deformation rate. Consequently, dynamic recrystallization can in many cases be precluded, even in heavy deformation, by lowering the deformation rate. Furthermore, a reduced rate of deformation can form a structure which will be stable against recrystallization in the subsequent heating at the deformation temperature.

For instance, no recrystallization occurs in pure nickel deformed 30% at 800°C at a rate of 10^{-3} s^{-1} and then held at that temperature for up to 10 minutes. For comparison, in XH77TЮP nickel-base alloy deformed 30% at 1080°C recrystallization begins after one-minute holding at that temperature. In 37X12H8Г8МФБ alloy deformed at a low rate at 1100°C, recrystallization begins after 30-40 minutes of holding at that temperature. In the same alloy deformed and heated at 1150°C, this time is 20-25 minutes.

In a low-carbon iron-nickel alloy (0.02% C, 29.5% Ni) rolled $< 10\%$ at 980°C and heated isothermally at that temperature, recrystallization is only observed after a holding time of 30 minutes [211].

As can be easily understood from the foregoing, this is due to dynamic recovery which takes place during slow deformation. Subsequent heating adds to perfection of subgrains and their boundaries for it diminishes the concentration of thermally unstable dislocation pile-ups and single dislocations in the bulk of subgrains. At a rather long time of holding, the conditions become favourable for the growth of subgrains and in-situ recrystallization.

Thus, while recrystallization during slow heating after hot deformation at low rates is undesirable, slow cooling after deformation or holding at the deformation temperature is not only safe, but, what is more, advisable as it ensures a substructure of the highest stability. In subsequent heating to temperatures well above the deformation temperature, recrystallization begins sooner in specimens which have been cooled more quickly after deformation.

This circumstance should be kept in mind in practice, especially when treating large-size articles. After hot deformation of such articles under common conditions, the rate of cooling will be dif

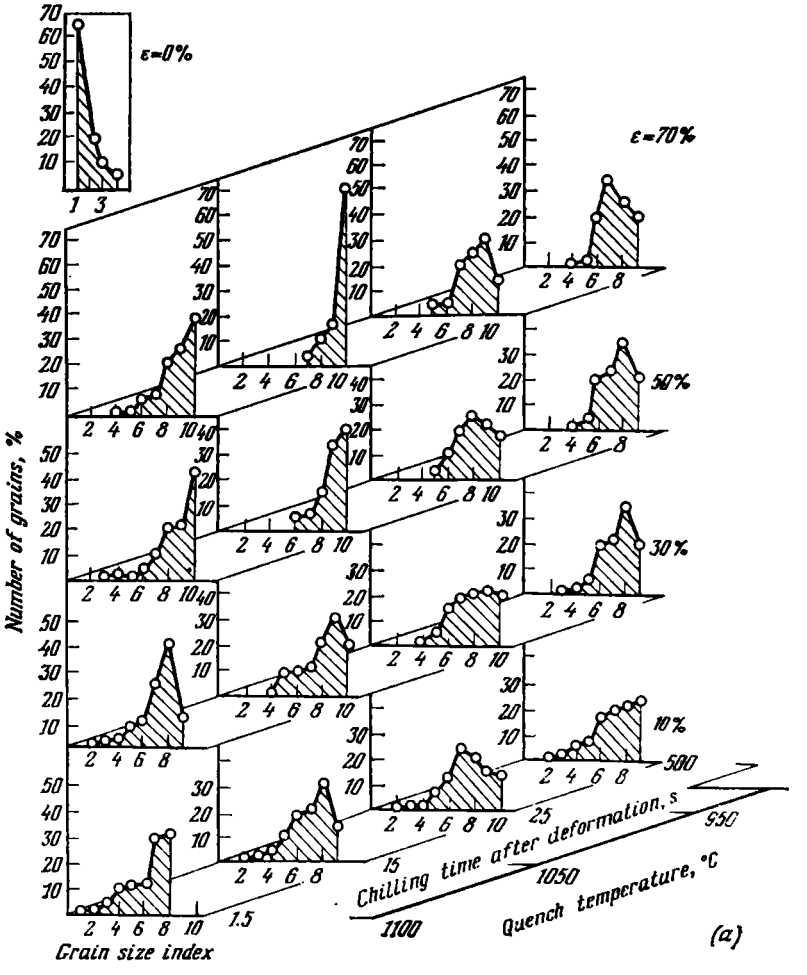

Fig. 102. Effect of post-deformation cooling on structural changes in

ferent in various sections and, accordingly, the thermal stability will also be different. The highest thermal stability will be in portions cooled at a lower rate. In subsequent heating, the external portions, which have been cooled faster and thus are more susceptible to recrystallization, will be heated earlier to the hardening temperature. This may result in an appreciable structural inhomogeneity.

Things are different with a metal deformed at a high rate. In that case, dynamic recovery is impeded and the conditions are more favourable for dynamic recrystallization. And what is very important is the fact that recrystallization is accelerated both in the course of deformation and in the subsequent cooling or isothermal heating. Even a few seconds' long holding after deformation causes noticeable recrystallization. Under definite conditions of cooling after hot deformation, even the process of grain growth can partially take place.

As an example, consider the results obtained in a study [212] of recrystallization in hot-deformed austenitic (18% Cr + 8% Ni) and ferritic (transformer type) steels in which no phase transformations took place. Treatment of preliminarily annealed specimens included the following stages: heating at 1200°C (10 minutes), air chilling to 1100°C, deformation at that temperature by single-stroke upsetting (at an average rate of approximately 10^2 s^{-1}) to a given degree, chilling to various temperatures, and water quenching. The degrees of deformation and the conditions of chilling are given in Fig. 102. Curves of grain size distribution were also plotted.

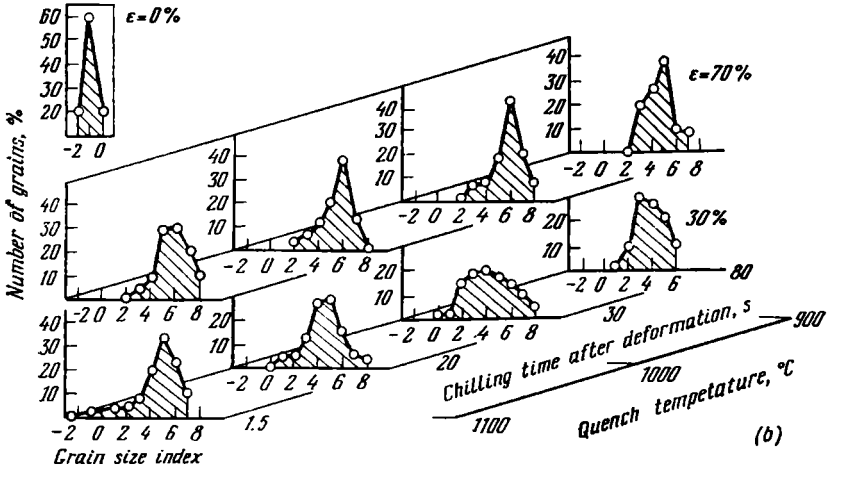

(*a*) hot-deformed austenite and (*b*) ferrite [212]

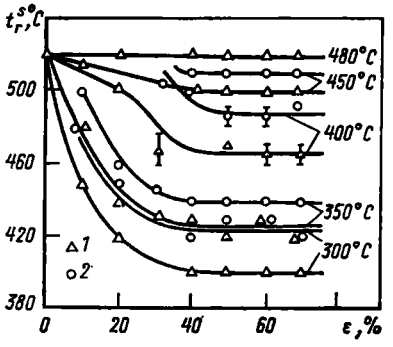

Fig. 103. Curves showing how the temperatures of the beginning of recrystallization [209] grow with deformation temperatures (numbers at curves)

1—recrystallized structure; *2*—original polygonized structure

The preliminary high-temperature annealing was used to form large original grains as well as to remove traces of prior deformation. In that case, the appearance of fine grains in the deformed structure, which were not observed prior to deformation, was indicative of primary recrystallization, while subsequent grain enlargement was an indication of grain growth.

An analysis of the curves of grain size distribution depending on the degree of deformation and the conditions of chilling (see Fig. 102) made it possible to conclude that a relatively large volume of the material had time to recrystallize during chilling. The process noticeably grew in intensity at an increased degree of deformation and did more so in the austenitic than in the ferritic steel. For instance, primary recrystallization in the austenitic steel deformed 50 to 70% was finished after a chilling time of only 15 s. On a deformation of 10-30%, this required more than 6 minutes. For the ferritic steel, hte required time was a few times longer. This agrees well with the fact that dynamic recovery occurs more easily in ferritic steel. Accordingly, the driving force of recrystallization diminishes.

Thus, to prevent recrystallization in high-speed hot deformation it is necessary to use accelerated cooling. It is not always feasible in practice, especially with large-size pieces. For that reason it is more preferable to use low rates of deformation.

A typical example of this approach is the method proposed by Yu. M. Weinblat *et al.* [12, 209] for manufacture of aluminium alloy parts of homogeneous polygonized structure.

A serious drawback of the common methods for making pressed aluminium alloy articles is that heating for hardening forms a very inhomogeneous structure in deformed articles; in some microregions where recrystallization is facilitated, a very coarse grain can form ('coarse-grained rim').

In Weinblat's method, this is prevented by deforming the metal slowly at an elevated temperature. The polygonized structure thus formed is rather stable and can recrystallize only at a temperature well above the temperature of hardening. In this method, both a low deformation rate and a high temperature of deformation are essen-

tial. As may be seen from Fig. 103, the temperature of the beginning of recrystallization rises substantially with an increase in deformation temperature.

Figure 104 shows the microstructures of two hardened pieces: one deformed by the common technology and the other by the method proposed in [12, 209].

The systematic study of the effect of various factors on the structural thermal stability of hot-deformed aluminium alloys [12, 209] has made it possible to conclude that it is not the pattern of stressed state, nor even so much the amount of deformation as the rate of deformation that plays the decisive role in this process.

Let us recall that the temperature of the beginning of recrystallization at a stable stage is independent of the degree of deformation, since at this stage a dynamically stable structure forms which practically does not change with a further increase in the amount of deformation. This means that unvarying conditions set in for subsequent recrystallization.

Hence, at relatively high degrees of deformation, this structure and these conditions can only be changed by varying the temperature and rate of deformation. As an example, let us consider the results obtained in [12] for an AK8 alloy (40% Cu, 0.6% Mg, 0.7% Mn, 0.70% Si, 0.25% Fe, balance aluminium).

The thermal stability of the structure of the alloy was determined by the temperature of the beginning of recrystallization t_r^s and by the least degree of deformation at which recrystallization begins during heating for hardening (500°C, 1 h). This degree of deformation was called the critical deformation, ε_{cr}, by the authors.

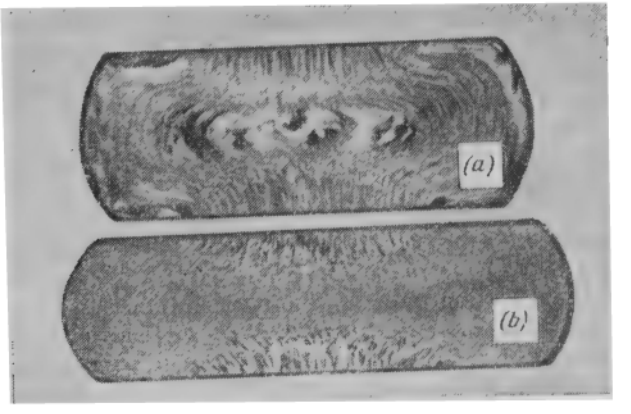

Fig. 104. Microstructures of metal parts after heat treatment
(a) by common technology; (b) special technique

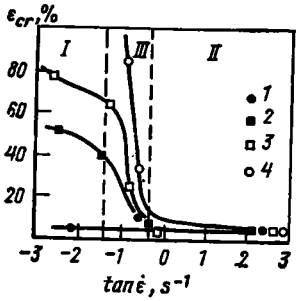

Fig. 105. Critical deformation ε_{cr} versus the logarithm of deformation rate at various deformation temperatures. AK8 alloy [12]

1—300°C; *2*—380°C; *3*—400°C; *4*—470°C

Figure 105 shows the logarithmic curves of ε_{cr} as a function of deformation rate plotted for various deformation temperatures.

For the lowest temperature of upsetting (300°C), the 'critical' deformation turns out to be practically independent of the rate of pressing (i.e. the case is similar to that observed in cold deformation).

For the specimens deformed at various rates at higher temperatures, the whole range of deformation rates can be divided into three intervals.

In interval *I* (low deformation rates), ε_{cr} is seen to depend heavily on the temperature of upsetting and only slightly on the deformation rate.

In interval *II* (high deformation rates), the structure is unstable and recrystallizes easily during heating for hardening. The instability is roughly the same for all upsetting conditions within this interval, i.e. practically independent of either the temperature or the rate of deformation. Thus, the process of structure formation in this interval is similar to that which takes place during low-temperature (300°C) deformation and subsequent heating.

Interval *III* that lies between the two intervals is most dangerous. Here, both the rate and the temperature of deformation have an appreciable effect on ε_{cr} and, therefore, on structure stability. Under real conditions, there always forms a gradient of deformation rates and often a gradient of temperatures. This is especially the case with articles of large size and intricate shape; the conditions of deformation that correspond to interval *III* will inevitably lead to zonal inequigranularity and inhomogeneous structure in subsequent heating.

According to [12], interval *III* of deformation rates is representative of the conditions of stamping as applied to aluminium alloys.

Using the experimental curves analogous to those described above, Weinblat *et al.* [209, 12] plotted generalized diagrams of structural states of alloys as a function of the rate and temperature of deformation. These diagrams give notion of the structure of an alloy immediately after hot deformation and the structure of deformed articles that forms in subsequent heating (Fig. 106*a*). Region *I* in Fig. 106*a* is typical for an unrecrystallized structure; region *III* for a structure recrystallized directly during deformation and subsequent cooling (i.e. without heating); region *II* for the structure that re-

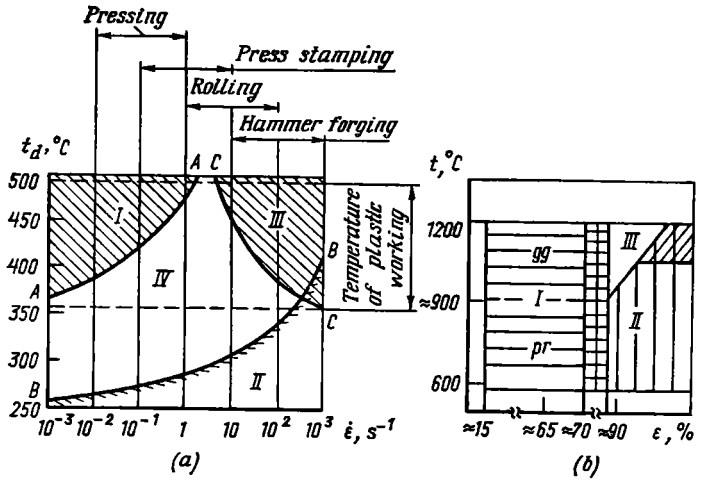

Fig. 106. Structural diagrams

(*a*) AMr6 alloy after hot deformation and heat treatment [12]; (*b*) f.c.c. precision magnetic alloys after cold deformation and heating: *I*—the structure of primary recrystallization (*pr*) and of grain growth (*gg*) without distinct texture; *II*—primary recrystallization structure with a cube texture; *III*—secondary recrystallization structure with a weak texture [255]

crystallized during heat treatment after deformation; and region *IV* for a mixed (partially recrystallized) structure.

The original state of a material also has a noticeable influence on the stability of the structure formed in hot deformation. If specimens with an unrecrystallized structure are deformed, i.e. with traces of prior deformation, the region in which the material can undergo recrystallization in subsequent annealing becomes markedly wider and the temperature of the beginning of recrystallization decreases.

These observations and conclusions are applicable not only to aluminium alloys but to other materials as well. Many similar facts have been established in studies on the structural changes in steel during high-temperature thermomechanical treatment. For instance, tensile deformation at a rate of 1×10^{-2} s^{-1} in steel Grade 40ХН3МС over the austenitic temperature range (900-950°C) results in a mixed (partially polygonized and partially recrystallized) structure that remains stable for a rather long time at the temperatures indicated.

Structural diagrams can also be constructed for cold deformation and subsequent heating (Fig. 106*b*).

It is therefore essential to analyse thoroughly the effect of the rate and temperature of deformation and of the conditions of subsequent annealing on the structure of various alloys and their thermal stability. In particular, it is of importance to construct struc-

tural diagrams like those given above. Naturally, in each case, one should consider properly the particular properties of an alloy. For instance, in alloys which are two-phase in deformation (i.e. contain carbides, intermetals or other secondary phases) the character of structural states will depend on the nature, concentration, shape, size and distribution of these particles.

An important feature of recrystallization in hot deformation is also the fact that the process often occurs in parallel with decomposition of the supersaturated solid solution and reverse dissolution of disperse phases. Hot deformation is often effected within temperature ranges corresponding to supersaturated state of the solid solution. Deformation usually accelerates decomposition. The degree of its completeness and homogeneity depends on the conditions of deformation. If decomposition has been nonuniform, the conditions for grain growth in subsequent heating for hardening will also be nonuniform. Heating can cause dissolution of disperse particles and thus form favourable conditions for secondary recrystallization and grain coarsening.

Structural diagrams cannot naturally be an adequate substitute for recrystallization diagrams (see Ch. 9) which give such an important structural characteristic as the average grain size. But they are often quite suitable for the purpose. For instance, the mechanical properties of hot-deformed and annealed aluminium alloys worsen markedly on changing from polygonized to recrystallized structure. On the other hand, the details of a polygonized structure (the size and shape of subgrains) and the size of recrystallized grains have in themselves an appreciably weaker effect.

In such cases, structural diagrams (which can be plotted much more easily than recrystallization diagrams) are quite informative for our purposes.

Chapter 7

Recrystallization on Critical Deformation

As noted in Ch. 3, the grain size of polycrystals after recrystallization annealing depends non-monotonically on prior deformation. The characteristic curve has at least one maximum, and for many alloys it features several maxima.

The first maximum which falls on the portion of low, so-called critical, degrees of deformation is practically typical of all metals and alloys. The causes and the mechanism of formation of this maximum will be discussed in this chapter.

Other maxima, which appear less frequently and fall within the intervals of moderate and heavy deformations, will be discussed in Chs. 8 and 10.

7.1. General Relationships

Strictly speaking, the critical deformation ε_{cr} is the minimal degree of deformation following which primary recrystallization nuclei appear and grow in subsequent heating. In that case, the effect of critical deformation ε_{cr} on the D-ε curves relating the degree of prior deformation to the average size D_{av} of recrystallized grains will be different for single crystals and polycrystals.

With single crystals, the appearance of first recrystallized grains results in a decrease of the average grain size; here ε_{cr} is the lowest deformation under the effect of which $\overline{D}$ begins to diminish (Fig. 107, curve *1*).

With polycrystals, the formation of a small number of recrystallization nuclei and their growth at the expense of the deformed matrix must cause an increase in the size of recrystallized grains $\overline{D}$ compared to the original size (prior to deformation); here ε_{cr} is representative of the moment at which $\overline{D}$ begins to increase, i.e. of the maximum on the curve $\overline{D} = f(\varepsilon)$, as seen from Fig. 107 (curves *2* and *3*).

In the range of low deformations, however, a maximum on the $\overline{D}$-ε curve can be caused not only by the appearance of first actual nuclei of primary recrystallization but also by the growth of some original grains at the expense of others. The deformation corresponding to the first maximum on the $\overline{D}$-ε curve will not then be the criti-

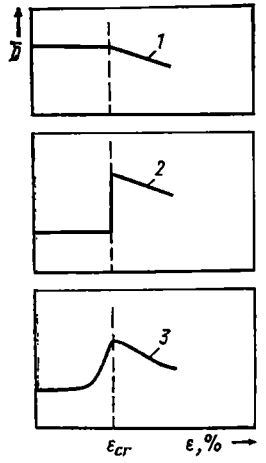

Fig. 107. Variations of grain size $\bar{D}$ during recrystallization after critical deformation
1—for single crystals; 2, 3—for polycrystals

cal deformation in the sense mentioned above.

On the other hand, the critical deformation of polycrystals is taken generally as the lowest deformation causing the appearance of the first maximum for grain size on the $\bar{D}$-ε curve, disregarding the cause of that maximum. Practically, it causes no complications since the deformations that favour grain enlargement due either to a low number of nuclei or to the consumption of some original grains by others are close to each other in magnitude.

Table 16 contains data on the critical deformation and the D_{cr}/D_0 ratio (the ratio of the size of recrystallized grains after critical deformation ε_{cr} to that in undeformed metal heated to the same temperature) for selected metals and alloys, as determined by various workers. As seen, the critical deformation is usually a few (up to ten) per cent.

If the time of heating is within the common range (1-2 h) and the temperature of heating is not excessively high (not above $0.9T_m$), the grain-coarsening factor D_{cr}/D_0 ranges from 4 to 10. It has been shown in many works that ε_{cr} depends on many factors, including the conditions of deformation and heating, the original microstructure, the nature and purity of the metal, etc.

Before analysing the effects of these factors, let us consider the shape of the first maximum in the $\bar{D}$-ε curve.

According to a number of reports, especially in the earlier studies, $\bar{D}$ changes jumpwise with an increase in the degree of deformation to ε_{cr} and immediately reaches a maximum (Fig. 107, curve *2*). As the deformation rises above ε_{cr}, $\bar{D}$ diminishes but rather smoothly. This shape of the curve agrees well with the assumption that the first maximum is associated with a low number of actual nuclei. The smaller the number of nuclei, the coarser the grain.

A number of later works have shown, however, that the $\bar{D}$-ε curve does not always change in a jumpwise manner (Fig. 107, curve *3*). The height of the peak depends on many factors, as does the magnitude of ε_{cr}.

In all cases, an increase in the temperature of annealing causes a decrease in ε_{cr} (Fig. 108*a* and Table 16) and a sharp rise in $\bar{D}$. A change in temperature (and in the rate of heating too) has a sharp effect on the form of the left-hand (ascending) branch of the $\bar{D}$-ε

TABLE 16. Critical Deformation of Various Metals and the Associated Structure Coarsening (after various authors)

Metal (alloy)	$\overline{D}_0$, μm	Type of deformation	t_h, °C	ε_{cr}, %	Grain coarsening on heating after ε_{cr}, $\overline{D}_{cr}/\overline{D}_0$
Fe	60	Upsetting	800*	4.5	10
		Rolling	800	5.5	9
			875	2.5	12
			800	3.1	8
			750	6.0	3
Fe + Si	120	Upsetting	900**	6.0	3.0
			900	8.0	2.5
		Rolling	900 (τ = 3 h)	8.5	13
		Upsetting	1200 (τ = 1 h)	5.0	10
Steel ШХ15	120	Hot forming	900	3	2.5
			1000	2	5
Cr		Upsetting	1020	7	1.5
			1500	2.5	6
Al (99.99%)	80	Upsetting	400	6.5	7.5
			500	5.5	5
	150		550	2.3	8
	770		550	1.0	7
Cu (99.99%)	70	Rolling	800	1.0	10
			500	4.3	3
		Tension	800	1.0	12
Cu + 0.065% Ni	70	Rolling	800	2.8	3
+ 0.040% O_2		Tension	800	2.0	4
Cu + 0.5% Cr	70	Rolling	1000	2.0	8-10
Cu + 0.05% Cr	70	Rolling after ageing at 700°C	1000	18.0	8
Cu + 0.013% Fe	70	Rolling	800	5.0	—
Cu + 0.1% Zr	70	Rolling	800	1.5	—
Ti	20	Rolling	815	8	—
Ti + 0.08% C	20	Rolling	650	10	—
Ti + 0.144% W	20	Rolling	815	10	—
Ti + 0.049% N	20	Rolling	600	12	—
Ti + 0.04% C	20	Rolling	815	10	—
Ti + 0.2% Fe	20	Rolling	600	12	—

Note: Heating in the furnace except where specially indicated.

* 200°C/s.
** Induction heating.

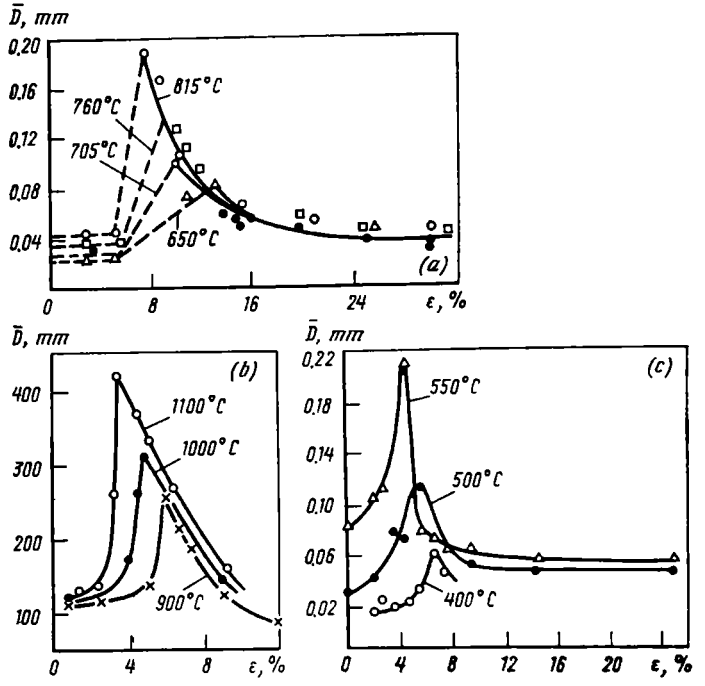

Fig. 108. Effect of the degree of deformation and the temperature of annealing on grain size after recrystallization annealing

(a) commercially pure titanium, (b) Fe + 3% Si alloy; (c) aluminium

curve (which becomes smoother with a decrease in the temperature or rate of heating), but has only a slight effect on the form of the right-hand (descending) branch (Fig. 108). Experimental points obtained at various temperatures of annealing practically fall on the same descending portion of the curve.

An increase in the rate of deformation lowers ε_{cr} (Fig. 109) and increases the size of 'critical grain' [213]. Unlike variations in the temperature and rate of heating, a change in the deformation rate has a strong effect on the right-hand descending branch of $\bar{D}$-ε curve. Besides, the rate of deformation can influence the shape of recrystallized grains and of their boundaries. At high deformation rates, recrystallized grains in f.c.c. metals and alloys have the shape of almost regular polyhedrons with straight boundaries and with angles close to 120°. At low deformation rates, the structure is less stable, grain boundaries are extremely curved and have numerous 'tongues' which are typical of the mechanism of strain-induced migration [156].

Figure 110 shows the effect deformation temperature in the subrecrystallization temperature range ('warm' deformation) on ε_{cr} for a Ni + 20% Cr alloy. This effect is opposite to that observed in hot deformation. An increase of the deformation temperature in the subrecrystallization range shifts ε_{cr} into the region of heavier deformations, i.e. makes itself felt so as if upsetting were accompanied by simultaneous recovery. A change in the deformation temperature has a stronger effect on the shape of the left-hand branch. The difference in the size of grain, when passing from the subcritical to the critical range, is less pronounced in 'warm' deformation than in cold deformation.

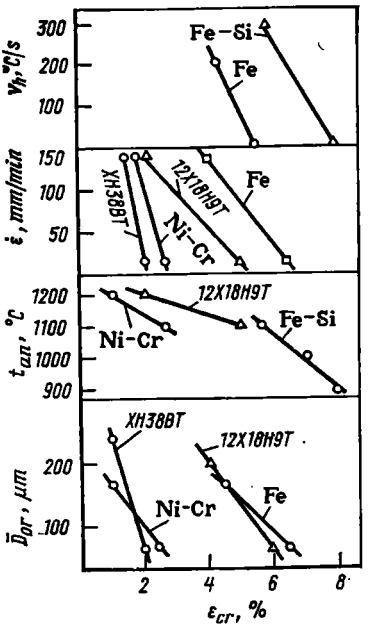

Fig. 109. Effect of various factors on critical deformation ε_{cr}

Figure 109 shows the dependence of ε_{cr} on the size of original grains for selected alloys [213, 214]. It is seen that ε_{cr} shifts into the region of lower deformations with an increase in the size of original grains.

The effect of the original grain size becomes even more pronounced if a metal has a high concentration of secondary phase disperse particles. This may be well illustrated by the results obtained for a chrome bronze Cu + 0.5% Cr [215]. Before rolling deformation intended to determine the critical degree, the original cold-rolled specimens ($\varepsilon = 80\%$) were heat-treated in four different modes. In three modes (I, II and III), specimens were heated at 1020°C to form coarse grain ($\bar{D} = 0.7$ mm) and then cooled at various rates. In mode IV, specimens were heated at 700°C, which produced an appreciably finer grain ($\bar{D} = 0.02$ mm) and a high concentration of excess chrome particles of a relatively uniform size (2 to 4 μm).

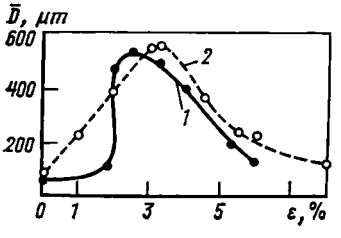

Fig. 110. Effect of deformation temperature on the shape of $\bar{D}$-ε curve for Ni + 10% Cr alloy deformed at 20°C (*1*) and 800°C (*2*) and annealed at 1100°C for 1 h

After rolling with slight deformations, specimens in four various sta-

tes were heated at 1000°C for 30 minutes. During the heating process, recrystallization occurred in parallel with dissolution of chromium particles. Since these particles had been present in a high concentration prior to deformation, they had a large influence on the dislocation structure of the matrix and, in heating at 1000°C, retarded boundary migration before being dissolved.

For fine-grained specimens (mode IV), the critical deformation turned out to be very high, 18-20% against 2% for specimens with coarse original grain.

For the same size of large original grains, an increase in the concentration of disperse chromium particles (mode III) had almost no effect on ε_{cr}, but the maximum size of grains was appreciably smaller (by a factor of 2 to 3).

Systematic data on the effect of impurities on ε_{cr} have been obtained for aluminium alloys. Copper and zinc have been found to have no effect on the critical deformation. On the other hand, iron and especially manganese shift ε_{cr} to higher values. A comparison of these results with the solubilities of these elements in aluminium has made it possible to attribute the sharp effect of iron and manganese to their low solubility in aluminium and, therefore, to the influence of excess phase particles ($FeAl_3$ and Al_6Mn).

This effect of disperse phase particles can obviously be observed only at temperatures at which they are not dissolved or are dissolved insignificantly. If, however, the recrystallization heating involves noticeable (but not excessively fast) dissolution of disperse particles, heating after ε_{cr} can cause vigorous grain coarsening, even more vigorous than in the absence of these particles. The shape of the corresponding maximum on the $\bar{D}$-ε curve then corresponds to a jumpwise change of $\bar{D}$ at ε_{cr}.

Since the shape of the first maximum of the D-ε curve and the type of the microstructure being formed and also the value of ε_{cr} depend in a complicated manner on various factors, it is reasonable to suppose that there are several causes and several mechanisms for the formation of that maximum. It may be supposed therefore that this maximum is a superposition of a few maxima each of which depends in a particular manner on various factors.

The results obtained on XH77TIOP alloy [356] are direct evidence in favour of this assumption. The experiments were based on the following reasoning. If actual maxima are superposed on one another, it might be possible, by deforming a specimen at a very low deformation gradient $d\varepsilon/dx$ (where x is the distance along the specimen), to shift various maxima a large distance apart and thus to detect separately the actual maxima instead of the common maximum.

In the experiments, this has been achieved by tensile tests of tapered specimens having a very small taper angle. Owing to this and also to the fact that the total deformation was very low, the

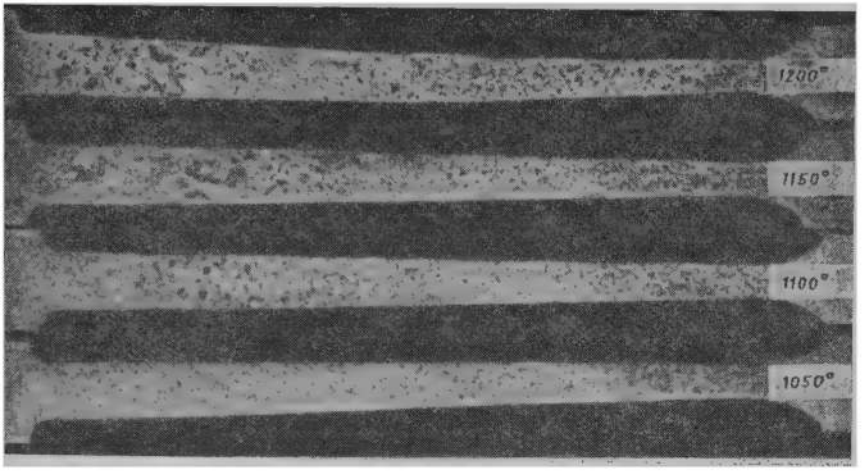

Fig. 111. Microstructure of tapered specimens of nickel alloys after tensile deformation and recrystallization annealing at various temperatures

region of the low deformations turned out to be extended along the length of specimen so that the deformation gradient $d\varepsilon/dx$ along the specimen was low.

Figure 111 shows the microstructures of the specimens after tension and recrystallization annealing. As may be seen, the structure in each has two maxima of grain size in the region of low deformations, which are shifted slightly one relative to the other (the picture is most clear in the specimen heated at 1150°C). With a slightly higher deformation gradient $d\varepsilon/dx$, the two maxima would merge together.

The existence of two maxima is convincing evidence that there are two various mechanisms of grain enlargement after low deformations, and, therefore, there are essentially discernible particularities in the nature of structural changes in the range of low deformations.

7.2. The Mechanism of Recrystallization after 'Critical' Deformation

Up to a recent time, there existed two different views on the mechanism of 'critical' recrystallization. One of them, which was formulated by S.S. Steinberg, G. Masing, M. Smith and some other researchers, reduces to the statement that recrystallization after 'critical' deformation does not differ principally from recrystallization after heavy deformations and also occurs by the formation of nuclei of new undistorted grains. A coarse-grained structure may

be due to a low number of these nuclei. Though being widespread, this standpoint has found no experimental support.

By another view, first formulated by D. Jaffrey and supported by E. M. Savitsky, Ya. R. Rauzin, A. P. Gulyaev, S. S. Gorelik, J. E. Burke and others, coarse grain forms by the growth of some original grains at the expense of others. Some workers in this group disagree on the problem of the causes and driving forces of grain coarsening in 'critical' recrystallization.

Burke and Shiau [216] have made direct observations of the mechanism of recrystallization in lightly deformed brass and concluded that the enlargement of the original grains after critical deformation and the nucleation are two competing processes which differ from each other in the length of the incubation period. On light deformations, the incubation period of nucleation is longer, because of which the growth of original grains has the decisive effect on the structure.

'Critical' recrystallization was not explained for a long time mainly owing to insufficient available experimental data on structural changes in light deformations. This gap has been filled in by a recent experimental study which has been briefly described in Ch. 2.

These experiments have shown that there is no special 'intergranular' mechanism of plastic deformation at low (subcritical) deformations. Plastic deformation at common rates, beginning from the lowest degrees and temperatures up to $0.7\text{-}0.8T_m$ is effected by intragranular shear, i.e. by dislocation movement. On the other hand, structural changes on low deformations have some features responsible for the mechanisms of 'critical' recrystallization. This relates, in the first place, to microinhomogeneous nature of the deformation and the effect of deformation rate on this inhomogeneity.

Table 17 gives the misorientation angles β in individual Ni-Cr crystallites after various modes of deformation. Even a rather light

TABLE 17. **Misorientation Angles β_{min} of Separate Ni-Cr Crystallites**

ε, %	β_{min}^{or}	β_{min} after deformation at a rate, cm/s	
		400*	0.03**
0	20-50	—	—
1	20-50	21-79	42-90
1	20-50	(22-51)***	(35-97)
8.5	20-50	(16-29)	(15-28)

* Hammer upsetting.
** Press upsetting.
*** Values in brackets were obtained after heating for 60 min at 1100°C.

deformation increases β, which is apparent from tangential blurring of reflections visible even to the naked eye on X-ray photographs and is indicative of a change in the intragranular substructure.

Upsetting at a higher rate is characterized by a greater inhomogeneity in the deformation of various grains. The range of angles β before upsetting was from 20 to 50 minutes ($\Delta\beta = 30'$), but changed to 21-79′ ($\Delta\beta = 58'$) on hammer upsetting and to 42-90′ ($\Delta\beta = 48'$) on pressing. Thus, after slight upsetting (on the hammer), the structure had both strongly deformed grains and practically undeformed grains. After pressing (low deformation rate), there were no undeformed grains and the maximum misorientation was even greater than after hammer upsetting.

In fine-grained specimens of nichrome and iron, it is also seen that the deformation due to pressing is more uniform and the inhomogeneous microstresses produced are more appreciable. In X-ray photographs, there was practically not a single distinct reflection after a press deformation of only 2%, whereas photographs taken after a 2.5-% deformation on the hammer had quite a few reflections.

On the other hand, radiographic lines were more blurred in radial direction after hammer deformation than after pressing. Deformation at a higher rate seems to produce additional structural changes (apart from structure dispersion and formation of inhomogeneous microstresses). One of the changes of this kind probably results from the effect of uniform microstresses first discovered by B. M. Rovinsky *et al.*

Using a method of local radiography, Gorelik and Spektor [217] revealed elastic distortions which were distributed non-uniformly over various microvolumes but were uniform in a given microvolume. Figure 112 shows two radiographs of deformed Fe + + 3% Si alloy. Arrows (*1*, *2*, *3*) indicate some reflections which pass well beyond the Debye ring. This effect can be interpreted as a result of elastic compression or tension of certain crystallites. The stresses obviously result from non-uniform deformation of various grains or groups of grains.

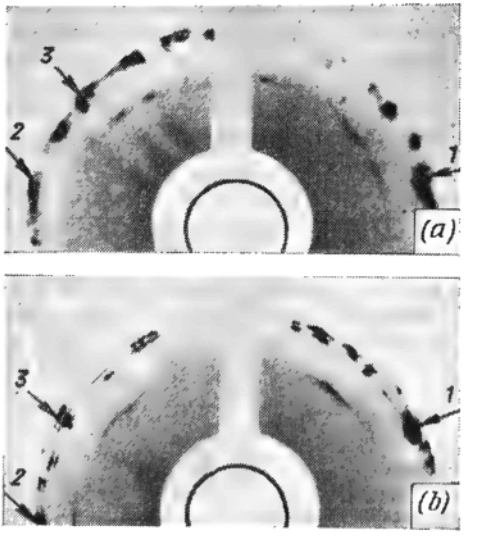

Fig. 112. Radiograms of Fe + 3% Si alloy after deformation to $\varepsilon < \varepsilon_{cr}$ (*a*) and subsequent heating at 900°C for 30 min (*b*). Local X-ray technique [217]

The highest deviations of the interplane spacing from the average value after hammer upsetting were found in silicon iron, smaller in iron and still smaller in nichrome and nickel. Calculation of the highest stresses in individual crystallites gave the following values: 30 kgf/mm² for Fe + Si, 15 kgf/mm² for iron, and 15 kgf/mm² for nichrome. These data correlate with the elastic limits of these materials which are respectively 32, 15-17 and 11-13 kgf/mm². The effect becomes less pronounced with a decrease in the deformation rate, which is obviously due to a more uniform deformation of variously oriented crystallites. In this case, homogeneous microstresses are localized in smaller volumes and the stress gradient decreases accordingly. As will be shown later, these stresses are very stable.

An analysis of the intensity of X-ray interference lines has suggested a conclusion that the formation of deformation textures begins already at low degrees of deformation (3-6%). This effect is naturally weak but shows up quite clearly after deformations at a low rate.

It can be concluded from the foregoing and from the material of Ch. 2 that at low (subcritical and critical) degrees of deformation there occurs intragranular dislocation flow which, however, is rather inhomogeneous in character.

Boundary regions are characterized by a high density of defects, in particular dislocations. On the other hand, the density of defects is, as a rule, different on the two sides of a boundary, i.e. in boundary regions of adjacent grains. Non-uniform conditions of deformation cause stresses in microvolumes comprising a few grains. This non-uniformity manifests itself stronger with an increase in the deformation rate.

Studies have been made in order to decide which of the two probable mechanisms—either the formation and growth of a small number of nuclei or the growth of some original grains—is responsible for the appearance of the first actual maximum after critical deformation or for the left-hand branch of the resultant maximum. Some of the results obtained will be discussed below.

Gorelik and Granik [218] made a quantitative metallographic analysis of recrystallization on commercial iron specimens with the same grain size ($\bar{D} = 60$ μm) in the original structure.

Cylindrical specimens were upset in a press to various degrees of deformation with an accuracy of ±0.2% and induction-heated to 800°C at a high rate (200°C/s). This made it possible to analyse structural changes after very short times of holding at 800°C (2-3 s), counting from the moment of full heating (4 s).

The obtained curve of the effect of annealing time on the average grain size (Fig. 113) suggests that structure coarsening after a critical deformation ε_{cr} of 4.5% begins with the growth of original grains. Only this mechanism can explain why $\bar{D}$ increases continuously in

time. Otherwise, the value of $\bar{D}$ should diminish temporarily after the formation of even a small number of new grains and the $\bar{D}$-ε curve should exhibit a bend as does the curve for $\varepsilon = 7\%$.

In heating of specimens deformed 10% (supercritical deformation), at first (for 1-2 min) the main process that can be revealed metallographically is grain growth, too, which occurs even at a higher rate than after critical deformation. But with a further increase in the time of annealing, $\bar{D}$ begins to diminish as nuclei of new recrystallized grains become discernible. The final structure in that case is the result of two competing processes: grain growth (of original grains) and recrystallization by nucleation. After a heavier deformation (up to 20%), recrystallization practically occurs only by the formation and growth of recrystallization nuclei. The rate of these processes is now so high that nuclei become discernible after a short time of heating (3-5 s).

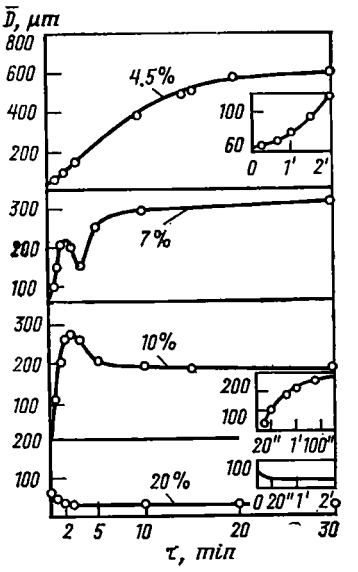

Fig. 113. Effect of time of heating at 800°C on the average grain size in iron (after various deformations) [218]

An analysis of grain-size distribution curves also confirms that recrystallization after deformation to ε_{cr} occurs by the mechanism of grain growth.

During heating of a specimen deformed to ε_{cr}, the number of small grains remains practically unchanged (or changes only insignificantly), but there appears ever increasing number of large grains whose size exceeds appreciably that in the original state.

After supercritical deformation, however, large grains also increase in size, but the number of small grains increases noticeably at the early moments of annealing. With a longer time of annealing, the number of the smallest and the largest grains begins to decrease and the number of moderate-size grains increases, so that the grain size distribution approaches the normal level.

Therefore, recrystallized grains, which have formed as nuclei, have a greater stability and partially grow at the expense of the larger grains formed by the mechanism of grain growth at the early stages of annealing. Thus, the structure of commercial iron deformed slightly above the critical deformation and annealed for a short time (up to 3-5 minutes) is unstable. This conclusion is very impor-

The above results of statistical analysis are confirmed by direct observations of structural changes.

It may be seen from the microstructures shown in Fig. 114 that some of original grains in deformed metal become 'centres' from which large grains grow. For instance, a large grain *A* marked by a dotted line in Fig. 114*c* has grown from an original grain *A* (Fig. 114*a*) and increased several times in size. During that time, however, the surrounding grains remained practically unchanged.

A similar result has been obtained by local radiography [217]. Figure 115 shows local radiograms of an Fe-Si specimen deformed to the critical deformation. The radiograms have been taken before and after heating. In the as-deformed state, there are blurred reflections (*1* and *11* in Fig. 115*a*). After heating, a small number of large point reflections appear (*1* and *11* in Fig. 115*b*).

Some of these reflections are in places which have been occupied by less blurred reflections (see, for instance, *9*, *4*, and *11* in Fig. 115. *a* and *b*). After supercritical upsetting deformation, it is impossible to establish any relation between the new and old reflections. Thus, radiographic analysis also shows that in heating after critical defor-

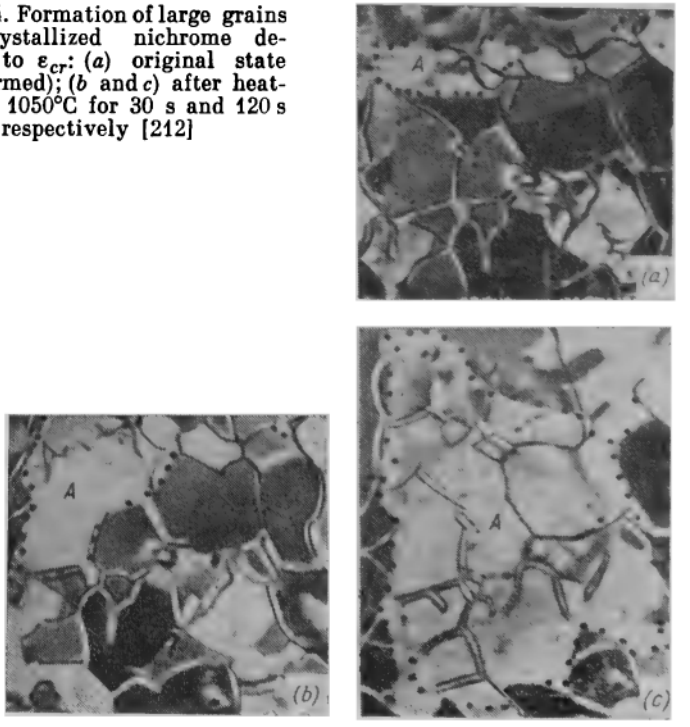

Fig. 114. Formation of large grains in recrystallized nichrome deformed to ε_{cr}: (*a*) original state (as-deformed); (*b* and *c*) after heating at 1050°C for 30 s and 120 s respectively [212]

mation large grains grow from original grains, in particular from least deformed ones.

What processes occur during heating of a metal the degree of deformation of which is less than the critical deformation?

As has been found by local radiography, reflections on radiograms taken from a metal deformed to $\varepsilon < \varepsilon_{cr}$ have the form of arcs blurred along the interference rings; after annealing, they split into small relatively sharp dots.

This splitting of blurred reflections can be interpreted as the result of stabilizing polygonization which takes place during annealing owing to the redistribution of dislocations into energetically more favourable groups.

Differences in the character of changes in the substructures of iron in heating after subcritical, critical, and supercritical deformation can also be revealed by analysing the extinction effect. Figure 116 shows the effect of deformation (before and after annealing) on the intensity of the (110) X-ray line and on the ratio of the intensities of the lines (110) and (220) in iron. These data suggest that polygonization during heating after subcritical deformation causes an enlargement of coherently reflecting regions and enhances slightly the extinction effect. Heating after critical deformation, which results in the formation of a very large grain, is not however accompanied by a sharp increase in extinction or by a noticeable coarsening of the substructure. On transition to supercritical deformations, in which case the grains formed in annealing from actual recrystallization nuclei are somewhat smaller than those formed after critical deformation, the extinction effect is not decreased, but is enhanced further.

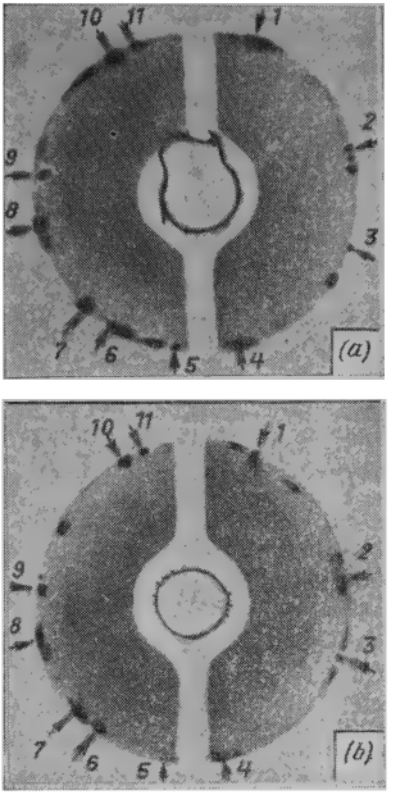

Fig. 115. Radiograms of a specimen of Fe + 3.0% Si alloy deformed to $\varepsilon_{cr} = 8.2\%$ before (*a*) and after (*b*) recrystallization annealing at 800°C for 30 min. Local radiography

Thus, in distinction to the process following critical deformation, heating after supercritical deformation produces finer grains, larger

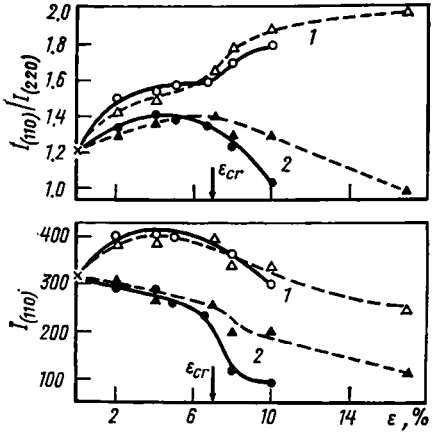

Fig. 116. Effect of deformation on intensity of X-ray reflections in iron [212]: dotted lines—hammer upsetting; solid lines—press upsetting

1—deformation; *2*—deformation and annealing at 800°C for 30 min

coherent regions and a more perfect substructure. This fact is another support of the assumption that the early stages of recrystallization after critical deformation occur by the mechanism of grain growth. It also explains well why in the region of deformations slightly above the critical value, in which case recrystallization occurs by two mechanisms—the growth of some of the original grains and the formation of recrystallization nuclei—the nuclei are more stable and partially grow at the expense of other grains formed at an earlier stage of the process by the mechanism of grain growth.

It seems probable that in heating after ε_{cr}, when some of the original grains increase in size owing to internal boundary migration at the same time, such processes take place as redistribution of dislocations and formation of substructures (polygonization).

X-ray structural analysis also shows that heating after $\varepsilon < \varepsilon_{cr}$ is accompanied by redistribution and release of uniform microstresses, though the rate of these processes is quite low.

In Figure 112, arrows indicate certain (211) reflections from individual elastically compressed crystallites in as-deformed Fe + + 3% Si alloy. The angles of these reflections correspond to a smaller interplane spacing than that for most of the other (211) reflections. Heating at 900°C for 30 minutes has caused a reflection to move to a position characteristic of smaller angles, which attests to an increase of corresponding interplane spacings, though not to a full extent. Heating for as long as 2 h has relieved uniform microstresses completely.

Stress relaxation in some stressed crystallites causes stress redistribution in adjacent grains and often changes somewhat their orientation. This is confirmed by the disappearance of some reflections after heating, which is due to a change in their orientation.

As noted earlier (see Table 17), a change in the deformation rate influences the character of structural changes caused by deformation. The effect is the same in heating.

In nichrome specimens subjected to subcritical deformation at a high rate, the polygonization decreased substantially the misorientation angles. The range of β angles changed from 27-79′ to 22-51′. In specimens upset at a low rate, the range of angles did not practically change from that observed in the as-deformed state (see Table 17).

But, as one would expect, polygonization causes an intensive narrowing of reflections in radial directions. Redistribution of dislocations with the formation of dislocation arrays normal to the slip planes must have only a weak effect on the total grain misorientation, but diminish substantially the non-uniformity of interplane spacings, which is the cause of radial blurring of X-ray reflections.

Heating of specimens upset to a supercritical degree of deformation leads to the formation of new grains through primary recrystallization. Misorientation angles for new grains lie in the range between 15 and 30 min (see Table 17) and do not depend on the rate of preceding deformation.

During heating after subcritical deformation, polygonization is accompanied by a slight frontal movement of individual boundaries. Examples of this movement are shown in Fig. 117. The main driving force of this movement is obviously the trend to decrease the grain-boundary energy and form more balanced joints, as in the case of grain growth. Most of these boundaries (for instance, 94 of the 100 boundaries observed in an aluminium specimen) move towards the centres of their curvature. A boundary usually moves frontally as a whole. The rates of movement of its individual portions differ only slightly, which is indicative of a low structural and energetic difference in the boundary volumes of adjacent grains along their boundaries. The distances through which boundaries move are not large, a few tenths or hundredths of the size of the 'devoured' grains. The path a boundary covers in 30 minutes at 400°C is approximately 0.01 mm.

In addition to this main mechanism, boundaries move in some cases under the action of another mechanism similar to that observed by P. A. Beck and P. R. Sperry. As an example, Fig. 117*b* shows successive positions of the boundary of the left-hand grain after annealing stages varying in duration. The movement of the boundary has certain specific features:

1. The boundary moves away from its centre of curvature (as indicated by the arrow).

2. Various portions of the boundary move extremely non-uniformly, so that the boundary which has been relatively straight initially becomes extremely curved (tooth-shaped) and its energy increases.

3. The distance through which such a boundary moves and the rate of its movement is 5 or 6 times longer than that for a boundary

which moves towards its centre of curvature as a result of a decrease in the grain-boundary energy.

4. The rate of movement varies very unevenly in time. Measuring the distances the boundary of the left-hand grain covers in the direction indicated by the arrow makes it possible to estimate its average minimal rate at various moments (the photographs are taken at various moments of heating). The minimal rates have turned out to be not less than 4×10^{-5}, 4×10^{-6}, 1×10^{-5}, and 5×10^{-6} cm/s.

This non-uniform movement of boundaries can be attributed to the effect of local differences in the elastic volume energy of

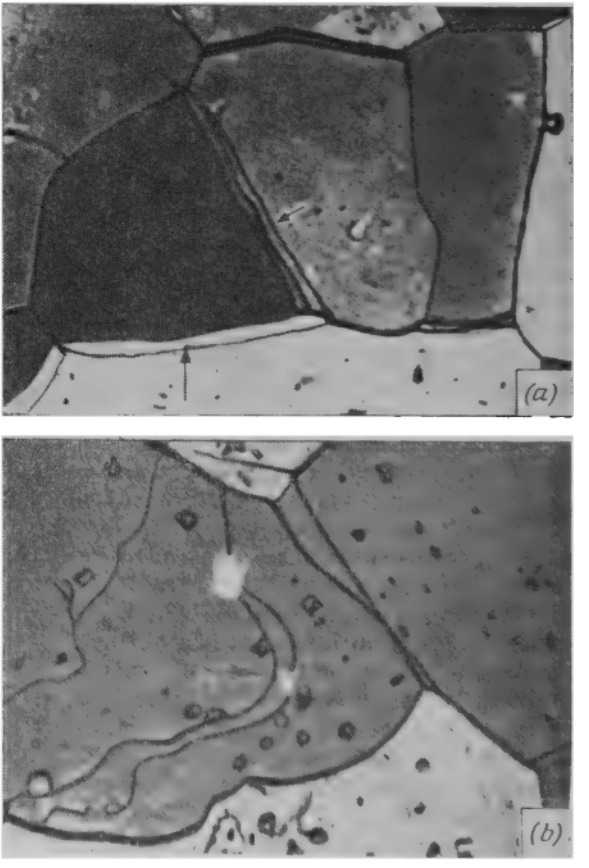

Fig. 117. Migration of boundaries of original grains in aluminium during heating after $\varepsilon < \varepsilon_{cr}$. Polarized-light microscopy. The pictures show successive positions of boundaries

(*a*) migration is stimulated by unbalanced grain-boundary tension, $\times 200$; (*b*) migration is stimulated by difference in volume energies between boundary regions of grains, $\times 400$

distortions of adjacent grains and of their microvolumes (differences in dislocation density) and also to a continuous redistribution of this energy during heating.

Thus, with $\varepsilon < \varepsilon_{cr}$ too, the frontal movement of a boundary in individual portions (which are few in number) can be due to a gradient in the elastic volume energy. In this process, the nature and rate of movement differ appreciably from those typical for more common cases of movement due to a decrease in grain-boundary energy.

In heating after $\varepsilon = \varepsilon_{cr}$, the process of structure formation differs sharply from that described earlier. The following specific features are worth mentioning.

1. A vigorous growth of grains follows an incubation period whose length depends on temperature. For aluminium, for instance, the incubation period in heating at 400°C (furnace heating) is three times longer than that at 500°C.

During the incubation period, some grains grow insignificantly through the frontal movement of their boundaries over short distances. Boundaries move either towards their centres of curvature or away from them. In the former case, a boundary moves uniformly almost parallel to itself and in the latter, with different rates in individual portions.

2. After the incubation period, vigorous grain growth occurs by frontal movement of boundaries. The regular correlation between the direction of migration and the position of the centre of curvature of a boundary now disappears. Boundaries move in both directions, either towards or away from the centres of curvature. The latter case is more frequent. The difference in the volume energies of adjacent grains obivously has a decisive effect on the nature of boundary migration.

3. The rate of deformation influences both the nature of the process and the final recrystallized structure.

In recrystallization after critical deformation at a low rate, the size of grains is smaller than in recrystallization after fast deformation (Fig. 118).

In addition, recrystallization of slowly deformed specimens is characterized by a sharp non-uniformity in the rate and direction of movement of various portions of the boundary of a growing grain. The boundary front is not straight and its direction varies unevenly in various portions. This results in the formation of 'tongues' protruding along the boundaries of 'devoured' grains (see the arrows in Fig. 118), where the elastic stresses and the density of dislocations and vacancies are higher than in the bulk of grain.

In high-purity aluminium, this phenomenon (strain-induced migration) was observed in some portions also after deformations well above the critical value.

The boundary migration caused by non-uniform strain in adjacent grains differs in its nature from the migration in grain growth. In the latter case a boundary migrates by its whole front, as 'a bubble wall in soap-suds', provided it encounters no disperse phase particles, while in the former case individual portions of a boundary are wedged in between adjacent grains.

A relatively low rate of deformation can obviously be characterized by a high non-uniformity of distortions in individual grains.

The boundary migration in recrystallization after fast deformation is slightly different in nature. A moving boundary has a smoother front, its individual large portions move at the same rate through adjacent grains (see Fig. 118), curving only insignificantly on passing from one grain to another.

This agrees well with the concept that fast deformation forms an appreciable stress gradient between individual adjacent grains or groups of grains and a low gradient within grains.

The rate of migration during vigorous grain growth is high, roughly 10^{-2} to 10^{-3} cm/s.

4. Boundary migration results in an interrupted and uneven growth of grains with time and in direction. While in heating after $\varepsilon < \varepsilon_{cr}$ this non-uniformity is rare and the paths of boundaries are short, in heating after ε_{cr} the jumplike migration of boundaries becomes a common case.

5. The boundaries of vigorously growing grains move through distances comparable with the size of grains. Boundary migration comes to an end when growing grains begin to collide. A further

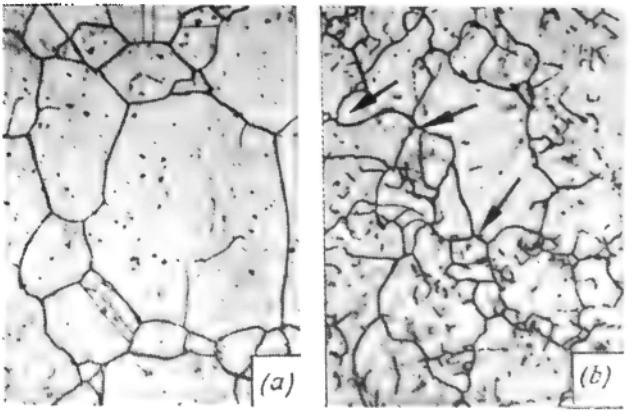

Fig. 118. Effect of deformation rate on ε_{cr} and the size and shape of grains formed in recrystallization annealing. Ni + 13% Cr alloy, hammer deformed (*a*) and press-deformed (*b*)

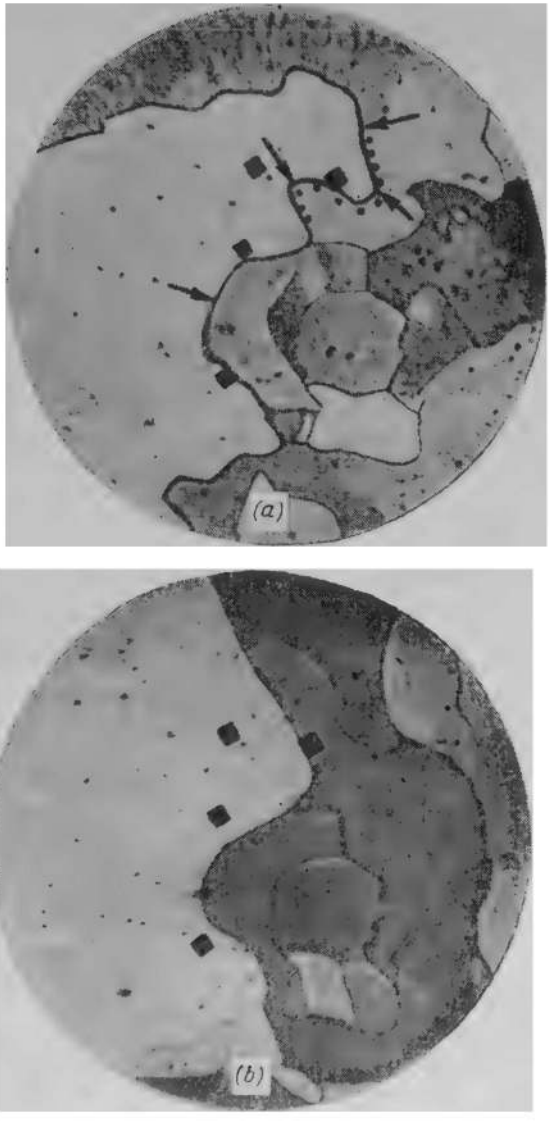

Fig. 119. Straightening of boundaries of large grains (grown during recrystallization after ε_{cr}) after collision. Iron. Vacuum metallography, ×200

(*a*) 900°C, 15 s; (*b*) 900°C, 25 s

isothermal heating causes straightening of the new boundaries, which is stimulated by their trend to lower the grain-boundary energy. Boundaries move towards their centres of curvature and straighten, tongues disappear, and the rate of migration decreases roughly by two orders of magnitude (10^{-4}-10^{-5} cm/s).

A typical example of how grain boundaries straighten and shorten is shown in Fig. 119. In the 'saddle' portion, the grain has consumed a portion of an adjacent grain and in a neighbouring portion it has been consumed by another grain.

It should be emphasized that in recrystallization after ε_{cr} a stable structure (as regards its grain-boundary tension) in metals and single-phase alloys is formed relatively quickly (after an annealing time of roughly an hour). This takes place at the process stage in which the grain has 5 or 10 times the size of the original grain (see Table 16).

After deformations not much above the critical, the structural changes in a heating process of common duration (30-60 minutes) occur in two ways, which can be easily detected metallographically. Firstly, in some portions the mechanism of growth by the migration of some boundaries of original grains is operative. Secondly, the process of the formation and growth of nuclei of new grains becomes more and more pronounced.

Nucleation requires an incubation period which, on the average is noticeably longer in duration than that of growth of original grains. It decreases with an increased amount of deformation. All nuclei appear in joints of original grains, i.e. in places of the highest distortion of the crystal lattice (Figs. 39 and 120).

The number of nuclei increases sharply with an increase in ε. In orientation they noticeably differ from the surrounding deformed grains.

It is typical that after a deformation slightly above the critical value recrystallization nuclei grow in 30 minutes of annealing to a size roughly equal to that of the original grains, i.e. they are substantially smaller than nuclei formed in annealing after critical deformation.

Thus, all the available data are evidence that a non-uniform nature of deformation in microvolumes is the decisive factor at the early stages of recrystallization after ε_{cr} under common conditions of heating.

After subcritical deformation, the total dislocation density and its gradient are low. Dislocations are only weakly associated in arrays and during heating are redistributed easily with the formation of low-angle boundaries and partially dissociate. The difference (gradient) in the energy state of various grains, which is slight before heating, decreases even more after heating.

On increasing the amount of deformation to the critical value, the average dislocation density and the number of operative slip systems increase, especially in portions at grain boundaries.

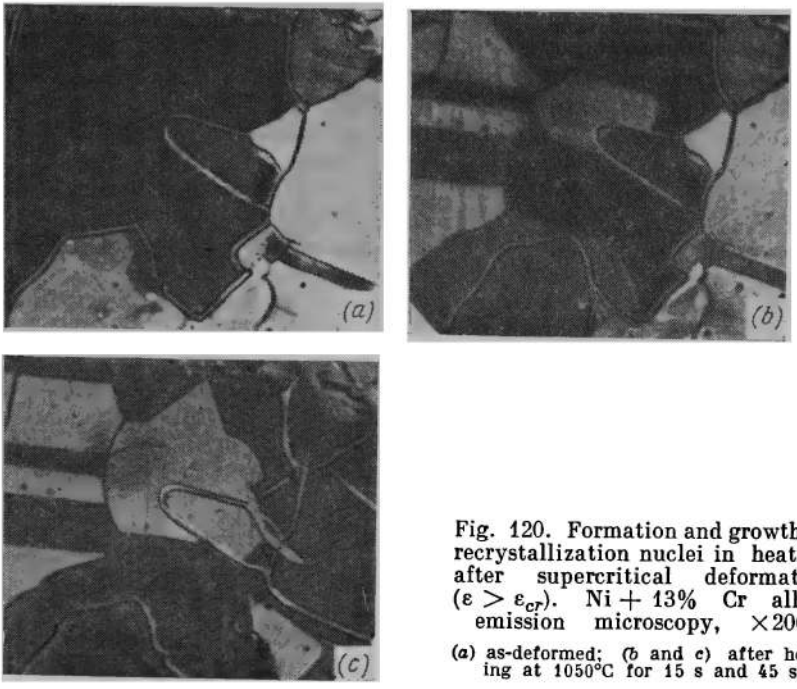

Fig. 120. Formation and growth of recrystallization nuclei in heating after supercritical deformation ($\varepsilon > \varepsilon_{cr}$). Ni + 13% Cr alloy, emission microscopy, ×200

(*a*) as-deformed; (*b* and *c*) after heating at 1050°C for 15 s and 45 s

This dislocation density is still low for the new boundaries that form during redistribution of dislocations in the course of heating to cause a misorientation sufficient for the appearance of primary recrystallization nuclei. Nevertheless, the tension of these boundaries is already high enough to attract a boundary of the original grain in a triple joint.

The migration of a boundary can also be accelerated if the boundary is attracted by low-mobile screw dislocations of an array. As noted by D. McLean [45], the force of attraction of a boundary to a screw dislocation can be very high, roughly 100 times that of grain-boundary tension. An elevated concentration of vacancies in a more heavily deformed grain will additionally facilitate boundary migration.

A boundary can migrate either towards or away from its centre of curvature and disturb the equilibrium of grain-boundary tension which has been established before deformation in some grain joints. This in turn must cause a rearrangement of the whole system of boundaries and joints.

With a high rate of deformation, the volumes in which uniform microstresses are equalized have the size of one or a few crystallites,

whereas with a low deformation rate these volumes are appreciably smaller. This can be the cause of a difference in the nature of boundary migration and the type of structure formed during heating after deformations at various rates.

The above-discussed mechanism can explain the shift of ε_{cr} to higher amounts of deformation on introducing minor additions to a metal. These additions can interact with boundaries of original grains, retard their migration and require a greater driving force to initiate migration. The interaction of impurities with dislocations retards the formation of recrystallization nuclei.

Thus, owing to inhomogeneous deformation at ε_{cr}, the difference in elastic energies between contacting boundary regions turns out to be sufficient to initiate the migration of some boundaries (i.e. the growth of some grains at the expense of their neighbours) under given conditions of heating, but the dislocation density and, what is most important, the excess of like-sign dislocations have not yet reached the values necessary to form new relatively short boundaries of high misorientation.

Proceeding from this, we can expect that if polygonization takes place prior to recrystallization, it should impede 'critical' recrystallization by diminishing the inhomogeneity of distribution of dislocations.

In addition, the long-range stress fields of dislocation arrays should become weaker after polygonization, and, therefore, the capability of dislocations for attracting grain boundaries should also diminish. Thus, polygonization plays the part of a structure stabilizer. Consequently, a change in heating rate and a preliminary recovery should influence the magnitude of ε_{cr} and the size of grains formed after the 'critical' deformation.

Indeed, as has been noted earlier, an increase in the heating rate facilitates 'critical' recrystallization and lowers somewhat the value of ε_{cr}. But if high-speed heating without isothermal holding is employed, i.e. if the time of keeping of the metal at a high temperature is shortened, the size of grains after ε_{cr} will decrease sharply and will depend only slightly on the amount of deformation ε (see Fig. 142*b*, Ch. 9).

Recovery increases somewhat ε_{cr} (Fig. 121) and decreases sharply $\bar{D}_{cr}$, provided that it is carried out at a sufficiently high temperature. For instance, heating of as-deformed aluminium at 300°C prior to recrystallization annealing had practically no effect on the $\bar{D}$ - ε relationship (curve *2* in Fig. 121). An increase of temperature up to 400°C (curve *4* in that figure) gave the expected result: ε_{cr} increased and the maximum grain size decreased. X-ray analysis showed that heating at 400° for 30 minutes caused polygonization, whereas no traces of polygonization were detected on heating at 300°C.

G. V. Indenbaum [219] also observed the suppressing effect of

recovery on the critical growth of grains. It turned out that the effect was enhanced by cyclic heat treatment.

A similar interpretation can be given to the results obtained by I. L. Maevsky [19] on a heat-resisting alloy XH77TIO. It turned out that heating for 2 hours at 900-1000°C, which corresponded to the stage of polygonization in lightly deformed specimens of XH77TIOP alloy, suppressed almost fully vigorous grain growth in the range of critical deformations.

Thus, with properly selected conditions of recovery, the peak on the $\bar{D}$ - ε curve almost disappears. This result is important practically. It is evident that in cases where coarse grain is undesirable and low degrees of deformation are inevitable, it is reasonable to employ recovery.

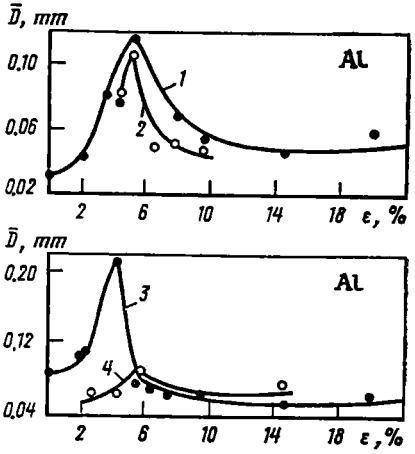

Fig. 121. Effect of isothermal recovery on the shape of $\bar{D}$ - ε curves and the position of ε_{cr} in aluminium. Heating for 30 min at various temperatures

1—500°C; *2*—300°C + 500°C; *3*—550°C; *4*—400°C + 550°C

When utilizing this effect practically, it should be kept in mind that prior recovery has an opposite effect in the range of heavy deformations and increases somewhat the size of final grain (see curve *4* in Fig. 121). With subcritical deformations, recovery increases the number of probable nuclei, since these are preferably less deformed grains; at supercritical deformations, on the contrary, recovery decreases the number of recrystallization nuclei, since these appear in most distorted regions.

The controversial results obtained by various workers as regards the effect of prior recovery can be explained, apart from other causes, by that the results were obtained after various degrees of deformation and at various temperatures of recovery, i.e. with different polygonization effects.

Since recrystallization can be initiated by the mechanism typical of ε_{cr} only if the distortions of adjacent grains are non-uniform, all the factors affecting this inhomogeneity (the rate and temperature of deformation, the size of original grains, etc.) should also influence ε_{cr}. The higher the inhomogeneity, the lower is ε_{cr}. At a higher temperature of recrystallization annealing, a lower degree of inhomogeneity is sufficient to initiate 'critical' recrystallization. The results of studies into the effect of various factors on ε_{cr} agree well with these conclusions.

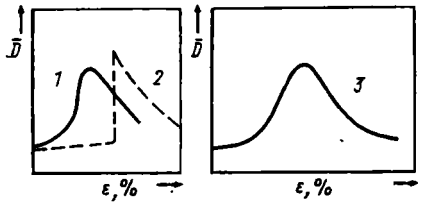

Fig. 122. Curves of elementary processes associated with the growth of original grains (*1*) and of new recrystallization nuclei (*2*); *3* is the resultant curve $\bar{D} = f(\varepsilon)$.

Therefore, the above considerations enable us to regard the $\bar{D}$ - ε curve (the curve relating the size of recrystallized grains to the amount of prior deformation) in the region of the first maximum as a resulting curve obtained by superposition of two curves corresponding to two various processes (Fig. 122): the process of changes in D_{av} due to the growth of some original grains and the process due to the formation and growth of recrystallization nuclei.

The first curve determines the left-hand ascending branch of the common curve. The ascending character of this curve is explained as follows. The growth of original grains is caused by a gradient of dislocation densities in adjacent grains. It is then clear that in the range $\varepsilon < \varepsilon_{cr}$ this gradient first increases and, on passing through its maximum, decreases.

With a further increase in the amount of deformation ($\varepsilon > \varepsilon_{cr}$), excess like-sign dislocations appear locally and a cell structure forms. Heating offers favourable conditions for the formation of new large-angle boundaries, i.e. of recrystallization nuclei. The effect of the processes of formation and growth of these nuclei is reflected in the descending right-hand branch of the common curve $\bar{D} = f(\varepsilon)$. The growth of the first actual recrystallization nuclei at the expense of the deformed matrix should produce a sharp rise in the maximum size of recrystallized grains and a sharp drop in that size with a further increase in the amount of deformation and the number of nuclei, i.e. curve *2* should fall down steeply from its maximum. Experimental curves have exactly this shape.

A maximum on the common $\bar{D}$ - ε curve is determined by the superposition of these two processes. By varying the conditions of deformation and heating, it is possible to influence the shape and position of each of the curves (*1* and *2*) and, therefore, the common curve (see p. 307).

From the results of macrostructure analysis of tapered specimens deformed by tension and heated at various temperatures (see Fig. 111) it can be concluded that a decrease in the heating temperature has a stronger retarding effect on the growth of original grains (the left-hand branch of the curve). The maximum of grain size associated with this process is seen clearly after heating at 1150°C, but is practically absent in specimens heated at 1100°C. On the other hand, the maximum associated with the formation and growth of a small

number of actual recrystallization nuclei is quite discernible in the latter case.

After heating at 1200°C, the two maxima merge together into a single blurred maximum corresponding to a wide range of deformations.

It should be emphasized again that the large grains formed by the process described by curve *1* are less perfect than the large grains formed from actual primary recrystallization nuclei (curve *2*). This offers additional possibilities for controlling the structure.

Annealing for a long time can provide conditions under which these nuclei will form later and will grow at the expense of the original grains which have enlarged earlier. This explains the mechanism and conditions of some special process, in particular, the process for growing single crystals by the strain-anneal method (see the next section).

The above-considered mechanism of recrystallization after ε_{cr} relates to metals and single-phase alloys. If other processes, such as phase transformations, are superposed on recrystallization after ε_{cr}, particularly the processes of precipitation and dissolution of disperse phase particles, then this introduces certain specifics in the formation of microstructure in the matrix.

These particularities can be illustrated by comparing the recrystallization diagrams of two chrome-nickel low-carbon (0.05-0.06%) austenitic steels X18H14M2 and X18H14M2Б1 (see Fig. 136*g* and *h*).

In steel X18H14M2, the disperse phase is type $Cr_{23}C_6$ carbide which is almost fully soluble in the temperature range of 1000-1050°C. In steel X18H14M2Б1, which additionally contains 1% Nb, the disperse phases are niobium carbide NbC and Fe_2Nb intermetal. Both phases are more stable than chrome carbide. Fe_2Nb particles dissolve intensively at temperatures above 1200°C and NbC particles, beginning from approximately 1250-1300°C.

The average grain size in steel X18H14M2 increases monotonically as the temperature of heating rises from 1050° to 1250°C. The average grain size $\bar{D}$ increases roughly twice at an increase of temperature from 1050° to 1150°C and from 1150°C to 1250°C. The value of $\bar{D}$ after a deformation of 5-6% exceeds that after 50-% deformation by a factor of not more than 2 or 3.

In steel X18H14M2Б1, the grain does not practically grow up to a temperature of 1150°C, and after any degree of deformation it remains much finer than in the steel grade without niobium. After heating at 1250°C, which involves dissolution of Fe_2Nb and NbC particles, the grain size in niobium-alloyed steel increases abruptly and becomes much larger than in the other grade (see Fig. 136*h*). After critical deformation, the grain size $\bar{D}$ increases almost by a factor of 20 (i.e. the area of grains increases 400 times). After heavy

deformations, linear dimensions of grains increase more than four times. The size of grains after critical deformation exceeds $\bar{D}$ at $\varepsilon = 50\%$ roughly 5 or 6 times.

Thus, recrystallization after ε_{cr}, if it is accompanied by dissolution of disperse particles, is characterized by a very large size of new grains and by the fact that grain enlargement takes place abruptly and only at temperatures above the point of dissolution of the particles.

The recrystallization diagrams for X18H14M2B1 alloy and for chromium given in Fig. 136*f* and *h* are typical for the case considered.

Another peculiarity, as noted at the beginning of this chapter, is that in alloys with soluble disperse particles the maximum on the $\bar{D}$ - ε curves appears in the range of heavier deformations than in steels containing no disperse particles. Besides, with an increase in the temperature of annealing, this maximum shifts not towards lower degrees of deformation, as is the common case, but to heavier deformations that reach in some cases 10-15%. It is then clear that recrystallization after such heavy deformations can only be realized by the growth of small number of new recrystallization nuclei.

New recrystallization nuclei possess an appreciably higher driving force for boundary migration and therefore have greater ability to overcome the barrier effect of disperse particles than do original grains (see Ch. 3). In that case, twin boundaries (and all coherent boundaries in general) seem to play an important part. This probable mechanism has been discussed thoroughly in Ch. 5.

This still insufficiently studied peculiarity of grain enlargement in alloys containing disperse particles during heating after relatively light deformations plays an important part in the formation of inequigranular and coarsened structures. The problem will be discussed in the next chapter.

7.3. Growing Single Crystals by Recrystallization after 'Critical' Deformation

In single-phase alloys, recrystallization after critical deformation, which occurs through migration of boundaries of some original grains, usually results in an increase of the grain size by not more than 6-10 times.

Recrystallization after ε_{cr}, can also be harnessed to increase sharply the grain size or even to transform a polycrystalline aggregate into a single crystal. The problem of single crystal growth is gaining in importance with the progress in the solid-state physics and ever expanding demands for single crystals to meet scientific and industrial purposes [220].

Growing of single crystals by this method (the strain-anneal process) takes very much time and is characterized by low rates and high temperatures of heating. The available data make it possible to assume that sharp enlargement of grains and the formation of single crystals or large-grained polycrystals occurs not by the growth of some original grains, but by the formation and growth of a single or a few nuclei. Some details of this process are still unclear.

Preparing single crystals by annealing of lightly deformed polycrystals is in many aspects advantageous over the conventional methods for growing single crystals by crystallization from solutions. Among the advantages are the possibility for obtaining single crystals of materials which can undergo phase transformations in the solid state, the possibility of making single crystals in the form of thin sheets or wire or of an intricate geometrical shape, the possibility of obtaining crystals of homogeneous compositions, etc.

On the other hand, the strain-anneal process has some disadvantages which make it inapplicable in certain cases. For instance, it cannot always allow for repeated fabrication of single crystals with a desired orientation. In a number of f.c.c. metals and alloys, annealing twins can form during annealing of deformed metal. These twins are difficult to eliminate. The probability of the formation of annealing twins is higher at a lower stacking fault energy. For that reason, the strain-anneal process fails to produce single crystals of copper and copper alloys (methods of secondary recrystallization are employed for these materials).

Additional difficulties appear where large-size single crystals are to be formed.

The first mention of the strain-anneal technique was made back in 1921 in the work of Carpenter and Elam who proposed this method for preparing single crystals and large polycrystals of aluminium. This method still retains its significance. It has served as a stimulus for many research works on aluminium, iron and other materials.

A detailed investigation of the process proposed by Carpenter and Elam and the structural changes involved was made by G. V. Indenbaum on pure aluminium (99.99-99.996% by mass) with the use of X-ray structural analysis. She provided a scientific substantiation for the process, though used a more pure aluminium. A homogeneous and very coarse original structure of a metal (grain size 3-5 mm) was found to be indispensable for preparing single crystals. With structures of common grain size (50-60 μm), recrystallization after ε_{cr} was effected by the migration of boundaries of original grains and failed to form single crystals or bicrystals.

A coarse original grain can be formed by annealing for 0.5-1.5 h at 550°C, depending on the purity of aluminium, after cold rolling to 60-75%.

The final deformation to the critical degree that comes to 1.2-1.8% is effected by tension. With a lower amount of deformation, subsequent annealing can cause only polygonization. The conditions of recrystallization annealing used by G. V. Indenbaum are practically identical with those employed by Carpenter and Elam.

A specimen is placed in a furnace at a temperature of 450°C. Heating in the range of 450-560°C is carried out at a rate of 100°C day and in the range of 560-640°C at a rate of 100°C/day. Finally, the specimen is held for 1.5-2.0 h at 600-640°C. Zone-refined specimens are heated at a rate of 70°C/h up to 600-640°C and held at that temperature for 1.5-2 hours.

As given in [219], an analysis of the structural changes has suggested a conclusion that no nucleation takes place in the temperature range of 450-535°C. Subgrains become more perfect and their subboundaries more distinct, i.e. only an intensive high-temperature recovery takes place, which diminishes the probability of nucleation. In this temperature range the average grain size remains practically unchanged.

In the range of 535-560°C, one or two nuclei form and grow vigorously. The nucleation mechanism of the process is confirmed by the fact that none of the crystals grown after anneal has an orientation coincident with the original one and their structure has high perfection, whereas large grains grown from fine ones by migration of the original boundaries have a polygonized structure.

More reliable and stable results can be obtained, however, as applied to aluminium and other metals, by heating specimens as they move in a furnace with a definite temperature gradient, rather than by heating a whole specimen simultaneously to a specified temperature.

The forward portion of a specimen is put into the high-temperature zone of a furnace. If the temperature and the rate of movement of the specimen are selected properly, one or two nuclei form in that portion and begin to grow rapidly. With further travel of the specimen, these nuclei consume the fine-grained matrix, which has been introduced into the high-temperature zone at the moment when new nuclei have not yet formed in it. The provision of the temperature gradient should prevent nucleation in other portions of the specimen.

For successful preparation of single crystals by this technique, it is necessary to determine experimentally the critical deformation for the given material (according to its composition, purity, etc.) and an appropriate ratio between the rates of nucleation and growth, and also the temperature relationship for this ratio. Knowledge of these characteristics is needed for establishing the optimal temperature gradient and the rate of travel of specimens in the furnace.

A special condition essential for growing single crystals by using a temperature gradient is that specimens before critical deformation

must have a fine-grained rather than a coarse-grained structure as is the case with stationary temperature conditions.

Some typical conditions for growing single crystals of various metals will be described below.

Aluminium (99.5-99.9%) single crystals a few millimetres in diameter and ten or more centimetres in length were prepared at a temperature gradient of 20-60°C/cm, maximum temperature 600-640°C, and the rate of travel of specimens a few decimetres per hour [220].

In another case, when monocrystalline plates of aluminium were grown, both a longitudinal and a radial temperature gradient were maintained in the furnace. The latter was needed to prevent the formation of excess nuclei in the ribs of a plate.

TABLE 18. **Conditions for Growing Single Crystals of Selected Single-phase Aluminium Alloys [220]**

Alloying addition	Annealing time, min	ε_{cr}	Rate of growth (travel) of specimen, cm/h	Temperature gradient, °C/cm
0.5% Ag	15	2	6.5	90
2.0% Ag	5	2	6.5	90
3.0% Cu	5	1.5	0.65	100
7% Zn	5	1.75	0.65	100

Note: The temperature of annealing prior to deformation was 500°C and the temperature of crystal growing 560°C.

Aluminium alloy single crystals are grown at different temperature gradients depending on alloying (see Table 18).

In view of the high stacking fault energy of aluminium, special measures are needed to prevent polygonization during heating of deformed metal. The danger of polygonization, which in this case competes with recrystallization, becomes greater with a higher purity of the metal.

One of the most effective methods for preventing polygonization in aluminium is addition of certain soluble impurities which can later be removed from single crystals by annealing in a special medium. According to [220], good results can be obtained by alloying aluminium (99.99%) with lithium (0.04% by mass) or iron (0.035% by mass).

Much experience has been obtained in using the method of temperature gradient for growing single crystals of iron and iron alloys, in particular silicon iron (roughly 3% Si) with a composition close to that of transformer steel.

The content of carbon in iron has a high importance for growing iron single crystals.

With a relatively high content of hydrogen (0.1% or more), it is impossible to prepare large crystals obviously because of the formation of numerous recrystallization nuclei, in carbide particles included, and also due to impeded migration of grain boundaries. Yet, single crystals of iron of high purity ($\geqslant$99.99%) cannot be prepared in view of the fact that stabilizing polygonization occurs quite easily and earlier than recrystallization.

Naturally, it is essential to determine the optimal content of carbon for growing single crystals of iron. The results reported in [119] indicate that this optimum is approximately at 0.03% C. i.e. slightly lower than the ultimate solubility of this element in α-iron. If the original iron contains more carbon than this optimal value, it must be decarbonized by annealing in a hydrogen atmosphere. The time of annealing depends on temperature. For instance. according to [221, 222], steel with 0.1-0.15% C should be annealed for 48 h at 950°C or for two weeks at 700°C (in moist hydrogen).

It should be remembered also that some other impurities can influence polygonization in the same manner as carbon. In iron grades of a lower purity, the optimal content of carbon is therefore less than 0.03%.

The critical degree of deformation for low-carbon iron and iron-silicon alloy is 3-2.5%. After critical deformation, the surface of metal must usually be etched to eliminate surface defects and prevent the formation of random nuclei in these places.

The final recrystallization annealing is usually carried out in a furnace with a sharp temperature gradient [223] and at a temperature just below the $\alpha \rightarrow \gamma$-transformation point, i.e. roughly at 880-890°C.

In order to clean iron of the slight additions of carbon which have been introduced to retard polygonization but are unwanted at the later stages of the process (the stage of migration of boundaries of the growing single crystal nucleus), the final recrystallization annealing should be carried out in hydrogen, but not in a vacuum or inert medium.

For silicon iron, in which no $\alpha \rightarrow \gamma$-transformation takes place, C. G. Dunn used a very sharp temperature gradient (approx. 1000°C/cm) which was formed by a special device; the maximum temperature was roughly 1050°C and the rate of travel 1 cm/h.

As noted earlier, a fine-grained original structure before critical deformation is essential for the temperature-gradient method of heating. A fine grain is usually obtained by a heavy deformation followed by recrystallization. This deformation can however produce a texture in the matrix. The rate of growth of nuclei in a textured matrix depends sharply on their orientation relative to the matrix.

For that reason, iron single crystals grown by the strain-anneal method usually have close orientations. The crystal axes are mostly oriented close to ⟨011⟩ directions and less often close to ⟨001⟩. Orientations of the type ⟨111⟩ are almost never encountered.

Single crystals of molybdenum and niobium, up to 12 mm in diameter, are grown by a process in which recrystallized specimens are annealed at a temperature gradient (the maximum temperature is roughly 2000°C); during the heating process, the specimens are deformed close to the critical value (1-2%).

Single-crystal tungsten wire is prepared by passing fine-grained wire through a high-temperature zone (2000-2200°C) in an atmosphere of dry hydrogen in which a steep temperature gradient is maintained.

Long crystals of tungsten can be prepared more easily by deforming the original wire in torsion (spiral winding) before annealing. The mechanism of this effect is still unclear. More detailed data on the conditions for growing single crystals of various metals and alloys by the strain-anneal method can be found in [220, 224].

Let us also consider the use of this method for preparing crystals of a desired orientation. There are a few particular techniques. The following one is employed most often. A specimen (a plate or wire) is deformed to a critical degree, after which one of its ends is annealed in a furnace zone with an appropriate temperature gradient. In this process, a few differently oriented nuclei form. Their orientation is determined by diffraction techniques, mostly by the microbeam X-ray method. After that a nucleus of a desired orientation is selected and its position in the specimen is marked. Other nuclei of unwanted orientations are removed (cut out, for instance) or treated so as to prevent their growth during annealing. For this, it is necessary to form locally an elevated density of defects by various methods, among which a method of indenting seems to be most suitable. An original but unfortunately not so widely applicable method has been proposed in [225]. It can be used where the selected nucleus is so oriented that only simple slip occurs in it after a light deformation, whereas multiple slip takes place in other nuclei. Upon forming recrystallization nuclei in one of the ends of a specimen, this is deformed lightly and annealed. During annealing, the selected nucleus of the desired orientation grows at the expense of both the earlier formed nuclei (now distorted by the light deformation) and the matrix.

If none of the nuclei formed during first heating in the temperature gradient zone has the desired orientation, a nucleus of a close orientation is selected and, before the final annealing, the specimen is bent or twisted so as to orientate the priming crystal properly relative to the specimen.

This technique was employed with success by Dunn [220]. It can also be used for preparing bicrystals.

Chapter 8

Inequigranular and Coarse Structures and Their Formation

In heat treatment of many alloys of practical importance (usually of a complicated composition), anomalously large grains can often form, which exceed tens or hundreds of times the size of original grains. They are much larger in size than recrystallized grains formed after critical deformation. This enlargement in grain size is sometimes called grain coarsening and the structure that results is termed coarse-grained.

Where grain coarsening occurs locally, but not in the whole volume of a metal piece, the structure formed has a sharply non-uniform grain size and is called inequigranular.

The causes and types of inequigranularity are quite diverse. As regards the size and position of coarse-grained portions in the main metal, the following three cases can be distinguished:

1. A region (or regions) of anomalously large grains is located in certain macroportions of a piece and has a size $L \gg D$ (D being the grain size) in two or three dimensions; this is what is called zonal inequigranularity.

2. If $L \gg D$ in one direction only, we have what is called 'lineage' inequigranularity.

3. Individual very large grains or groups of very large or very fine grains are distributed randomly over the volume; this is islet inequigranularity, or microinequigranularity.

Inequigranularity can be estimated quantitatively using certain characteristics which are determined by metallographical statistics. Making a large number of measurements (800-1000) it is possible to calculate the number of grains N_i of a given diameter D_i and the average grain diameter $\bar{D} = \Sigma (D_i N_i)/N$, where N is the total number of measured grains of all sizes.

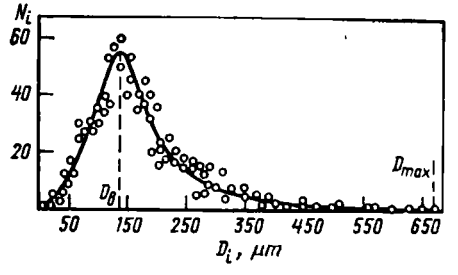

Fig. 123. Grain size distribution curve $N_i = f(D_i)$

A curve of grain size distribution $N_i = f(D_i)$ (Fig. 123) can be used to determine the size D_c of the most common

grains (the maximum of the curve) and the maximum size D_{max} which is determined by the right-most portion of the curve.

The curves of grain size distribution plotted from the results of measurements on plane microsections do not resemble in shape the curves of normal grain size distribution even if the structure is homogeneous [188, 190]. They are always asymmetric and stretched in the region of larger grain sizes (see Fig. 123) and become symmetrical only when plotted in semilogarithmic coordinates. This is why the values of $\bar{D}$ and $\bar{D}_c$ never coincide.

A. G. Spektor [226] proposed the ratio $\Delta D/\bar{D}$ to characterize the proportion of grains whose size differs from the average value

$$\Delta D/\bar{D} = [(\sum_{i=1}^{K_{max}} |\bar{D} - D_i| N_i)/\bar{D}N] \ 100\%$$

where K_{max} is the total number of groups of grain sizes.

For homogeneous (equigranular) structures, $\Delta D/\bar{D} \approx 30\text{-}35\%$. A higher ratio is indicative of inequigranularity. This characteristic, however, gives no notion of the maximum deviation from the average size or from the size D_c that is most probable statistically. For this purpose, use may be made of another characteristic, D_{max}/D_c, which determines the asymmetrical nature of the distribution curve.

For structures composed of grains of equal size, the ratio D_{max}/D_c is 2.5 to 3. For inequigranular structures it is greater than 3 and may reach 9-10 or more. This characteristic is also insufficient, however, since it does not indicate the proportion of large grains in the structure (or the area occupied by them).

Thus, the two characteristics given above complement each other.

A clear graphic demonstration of inequigranular structures and their nature is offered by curves of distribution of the areas occupied by grains of definite size ranges, i.e. $S_i = f(D_i)$ or $\sqrt{S_i} = f(D_i)$.

In the latter case, the quotient $\sqrt{S_i}/D_i$ characterizes the concentration of grains of a given size occupying an area S_i.

For inequigranular structures it is typical that the S_i-D_i relationship is described by a curve with two maxima or often even by two individual curves with their maxima being separated by a wide interval of medium grain sizes. This interval is wider at a higher degree of inequigranularity. The ratio of the areas under the two curves characterizes the relative area occupied by large grains, and the ratio $D_{max(1)}/D_{max(2)}$ determines the excess in size of large grains over small grains.

This graphical representation is especially useful where the size of large grains greatly exceeds the size of the main mass of grains. In recrystallization diagrams for such materials, it is reasonable to give two curves (but not one) which describe accordingly the average size of two groups of grains: large and small.

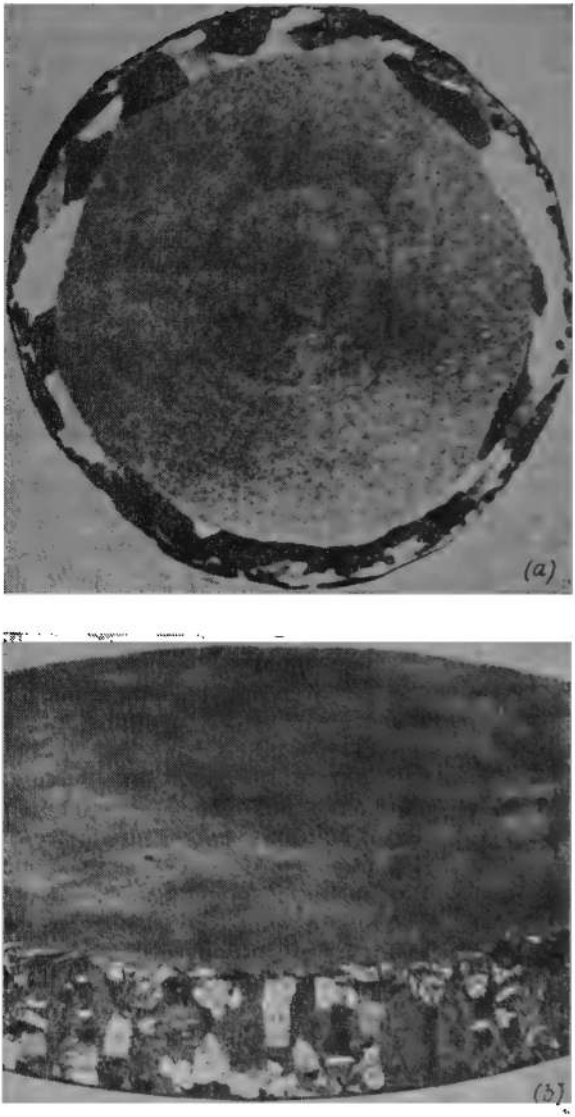

Fig. 124. Zonal inequigranularity

(*a*) in pressed aluminium alloy ('large-crystalline rim'); (*b*) low-carbon steel

When choosing an area in a microsection to calculate the number of grains and determine their sizes in order to plot S_i-D_i curves, one should consider the type of inequigranularity (zonal, lineage or islet).

Structure coarsening is often found in nickel, aluminium, magnesium and other non-ferrous alloys [227, 228]. It can also appear during high-temperature heating of 'killed' carbon steels which are deoxidized by aluminium. Coarse-grained fracture is often found in alloy steels [40-42].

Typical examples of zonal inequigranularity are coarse-grained peripheral zones appearing during heating for hardening in pressed articles made from some popular aluminium alloys (Fig. 124*a*) and also in hot-deformed low-carbon steel pieces (Fig. 124*b*). Zonal inequigranularity is also encountered in heat-resisting alloys based on nickel (type ЭИ437 alloys), iron (37Х12Н8, Г8МФБ), etc. Lineage and islet types of inequigranularity are also quite common in these alloys (Fig. 125).

The problems of formation of inequigranular and coarse structures attract much practical interest, since these structures adversely affect the properties of metal (see Ch. 1).

Coarsened structures in final products made of alloys undergoing no phase transformations cannot be amended. For that reason, a coarse-grained zone must be often removed by machining, which involves high economic losses.

Various workers attribute the effects of structure coarsening and inequigranularity to different causes. Most of them explain structure coarsening by dissolution of disperse phases, but associate this with different particular mechanisms.

V. I. Dobatkin *et al.* [229] examined recrystallization in type АМГ alloys (2.5% Mg, 0.27% Mn, 0.16% Si, 0.1% Fe, 0.024% Cu,

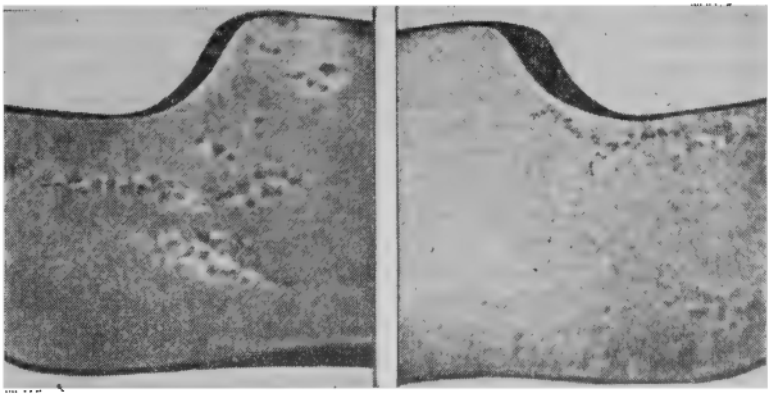

Fig. 125. Lineage and islet inequigranularity in parts of complex nickel alloy

balance aluminium), in which heating within 500-550°C causes a sharp structure coarsening. They explained this by the dissolution of disperse particles of magnesium silicide and Al_6Mn compound. In their view, an uneven distribution of these particles and the associated non-uniform coagulation are responsible for nucleation only in some individual sites, which results in the formation of large grains. It is of interest to note that, according to their results, the temperature range of coarsening does not depend on either the amount of deformation (within 76-92%) or the type of deformation. These factors can only influence slightly the size of grains. Structure coarsening results in weakening of recrystallization textures.

V. S. Mes'kin [230] explained anomalous grain coarsening in a different way. He also attributed it to the dissolution of disperse particles, but used a different approach. In his view, the dissolution of, say, aluminium nitrides in aluminium-deoxidized killed steel weakens interatomic bonds in the solid solution and increases accordingly the coefficient of self-diffusion which is responsible for the high rate of boundary migration.

This weakening of interatomic bonds, in Mes'kin's opinion, is in general responsible for the intensive grain growth in steel at temperatures corresponding to the beginning of dissolution of carbides and nitrides.

McLean [45] also holds that secondary recrystallization is associated with dissolution of disperse phases, but stimulated by the free energy of grain boundaries. The formation of very large grains is obviously linked with the fact that the rate of liberation of boundaries from impurities (i.e. the rate of dissolution of disperse particles) is low compared to the rate of boundary migration, so that only a few of the nuclei have had time to become free in the period during which a grain expands over the whole specimen or its large portion.

Some authors, such as A. P. Gulyaev [41, 366], M. A. Krishtal et al. [193], K. M. Zhak and E. N. Pogrebnoy [194], support the idea that structure coarsening at the stage of secondary recrystallization is realized by coalescence of large groups of grains rather than by boundary migration. They deny the possibility of grain coarsening by boundary migration, stating that this cannot lead to such a high rate of coarsening.

The effects of various modes of heat treatment and plastic working on structure coarsening have yet to be studied thoroughly.

K. A. Malyshev, one of the few workers who studied this effect in steels, concludes that any type of treatment (either heat treatment or thermomechanical treatment) can exert its influence on the kinetics of growth of austenitic grain inasmuch as it changes the shape and distribution of particles which can be obstacles to grain boundary migration.

Eyre [231] notes that structure coarsening in aluminium alloyed with manganese can be eliminated if the alloy is first subjected to a high-temperature homogenizing treatment (579°C, 12 h).

The mechanism of formation of inequigranularity has been studied even less thoroughly. In a few Soviet works on the problem, the main attention is paid to conditions of deformation. Morokhovets, Kaplin and Gaideburov [232] analysed inequigranularity in nimonic alloys after hot closed-pass rolling of bars and after hot open upsetting. It turned out that the latter process produced an appreciable inequigranularity. The authors explained this effect by a less uniform character of deformation that resulted in a poorer structural homogeneity.

In their work, they analysed inequigranularity immediately after hot deformation, i.e. without any subsequent heat treatment. An example of inequigranularity of this type is shown in Fig. 140. Such a structure forms on low and moderate degrees of hot deformation and consists of large original grains surrounded by fine new grains which have grown from nuclei. In other words, this is the case of incomplete primary recrystallization.

This type of inequigranularity can be eliminated easily by a heat treatment process in which primary recrystallization is allowed to proceed to an end. In that case new grains grow at the expense of the large original grains and the structure gets homogenized.

The case of inequigranularity formed after primary recrystallization during subsequent heating is of much practical interest. It is still unclear how the conditions of deformation can influence this type of inequigranularity.

I. L. Mayevsky [197], who studied some alloys of a composition similar to the composition of alloys used in [232], holds that inequigranularity is mainly caused by a low critical degree of deformation and uneven deformation of various grains.

This opinion is shared by F. F. Khimushin [33] who states that inequigranularity "... forms in products during hot plastic working when a critical degree of deformation is reached in a portion of the metal, so that after heat treatment a coarse-grained structure forms in that portion along with a fine-grained structure".

In the works mentioned, however, the role of the deformation mode was analysed on alloys of the same composition and no analysis was made of the effect of alloy composition at unvarying conditions of deformation. For this reason, obviously, the authors attribute inequigranularity only to the conditions of deformation.

The effect of deformation temperature on the formation of coarse and inequigranular structures has been studied poorly. On the other hand, the results suggesting that such structures are only formed in regions deformed to low (critical) degrees were obtained on specimens usually deformed at room temperature.

Of principal importance are the results obtained recently by Yu. M. Weinblat et al. [118, 208, 209, 12] which show that the rate of hot deformation has a decisive effect on the type of structure.

Considered below are the results of a number of research works [233, 234] which characterize the role of the composition of alloys and disperse phases and also the conditions of deformation in the formation of inequigranular and coarsened structures in nickel, iron and aluminium alloys.

8.1. Nickel and Iron Alloys with Disperse Phases

The effect of disperse phases and of their dissolution on grain growth and inequigranularity was examined on three groups of alloys: (1) nichrome (87% Ni + 13% Cr) and nichrome-base heat-resisting alloys; (2) killed and rimming steel Grade 08; and (3) Fe-W and Fe-Si alloys.

Nichrome and heat-resisting nichrome-base alloys (grades XH77TIOP and XH70BMTIO of the nimonic type) were melted in vacuum or in air in laboratory and industrial furnaces. To determine the role of various disperse phases, various concentrations of nitrogen and carbon were added to Ni-Cr alloys. Besides, some selected melts with varying concentrations of oxygen and aluminium were tested.

The compositions of the Fe-W and Fe-Si alloys used in the tests and the results obtained are given partially in Ch. 5.

Vacuum-melted nichrome specimens were distinguished by a sharp susceptibility to grain coarsening (Fig. 126). An intensive grain

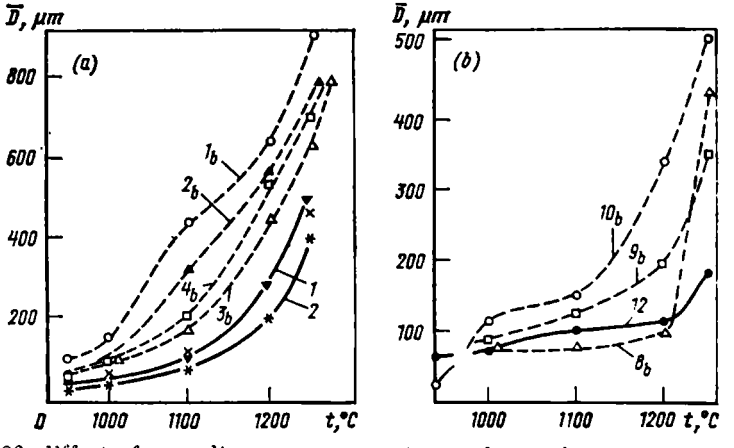

Fig. 126. Effect of annealing temperature (τ = 1 h) on the average grain size in Ni-Cr alloy (*a*) and type XH77TIO alloy (*b*). Vacuum melts are denoted by *b*; numbers at curves are melt numbers

growth in these specimens began at 1050-1100°C against 1200°C in air-melted specimens (melt *1*) and even 1250°C in the most contaminated melts (melt *2*). In vacuum-melted nichrome with various contents of the elements (C, N_2, O_2) forming stable compounds with chromium, grain growth began at a lower temperature in less contaminated melts (melt 1_b in Fig. 126).

At high temperatures of heating the rate of grain growth in less pure melts was very high. The difference in grain size between vacuum- and air-melted specimens with various contents of carbon was smaller after heating at 1200-1250°C and practically disappeared at 1275°C.

Similar relationships were found for nimonic alloys. It should be noted that the average grain size in a vacuum-melted nimonic alloy with an elevated content of nitrogen (after heating at 1250°C) was equal to the grain size in vacuum-melted nichrome. But interatomic bonds in XH77TIOP alloy are undoubtedly stronger than in nichrome and the diffusion mobility is lower. Therefore, if these characteristics had been decisive, the grain size in nichrome would have been greater than that in nimonic alloys (under the same conditions of heating).

The early stages of grain growth are accompanied by islet inequigranularity. The highest degree of inequigranularity always appears just before the onset of intensive total grain growth.

The inequigranularity in air-melted specimens is appreciably greater in magnitude and reaches $D_{max}/D_c = 4$ or even more.

In vacuum-melted specimens the highest inequigranularity at 950-1000°C is $D_{max}/D_c = 3.5$.

In the temperature range of 975-1050°C where inequigranularity increases, air-melted specimens show a sharp rise in resistivity. In that temperature interval, the lattice spacing of the solid solution, as has been found radiographically, increases from 3.548 Å to 3.551 Å. This makes it possible to suppose that the dissolution of disperse particles begins in that temperature interval, which obviously accelerates the growth of some grains and thus causes inequigranularity.

In vacuum-melted metal, the effect of an increase in resistivity with temperature is negligible. The dissolution of disperse particles has a more noticeable effect on the lattice spacing. On heating at 1050°C, the spacing increases only slightly, from 3.544 Å to 3.544_5 Å. Obviously, dissolution of disperse phases occurs also in vacuum-melted metal, but in appreciably less quantities.

Metallographic and electron-microscopic analyses confirm the conclusion that coagulation and dissolution of disperse phases take place during heating. The character of distribution of disperse phases in the matrix is of much importance. Even in vacuum melted nichrome, undissolved disperse particles are found in the form o

almost continuous chains (barriers) along grain boundaries, and therefore they lock the latter. The growth of grain can only proceed as the disperse phases dissolve and coagulate.

It is important for practice to know what phases in nichrome alloys cause inequigranularity and intensive grain growth as they dissolve and coagulate. Analysis shows that grain growth in nichrome is impeded by phases capable of dissolution and coagulation rather than by 'primary' phases which form directly during crystallization.

In vacuum-melted metal, grain growth is inhibited mainly by nitride, CrN, and carbide, $Cr_{23}C_6$. A carbide phase requires a lower temperature (1000-1100°C) for coagulation and dissolution than does a nitride phase. Thus, the inhibiting effect of carbides is eliminated on heating above 1100°C and an intensive structure coarsening then takes place. In melts with an elevated content of nitrogen, the retarding effect of disperse phases is noticeable at higher temperatures (up to 1200°C).

The phase composition of precipitates obtained from air-melted metal includes at least four phases: CrN, $Cr_{23}C_6$, Cr_2O_3 and a small amount of AlN. The phases are present in various proportions. High-carbon melts have the highest content of carbide, $Cr_{23}C_6$. With a high concentration of aluminium in the melt, nitrogen is partially used to form aluminium nitride, whose affinity for nitrogen is higher than that of chromium. The AlN phase is more stable against coagulation and dissolution than CrN.

Thus, there is a direct interrelation between the growth of grains and inequigranularity in nichrome-type alloys, on the one hand, and the dissolution of disperse phases, on the other.

This is also true of iron-base alloys. At high temperatures of heating, the size of grains in aluminium-deoxidized killed steel turns out to be higher (owing to an intensive grain growth) than in rimming steel. The picture is different on heating at lower temperatures. In killed steel, an intensive grain growth is preceded by an increase in inequigranularity. In this type of steel, aluminium nitride is the main phase that inhibits the growth of grains [230].

Yet, the fact that both disperse phases are found in the precipitate even after heating at 1250°C and the lattice spacing remains practically the same indicates that only a small quantity of aluminium and nitrogen pass into the solution. One can hardly suppose that this can markedly alter the diffusion mobility and the strength of interatomic bonds in the solution and thus accelerate boundary migration.

Referring to the material of Ch. 4, we can state that in the case considered an unbalanced grain-boundary tension of joining boundaries and the trend of the system to lower its total boundary energy are the decisive factors which cause an accelerated boundary migration.

As has been shown in Ch. 5 (see Fig. 83), boundaries at unbalanced joints can move tens of times faster than those adjoining balanced joints. In this process, the speed of atomic movements is substantially higher than would be found in dissolution. Uneven dissolution also causes inequigranularity and accelerates the growth of large grains.

If disperse particles are present in high concentrations and do not dissolve up to very high temperatures above, say, $0.73\text{-}0.8T_m$, as is the case with Fe-W alloys, dissolution that takes place in heating over the given temperatures can cause vigorous growth of grains and structure coarsening. A high value of grain-boundary energy also aids in the process.

If disperse particles dissolve at lower temperatures, in which case the diffusion mobility is low, and, moreover, if the concentration of disperse particles is not high, as in Ni + Cr alloys and nimonic-type alloys melted in open air, the stage of structure coarsening does not set in. The process reduces to an increase in inequigranularity at the early stages of dissolution, after which large (but not coarse) grains are formed.

Thus, inequigranularity can appear in alloys during the growth of grains due to uneven distribution and dissolution of disperse phases, irrespective of prior deformation.

Under definite conditions, however, deformation can promote inequigranularity and the formation of a coarse structure. This can be illustrated by experimental results obtained on nickel alloys of the composition given earlier.

Light deformations at temperatures within the temperature interval of dissolution of disperse phases are most unfavourable as regards inequigranularity. With light deformations, inequigranularity is at the highest level immediately after upsetting and then diminishes in subsequent heat treatment.

Things are different on heavy deformations. With $t_{def} \gg t_r^s$, inequigranularity is at a minimum immediately after deformation and increases during high-temperature heating.

Figure 127 shows the microstructure of commercial XH77TIOP alloy deformed 40% by upsetting in the temperature range of dissolution of disperse phases (1100-1150°C) and heat-treated by a standard technique. It is seen clearly that inequigranularity has increased in the course of heating.

In this case, primary recrystallization has enough time to come to completion during upsetting and subsequent cooling. When the metal is then heat-treated, grain growth takes place. In portions free of disperse particles, new grains can grow unobstructedly; in other portions their growth is retarded so that inequigranularity results.

At low degrees of hot deformation, the structure in portions free from disperse particles is coarsened quickly because of the growth of

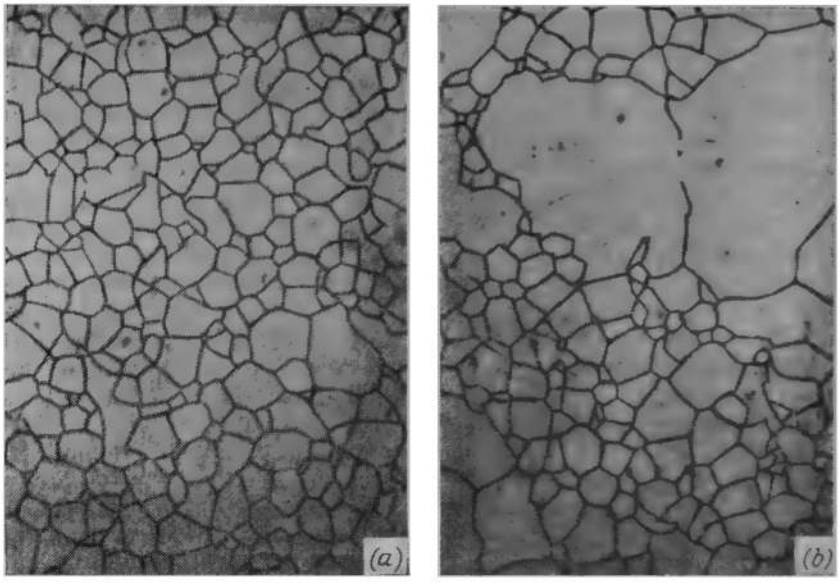

Fig. 127. Increase of local inequigranularity in ХН77ТЮР (ЭИ437Б) alloy during heat treatment

(*a*) after 40-% deformation and heating at 1000-1100°C; (*b*) after deformation and heating at 1080°C for 8 h

some original grains at the expense of other, less distorted, grains. But the crystal lattice in such crystallites is insufficiently perfect. During heating, these crystallites cannot grow by the mechanism of primary recrystallization at the expense of other less perfect grains which have formed in other portions of the alloy. The growth of small perfect nuclei at the expense of these large grains is even more probable (see p. 327). In this case, inequigranularity even becomes slightly lower.

In metal pieces of an intricate shape, the deformation may be quite non-uniform and, accordingly, grains formed in various portions may differ appreciably in size. The expected inequigranularity can be estimated here using the curves of grain size distribution $N_i = f(D_i)$ for heavy (ε_1) and light (ε_2) deformations. The ratio $D_{\max(\varepsilon_2)} / D_{c(\varepsilon_1)}$ will characterize the highest probable inequigranularity due to uneven deformation.

Figure 128 shows typical N_i-D_i curves taken at $D_{\max(5\%)}$ $D_{c(40\%)}$. Thus, deformations within the common practical range do not cause high inequigranularity. It is close to the usual difference in the size of grains obtained after critical and heavier deformations (see Table 16). This inequigranularity is lower than that found in heat-resisting nickel alloys.

Inequigranularity is likely to increase if deformation is uneven and the distribution of disperse excess phases is non-uniform. The most unfavourable cases are those when lightly deformed microportions are most free from disperse phases and those deformed most heavily are most contaminated.

For the case considered, the highest possible inequigranularity can be determined by the ratio between D_{max} for the lightly deformed vacuum-melted metal and D_c for the same but heavily deformed air-melted metal. Apart from the N_i-$\bar{D}_i$ for the air-melted metal, Fig. 128 shows the distribution curve for the same metal but melted in vacuum after 5-% upsetting and the same heat treatment. The ratio that characterizes the inequigranularity in this case is $D_{max(melt\ 11b,\ \varepsilon=5\%)}/D_{c(melt\ 13,\ \varepsilon=40\%)}=10$, i.e. it is quite high and approaches the values found in practice.

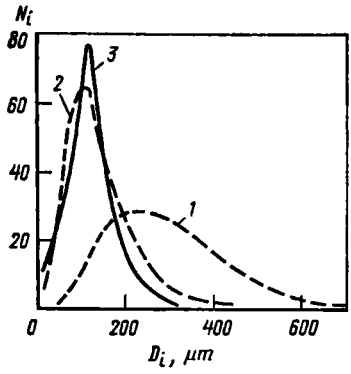

Fig. 128. Grain size distribution curves. XH70BMTIO alloy melted in vacuum (*1*) and in open air (*2*, *3*). Deformation of 40% (solid lines) and 5% (dotted lines)

The results considered suggest the following conclusion: the most important cause of inequigranularity in nickel alloy products is superposition of the effect of an uneven deformation on that of non-uniform distribution of disperse phases.

A clear illustration in support of this conclusion is the macrostructure of an intricate part made of XH77TIOP alloy, which is shown in Fig. 125. Various portions of the part were deformed differently by hot-die-forging, since the original workpiece was of the same thickness everywhere. The part is symmetrical and, assuming that inequigranularity is caused only by a difference in the amount and type of deformation, coarse-grained portions of the part would be expected to be located symmetrically relative to the centre. As can be seen from the figure, however there is no symmetry at all. Chemical analysis of the metal in various local microvolumes has shown that there is a certain difference in the chemical and phase composition of the metal in the zones of coarsened and normal structure.

Thus, the effect of deformation is large, though not independent in nature. This conclusion is confirmed by the data on recrystallization of two steel grades X18H14M2 and X18H14M2B1 after various degrees of deformation (see Chs. 5 and 7) and by the recrystallization diagrams for these steels (see Fig. 136*g* and *h*).

Both diagrams have a maximum of the size of recrystallized grains after critical deformation, but the maximum grain size in

steel X18H14M2Б1, which contains disperse phases, is many times greater. This indicates that a low degree of deformation in this case is necessary for anomalous grain enlargement. It should be noted also that in the absence of soluble disperse phases particles, common annealing would not have produced such high grain coarsening.

Thus, abrupt grain coarsening after light deformations is obviously due first of all to a high concentration of disperse particles which are stable to temperatures close to $0.8T_m$ and due to superposition of recrystallization on the dissolution of these particles.

A number of researchers have established, however, that the curves for certain, yet not numerous, metals and alloys have a second maximum of grain size in the region of heavier deformations (60-70%).

Some authors hold that the formation of this second maximum is favoured by a texture formed on heavy deformation. In our opinion, this is only substantiated for cases where the matrix before coarsening mainly consists of grains of the same orientation (a distinct monotexture). High-temperature heating can produce in this matrix favourable conditions for the preferable growth of some, not numerous, grains of a different orientation. An illustration of this case is probably the effect of sharp grain coarsening after 80-% deformation and annealing at 1040°C of originally fine-grained chrome bronze (0.5% Cr) [215]. After this type of heat treatment, the specimens become almost monocrystalline. The effect is not observed in originally coarse-grained specimens.

As found by analysis, a fine-grained original structure has a different type of texture after deformation and recrystallization as compared to a coarse-grained structure. The texture in the originally coarse-grained state after primary recrystallization has several components, whereas the originally fine-grained bronze acquires a distinct (100) [001] cube texture after primary recrystallization. During heating at 1040°C, secondary recrystallization takes place and the cube texture disappears; instead, a small number of gigantic grains with an orientation of the type (110) [*uvw*] grow at a high rate. The cubic orientation of the matrix seems to be favourable for accelerated growth of grains with orientations of the type (110) [*uvw*] (see Ch. 10).

On the other hand, it has been found from a number of studies carried out on certain popular alloys that a second maximum also appears after moderate or light deformations. Such cases are obviously more common than grain coarsening after heavy deformations.

Given below are the experimental results for recrystallization of a number of nickel- and iron-base alloys [10]. As a typical example, only the data for two alloys, ХН77ТЮР (nickel-based) and 10Х12Н20Т3Р (iron-based), are discussed. Figure 129 shows the recrystallization diagrams for these alloys, which have been plotted from the results of tensile tests of tapered specimens.

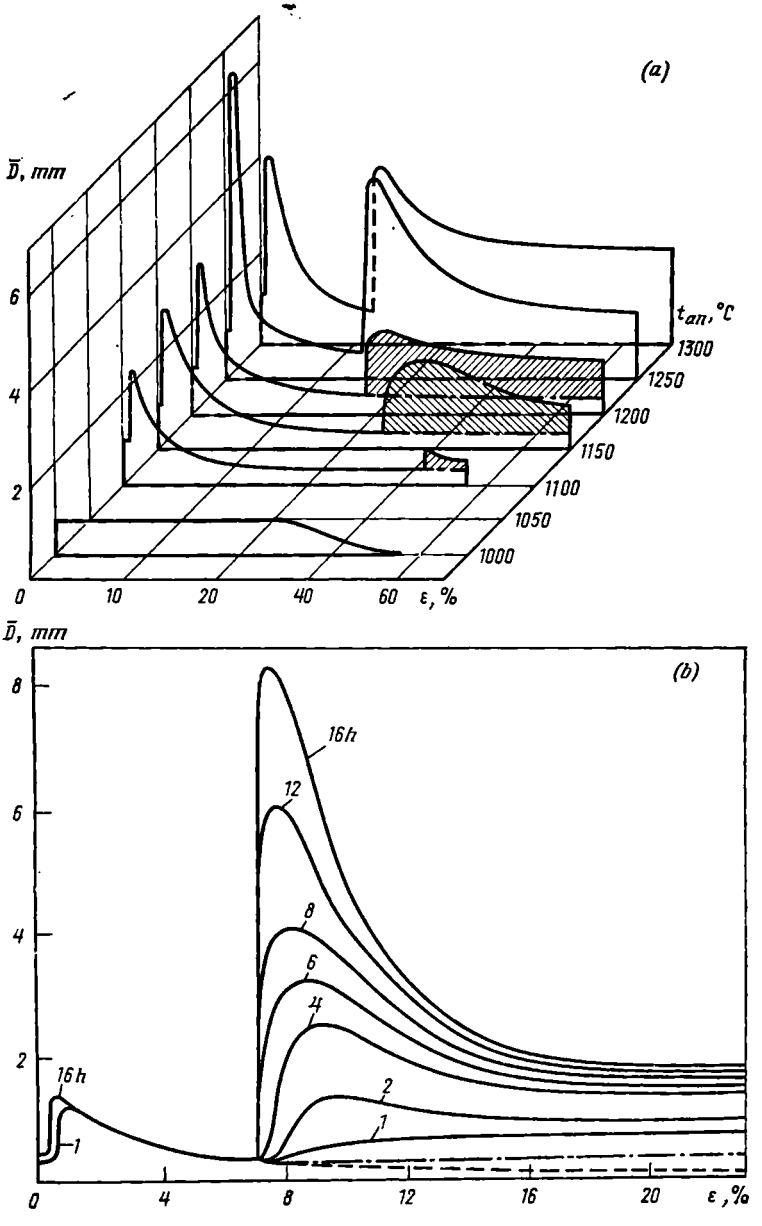

Fig. 129. Recrystallization diagrams constructed from the results of tension of tapered specimens [10]

(a) XH77TЮP alloy deformed at 1000°C and annealed for 2 h; (b) 10X12H20T3P alloy, hot-rolled rod annealed at 1100°C and then cold-deformed and annealed at 1200°C

The second grain-size maximum and the associated inequigranularity turn out to depend on certain technological factors: the degree and temperature of deformation, the temperature and time of annealing, prior treatment, original grain size, heating rate, etc.

The second maximum may fall within a wide interval of deformations (from 10 to 60% and more) depending on the conditions of a particular experiment, whereas the first maximum is always detected in the range of light 'critical' deformations. Since the position of the second maximum in the deformation range is indeterminate. it confirms once more that deformation is not a decisive factor, though it may be quite important. It is typical that the second maximum is often representative of a more coarse-grained structure than the first maximum, especially after light or moderate deformations. The second maximum emerges on completion of primary recrystallization and its appearance is associated with the process of secondary recrystallization. The dissolution and coagulation of disperse particles (which inhibit the growth of grains) are indispensable for secondary recrystallization to set in.

The disperse phases in XH78T alloy are mainly Cr_7C_3 and $Cr_{23}C_6$ carbides; in XH77TIOP and 10X12H20T3P alloys these are the same chromium carbides and respectively boride phases of Cr_5B_4 and TiB_2 types. In addition, titanium carbonitrides Ti(C. N) have a definite effect. The temperatures at which sharp grain coarsening takes place (a distinct second maximum appears) fall within the temperature range of dissolution of these phases in the respective alloys. They usually lie between 0.8 and $0.85T_m$ of the matrix.

There is a clear correlation between the tendency to formation of the second maximum in a particular region of the recrystallization diagram and the average grain size that forms in the matrix at the end of primary recrystallization [10]. With a larger grain in the matrix at the end of primary recrystallization. the total surface area of grain boundaries per unit volume is lower and the density of disperse phases on grain boundaries is higher. Therefore, these phases can more strongly stabilize the matrix and retard the growth of grains. This retarding effect diminishes during annealing because of coagulation or dissolution of the phases. It is lower at higher temperatures of annealing.

At the same time, the driving force for the growth of grains (i.e. the grain-boundary energy) diminishes with an enlargement in the grain size of the matrix. These grains grow larger at an increased temperature of annealing. So, at a definite temperature a critical grain size in the matrix should exist, at which the driving and the retarding force (for 'stabilization' of the matrix) will be balanced. After a definite time interval (incubation period), the coagulation and dissolution of unevenly distributed disperse phases cause the retarding force in some portions to decrease against the driving

force, so that some grains will start growing, i.e. secondary recrystallization will take place. Since the main mass of grains in the matrix (which have a critical size) is 'stabilized', the driving force of secondary recrystallization increases in time, since the difference in the size of the growing grains and the grain size of the matrix increases. Whenever the matrix has larger grains, the experimental conditions being the same, the retarding force exceeds appreciably the driving force, with the result that an anomalous grain growth and, what is more, mass grain growth (matrix 'restabilization') are impossible. In that case the structure formed at the end of primary recrystallization is retained even after a long time of annealing. Yet, the reverse is true if the grain size of the matrix at the end of primary recrystallization proves lower than the critical value: the driving force will dominate the retarding force and cause mass growth of grains in the matrix.

If one provides for such manufacturing conditions as can preclude the formation of the critical size of grains at the end of primary recrystallization, it will be possible to avoid coarse inequigranularity (i.e. appearance of the second maximum). Proper conditions can be selected by using recrystallization diagrams, as those shown in Fig. 129. In particular, since the height of the second maximum decreases sharply with a decrease in the temperature and time of annealing, it is advisable to lower this maximum to obtain lower inequigranularity, if this is admissible technologically.

The results obtained for many heat-resisting alloys show that inequigranularity due to secondary recrystallization (the second maximum of grain size) is much more common than inequigranularity caused by other factors.

In the cases discussed above, deformation had practically no effect on the volume concentration, dispersity and distribution of disperse phases. In age-hardening alloys, however, all these characteristics can depend substantially on the temperature, amount and type of deformation. This in turn can entail the formation of uneven grains in primary recrystallization and the subsequent coarse-grained structure and inequigranularity. This can be clearly seen from the examples that follow.

Example 1. Specimens of XH70BMTIO alloy were upset 5% and 40% at various temperatures corresponding to either single-phase or two-phase state and then heated under the same conditions (1200°C for 2 h and then 1050°C for 4 h).

For comparison, single-phase nichrome specimens were upset at two various temperatures and subjected to recrystallization annealing.

For XH70BMTIO alloy after a light deformation (5%) and for nichrome deformed 5% and 40%, the two curves describing the effect of deformation temperature on grain size immediately after defor-

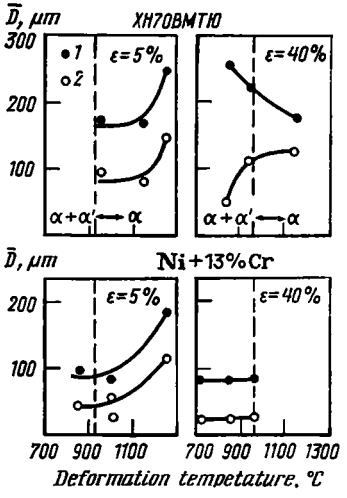

Fig. 130. Effect of the temperature and rate of deformation on the average grain size of XH70BMTIO alloy and nichrome (13% Cr)

1—as-deformed; *2*—deformed and heated

mation and after high-temperature heating, pass parallel to each other (Fig. 130). Heating after deformation causes an increase in the grain size roughly by one index, irrespective of the deformation temperature. $\bar{D}$ either increases with deformation temperature ($\varepsilon = 5\%$) or remains unchanged (nichrome, $\varepsilon = 40\%$).

A different pattern of grain size variation has been found in age-hardening XH70BMTIO alloy after heavy deformations. The size of grains turns out to be larger in the specimens deformed at a high temperature corresponding to the single-phase region. After heating, however, the specimens deformed at a temperature of the two-phase state of the alloy are found to have a coarser grain, with $\bar{D}$ increasing five-fold or more (from 50 to 250 μm). Thus, with age-hardening alloys, the relation of the deformation temperature to the temperature point between single- and two-phase states is essential.

At a temperature corresponding to the two-phase state, deformation accelerates the decomposition of the solid solution and increases the volume concentration of the second phase. Particles of this phase lock boundaries of nuclei and grains, so that an inequigranular structure forms by the end of primary recrystallization, though without especially large grains. In subsequent heating to a temperature at which the disperse phase begins to dissolve, grains grow extremely non-uniformly; some overtake the neighbours and grow further at the expense of fine grains. The conditions for this process are more favourable at a higher temperature of complete dissolution of disperse particles.

It should be noted that this type of structure coarsening involves only a slight increase in $\Delta D/D$ and a more noticeable increase in the D_{max}/D_e ratio, from 3.75 to 5 (see Fig. 127), which is due to the formation of a small number of extremely large grains.

Example 2. Tapered specimens of XH77TIOP alloy were fractured by tension at 20°, 900° and 1100°C. Owing to the tapered shape of the specimens, it was possible to obtain a whole range of deformation degrees, from zero to a maximum. The specimens were then heated at 1080°C for 8 h at two different modes: quickly in a furnace heated

up to 1080°C and more slowly, in 20 minutes from 900° to 1080°C. The second mode imitated the rate of heating of internal layers of the metal in large-size parts.

The results of microstructure analysis of the specimens are shown in Fig. 131*a* and *b*. The worst results were obtained after deformation at 900°C which was accompanied by decomposition of the solid solution. The maximum grain size and the highest inequigranularity turned out to be 3-4 times the values obtained after deformation at 20° or 1100°C. D_{max} was equal to 3 mm and the D_{max}/D_c ratio was very high, from 15 to 20. In the specimens broken at 900°C, the degree of deformation corresponding to the maximum grain size was 6-8%. In addition, in these specimens, as in those tensioned at 1100°C a slight increase of inequigranularity after heavy deformations

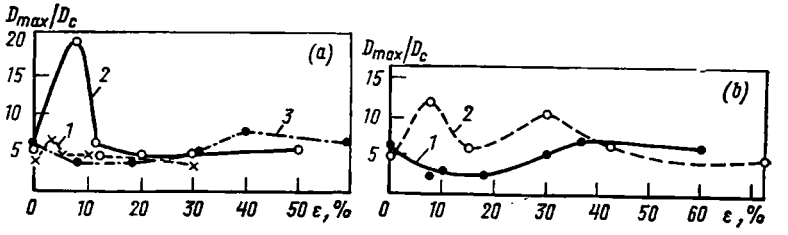

Fig. 131. D_{max}/D_c for XH77TIO alloy after heating at 1080°C for 8 h as a function of

(*a*) the amount of prior tensile deformations (*1*—20°C, *2*—900°C, *3*—1000°C) and (*b*) the rate of subsequent heating (*1*—heating in a furnace preheated to 1080°C, *2*—slow heating)

was noted. The effect of the rate of subsequent heating was also essential. Under the same conditions of deformation, the worst structure was found in specimens heated slowly up to 1080°C. In these specimens, inequigranularity and structure coarsening were more pronounced in the region of light deformations.

Besides, slow heating caused the shift of the 'critical' deformation region towards higher deformation degrees (10-12%) and the appearance of inequigranularity and coarsened structure in the deformation range of 30-35%. The degree of inequigranularity and coarsening in the range of heavy deformations was not less than in the light-deformation range.

Thus, hot deformation, which favours the decomposition of the solid solution direcly during deformation, promotes the formation of a coarse-grained structure in the subsequent recrystallization annealing if the temperature of annealing corresponds to the temperature of reverse dissolution of the phases which have precipitated during deformation.

It can be concluded from these results that a non-uniform deformation in intricate-shape articles at temperatures corresponding to

the two-phase region (this non-uniformity being due to different rate of metal flow in various portions) must cause a non-uniform decomposition of the solid solution directly during the deformation and, therefore, produce an inequigranular structure after heat treatment. This conclusion is confirmed by some industrial data.

For instance, a coarse-grained peripheral zone often appears after heat treatment in parts made of nimonic type alloys. Such structure defects usually form when the temperature of die-forging is too low (underheated dies). It may be supposed that the peripheral portion of a forged part is chilled in a cold die to a temperature of the two-phase region and, therefore, the deformation causes in that region the decomposition of the solid solution and the associated effects.

It is known from experience that coarse-grained structure zones sometimes form at the periphery of low-carbon steel forgings. As a rule they appear in a metal which is subjected to high-temperature heating in the austenitic range before hot deformation. This heating is accompanied by intensive dissolution of carbide and carbonitride phases. Before deformation, a part becomes chilled somewhat and its peripheral zone cooled from contact with die tools. Upsetting then causes noticeable decomposition of austenite in this zone and precipitation of disperse phases. In subsequent heat treatment, this may result in secondary recrystallization by the mechanism described earlier. Zonal inequigranularity, as shown in Fig. 124*b*, may probably originate just in the same manner.

The following common conclusion can be made from the above discussion. The type of inequigranularity in age-hardening alloys is determined not only by the presence of excess disperse phases, but also by the conditions of heating prior to and during deformation, by the shape of deformed parts and the associated non-uniformity of deformation over the cross section. These factors can influence the nature and intensity of decomposition of the solid solution and, accordingly, the conditions of growth of recrystallization nuclei (grains) in subsequent high-temperature heating.

8.2. Aluminium Alloys

Hot pressing, which has certain advantages over other methods of plastic working, is used extensively for making parts of aluminium alloys. The method ensures a favourable combination of high mechanical properties (due to the extrusion effect) and a high surface finish.

On the other hand, it has a serious drawback. After heating for hardening of pressed parts made of Avial, Д16, and other types of aluminium alloy, a coarse-grained structure often forms, with grains exceeding tens or hundreds of times the size of original grains. As a rule, such coarsening appears not over the whole volume or cross

section of parts, but only in certain microregions (zonal inequigranularity). The most typical and commonest example of local structure coarsening is a coarse-grained zone (called 'large-crystalline' rim) appearing on the periphery of pressed parts. In some cases, the rim may occupy a substantial portion of the cross section and spoil many parts (see Fig. 124*a*). Aluminium-base alloys undergo no phase transformations, so that structure coarsening in finally shaped products cannot be amended.

The mechanism of 'rim' formation and the factors that allow for prevention of this effect have been under extensive study and are now clear in principle.

Commercial aluminium alloys are complicated multi-component compositions, the commonest components being copper, magnesium, manganese, iron, nickel, silicon and other elements.

In order to collect systematic information on the role of chemical and phase composition in the formation of zonal coarse structures, experiments were made on pure aluminium Grade A99 and alloys based on this grade, such as binary alloys of the systems Al-Cu, Al-Mn, Al-Mg, Al-Si, Al-Fe, Al-Ni, Al-Co; ternary alloys Al-Cu-Mn, Al-Cu-Fe, Al-Mn-Fe; a quaternary alloy Al-Cu-Mn-Fe; and alloys of the Avial type (Al-Cu-Mg-Mn-Si) and Д16 grade both free of iron and with 0.3% Fe (by mass).

These materials were chosen from the following considerations. Manganese is noticeably soluble in aluminium at the eutectic temperature (the solubility limit is about 1.82%). With a reduction of temperature, its solubility decreases sharply. In contrast to this, the solubilities of iron, nickel and cobalt in aluminium are very low even at elevated temperatures (0.06-0.05% at the eutectic temperature) and are practically equal to zero below 400°C. In addition, the alloys have different rates of precipitation and reverse dissolution of disperse phases. The intermetallic phases in the Al-Mn system are characterized by an appreciably lower rate of these processes compared to the phases in the Al-Cu system. Because of these differences, the alloys selected are convenient for the purposes of this examination.

Ingots were cast at 690-710°C by the continuous casting technique into water-cooled moulds and then pressed at different temperatures into rods 90 mm and 40 mm in diameter (direct pressing without lubrication, at a rate of 1-1.5 m/min).

The following relationships are established.

Coarse-grained or coarsened structures sometimes form not only at the periphery of specimens, but, given definite conditions (the composition of a metal and the mode of deformation), also in the core portion of rods or even occupy the whole cross section.

A large-crystalline 'rim' forms in age-hardening alloys during heating for hardening, but only when the temperature of pressing

fell within the two-phase region. In Al + 0.28% Mn rods, no marked inequigranularity is observed, irrespective of the temperatures of pressing and subsequent recrystallization annealing. With an increase in the content of Mn up to 0.7%, a 'rim' appears after heat treatment in rods pressed at 300° and 350°C. Pressing at 420° and 500°C and subsequent heat treatment give a homogeneous structure over the whole cross section of rods.

No large-crystalline 'rim' appears in rods of pure aluminium; in rods of Al + 2.42% Mg alloy when the temperature of pressing falls within the single-phase region; and in rods of alloys Al + + 3.8% Cu, Al + 0.30% Mn, Al + 3.67% Cu + 0.24% Mn, Grade Д16 (iron-free), etc., when the temperature of pressing is close to the temperature of transition from the two- to the single-phase region.

Furthermore, in pure-aluminium rods pressed and heated at 400°, 500° and 560°C, the grain size in peripheral zones proves much smaller than in the core.

This peculiarity is even more pronounced in the binary alloys with low-soluble additions (Fe, Ni, Co). As with the addition of manganese, the structure of these alloys tend to coarsen beginning with a definite content of the addition (approximately 0.12-0.17% or higher). In contrast to Al-Mn alloys, a preferable zone of coarsening is the core rather than the periphery of rods. For instance, in alloys with 0.20% of Fe or Ni, coarsening appears only in the core zone, and with an increase in the concentration of these elements roughly to 0.40% it expands practically through the entire cross section.

The dependence of structure coarsening on pressing temperature is determined by the nature of dissolution of elements in aluminium. As noted earlier, an increase of the temperature of pressing diminishes the probability of zonal inequigranularity in Al-Mn alloys and, on the contrary, increases this probability in Al-Fe and Al-Ni alloys.

Irrespective of the alloy composition and the position of coarse-grained zones in the cross section of rods, coarse grains always have an anisotropic shape and are strongly stretched along the axis of pressing.

In Al-Cu and Al-Si alloys, and also in Al-Mn, Al-Cu-Mn and Д16, which contain not more than 0.4% Mn, a large-crystalline rim appears only when the content of iron reaches 0.2-0.25% or more. Besides, grains in peripheral zones are larger with a higher content of iron in an alloy.

The peripheral zones where a 'rim' forms after heating for hardening have a higher etchability already in as-pressed state. Often, they are dull after etching. This fact says in favour of the assumption that though a rim usually forms during heating for hardening the

conditions for its formation set in already at the pressing stage. Hence, to clarify the mechanism of rim formation, it is necessary, in the first place, to establish the difference in the structures of peripheral and core zones of rods in as-deformed state.

X-ray and macrostructural analysis and also resistivity measurements have showed that in aluminium and aluminium-alloy rods in which no rim (dull zone) appears the structures of peripheral and core regions differ only slightly. In binary and more complex alloys, where a dull zone has formed after pressing, there is an appreciable difference between the core and peripheral structures.

Measurements of the resistivity and the lattice spacing of the solid solution made on binary Al-Mn alloys with 1.38% and 0.77% Mn (Fig. 132) have showed that the solid solution in these alloys decomposes during pressing, the intensity of decomposition being appreciably higher in peripheral zones than in the core. Besides, the difference in the intensities of decomposition is greater with a higher content of manganese in the alloys. Similar results are obtained on the avial alloy.

The lattice spacing of the solution of Al + 1.38% Mn alloy in the peripheral zone immediately after pressing is 4.0538 Å against 4.0525 Å in the core. In avial, the respective values are 4.0487 Å and 4.0475 Å. The hardness in as-pressed state has proved lower at the periphery and higher in the core (40 *HB* and 49 *HB* in Avial).

In order to check whether the presence of disperse phase particles before heat treatment (annealing) is important in itself or only their precipitation from a supersaturated solution just during deformation is essential, ingots of Al + 0.7% Mn alloy were homogenized prior to pressing for a long time at 590°C (50 h) or 500°C (120 h). This gave a different content of manganese in the solid solution. At 500°C, a large quantity of acicular particles of Al_6Mn phase precipitated from the solution*.

Large-crystalline rim was only found in rods homogenized at 590°C. Coarsening took place only in regions where an intensive decomposition occurred during pressing.

Thus, the coarsening of peripheral zones of rods during annealing is preceded by intensive decomposition of the solid solution during pressing and precipitation of a large amount of fine-disperse particles. The size of particles in Al-Mn alloys is less than 0.3 μm, the average distance between them being 1.0-1.2 μm.

Structure coarsening in the rim zone is promoted by an increase of the manganese content in an alloy, a decrease of the pressing temperature and an increase of the temperature of homogenizing annealing prior to pressing, i.e. by the factors which cause super-

* The atomic radius of manganese is smaller than that of aluminium, so that the precipitation of Al_6Mn increases the lattice spacing of the solid solution.

saturation of the solid solution before pressing and intensify decomposition during deformation.

The more intensive decomposition of the supersaturated solid solution at the periphery of rods is undoubtedly associated with the type of plastic working. The degree of deformation in peripheral regions is higher than in the core and the flow of metal has a more intricate turbulent nature owing to friction against the die walls.

It is well known from the practice that the width of large-crystalline rim decreases along the length of a rod towards its front end.

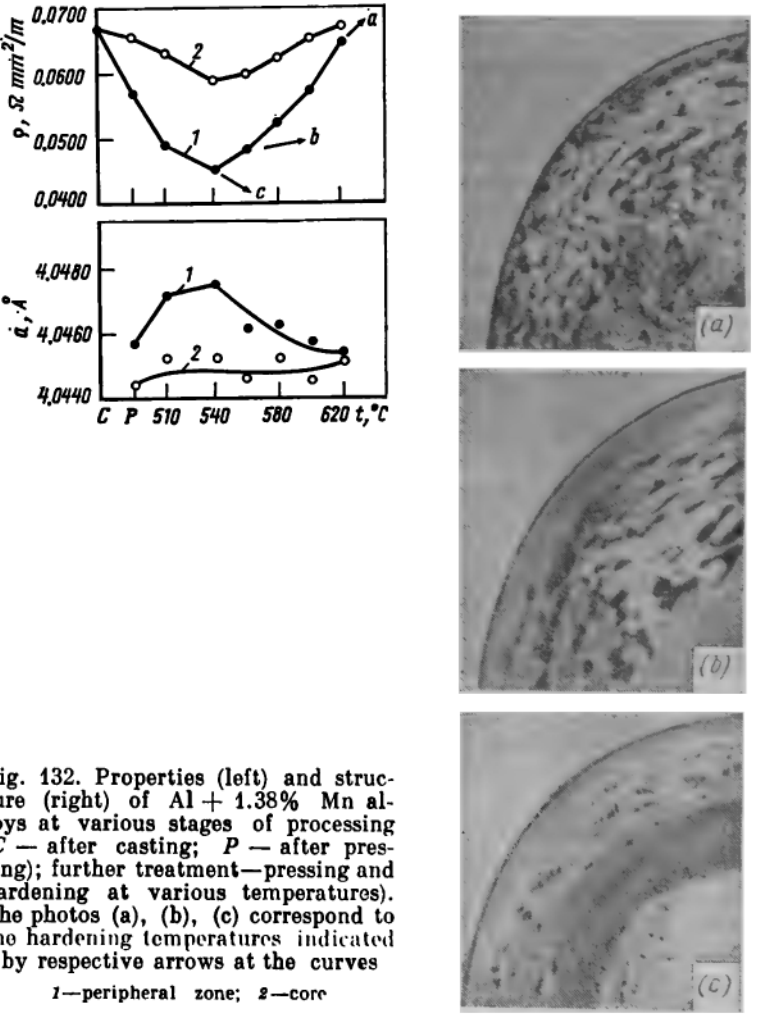

Fig. 132. Properties (left) and structure (right) of Al + 1.38% Mn alloys at various stages of processing (*C* — after casting; *P* — after pressing); further treatment—pressing and hardening at various temperatures). The photos (a), (b), (c) correspond to the hardening temperatures indicated by respective arrows at the curves

1—peripheral zone; *2*—core

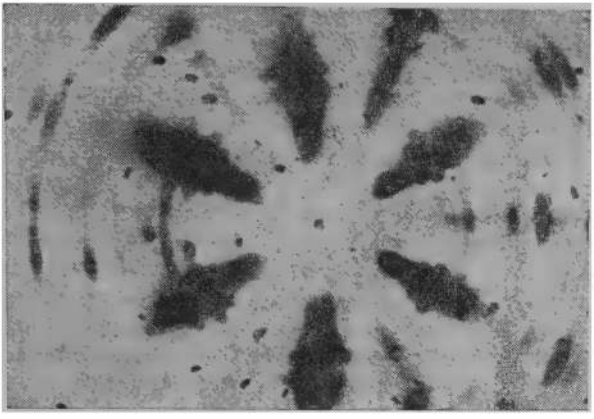

Fig. 133. X-ray photograph of a peripheral portion of pressed aluminum alloy containing iron and manganese

It has been also found that the intensity of decomposition of the solid solution in the peripheral zones also diminishes towards the front end of rods. This can be explained easily if we recall that the peripheral zone of the front end of rods is subjected to friction only in the plastic working zone (i.e. for a very short time). Towards the rear end of rods, the metal is subjected more and more to friction against the die walls. In this case the time of action of the forces which accelerate decomposition of the solid solution is longer and the decomposition proceeds more deeply.

Another difference between the rim and core portions of rods in as-pressed state is associated with the nature of microstructure. The core of rods is recrystallized. As a rule, primary recrystallization in the core is completed and in some cases the early stage of grain growth has started. X-ray photographs of the peripheral (dull) zone of a rim have the appearance typical of a textured unrecrystallized material in which only polygonization has taken place*. Micro-bundle radiography also reveals polygonized structure.

In very rare cases, radiograms of the dull rim show Laue spots from large grains grown locally during pressing and subsequent cooling against the background of blurred texture maxima of the deformed (polygonized) matrix (Fig. 133).

The stability of the polygonized structure in peripheral zones is favoured by particles of Al_6Mn phase precipitated during pressing

* It should be noted that relatively large subgrains can produce point reflections on radiograms and these can be mistaken for trails of primary recrystallization.

and subsequent heating and concentrated preferably on subboundaries.

A third peculiarity is associated with the type of texture. The axial texture with ⟨111⟩ and ⟨100⟩ directions is typical of the core portion of pressed rods. The peripheral portions show a rolling texture with the main components {110} ⟨111⟩, {100} ⟨001⟩ and {310} ⟨001⟩, i.e. in peripheral zones grains are oriented in the directions ⟨100⟩ and ⟨111⟩ which are parallel or almost parallel to the pressing axis. The angles of misorientation between adjacent grains in various texture components differ only slightly and are relatively small (approx. 1°).

After annealing which resulted in a large-crystalline rim, the orientations of individual grains were determined radiographically on reflected-light Laue photographs. The rolling texture was retained in the rim too. All grains in the rim were grouped around the orientations {215} ⟨120⟩ and {435} ⟨101⟩.

In large-crystalline rims, grains with the main orientations typical of the deformed state were absent.

Grains with the orientations ⟨110⟩-⟨210⟩ were not detected in as-deformed state and appeared only after annealing.

Thus, nuclei of large grains are not formed from the main mass of textured deformed material. Only the processes of the polygonization type take place in the main mass of metal during heating. At the end of the incubation period, the rate of growth of new grains rises abruptly and becomes anisotropic, the maximum rate being along the pressing direction. An important feature of new grains is their higher structural perfection compared to the surrounding polygonized matrix from which they are separated by highly mobile large-angle boundaries from the very moment of their detection.

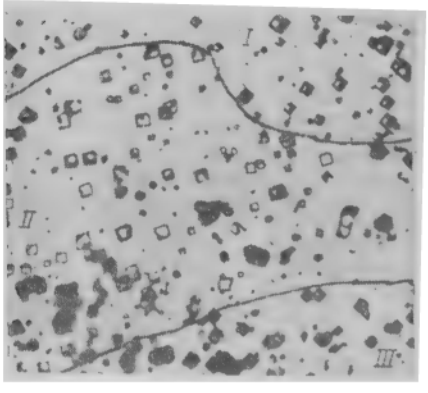

Fig. 134. Microstructure of large-crystalline rim. The boundaries outline the region which differs in the shape and orientation of etch pits from adjacent regions. ×300 [228]

Figure 134 shows a portion of the microstructure of a large-crystalline rim at a stage close to the completion of coarsening. The same orientation of etch pits in recrystallized grains of the rim (regions *I* and *III*) is indicative of their high perfection. In contrast to this, in the remaining portions of deformed material (region *II*) there is an appreciable angle of turn between adjacent etch pits (5-10°). This

is a direct indication that the substructure of the polygonized matrix is less perfect and contains rather misoriented subgrains separated by low-angle boundaries. The size of subgrains is 5-10 μm. This difference in the volume energies between new grains and the matrix and a favourable orientation of these grains relative to the matrix obviously ensure a high rate of growth of differently oriented grains.

Thus, there is no intermediate stage between the as-deformed and the coarse-grained recrystallized state of the matrix. The imperfect polygonized matrix is consumed during the whole time of the coarsening process. This suggests that coarsening is the result of primary but not secondary recrystallization. On the other hand, the process has some features typical of secondary recrystallization; namely, there are few nuclei in the stabilized matrix.

Consequently, the principal feature of zonal structure coarsening ('rimming') in the case considered is that the process of primary recrystallization takes place in the stabilized matrix by the growth of a small number of nuclei. If the conditions of deformation are favourable for primary recrystallization with the formation of numerous nuclei, subsequent annealing will cause no structure coarsening.

In the alloys considered, despite a high degree of deformation, a particular pattern, rate and high temperature of deformation stabilize the structure as a result of polygonization. Disperse-particle precipitates play the principal part in the polygonization and stabilization of the substructure. As follows from the material of Ch. 3, disperse particles produce a higher barrier effect on low-angle boundaries than on large-angle ones.

So, to stabilize the matrix by disperse particles, these must precipitate from the supersaturated solid solution either during hot plastic working (pressing) or in subsequent prerecrystallization heating. But the structure begins to coarsen only if recrystallization heating eliminates the stabilizing effect all over the whole volume and not in individual portions. The stabilizing effect is eliminated by the dissolution of precipitated disperse particles and/or their coagulation. Dissolution of disperse particles is indispensable for initiation of structure coarsening in alloys whose matrix has been stabilized by these particles. We can illustrate the point by considering the results obtained on the Al + 1.38% Mn alloy (see Fig. 132).

When the structure coarsens at the periphery and in the core, the process retains the principal features typical of the formation of large-crystalline rim. Large grains are also anisotropic in shape and have the same ⟨110⟩-⟨210⟩ orientations along the pressing axis. The process is also realized by the growth of a small number of nuclei into the stabilized matrix.

The principal difference is that the process features less rigid limitations on the radial orientation of new grains or even no limitations at all. The latter circumstance may be associated with a difference in the textures of the core and peripheral portions in the as-pressed state (there is an axial texture in the core and a rolling texture at the periphery).

Let us consider the fact why in pressed aluminium alloys with low-soluble additions (Fe, Ni, Co, etc.), where secondary phase particles precipitate during crystallization, but not during pressing, the process of structure coarsening begins in the core rather than in the peripheral portions of rods.

To understand this, one should remember that structure stabilizes through polygonization of the matrix and with the aid of disperse particles.

For stabilizing polygonization, the conditions are more favourable in the core portions of a rod, where the deformation is more laminar, so that a lower concentration of disperse particles is needed to produce the stabilizing effect. In the peripheral zone, where plastic flow is more turbulent, the conditions for stabilizing polygonization are less favourable.

In addition, it should be noted that Al-Fe, Al-Ni and Al-Co alloys contain secondary phase particles prior to pressing, whereas Al-Mn alloys do not. These particles can produce local inhomogeneities in the character of plastic flow of the matrix. For that reason, the conditions for stabilizing polygonization in core portions of ingots are more favourable in Al-Mn alloys than in Al-Fe and other alloys.

In Al-Fe, Al-Ni and Al-Co alloys, the density of disperse particles is practically the same over the cross section of a pressed rod and is determined by particle distribution in the ingot. For this reason, the turbulent plastic flow in peripheral zones, which is enhanced by the presence of primary disperse particles, ensures favourable conditions for recrystallization but not for polygonization.

In Al-Mn alloys, particles precipitate during pressing preferably in peripheral zones; the intensity of precipitation rises with increased supersaturation of the solution. Therefore, coarsening in these alloys takes place during heating preferably in peripheral zones and intensifies as the conditions for matrix stabilization prove favourable. These conditions include an increased content of manganese in the alloy, increased temperature of homogenizing, and decreased temperature of pressing (this drop in temperature must be relatively smooth to avoid the formation of numerous recrystallization nuclei). In core portions of Al-Mn rod, even a low content of manganese is sufficient to stop recrystallization at the in-situ stage.

In aluminium alloys containing iron and its analogues, an increase in the content of the secondary element produces a noticeable structure coarsening first in the core portion of rods (with approximately

0.15% Fe or Ni). With a further increase in the concentration of these additions (roughly 0.40% Fe or Ni), the number of secondary phase particles increases and becomes sufficient to stabilize the structure and promote structure coarsening in the rim portion of rods during heating.

These considerations can clarify the effect of pressing temperature. In pressing at 500°C, structure coarsening in the core portion of Al-Fe and Al-Ni rods is observed at a lower concentration of the secondary element than is the case in pressing at 350°C.

At a lower temperature of pressing, the conditions are obviously less favourable for stabilizing polygonization. In that connection it is essential to enhance the second stabilizing factor, i.e. increase the number of disperse particles.

If the temperature of pressing becomes so low that numerous recrystallization nuclei form during heating, no structure coarsening will take place.

This explains the effect of preliminary (prior to pressing) annealing, which involves changes in the size and shape of secondary phase particles. If particles become larger or change their shape from an oval to a less regular one, they act more as stress concentrators than as barriers. This facilitates nucleation and inhibits structure coarsening.

A generalization of the observed relationships makes it possible to conclude that the effect of pressing temperature on the size of recrystallized grains can be described by a curve with a maximum. The largest grain size is observed if the stabilized structure of a deformed metal is not recrystallized, but heating ensures favourable conditions for the appearance of a few recrystallization nuclei, with the matrix remaining stabilized.

An insufficient stabilizing effect will cause the formation of numerous recrystallization nuclei and grain refinement, while a stronger stabilizing effect will result in retention of the unrecrystallized structure after annealing (i.e. retention of what is called the extrusion effect).

Heating of an alloy after pressing at 500°, 510°, 520° and 540°C (isothermal holding for 1 h) caused no essential changes in the macrostructure and the pattern of radiograms as compared to the as-pressed state. The periphery of rods was dull. X-ray analysis showed that primary recrystallization was complete. The core had uniform grains and the periphery had grains of various sizes. Parallel measurements of the resistivity and lattice parameter showed, however, that the decomposition of the solid solution proceeded up to 540°C and was more intensive at the periphery. At 540°C the highest degree of decomposition was attained; the resistivity was at its minimum and the lattice parameter of the solid solution at the maximum.

After heating for hardening at 560°C, a rim first appeared at the periphery and at the same time a bend was noticed on the temperature curves of resistivity and lattice parameter, which was an indication of the onset of reverse dissolution of secondary phase precipitates. After that moment, resistivity began to rise and the lattice spacing to diminish.

The correlation between the formation of a rim and the beginning of reverse dissolution of disperse phases explains why the temperature of the formation of a rim depends on alloy composition. As found for Al-Mn alloys, the temperature of rim formation increases continuously with an increase in Mn content. For instance, in an alloy with 0.56% Mn a rim appears after heating at 500°C and in an alloy with 1.38% Mn only at 560°C. The matter is that as the concentration of manganese increases, the temperature at which the same concentration of Al_6Mn particles remains in alloys becomes higher, with the result that the temperature of the beginning of intensive growth of recrystallization nuclei changes.

Thus, an increase of the manganese content in an alloy cannot make it possible to avoid the formation of a rim, but only raises the temperature of rim formation. Therefore, keeping the same temperature of heating for hardening, one can preclude the formation of a rim by increasing the content of manganese.

On the other hand, it is now clear why there appears no rim in rods of the alloy with a reduced content of manganese (0.3%) and accordingly with a low temperature of dissolution of Al_6Mn.

In rods of Al + 0.3% Mn alloy, after pressing and hardening from various temperatures the resistivity is the same in the core and at the periphery. Therefore, no noticeable decomposition of the solid solution takes place in the alloy during pressing, since the temperature of pressing is close to the point of transition into the single-phase region. Accordingly, in that case there are no favourable conditions for the formation of inequigranular structure in the course of primary recrystallization.

How can we explain the fact that a small (0.3% or more) addition of iron (which is poorly soluble in aluminium) to the Al + 0.4% Mn alloy causes rimming? It may be supposed that the solubility of manganese decreases in the presence of iron and the aluminium solution becomes more saturated with manganese than is the case in the absence of iron. This explanation certainly requires verification.

At the same time, one should be cautioned against supposing that whenever the deformation involves decomposition of the supersaturated solid solution, the subsequent heating for hardening and the dissolution of disperse phases inevitably cause intensive secondary recrystallization and structure coarsening. This is only the case where the concentration of disperse phase particles is sufficiently high, the rate of their dissolution is low compared to the rate of

recrystallization, and the temperature of annealing is high.

For instance, a high rate of disolution of disperse phases during heating for hardening precludes structure coarsening in Al + 3.8% Cu and Д16 alloys which contain no iron.

Figure 135 shows the effect of heating temperature (in hardening) on the resistivity of pressed Al + 3.8% Cu alloy. Pressing was done at 420°C, i.e. in the two-phase temperature region, and involved an intensive decomposition of the solid solution.

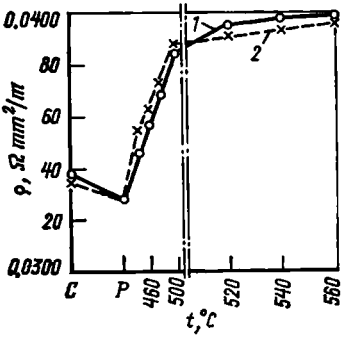

Fig. 135. Effect of temperature of heating on resistivity of pressed Al + 3.8% Cu alloy (*C* — as-cast; *P* — as-pressed)

1 – rim; *2* – corn

In contrast to Al-Mn alloys, where decomposition does not come to completion during pressing and a minimum of resistivity on the curve (see Fig. 132) appears only in subsequent heating to a temperature above the pressing temperature, in Al-Cu alloy the process of decomposition is accomplished during pressing and subsequent cooling. The resistivity of this alloy is at a minimum in as-pressed state. Heating above the temperature of pressing immediately causes an increase in the resistivity of Al-Cu alloy, i.e. the reverse dissolution of disperse phases. The dissolution in this alloy occurs much more intensively than in Al-Mn alloys and is practically completed at 500°C when the rate of boundary migration is still too low.

This difference in the behaviour of Al-Mn and Al-Cu alloys is obviously associated in the first place with the different rates of diffusion processes of decomposition and dissolution, i.e. with the different rates of diffusion of copper and manganese in aluminium. The fact that the temperature of transition from the two-phase to the single-phase in Al-Cu alloys is lower than in Al-Mn alloys can also play a certain role; therefore, with the same temperature of annealing, the excess of this temperature over the temperature of intensive dissolution and coagulation of disperse phases, ΔT, is higher in Al-Cu alloys than in Al-Mn alloys.

It should be also emphasized that the proposed scheme is not obviously the one that can be universally applicable.

Up to this point, we have not considered the causes of anisotropy of grain shape in coarsened structures. This anisotropy appears in the course of growth of grains and therefore is due to anisotropy of the rate of this process. As is known, this anisotropy may be associated with a favourable orientation of growing grains relative to the textured matrix or with a lineage distribution of secondary phase particles. The role of these factors was studied by Yu. S. Safonov

on an Al + 0.22% Ni alloy. He has determined the orientations and the coefficients of shape anisotropy (the length-to-width ratio) for various grains in coarse-grained structures formed on annealing after pressing at 500°C. Analysis has showed that grains with the ⟨210⟩ direction along the pressing axis have the highest coefficient of anisotropy, up to 8-12. With a deviation of the crystallographic direction from ⟨210⟩ towards the orientation ⟨100⟩-⟨111⟩, the coefficient of anisotropy drops to 2-5. In annealing of rods of the same alloy after pressing at 350°C, when recrystallization involves no structure coarsening, but retains a lineage distribution of disperse particles, new relatively fine grains have no preferable orientations and their shape is practically isotropic. This makes it possible to suppose that the anisotropy of the rate of growth is due to a favourable orientation of growing grains relative to a component of the deformation texture.

However, in Al-Fe and Al-Ni alloys, grains in coarsened zones with the orientation ⟨210⟩-⟨110⟩ are gradually stretched along the pressing axis as the content of the secondary component is increased (i.e. with an increase in the concentration of disperse particles). Therefore, an increase of the density of particles in the longitudinal direction additionally promotes anisotropy of the rate of growth and shape of grains.

Thus, anisotropy of grain shape in pressed aluminium alloys is due to the combined effect of two factors: the orientation factor and the barrier factor which is caused by a lineage distribution and high density of disperse particles.

In this chapter we have not considered the important results obtained by Yu. M. Weinblat et al., which show that the rate of hot plastic working plays a large part in recrystallization of alloys and coarsening of their structure. The main results of their work have been discussed briefly in Ch. 6.

Chapter 9

Recrystallization Diagrams

As has been shown in Ch. 1, the size and uniformity of grains are important characteristics which determine the structure-sensitive mechanical and physical properties of metals and alloys. In addition to the composition of metals and alloys, their grain size and the degree of inequigranularity are in many cases specified by state standards and technical specifications. In some cases, it is essential to know the size of grains and the type of structure not only in final products, but also at some intermediate stages of the technological process. For instance, for many poorly deformable materials it may be quite essential to know the grain size at the moment of plastic working, since the plasticity of metals usually worsens with an increase in grain size. It is therefore not by accident that these problems were the first stimulus for studies into recrystallization of metals and alloys and the published results of measurements of grain size and its variations in various technological procedures were among the earliest numerous publications relating to recrystallization.

The most common form of graphical representation of these results is a tridimensional diagram which gives the average size $\bar{D}$ of grains as a function of deformation (ε, %) and the temperature of annealing or deformation (t, °C); this is what is called a recrystallization diagram (Figs. 136-138).

Two types of recrystallization diagram are used most often. The first type of recrystallization diagram is plotted when recrystallization annealing is carried out after cold deformation (see Fig. 136). It illustrates the dependence of the average grain size on the degree of deformation and the temperature of subsequent recrystallization annealing for a given time taken to be the same for all temperatures. The second type of recrystallization diagram is constructed for hot deformation. It shows the dependence of the average grain size on the degree and temperature of hot deformation, without subsequent annealing (see Fig. 137).

Modern engineering extensively employs novel high alloys based on iron, nickel, molybdenum, titanium, aluminium, copper, etc. and intended for use at high temperatures and stresses, in aggressive media, etc. Because of their low plasticity, these alloys are mostly deformed by hot plastic working. After hot deformation, these metals

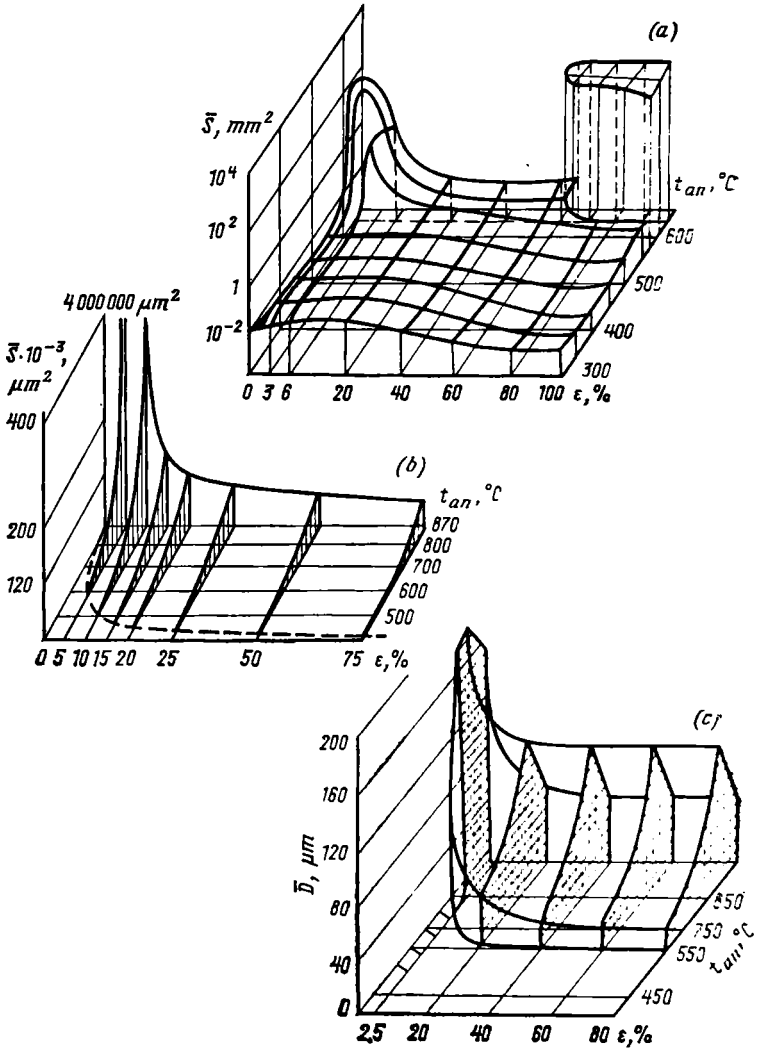

Fig. 136. First-order

a) aluminium (99.6%); (*b*) electrolytic iron; (c) commercial-purity titanium; (*d*) niobium Cr, 14% Ni, 2% Mo); (*h*) austenitic steel X18H14M2B1 (0.1% C, 18% Cr, 14% Ni, 2% 136*g* and *h*,

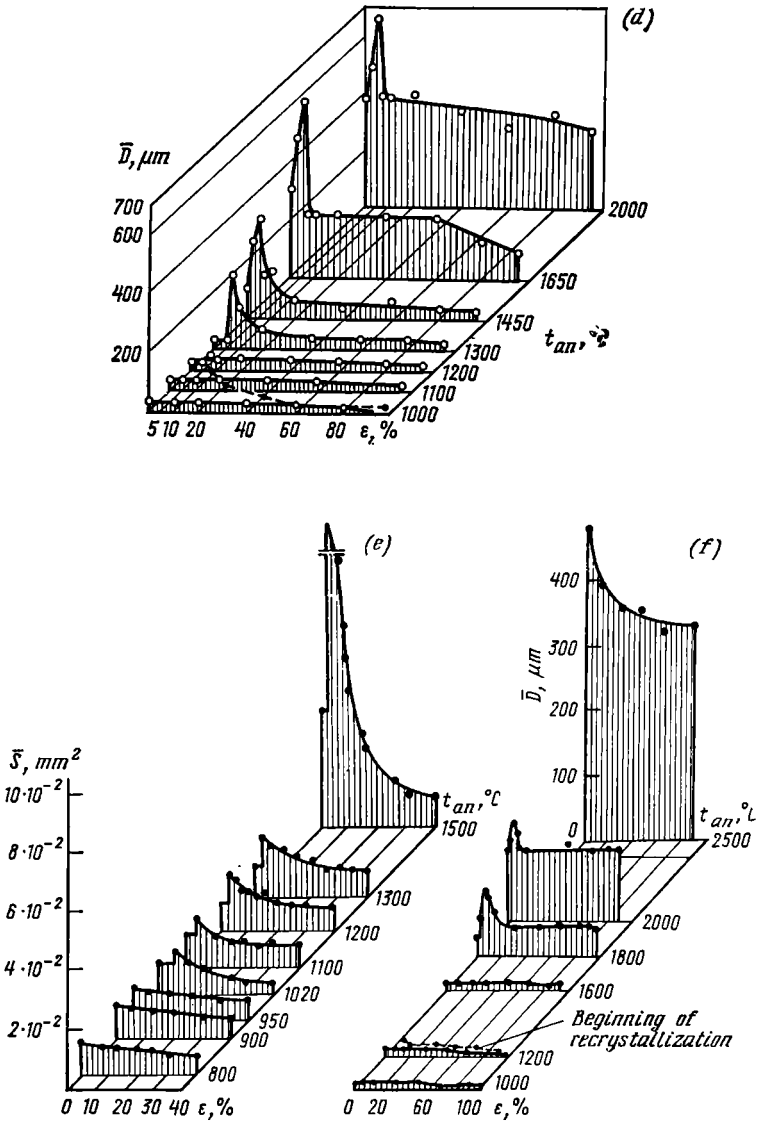

recrystallization diagrams

[236]; (*e*) tantalum [237]; (*f*) chromium [235]; (*g*) austenitic steel X18H14M2 (0.1% C, 18% Mo, 1% Nb) containing NbC carbides and Fe_3Nb_2 intermetals soluble above 1150°C (Figs.

see p. 292)

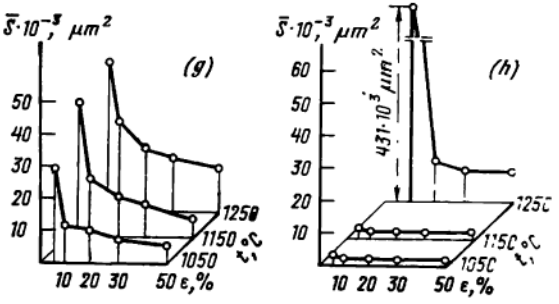

Fig. 136 (*g*, *h*)

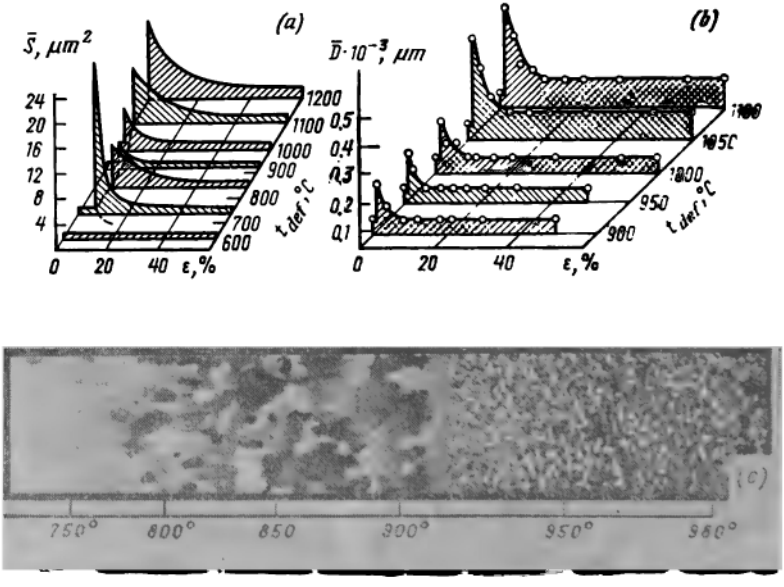

Fig. 137. Second-order recrystallization diagrams

(*a*) low-carbon steel (0.06% C), hot-rolled, annealed for 5 min at the rolling temperature, and cooled in furnace [7]; (*b*) ~ЭИ437 alloy press-forged and cooled in sand [8]; *c*—microstructure of low-carbon steel after light deformation and gradient heating at 700–1000°C to illustrate the diagram in (*a*)

are subjected to the final heat treatment (hardening and often age-hardening) to produce the desired microstructure. As mentioned above, however, the conditions of hot deformation substantially influence the type of structure formed during heat treatment.

This necessitates the use of a third type of recrystallization diagram to determine the grain size not only after hot deformation but also after heating for hardening. The idea was first expressed by S. I. Gubkin and later such diagrams were proposed and constructed by a number of workers [9]. Such a diagram contains two curves for each deformation temperature: one for the grain size immediately after deformation (as in the second-type diagrams) and the other for the grain size after final heat treatment. An example of this diagram is shown in Fig. 138.

When plotting a recrystallization diagram, all the factors which can affect grain size must be maintained constant and the numerical data on them should be added. These include: the chemical and phase composition of an alloy and, for pure metals, the degree of purity

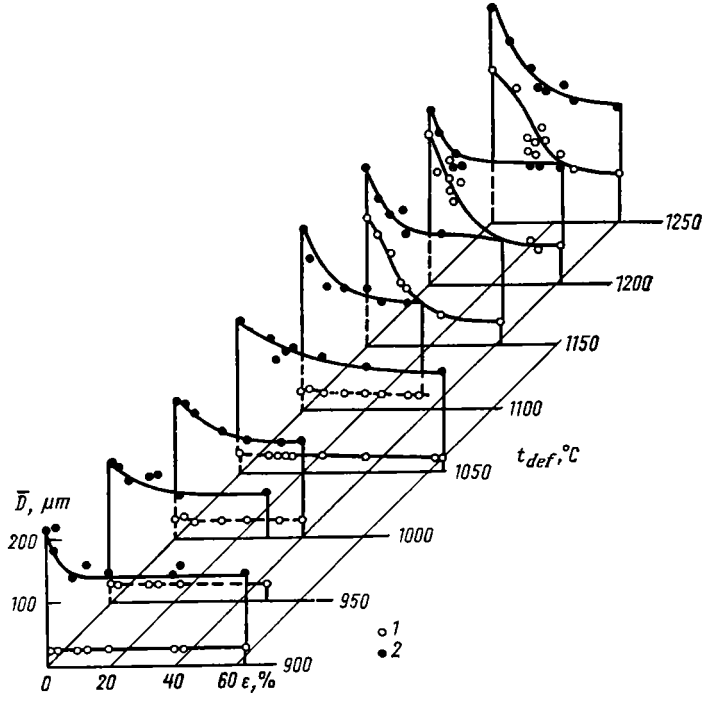

Fig. 138. Third-order recrystallization diagram. ХН70ВМТЮ alloy

○—hot upsetting in press; ●—hot upsetting in press and heat treatment at 1200°C for 2 h and at 1050°C for 4 h

and the content of impurities; the original grain size and texture; the type and rate of deformation; the rate of heating; the time of isothermal heating; the rate of cooling, etc. The size and position of the microsection on which grain size measurements are made should also be specified.

It should be remembered that recrystallization diagrams in their common form give only limited information on the type of recrystallized structure and do not reflect many structural peculiarities. For instance, we have mentioned that the degree of inequigranularity is quite important, but recrystallization diagrams usually give only the average size of grains $\bar{D}$. If, for instance, a structure has the main mass of grains of index 8 and a few very large grains, the structure may be estimated on a recrystallization diagram by index 2 or 3, which is far from being the actual characteristic of the structure. Besides, a recrystallization diagram fails to characterise the type of inequigranularity—micro- or macro-inhomogeneous, zonal, lineage, etc.

Berezhkovsky [9] has suggested special symbols to characterize the type of structure (equiaxiality and uniformity of grains, presence of twins, etc.) on $\bar{D}$-ε curves of recrystallization diagrams, as illustrated in Fig. 139.

It is desirable for the practice that recrystallization diagrams should contain exhaustive information on the structure and, in particular, on the extreme sizes of grains present in it, the type of inequigranularity, perfection of grains, grain textures, etc.

The lower of the two curves on a third-order recrystallization diagram describes the structure of as-deformed metal (after hot deformation). Such a structure very often consists partially of new recrystallized grains and partially of original grains, as shown in Fig. 140. Large original deformed grains are surrounded by fine new grains. The concentration of new grains is greater (and, accordingly, the concentration, or the area occupied by the rests of original grains, is smaller) after heavier deformations and at a slower rate of cooling. But grains differ from one another not only in size but also in the degree of perfection (volume energy). Large original grains are deformed and disappear in subsequent heating or in the course of slow cooling immediately after hot deformation. Fine, more perfect, new grains grow at the expense of these large grains; the picture here is quite opposite to that observed during heating of a common inequigranular metal where large grains grow at the expense of finer ones. This can be illustrated by the data on variations in grain size distribution in austenitic and ferritic steels during continuous cooling after hot deformation, which are given in Ch. 6 (see Fig. 102).

For instance, austenitic steel type 12X18H9 had a large number of grains of index 1 and 2 in the original state. After plastic working at 1 100°C and chilling for 1.5 s before hardening, grains of index 1

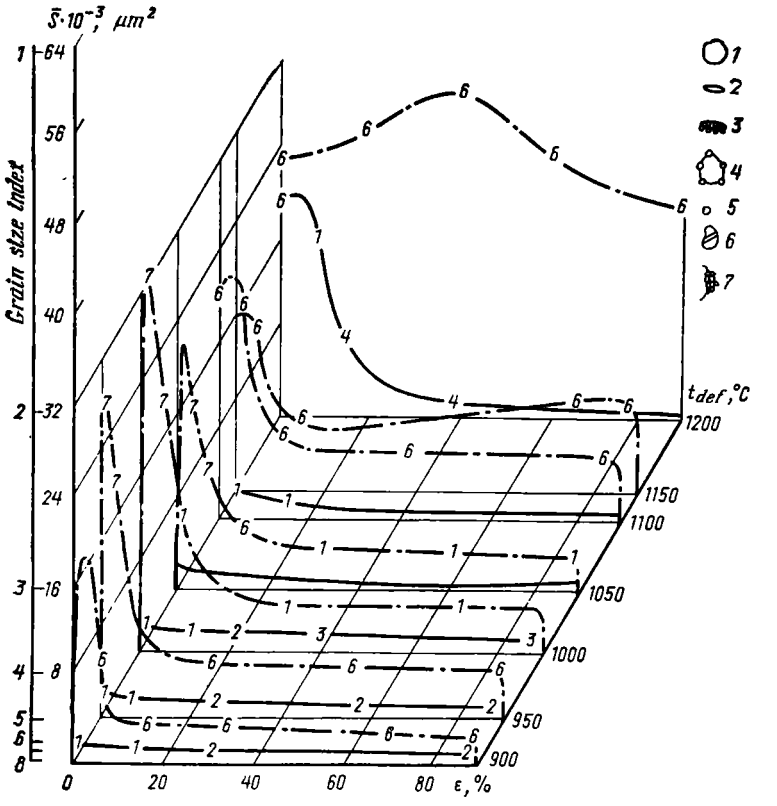

Fig. 139. Third-order recrystallization diagram characterizing the structure [9]

1—equi-axed uniform grains; *2*—inequi-axed uniform grains; *3*—stretched old grains and fine equi-axed grains on their boundaries (beginning of primary recrystallization); *4*—equi-axed old grains and new individual fine grains (occupying 5% of the area) on their boundaries (inequigranularity, beginning of primary recrystallization); *5*—new equi-axed grains occupy 100% of the area (beginning of grain growth); *6*—twin in most grains; *7*—inequigranularity (solid lines—after upsetting, dot-and-dash lines—after upsetting and heat treatment)

disappeared, but a small number of grains of index 3 and 4 were detected. After the same deformation and 15 s of chilling, the structure got refined (index 6 grains became the largest). After chilling for 500 s, grains of index 5 and 4 appeared again.

Therefore, large grains of index 3 or 4 in the metal chilled for 1.5 s were actually deformed grains which disappeared in subsequent heating.

It is then clear that the properties of these strain-hardened grains differ appreciably from those of recrystallized ones. For that reason it is important that a third-order recrystallization diagram should

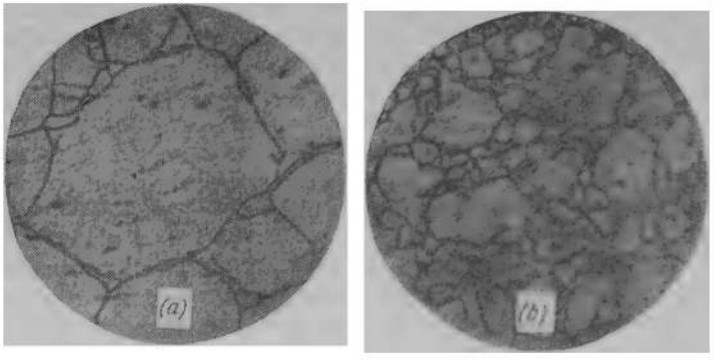

Fig. 140. Microstructure of H36XTIOM8 alloy after hot plastic deformation to 6% (*a*) and 20% (*b*). Large regions are deformed grains

indicate the nature of grains (deformed, recrystallized or both) that constitute the structure. Data on the presence or absence of textures would also be of much importance.

Figure 139 shows the system of symbols recommended in [9] to designate various structures on recrystallization diagrams and a third-type recrystallization diagram constructed with the use of these symbols.

A simpler, but illustrative and practically useful method for depicting inequigranularity in first-order recrystallization diagrams has been proposed in [10]. Inequigranular structures are characterized by two parameters: the average grain size of fine-grained matrix and the average size of large grains (see Fig. 129). Accordingly, two experimental curves, instead of one, are drawn in the portions of the diagram having an inequigranular structure. For more graphical clearness, the portions of inequigranular structure in the diagram between the two curves may be shown hatched (see Fig. 129). This method gives clearer information on the real microstructure and makes it possible to reveal more distinctly a second maximum of grain size.

Another drawback of the common recrystallization diagrams is that they do not always represent the actual degree of deformation. This circumstance was first emphasized by I. M. Pavlov et al. who proposed to construct the so-called actual recrystallization diagrams.

Recrystallization diagrams are usually constructed by testing flat or cylindrical specimens which are deformed by upsetting or rolling and heat-treated, after which the average grain size over the height of specimens is determined (at the intersection of diagonals in a rectangular specimen) and the degree of deformation is calculated by the formula $\varepsilon = (H_{or} - H_f)/H_{or}$. Yet, the degree of

deformation may vary appreciably along the height of specimen owing to the friction between it and deforming tool, especially with light deformations and high rates of upsetting. The difference in the temperature of the beginning of recrystallization between various points along the height of a specimen may be as high as 100°C.

I. M. Pavlov has suggested the screw method for determining the actual degree of deformation. A threaded bore is made along the axis of a cylindrical specimen to receive a screw made of the same material. After deformation and heat treatment (for constructing first- and second-order diagrams) or immediately after hot deformation (for constructing a third-order diagram), the specimen is cut in the direction of upsetting. The actual degree of deformation in various points along the specimen height is then determined by the change in the screw pitch: $\varepsilon_{act} = (S_0 - S_n)/S_0$, where S_0 is the screw pitch before upsetting and S_n is the pitch in the given cross section after upsetting. Then, the average grain size in the corresponding cross sections is found and the actual recrystallization diagram is constructed, on which the average grain size is laid off with due regard for the actual degree of deformation in the section where this size has been determined.

Figure 141 shows such a diagram constructed by I. M. Pavlov [6]. The size of grains is given by two contours. The upper corresponds to the actual degree of deformation and the lower to the average deformation calculated by common methods. Under common conditions, the difference in the values of D_{av} is not high, but would be

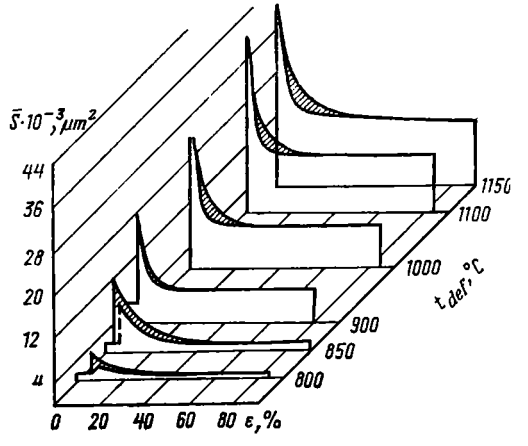

Fig. 141. Recrystallization diagram of medium-carbon steel (0.40% C, 0.65% Mn, 0.29% Si, 0.24% Ni, 0.14% Cr). Hot deformation in hammer, annealing for 40 min at the deformation temperature. Upper contours are actual diagrams and lower ones are common diagrams (after I. M. Pavlov)

greater if other structural characteristics were indicated on the diagram.

The most economic and quickest method for constructing actual recrystallization diagrams is based on the use of tapered specimens (see Fig. 111) which are deformed by tension [10]. Marks are made on a specimen before deformation. The actual deformation is determined by the changes in the distance between adjacent marks.

After deformation of this specimen, one obtains a set of deformation values from the values close to zero at the base to the maximum value at the neck (or in the broken section). The highest degree of deformation is determined by the plasticity of the specimen under the given conditions of plastic working. The gradient of deformations along the length of specimens can be varied by varying the inclination angle at the base and the total deformation of the whole specimen. For instance, in analysing the interval of critical deformations, it is reasonable to decrease the angle of inclination and thus to extend the region of low degrees of deformation.

By testing a single specimen (deformed and annealed at a given temperature), an isothermal section of recrystallization diagram can be determined and the whole diagram constructed from the results obtained on about 10 specimens. Furthermore, the method is quite illustrative, especially in cases where coarse-grained or inequigranular structures appear in definite intervals.

The method of tapered specimen is inapplicable to low-plastic materials where fracture occurs after a very small amount of plastic deformation. Besides, it should be kept in mind that the relations specific to tensile-deformed specimens are not always fully applicable to other types of deformation. Where slight variations in the grain size are inessential and the conditions for the formation of inequigranularity are absent, the common method for constructing recrystallization diagrams can give satisfactory results.

One more drawback of common recrystallization diagrams is that they represent the grain size after various degrees of deformation and at various temperatures of annealing for the same time of annealing, i.e. essentially for different stages of recrystallization. It is clear that for the same time of heating or cooling recrystallization can proceed more deeply after a higher degree of deformation or a higher temperature of annealing.

Of practical importance could be diagrams showing the grain size by the end of primary recrystallization and, when desired, at various stages of the subsequent recrystallization processes. Such diagrams could be used effectively for selecting the appropriate process conditions to form a desired structure. Unfortunately, the construction of such diagrams is quite a labour-consuming procedure, which requires a large number of annealing operations at various temperatures.

A large number of recrystallization diagrams for the most popular metals and alloys based on iron, nickel, copper, aluminium, etc. have been published in the specialist literature.

For selected alloys, in particular for structural steels, a few diagrams have been plotted (for various types and conditions of deformation, various size of original grains, various heating rates, etc.).

An appreciable portion of the diagrams constructed up to 1950 has been collected in [7]. Some of them are shown in Figs. 136 and 137.

As novel alloys and novel techniques and processes are developed, new recrystallization diagrams are constructed. For instance, E. M. Savitsky et al. have published in recent years many recrystallization diagrams for refractory and rare metals, such as chromium [235], niobium [236], tantalum [237], zirconium [238], hafnium [239], etc. Some of them are illustrated in Fig. 136.

In connection with the ever increasing use of heat-resisting alloys and higher requirements for their structure, recrystallization diagrams of a number of complex alloys based on nickel, iron and molybdenum have been developed [17, 10, 240, 241]. Typical recrystallization diagrams in this group have been shown earlier.

Despite their drawbacks mentioned above, recrystallization diagrams are used widely in selecting the process conditions of plastic working of metals and the intermediate and final procedures of annealing.

Using a recrystallization diagram, one can follow the variations in the size of recrystallized grains depending on the degree of deformation ε at a constant temperature of annealing (or deformation) or on the temperature of annealing (deformation) t at a constant deformation ε.

If we proceed from what has been said in Ch. 3, namely, that an increase in the degree of deformation increases sharply the nucleation rate in recrystallization, it could be expected that the grain size in recrystallization diagrams would decrease continuously with an increase in deformation. This would actually be the case if recrystallization diagrams showed the size of grains by the end of primary recrystallization. As has been noted earlier, however, the diagrams give the size of grains after annealing procedures of the same time length for all deformations and temperatures. In other words, various portions of a diagram represent various stages of recrystallization.

At a heating temperature above t_r^s in annealing procedures that take a common length of time, primary recrystallization has enough time to come to completion and, moreover, a certain stage of grain growth or secondary recrystallization can take place. In this connection, the dependence of grain size on deformation in recrystallization diagrams is described not by a monotonic curve, but by one

having one or more maxima. The number, position and height of these maxima, and also the mechanism by which they appear, depend on numerous factors (see Chs. 7 and 8).

The most widespread is the first maximum of grain size in the region of low, so-called critical, degrees of deformation. It is present in all recrystallization diagrams.

Another, less widespread maximum is found in the region of moderate deformations. It can be observed within the deformation range of 20 to 50% depending on alloy composition, original grain size, the temperature and degree of deformation, etc. As a rule, it is associated with sharp inequigranularity. This maximum is typical of many popular heat-resisting alloys in which coarse grain and inequigranularity are detrimental.

Finally, the third maximum of grain size is observed very rarely. It lies in the range of heavy deformations if a distinct deformation texture is present prior to recrystallization. A few grains that have a different orientation than that of the matrix grow at the expense of the latter.

The dependence of grain size $\bar{D}$ on annealing temperature at a constant degree of deformation ε is still simpler. If an alloy (metal) undergoes no polymorphous transformations, an increase in annealing temperature above t_r^s results in a monotonic increase of grain size (see Fig. 136*b*, *c*, and *d*).

In the presence of disperse phases soluble at high temperatures only (nitrides, carbides, oxides, intermetals), recrystallized grains remain fine up to the temperature of dissolution of these phases.

Heating to a temperature close to the beginning of this dissolution causes a jumpwise growth of grains to a very large size. This grain enlargement occurs especially sharply in the range of critical deformations. The higher the temperature at which the dissolution of disperse phases begins, the more intensive is the growth of grains in heating above this temperature. Typical diagrams of this kind are shown in Fig. 136*g* and *h*.

Note that the jumpwise grain growth observed for a number of metals and alloys on recrystallization diagrams beginning from a definite temperature, as in Fig. 136*f* and *h*, is always the result of an intensive dissolution of disperse phases and can be regarded as the sign of this dissolution.

The relationship $\bar{D} = f(\tau)$ is more complicated if polymorphous transformation, say $Fe_\alpha \rightarrow Fe_\gamma$ transformation, takes place in a metal. This transformation refines the original grain; therefore, in heating to a temperature much above or below the transformation point, a coarser grain can form (see Fig. 137*a*) than in heating to a temperature slightly above the transformation point.

A special type is recrystallization diagrams for high-speed heating (induction or electric-contact heating) without isothermal holding

[132, 367] (Fig. 142). They are constructed for various rates of heating.

An important feature of recrystallization during high-speed heating, which is reflected in recrystallization diagrams, is that the size of grains depends much less on the degree of deformation than it does in heating at common rates (see Figs. 136 and 142). For deformation degrees above the critical value, the recrystallization diagram actually gives the size of grains by the end of primary recrystallization since the processes of grain growth by boundary migration essentially have no time to develop or take place only at an early stage, so that their effect on the final structure is incomparably lower than the effect of primary recrystallization.

In conclusion it should be emphasized once more that the type of structure formed in the final annealing heavily depends not only on the conditions of this annealing and prior deformation, but also on the parameters of the structure formed in the earlier operations. Among the most important structure parameters are the size and uniformity of grains, texture, presence of particles of secondary phases and the size, concentration and distribution of these particles.

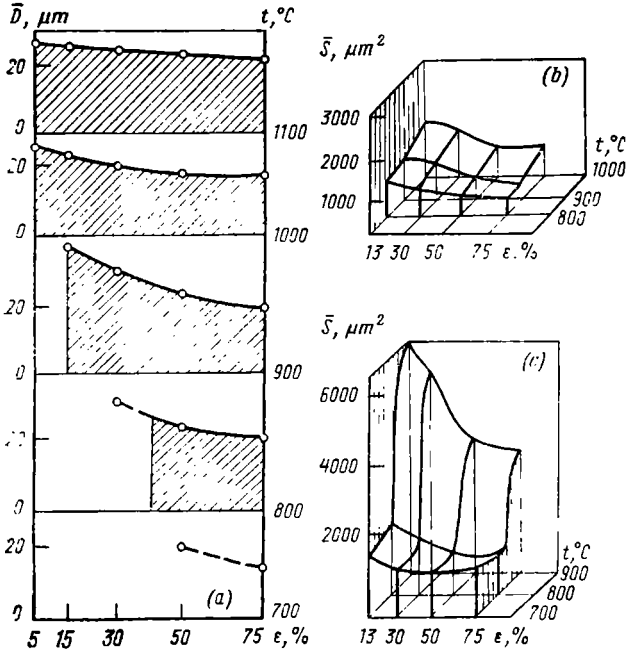

Fig. 142. Recrystallization diagram for high-speed electric heating

(*a*) commercial iron, induction heating, 50°C/s; (*b*) steel 10, contact electric heating for 1 s, air cooling; (*c*) steel 10, furnace heating for 10 min, air cooling (see Fig. 141)

The importance of these factors can be illustrated by the recrystallization diagrams (Fig. 143) for chrome bronze (Cu + 0.5% Cr) which have been constructed by I. G. Ravich and V. M. Rosenberg [73] for two various original states with different grain size.

State *1* was formed by hardening from 1 020°C and subsequent age-hardening at 500°C for 20 h. The average grain diameter was 0.7 mm, the size of chromium particles, d_{Cr}, approximately 500 Å, and the concentration of chromium, x, in the solid solution approximately 0.02% (by mass).

State *2* was obtained by hardening from 700°C (with holding for 1 h at that temperature). The respective parameters were: $\bar{D} = 0.002$ mm, $d_{Cr} = 2\text{-}4$ μm, and $x = 0.04\%$ (by mass). The two states differed also from each other in deformation textures and especially in primary recrystallization textures. State *1* had three cube texture components and state *2* one cube texture component.

Specimens were then cold-rolled at deformations of 20, 40, 60 and 80% and annealed at 800, 900, 1000 and 1040°C. Recrystallization diagrams were then plotted from the results of the tests (see Fig. 143). As seen, the diagrams greatly differ from each other.

Recrystallization at 800° and 900°C after moderate deformations refined the grain in state *1* and practically did not change it in state *2*. In heating at 1000°C, there was an inverse relationship. For the specimens in state *2* deformed 80%, heating at 1 040°C produced a sharply pronounced maximum of grain size due to secondary

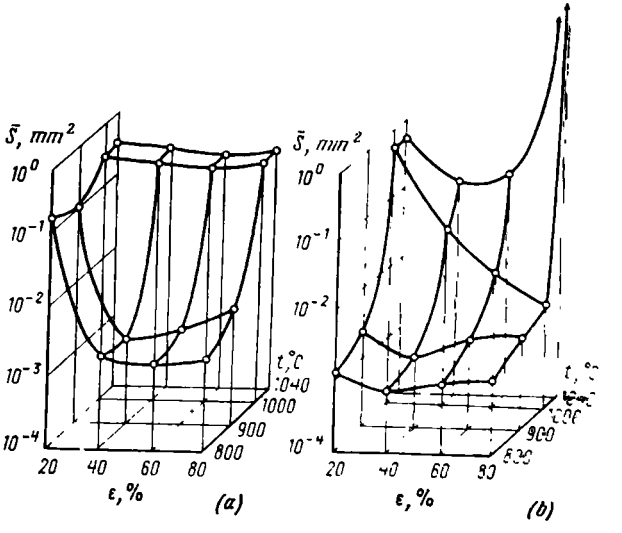

Fig. 143. Recrystallization diagram for chrome bronze
(a) hardening from 1020°C and heating at 500°C for 20 h; (b) hardening from 700°C

recrystallization in the cube texture matrix. Specimens in state *1* did not give such a maximum.

This example shows that one should not rely on recrystallization diagrams of particular metals or alloys without considering the original (prior to the last deformation) state of the material and the conditions of final deformation and heat treatment.

Since the structure characteristics determined by the recrystallization process are quite numerous and important, but cannot be reflected in common recrystallization diagrams, special recrystallization diagrams have been developed to represent some particular features of the process. The following types of special diagrams deserve mentioning.

V. I. Iveronova and G. S. Zhdanov [242] have suggested a diagram which gives the notion of the rate of the process and the temperature or time interval of its occurrence. This type of diagram shows the time of the beginning and end of primary recrystallization depending on the temperature of annealing and the degree of prior deformation.

With hot deformations, especially in view of high-temperature thermomechanical treatment processes, it is reasonable to construct diagrams showing the dependence of the temperatures of the beginning and end of recrystallization on the degree of hot deformation and the time of subsequent annealing (see Fig. 41*a*) or the dependence of recrystallized volume on deformation temperature (at a given degree of deformation) and the time of subsequent holding at the temperature of deformation (see Fig. 41*b*).

Of special use for hot deformations are the generalized diagrams ('structural state diagrams') proposed by Yu. M. Weinblat [12] (see Fig. 106*a*). They characterize the structural state (unrecrystallized, polygonized, recrystallized) as a function of the rate and temperature of deformation. This type of diagram has been discussed in more detail in Ch. 6.

Technologists can utilize diagrams of the type proposed by B. V. Molotilov *et al.* [11] for f.c.c. precision alloys whose properties are largely texture-dependent. Such a diagram is a projection of a first-order recrystallization diagram onto the deformation-heating temperature plane. This projection determines the regions having particular types of structure and texture. A schematic example of this diagram for f.c.c. alloys is shown in Fig. 106*b*.

Chapter 10

Recrystallization Textures

If a deformed material with a deformation texture is annealed, a recrystallization, or annealing texture usually forms in it, which is either identical to or differs regularly from the deformation texture. Recrystallization textures have a high practical significance since they cause anisotropy in the physical and mechanical properties. Examples of positive and adverse effects of textures on metal properties have been considered in Ch. 1.

The interest of metallurgists to recrystallization textures is not limited to their practical importance. Analysis of recrystallization textures provides us with valuable information on the mechanism of recrystallization as a whole. Texture formation, especially in transformer steel, is more associated with the mechanism of all stages of recrystallization than any other phenomenon of structural changes. Ways of controlling recrystallization textures essentially come to controlling certain recrystallization stages. It is not by chance that the progress in texture control goes parallel with the progress in understanding the mechanism of recrystallization.

In works published before the middle of 1950's, the processes of texture formation were discussed only indirectly; namely, they were judged from the results of statistical analysis of orientations, i.e. from pole figures (see Ch. 15) and from magnetometric measurements. Though the works mentioned were important for many purposes and especially for establishing the correlation between textures and metal properties, they were of limited value for understanding the mechanism of texture formation.

First of all, the methods employed at that time gave only an averaged picture for a relatively large volume of material (magnetometry) or a large surface (X-ray analysis). Further, they featured low sensitivity and did not enable one to detect the orientations of local regions of small size ($<$1-2%), which are exactly the regions largely responsible for the appearance of new orientations at various stages of recrystallization. For that reason, metallurgists were for long uncertain of what governs the appearance in a recrystallized metal of new orientations which seem to be absent in as-deformed state, the variations of these orientations with the conditions of deformation and heating, the addition of impurities, etc.

A qualitative change in the concepts has taken place in the last two decades, mainly as a result of the development of new experimental methods for the analysis of structure (its perfection and orientation in localized volumes of fractions of a micrometre in size) and, in the first place, of transmission electron microscopy techniques. These methods have enabled us to understand more clearly the fine details of the mechanism of recrystallization, in particular the mechanism of texture formation.

Another obstacle in establishing the regularities of texture formation was a low and uncontrollable purity of materials. This circumstance was in many respects responsible for the fact that the results of earlier works were unstable and even controversial.

Some later studies have shown that the history of a specimen has a strong effect on the type of recrystallization texture (the size of grains, the state and distribution of disperse phases, the deformation texture and its peculiarities).

The type of recrystallization texture is influenced by a larger number of factors than the type of deformation texture. The latter is formed in the course of shear deformation under the action of oriented external forces. The conditions of deformation, the operative slip systems, and the behaviour of dislocations in the given material have a pronounced effect on deformation textures.

The formation of recrystallization textures is associated with spontaneous structural changes whose direction is determined by the tendency of the system to lower its energy and by certain internal locally inhomogeneous driving forces of the process. This tendency is realized through the thermally activated processes of the formation of primary recrystallization nuclei and their growth at the expense of the deformed matrix and other nuclei. Dislocation slip takes place only at the earliest stage of nucleation. The further stages of the process are associated with dislocation climb, migration of large-angle boundaries, collective atomic displacements and diffusion of single atoms.

For that reason, the crystallography of slip has only a slight effect on the type of recrystallization texture. More essential factors are the composition of metal, the presence of impurities and especially of undissolved particles of secondary phases, their dispersity, distribution and capacity, in some cases, to interact selectively with various boundaries; local variations of dislocation density; the original deformation texture and the substructures of its components, i.e. the previous history of the specimen; the temperature and time of annealing, and even the atmosphere in which annealing is done, the thickness of metal piece, etc.

The influence of the metal composition can be seen clearly by comparing the data for various isomorphous materials with identical slip systems and, therefore, with identical deformation textures.

The majority of the workers who have analysed the effect of minor additions on deformation and recrystallization textures [23-25, 243] conclude that minor additions only slightly influence the deformation texture, but affect extremely strongly the type of recrystallization texture.

The cube texture mentioned earlier is found very often in f.c.c. metals and alloys. It is formed during recrystallization after rolling in pure copper, nickel, gold, lead, silver [with the concentration of impurities $<(5\text{-}10)\cdot10^{-3}$% (at.)], in Fe-Ni alloys (30-100% Ni), Ni-Mn (1%), Cu-Zn (up to 1% Zn), and some ternary alloys of iron, nickel and copper.

Cube texture is very sensitive to minor additions. Additions of aluminium (0.2%) and cadmium (0.1%) to copper are favourable for the formation of cube texture, whereas an addition of 0.0025% (at.) of phosphorus to pure copper (99.999% by mass) suppresses the formation of cube texture and ensures complete dissolution of the recrystallization texture upon annealing (rolling with 95% deformation, annealing at 300°C for 1 h). On the other hand, phosphorus has no noticeable effect on the texture in cold-rolled copper.

Green et al [244] have found that a minor quantity of iron dissolved in commercially pure aluminium (99.8%) eliminates the recrystallization texture, whereas a higher concentration of this element, at which it precipitates as an excess secondary phase, has no such effect.

These examples agree well with the general relationships established in [243] for the conditions necessary for minor additions to eliminate recrystallization textures. To do this, the additions should be (*a*) surface-active; (*b*) non-isomorphous to the main metal and (*c*) dissolved in the metal. Some elements which are soluble in copper and increase intensively its hardness, produce in copper alloys a complicated type of recrystallization texture with less regular orientations.

The type of recrystallization texture can also be influenced to a high extent by the temperature and time of annealing. At present, however, it is still impossible to formulate the conditions which would be necessary and sufficient to produce changes in the type of recrystallization texture.

The analysis of the mechanism of recrystallization (Ch. 3-5) suggests two conclusions which are important for understanding texture formation. Firstly, the course of recrystallization is determined by the structure formed in deformation and, in particular, by the specific features and differences of this structure in neighbouring local volumes of the material. Secondly, recrystallization cannot form orientations which were not present in the deformed state, or, more strictly, which would differ somewhat from those found in the deformed material.

As seen from the above examples, however, this by no means implies that the texture formed in deformation definitely predetermines the recrystallization texture.

Experience shows that for the same original deformation texture, including its weaker components which cannot be detected by common techniques, it is possible to obtain on annealing various recrystallization textures. This can be achieved by varying the conditions of heating, the purity of metal, by making use of phase transformations, etc.

Thus, the principal problem in the theory of texture formation is to know the stage at which the orientations causing the formation of a particular recrystallization texture are chosen, i.e. the stage of nucleation or the stage of grain growth.

10.1. The Principal Theories of Formation of Recrystallization Textures

The *theory of oriented nucleation* reduces to the statement that primary recrystallization nuclei possess a particular orientation which crystallographically is regularly associated with the deformation texture. A recrystallization texture results from the growth of these oriented nuclei at the expense of the deformed matrix.

This theory was developed most consistently by W. G. Burgers [245]. He suggested several possible mechanisms of oriented nucleation on the basis of the dislocation concepts of the nucleation mechanism. According to one of these mechanisms, nuclei are some of the blocks that have appeared through polygonization. Because of non-uniform polygonization and different length of the incubation period, conditions are likely to set in under which some regions arranged in a definite manner in the deformed matrix will be polygonized more quickly than others. In order to play the role of nuclei, these polygonized regions must be strongly misoriented relative to the surrounding matrix.

Since subgrains (polygons) formed in polygonization retain locally, with only slight deviations, the orientations of cells (regions) existed in as-deformed state, this means that the orientations of recrystallization textures formed by this mechanism must exist already in as-deformed state.

By changing the conditions of heating (temperature and rate) and using the effect of disperse phases, it is possible to vary the relation between the incubation periods for nuclei in differently oriented regions and thus change the recrystallization texture.

It is also worthy to mention a special mechanism proposed by Burgers. By this mechanism, some nuclei can form with an orientation non-existent in the deformed matrix.

As a sole particular example of this mechanism, Burgers and Verbraak [246] proposed a model of the formation of cube texture on primary recrystallization in rolled copper. In their view, this texture can form by a shear mechanism which is the inverse of the mechanism known in the specialist literature as Rowland's transformation and consists in the following. Let a cube be compressed along one of its axes, say AC (Fig. 144). One of its planes having the AC [100] axis will then remain stationary. In Fig. 144*a*, the whole hatched plane ACE remains fixed. The other two axes, [010] and [001], of the cube are stretched so that two tetrahedrons are formed which belong to two cubic lattices and are in a twinning position relative to each other. The ⟨100⟩ directions of the original lattice are now transformed into the directions [100], [111] and [112] of the

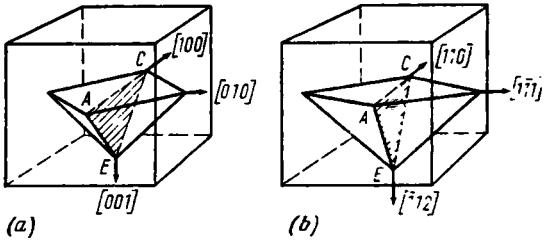

Fig. 144. Rowland transformation [246] (schematic)

two new lattices (Fig. 144*b*). The twinning plane is the (111) plane.

Such twinning configurations can appear, for example, in f.c.c. metals with axial textures ⟨111⟩ and ⟨100⟩ when deformed by drawing.

According to [246], these regions of a twinning configuration can serve as preferable nuclei of the cube texture in recrystallization, since this texture can be formed as a result of the inverse Rowland transformation by successive movements of dislocations on (112) planes. This mechanism, however, has found no experimental support and, in our view, is hardly probable.

The main weak point in the theory of oriented nucleation is that this theory fails to explain the facts of texture variation in the course of recrystallization which are often encountered in practice and, for that sole reason, is not universally applicable.

The *theory of oriented growth*, first proposed by Beck [247], proceeds from the assumption that the boundary mobility M, and therefore the rate of migration of grain boundaries depend sharply on the mutual orientation of adjacent crystallites and on some other factors. By this theory, nuclei with diverse orientations exist at the early stage of primary recrystallization, but then a 'selection' occurs in the process. Only the nuclei whose orientation relative to the

textured deformed matrix corresponds to the highest mobility of their boundaries survive in the process and can grow further.

Numerous experimental data accumulated in the field prove irrefutably that the rate of boundary migration does depend on orientation. The problem has been analysed in Ch. 5.

The mobility of grain boundaries increases with an increase in misorientation angles not monotonically (see Fig. 70). There are discrete values of misorientation angles at which boundaries possess the highest mobility. An important characteristic of these boundaries in contrast to common ones is that their mobility is influenced less appreciably by impurities and temperature.

The theory of oriented growth is based on experimental facts and explains well many relationships. On the other hand, it fails to clarify some particular facts, for instance, why there is a correlation between recrystallization textures and deformation textures.

The *combined theory of oriented nucleation and growth* is based on the results of electron-microscopic analysis of dislocation structures and crystallographic orientations in very small volumes.

These results have shown that the orientation of recrystallization nuclei almost always repeats the orientation of the deformed matrix in the local volumes where these nuclei appeared. The rate of growth of various nuclei in the textured matrix may however be different.

This rate is the result of the competing effect of the driving and retarding forces, which is determined by the interaction of numerous factors. One or another of these factors may be decisive under particular conditions and at various stages of the process. Consequently, in each particular case it is required to make a comparative analysis of the local orientations and averaged textures in as-deformed state and at various stages of recrystallization and collect data on the kinetics of enhancement of some orientations and attenuation of others and also on the presence and distribution of impurities in order to decide which of the two processes, either nucleation or grain growth, plays the leading part.

Thus, the modern theory of recrystallization textures is a combination of the two earlier theories.

As will be shown later, the generalized theory explains well many complicated cases, including the formation and consecutive changes of textures at various stages of recrystallization under the action of various factors.

The new experimental data (in the first place the results of electron-microscopic analysis) on the mechanism of recrystallization considered in Chs. 3-5 make it possible to analyse the problem of the particular mechanisms of oriented nucleation and growth (which are responsible for changes in certain textures) in a broader manner than this was done by Burgers and Beck. It is methodologically reasonable to discuss the problem in relation to the following three types of

texture variations which are likely to occur in annealing of deformed textured materials:

(a) the deformation texture is not changed by recrystallization annealing;

(b) the deformation texture is replaced in recrystallization, fully or partially, by a different texture composed of one or more components; this replacement can occur at various stages of recrystallization: primary, secondary, or ternary recrystallization; in many cases, the texture formed at an early stage of recrystallization is replaced by another texture at a later stage;

(c) the deformation texture is replaced in recrystallization fully or partially by randomly oriented new grains; this case is less common than the former two.

10.2. The Principal Types of Texture Changes in Recrystallization

10.2.1. Retention of Deformation Texture in Annealing

The simplest explanation of the mechanism of retention of a deformation texture after annealing is that the decisive process here is the oriented nucleation of recrystallization centres having the same orientation as that of the deformed matrix. As will be shown later, this concept is true, but not exhaustive.

Let us consider the particular conditions under which the oriented nucleation plays a leading part and the ways of retention of the deformation texture after recrystallization. It is possible to indicate at least five cases, the first three being probably quite common and the other two more special.

1. Short-time annealing of a material deformed to a high degree under the conditions of high-speed heating (say, induction or electric-contact heating) to a temperature which exceeds the value of t_r^s for common heating rates.

Under these conditions, a short period of time is enough for recrystallization nuclei to form from subgrains not only in portions having the highest distortion of the lattice, but also in places less favourable for nucleation. The orientation of nuclei corresponds to the orientation of the respective portions of deformed material in which they have originated (here, oriented nucleation in its pure form is realized). But since the time of action of high temperature is short, neither grain growth nor secondary recrystallization can develop well enough. In this way, it is possible to preserve the deformation texture completely or at least its prevailing part with a small share of other orientations.

Izbranov, Pavlov and Rodigin [248] analysed qualitatively variations in the recrystallization texture of transformer steel (3.54% Si by mass) with the time of annealing at high heating rates (1000-1100°C/s). At the first recrystallization stage, the recrystallization texture was the same as the deformation texture, though more distinct. In the course of further isothermal holding, this texture disappeared almost fully, after which a new orientation appeared and became more and more distinct.

A similar result was obtained by Ts. N. Rafalovich for deformed steel grade 10 heated at different rates.

Lainer and Krupnikova-Perlina [243] studied the textures in copper and copper-nickel alloys with various additions after heavy rolling deformations (96%) and annealing of various duration at 400° or 600°C.

At the early stages of primary recrystallization, the structure had the deformation texture and weak additional orientations which were absent in as-deformed state. In the later stages of recrystallization (grain growth and/or secondary recrystallization) the number of orientations diminished and the deformation texture disappeared; after 1 h of annealing, cube texture was the sole texture in the material.

2. Heating at common rate to relatively low temperatures at which primary recrystallization has enough time for its completion by nucleation from a large number of centres, but grain growth does not practically develop at all. This case can be illustrated by the following examples.

E. Schmid and G. Wassermann et al. conducted experiments on cold-drawn aluminium wire (99.95% Al) annealed at 500° and 600°C. The axial deformation texture ⟨111⟩ was retained after annealing at 500°C and changed to the ⟨112⟩ texture at 600°C.

A Fe + 3% Si alloy was annealed at 650°C and 925°C [249]. In the former case, the recrystallization texture was identical to the deformation texture; in the latter, a different texture was formed.

With heavier deformations and more distinct deformation textures, the latter are repeated more clearly in the recrystallization textures formed after low-temperature annealing.

3. Recrystallization by migration of local portions ('tongues') of large-angle boundaries of the original grains (by Beck and Sperry) [156].

In cold deformation, migration by the formation of tongues is observed on relatively light deformations. In hot deformation, the range of deformations is wider and extends to moderate and heavier deformations if the deformation texture is sufficiently distinct.

In [118], variations of orientation relationships in hot pressed and rolled aluminium after recrystallization annealing were analysed by radiographic and metallographic methods.

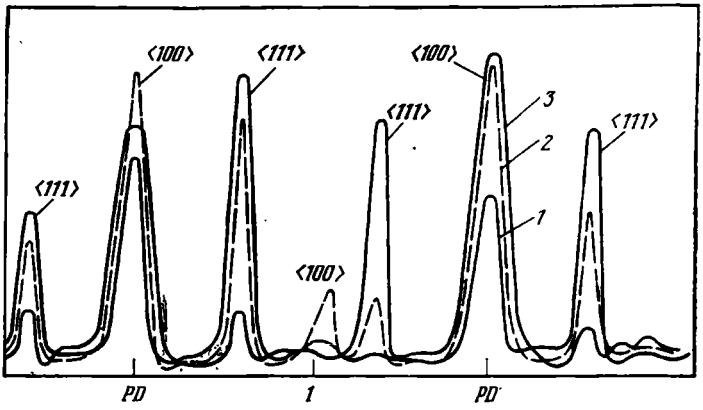

Fig. 145. Sections of (100) pole figures of pressed aluminium

1—as-pressed; *2*—annealed at 300°C for 45 min; *3*—annealed at 300°C for 90 min; $\alpha = 90°$ [118]; *PD*—pressing direction

Deformed specimens were annealed directly on the texture attachment of a diffractometer, which made it possible to obtain more reliable data on changes in the intensity of various diffraction lines caused by texture variations.

Figure 145 shows the pole figure sections for (100) planes in pressed aluminium (deformation textures ⟨111⟩ and ⟨100⟩) after annealing for 45 and 90 minutes at 300°C. Annealing for 45 minutes changed the deformation texture only slightly. Larger changes were noticed after annealing for 90 minutes, though the recrystallization texture repeated qualitatively the deformation texture. The changes were due to an increase in the volumes having the ⟨100⟩ orientation at the expense of those having the ⟨111⟩ orientation. A metallographic analysis based on the use of polarized and oblique light and analysis of pole figures gave interesting results.

As seen, recrystallization occurs under these conditions by migration of tongues of original grains. Adjacent grains belonging to the components ⟨111⟩ and ⟨100⟩ grow at the expense of one another (Fig. 146).

Thus, the repetition of the deformation texture in the recrystallization texture in this case does not mean that a volume which has had a given orientation in as-deformed state has retained it after recrystallization.

The resultant decrease in the volume having the ⟨111⟩ orientation stems from the fact that ⟨100⟩ volumes grow faster at the expense of ⟨111⟩ volumes than ⟨111⟩ volumes at the expense of ⟨100⟩ ones. The difference in the rates of growth is associated with a difference in the driving force of migration. As has been noted in Ch. 4, the driving force of recrystallization by migration of boundary tongues

of original grains is a difference in dislocation densities on the two sides of a boundary. As applied to the case considered, this means that the dislocation density in ⟨111⟩ grains is statistically higher (or the size of cells and, respectively, of subgrains is lower) than in ⟨100⟩ grains.

Measurements of grain sizes in pressed rods immediately after deformation [118] showed that subgrains with the component ⟨100⟩ were roughly 2.5 times larger than those with the component ⟨111⟩ (3 μm against 1.3 μm).

Though the problem of the differences in the strain-hardening and substructure of various texture components has been studied insufficiently, these differences should principally exist. In special studies devoted to the problem they were usually detected. For instance, S. N. Kaverina et al. in a recent work [250] reported that of the two principal texture components, (001) [110] and (111) [112] in heavily rolled molybdenum sheets, the former was strain-hardened less than the latter.

I. D. Seidman has found that crystallites with the orientations (001) [110] and (112) [110] in cold-rolled transformer iron are strain-hardened less than other components, do not recrystallize by themselves during heating (the existing distortions are eliminated by polygonization), but, owing to a lower stacking fault energy, grow by the formation and migration of tongues at the expense of differently oriented grains.

It is then clear that a recrystallization texture should repeat the deformation texture more distinctly when there is little difference in strain-hardening of various texture components.

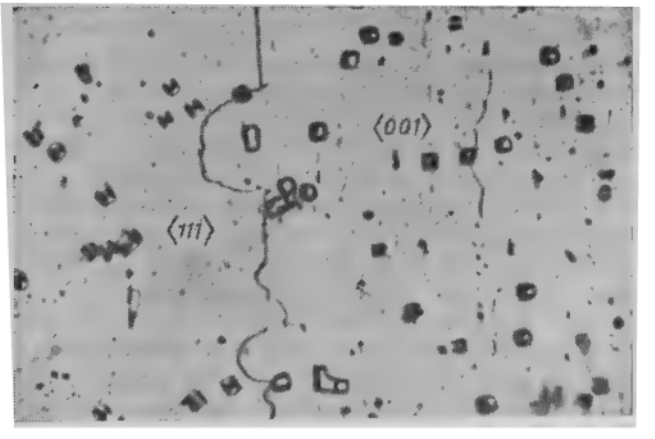

Fig. 146. Recrystallization in pressed and annealed aluminium by migration of tongues of original grains, ×320 [118]

Some other examples of how differences in substructure of various components of deformation textures can influence the formation of recrystallization textures will be given below.

In the light of the foregoing, it should be emphasized that substructures of metal volumes belonging to various components of deformation textures deserve a deeper and more systematic examination.

4. In-situ recrystallization. If deformation is quite uniform in nature and the deformation texture contains only one component, annealing will cause only in-situ recrystallization, i.e. the appearance and growth of subgrains to an appreciable size (of an order of a micrometre) without the formation of large-angle boundaries and, therefore, without any substantial change in orientation. This effect is especially pronounced in single crystals with an orientation favourable for easy slip, such as (001) [110] for b.c.c. metals, (110) [112] for f.c.c. metals, (0001) [11$\bar{2}$0] for c.p.h. metals, etc. The corresponding examples were analysed in Ch. 2.

5. Recovery and the early stages of recrystallization occurring parallel with the decomposition of supersaturated solid solutions. In that case, the growth of subgrains and recrystallization nuclei and the associated 'consumption' of grains of a certain orientation by the faster growing grains of another orientation become impossible due to the barrier effect of particles.

This mechanism can be illustrated by the results obtained for sheets of low-carbon steel with additions of niobium (0.015% C, 0.126% Nb) [251]. Cold-rolled sheets deformed 40-90% were annealed at 800°C for 10 h. The recrystallization texture turned out to be identical to the rolling texture, with the type {111} component being the main one in both. The development of the {110} ⟨001⟩ component was retarded by niobium-containing precipitates of a size of approximately 150 Å. This effect was not observed in a steel with lower concentrations of niobium and carbon (0.039% Nb, 0.003% C).

Thus, the condition favourable for retention of a deformation texture in age-hardening alloys is a high concentration of highly disperse particles stable against coagulation. But disperse phase particles must not be coherent with the matrix, since otherwise they will precipitate on dislocations, retard the redistribution of dislocations and thus inhibit the formation of recrystallization nuclei as well as their growth.

In practice, some of the cases considered, for instance, short-term high-speed heating, low-temperature heating, decomposition of the solid solution occurring parallel with recrystallization, etc. are technologically inevitable. As a consequence, the recrystallization textures formed will be identical with deformation textures. In

ch cases, the textures of recrystallization can be controlled by rying the deformation texture, i. e. by changing the conditions of astic working.

.2.2. Texture Variations at Various Stages Recrystallization

A variation of texture in the course of recrystallization, especially multiple variation, is usually associated with the effect of oriented cleation and oriented growth (one of these two processes being edominant) or only with oriented growth.

Oriented growth is predominant where nuclei of various orientations 'm at the early stage of annealing and the conditions are such that eferably a given texture component develops.

Oriented nucleation plays a prevailing role where the nucleation an unwanted component is inhibited by special techniques.

(*a*) *Texture Variation by the Prevailing Effect of Oriented Growth*

Formation of a cube texture in recrystallization of f.c.c. metals d alloys. Many workers [73, 243, 252] have shown that in some tals and alloys (copper and copper-base alloys, commercial alumi- ım and aluminium alloys, alloys of the system Fe-Ni, etc.), where e copper-type texture (110) [112] + (112) [111] forms as the prin- ɔal texture on deformation, the (100) [001] texture appears on rystallization either as the main texture or more often in combin- on with a texture repeating the deformation texture.

The mechanism of the formation of cube textures deserves a serious amination, since they cause sharp anisotropy of mechanical pro- rties ('earing') and physical (magnetic) properties in metals.

As found, the cube texture forms in annealing only when the formation texture contains the {112} ⟨111⟩ component as one of e main components. The cube texture formed in recrystallization more distinct with a heavier degree of deformation and finer e of grains before the last stage of cold rolling. According to [73], recrystallization of copper the cube texture forms at a deformation no less than 80% (which forms the (100) [001] and (011) [100] nponents in addition to the main two mentioned above) and at ize of original grains of no more than 20 μm. With an increase in e degree of deformation, the required minimal size of grains in- ɔases.

As seen from Table 19, a cube texture forms in recrystallization o when its trails in the deformation texture are not detected by nmon methods. This circumstance has probably stimulated Bur- s and Verbraaks to propose a theory [246] according to which

nuclei of a cube orientation form in a diffusionless shear-type manner by the mechanism which is the inverse of Rowland's transformation. For this mechanism to be operative, the deformed structure must contain regions with a twinning orientation (112) [111]. With a finer grain, there is a higher probability that regions with the twinning

TABLE 19. Effect of Minor Additions on Changes in Copper Textures After Isothermal Recrystallization

Composition, % by mass	τ_{an} at 600°C	Recrystallization texture
Cu (100%)	1 s	(112) [111]+(110) [1$\bar{1}$2]+(110) [1$\bar{1}\bar{1}$]+ +(001) [100]
	1 h	(001) [100]
Cu + 0.18% Cd	10 s	(112) [11$\bar{1}$]+(110) [1$\bar{1}$2]+(130) [001]+ +(001) [100]
	1 h	(110) [1$\bar{1}$2]+(001) [100]
Cu + 0.24% Si	3 s	(112) [11$\bar{1}$]+(110) [1$\bar{1}$2]+(130) [001]+ + (111) [1$\bar{1}$2]+(001) [100]
	1 h	(112) [11$\bar{1}$]+(110) [1$\bar{1}$2]+(001) [100]
Cu + 0.47% Sn	10 s	(112) [11$\bar{1}$]+(110) [1$\bar{1}$2]+(130) [001]+ (001) [100]
	1 h	(110) [1$\bar{1}$2]+(001) [110]+(001) [100]

Note. Cold rolling with 97-% deformation; deformation texture (112) [11$\bar{1}$]+ (110) [1$\bar{1}$2].

texture components (112) [11$\bar{1}$] will be in contact and form a cube texture. As has been noted earlier, however, this hypothesis has not yet get a direct experimental support.

The mechanism proposed by Barrett and Beck et al., which relies on the concept of oriented growth, seems more probable. By this mechanism, among the nuclei of various orientations, the nuclei which are oriented favourable relative to the matrix lattice have the highest rate of growth. For f.c.c. metals and alloys these are the nuclei whose lattice is turned approximately 40° about ⟨111⟩. Each pair from the four components of an ideal rolling texture has a favourable orientational relationship (the common ⟨111⟩ pole). The cube texture, however, has a favourable orientation relative to all the four components of the rolling texture. This is why the cube texture is usually accompanied by the rolling texture, but the former is predominant. With a finer grain, it is more probable that growing grains of a cube orientation will be in contact with all the four

components of the rolling texture. This is how the hypothesis mentioned explains the favourable role of fine original grains before the last rolling procedure.

The formation of cube texture can also be inhibited by the presence of highly disperse particles of a secondary phase in the alloy.

These theoretical concepts have been well supported by the results of many experimental studies. For instance, I. G. Ravich and V. M. Rosenberg [215] have found that the cube texture component and 'earing' spoilage in chrome bronze can be diminished sharply by heating the metal before the final rolling procedure at least at 900-1000°C so as to form large original grain ($\geqslant$0.5 mm).

The *formation of the brass texture* (30% Zn). The ideal texture in brass is (110) [112]. In sheet brass, the (225) [73$\bar{4}$] texture usually forms in recrystallization, which is very close to the ideal orientation, as seen from the comparison of their crystallographic indices.

The (225) [73$\bar{4}$] texture has a favourable orientational relationship with the principal deformation texture components (110) [11$\bar{2}$] and (110) [001] in brass. The former changes to the (225) [73$\bar{4}$] orientation by rotation through 30° and the latter by rotation through 45° about the common ⟨111⟩ pole [253]. In addition, the (225) [73$\bar{4}$] texture is oriented favourably relative to the region of scatter around the main texture components.

The *effect of temperature on oriented growth.* Several causes of this effect can be mentioned.

Let a small number of differently oriented nuclei be present in the metal after primary recrystallization in addition to the distinct main texture. The activation energy of migration of differently oriented nuclei is different. Nuclei with a lower activation energy Q will grow preferably at low temperatures and those with a high value of Q at higher temperatures. In this respect, the following example is of interest [254]. A copper-type texture forms in deformed steel grade X18H9 which changes to a cube texture in heating at 1000°C (τ = 30 min). With a longer time of annealing, the cube texture partially changes to the type (025) [100] as a result of rotation around [100]. If the temperature of heating is raised up to 1200°C, the (123) [14$\bar{2}$] texture forms by rotation around [111] in addition to the (025) [100] texture. This can be explained by the fact that the (025) [100] nuclei have a lower activation energy of migration in the cubic matrix than the (123) [41$\bar{2}$] nuclei.

A similar effect can be obtained if the growth of nuclei is inhibited up to a definite temperature by disperse phase particles which are dissolved at a higher temperature and their barrier effect is thus eliminated.

It is also known from experience that successive changes of textures in annealing are sometimes caused by alternate processes of

primary, secondary, and ternary recrystallization. Such effects are examined in most detail in thin (approx. 0.3 mm) sheets of transformer steel. A multi-component texture of primary recrystallization changes here essentially to a rib texture in the course of secondary recrystallization and the latter passes into a cube texture during annealing (at 1100°C) in a deep vacuum ($5 \cdot 10^{-4}$ mm Hg).

(*b*) *Texture Variation under the Prevailing Effect of Oriented Nucleation*

Two practically important cases will be considered here.

The *texture of low-carbon steel for deep drawing*. As has been noted in Ch. 1, the suitability of a material for deep drawing is estimated in terms of the coefficient of plastic anisotropy, R, which characterizes the change in the width of a flat tensile-deformed specimen relative to the change in its thickness. Any material with $R > 1$ is suitable for deep drawing.

The coefficient R is determined by the type of texture. The (111) [*uvw*] orientation is most favourable, but the (001) [110] orientation is least so. Any change in the relation between these components sharply changes R.

Thus, the problem reduces to the need to change a deformation texture (rolling texture) in annealing to a texture with the (111) [*uvw*] component.

If no special measures are taken, then during recrystallization the nuclei usually have two types of principal orientations, (100) and (111). The former usually appear on the boundaries and the latter in the bulk of original grains. It is shown in a number of works that, for instance, in killed steel Grade 08IO deoxidized by aluminium, the development of the (100) orientation can be inhibited by preventing the precipitation of aluminium nitrides (or their preprecipitates) before the final procedure of cold rolling. For this, it is advisable to coil hot-deformed strip at the lowest possible temperature (550-600°C). The subsequent heat treatment must effect decomposition of the solid solution along with early stages of recrystallization. This decomposition inhibits the formation and growth of {100} nuclei and offers favourable conditions for the growth of {111} nuclei.

These results were confirmed by research studies [368, 369]. In [368], the effect of aluminium nitride precipitates was analysed and in [369] the process was simulated on copper precipitates. These studies showed that the recrystallization textures of these alloys were very sensitive to the heating conditions for the final annealing stage which was carried out at a temperature close to 700°C. Slow heating, much like long preliminary holding at 500°C, gave a strong

{111} texture or a similar texture. At a higher heating rate or a higher temperature of preliminary heating, {100} components appeared in addition to the {111} component. Direct heating at 700-725°C suppressed the component {111} and caused an appreciable scatter in recrystallization textures.

The mechanism of this effect reduces essentially to the following [368, 369].

With slow or stepwise heating (500°C), decomposition takes place quicker than recrystallization. Decomposition is especially intensive on subboundaries, which get locked. In the course of coagulation and coarsening of AlN or copper particles, some subboundaries become free earlier than the others and begin to migrate.

Analysis of the substructure of components {111} and {100} in deformation textures and also direct observations have shown, that under these conditions, subgrains within the {111} component are first to start growing. In essence, it is in-situ recrystallization that is realized here. In the process of their growth, these subgrains become recrystallization nuclei. With a further rise in temperature and enlargement of precipitates, they grow intensively at the expense of {100} grains which have been locked until this moment.

The boundaries of {111} grains are free to migrate when the size of AlN particles becomes equal to 170-200 Å, with their volume concentration $f \approx 10^{-4}$. The preferable growth of {111} subgrains can be explained as follows.

From the equality of the driving force P_{dr} and the braking force P_{br} [see expressions (6) and (7) in Ch. 3], we can obtain an expression for the critical size of precipitate particles

$$d_{cr} = D_1 \sqrt{f(D_2/\Delta D)}$$

which implies that for particles with $d < d_{cr}$ (for a given volume concentration of precipitates) the braking force is greater than the driving force and the boundaries are locked, whereas for particles with $d > d_{cr}$ the driving force exceeds the braking force and the boundaries can migrate. As precipitate particles grow larger in size, the boundaries with a higher driving force get free earlier.

Electron-microscopic studies [375, 373] of substructures in deformed steel volumes with {111} and {100} components have shown that the average size of subgrains in the {111} component is roughly one-half that in the {100} component (0.5-1 μm against 1-2 μm) and, besides, the curve of size distribution of subgrains for the {111} component is appreciably wider than that for the {100} component. Therefore, the statistically average value of ΔD is higher in the {111} component.

Owing to these peculiarities, the driving force of growth of subgrains of the {111} component must be predominant. By an estim-

ation [367], it is roughly four times that for the {100} component, which ensures the preferable growth of {111} subgrains.

With an increase in the heating rate or the temperature of preliminary heating, the barrier effect of particles diminishes, recrystallization proceeds faster than decomposition. Further, in direct and relatively fast heating to 700-725°C, the original large-angle boundaries adjacent to the metal volumes with the preferable {100} orientation become free and are able to migrate.

If another type of steel is taken, instead of grade 08Ю, for deep drawing, in which a different phase plays the same part as does the AlN phase in 08Ю steel, the particular conditions for the precipitation of that phase during post-deformation annealing must naturally be different.

The *texture of transformer steel.* In commercial transformer steel, the (110) [001] component, which is practically absent in the deformation texture, appears at the stage of primary recrystallization. This component develops from subgrains of the same orientation located in the middle portion of microbands.

B. V. Molotilov et al. [255] note the following fact indicative of oriented nucleation.

Polycrystalline specimens with the original (110) [001] texture have the same {111} ⟨112⟩ texture after deformations ranging from 53% to 87%. Upon recrystallization, the specimens obtain the $\{h10\}$ ⟨001⟩ texture in which the value of h varies from 1 for 53-% deformation to 5 for 87%.

The formation of various recrystallization textures in the matrix with the same type of deformation texture confirms, in the authors' view, the concept of oriented nucleation.

V. Yu. Novikov and I. V. Semenovskaya [256] analysed the effect of nitride particles on texture formation. Nitrides were introduced into (110) [001] single crystals of deformed silicon iron by nitriding at a temperature 100°C below the temperature of the subsequent recrystallization annealing. In the presence of nitrides, the rate of formation of recrystallization nuclei diminished sharply, but the rate of their growth remained almost unchanged. In microbands, a drop in the rate of formation of (110) [001] nuclei was especially sharp. The presence of nitride particles had virtually no effect on nucleation at boundaries of Neumann bands where the subgrains from which nuclei grow, have the $\{hk0\}$ ⟨001⟩ orientation and show a heavier misorientation than those in microbands. As a result, the proportion of the $\{hk0\}$ ⟨001⟩ component in the primary recrystallization texture was 80% in the crystal with nitrides against 20% in the one free from nitrides. Thus, the secondary phase particles produced a selective effect on oriented nucleation and changed the texture at the primary recrystallization stage.

10.2.3. Weakening of Texture in Recrystallization

The possibilities of weakening deformation textures or preventing the formation of distinct recrystallization textures by recrystallization annealing are not yet sufficiently studied. Yet, they are examined in more detail as regards the manufacture of electric (dynamo) steels. On the whole, the earlier discussion of the conditions favourable for producing various types of texture enables us to recommend several methods for texture weakening.

(1) Addition of an appreciable concentration of coarse secondary phase particles (>0.1 μm in size) with simultaneous use of high rates of heating. In this case, plastic working forms a distinct multicomponent texture. The high rate of heating gives rise to the highest possible number of nuclei (counting in those near secondary phase particles). The nuclei formed are chaotically oriented.

If secondary phase particles strongly differ from the matrix in the coefficient of thermal expansion, randomly oriented nuclei can additionally form as a result of structural thermal strain-hardening. In this case, thermocycling should be quite effective.

It should be noted that the method discussed gives a desired effect only when the concentration of particles is high, and thus the spacings between them are small. As has been shown by V. Ya. Goldstein, recrystallization nuclei formed on secondary phase particles by structural strain-hardening are less perfect than those formed in other portions of the lattice. Therefore, with a low concentration of particles, the nuclei which form near them will be consumed during annealing by more perfect nuclei.

(2) The suppression of unwanted texture components having a short incubation period by an intermediate annealing procedure to cause partial recrystallization and subsequent deformation to a low degree.

This method, proposed in [225], is based, firstly, on the different length of incubation period of nucleation in various texture components, secondly, on the orientation relationship of strain-hardening effect in these nuclei, and, thirdly, on the dependence of thermal stability of structure defects on the type and density of these defects.

The method is especially effective where unwanted nuclei formed during intermediate annealing have an orientation favourable for multiple slip. Then, even a slight strain-hardening and subsequent heating can cause their recrystallization, during which the nuclei lose the orientation they have had after the intermediate heating.

(3) Utilization of phase transformations. This method is applicable only to alloys undergoing phase transformations at temperatures close to the recrystallization temperature. In some cases a phase transformation can be initiated on addition of a very small quantity of an impurity. A typical example is dynamo steel which is manufactured by the method mentioned. An addition of a small quantity of

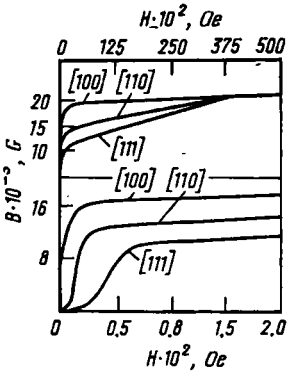

Fig. 147. Magnetization curves of Fe + 3.8% Si single crystals in various crystallographic planes

carbon (>0.03%) to a Fe + (2.5-3.0)% Si alloy causes the $\alpha \rightarrow \gamma$-transformation at a temperature near 800°C.

The $\alpha \rightarrow \gamma$-transformation which takes place in quick heating and the reverse $\gamma \rightarrow \alpha$-transformation in cooling weaken appreciably the texture.

10.3. Texture Formation During Recrystallization in Electric Steel

The manufacture of textured electric steel with favourable anisotropy of properties is one of the most important aspects in practical application of recrystallization textures.

The magnetic properties of iron and transformer steel are strongly anisotropic. Figure 147 shows the magnetization curves for single crystals of a Fe-Si (3.8%) alloy. It is seen that the crystallographic directions are arranged in the decreasing order of easy magnetization and the maximum permeability as follows: ⟨100⟩ → ⟨110⟩ → ⟨111⟩.

Enormous savings that are likely to result from the utilization of anisotropy in transformer steel have been the cause of an intensive search into the methods for making textured steel based on Fe + + 3.5% Si in which all or most of the grains would have their planes {110} or {100} and directions ⟨001⟩ oriented parallel to the plane and direction of rolling. The work has been a success. Now, transformer steel with the rib texture (Goss texture) {110} ⟨001⟩ and cube texture {100} ⟨001⟩ is widely employed all over the world (Table 20). These steels lower power losses by a few tens of a per cent.

TABLE 20. **Magnetic Properties of Textured Transformer Steel 0.32 mm Thick**

Steel texture	μ_m, G/Oe	$P_{15/16}$, W/kg	H_c, Oe	B_r, G
Cube texture:				
lengthwise	116 000	0.97	0.07	12 200
crosswise	65 000	1.13	0.08	11 500
Rib texture:				
lengthwise	55 000	1.04	0.08	9 500
crosswise	8 000	2.78	0.27	1 750

At present, cold-rolled transformer steel has replaced almost fully hot-rolled steel, particularly, in the field of manufacture of high- and medium-power transformers in which the magnetic flux goes parallel to the rolling direction of sheets almost along its whole path.

The degree of perfection of the rib texture in commercial transformer steel and, accordingly, the power losses and the stability of properties have not yet been brought to the optimum level. The difficulties in the manufacture of transformer steel with most effective texture are associated, in the first place, with the fact that the mechanism of the formation of (110) [001] texture and, especially, of (100) [001] texture and also the conditions for their formation are not yet clear enough. Many principal details of this mechanism still remain controversial.

The cube texture has a number of advantages over the rib texture, especially in thin sheets (<0.3 mm), but has still not found wide practical application. Unfortunately, all the existing processes for making cube texture steel are quite complicated and, besides, cannot ensure the desired stability of properties.

The principal technological feature of both textures is that they are produced by the processes of secondary recrystallization, though the driving forces of these processes are different and, therefore, the required technological conditions are also different.

10.3.1. Transformer Steel with {110} ⟨001⟩ Rib Texture

The typical technology for making sheets (0.30-0.35 mm) of rib-texture transformer steel is as follows [257]:

(a) hot rolling into strips 2.5 mm thick;

(b) cold rolling to 0.62-0.80 mm;

(c) annealing at 925-980°C (for 3-5 min) to cause decarbonization and primary recrystallization;

(d) cold rolling to 0.30-0.36 mm;

(e) annealing at 790-845°C (3-5 min) for decarbonization;

(f) annealing at 1150-1180°C in moist hydrogen (25-30 h) to cause secondary recrystallization and remove harmful impurities;

(g) annealing at 760-820°C to relieve stresses.

The sequence in which the main orientations in transformer steel are changed at various stages of the process is given in Table 21.

Let us consider the principal conditions for producing the (110) [001] rib texture.

The first requirement is evidently that the original deformation texture should contain the (111) [11$\bar{2}$] orientation, which can be ensured by appropriate rolling conditions. N. P. Goss obtained a rib texture by double cold rolling with intermediate low-temperature

TABLE 21. **Orientation Changes in Silicon Iron Upon Recrystallization**

Process stages	Orientation		
	main	medium	weak
Cold rolling	{111} ⟨112⟩	{112} ⟨110⟩	{001} ⟨110⟩
Primary recrystallization (low-temperature annealing)	{111} ⟨112⟩	{110} ⟨001⟩	{100} ⟨001⟩
Secondary recrystallization	{110} ⟨001⟩	{100} ⟨001⟩	

annealing at 850-900°C and final high-temperature annealing at 1100-1200°C. The low-temperature annealing is needed to initiate primary recrystallization in which the (110) [001] orientation forms along with other orientations from subgrains located in the middle of microbands in deformed crystallites relating to the (111) [112] component of the deformation texture. The high-temperature annealing ensures secondary recrystallization in which (110) [001] grains serve as recrystallization nuclei.

The correlation between grains with the (111) $[11\bar{2}]$ orientation in the deformation texture and those with the rib texture orientation at the stage of primary recrystallization has been established in many studies on polycrystals and single crystals.

According to [75], at least five types of microzone can be distinguished in (111) [112] crystallites, which differ from one another in the orientation and the nature of local misorientations and thus in the nature and kinetics of the processes occurring during annealing (see Ch. 2). These are deformation bands (matrix bands), microbands, Neumann bands (deformation twins), regions near boundaries of original grains, and regions surrounding inclusion particles. Single crystals can contain only the first three types.

Deformation bands occupy the largest volume, make the main contribution to the deformation texture, and are distinguished by a slight misorientation within a band (see Fig. 22).

Microbands occupy very small volumes (1-3 μm in width), which often make no contribution even to common pole figures. They have typically large misorientations from subgrain to subgrain, which ensure the structural link between adjacent deformation bands, say, between the $(11\bar{1})$ [112] and the (111) $[11\bar{2}]$ deformation band separated by a given microband.

The core volumes of microbands have an orientation close to the (110) [001] rib texture and are misoriented relative to the adjacent deformation bands by approximately 30° on the common ⟨110⟩ direction, i.e. by an angle corresponding to the maximum mobility of their boundaries.

The orientation of deformation twins is also different in various grains and differs substantially from the orientation of deformation bands. For instance, it corresponds to {100} ⟨011⟩ and {114} ⟨221⟩ for {111} ⟨112⟩ bands.

Regions near the boundaries of original grains and near inclusions (and, at high degrees of deformations, near twin boundaries too) are also characterized by large misorientations between adjacent cells, but these misorientations are not so regular as in microbands.

The relative volume occupied by any of these zones may be different depending on a number of factors. For instance, with a decrease in grain size, the volume of boundary zones increases and that occupied by microbands decreases. The contribution of deformation twins increases with transition of a portion of disperse phases into the solid solution as it does with an increase in the rate of deformation and a decrease in deformation temperature. A higher concentration of disperse particles increases the scatter of the principal components of deformation textures.

The differences in the structure of local microzones also cause differences in the rate of nucleation and in the orientation of recrystallization nuclei.

Nucleation obviously begins most early at boundaries of original grains, on inclusion particles and also in Neumann bands where the orientation is usually different to the rib orientation. Nuclei are formed less quickly in microbands and most slowly (by the mechanism of in-situ recrystallization) in deformation bands. In the last case, a recrystallization texture repeats the texture of deformation bands.

In contrast to this, the growth of subgrains in microbands involves intensive misorientation. It has been found statistically that the {110} ⟨001⟩ orientation for the nuclei which form in microbands accounts for the highest percentage of all the possible orientations from {111} ⟨112⟩ to {110} ⟨001⟩. This can be explained by the fact that the misorientation angle of these nuclei increases faster than in other nuclei. These are the very nuclei that are separated from the matrix (into which they grow) by boundaries of the highest mobility.

Figure 148 shows a recrystallization nucleus of rib orientation which has formed in a microband and grows into the neighbouring deformation bands of the type {111} ⟨112⟩. At a low magnification, the microband looks like a linear boundary.

In that connection, the contribution of {110} ⟨001⟩ nuclei to the texture must be greater in a coarse-grained material, i.e. in the material with a higher volume percentage of microbands. In fine-grained materials, the nuclei that have appeared at grain boundaries can grow into the depth of grains before most nuclei of rib orientation in microbands have a chance to form adequately.

Koksharova, Lyasko and Mironov [258] note that, for a rib texture to be prevailing, the degree of cold deformation should not exceed a definite limit. This agrees well with the material of Ch. 2 and with the results obtained by S. V. Afanasyev and B. V. Molotilov who have found that, after heavy deformations (above 70-80% depending on the size of original grains), the orientations of the {112} ⟨110⟩ and {001} ⟨110⟩ types develop in a rolling texture at the expense of the {111} ⟨112⟩ orientation, so that the conditions for the formation of a rib texture worsen. The optimum degree of deformation is 40 to 70%.

This problem is closely associated with the effect of the number of rolling passes on the perfection of rib texture. Most workers hold that the deviation of the orientation of 'rib' grains from the ideal {110} ⟨001⟩ orientation is greater after single-pass rolling than after two-pass rolling. Rolling in two passes obviously produces a more perfect orientation {111} ⟨112⟩, and thereby gives a more regular orientation of rib-texture nuclei after repeated recrystallization.

I. D. Seidman shows another advantage of two-pass rolling. The deformation texture in sheets rolled in one pass contains a high percentage of the above-mentioned components {100} ⟨110⟩ and

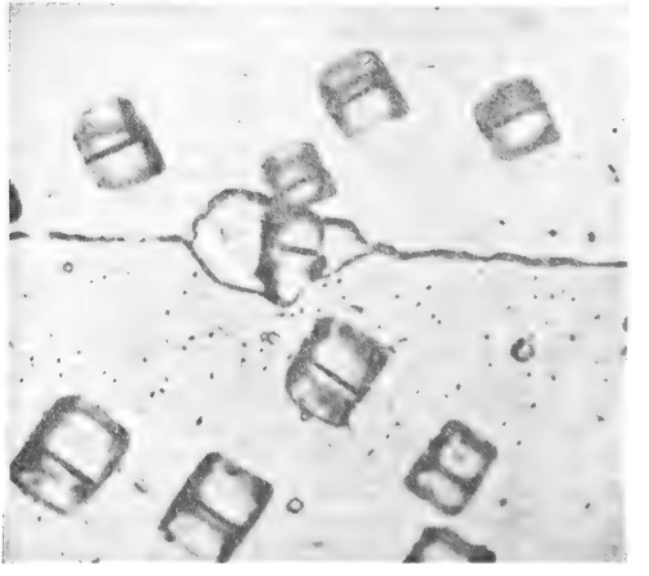

Fig. 148. Rib-oriented recrystallization nucleus in transformer steel. It forms in a microband and grows into adjacent, type {111} ⟨112⟩, deformation bands [71]

{112} ⟨110⟩ (50% or more), which are strain-hardened to a lesser extent than the other components of the texture and are recrystallized in primary recrystallization preferably by migration of boundaries of the original grains. This results in a sharply inequigranular structure ($D_{max}/\bar{D} \approx 10$) by the end of primary recrystallization. This structure diminishes the difference in the rates of growth of 'rib' grains and other grains at the stage of secondary recrystallization. Two-pass rolling with an intermediate annealing weakens the {112} ⟨110⟩-{100} ⟨110⟩ components in the texture.

As follows from the foregoing, primary recrystallization only results in the appearance of a distinct {110} ⟨001⟩ component in the texture, though this component is still not predominant, but becomes so largely at the stage of secondary recrystallization when {110} ⟨001⟩ nuclei grow faster than nuclei of other orientations (see Table 21). For this to occur, the boundaries of the main mass of grains should be stabilized by disperse particles of a secondary phase ('inhibitor').

It is further essential that secondary phase particles stabilize the matrix only to a definite temperature. Above that temperature, disperse particles must start dissolving in order that secondary recrystallization should take place. The concentration and dispersity of precipitates should be high enough to inhibit premature mass growth of grains, but not so high as to impede the growth during high-temperature heating and thus bring about 'overstabilization' of the matrix. The rate of dissolution of disperse particles is also of importance. It should be low in order to preclude mass growth of grains.

Thus, another important condition for producing a rib texture is to select properly the composition of alloys and the mode of treatment to ensure the optimal stabilization of the structure.

Two processes, the nitride and the sulphide process, are employed most widely for making transformer steel. In the former process, the matrix is stabilized by nitrides of aluminium, silicon, manganese and other elements. Among them, aluminium nitride is most important, since it is most stable against coagulation. In the sulphide process, the matrix is stabilized by sulphides of manganese and other elements.

According to a number of reports, the optimum concentration of nitrogen that is needed to form a perfect rib texture is approximately 0.001%. It should be emphasized, however, that the problem of optimal composition cannot be treated without regarding the process conditions of deformation and heat treatment. To illustrate the point, consider, for example, the use of aluminium, more correctly aluminium nitride, AlN, for matrix stabilization and improvement of the magnetic properties of transformer steel.

Up to quite recently, there have been controversial views on the optimum concentration of aluminium in transformer steel and the

conditions of steelmaking, in particular, of hot rolling. Important results have been obtained in the studies carried out by B. V. Molotilov et al. [260], I. D. Seidman, I. A. Shestakov et al. [261].

Particles of AlN can have a strong effect on the texture when their size is a few hundredths of a micrometre (300-500 Å) and their concentration is $(3\text{-}5)\cdot 10^{13}$ cm^{-3}.

This state can be obtained if particles can precipitate during hot plastic working and subsequent cooling, cold rolling and heat treatment. For this, at least 0.011-0.015% Al must be dissolved in the metal during heating before hot deformation; approximately one-third of this concentration (0.004-0.005%) precipitates from the solution during hot deformation. These requirements should be taken into account in selecting the heating conditions for slabs (the temperature T_{opt} and the heating time τ_{opt}). The total amount of aluminium, Al_{tot}, determines in every case the optimum values of T_{opt} and τ_{opt} that make for the best magnetic properties in rolled sheets. The higher the concentration of aluminium in steel, the lower must be T_{opt} and the shorter the value of τ_{opt}.

With $Al_{tot} = 0.011\text{-}0.013\%$, magnetic losses have been the lowest in a steel rolled from slabs heated at about 1250°C for 2.5 h [261]. A higher temperature of heating or a higher content of aluminium results in overstabilization. With an overstabilized matrix, a small number of nuclei form in primary recrystallization and thereby the sheets have an excessively coarse grain. Besides, all properly oriented rib-texture nuclei are excluded from the process of secondary recrystallization. These factors increase the magnetic loss in final steel. With a further increase in the total concentration of aluminium, the number of nuclei for secondary recrystallization becomes equal to zero.

If the actual concentration of aluminium or the temperature of heating of slabs is below the optimal values, high-temperature heating for secondary recrystallization will cause an intensive growth of nuclei not only of the {110} ⟨001⟩ orientation but also of other orientations.

The conditions of heating and of hot and cold rolling can influence the final texture not only through the concentration of secondary phase particles, but also through the size of these particles (particles of aluminium nitride in the case considered). According to [261], if the size of AlN particles in slabs is about 10 000 Å and the conditions of heating are selected properly, their size will be 1000-1500 Å in hot-rolled strip and 300-500 Å in cold-rolled steel. In this process, the size of grains in the matrix after primary recrystallization is about 13 μm, the degree of inequigranularity is $D_{max}\,D_c = 4.5\text{-}5.5$, and the perfection of the rib texture after secondary recrystallization is approximately 85%.

It can be mentioned for comparison that, for the same concentration of aluminium in steel, but with a lower temperature of heating of slabs, i.e. with incomplete dissolution of the secondary phase before hot rolling, the average size of grains increases up to 20 μm and D_{max}/D_c up to 4.8-6.3.

In the sulphide process, a high temperature of heating of slabs before hot rolling (>1300°C) should also ensure the maximum dissolution of sulphides and their precipitation from the solution in subsequent procedures. The temperature at the end of rolling should not be less than 960-1000°C to ensure the precipitation of high-temperature sulphides during cooling, which are more stable against coagulation than the sulphides precipitating at lower temperatures.

The optimum concentration of sulphide particles is $(2\text{-}4)\cdot 10^{12}$ cm^{-3}.

B. V. Molotilov et al. [260, 262-264] have analysed the role of stabilizing phases ('inhibitors'). As has been found [262], titanium nitrides, apart from aluminium nitrides, can play an essential part in the nitride process. Titanium nitrides have a higher affinity for nitrogen than aluminium nitrides. The concentration of titanium should be strictly specified and must not exceed 0.3%. A higher concentration or the presence of titanium together with aluminium can overstabilize the matrix.

In the sulphide process [263, 264, 260], silicon sulphide can also have an important role in addition to manganese and iron sulphides. Complex sulphides are less effective.

An excess of carbon over 0.015-0.020% has a strong adverse effect on texture formation and magnetic properties [265]. It causes grain refinement, increases power loss and lowers remanent induction. This effect of carbon is associated not with the role of carbides, but with a change in the phase composition of steel, since at high concentrations of carbon a steel becomes two-phase ($\alpha + \gamma$) at elevated temperatures. The austenite thus formed retards the growth of ferritic grains during heating and precludes the preferable growth of grains with the (110) [001] orientation. The concentration of carbon is sometimes lowered by annealing in moist hydrogen.

In order to prevent mass growth of grains before reaching a definite temperature, it is possible to utilize the effect of the rate and temperature of heating on the course of recrystallization, the size of grains, and the perfection of rib texture. An increase of the heating temperature [265] increases the area occupied by grains with the (110) [001] orientation. This effect is stronger at a lower rate of heating. With an increase in heating rate, the preferable growth of these grains is suppressed, probably on account of a more intensive dissolution of disperse phases and vigorous growth of all grains irrespective of their orientation.

It follows from the foregoing that the conditions of heat treatment should be such as to ensure a slow passage through the tempe-

rature interval of the beginning of dissolution of disperse phases and the initial preferable growth of secondary recrystallization nuclei with the (110) [001] orientation.

Thus, crystallites with the {110} ⟨001⟩ orientation are almost absent in the deformation texture. Only subgrains (more strictly, cells) of microbands of {111} ⟨112⟩ grains possess this orientation, but their volume concentration is low and is beyond the sensitivity of common methods of analysis. Grains with the {110} ⟨001⟩ orientation appear at the stage of primary recrystallization and later become the 'centres' of secondary recrystallization.

What accounts for this role of grains with the {110} ⟨001⟩ orientation? Why do these grains grow faster at the stage of secondary recrystallization than other grains?

Dunn and Koch have supposed in an early work [266] that {110} ⟨001⟩ grains are more perfect in their structure and for that reason they grow during secondary recrystallization at the expense of differently oriented grains.

Livshits and Novikov [267] have not confirmed this view. They measured the dislocation density and found that in {110} ⟨001⟩ grains it was not lower than in other grains. They even observed a definite tendency to a higher dislocation density in 'centres' of secondary recrystallization. The authors have concluded from the results of their experiments that the 'centres' of secondary recrystallization are essentially the grains which have formed earlier than other grains during primary recrystallization in regions of the highest distortion. They have also found that {110} ⟨001⟩ grains are the largest at the moment of completion of primary recrystallization. An indirect conclusion has been made on this basis that these grains form earlier than others, though this has not been confirmed by direct observations. As has been mentioned above, nuclei form most early at boundaries of grains and inclusions and in Neumann bands.

G. M. Vorobyev and some other workers hold that the accelerated oriented growth of {110} ⟨001⟩ nuclei at the expense of grains with the {111} ⟨112⟩ orientation is the decisive factor that causes transformation of these nuclei into 'centres' of secondary recrystallization.

This standpoint is gaining more and more recognition. There is much evidence [268, 269] that {110} ⟨001⟩ grains actually become centres of secondary recrystallization when they are found to be linked with adjacent {111} ⟨112⟩ grains by rotation through 35° about the common ⟨110⟩ axis lying in the rolling plane across the rolling direction. Thus, an increase in the scatter of the rib component diminishes the difference in the rates of growth of 'rib' grains and other grains upon removal of the retarding effect of disperse phase particles.

In transformer steel, particles of stabilizing phases produce an effect in the first place on common boundaries. The authors of the work [261], who have studied the effect of overstabilization, point out that an increase in the concentration of aluminium (AlN) has a stabilizing effect primarily on grains whose orientation is closest to the ideal (110) ⟨001⟩ orientation*.

V. Yu. Novikov [268] and D. B. Titorov [269] have analysed their own results and some literature sources and come to a conclusion that the boundaries having a high mobility possess a wider range of misorientation angles than was supposed earlier. In Titorov's view, what is only important is that misorientation angles should be large in magnitude (30-40°), the role of crystallographic direction around which adjacent grains are misoriented being inessential.

Thus, many details of this problem are still unclear. But even if we assume that the boundaries separating the {110} ⟨001⟩ and {111} ⟨112⟩ components are actually most mobile, it is unclear, on the face of it, why {110} ⟨001⟩ grains, which have the same size as {111} ⟨112⟩ grains at the end of primary recrystallization, grow at the expense of the latter, but not the other way round. This would be quite understandable if the volume energy of 'rib' grains were lower than that of other grains, as has been supposed by Dunn and Koch. A more careful analysis shows, however, that a difference in volume energies is not an essential condition.

Indeed, let a texture be composed of two components formed by grains of an identical grain-size distribution pattern and oriented favourably for mutual growth. Let one of the components be very strong and represent the main orientation and the other be weak and formed by a small number of grains.

Then, with the same probability of migration of a boundary (which separates two differently oriented grains) into one or the other of the two grains, in the process of growth a portion of the grains of the weak component must inevitably grow to a greater size and become centres of secondary recrystallization. Indeed, after the grains of the main component, which surround a grain of the weak component, have grown at the expense of that grain, their further growth will be stopped or retarded, since their neighbours are now grains of the same orientation. This retardation of growth should be stronger at a lower texture scattering in the main component. As regards the few grains of the weak component which grow at the expense of the surroundings, the boundary mobility will increase, but not decrease, in the course of their growth, since the

* It should be noted that this case relates to the effect of precipitated particles, whereas in the works dealing with the pure effect of impurities on the mobility of conjugate boundaries, the results were obtained for dissolved impurities (see Ch. 5).

driving force associated with a difference in surface energies (difference in grain size) continuously increases.

Thus, the general rule for texture changes at the stage of secondary recrystallization in a system composed of the main and the weak component is that a portion of grains of the weak component are transformed into centres of secondary recrystallization and this weak component is finally transformed into the main one.

If there is a favourable difference in volume energies, the process will be stimulated additionally. In the case of transformer steel, the problem of the differences in volume energies of {110} ⟨001⟩ and {111} ⟨112⟩ grains by the end of primary recrystallization still cannot be regarded as being perfectly clear.

A later work [270] makes it possible to suppose that the volume energy plays a definite part in the formation of 'rib' centres of secondary recrystallization and in their preferable growth at the expense of {111} ⟨112⟩ grains.

Figure 149 shows the distribution of microhardness in silicon iron microcrystallites oriented with the (111) and (110) planes in the sheet plane at an early stage of secondary recrystallization [270]. As may be seen, (111) grains have a higher hardness on the average. Besides, the curve of microhardness distribution in (110) grains has an intricate shape. It may be supposed that there are two groups of (110) grains which differ one from the other in the volume energy and probably in the mechanism of their formation. Grains formed by coalescence of subgrains are less perfect and those formed by migration of their boundaries are more perfect. The latter include (110) grains formed from subgrains in microbands. Nuclei appear through coalescence on secondary phase particles and in boundary regions — on grain boundaries and Neumann bands.

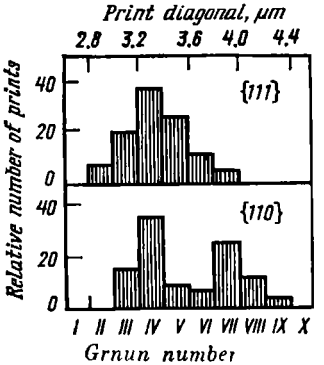

Fig. 149. Distribution of microhardness of primary recrystallization grains in silicon iron oriented with their {111} and {110} planes in the plane of sheet

An elevated volume energy of grains formed near inclusions is also associated with the fact that these grains are strain-hardened during heating and cooling due to a difference in unit volumes and in coefficients of thermal expansion between inclusion particles and the matrix. Thus, though these nuclei appear earlier than other nuclei (including 'rib' nuclei), they are finally consumed by the younger but more perfect grains.

Still another standpoint deserves mentioning. Yu. S. Avraamov [271] and N. L. Bryukhatov [272] have advanced a different supposition; namely, that the driving force of the preferable growth

of 'rib' grains is the reduced surface energy of atomic {110} planes in b.c.c. crystallites (see Table 11).

This might be the reason why the grains whose {110} planes come out to the surface of sheets must grow at the expense of neighbouring grains which show a higher surface energy and have their {111} planes coming to the surface of sheets. Yu. S. Avraamov has shown that this actually can take place under particular conditions.

V. V. Sosnin and T. Ya. Yastrebov [273] examined the effect of surrounding media on the growth of grains with various deviations from the rib orientation in secondary recrystallization. Three types of medium were examined: vacuum ($5 \cdot 10^{-5}$ mm Hg), hydrogen, and helium. The content of oxygen in the vacuum medium was $2.16 \times \times 10^{-11}$ g/cm^{-3} and that in hydrogen and helium, $8.9 \cdot 10^{-9}$ g/cm^{-3}. In all cases, grains with an orientation closest to the rib orientation had the highest rate of growth. The highest difference in the rates of growth, and therefore the preferable formation of the rib texture, were obtained by annealing not in vacuum, where the anisotropy of the surface energy shows up in the purest form, but in hydrogen and in helium, where the concentration of oxygen was two orders of magnitude higher. Annealing in the medium with an elevated concentration of oxygen lowered markedly the absolute rate of grain growth, and especially so the rate of growth of less favourably oriented grains.

These results and the results of metallographic analysis have enabled the authors to conclude that this role of oxygen is associated not with a change in the anisotropy of surface energy, but with the fact that oxygen accumulates preferably on grain boundaries and, in particular, on boundaries of grains whose orientation differs to a greater extent from the ideal rib orientation, with the result that it strongly decreases the rate of their growth.

It should be added that in industrial processes of making transformer steel, {110} nuclei are usually formed not directly on the surface of sheets, but in a subsurface layer, i.e. at a certain depth under the surface [90], in a region of the cross section where the most distinct {111} ⟨112⟩ component of the deformation texture forms in plastic working. This fact implies that, under industrial conditions, the surface energy does not seem to play a decisive part in the formation of rib texture, at least at an early stage of the process.

Let us mention some other aspects essential for the formation of rib texture.

As has been shown in a number of works [274, 275], a sufficiently perfect rib texture can form in secondary recrystallization only when the average size of grains, $\bar{D}$, at the end of primary recrystallization does not exceed a definite value which is smaller for a smaller

thickness H of sheets. For sheets 0.35-0.5 mm thick, it is necessary that $\overline{D} \leqslant$ 0.02-0.04 mm.

With a decrease of the sheet thickness below a definite 'critical' value, H_{cr} (according to some authors, below a definite value of the $H/\overline{D}$ ratio), the rib texture becomes less perfect, magnetic induction decreases, and power losses increase.

As has been shown in [261], the critical value of H_{cr} for transformer steel decreases with an increase in the concentration of aluminium (and, thus of AlN particles) and with a decrease in the size of grains by the end of primary recrystallization. H_{cr} is equal to 0.36 mm at 0.004% Al and becomes less than 0.30 mm at approximately 0.016% Al. These effects of $\overline{D}$ and H on the texture and properties of steel have still not found a reliable explanation.

The conditions of friction between the rolls and the surface layers of rolled metal are also of importance. With improper lubrication and, therefore, high friction forces, the surface layer of sheets has a less distinct deformation texture and thus a less distinct rib texture after recrystallization [90]. A lubricant, say, castor oil, enhances the (111) component in the surface layer and thereby increases the probability of formation of rib-oriented nuclei of secondary recrystallization in that layer.

Uneven heating of slabs should also be considered. In continuous heating furnaces, the regions of contact of slabs with skid pipes become less heated than the remaining mass of metal (Fig. 150). Accordingly, these portions turn out to contain a smaller amount

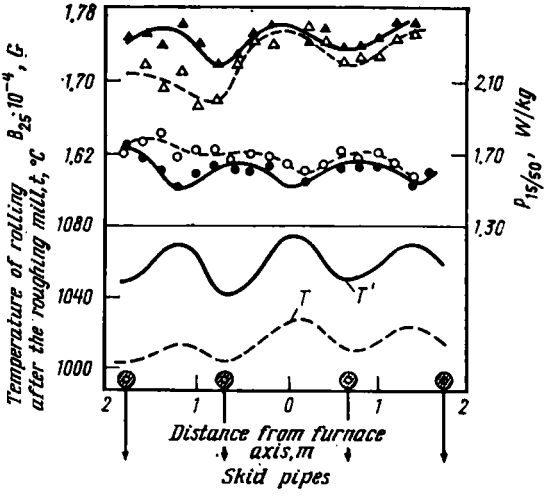

Fig. 150. Distribution of temperature (T) and variations of magnetic properties along the length of strips of transformer steel containing aluminium [261]

T'—maximum temperature; T—minimum temperature

of dissolved aluminium and, subsequently, a lower concentration of the stabilizing secondary phase [261]. The result is that sheets rolled from these portions of slabs have poorer magnetic properties.

The results given in Fig. 150 show that the effect of local chilling of slabs can be prevented by raising the average temperature of heating (to its upper limit) and also by increasing the concentration of aluminium in steel. This may be illustrated by the data from [261]. In specimens of steel from a melt with 0.004% Al (with the temperature of heating of slabs 1040-1075°C), the scatter of magnetic characteristics was approximately 3% (for B_{25}) and 12.5% (for $P_{15/50}$). For comparison, the magnetic characteristics in specimens from a melt with 0.010% Al were practically uniform along the length of sheets already at the heating temperature of 980-1010°C.

Thus, many details of the mechanism of formation of rib texture have still to be investigated.

10.3.2. Transformer Steel with {100}⟨001⟩ Cube Texture

Ways for reliable making of steel with the cube texture are still known insufficiently.

The most favourable conditions for the formation of this texture are obviously those at which the texture already contains the {100} ⟨001⟩ component before the final rolling procedure. For instance, Wiener [276] obtained the cube texture by rolling and recrystallization of an ingot which was cooled under the conditions in which columnar crystals grew in the direction of the temperature gradient and the ⟨001⟩ direction was parallel to the ingot length. Wiener found that a perfect cube texture could be formed by high-temperature annealing of cold-rolled polycrystalline silicon iron with the {100} ⟨001⟩ texture.

The degree of deformation should not be high in order to preserve the {100} ⟨001⟩ orientation in subsequent rolling. Besides, measures should be taken to lower the contact friction forces and prevent the associated non-uniform flow of metal in the surface layers of strips [277]. In hot plastic working, recrystallization directly during deformation should be avoided.

The temperature of rolling is also essential. The highest stability of the cube texture is observed at 1000°C, and the lowest at 1200°C [277].

The cube texture can also be obtained by rolling and annealing a metal with the rib and axial textures. In that case, by varying both the number of intermediate annealing operations in cold plastic working and the conditions of the final heat treatment, it is possible to form the cube texture either in secondary recrystallization (one- or two-pass rolling plus annealing at 1200-1350°C) or in primary

recrystallization (two- or three-pass cold rolling plus annealing at 1000-1300°C).

Ingots cast by common methods should have the {111} ⟨112⟩ component in the deformation texture before rolling. After primary recrystallization, the {110} ⟨001⟩ and {100} ⟨001⟩ components appear: their presence in the metal before the final rolling operation is indispensable.

What factors can prevent the development of the rib texture and ensure the preferable development of the cube texture in high-temperature heating of this metal?

In the first place, the metal should contain no inhibitors, i.e. impurity phases which can stabilize the matrix and thus promote the formation of the rib texture. A high purity of the metal is the most important condition for obtaining the cube texture.

The conditions for stabilization of the matrix, along with the causes for preferable growth of {100} ⟨001⟩ grains, are in this case different to those required for obtaining the rib texture. According to [278], matrix stabilization in the formation of the cube texture is ensured by thermal etch pits in the surface of sheets (see p. 112): they retard the growth of the main mass of grains as soon as these reach a size comparable with the thickness of sheets. With these conditions observed (and, first of all in the absence of stabilization by impurities), grains of all orientations become roughly of the same size by the end of primary recrystallization.

The available data allow us to state that the preferable growth of grains with the {100} ⟨001⟩ orientation in secondary recrystallization is determined by the fact that the {100} faces have the lowest surface energy compared with other crystallographic faces.

In pure metal, it is the planes of the most dense packing that must have the lowest surface energy. In b.c.c. metals, these are the {110} planes. But because of the effect of selective adsorption of impurities, certain planes in alloys, particularly the {100} and {110} planes, may change places as regards their surface energy. This has been confirmed by some direct experiments.

Walter and Dunn [278] have analysed the growth of grains whose {100} and {110} planes come to the surface of a sheet during annealing at 1200°C in various atmospheres. It turns out that {110} grains grow preferably in vacuum ($5 \cdot 10^{-4}$ mm Hg) and {100} grains in the atmosphere of argon with an addition of oxygen. A change from one to another atmosphere during annealing of a specimen causes a change in the direction of migration of a boundary. The authors of [278] have also shown that, apart from the oxygen in the atmosphere, the oxygen in the metal proper may play an important part.

Yet, an excess of oxygen is also undesirable. It is obvious that in the given case a selective concentration of oxygen at certain boundaries is essential, but not the effect of oxygen on the surface

energy. This agrees well with the data of V. V. Sosnin and T. Ya. Yastrebov [273] on the role of excess oxygen in hydrogen and helium atmospheres. It is also probable that, at an elevated concentration of oxygen, an oxide film formed on the surface of metal can play an important role. According to N. F. Dubrov and Yu. M. Gartman, the absence of oxide film is one of the requirements for obtaining the minimal surface energy on {100} planes.

This explanation is confirmed by the favourable effect of annealing in high-purity dry electrolytic hydrogen with the dew point at —75°C.

As has been noted [275, 279], the formation of a reducing atmosphere, which is more favourable for obtaining the cube texture, is promoted by transforming molecular hydrogen into the atomic form by means of catalysts, such as nickel and nickel alloys.

The effect of sulphur is similar to that of oxygen. Wiener [276] has found that sulphur in a concentration of $5 \cdot 10^{-5}$—$6 \cdot 10^{-4}$% (by mass), i.e. below its solubility limit in the solid state, promotes the growth of cube-oriented grains. An excess of sulphur, however, like an excess of oxygen, inhibits grain growth.

It is worthy to mention still another fact in favour of the leading role of the surface energy in the formation of cube texture. According to Mullins [139], the driving force associated with the difference in the energies of free surfaces of adjacent grains should be inversely proportional to the thickness of sheets. As has been determined experimentally, the {100} ⟨001⟩ texture actually forms more easily, under comparable conditions, in thinner sheets.

The problem of the most favourable composition of transformer steel, which is required to form the cube texture, still requires further examination. Molins and Pawlek [280], who have analysed the effect of silicon, state that its optimal concentration lies within 1.8-2.2%. At a lower concentration, a steel becomes two-phase (ferrite plus austenite) at elevated temperatures, which is unfavourable for secondary recrystallization and texture formation. At the silicon concentration above 2.2%, the cube texture becomes weaker, which is attributed to a higher slip resistance of the steel and a change in deformation texture. In practice, steels having up to 3% Si are often used.

Favourable conditions for the development of the cube texture can also be formed by additional alloying of Fe-Si alloys. There are certain indications of the favourable effect of manganese and some other elements. It is still unclear how these elements influence the cube texture, whether by changing the difference in surface energies or by altering the deformation texture.

10.3.3. Low-textured Dynamo Steel

In contrast to transformer steel, a steel for making magnetic circuits of a.c. electric machines with an intricate path of the magnetic flux must show the least anisotropy of magnetic properties in the plane of sheets (in particular of magnetic induction B_{25}). Besides these properties must be sufficiently stable and high.

These requirements are met by a steel grade whose composition is close to that of transformer steel, but with a less pronounced texture. The rib component of the texture of this steel must not exceed 15-20%.

A weaker texture is obtained by controlling the conditions of secondary recrystallization.

In the most popular method, this is effected by deformation to the critical degree (6-10%) during the last (third) cold-rolling procedure before the final annealing. This deformation deprives the primary recrystallization nuclei with the rib orientation of the advantage of growing preferably in secondary recrystallization [281].

Another, more efficient, method consists in that hot-rolled (not decarbonized) strips are cold-rolled in one pass and then annealed.

In this process, secondary recrystallization is suppressed, firstly, by the $\alpha \rightarrow \gamma$-transformation during the final annealing (though some details of the mechanism of this suppression are still unclear) and, secondly, due to a less perfect orientation of 'rib' nuclei after one-pass rolling as compared to two-pass rolling. An important point for obtaining satisfactory results in this process is to prevent premature decarbonization of the metal. This process ensures more isotropic properties in the sheet plane compared with the former method, though the absolute characteristics may sometimes be somewhat poorer.

Chapter 11

Effect of Alloying on the Temperature Level and Rate of Recrystallization in Metals and Single-phase Alloys

The temperature level and rate of recrystallization in various metals and alloys have been studied by many researchers, but only a few works are concerned with the effect of alloying in a wide range of concentrations and in various phase states.

A reliable generalization is difficult to make because the studies were usually conducted on insufficiently pure materials, so that many results obtained do not prove suitable enough for the purpose. As is known, the effect of alloying additions on the rate of recrystallization is stronger in less alloyed metals.

Large difficulties arise in generalizing the available results. The fact is that various workers use different criteria to estimate the effect of impurities on recrystallization in metals. The characteristics which are used most often for comparative analysis are the temperature of the beginning and end of recrystallization, the temperature of 50-% softening, the rate of nucleation, the rate of growth, the effective activation energy, etc.

11.1. The Criteria for Estimating the Susceptibility of Metals and Alloys to Recrystallization

The selection of a simple criterion which could reliably characterize the rate and temperature level of recrystallization and make it possible to compare the susceptibility of various alloys to recrystallization is far from being an easy task.

The temperature of the beginning of recrystallization (t_r^s, °C, or T_r^s, K) depends on many factors, in the first place on the type of the dislocation structure formed by the prior deformation ε and the temperature and time of annealing before the onset of recrystallization, τ_r^s, with the relationship between τ_r^s and T_r^s being of an exponential nature:

$$\tau_r^s = \tau_0 \exp (Q/RT_r^s) \qquad (14)$$

With a decrease of temperature, the time of isothermal annealing until the onset of recrystallization, τ_r^s, becomes so long that it

cannot be practically used for estimating the susceptibility of various alloys to recrystallization.

It is much more convenient to use the temperature of the beginning of recrystallization in isochronous annealing. Since the value of t_r^s decreases attenuatedly with an increase in ε and τ (see Fig. 41), most workers estimate the susceptibility to recrystallization by the temperature of the beginning of recrystallization after an appreciably high degree of deformation and after isochronous annealing for at least 1-3 h. The temperature of the end of recrystallization is determined in a similar manner. These temperatures can be regarded as the thresholds of the beginning and end of recrystallization, i.e. the temperatures of annealing below which recrystallization does not start or, respectively, does not near completion within a practically reasonable time of annealing (2-3 h). Curves of the type shown in Fig. 41 can also be used to estimate the rate of a recrystallization process by the width of the interval between t_r^s and t_r^f.

Since recrystallization consists of two stages—the formation of recrystallization nuclei and their growth by boundary migration—some workers have analysed separately the effect of impurities on the rate of each of these stages. It should be noted however that the moment of the end of nucleation cannot be determined definitely. Most nuclei grow by that moment to an appreciable size (which may vary with the sensitivity of the method used for analysis).

The rate of growth of nuclei or grains during recrystallization can be determined more definitely, though usually a time-averaged value, but not the actual rate, is obtained, since the process of growth occurs not monotonically, but interruptedly.

In view of these drawbacks, the susceptibility of alloys to recrystallization is often determined in terms of what is called the activation energy of recrystallization, Q. It is found from the above-mentioned exponential expression relating the time of the beginning of recrystallization, τ, to temperature T (K). In many cases, however, the experimentally found value of Q does not represent the actual activation energy of the process. For a number of alloys there is no regular relationship between t_r^s and Q and the latter may vary by a factor of two or more depending on the temperature interval in which it has been determined. This effect is especially pronounced in multi-phase alloys, but can also make itself felt in single-phase alloys and even in pure metals [132].

This consideration may be illustrated by the semi-logarithmic curves relating the time of the beginning of recrystallization to $1/T$ for selected alloys (Figs. 151 and 152). For age-hardening alloys (XH77TIOP, Ni-Cr-Al-Ti), the experimental points found in a wide range of temperatures fall on the sections of a broken line, where each of the straight sections corresponds to a narrower temperature

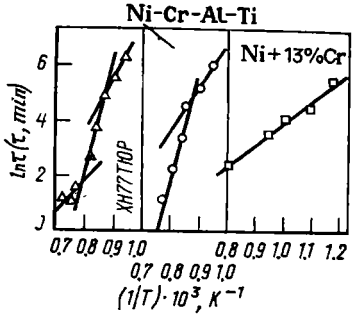

Fig. 151. Logarithm of the time of beginning of recrystallization versus $1/T$ for a nickel-base alloy

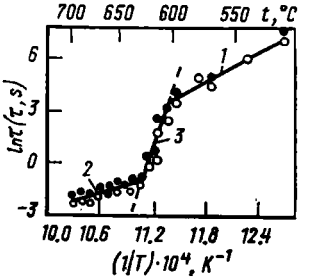

Fig. 152. Logarithm of the time of beginning of recrystallization versus $1/T$ for iron [132]

interval. The values of Q calculated for these narrower intervals (Table 22) differ sharply from one another. The highest values of Q for age-hardening alloys are much greater than they are for single-phase alloys of the same base.

TABLE 22. **Effective Activation Energy (Q) of Recrystallization of Age-hardening Alloys in Various Temperature Intervals**

Alloy	t_r^s, °C	t_b, °C *	Temperature interval, t, °C	Q, kcal/g-atom
XH77TIOP	950	950-975	1100-1000	35
			1000-900	78
			900-830	42
Ni + 13% Cr + 2.4% Ti + 2.2% Al	900	875	1030-830	78.2
			830-730	42.2
Cr + 13% W	920	920	940-900	113
			890-850	60

* t_b is the boundary in temperature between the single-phase and two-phase regions; is the temperature interval in which Q is determined.

Figure 152 shows the curve $\ln \tau = f(1/T)$ for iron [132]. The authors have calculated Q only for two temperature intervals, (1) 520-620°C and (2) 630-720°C, and found it to be sharply different (57.2 kcal/g-atom and 26.9 kcal/g-atom). They have not determined Q for an intermediate temperature interval of 600-650°C (3), though the experimental points fall on the straight line in that interval not less accurately than in the other two intervals.

If a straight line is drawn for the intermediate interval (dotted line *3* in Fig. 152), the respective value of Q will be 150 kcal/g-atom.

Some literature data show that Q for aluminium also decreases in higher temperature intervals; it has been found, for instance, that $Q = 59.0$ kcal/g-atom at 310-370°C and 34 kcal/g-atom at 425-540°C.

The results obtained by some workers [282] for purest copper and aluminium show that their activation energies and temperatures of the beginning of recrystallization vary quite differently on addition of minor impurities; in particular, t_r^s increases in both metals, whereas Q for copper increases and that for aluminium decreases.

In many studies, analysis of the values of Q is used to clarify the mechanism of recrystallization. In that connection, it is essential to understand the physical sense of Q and the factors which can affect it.

In expression (14), Q actually has a double sense. On the one hand, it determines the energy barrier to be overcome by atoms (or a group of atoms) to pass from a metastable into a stable state. In this sense, the concept of activation energy Q is applicable to elementary processes. It can be determined correctly if the state of the system in regions where transformations have not yet taken place remains stable in the course of the process. This is however not the case with recrystallization which includes a number of elementary processes the rate of each of which depends in its own manner on the alloy composition and the conditions of deformation and heating.

Each preceding process, be it complete to a greater or smaller extent, correspondingly changes the conditions for the occurrence of the subsequent elementary processes and their activation energies. Therefore, Q loses its actual sense of activation energy and can be regarded only as a conditional effective activation energy of a complicated common process. B. Ya. Pines [145] has shown that the experimentally found activation energy for a sintering process (in which case the system changes less than it does in recrystallization) is not adequate to characterize the essence of the phenomena. This conclusion is even more applicable to recrystallization.

At the same time, Q characterizes the effect of temperature on the rate of the process. If Q is different in various temperature intervals, this implies, first of all, that the rates of individual elementary processes depend differently on temperature.

Consider for example an age-hardening alloy type ХН77ТЮР. The value of Q for this alloy is low when the time of the beginning of recrystallization is determined in the interval of low temperatures corresponding to the two-phase region of the equilibrium diagram (interval *1* in Fig. 151). For the interval *2*, which falls partially into the two-phase region and partially into the single-phase region, Q is very high. For the interval *3*, which is completely in the high-temperature single-phase region, Q is low again.

This result can be explained easily if we recall that disperse phase particles sharply inhibit nucleation at annealing temperatures corresponding to the two-phase state of the system; this inhibiting effect is eliminated at temperatures of the single-phase state. An increase in the rate of recrystallization is determined by the increased temperature proper and additionally by elimination or weakening of the inhibiting effect of a disperse phase. It follows that the effect of temperature on the rate of recrystallization and, correspondingly, the value of Q can be found to be very high if the time of the beginning of recrystallization, τ, is determined within a temperature interval in which lower temperatures correspond to the two-phase region and higher values to the single-phase region.

In pure metals and single-phase alloys, some other factors can influence Q. As has been shown in Ch. 4, the formation of recrystallization nuclei is controlled by the diffusion process of dislocation climb. With a lack of free vacancies, the activation energy of climb is determined by the sum of the activation energies of the formation and migration of vacancies. With an excess of vacancies, it is determined only by the activation energy of their migration.

If the concentration of vacancies varies sharply in the temperature interval in which Q is being determined, the rate of the process becomes more dependent on temperature and the value of Q tends to grow.

Thus, preliminary recovery, which diminishes the concentration of vacancies, should make the rate of recrystallization less dependent on temperature and give a lower value of the effective activation energy Q_{ef}, though the temperature of recrystallization may increase in that case.

Dahl and Geisler [282] have made use of the fact that the concentration and mobility of vacancies are different in various metals and alloys in order to explain in their own way why minor additions have opposite effects on the activation energy of recrystallization in copper and aluminium. By their results, the activation energy of heavily deformed pure copper is of the same order of magnitude as the activation energy of diffusion of vacancies (approximately 30 kcal/g-atom). On adding minor impurities, Q increases. This result is principally different to that obtained for purest aluminium (99.999%), whose activation energy Q has proved to be very high, approximately 75 kcal/g-atom. In less pure aluminium (99.99%) it lowers to 52 kcal/g-atom and, on addition of 0.1% Cu, to 48 kcal/g-atom.

Dahl and Geisler explain this difference by stating that vacancies in cold-deformed aluminium are highly mobile and disappear at room temperature, whereas in cold-deformed copper they are less mobile and are partially preserved in the structure. Therefore, the diffusion of vacancies required to initiate recrystallization is asso-

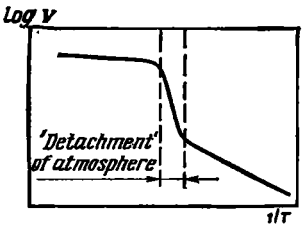

Fig. 153. Variation of the rate of nucleation and growth (the rate of grain boundary migration) with temperature in metals with minor additions (after Lücke)

ciated in pure aluminium with the energy of activation of the formation and migration of vacancies, i.e. with the activation energy of self-diffusion. Minor additions can interact with vacancies and lock the latter, so that the migration of vacancies occurs at a rate which is limited by the diffusion of foreign impurity atoms (more strictly, by the diffusion of impurity atom-vacancy complexes). The activation energy of recrystallization is now determined by the activation energy of diffusion of these complexes, which differs from the activation energy of self-diffusion, as has been observed in aluminium.

In pure copper, where a small portion of vacancies remain in the structure, the activation energy of recrystallization must be close to the activation energy of vacancy diffusion. On addition of impurities which lock vacancies, the activation energy Q of recrystallization increases over the value found for pure copper.

When alloying pure metals with low-soluble additions, one should also consider the influence of impurity atoms on the mobility of subboundaries. The interaction of impurity atoms with boundaries becomes weaker with increased temperature. Hence, the activation energy of the growth of nuclei and grains in metals with minor additions must diminish with an increase in temperature up to a definite temperature interval. This is shown schematically in Fig. 153 (after K. Lücke) in the $1/T$-log v coordinates, where T is the absolute temperature and v is the rate of growth. At high temperatures, boundary mobility is determined by boundary diffusion. Since the activation energy of boundary diffusion (Q_b) is low, the slope of the straight portion is rather flat. At low temperatures, the slope increases; it depends on the activation energy Q_v of volume diffusion of foreign atoms which form a cloud behind the boundary. This energy is higher than Q_b. In the middle portion, the curve is even steeper, since the growth of nuclei is associated here with several activated processes and the contribution of each of them to the process of growth of nuclei varies differently with temperature.

For single-phase alloys with a higher concentration of a second component, rearrangements of atoms in the phase may have a significant effect on the temperature-recrystallization rate relation.

Thus, when analysing the activation energy Q, one should consider the nature of the processes that accompany recrystallization in the temperature interval within which Q is being determined.

Analysis of a large volume of experimental data shows that the

data on t_r^s (for prolonged annealing) give a relatively more stable characteristic of the susceptibility of an alloy to recrystallization. It is thus more reasonable to use t_r^s to characterize the recrystallization capacity of alloys.

Neither this quantity, however, nor any other can characterize completely the process of recrystallization; one must additionally use such quantities as the temperature of the end of recrystallization, t_r^f, the effective activation energy, Q_{ef}, the preexponential τ_0, the rate of formation of recrystallization nuclei, and the rate of their growth. In all cases, the temperature interval and the conditions of determining these characteristics should be indicated.

Caution is advised in judging the mechanism of recrystallization and its individual stages by the data on the effective activation energy.

11.2. The Temperature Level of Recrystallization in Metals

Bochvar [13] was the first to point out back in 1927 that the temperature level of recrystallization in commercially pure metals constitutes a certain, though not strictly definite, fraction of the melting point. He proceeded from the assumption that melting bears a definite analogy to recrystallization, since in both processes a certain energy is required to cause changes in the coordination of atoms in the crystal lattice.

At the melting point, the amplitude of oscillations of atoms, α_m, is a certain fraction $1/m$ of the average interatomic spacing r, i.e. $\alpha_m = r/m$. Accordingly, for recrystallization, $\alpha_r = r/n$.

The frequency of oscillations of atoms at the melting point, f_m, in the first approximation is

$$f_m = C_m (1/\alpha_m) \sqrt{T_m/M} \tag{15a}$$

where C is a constant and M is the atomic mass.

Similarly, for recrystallization

$$f_r = C_r (1/\alpha_r) \sqrt{T_r/M} \tag{15b}$$

Dividing (15*a*) by (15*b*) we obtain

$$\alpha_r/\alpha_m = C' \sqrt{T_r/T_m} \text{ or } m/n = C' \sqrt{T_r/T_m} \tag{16}$$

whence $T_r = \delta T_m$, where δ is a coefficient.

Bochvar noted in the same work and in later works that this relationship was not strict and δ was not strictly a constant, since the derivation was made in a rough approximation and without due knowledge of the mechanism of the process.

Based on the experimental data for the minimal temperatures of recrystallization in commercially pure metals after heavy deformations and annealing for 60 min, A. A. Bochvar found that the above ratio held for $T_r = (0.35\text{-}0.4)\ T_m$.

It became possible to obtain lower values of δ with the production of more and more metals of higher purity (Table 23). The progress in the theory of dislocations enabled us to gain a more intimate knowledge of the mechanism of recrystallization. Yet, the relationship proposed by A. A. Bochvar is still quite applicable for evaluat-

TABLE 23. Values of $\delta = T_r/T_m$ for Selected Metals of Commercial and High Purity *

Metal	T_m, K	Commercial purity		High purity	
		T_r, K	T_r/T_m	T_r, K	T_r/T_m
Al	933	423-500	0.45-0.5	220-275	0.24-0.29
Au	1336	475-525	0.35-0.4	—	—
Ag	1234	475	0.38	—	—
Be	1553	950	0.6	—	—
Bi	554	—	—	245-265	0.51-0.52
Co	1765	800-855	0.4-0.46	—	—
Cu	1357	475-505	0.35-0.37	235	0.20
Cr	2148	1065	0.50	1010	0.46
Fe	1808	678-725	0.38-0.40	575	0.31
Ni	1729	775-935	0.45-0.54	575	0.30
Mo	2898	1075-1175	0.37-0.41	—	—
Mg	924	375	0.4	250	0.27
Nb	2688	1325-1375	0.49-0.51	—	—
V	1973	1050	0.53	925-975	0.45-0.49
W	3653	1325-1375	0.36-0.38	—	—
Ti	1933	775	≈ 0.4	723	0.37
Ta	3123	1375	≈ 0.44	1175	0.37
Pb	600	260	0.42	165	0.28
Pt	2042	725	0.25	—	—
Sn	505	275-300	0.35-0.38	—	—
Zn	692	300-320	0.43-0.46	—	—
Zr	2133	725	0.34	445	0.21
U	1403	625-705	0.44-0.50	545	0.38

* When using these data, it should be remembered that the purity of various metals may be different depending on the refining process. In particular, the purity of a number of transition metals, which are difficult to purify from larbon and some other elements (Cr, Nb, Mo, W, etc.) is always lower than that of f.c.c. metals.

ing the temperature level of recrystallization. It should only be remembered that, as seen from Table 23, for high-pure metals $T_r = (0.25\text{-}0.35)\ T_m$ or even lower.

Some authors attempt to determine more accurately, in a formal way, the temperature level of recrystallization and the values of δ in formula (16). But they usually proceed from energetic considerations and disregard the actual dislocation structure of materials.

As follows from Table 23, the T_r/T_m ratio for various metals of roughly the same purity are quite different. One of the probable causes is a difference in the structure in as-deformed state. The effect of the structure is noticeable even in one and the same material since t_r^s heavily depends on the temperature of deformation. A lower temperature of deformation results in a lower temperature of the beginning of recrystallization. For instance, commercially pure aluminium deformed 20% at room temperature recrystallizes at 520°C and that deformed at 78 K recrystallizes at 390°C. For copper, these temperatures are respectively 450° and 415°C. High-pure iron and nickel deformed heavily at 78 K recrystallize at 20°C, but after deformation at room temperature, they recrystallize at 450° and 325°C respectively. Bismuth deformed roughly at 5 K recrystallizes at 242 ± 1 K, which is 25°C less than the recrystallization point after strain-hardening at 200 K. For high-pure lead, the respective difference is around 15 K.

With the same purity, brittle metals recrystallize at higher temperatures than ductile.

11.3. The Temperature Level of Recrystallization in Single-phase Alloys

The standpoint according to which the temperature level of recrystallization is completely determined by the energy of atomic bonds and the amplitude of thermal oscillations of atoms becomes especially vulnerable to criticism on passage from pure metals to alloys.

For instance, it fails to explain the complex effect of alloying, particularly a sharp rise in t_r^s caused by minor additions in pure metals (see later).

One of the first attempts to analyse the mechanism of the effect of alloying on the temperature level of recrystallization was made by J. A. M. Van Liempt [283] in his theoretical study, where he put forward an idea of the decisive role of the ratio between surface tensions of a solvent and a solute, disregarding the concentration of the solution. A similar conclusion was later drawn by V. K. Semenchenko.

According to Van Liempt and Semenchenko, a soluble element whose surface tension* σ is lower than that of a solvent should inhibit recrystallization of the latter, since it is concentrated on the surface of grains and thus lowers the thermodynamic stimulus for diminishing the length of a boundary. In the opposite case, the solute element should lower the temperature of the beginning of recrystallization in the solution.

In view of the lack of experimental data, Van Liempt proposed for solid metals an approximate formula to determine σ:

$$\sigma = K \frac{T_{b.p}}{(M/D)^{2/3}} \qquad (17)$$

where $T_{b.p}$ is the boiling point, K; M is the atomic mass; and D is the density.

If σ is calculated for selected elements by this formula, the elements can be written in the following order of increasing σ: Cd, Bi, Sb, Pb, Zn, Al, Be, Fe, Cu, and Ni.

According to Van Liempt, all the elements to the left of a given element in the row must increase the temperature of recrystallization of that element upon dissolution; those on the right must decrease that temperature. Yet, Van Liempt himself has discovered that some elements disobey that rule. Later works have found still more elements of this kind.

In most works concerned with minor additions, it has been demonstrated that these additions raise the temperature of the beginning of recrystallization of the solvent irrespective of the ratio of surface tensions.

Van Liempt's ideas contradict the experimental results concerning the mutual effect of pairs of elements such as W-Nb, Fe-Cr, Fe-Ni, and Ni-Cu on the temperature of the beginning of recrystallization. As has been found, minor additions of a second component always raise the temperature of the beginning of recrystallization (Fig. 154).

One can take it as an established fact that the tendency toward concentration in distorted boundary regions is also typical of the elements whose σ is not less than that of the base metal, but whose dissolution is accompanied by a strong distortion of the solvent lattice and by an increase in the volume free energy.

In this case, as has been correctly noted by L. N. Larikov [16], the derivative of the free surface energy with respect to the concentration $(\partial\sigma/\partial C)$ must not necessarily be negative.

As applied to an elementary act of recrystallization — the growth of nuclei and grains — Van Liempt's concepts in many cases are not unfounded. They agree well with V. I. Arkharov's concepts of

* This implies the grain-boundary energy rather than the surface energ

horophilic elements which, while concentrating in boundary layers of crystallites, decrease the total surface energy and, accordingly, the stimulus to grain growth. But since minor additions almost always inhibit recrystallization and shift it into the region of higher temperatures, one can only conclude that they simultaneously influence some other parameters of the state of alloys, which affect the rate of recrystallization more strongly than does the surface tension. Thus, the role the surface tension plays at the stage of nucleation by redistribution of dislocations is obviously much less significant than at the stage of growth and is not decisive for the rate of this redistribution.

Another extreme viewpoint as regards the mechanism by which alloying can influence recrystallization is the concept which directly relates this mechanism to the influence on the diffusion mobility of matrix atoms.

Gruzin and Tyutyunnik [284] affirm that the temperature of recrystallization in metals and alloys corresponds to a definite level ('threshold') of diffusion mobility in undeformed material. Solid solutions have a higher temperature of recrystallization than pure metals supposedly because deformed-matrix atoms in the former must cover an appreciably greater diffusion path for the growth of recrystallization nuclei. In the general case, however, recrystallization involves no differentiation of atoms of different kinds. Statistically, atoms which have been in neighbouring positions in as-deformed material remain in the same positions in the recrystallized material too.

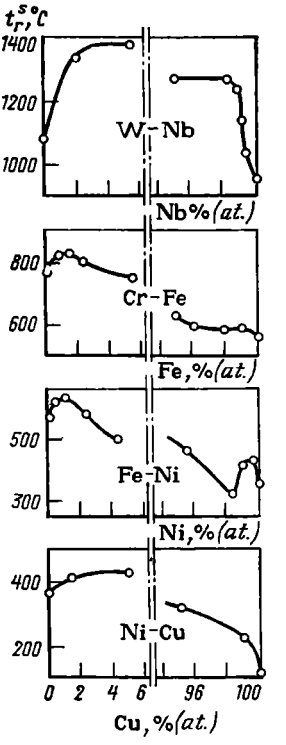

Fig. 154. Effect of mutually soluble elements on the temperature of the beginning of recrystallization

Smith [285] reduces the causes responsible for an increase in the temperature of recrystallization and a decrease in the rate of flow in alloys as against metals to the statement that impurities and alloying elements in a solid solution as a rule inhibit diffusion, though it is well known that alloying often gives an opposite effect.

We shall consider below the results of some experimental studies carried out to clarify the question whether there is a unique correlation between the diffusion mobility in undeformed state and the temperature level of primary recrystallization.

In this respect, it is interesting to analyse the results for six alloys of the Fe-Co system given in Table 24.

The diffusion coefficients of the two elements, Fe and Co, were determined by the 'imprint' technique [170] at 875°C on 35/65 and 15/85 alloys; at the temperature indicated, the former has a b.c.c. lattice and the latter an f.c.c. lattice.

For alloys with a closer packed lattice (f.c.c.), the coefficient of ^{60}Co turned out to be only 0.06 and that of ^{59}Fe, 0.32 of their respective values in b.c.c. alloys.

Yet, the results in Table 23 show that t_r^s is only slightly dependent on the type of crystal lattice and on the composition of single-phase alloys of the Fe-Co system. For instance, t_r^s of α-lattice alloys, which contain 25 to 99% Fe, varies in the experiments only from 560° to 575°C.

Thus, the diffusion mobility decreases sharply with a change from b.c.c. to f.c.c. alloys, but the rate of recrystallization diminishes only insignificantly. This can obviously be attributed to an opposite effect of some other factors.

Among the other factors which can influence recrystallization, the most important ones are the variations in the strength of interatomic bonds and in the structure of alloys in the deformed state.

The estimates of $m\theta^2$ (proportional to the quasi-elastic force f, which returns deviated atoms to their normal positions in lattice sites) show that the strength of interatomic bonds in f.c.c. lattices is markedly higher than that in b.c.c. lattices (see Table 24). Con-

TABLE 24. Values of D_{Co}, D_{Fe}, t_r^s, θ and $m\theta^2$ for Various Fe-Co Alloys

Alloy composition (Fe/Co)	Phases	D^*_{Co}, $(cm^2/s)\cdot 10^{10}$	D^*_{Fe}, $(cm^2/s)\cdot 10^{10}$	t_r^s, °C	θ, K	$m\theta^2$, $K\cdot(^\circ C)^2$
5/95	γ	—	—	585	360	7.7
15/85	$\alpha+\gamma$ (up to 770°C) γ (above 770°C)	10.9	5	665**	365	7.9
25/75	α (up to 700°C) γ (above 900°C)	—	—	560	—	—
30/70	α	—	—	505	340	6.5
35/65	α	175	15.5	—	325	6.0
99/1	α	—	—	575	—	—

* At 875°C.

** The sharp rise of t_r^s of the γ-phase in 15/85 alloy is associated with a special phenomenon — veiling of recrystallization by decomposition of the solid solution — and has no relation to the problem considered.

sequently, in view of this difference in interatomic bonds too, f.c.c. alloys might be expected to have a noticeably higher value of t_r^s than b.c.c. alloys.

A different result was obtained by comparing the processes of strain-induced hardening in alloys of various lattices. This comparison indirectly characterizes the differences in structure changes caused by deformation. After a 60-% deformation, a b.c.c. alloy was hardened by a factor of 1.83 and an f.c.c. alloy by a factor of 3.17.

The higher hardenability of f.c.c. alloys agrees well with the data in Ch. 2 and is associated with impeded dynamic recovery and a lower number of slip systems, and therefore, with a higher dislocation density, less uniform distribution of dislocations, and their higher local misorientations.

These factors facilitate recrystallization in f.c.c. alloys and thus compensate (to some extent or other) the opposite effect due to the lower diffusion mobility.

The comparative results obtained for nickel and nichrome (13% Cr), which have the same type of lattice, are also indicative of a distinct correlation between the strain-hardening effect during deformation and the temperature level of recrystallization. The diffusion mobility is lower in nichrome and higher in nickel. Nichrome has a higher hardness in the original state, but nickel is strain-hardened more intensively. With a change from 10-% to 40-% deformation, the gain in hardness is 35 HRB for nickel and 20 HRB for nichrome.

The temperature of the beginning of recrystallization in this interval of deformations drops by 175°C for nickel and only by 100°C for nichrome.

The results of analysis of the relationship between D and t_r^s for a number of pure elements and their binary alloys have also shown that there is no definite correlation between the effect of alloying on diffusion mobility, on the one hand, and the susceptibility to recrystallization, on the other.

An analysis of t_r^s in various binary alloys of the systems Cu-Ni, Cu-Al, and Fe-Ni [1] and a similar analysis of the diffusion coefficient and activation energy of diffusion in these alloys [297] have shown that there is no strict correlation between the composition and diffusion in these alloys. This is seen most clearly when introducing minor additions, which always raise the temperature of recrystallization, but influence differently the diffusion coefficient D.

An addition of 1-4% (at.) of molybdenum and 1-2% (at.) of tungsten to iron increases almost twice the rate of self-diffusion and at the same time raises the temperature of recrystallization by 150°C and gives an increase in the effective activation energy of recrystallization.

Thus, it can be concluded that there is no definite correlation between the temperature level of recrystallization in alloys and the level of their diffusion mobility in non-deformed state.

When comparing the temperature levels of recrystallization of various alloys, the diffusion mobility can obviously be regarded as having the decisive role if the difference in diffusion mobilities of two alloys is a few orders of magnitude. With a lower difference, the effect due to diffusion mobility can be masked by the effects of other factors, in the first place, of the structure in as-deformed state and the surface energy (more strictly, grain-boundary energy).

It is also possible that the effect of alloying on the rate of diffusion in as-deformed alloy may be quite different to this effect in non-deformed state. Alloying can also influence the structure formed on deformation in such a manner that the difference in diffusion mobilities of two alloys due to the peculiarities of the structure will overbalance the difference in their diffusion mobilities in undeformed state. Unfortunately, there are virtually no experimental data on the diffusion in as-deformed metals and alloys.

The above discussion relates to the process of growth of recrystallization nuclei. As regards the temperature level of nucleation, there is even a smaller probability that it may be explained by diffusion mobility only.

Diffusion mobility is necessary to disturb the elastic equilibrium of dislocation arrays. The start of redistribution of dislocations and of nucleation depends however on the level of internal local stresses and on the mobility of dislocations.

The above-discussed viewpoints are inconsistent since they attempt to explain the complex laws of the effects of alloying on the temparature level of recrystallization by considering only their effect on a single characteristic.

This approach is unjustified in view of the complexity of the phenomenon and the multitude of factors which are essential for recrystallization.

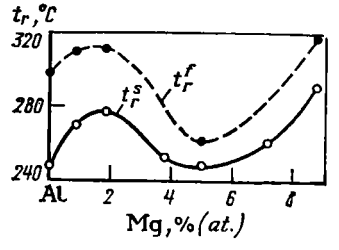

Fig. 155. Effect of Mg concentration on temperatures of the beginning and end of recrystallization in Al-Mg system (after V. I. Iveronova)

One of the earliest works where this idea was reflected was the systematic study of a few systems, such as Cu-Zn, Cu-Sn, Cu-Al, Al-Zn, Al-Mg in a relatively wide range of concentrations, carried out by V. I. Iveronova [14].

According to her results, the general relationship between the temperature of the beginning of recrystallization and the concentration of alloys is of a complicated nature (Fig. 155). At low concentrations of a second component, t_r^s rises sharply, then ceases to grow at a further

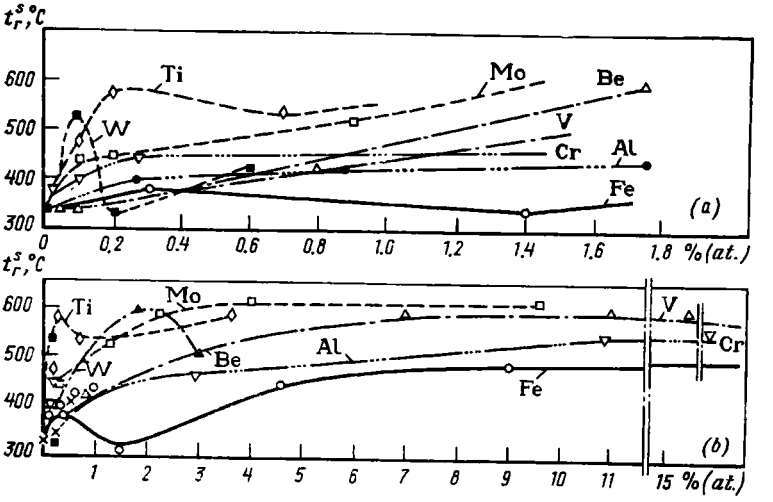

Fig. 156. Effect of concentration of elements on t_r^s in nickel-base binary alloys ($\varepsilon = 50\%$). Alloys with low (*a*) and high (*b*) concentration of second component

increase in concentration or even decreases somewhat. Another rise in t_r^s is observed in the range of high concentrations near the saturation of the solid solution.

In Iveronova's work, however, the number of alloys and systems analysed and the range of their compositions were not large enough to conclude definitely whether the established pattern of the variation of t_r^s is universal.

V. I. Iveronova put forwad an idea that the effect of alloying elements on t_r^s in alloys was due to a number of factors, the decisive role of each being dependent on the concentration of the solid solution.

At that time, however, it was impossible to draw convincing conclusions on the particular factor that determines the complex pattern of variations in t_r^s.

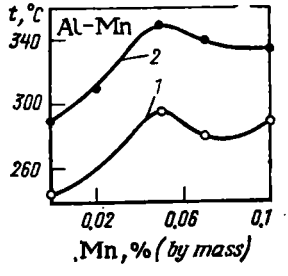

Fig. 157. Effect of Mn concentration on t_r^s (*1*) and t_r^l (*2*) in single-phase Al-Mn alloys ($\varepsilon = 50\%$)

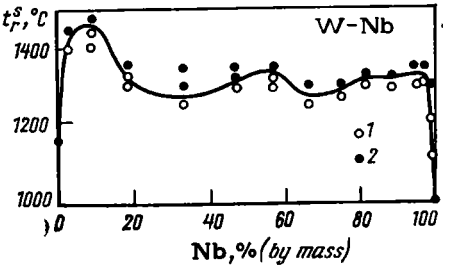

Fig. 158. Effect of Nb concentration on t_r^s in W-Nb system

1—no signs of recrystallization; *2*—signs of recrystallization

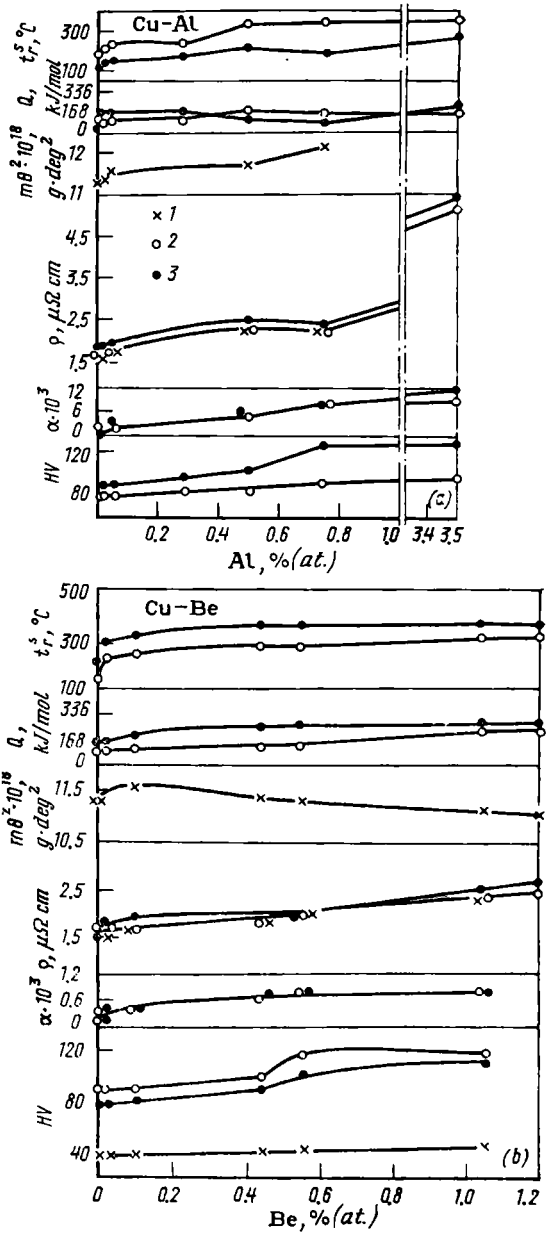
Cu–Al
t_r^s, °C
300
100
Q, kJ/mol
336
168
0
$mB^2 \cdot 10^{18}$, g·deg^2
12
11
× 1
○ 2
● 3
ρ, μΩ cm
4.5
3.5
2.5
1.5
α·10^3
12
6
0
HV
120
80
(a)
0.2
0.4
0.6
0.8
1.0
3.4
3.5
Al, %(at.)
Cu–Be
500
300
100
336
168
0
11.5
10.5
2.5
1.5
1.2
0.6
0
120
80
40
(b)
0
0.2
0.4
0.6
0.8
1.0
1.2
Be, %(at.)

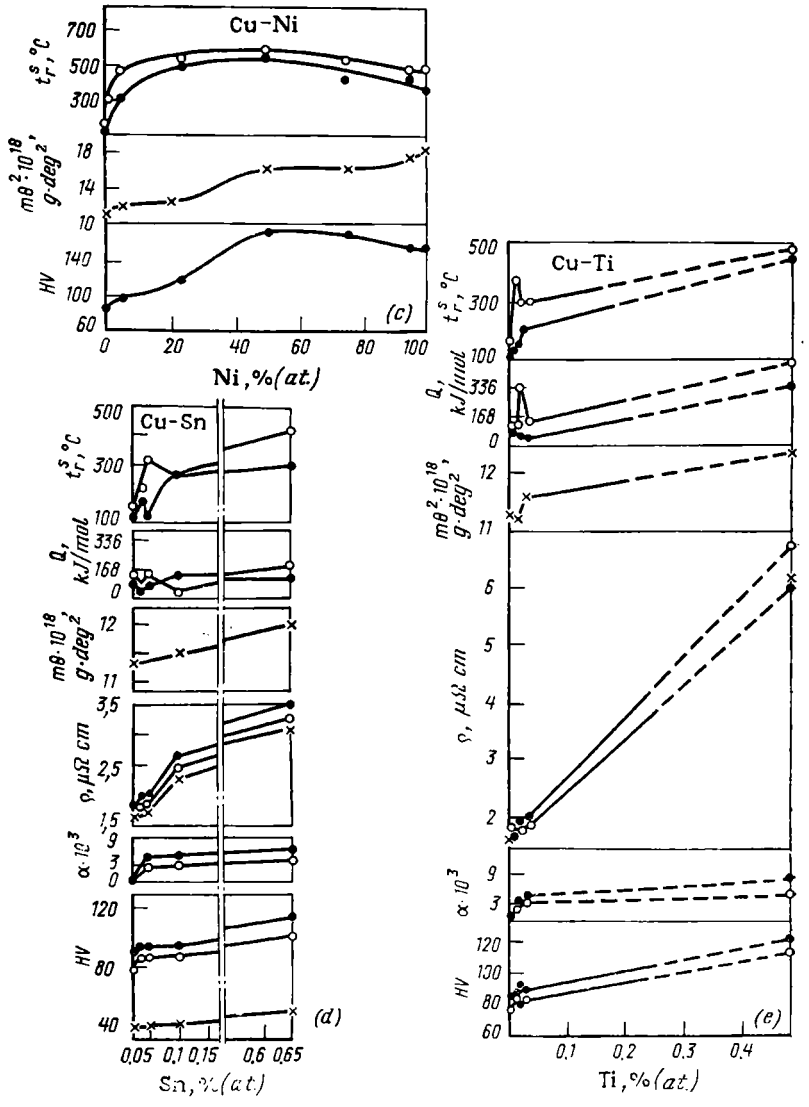

Fig. 159. Dependence of t_r^s, θ, $m\theta^2$, ρ, α and HV on the concentration of a second component in binary single-phase copper-base alloys

1—prior to deformation; *2*—after 20-% deformation; *3*—after 70-% deformation

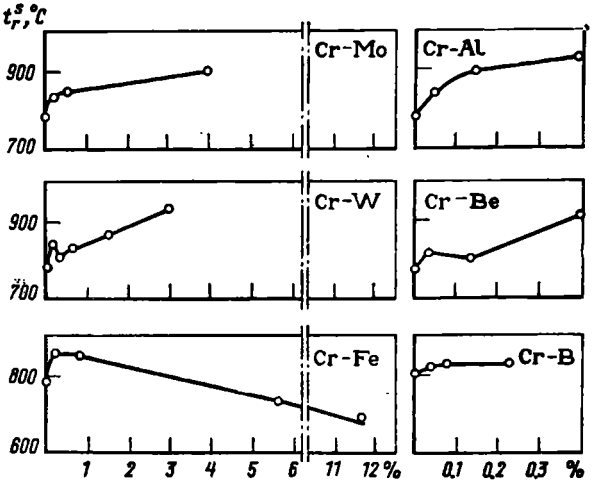

Fig. 160. Dependence of t_r^s on the concentration of a second component in two-component single-phase chromium-base alloys

Later, the progress in the theory of dislocations, as applied to the structure of deformed metals, provided a new approach to clarifying the mechanism by which alloying elements influence the rate and temperature level of recrystallization. Apart from the fact that alloying has an effect on the strength of interatomic bonds, the diffusion mobility and the energy of interfaces, also it exerts an influence on some other characteristics of alloys that are essential to the rate of recrystallization, such as the dislocation structure in as-deformed state, the distribution and density of dislocations, the stability of dislocation pile-ups, the rate and type of movement of dislocations and point defects during heating. It is quite probable that the effect of alloying on certain of these characteristics may be definitely prevailing in a particular range of concentrations.

This approach seems to be most suitable for understanding the effect of alloying on the tendency of alloys to recrystallization. In the further discussion of a number of works in the field we shall reason from this position. Figures 156-161 show the curves of t_r^s at various concentrations in binary alloys based on nickel (Fig. 156), aluminium (Fig. 157), tungsten (Fig. 158), copper (Fig. 159*a* and *b*), chromium (Fig. 160), and iron (Fig. 161). The pattern of these curves is in general similar to that established earlier by Burkhardt and Iveronova [14]*. Yet, the results obtained enable us to make certain amendments and explain the relationships found.

* The results for iron-base alloys at low concentrations are approximate in view of the low purity of iron used. At high concentrations, the results for iron-base alloys are quite reliable.

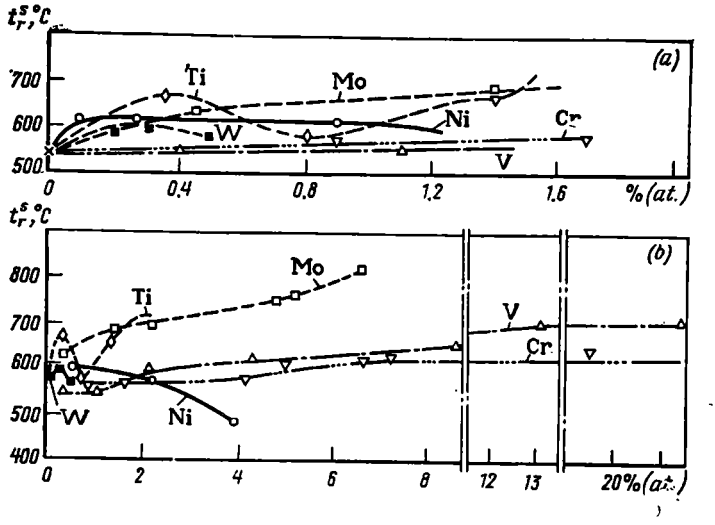

Fig. 161. Dependence of t_r^s on the concentration of a second component in two-component iron-base alloys

The differences in the regularities of variation of t_r^s in alloys with low and high concentration of a second component suggest a conclusion that the effects of minor and large additions on the temperature of recrystallization are due to different causes. In that connection, let us discuss separately the effects of minor and large additions on t_r^s.

11.3.1. Effect of Minor Concentrations of Impurities on t_r^s of Alloys

The effect of minor concentrations of impurities on t_r^s in single-phase alloys can be characterized by the following specific features.

Minor impurities never decrease the temperature of the beginning of recrystallization of the solvent (except in some special cases). In the majority of cases they raise that temperature and in rare cases they leave it unchanged.

The effect of various elements on t_r^s increase may be quite different. Low-soluble impurities raise t_r^s most heavily. A few hundredths of a per cent of such a substance can raise t_r^s by 200°C or even more (see the data for Cu-Be, Cu-Ti, etc.). With a high solubility and a low difference in atomic radii, minor additions have almost no effect on t_r^s.

The effect of minor additions also shows up in a sharp dependence of the temperature of recrystallization of a metal on the method of

melting. If melted in open air, a metal is saturated heavily with gases and its temperature of recrystallization greatly rises (see Table 25).

TABLE 25. Values of t_r^s and T_r/T_m for Some Metals Melted by Various Methods

Melting method	Ni		Fe		Cr	
	t_r^s, °C	T_r/T_m	t_r^s, °C	T_r/T_m	t_r^s, °C	T_r/T_m
In vacuum furnace	300	0.32	375	0.36	750*	0.45
In atmospheric induction furnace	550	0.45	500	0.45	790	0.50

* Cr remelted by crucibleless method.

The stronger the interaction of molten metal with gases, the higher quantity of an impurity dissolves under the same conditions of melting and the more difficult it is to lower the t_r^s to 0.25-0.30 T_m. This follows from the comparison of the data for chromium and other metals.

The effective activation energy of recrystallization, Q_{ef}, in the range of minor concentrations varies with the concentration and the degree of deformation in a complicated pattern and does not follow the variations in t_r^s. In contrast to pure metals and high alloys, Q_{ef} in low-concentration alloys often increases with the degree of deformation. In some low-concentration copper alloys, Q_{ef} turns out to be even lower than in pure copper. A similar effect has been found in aluminium on moderate deformations.

Complex alloying with several elements, each taken in a concentration corresponding to its first maximum on the t^s-%C curve (C being the concentration) usually raises t_r^s as much as does the addition of a single, strongest, impurity. This is also evident from the fact that the influence of minor additions on t_r^s of metals and alloys melted in open air is appreciably weaker than its influence on t_r^s of pure vacuum-melted metals.

The pattern of the t_r^s-% C curve changes with an increase in the concentration of the second component up to a few hundredths or, sometimes, a few tenths of a per cent (at.); t_r^s rises less intensively or does not rise at all, and in some systems it even decreases against its level at lower concentrations and then begins to rise again. This decreasing effect is stronger after moderate deformations. As a rule it is more distinct in systems where the first rise in t_r^s is especially high, i.e. in systems with low solubility of the second component

(Ni-Ti, Ni-W, Cu-Ti, Cu-Sn, Al-Mn, Fe-Ti, Fe-W, Cr-W, Cr-Be, etc.). In systems with high solubility (Cu-Al etc.), t_r^s drops less sharply and at higher concentrations.

Further, it is essential to determine in the analysis which of the two principal processes, whether the nucleation by redistribution of dislocations or the growth by boundary migration, is more subject to the effect of minor impurities and is decisive in increasing t_r^s.

Some workers [286-288] point to the complexity of experimental analysis of nucleation, but at the same time assume, without sufficient reason, that impurities mainly influence the processes of boundary migration, i.e. the processes of growth.

As has been noted earlier, the sharp increase of t_r^s with minor soluble impurities cannot be attributed to a change in the interatomic bonds and diffusion mobility of atoms or to the fact that the additions are horophile. It is most natural to suppose that the effect of small additions is associated with retardation of the formation and growth of recrystallization nuclei by the elastic and probably chemical interactions of impurity atoms with dislocations and boundaries.

Under the effect of elastic stress fields around dislocations, foreign atoms must tend to move into regions near dislocations and form there impurity atmospheres ('clouds'). According to Cottrell, the attraction of impurity atoms must be stronger at higher stresses around dislocations and, at the same time, at a higher difference in the radii of the impurity and solvent. Impurity atoms diminish the lattice distortion and the stress field forming a 'cloud' around dislocations and thus lower the mobility of dislocations. If this interaction occurs between impurity atoms and individual dislocations or dislocation arrays, it must exert its influence on the redistribution of dislocations, i.e. retard the formation of recrystallization nuclei.

The above conclusion (i.e. that minor impurities retard recrystallization mainly as a result of their elastic interaction with dislocations) can be confirmed by the results obtained in [98], which deals with the analysis of the effect of minor additions of aluminium and beryllium on recovery and recrystallization in pure copper. The compositions of the alloys used are given in Table 26.

As seen from the table, the differences in the atomic radii of aluminium and the base and of beryllium and the base ($\Delta R = R_{Cu} - R_{imp}$) are roughly equal in magnitude, but are of opposite sign. It is known however that the atomic (more strictly, ionic) radii can change substantially in the formation of solid solutions; this circumstance should be considered properly.

It should be noted, in passing, that some workers compare the values of Δt_r^s with the tabulated values of atomic radii taken for different coordination numbers, which is erroneous. Even the tabulated data taken for one and the same coordination number should

TABLE 26. **Effect of Minor Additions of Aluminium and Beryllium on Resistivity of Copper**

Alloy No.	Composition, % (at.)	ΔR_{tab}, Å	ΔR_{exp}, Å	ρ at 78 K, μΩ/cm	Δρ*
1	Cu (99.995%)	—	—	0.208	0.020±0.01
2	Cu+0.04% Al	+0.15	+0.09	—	—
3	Cu+0.02% Al	+0.15	+0.09	0.449	0.020±0.01
4	Cu+0.04% Be	—0.14	—0.11	—	—
5	Cu+0.2% Be	—0.14	—0.11	0.399	0.022±0.01

* Upon 14-% deformation.

be used with much care. A more correct method is to use the actual or effective atomic radii and experimentally found values of ΔR_{exp}.

Along with tabulated values of ΔR_{tab}, Table 26 also gives experimental values of ΔR_{exp} as determined in [112]. The difference between the two is quite large. For instance, the absolute value of ΔR by tabulated data for beryllium is somewhat lower than that for aluminium, whereas the effective value of ΔR_{exp} for beryllium is even higher than that for aluminium.

Apart from the analysis of the pattern of distribution of microdeformations, the size of coherent scatter regions, and the onset of recrystallization, studies were also made of the variation of the cold-deformation induced gain in resistivity after annealing $(\rho_{an} - \rho_r)/(\rho_d - \rho_r) = \Delta\rho/\Delta\rho_0$. The corresponding results for copper and its alloys (alloys 3 and 5) are given in Table 26.

Figure 162 shows variations in $\Delta\rho$ $\Delta\rho_0$ of the tested materials after annealing at various temperatures. Arrows indicate the temperatures of the beginning of recrystallization (t_r^s) as determined by radiographic analysis.

The values of t_r^s are given below; it is also shown how the strain-induced resistivity gain $(1 - \Delta\rho/\Delta\rho_0) \cdot 100\%$ decreases by the moment of beginning of recrystallization

Alloy No. (see Fig. 162)	1	2	3	4	5
t_r^s, °C (τ = 40 min)	120-140	180-200	180-200	220-240	240-260
$(1 - \Delta\rho/\Delta\rho_0) \cdot 100\%$	7.5-10	11-12.5	7.5-10	15.5-20	25.5-37

Minor additions of beryllium retard the onset of recrystallization in copper much more strongly than do aluminium additions. In copper-beryllium alloys the strain-induced resistivity gain decreases by the beginning of recrystallization much more strongly than in

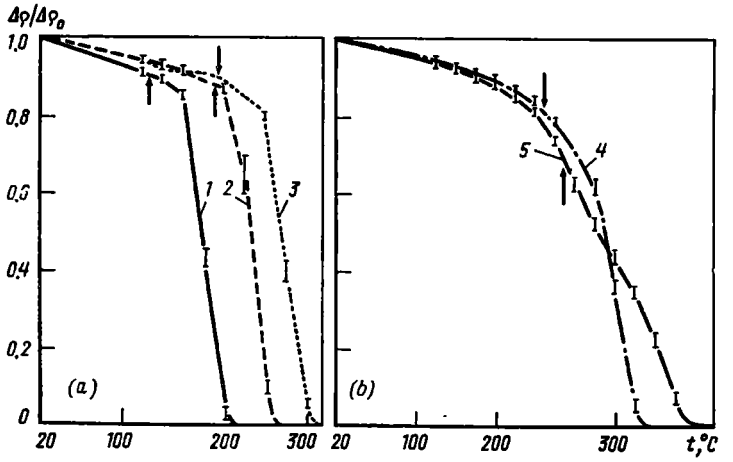

Fig. 162. Variations of the strain-induced gain in resistivity during heating of copper and copper-base alloys. Numbers at curves are numbers of alloy grades (see Table 26)

copper-aluminium alloys (by about 30% in alloy 5 and roughly 10% in alloy 3, Table 26). This means that at the moment of appearance of first recrystallized regions the total decrease in the concentration of defects in copper-beryllium alloys is roughly three times that in copper-aluminium alloys.

The curves of $\Delta\rho/\Delta\rho_0 = f(\tau)$ for Cu + Al alloys have two characteristic portions. The first portion is associated with the loss of resistivity during recovery and the second during recrystallization. These portions are separated by an interval representative of an attenuation in the resistivity drop at the end of recovery.

In Cu + Be alloys, resistivity decreases more smoothly, and the two portions are not seen distinctly.

X-ray structural analysis has shown that no substantial redistribution of dislocations occurs in Cu + Al alloys before reaching the temperature of the beginning of recrystallization. This redistribution starts and develops quickly only immediately before the onset of recrystallization and causes a jumpwise change in the pattern of distribution of microdeformations and enlargement of coherent scatter regions d_{coh}.

In Cu + Be alloys, slight variations in the dislocation structure and a slight increase of d_{coh} are also observed at temperatures below t_r^s, but in this case too a jumpwise enlargement of d_{coh} takes place at the level of t_r^s.

These results can be interpreted as follows. Dislocations and low-angle boundaries surrounded by foreign-atom clouds can move either

after detachment from their clouds or together with these clouds by way of diffusion.

For the examined range of concentrations of aluminium and beryllium in copper, the coefficient of diffusion of aluminium at 200°C turns out to be two orders of magnitude smaller than that of beryllium ($1.3 \cdot 10^{-19}$ and $2.3 \cdot 10^{-17}$) [289]. Therefore, in 40 min at 200°C a dislocation with a cloud of aluminium atoms can move a distance of around 2 Å, i.e. it virtually remains immobile, whereas a dislocation with a cloud of beryllium atoms will move through 100 Å and even approximately 0.5 μm at 260°C.

Thus, if dislocations moved together with clouds, the temperature of the beginning of recrystallization in Cu-Al alloys would be higher than in Cu-Be alloys. Experiments, however, prove that the reverse is true. It can be assumed therefore that the formation of recrystallization nuclei by redistribution of dislocations occurs in Cu-Al alloys after detachment of dislocations and low-angle boundaries from impurity-atom clouds. This detachment becomes possible at a temperature near 200°C.

In Cu-Be alloys, say, Cu + 0.2% Al, where the diffusion mobility of beryllium is high, the movement of dislocations together with the surrounding clouds of beryllium atoms becomes possible at a temperature below t_r^s. This point is confirmed by X-ray analysis; it enables one to detect at slight increase in the size of coherent scatter regions and in the redistribution of microdeformations, and also a slightly more intensive drop in resistivity before the onset of recrystallization, as compared to Cu-Al alloys.

In Cu-Be alloys, as in Cu-Al alloys, the beginning of recrystallization proper is obviously determined by the slip and climb of free dislocations. This is confirmed by the jumpwise change in microdeformations and coherent scatter regions at the temperature of the beginning of recrystallization.

Therefore, the retarding effect of impurities on recrystallization in copper is mainly associated with a delay of the stage of nucleation, but not of the stage of growth of nuclei by boundary migration, as has been postulated in [286-288].

Smart and Smith [20], who were the first to study the effect of minor additions on the kinetics of recrystallization in pure metals, analysed the effect of soluble impurities on the temperature at which the deformation-induced hardness increment decreases by half (they took this temperature as that of the beginning of recrystallization) and on resistivity in copper. They detected a distinct correlation between a rise in the temperature of recrystallization due to an impurity and the difference in atomic radii of the base and impurity. They also noted some exceptions from the general rule.

The correlation between Δt_r^s and the difference in atomic radii has been confirmed by a number of later studies.

Figure 163 gives data on the rise in recrystallization temperature by minor additions as a function of the absolute difference in atomic radii (tabulated and effective) between the base and addition for a large group of nickel, copper, chromium, and iron alloys. As may be seen, ΔR_{ef} follows more accurately a linear relationship.

Yet, as in the work of Smart and Smith, one can see noticeable deviations from the linear law. These deviations relate to the elements which, despite a high value of ΔR, are readily soluble in the matrix (up to 10% or more, for instance, aluminium in copper or copper in nickel). These deviations are still greater as regards the elements whose atomic radius is appreciably smaller than that of the solvent (for instance, beryllium in copper, beryllium in nickel).

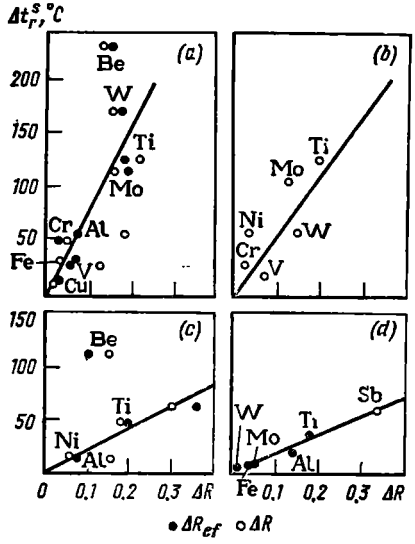

Fig. 163. Correlation between Δt^s_r (the rise of the temperature of beginning of recrystallization of pure metals upon alloying with minor additions) and the absolute difference $|\Delta R|$ of the atomic radii of the base metal and additions. The base is

(*a*) nickel; (*b*) iron; (*c*) copper; (*d*) chromium

Back in 1930, A. A. Bochyar and N. E. Merkuryev, in studying the susceptibility of tin-base binary solid solutions to recrystallization, found a certain correlation between the recrystallization retarding effect produced by an impurity and the solubility of that impurity. The elements of lower solubility in tin showed a stronger retarding effect. This correlation was later confirmed by many workers.

V. I. Elagin [18] analysed the effect of minor additions of transition metals of groups IV and V on t^s_r in commercial aluminium (Grade A7). He found that impurities of low-soluble metals (Zr, Fe, Cr, etc.) increased t^s_r most heavily. The effect of these impurities was higher at a higher difference in the atomic radii of the impurity and aluminium, especially when an impurity had a greater radius. The only exception was nickel which is poorly soluble in aluminium and does not form in it a supersaturated solid solution. Additions of nickel had practically no effect on t^s_r in aluminium.

Olsen [290] analysed the effects of a large group of impurities on the temperature level of recrystallization in high-purity nickel (99.9%). The group included readily soluble elements (Co, Mn, W), limitedly soluble (Si, Ti, Al), and poorly soluble (C, Mg, B, Zr).

The elements of the last group, especially zirconium and magnesium, had the highest effect on t_r^s in nickel (Table 27). A low solubility, especially when complemented by a large difference in atomic radii ΔR, probably serves as an additional stimulus for the movement of impurity atoms into defective portions of the lattice, which thus increase t_r^s most markedly. With a high solubility, the tendency

TABLE 27. **Effect of Low Concentrations of Dissolved Impurities on Recrystallization in Nickel**

Impurity	ΔR, Å	Maximum solubility, % (at.)	Δt_r^s, °C	Drop of t_r^s after maximum, °C
Cu	+0.020	100	10	—
Mn	+0.037	30	50	—
Co	+0.051	30	40	40
V	+0.062	25	20	—
Al	+0.057	10	60	—
Mo	+0.163	10	100	—
Be	−0.150	5	250	100
W	+0.182	4	100	150
Ti	+0.177	4	250	60

of impurity atoms to move into portions near dislocations and boundaries is appreciably less strong. Even in low concentrations, these atoms easily dissolve in the volume of crystallites too. For that reason, t_r^s in that case rises less steeply to the first maximum.

These considerations are obviously applicable also to systems Ni-Al, Ni-Cu, Cu-Al, etc.

The data given in Table 27 illustrate the above discussion of the effect of solubility on the change of t_r^s in the range of low concentrations of impurities.

Thus, there is a definite correlation between the solubility of a given element in a solvent and its effect, in low concentrations, on increasing the temperature of recrystallization in the solvent.

The effects of minor additions on t_r^s cannot, however, in all cases be attributed to their solubility, as may be seen from the above-discussed example of beryllium dissolved in copper or nickel since its atomic radius is 11-13% smaller than that of these elements.

Beryllium has even a stronger influence on t_r^s than titanium, though the solubility of beryllium in nickel is somewhat higher than that of titanium, and $|\Delta R_{Ti}| > |\Delta R_{Be}|$ (see Table 27). Besides, the range of concentrations of berrylium within which it sharply raises t_r^s of a solvent (Cu, Ni) is wider than it is for other elements.

Apart from raising t_r^s, an addition of 0.1% Be to copper causes a higher increase in the effective activation energy of recrystallization than the additions of other elements with the atomic radius greater than that of copper (Ti, Sn, Al). In contrast to these elements, beryllium in a concentration up to 0.1% does not raise the resistivity after heavy deformations (see Fig. 159). With an addition of beryllium up to 0.1%, the intensity of variations in the lattice spacing of the solution is initially low, but then increases with concentration. An inverse phenomenon is observed with titanium, aluminium and tin.

There are not yet enough experimental data for a definite interpretation of these effects. It may be assumed that, apart from the elastic interaction of impurity atoms with dislocations on addition of beryllium, there also occurs a chemical interaction, i.e. the formation of Suzuki atmospheres on dissociated dislocations.

Suzuki atmospheres require a higher concentration of impurity atoms for saturation than Cottrell atmospheres. Besides, Suzuki clouds form more easily when an impurity differs from the matrix not only in valency but also in the type of lattice. These conditions are met, for instance, when f.c.c. copper or nickel is the matrix and hexagonal beryllium is the impurity.

Rolling and Winegard [291] analysed the effect of minor impurities (10^{-3}-10^{-2}) on grain growth in zone-refined lead and proved that the retarding effect of tin, silver and gold on grain growth increased in the sequence from tin to gold. Thus, in the case considered, the effect of an impurity was proportional to the difference in atomic radii. But this conclusion proved valid only at relatively low temperatures. At temperatures close to the melting point, the rate of grain growth in all these alloys was roughly the same.

R. H. Harrington [292] studied the combined effect of minor impurities on the rate of nucleation and growth during recrystallization. In particular, he analysed the effects of silver, copper, titanium, chromium, manganese, iron, nickel, zirconium, silicon, magnesium, and beryllium in concentrations of a few fractions of a per cent on the temperatures of the beginning and end of recrystallization in aluminium. The t_r^s was 250°C in pure aluminium, 460°C in an Al + 0.1% Fe alloy, 550°C in Al + 0.3% Be alloy, and 600°C in Al + 0.32% Zr alloy. These impurities had roughly the same effect on the temperature of the end of recrystallization.

The results considered above are as a rule indicative of a retarding effect of impurities on the formation of recrystallization nuclei. Enormous experimental data prove beyond doubt that impurities also inhibit the migration of boundaries of recrystallization nuclei and of grains in general.

Aust and Rutter [182] have found that one atom of tin per million atoms of lead diminishes the boundary migration in the latter

roughly by a factor of four. Additions of silver and gold to lead have even a stronger effect.

The effect of impurities on boundary migration depends in a rather complicated manner on many factors such as the type of boundary, the boundary mobility and the driving force of migration, the type and concentration of impurity, the rate of diffusion of impurity in the matrix, the temperature of the process, etc.

The problem has been analysed theoretically by Lücke [74] and later by Cahn [64].

The model proposed by K. Lücke is based on the assumption that there exist interaction forces between atoms of a dissolved impurity and the boundary which separates a growing recrystallization nucleus from the deformed matrix (in primary recrystallization) or one grain from another (in grain growth).

As with impurity atmospheres around dislocations, the energy gain that stimulates this interaction increases the concentration of an impurity on a boundary. This concentration C_b is determined by the expression $C_b = C \exp(\Delta U/kT)$, where ΔU is the energy gain on transition of a foreign atom from the bulk of a crystal to its boundary. By Lücke, ΔU is close to 0.1 eV (2.2 kcal g-atom).

In the absence of impurities, the rate of migration is controlled by boundary diffusion. Atoms of the matrix move through distances which are fractions of the interatomic spacing. In the presence of impurities, however, foreign atoms in the boundary layer of a nucleus will be within the grain at the beginning of migration, which will increase the total free energy. To prevent this, the diffusion of impurity atoms must follow the migration of a boundary. The mobility of that boundary will be controlled not by the boundary diffusion, as in pure metals, but by a slower process of volume diffusion of foreign atoms. The rate of movement of a boundary then is

$$v = (D_0/\delta T) \exp[-(U_D + \Delta U)/kT]$$

where δ is the thickness of the boundary, and U_D is the activation energy of volume diffusion.

With rising temperature, clouds of impurity atoms are scattered gradually due to enhanced thermal motion and ΔU accordingly decreases. As U_D changes to U_b, the retarding effect of the impurity on the boundary decreases or disappears.

Experimental data, however, were not always in good agreement with this. For instance, the results obtained in [291, 294] agree quite well with this assumption, but those given in [295], do not.

In [294], the authors analysed the effect of minor concentrations of impurities on recrystallization in tin. The distribution of minor additions of ^{110}Ag in as-cast and recrystallized tin was determined by autoradiographic methods. It was found that, irrespective of the total content of silver (either above or below the solubility limit,

0.02%), the ^{110}Ag isotope was concentrated after recrystallization on boundaries of grains and subgrains.

A different result was obtained by S. Z. Bockstein and S. T. Kishkin [295] in their analysis of grain growth in iron enriched with radioactive carbon on grain boundaries. After annealing at 650°C for 40 minutes, a network of new boundaries was detected metallographically, whereas autoradiographic analysis showed that carbon remained in places of old boundaries. After annealing at 700°C for 30 minutes, part of the carbon moved by diffusion to new boundaries, but another part remained in the initial positions. After annealing at 750°C for 1 h, almost all the carbon moved by diffusion to new boundaries.

These results naturally suggest that, with impurities concentrated on grain boundaries, two extreme cases of migration of these boundaries are possible: either a boundary drags behind impurity atoms and then the rate of its movement is limited by the rate of diffusion of impurity atoms, or, if the driving force of boundary migration is very high and exceeds the retarding effect of the impurity, a boundary 'detaches' from the impurity atmosphere and moves in the same manner as in the absence of 'atmospheres'.

It is then clear that the retarding effect of an impurity, all other conditions being the same, is proportional to its concentration (before the 'saturation' of a boundary). Accordingly, the driving force to detach a boundary must diminish as the concentration of the impurity decreases below the saturation concentration.

In view of the foregoing, the rate of boundary migration can be determined as $v = M(P - P_i)$, where M is the boundary mobility, P is the driving force of migration due to the gain in energy of the system offered by boundary movement, and P_i is the retarding force caused by impurity atoms in an 'atmosphere'.

The value of P_i is determined by the forces of interaction between the impurity and boundary and by the impurity concentration.

K. Lücke and R. Stüwe [74] and also R. Cahn [64] have proposed expressions to determine the rate of boundary migration in the two extreme cases mentioned.

The expression for v can be rewritten as $P = v/M + P_i$. In the general case, $P_i = \alpha Cv/(1 + \beta^2 v^2)$, where α is a parameter depending on variation in the energy of interaction between a boundary and impurity atoms and on the diffusion mobility of impurity atoms, which in its turn depends on the distance from the impurity atom to the boundary; β is the reciprocal of the average rate of diffusion of impurity through a boundary; and C is the concentration of impurity.

For sharply different rates of migration, the dependence of the rate of boundary migration v on the driving force and the concentration of impurity is expressed, according to R. Cahn, as follows.

1. A *low rate of boundary migration.* This can take place at a low driving force P and/or a high concentration of an impurity. Then

$$v = P/(1/M + \alpha C)$$

It follows from this expression that, with a low rate of boundary migration in an alloy of a given composition, the rate v is proportional to the driving force P and that an increase in the concentration of impurity lowers v by a linear law. The concentration of impurity at the boundary is higher (compared to its value in the bulk of grain) at a lower diffusion mobility. Impurity atoms with a lower rate of diffusion retard boundary migration more strongly.

The activation energy of boundary migration may vary in a range from the activation energy of volume diffusion of impurity to the sum of activation energies of the boundary diffusion and the adsorption of the impurity on the boundary.

2. A *high rate of boundary migration*, i.e. a high driving force and/or a low concentration of impurity. Then

$$v = PM - (\alpha/\beta^2)\,(C/P)$$

where the coefficient α/β^2 is proportional to the diffusion rate.

Therefore, at a high rate of migration, v ceases to be proportional to the driving force (except for cases of a very high P or a very low C, when the second term becomes negligible). The relative concentration of the impurity on a boundary is higher at a higher rate of diffusion of the impurity. Impurity atoms with a higher rate of diffusion can retard boundary migration more strongly.

In this case the activation energy of boundary migration is close in magnitude to the activation energy of boundary self-diffusion.

Thus, the effect of increasing temperature of recrystallization produced by minor concentrations of impurities is associated with the retarding effect on the formation of recrystallization nuclei and on the rate of their growth, and is quite complicated in its nature. This complexity is not however exhausted by the examples considered earlier. All those examples relate only to cases where t_r^s of the solvent is raised by minor additions of an impurity. As has been noted earlier, however (see p. 358), in some rare cases an increase in the impurity concentration up to a few hundredths or sometimes a few tenths of a per cent (at.) gives a less intensive rise of t_r^s compared with lower concentrations or, in some systems, can even diminish the value of t_r^s. At higher concentrations, t_r^s then rises again. In such cases, there is a maximum in the region of low concentrations on the t_r^s-concentration curve (see Figs. 156 and 161). This maximum is more distinct after moderate deformations.

The mechanism by which t_r^s drops after reaching its maximum is still not clear. According to some indirect features, it can be assumed to be associated with the dissolution of an impurity in the bulk of

grains, and therefore with its influence on the structure in as-deformed state.

Indeed, if we take it that the first rise in t_r^s is due to the interaction of impurities with dislocations, this effect should be exhausted as soon as the regions near dislocation clouds are saturated with impurity atoms. A further increase in the impurity concentration will result in the dissolution of impurities in the bulk of crystallites (blocks), and this in turn must change the pattern of the concentration-t_r^s relationship.

For copper alloys, the correlation between the bend on the t_r^s-C curve and the beginning of dissolution of impurity atoms in the bulk of grains was examined by measuring the resistivity. A very good coincidence was found for alloys of the Cu-Sn system (see Fig. 159*d*). The bend on the t_r^s curve coincided accurately with the sharp increase in ρ after changing the concentration from 0.015% to 0.025% Sn. With alloys of the Cu-Al system, the correlation was less evident (see Fig. 159*a*); the resistivity increased noticeably already on adding 0.01% Al.

Alloys of th Cu-Be system are of a special case (Fig. 159*b*). At concentrations up to 0.1%, beryllium has no effect on the resistivity (at room temperature) of annealed and deformed (70%) copper, though a bend on the curve $t_r^s = f$ (% Be) is noticeable at very low concentrations of beryllium (0.01%).

For nickel alloys, the correlation between the bend of the curve $t_r^s = f$ (% x) and the start of marked dissolution of the impurity in the bulk of grains was examined by radiography*. The coincidence was quite good for the systems Ni-W and Ni-Ti and less distinct for Ni-Mo and Ni-Al.

These deviations established for nickel and copper alloys are obviously associated with a large number of factors which can influence the distribution of minor impurities between defective portions of the lattice and the bulk of grains, and therefore can vary the pattern of the t_r^s-C relationship.

The general relationship seems to be as follows. At a lower equilibrium solubility, impurities are dissolved preferably in defective places. As soon as these are saturated, new portions of the impurity will be distributed over the bulk of grains and the rise of t_r^s will be stopped or slowed down.

---

* The work has been carried out with the use of the effect employed more than once by V. I. Arkharov [296]. The effect consists in the following. The lattice spacing of the solution in alloys with minor additions of horophilic impurities depends on the size of grains. With fine grains and a large total extent of grain boundaries, all impurity atoms occupy positions in boundary regions (intercrystalline joints) and have almost no effect on the lattice spacing of the solvent. With larger size of grains, more and more impurity atoms are dissolved in the bulk of grains and the lattice spacing of the solvent changes respectively.

Thus, many experimental, though indirect, data enable us to assume that a bend of the curve $t_r^s = f(\% x)$ after the first maximum is associated with the saturation of regions near dislocations by impurity atoms. The concentration of impurity corresponding to that bend is determined by the equilibrium solubility of the impurity and by the nature of its interaction with lattice defects.

The mechanism of the reduction of t_r^s after that bend is less clear. There is much evidence that alloying of copper or nickel-base systems almost always lowers the stacking fault energy. This, however, must inhibit dynamic recovery and thus facilitate subsequent recrystallization. Therefore, the drop of t_r^s can be associated with a particular concentration of dissolved foreign atoms at which a decrease in γ_{sf} has a stronger effect on t_r^s than the interaction of impurity atoms with lattice defects.

The theory of the effect of alloying on the stacking fault energy has not yet been developed thoroughly and only the experimental results are reliable.

The concentration of stacking faults, α, was determined radiographically for a few systems of copper-base alloys (Cu-Al, Cu-Be, Cu-Sn, Cu-Ti), in which recrystallization was also analysed. It was assumed that the concentration of stacking faults was higher at a lower stacking fault energy. The value of α was determined by using the effect of displacement of interference maxima, which is typical of stacking faults only [68].

In pure copper, the stacking fault concentration was so low that stacking faults could not be revealed by the method employed. For that reason, α of pure copper was taken equal to zero. The results of calculation and the data on the measured temperatures of recrystallization and hardness at various concentrations are given in Fig. 159.

As may be seen from the figure, minor additions of all the four elements (Al, Be, Sn, and Ti) increased somewhat the concentration and stability of stacking faults, i.e. decreased their energy, which agrees well with the available literature data. The variations in hardness in as-deformed state followed quite accurately the variations in α.

In the systems Cu-Al and Cu-Be (Fig. 159*a*) there was a distinct correlation between the patterns of variation of α and hardness and the drop of t_r^s.

In alloys of the systems Cu-Sn and Cu-Ti, the correlation between the variations of α, HV, and t_r^s was less distinct.

The principal result obtained with the Cu-Al and Cu-Be systems is that the drop of t_r^s after the first maximum is obviously caused mainly by specific structural changes in deformed metal with an increase of the concentration of the alloying addition. With f.c.c. alloys, this is clearly associated with a decrease in the stacking fault

energy and an increase in the concentration of stacking faults, which results in impeded cross-slip at heavy deformations, a different distribution of dislocations, and a stronger strain-hardening effect.

The fact that the correlation between t_r^s and hardness and α is less distinct in alloys with low solubility of an impurity can be explained by a more intensive effect of other factors, such as variations in the forces of interatomic bonds, the formation of segregates by ascending diffusion, etc. These factors will be later discussed in more detail.

Finally, it is reasonable to mention still another factor which can promote the drop in t_r^s after the first maximum. When the concentration of an impurity becomes sufficient for saturation of defects, its further rise in the whole volume of grains can weaken the locking of dislocations and boundaries by 'clouds' of impurity atoms, since this decreases the difference of impurity concentrations in defective and more perfect regions of the lattice.

11.3.2. Effect of High Concentrations of Impurities on t_r^s in Single-phase Alloys

The dependence of t_r^s on the composition of single-phase alloys in the region of high concentrations can be characterized as follows.

In contrast to minor concentrations, with a large quantity of a second element dissolved in the matrix, t_r^s of the matrix can either rise or drop. A decrease in t_r^s takes place if the melting point of the dissolved element is lower than that of the solvent. This effect is observed in chromium with 6-12% Fe (Fig. 160), in iron with 4% Ni (see Fig. 161), etc.; in these cases, t_r^s of the alloy turns out to be lower than that of the solvent.

The change in t_r^s on addition of one per cent (at.) of a second element is very low, a few degrees or, more rarely, a few tens of degrees, against hundreds of degrees in the region of low concentrations. If the single-phase region of a solid solution can exist within a wide range of concentrations, t_r^s of the alloys in that region remains practically invariable with a change in the concentration of the dissolved element by 5-10% (at.) or more. Examples are alloys of the systems W-Nb (see Fig. 158), Ni-Cr, Ni-Mo, Ni-Fe, Ni-V (see Fig. 156), Cu-Al (see Fig. 159*a*), Fe-Cr, Fe-V (Fig. 161), etc.

Exceptions from this rule are alloys with a composition close to the solubility limit (see alloys of the systems Ni-Ti and Ni-Mo in Fig. 156 and Fe-Mo in Fig. 161), and also single-phase alloys with an equiatomic or, in general, a multiple proportion of the components (see alloys of the systems W-Nb, Fig. 158 and Cu-Ni, Fig. 159*c*). These alloys are characterized by an intensive rise of t_r^s.

The intensity of the rise in t_r^s produced by various additions is different. As a rule, the elements which show a greater difference

in valency or have an appreciably higher melting point than that of the matrix cause a more intensive rise in t_r^s.

In nickel-base alloys, the lowest effect on t_r^s is produced by iron and cobalt, and the highest by the elements of groups IV, V, and VI (molybdenum, titanium, vanadium, chromium, etc.).

The temperature of recrystallization of chromium in single-phase state is changed only weakly by iron and boron and sharply by tungsten, molybdenum and aluminium. Accordingly, additions of

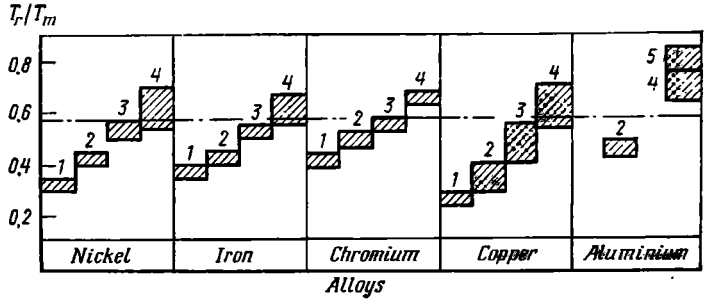

Fig. 164. Relative temperature levels of recrystallization of selected metals and their alloys

1—high-purity metal; *2*—commercial-purity metal; *3*—single-phase alloys; *4*—age-hardening alloys; *5*—sintered aluminium powder with Al_2O_3 oxides (SAP)

molybdenum and vanadium influence intensively the temperature of recrystallization, t_r^s, in iron, while chromium has a negligible effect.

In contrast to low-concentration solid solutions, in single-phase alloys there is a more distinct correlation between the pattern of variations of t_r^s and the effective activation energy.

In high-concentration solid solutions, t_r^s is practically independent of the method of melting (either vacuum melting or open-air melting), as may be seen from the data on t_r^s in Ni-Cr alloys.

The T_r/T_m ratio increases from 0.35-0.45 in commercially pure metals to 0.5-0.58 in high-concentration solutions (Fig. 164 and Table 29). Experiments were carried out on a large group of single-phase alloys in order to check whether it is possible to obtain a higher T_r/T_m ratio by complex alloying with several elements (Table 28).

For all the alloys tested, the T_r/T_m ratio was not higher than 0.58, i.e. was close to 0.6, the value that was indicated by A. A. Bochvar [298] as the temperature limit of strain-hardened state in single-phase solid solutions.

It can be stated that the main effect on changes of t_r^s in high-concentration alloys is due to variations in the strength of interatomic bonds and diffusion mobility caused by an impurity. This circumstance was also noted by other workers.

TABLE 28. **Values of T_r/T_m for Single-Phase Nickel-Base Alloys ($\varepsilon = 70$ to 90%; $\tau_{ann} = 2$ h)**

System	Cr, % (at.)	Addition, % (at.)	t_r^s, °C	T_r/T_m
Ni_{vac}	—	—	350	0.35
Ni-Fe	—	21	525	0.47
Ni-Ti	—	15.5	600	0.5
Ni-W	—	8.6	600	0.51
Ni-Mo	—	0.6	425	0.40
Ni-Co	—	9.6	620	0.58
Ni-Cr	14.5	—	620	0.53
Ni-Cr-B	15.1	0.03	630	0.53
Ni-Cr-Co	11.2	9.74	700	0.54
Ni-Cr-Al	14.7	4.57	690	0.54
Ni-Cr-Ti	14.4	3.34	730	0.55
Ni-Cr-Mo	14.7	2.46	650	0.52
Ni-Cr-W	16.0	0.17	670	0.53

A certain correlation undoubtedly exists between these characteristics. The role of interatomic bonds is most clear in alloys of the Cu-Ni system, where an alloy of the equiatomic composition has the corresponding distinct maxima of t_r^s and $m\theta^2$. This alloy also has the lowest diffusion mobility. It has a sharply elevated hardness in undeformed state, like the equiatomic alloy in the W-Nb system.

In high-concentration solutions, the relative positions of t_r^s and of the effective activation energy Q usually remain unchanged after different degrees of deformation. This means that the effect of the structure changes after various degrees of deformation is in these alloys weaker than the effect of alloying on interatomic bonds, and, therefore, on the temperature level of recrystallization.

This does not imply however that variation of t_r^s in high-concentration single-phase alloys can be fully explained by the pattern of variations of interatomic bonds.

For instance, as may be seen from Fig. 156, t_r^s in Ni-Mo, Ni-V and Ni-Cr alloys remains practically the same with a change of the concentration of chromium from 1% to 13%, molybdenum from 5% to 10%, and vanadium from 7% to 16%, whereas $m\theta^2$ increases markedly and the coefficient of diffusion, D, decreases.

In Cu-Be alloys (see Fig. 159*b*), a decrease in $m\theta^2$ is not associated with a noticeable drop in t_r^s. In Cu-Ni alloys with more than 50% Ni, t_r^s and $m\theta^2$ vary in opposite directions (see Fig. 159*c*).

Why is the effect of changes in interatomic bonds weaker here? At least two causes can be indicated: (1) a change in the structure of

as-deformed state associated, in particular, with the energy and concentration of stacking faults and (2) a change in the free energy of interfaces (grain-boundary energy).

The contribution of the structure change in as-deformed state is especially important when alloying changes the type of the lattice. An example has been discussed earlier in this chapter (Fe-Co alloys).

From the data on the strength of interatomic bonds ($m\theta^2$ and D), one should expect a progressive rise in t_r^s of copper with an increase in the concentration of dissolved aluminium. Actually, however, a change in aluminium concentration from 0.5% to 0.75% even lowers slightly t_r^s, which can be attributed to a loss in the stacking fault energy. This can also occur in many other systems, especially at high concentrations.

As has been given in Ch. 3, an increase in the grain-boundary energy should accelerate recrystallization at all its stages, though with various intensities.

In a first approximation, grain-boundary tension is regularly associated with the strength of interatomic bonds. Therefore, alloying with elements which strengthen interatomic bonds should have a double effect on recrystallization. On the one hand, it should decrease the thermal mobility of atoms and thus raise t_r^s. On the other hand, as it increases the free energy of interfaces, alloying should accelerate recrystallization.

According to B. Ya. Pines and the material of Ch. 3, boundary migration under the effect of grain-boundary tension occurs by redistribution and diffusion of vacancies. The required mobility of vacancies can obviously be obtained at a temperature of 0.55-0.67 T_m.

Therefore, complex alloying of single-phase alloys can be effective only to a definite limit; if the grain-boundary energy increases with a simultaneous decrease of diffusion mobility, t_r^s stops to rise.

The above considerations are also valid for cases where alloying weakens the interatomic bonds and lowers the temperature of recrystallization. This decrease in t_r^s should be less intensive than the weakening of interatomic bonds, since the latter effect is compensated to some extent or other by a decrease in the interface energy. This is obviously the case in Cu-Be alloys. According to the data on the changes in the lattice spacing in fine- and coarse-grained state, beryllium behaves like a surface-active element (it is concentrated in boundary layers) up to rather high concentrations, 2.3% (at.).

If the above considerations are true, a further increase in the temperature level of recrystallization in alloys as against the maximum possible level for solid solutions can be attained by forming obstacles (such as disperse phase particles) to boundary migration. These particles can ensure a high temperature level of recrystalli-

zation in age-hardening and some heterophase alloys (see the next chapter).

Also a sharp rise of t_r^s in single-phase alloys of a composition approaching the solubility limit is obviously associated with this effect. An example is a Cu + 0.45% Ti alloy whose characteristic features (in comparison with alloys of a lower concentration) are as follows (see Fig. 159*e*):

(1) a sharp rise of t_r^s;

(2) a very high effective activation energy of recrystallization (80-100 kcal/g-atom); here as in age-hardening alloys, the linear relationship $\ln \tau = fCT^{-1}$ is less pronounced;

(3) a weak dependence of t_r^s on the amount of deformation; this feature is also typical of age-hardening alloys;

(4) absence of the effect of sharp increase in the hardness in undeformed state (this effect is typical of alloys of an equiatomic composition in which the strength of interatomic bonds is very strong);

(5) a more intensive rise of resistivity after light and moderate deformations than after heavy deformations; the resistivity of the alloy after a 70-% deformation turns out to be lower than that after 20-% deformation (actually, ρ is almost the same as in undeformed state).

These data in combination with the material of the next chapter make it possible to state that the sharp rise of t_r^s in such alloys is caused by the formation of preprecipitates (segregates) during plastic working; in some cases with heavy deformations, precipitation from the solid solution can also take place. These preprecipitates can appear either directly during plastic working or partially in subsequent heating. They inhibit the redistribution of dislocations and the growth of recrystallization nuclei until the dissolution of precipitates or dissociation of segregates begins.

Figure 165 shows schematically variations of the temperature of the beginning of recrystallization in binary alloys when their composition varies under the effect of the various factors discussed in this chapter. The figure also gives the dependence of t_r^s on total concentration. The diagrams are given for several typical cases with various proportions of A and B components under the assumption that the temperature level of recrystallization is determined by several characteristics of the material. At least four of these characteristics can be indicated:

1. The diffusion mobility in undeformed state (which is determined by forces of interatomic bond, the type of lattice, and the interaction of impurity atoms and vacancies).

2. The structure that forms as a result of plastic working, in other words, the pattern of distribution and concentration of dislocations, stacking faults and vacancies.

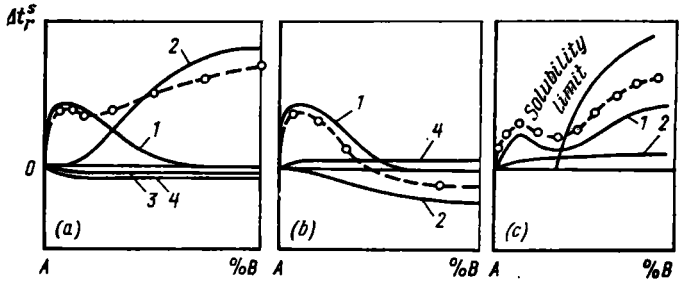

Fig. 165. Relation between changes in the temperature of beginning of recrystallization, t_r^s, of binary alloys consisting of components A and B (dotted line) and also changes in t_r^s due to such factors as interaction of impurity atoms and disperse particles with dislocations (*1*); strength of atomic bonds (*2*); grain-boundary energy (*3*) and conditions of dynamic recovery (*4*), on the one hand, and the compositions of alloys, on the other

(*a*) $\Delta R = R_B - R_A$ is high, component B increases interatomic bonds and lowers diffusion mobility; (*b*) ΔR is high, B weakens interatomic bonds; (*c*) B is limitedly soluble in A

3. The movement of dislocations by slip (including cross slip) and climb during heating.

4. The free energy of interfaces (grain-boundary energy).

Alloying can influence all these characteristics, though to a different extent. In various concentration ranges, a change of a particular characteristic can be decisive for variations of t_r^s in a metal or alloy.

In high-purity metals, $t_r^s = (0.25\text{-}0.35)\ T_m$. Within this range, the temperature level of recrystallization is obviously associated with the type of lattice and the structure in as-deformed state. Plastic working below room temperature can lower t_r^s substantially in metals where cross slip and dynamic recovery can occur easily at room temperature (since they have a high stacking fault energy γ_{sf}). In metals where cross slip is impeded (a low stacking fault energy γ_{sf}), plastic working at a lower temperature only slightly decreases t_r^s (see the data on aluminium and copper on p. 347).

In commercially pure metals, $t_r^s = (0.35\text{-}0.45)\ T_m$, i.e. it is higher than in the former case, which is due to the effect of minor impurities. Soluble minor impurities (in a concentration of a few tenths, hundredths or sometimes thousandths of a per cent), almost always raise the temperature level of recrystallization of pure metals, except for some rare cases where they change noticeably the structure of the matrix in as-deformed state and thus inhibit cross slip. Impurity atoms interact with dislocations and vacancies, diminish the elastic energy and mobility of dislocations, and thus impede nucleation. The effect of minor impurities is greater at a higher difference in atomic radii of the matrix and impurity, at a lower solubility of the impurity, and higher purity of the original metal.

Under favourable conditions, an impurity in a concentration of only 0.01-0.1% (at.) can raise t_r^s by a few hundred degrees.

As the concentration of an impurity increases, regions near dislocations are saturated with the impurity element, after which the difference in the concentrations in these regions and in the bulk of crystallites begins to decrease. The curve of t_r^s becomes more smooth and, in some systems, t_r^s may even diminish compared with alloys of lower concentration. This decrease of t_r^s is more probable if impurity atoms have a strong effect on the structure in as-deformed state (by lowering the stacking fault energy) and low effect on increase in the strength of interatomic bonds.

In the range of high concentrations, t_r^s only weakly depends on the composition of single-phase alloys. A change of concentration by 1 per cent varies t_r^s by a few degrees only. The value of t_r^s may either rise or lower depending on the effect of the impurity on the diffusion mobility and the strength of interatomic bonds in undeformed state. However, the temperature of the beginning of recrystallization varies less intensively than the two characteristics mentioned. Other characteristics (the structure in as-deformed state and the boundary energy) can probably play a definite part, because of which even complex alloying fails to raise t_r^s in single-phase alloys above (0.55-0.60) T_m.

Chapter 12

Recrystallization in Supersaturated Solid Solutions and Heterophase Alloys

Recrystallization and decomposition of supersaturated solid solutions and also recrystallization and reverse dissolution of precipitated disperse phases very often accompany each other in real alloys during heat treatment processes. The effect of superposition of one process on the other causes appreciable changes in the kinetics of each, so that the final structure and, consequently, the properties of the alloy change significantly.

The role of precipitates in the primary and later stages of recrystallization is very important.

When precipitates are present in an alloy prior to deformation, they alter the density and the nature of distribution of dislocations generated by deformation and thus affect radically the subsequent recrystallization.

Particles which precipitate during the deformation or in the subsequent recrystallization heating can retard or stop fully the movement of dislocations and boundaries and thereby make the process of recrystallization come to a halt. Reverse dissolution of precipitates liberates dislocations and boundaries and allows recrystallization to proceed freely. The particular result of the influence of these processes on microstructure depends on many factors.

At the same time, the early stages of recrystallization, being themselves affected by precipitates, in turn affect the rate of decomposition and the coagulation of disperse phases, as they accelerate the diffusion processes. This circumstance, which has been neglected until recently, is of a high practical importance.

The most common cases of secondary recrystallization are closely associated with the role of precipitates, the nature of their distribution, and the rate of dissolution.

Proceeding from the above, it is reasonable from the methodological and practical viewpoint to discuss separately the following aspects.

1. The mutual effects of recrystallization and decomposition of supersaturated solid solutions, namely:

(a) the effect of precipitates formed in deformation or in subsequent heating on primary recrystallization;

(b) the effect of primary recrystallization on the decomposition of a solid solution;

(c) the effect of precipitates and their dissolution on grain growth and secondary recrystallization (see Chaps. 5 and 8).

2. The effect of precipitates existed in an alloy prior to deformation, and of heterophase structures in general, on primary recrystallization.

12.1. Mutual Effects of Primary Recrystallization and Decomposition of Supersaturated Solid Solutions

Even the early studies into recrystallization of copper and aluminium-based supersaturated solid solutions point to the fact that these exhibit a higher temperature level of recrystallization than single-phase alloys closest to the former in composition. Burkhardt was among the first to observe an intensive retardation of recrystallization in supersaturated copper-base solid solutions. V. I. Iveronova [14] has shown later that t_r^s of copper- and aluminium-base systems

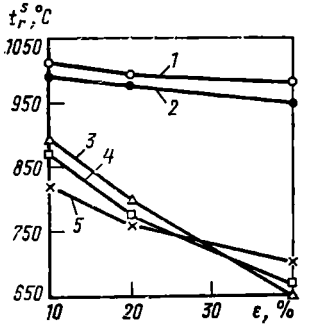

Fig. 166. Effect of deformation on t_r^s in nickel-base alloys

1, 2—age-hardening alloys, Ni-Cr-Al-Ti-Co and Ni-Cr-Al-Ti; *3, 4, 5*—single-phase alloys Ni-Cr, Ni-Cr-W, and Ni-Cr-Co

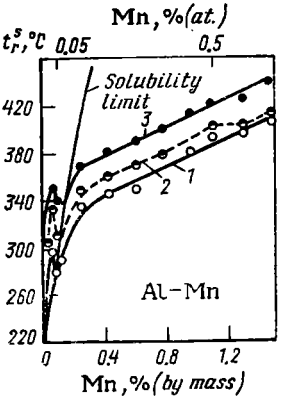

Fig. 167. Effect of Mn concentration on recrystallization temperatures of Al-Mn alloys

1—t_r^s; *2*—$t_r^{0.5}$ [(50% of recrystallized volume); *3*—t_r^f

of limited solubility begins to rise as the composition of a solid solution approaches the solubility limit. The increase in t_r^s becomes especially high in the region of supersaturated solid solutions.

Similar effects were later observed by many researchers. The author of the present book and co-workers studied recrystallization in supersaturated solid solutions and nearly saturated single-phase solutions in alloys based on nickel, copper, iron, chromium, and

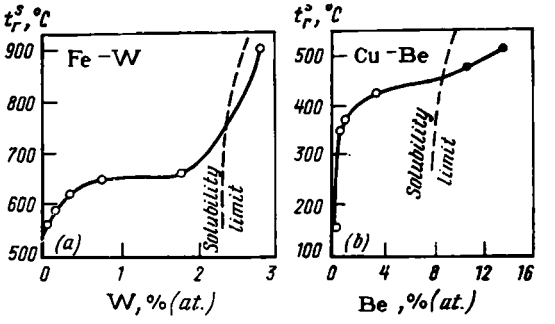

Fig. 168. Dependence of t_r^s on composition in systems Fe-W (*a*) and Cu-Be (*b*)

aluminium. The experiments were carried out on binary alloys, Al-Mn, Cr-Ta, Cr-Ti, Cr-Zr, Cr-Nb, Cr-Sb, Cu-Be, Cu-Sn, Fe-W; ternary alloys, Cu-Ni-Co, Ni-Cr-Ti, Ni-Cr-Al; quaternary and more complex alloys of the nichrome type: Ni-Cr-Al-Ti, types ЭИ437, XH70BMTIO, etc.

The temperatures of the beginning of recrystallization (t_r^s and T_r/T_m ratios) for selected age-hardening and single-phase alloys (close in composition to the solubility limit) after 40 to 70% deformation and annealing for 1 h are given in Table 29 and in Figs. 166-168. These data are obtained by using the common methods of X-ray structural analysis with a light beam 0.6-0.8 mm in diameter (by the appearance of the first point reflections). The results show that age-hardening alloys have a high level of recrystallization temperature. The increase in t_r^s on transition from single-phase to age-hardening alloys reaches 200 to 300°C. The T_r/T_m ratio is usually above 0.60 and in some cases comes to 0.75-0.80.

The highest relative level of recrystallization is shown by alloys in which a new phase, isomorphous to the matrix, precipitates from the supersaturated solid solution (alloys of the types cunico, nimonic, etc.), and also by alloys in which the two-phase to single-phase transition occurs at a temperature very close to the melting point (Al-Mn alloys in Fig. 167, etc.). For these alloys $T_r/T_m \approx 0.85$.

Another feature of supersaturated solid solutions is that their t_r^s is far less dependent on deformation than that of single-phase alloys (Fig. 166). That is why the higher value of t_r^s of age-hardening alloys is especially noticeable in strongly deformed specimens.

What are the reasons for such a high rise in the temperature level of recrystallization on transition from single-phase solid solutions to age-hardening alloys?

This temperature increase cannot evidently be explained by changes in atomic interactions since the composition of a solid solution

TABLE 29. **Temperature Levels of Recrystallization of Selected Alloys**

System	Composition, % (at.)	Alloy type	t_r^s, °C	T_r/T_m
Al-Mn	0.01 Mn	Single-phase	295	0.58
	0.35 Mn	Age-hardening	365	0.70
Cu-Be	3.7 Be	Single-phase	425	0.52
	10.8 Be	Age-hardening	475	0.70
	14.3 Be	Age-hardening	500	0.68
Cu-Sn	2.1 Sn	Single-phase	300	0.45
	3.8 Sn	Age-hardening	300	0.50
Cu-Ni-Co	20-80-10*	Single-phase	500	0.48
	50-20-30*	Age-hardening	800	0.75
Cr-Ta	0.03 Ta	Single-phase	950	0.58
	0.12 Ta	Age-hardening	1035	0.61
Cr-Ti	0.04 Ti	Single-phase	905	0.55
	0.15 Ti	Age-hardening	1060	0.63
Cr-Sb	0.02 Sb	Single-phase	905	0.57
	0.13 Sb	Age-hardening	1040	0.62
Fe-W	0.7 W	Single-phase	640	0.51
	1.7 W	Age-hardening	650	0.54
	2.7 W	Age-hardening	900	0.66
	4.9 W	Age-hardening	1025	0.73
Ni-Cr	22 Cr	Single-phase	660	0.52
Ni-Cr-Al-Ti	75-20-2.4-2.5*	Age-hardening	900	0.68-0.7
Ni-Cr-Al-Ti-Co	65-20-2.5-2.5-10*	Age-hardening	1000	0.75

* Per cent by mass.

after decomposition is the same as that of a single-phase alloy of the ultimate concentration.

One of the explanations for the high temperature level of recrystallization of age-hardening alloys has been suggested by V. I. Iveronova.

A deformed supersaturated solid solution undergoes decomposition if heated to a temperature corresponding to the two-phase region. The process of decomposition is more intensive in regions of the highest deformation distortions. In the course of decomposition in the regions having the strongest lattice distortions, the quantity of accumulated stresses in the alloy diminishes, which retards the process of recrystallization. Iveronova called this mechanism the diffusion stress relaxation.

Yet the concept of the diffusion stress relaxation fails to explain many peculiarities of recrystallization in supersaturated solutions.

If the diffusion decomposition could diminish deformation distortions, this would result in a reduced rate of nucleation and growth of recrystallization nuclei; the process of recrystallization would occur at a lower rate and the recrystallization interval would be wider than is the case with single-phase alloys. Experimental evidence, however, proves that the opposite is true.

Figure 169 shows the recrystallization intervals for a single-phase Ni-Cr alloy and age-hardening Ni-Cr-Al-Ti-Mo-W alloy after various degrees of deformation, and Fig. 167 shows this interval for Al-Mn alloys. The recrystallization interval of the age-hardening alloys is one-half that of the single-phase alloys. This points to a high rate of primary recrystallization and contradicts the concept of diffusion stress relaxation.

A comparative analysis of the dependence of the number of new recrystallized grains on heating temperature for non-age-hardening and age-hardening alloys reveals that primary recrystallization in age-hardening alloys originates at a higher temperature than in single-phase alloys, but, once it sets in, it proceeds very vigorously.

If the sharp rise in t_r^s in age-hardening alloys were to be due to diffusion stress relaxation through decomposition of the solid solution, the process of recrystallization would have to start at a lower temperature in cases where decomposition is precluded by prior age-hardening.

This supposition was checked on beryllium bronze with 14.3% Be (at.), or 2.3 mass % Be.

The first traces of recrystallization in age-hardened specimens were discovered on heating to 650°C (τ = 30 min), against 500°C for the specimens that were not age-hardened (the deformation degree was 50%). Thus, it was found radiographically that the temperature of recrystallization rose, but not decreased as would be expected.

The hardness of age-hardened and deformed specimens became equal to that they had prior to deformation already in heating up to 450°C, i.e. to a temperature 200°C below the temperature of recrystallization as revealed by radiographic techniques. In most cases, however, even 50-% softening in single-phase alloys roughly coincides with the temperature of the beginning of recrystallization. It follows that in this case the common radiographic methods can detect traces of recrystallization only at rather a late stage.

The heating of a deformed supersaturated solid solution involves two opposite processes: (a) elimination of the deformation distortions in the structure and, hence, softening due to recovery and recrystallization and (b) dispersion of the structure and hardening due to the decomposition of the supersaturated solid solution. This strain-hardening effect causes such changes in the radiographic pattern, microstructure, and physico-mechanical properties that they mask the effect of structural changes due to recovery and recrystallization.

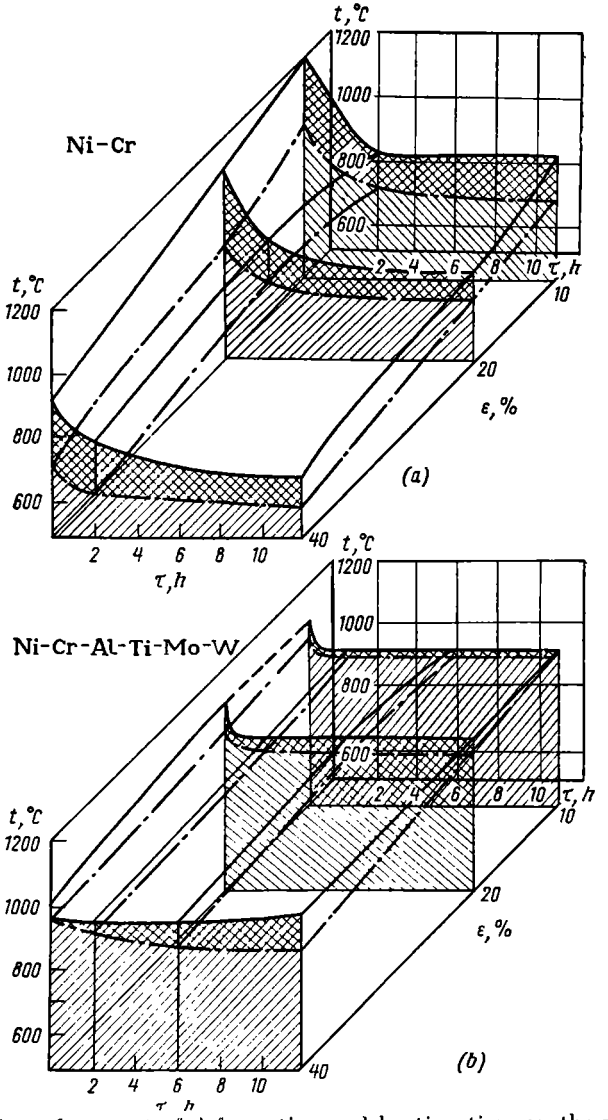

Fig. 169. Effect of amount of deformation and heating time on the recrystallization interval in (*a*) single-phase and (*b*) age-hardening nickel-base alloy

In that case the initial traces of recrystallization can be revealed by the common methods only after heating to a temperature at which the reverse dissolution of the disperse phase begins and recrystallization nuclei become capable of growing intensively. This temperature should however be regarded as the temperature of the beginning of intensive growth of recrystallization nuclei. The actual temperature of the beginning of recrystallization (the temperature of nucleation) is appreciably lower.

Recrystallization in supersaturated solid solutions has been studied by E. Hornbogen and co-workers [44]; he has also made a review of the research work in the field.

Hornbogen starts from an analysis of the effect of temperature on the rates of both processes, i.e. recrystallization and decomposition.

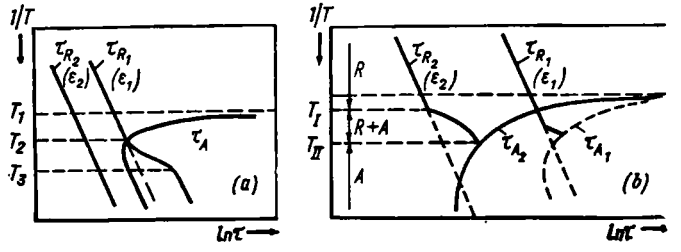

Fig. 170. Temperature curves of the beginning of recrystallization, τ_R, and of decomposition, τ_A, for two various deformations ($\varepsilon_2 > \varepsilon_1$): (*a*) without interaction of the two processes; (*b*) with their interaction

The time of the beginning of recrystallization τ_r is determined only by kinetic factors and, in the general case, as has been noted earlier more than once, depends exponentially on temperature: $\tau_r = \tau_{r0} \exp(Q_r/kT_r^s)$, where Q_r is the effective activation energy of recrystallization.

The expression for the time of the beginning of decomposition τ_A is of a more complicated form, since it is determined, apart from the kinetic factors, by a thermodynamic factor, too, which accounts for the effect of temperature on the gain in free energy of the system during decomposition. The resultant expression for τ_A is $\tau_A = \tau_{A0} \exp(-\Delta F/kT) \exp(Q_D/kT)$, where ΔF is the free energy change in the system during decomposition of the solid solution, and Q_r is the activation energy of diffusion.

The temperature relations for τ_r and τ_A are shown schematically in Fig. 170*a*, without considering the interaction between the two processes in question.

Given such an interaction, the kinetics of each of the processes and thus the above relations must change. Beginning from the moment at which the lines τ_r and τ_A intersect, precipitates retard recrystallization. The particular nature of this interaction may be

different. A higher deformation must shift the curves of the two processes into the regions of shorter time periods. The degree of shift of each of the curves is undoubtedly different and depends on many factors.

One of the possible variants proposed by Hornbogen and co-workers is shown in Fig. 170*a*. In our opinion, Hornbogen has analysed an extremely rare case where an increase in the degree of deformation shortens the time of the beginning of recrystallization, τ_r, and does not change the time of the onset of decomposition, τ_A. As the degree of deformation increases, a situation becomes probable in which recrystallization turns out to be fully complete before the start of decomposition and the latter begins, in Hornbogen's view, only after full completion of primary recrystallization.

If such a scheme is realized, it should then be inferred that the precipitates which appear in heating after heavy deformations must have no effect on the rate of recrystallization or at least the effect must be much weaker than would be the case after light deformations.

According to Hornbogen and co-workers [44], this scheme must be realized in systems where precipitation from the solid solution occurs very slowly and the precipitated particles do not interact either with dislocations or with various types of boundaries, and stay in active in the bulk of grains. By the authors' data, these conditions are observed in the decomposition of a copper-cobalt alloy which they have studied by various methods. According to these data, at deformations up to 10%, precipitates fully inhibit recrystallization; at deformations of 20% or more decomposition proceeds along cell boundaries and retards, but does not prevent, recrystallization. At deformations above 50%, recrystallization with the formation of new grains is sharply accelerated and has had time to go along through before the start of decomposition.

An analysis of the results of other research studies in the field suggests, with good reason, that the cases in which decomposition is very sensitive to the effect of deformation and recrystallization are more common in practice.

First, an increased degree of deformation and thus increased density of structural defects intensify decomposition either directly during deformation [299] or in subsequent heating. Second, the accelerating effect of (primary) recrystallization on decomposition should also be considered. The effect must be due to vacancies formed at the stage of primary recrystallization (see Ch. 4). This peculiar 'injection' of vacancies, which accelerates diffusion, should accelerate the coagulation of precipitates (for more detail see Ch. 4) as well as the decomposition of supersaturated solutions. Unfortunately, the authors [44] do not analyse the process peculiarities which are associated with the generation of vacancies at the stage of primary recrystallization.

The mutual effects of recrystallization and decomposition are also observed in heterogeneous (two-phase) decomposition of deformed supersaturated solid solutions. According to [300], when a migrating boundary leaves behind a recrystallized and decomposed volume, the chemical energy of decomposition becomes an additional driving force of recrystallization. It may be expressed by the formula $P_x = \alpha RT \ln (C_1/C_0)$, where α is the number of moles, and C_1 and C_0 are the concentrations of the solid solution respectively before and after the decomposition under given conditions of annealing.

Experiments have been carried out to determine whether and when the recrystallization of a supersaturated solution is possible without its decomposition. The results of experiments are discussed below. The following groups of alloys have been tested:

1. Alloys having no structural similarity between the matrix and the phase precipitated (Cu-Be, Fe-W) and also alloys in which there is such a similarity (of the cunico and nimonic types).
2. Alloys of one and the same system, but with different degrees of supersaturation and with different amounts of the precipitated phase (Fe-W and Al-Mn).
3. Alloys in which decomposition can occur with a different rate—relatively low for Cu-Be and relatively high for Cu-Sn—and also with a different ability of the precipitated phase to coagulation—higher for Ni-Cr-Al-Ti and lower for Ni-Cr-Al-Ti-Co.

The principal results of the experiments are as follows.

Cu-Be alloys. For an age-hardening alloy (10.8% Be) and single-phase alloy (3.7% Be) that approaches the solubility limit, the temperatures of the beginning of recrystallization as determined by common methods, after rolling with 55% deformation are respectively 475° and 425°C.

Special methods have been used to check for overstatement of the first temperature due to some screening factors and for occurrence of the actual formation of recrystallization nuclei in the age-hardening alloy at the same temperature as in the single-phase alloy, i.e. at 425°C.

Heating to 425°C, i.e. 50°C below the established value of t^s_r, has proved to eliminate almost fully the traces of the structural changes caused by the deformation. The coherent scatter regions after such heating have 3.5 times the size of regions in as-deformed state.

Micro-beam radiography has revealed that the process of nucleation in a 10.8-% Be age-hardening alloy becomes complete during heating to 425°C: individual reflections are seen on the line (111) of a specimen rolled and heated to 425°C. Further, the scattering of texture maxima on the radiogram has increased noticeably.

These experiments make it possible to suppose that the actual value of t^s_r for the age-hardening alloy Cu + 10.8% Be, in which

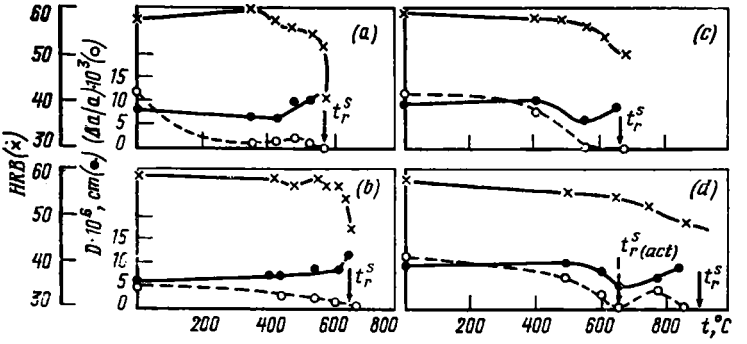

Fig. 171. Effect of temperature of heating (τ = 60 min) on microstresses ($\Delta a/a$), size of coherent scatter regions, D, and hardness HRB

(*a*) Fe; (*b*) Fe + 0.7% W; (*c*) Fe + 1.8% W; (*d*) Fe + 2.7% W

the crystal structure of the disperse phase strongly differs from that of the matrix, is at least not higher than in the single phase alloy with 3.7% Be.

Fe-W alloys. The compositions of these alloys and the values of t_r^s determined upon 50-% upsetting deformation are shown in Fig. 171. The maximum rise in the temperature of recrystallization of age-hardening alloys over that of a single-phase Fe-W alloy may be as high as 400°C.

The results of analysis of changes in the fine structure of the matrix by broadening of lines (110) and (211) are shown in Fig. 171. Vertical arrows indicate the position of t_r^s as found by a common technique.

What is typical for pure iron and Fe + 0.7% W alloy is that the beginning of recrystallization, as detected experimentally, is preceded by simultaneously occurring processes of reduction of microstresses and a certain growth of the regions of coherent scatter. The beginning of recrystallization practically coincides with the complete elimination of microstresses, as detected radiographically, though the size of coherent scatter regions remains still small (600-800 Å). By this moment, the main portion of dislocations, which produce the effect of non-uniform variations in interplane distances, has obviously enough time to dissociate or migrate to the boundaries of growing nuclei.

The fine structure in the age-hardening alloys changes by a different pattern. A reduction of microstresses occurs together with diminution of blocks, rather than with their growth as is the case in single-phase alloys. Resistivity measurements and metallographic data show that the drop of $\Delta a/a$ and the reduction of D correlate with the decomposition of the solid solution and are obviously due to this decomposition. In an alloy with 2.7% W, microstresses decrease

in the range of 600-650°C, then grow at 680-770°C and further drop to zero at 830°C.

The analysis of broadening of radiographic lines suggests a reasonable conclusion that the established temperature t_r^s is by far overstated and that the actual temperature of nucleation corresponds to the initial moment of release of microstresses in the alloy, i.e. as with single-phase alloys, this temperature lies at roughly 630-650°C, i.e. 250-270°C below the value of t_r^s as found by common methods. Another growth of microstresses on heating to 680-770°C is caused by structural strain hardening (owing to an increasing amount of the secondary phase).

Using the micro-beam technique, it has become possible to detect point reflections upon heating to 830°C, i.e. only 80°C below the value of t_r^s found by the common methods. An additional analysis has shown that the actual temperature of the beginning of recrystallization—in full accordance with the data on variations of microstresses—lies at roughly 610-630°C rather than at 910°C. In the single-phase Fe + 0.7% W alloy, the temperature of the beginning of recrystallization is 630-650°C. The low sensitivity of the micro-beam is evidently associated with a large number of Fe_2W particles, small size of recrystallization nuclei and, undoubtedly, with structural strain hardening of the nuclei.

The fact that incoherent decomposition and formation of recrystallization nuclei occur practically at the same time can be explained as follows.

Incoherent decomposition of a solid solution occurs primarily on boundaries and subboundaries. The precipitates which differ from the matrix in structure and in unit volume increase the misorientation angles of adjacent grains and also cause stresses within these blocks. These stresses obviously play an important part by accelerating the movement of dislocations, their migration to subboundaries and partial dissociation of dislocations; in the final result, they accelerate the formation of regions which are almost free of dislocations (and, therefore, free of inhomogeneous microstresses) and are confined within large-angle boundaries.

As the amount of the precipitated phase increases, new stresses, which are caused by decomposition and associated with the difference in unit volume and in thermal expansion between the matrix and the secondary phase, become more and more effective. They can and often do produce an effect of a new rise in microstresses and of blurring of lines in radiograms, as has been found on Fe-W alloys (Fig. 171).

As the dissolution of a disperse phase begins, the stresses that arise during decomposition get relieved, and the boundaries are freed from the particles and can migrate.

Cunico alloy (50% Cu + 20% Ni + 30% Co). During heating of this alloy to 600-650°C after quenching from the single-phase region temperature, the decomposition occurs with the separation of the original solid solution into two isomorphous solutions whose lattices are coherent with that of the matrix (Fig. 172). Above the temperatures indicated, decomposition disturbs the coherence.

In heating upon cold rolling with 70-% deformation, the temperature of the beginning of recrystallization, as found by common techniques, is $t_r^s = 800°C$, i.e. 0.75 of T_m.

Such a high T_r/T_m ratio is associated with the fact that the actual beginning of recrystallization coincides with the moment of disturbance of coherence.

Thus, in heating of deformed cunico-type alloys, the supersaturated solid solution first decomposes coherently. After that the coherence is disturbed and then recrystallization begins. This fact obviously explains the high level of t_r^s in these alloys. Even assuming that the actual value of t_r^s for cunico alloys is 740-750°C, the T_r/T_m ratio is equal to 0.7, i.e. is still very high.

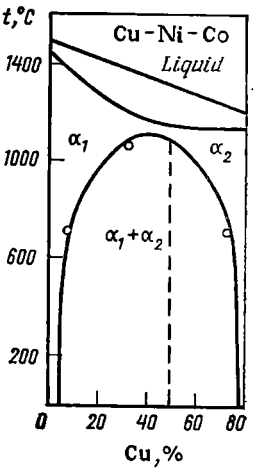

Fig. 172. Pseudobinary section of the binary equilibrium diagram of Cu-Ni-Co system. Dotted line gives the composition of the tested alloy (50 + 20 + 30%)

Nimonic-type alloy. The interrelation between the nature of decomposition and recrystallization has also been found for a nimonic alloy, namely, on quenched specimens rolled 50% and 75% and then annealed for a long time at 800, 700 and 600°C.

An analysis of the microstructure has shown (Fig. 173) that the decomposition and coagulation of the α' phase during heating are most intensive along slip bands (places of concentration of dislocations). The high local dislocation density in these regions disturbs coherence from the very beginning of decomposition. Recrystallization of the matrix occurs in these same places, whereas recrystallization is absent in the remaining volume of crystallites where the decomposition has proceeded according to normal kinetics, i.e. with long retention of coherent bonding between the phases. Thus, incoherent decomposition in nimonic alloys, too, goes parallel to recrystallization.

R. M. Lerinman and M. I. Turchinskaya observed parallel decomposition of the solid solution and recrystallization of the matrix in heating of a cold-deformed Al-Ag alloy.

Small regions in which decomposition has occurred with the formation of γ'-phase are always in the form of pearlitic colonies of

the γ′-phase in recrystallized matrix. In places where no decomposition has occurred, no effects of recrystallization are found.

Retardation of recrystallization by coherent decomposition can be readily explained by assuming that coherent precipitates 'settle down' preferably on individual dislocations and thus make difficult or even impossible the movement and redistribution of the latter. This is due to an essential reduction in the elastic energy of dislocations. Another reason is that moving dislocations must cut through coherent precipitates. Calculations made for age-hardening alloys of the systems Al-Cu [299], Al-Zr, Ni-Al [301], etc., in which the precipitates are of a coherent nature, show that the activation energy of recrystallization increases in this case 1.5 to 2 times and the rate of the process diminishes by two or more orders of magnitude.

As coherence disappears, dislocations get free for redistribution, which enables the formation and growth of recrystallization nuclei.

In most of the cases discussed above, the incoherent decomposition of the solid solution and recrystallization practically occur at the same time, though the former process leads the latter.

A question naturally arises: can a supersaturated solution recrystallize prior to decomposition and what effect has the process of recrystallization on subsequent decomposition?

To clear up the question we have carried out experiments on a Cu + 3.85% Sn alloy which has a typically low rate of decomposition and rather a high difference between the atomic radii of the constituents. This has eased the task of determining the onset of decomposition by a change in the lattice spacing of the original solid solution.

After 90-% deformation, specimens of the alloy were subjected to heating of various duration at 290°C. Recrystallization started simul-

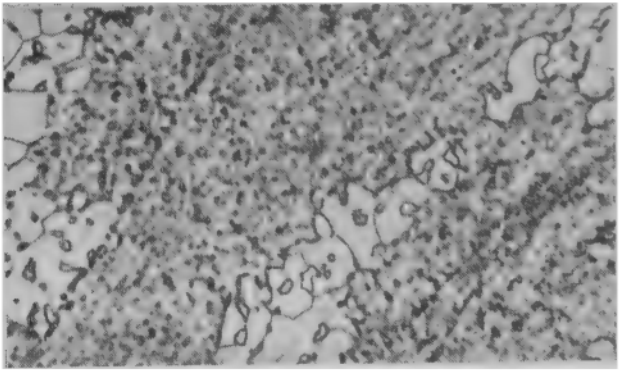

Fig. 173. **Microstructure** of X1177T10 (301437) alloy rolled 50% and heated at 800°C for 5000 min

taneously with decomposition of the solid solution, but not earlier.

The specifics of recrystallization in a solution of high supersaturation and of an elevated amount of an excess phase were studied on alloys of the systems Al-Mn and Fe-W. Among the alloys of the former system, an alloy with 0.59% Mn (at.) was tested, which contains about 5% of Al_6Mn phase (vol.) in the equilibrium state. Upon 80-% deformation, the temperature of the beginning of recrystallization, as determined by a common radiographic technique, was found to be 397°C. In contrast to the alloys of lower supersaturation the analysis of texture scattering and differential-hardness techniques gave the same result for this alloy.

According to the results, the lattice spacing of the solid solution increases up to 380°C and then drops beginning from 390°C. Narrowing of the radiographic lines is noticed from 390°C. Decomposition of the solid solution in heating to 380°C obviously occurs with precipitation of a large amount of Al_6Mn phase ($R_{Mn} < R_{Al}$). Above 390°C, the reverse dissolution of the precipitated phase begins, which is associated with intensive and extremely non-uniform growth of subgrains and recrystallization nuclei.

Consequently, if a disperse phase precipitates in a large amount, the process of intensive disintegration of coherent scattering regions and redistribution of the dislocations formed by prior deformation (which process is associated with reduction of microstresses) occurs parallel with the appearance of new microstresses due to phase strain hardening. In view of the large amount of a disperse phase, the matrix lattice regions rimmed by particles of this phase are extremely small. Each of these regions transforms into a nucleus whose growth is impossible since the disperse phase particles produce a barrier effect. This is why no noticeable change in the texture scattering takes place.

The growth of nuclei becomes possible as soon as the dissolution of the excess phase begins. Selective dissolution results in selective growth of nuclei. In places where the growth of nuclei becomes possible, it occurs at a very high rate since the grain-boundary tension at the joints between nuclei and grains is highly unbalanced (unstable boundaries are 'fixed' by particles of the secondary phase).

A different behaviour should be expected of an alloy of low supersaturation where the rate of decomposition is small, but the conditions for recrystallization are favourable. These conditions are found in annealing of deformed alloys at relatively high temperatures which, however, are still within the two-phase region.

Such an experiment was made for XH77TIOP and Cu-Be [14.3% (at.) Be] alloys. Specimens were deformed and annealed, after which their hardness was measured and the course of recrystallization in them was studied radiographically.

During heating of the specimens deformed 40%, the recrystallization and decomposition occurred simultaneously. Heavy deformations accelerated both processes to such an extent that the beginning of each of them could not be detected separately by the experimental methods applied.

In lightly deformed specimens (10-20%) the process of recrystallization was leading at the early stages of the isothermal annealing. The hardness of these specimens decreased, radiographic lines became narrower, and point reflections from new recrystallized grains appeared. Decomposition, however, started immediately after the beginning of recrystallization. As the time of annealing was increased to 10-15 minutes, the hardness of specimens rose again and the lattice spacing of the solution changed, which was indicative of decomposition; the clear point reflections that had appeared earlier became blurred again.

This effect is essentially analogous to that described earlier for the deformed age-hardening Fe + 2.7% W alloy in which the microstresses that fully disappear on low-temperature heating grow again in heating to higher temperatures.

So, at low supersaturations, too, decomposition and recrystallization affect each other, but the latter retains the leading role.

Thus, in systems where at temperatures near t_r^s for single-phase alloys of the ultimate concentration there is neither structural nor dimensional similarity between the crystal lattices of the matrix and the secondary phase and where the secondary phase lattice is incoherent with the matrix lattice in that temperature interval, the actual temperature of the beginning of recrystallization may be even lower than the temperature of recrystallization of a single-phase alloy of the ultimate concentration. This case is typical of alloys of the Fe-W system and partially of a Cu + 2.7% Be alloy.

If, however, decomposition takes place so that the lattices of the matrix and a precipitate remain coherent, the actual t_r^s may be noticeably higher than the corresponding t_r^s of a single-phase alloy of the ultimate concentration.

If the growth of recrystallization nuclei is inhibited by particles of a secondary phase, no essential softening occurs in supersaturated solutions at the actual temperature of the beginning of recrystallization (the temperature of nucleation). Softening only begins with an intensive growth of recrystallization nuclei. This circumstance appears to be important practically, in particular for thermomechanical treatment.

As regards the temperature of the beginning of intensive growth of nuclei, which coincides with the temperature of recrystallization as found by common methods, it depends on a number of factors, such as the temperature of two-phase to single-phase transition in an alloy, the shape of the solubility curve, the quantity, dispersity,

and coagulation resistance of an excess phase, the extent and stability of the strain-hardening effect produced by that phase, etc.

The effects of these factors can only be determined by special experiments. Some particular examples will be given below.

1. An addition of cobalt increases the temperature of recrystallization of an age-hardening Ni-Cr-Al-Ti alloy, as found with common techniques, by 50-75°C. But t^s_r of a single-phase Ni + 13% Cr alloy remains practically unchanged on addition of 10% Co to the solid solution.

The mechanism of this effect may be clear by referring to electron micrographs in Fig. 174. In a Ni-Cr-Al-Ti alloy (Fig. 174*a*, *c*) deformed 40% and heated for 2 h at 900°C, precipitates are quite large and the solid solution regions surrounded by them have a size of 1-2 μm (Fig. 174*a*). Point reflections from grains of such a size do not merge together on radiograms. In a Ni-Cr-Al-Ti-Co alloy (Fig. 174*b*), after the same treatment the size of α'-phase particles and the solid solution regions between them are much smaller

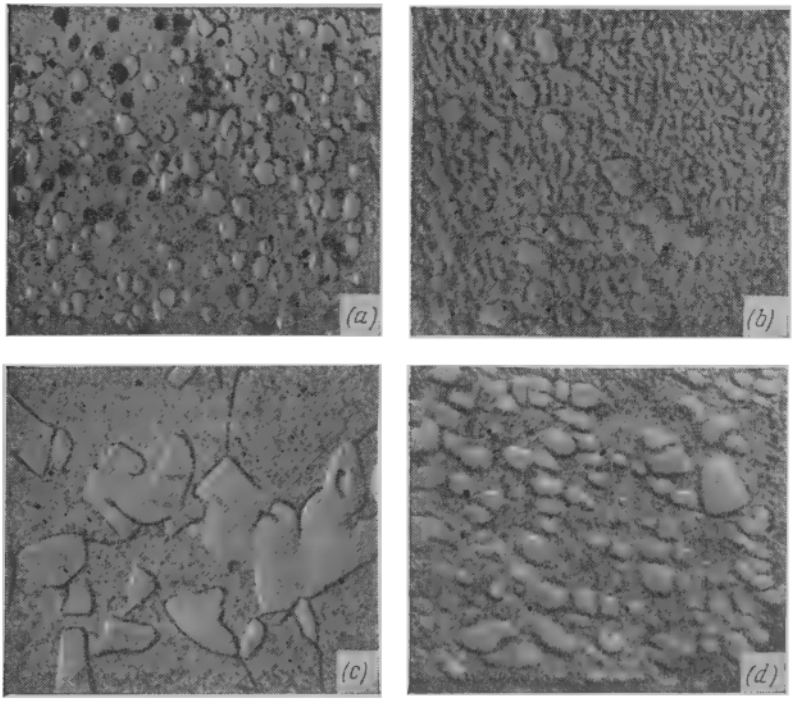

Fig. 174. Structures of various alloys after 40-% deformation and heating at 900°C for 2 h (*a*, *b*) and at 1000°C for 1 h (*c*, *d*) ×10 000

(*a*, *c*) Ni-Cr-Al-Ti alloy; (*b*, *d*) Ni-Cr-Al-Ti-Co alloy

(Fig. 174*b*, *d*) and the recrystallized regions of the solid solution cannot be resolved by the common radiographic technique. The temperature of single-phase transition of this alloy is higher and the rate of coagulation of α'-phase particles is lower than in the former alloy. This is also evident from the analysis of the structure after heating at 1000°C (Fig. 174*c*, *d*). Therefore, the growth of recrystallization nuclei is retarded up to a higher temperature.

2. At a greater saturation of the solid solution there is a greater difference between the temperature of single-phase to two-phase transition, t_b, and the temperature at which an intensive coagulation of the disperse phase begins or the coherence is disturbed. As the degree of supersaturation increases, the difference $\Delta t = t_b - t_r^s$ correspondingly increases. This can be well illustrated by the data on t_r^s for Al-Mn and Fe-W systems.

3. Table 30 gives the temperatures of the beginning of recrystallization and the temperatures of two-phase to single-phase transition for a number of age-hardening alloys in which the concentration of

TABLE 30. Values of t_r^s and t_b for Selected Age-hardening Alloys

Alloy	Composition, % (by mass)	t_b, °C	t_r^s, °C	$\Delta t = t_b - t_r^s$	Precipitating phase
1	Ni+13Cr+22Al+2.4Ti	1000	850	150	$Ni_6(Al, Ti)$
2	Al+0.5Mn	480	340	140	Al_6Mn
3	Cu+2.3Be	830	480	350	CuBe
4	Fe+3.8W	850	650	200	Fe_2W

the secondary phase is roughly the same, but the structural conformity between the matrix and the precipitated phase is different.

If a secondary phase has a lattice that differs appreciably from that of the matrix, the difference between t_r^s and t_b is greater and the former is appreciably lower than the latter. If, however, there is a definite structural conformity between the secondary phase and the matrix, the temperature of recrystallization increases and the difference $\Delta t = t_b - t_r^s$ becomes smaller. Coagulation of disperse particles then goes on rather languidly because of the low interfacial energy of the conjugated phases.

For Al-Mn alloys, it may be supposed that a coherent bond exists between the matrix and Al_6Mn phase, which is obviously responsible for the extrusion effect observed in these alloys. For this system, $\Delta t = 50$ to 120°C.

In alloy 1, the secondary phase is isomorphous to the matrix and $\Delta t = 150$°C.

The lattices of the matrix and secondary phase in Cu-Be alloys are quite different (K12 and K8 and, respectively, $a_1 = 3.607$ Å and $a_2 = 2.795$ Å) and the coherent bonding is retained only at a very early stage of decomposition; correspondingly $\Delta t = 350$°C.

In the Fe-W system, Fe_2W phase has a hexagonal lattice ($a = 4.739$ Å, $c = 7.715$ Å), and the matrix has a b.c.c. lattice ($a = 2.930$ Å); accordingly, $\Delta t \geqslant 200$°C.

All the examples given above make it possible to modify Hornbogen's scheme for a case where deformation and recrystallization accelerate decomposition, i.e. for the case that is most typical of supersaturated solid solutions (Fig. 170*b*).

Firstly, a heavier deformation should shorten the time of the beginning of recrystallization (line τ_r in Fig. 170*b*) and the time of the beginning of decomposition (curve τ_A).

Secondly, as recrystallization begins to develop locally in certain places, it is immediately followed by local decomposition which impedes further recrystallization in those places. Recrystallization must slow down at a temperature slightly below the temperature corresponding to the solubility limit T_b, but above the intersection of lines τ_r and τ_A.

Thirdly, both recrystallization and decomposition must be realized in the temperature interval between T_b and the temperature corresponding to the intersection of lines τ_r and τ_A (between the horizontal dotted lines), with one of the two processes playing the leading part. In the upper portion of that temperature interval, recrystallization is the leading process. Decomposition which starts immediately after recrystallization, temporarily decelerates the latter.

Recrystallization nuclei can often be detected only at the beginning of coagulation of precipitates, i.e. when the retarding effect of precipitates is terminated. The effect of retarding the formation of recrystallization nuclei is stronger at a lower temperature within that interval. The leading role of recrystallization thus becomes less and less pronounced.

The temperature interval *A* corresponds to such a state of a system that the decomposition of the solid solution goes on rather intensively (because of deep supersaturation) even at the initial moments of annealing and fully blocks the structural defects formed by the prior deformation. No recrystallization can start within a practically reasonable time of annealing

Such is the general scheme. It follows that the effect of decomposition in various alloys may be different depending on the nature of the interaction of precipitates with various defects and on the retarding effect at various stages of recrystallization.

The following principal cases are obviously possible:

1. Precipitates interact with individual dislocations and dislocation clusters. This case relates, in the first place, to coherent precipitates which inhibit the earliest stage of the formation of recrystallization nuclei, i.e. they act most effectively.

A similar result is obviously obtained when only the earliest stages of decomposition take place, resulting in the formation of precipitates and segregations of solute atoms on dislocations and dislocation pile-ups.

2. Precipitates settle down on low-angle boundaries. In this case, precipitates slow down the growth of subgrains, i.e. retard the last stage of formation of recrystallization nuclei. Usually, incoherent or partially coherent precipitates settle out on subboundaries, as they do on large-angle boundaries. Since, however, the energy of low-angle boundaries is lower than that of large-angle ones, the retarding effect on low-angle boundaries is greater.

3. Precipitates settle down preferably on large-angle boundaries; in that case, during heating after light deformations, recrystallization by boundary migration of original grains is retarded.

In heating after heavy deformations, the growth of recrystallization nuclei is retarded (i.e. the retarding action is effected at the end of primary recrystallization and the beginning of grain growth). This means that the two stages of primary recrystallization—the formation of nuclei and their growth—which follow one another without interruption in single-phase alloy, turn out to be separated by a large temperature-time interval in supersaturated solid solutions. The beginning of recrystallization as detected by common methods is essentially the beginning of intensive growth of nuclei.

Therefore, the dependence of the temperature level of recrystallization on the composition of supersaturated solutions of this type can be described by two curves, of which the lower curve corresponds to the temperature of formation of nuclei and the upper one to the temperature at which growth of these nuclei begins.

The possibility of interaction between precipitates and the described types of imperfections is determined by crystallochemical characteristics of the precipitates, more exactly by the degree to which the crystallochemical structure of the matrix conforms to a precipitate, including its possible metastable states (Guinier-Preston zones etc.). With a greater crystallochemical non-conformity of the matrix to precipitates there is a greater probability for interaction with imperfections in the sequence: dislocations → → low-angle boundaries → large-angle boundaries.

Useful information on the nature of interaction between precipitates and various imperfections can be obtained from the analysis of recrystallization textures (see Ch. 10).

Where age-hardening changes the deformation texture, precipitates obviously interact more intensely with low-angle boundaries

and facilitate the leading growth of the nuclei separated from the matrix by boundaries of large misorientation. Where the recrystallization texture repeats the deformation texture, precipitates obviously interact more intensely with large-angle boundaries.

For prediction and practical utilization of the effects of interaction between recrystallization and decomposition processes, more data should be accumulated on the crystallochemistry of precipitates and the nature of their interaction with various imperfections.

12.2. Recrystallization in Heterophase Alloys

The absolute majority of commercial alloys are mixtures of a few phases. Until the recent time, the available information on recrystallization in heterophase alloys was scarce and ambiguous, largely because recrystallization in these alloys heavily depends on the nature of phases, their thermal stability, dispersity, the shape and relative volume of particles, etc. Where the temperature intervals of recrystallization and dissolution of secondary-phase particles coincide, any conclusions on the role of the secondary phase become even more ambiguous.

The situation has changed drastically in the last decade due to the appearance and wide application of metal ceramic alloys belonging to metal-and-high-melting disperse phase systems in which the disperse phases increase the strength and raise the temperature level of softening. This circumstance has stimulated extensive research into the mechanism of recrystallization in heterophase alloys and the effect of secondary phase particles on the nature of the dislocation structure which forms in deformation and subsequent heating.

Two-phase alloys in which both phases are present in approximately equal quantities and resemble each other in properties and structure have yet to be studied more thoroughly. Examples are $(\alpha + \beta)$-brasses, titanium alloys, etc.

Studies into the recrystallization of alloys containing hard particles of a secondary phase have shown that these particles may either accelerate or impede or even block up recrystallization.

For instance, in one of his earliest works in the field A. I. Kitaigorodsky found that a small quantity of Cu_2O particles in copper (approximately 0.02% by volume) decreased t^s_r by 80-100°C. He discovered a similar effect after adding titanium carbide particles to a solid solution of nickel and titanium. Two non-ageing alloys were analysed: (1) single-phase Ni + 3.05% Ti alloy and (2) Ni + 3.4% Ti + 0.4% C alloy containing roughly 2.0% (vol.) of primary titanium carbides. Though the latter alloy had a higher content of titanium, it began to recrystallize earlier than the former. The time to recrystallization was respectively 20 and 50 minutes at 600°C, and 50 and 200 minutes at 575°C.

A number of research works published in the middle of 1950's have shown that the temperature of recrystallization and the effective activation energy increase with the concentration of a secondary phase. For instance, an addition of certain insoluble impurities (Al_2O_3, SiO_2) to tungsten raises t_r^s by a few hundred degrees (from 1680°C to 2115°C) [302].

In a heterophase alloy, Al + Al_2O_3 (SAP), produced by sintering aluminium powder particles coated by a thin layer of an oxide, recrystallization of aluminium occurs at appreciably higher temperatures than in the absence of Al_2O_3 particles (see later in this chapter).

The temperature level of recrystallization in chromium bronze, Cu + 0.5% Cr (by mass), turned out to depend appreciably on the size of excess chromium particles (I. G. Ravich). With particles 2 to 4 μm in size, the temperature level of recrystallization was 200 to 400°C; with more disperse particles (tenths of a micrometer) present in the metal prior to deformation, the temperature level shifted up to 400-800°C.

Using common methods of X-ray analysis (see Ch. 15), I.A. Sobolevsky [303] found that the temperature of recrystallization of ferrite in carbon steels increased steadily with the content of cementite (from 250°C for a steel with 0.1% C to 570°C for a steel with 0.8% C). The 'activation energy' of recrystallization increased accordingly from 232 to 294-336 kJ/mole.

V. K. Babich [304] has studied separately the recrystallization of excess ferrite and of ferrite in pearlitic colonies. In the excess ferrite after relatively light pressing (up to 20%), the nucleation and growth of recrystallization centres have proved to begin in heating to approximately 500°C, i.e. at a lower temperature than in carbon-free iron deformed to the same degree. The process starts to develop as a rule near pearlitic colonies, i.e. on ferrite-pearlite boundaries.

Ferrite in pearlitic colonies behaves in a different manner. As long as the cementite in these colonies remains lamellar, the primary recrystallization of the ferrite in the pearlitic structure does not start even on heating up to 550°C and does not come to an end on heating to 600°C, whereas excess ferrite undergoes even the stage of grain growth in heating to this temperature. Spheroidization and coagulation of cementite platelets facilitate recrystallization of the ferrite in pearlite.

Thus, cementite particles facilitate recrystallization in some microportions of a specimen and produce an inhibiting effect in other microportions.

It is worth while to mention the work of R. D. Donerty and I. W. Martin [305] who studied recrystallization in age-hardened Al-Cu alloys containing Cu_2Al particles (θ-phase). The authors showed that this phase could either accelerate or decelerate recrystalli-

zation, the decisive factor being the distance between particles, rather than their volume concentration. Particles of this phase produced a decelerating effect at distances of 2000-3000 Å between them and an accelerating effect at distances larger than 3000 Å.

In order to understand these results, we should analyse how the principal factors that determine susceptibility to recrystallization can be affected by disperse particles of other phases present in the matrix. Particles of other phases can:

(a) change the type of the dislocation structure of the matrix that appears in deformation;

(b) change the conditions of redistribution of dislocations and boundary migration in heating by virtue of the barrier mechanism, i.e. change the conditions of formation and growth of recrystallization nuclei;

(c) cause strain-hardening of the matrix in heating owing to the different linear expansion of the matrix and secondary phase;

(d) mask the actual beginning of recrystallization as a result of disintegration of excess particles during plastic deformation and a higher barrier effect, and also due to structural strain hardening.

The contribution of some or other of these effects depends in the first place on the size and shape of particles, and also on the distance between adjacent particles.

Let us analyse how the dislocation structure of alloys with excess phases changes during deformation.

In the general case, excess particles serve as barriers for the dislocations that move in the matrix during deformation. This results in a local increase of the dislocation density in microvolumes of the matrix near excess particles, an increase in the excess of dislocations of one sign and, consequently, in an increased local curvature of the crystal lattice in these microregions. In heating, these regions become preferable sites of nucleation. These are the sites where large-angle boundaries form more readily than in other places. Larger particles of irregular shape produce a greater effect on local curvature, especially at lower deformations.

I. W. Martin et al. [306] studied local curvature of the lattice on deformation of Cu + SiO_2 alloys with spheroidal SiO_2 particles and of Al + $CuAl_2$ alloys with $CuAl_2$ particles (θ-phase) in the form of disc platelets, 0.25-1.2 μm in diameter and about 500 Å thick. In the latter case the regions near platelets had a greater curvature, which was detected by electron microdiffraction and by asterism in Laue photographs.

M. F. Ashby has analysed the effect of particle shape and found that particles of different shape produce different types of dislocation structure in adjacent regions of the matrix. With particles of lamellar or acicular shape, the glide of dislocation loops plays the leading

part in the formation of dislocations in the matrix, which causes sharp local misorientation. With small equi-axed particles, the leading role belongs to prismatic dislocations which cause no appreciable misorientation.

This explains well the above considered cases of the reduction of recrystallization temperature by inclusions and also the fact of the preferable nucleation in local excess ferrite regions near pearlitic colonies, non-metallic inclusions (see Fig. 54), etc.

Ashby's conclusions are however valid only for cases where the size of particles and the distances between them are sufficiently large (of a few tenths of a micrometre or more) and the volume occuied by the particles is relatively small (not more than 4-5%).

An utterly different dislocation structure appears if disperse phase particles and the distances between them are smaller and their volume concentration is higher. Exactly this circumstance is responsible for retarded recrystallization and not only the locking effect of particles on the distribution and migration of dislocations during heating.

The dislocation structure of heterophase alloys and its variation in recrystallization were analysed in the last decade in the works of E. Hornbogen et al. and by other researchers [308-311]. In most cases these studies were made on alloys in which the secondary phase was an oxide formed through internal oxidation. Owing to their negligible solubility and low liability to coagulation, these phases are convenient for determining the role of particles proper.

A typical research work of this kind in its technique and the results obtained is the work [310] concerned with the studies on deformed, internally oxidized, Ag-Mg alloys (oxide phase, MgO) and Cu-Al alloys (with Al_2O_3 oxide). The size of and the distance between MgO particles in the former alloy were approximately 60 Å and 200-300 Å respectively. For Al_2O_3 particles in the latter alloy, these values were 500 Å and 1800-2500 Å.

Oxidized strip specimens were deformed by rolling at room temperature to a deformation of 5 to 75%, after which their dislocation structure was examined. For comparison, reference specimens of pure silver and pure copper were rolled to the same deformation and examined.

In alloy specimens containing oxide particles, the dislocation density was even appreciably higher than in the corresponding pure metal specimens after light deformations (roughly 5%).

The dislocations had a large number of jogs and were of a complicated form. They were distributed uniformly and chaotically over the matrix. Signs of cell structure appeared in alloys much more heavily deformed than pure metals. This was especially the case where the alloys contained smaller particles and had smaller interparticle distances.

V. K. Babich observed a similar effect in a carbon steel with lamellar pearlite colonies. A distinct cell structure formed in excess ferrite deformed to roughly 10%, whereas a deformation of 20 to 30% was needed to produce the same effect in the ferrite of pearlite.

In the presence of oxide particles, cells are smaller in size and more uniform than in pure metals (Table 31). Cell walls in hetero-

TABLE 31. **Structural Characteristics of Pure Silver and Copper and Heterophase Ag-MgO and Cu-Al_2O_3 Compositions after Rolling (ε=75%)**

Material	Average size of cell, μm	Cell size range, μm	Misorientation across cell walls, degrees	Change in lattice orientation at distance 3 μm, degrees
Ag	0.45	0.2-1.0	5-13	28
Ag-MgO	0.15	0.08-0.4	2-4	10
Cu	0.5	0.3-1.2	2-6	14
Cu-Al_2O_3	0.35	0.2-0.5	2-4	12

phase systems are rather less distinct and have a lower excess of like-sign dislocations, so that they feature a smaller misorientation relative to one another than in the absence of disperse particles.

In an Ag-MgO alloy, which is characterized by a very small size of particles, the thickness of cell walls after heavy deformation (75%) exceeds the interparticle distance and the dislocation density in the walls is lower than in an alloy with larger particles. In pure silver deformed to the same degree of deformation, cell boundaries are almost flat and the cells are essentially subgrains. A typical dislocation structure of this type is shown in Fig. 175.

A series of electron micrographs were taken to determine the average variations in the lattice orientation in pure silver and copper and Ag-MgO and Cu-Al_2O_3 alloys over a length of 3 μm. The structural characteristics obtained are given in Table 31.

The textures of heterophase alloys also greatly differed from those of the respective pure metals. The orientations {100} ⟨112⟩, typical of pure silver and copper, were not detected at all in heterophase materials. The texture of heterophase alloys was poorly distinct and multicomponent. The Ag-MgO alloy was found to have the main orientations {110} and {112} and supplemental orientations {130} and {111}.

These observations cannot be explained properly if the excess particles are regarded only as barriers for dislocation movement. Indeed, as noted in [310], in that case one could expect the appearance of dislocation pile-ups generated by a limited number of sour-

ces. Actually, however, a high density of rather uniformly distributed dislocations is observed even on light deformations.

For such a distribution, a material should contain a large number of internal dislocation sources. In [310], it is assumed that particles proper perform the function of such sources; thus, excess particles have a double role, i.e. they act as dislocation generators and as barriers for dislocation movement.

It is still impossible to decide definitely what actual mechanism it is by which particles can act as dislocation generators. One of the most probable mechanisms is related to the fact that a stress dield must always exist around particles, this field being due to the difference in specific volumes between the particles and matrix and the difference in their linear expansion. On application of an external stress, a stress concentration at a particle-matrix boundary

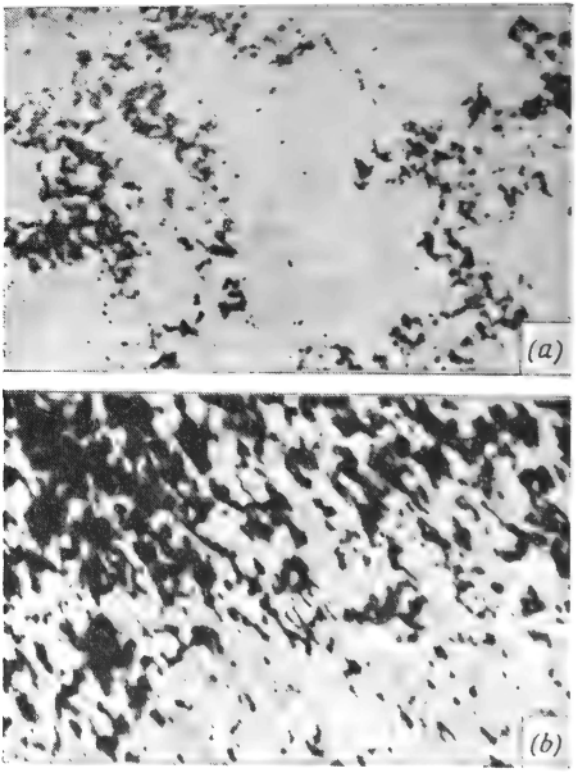

Fig. 175. Dislocation structures illustrating the effect of oxide particles on the formation of a cell structure, ×40 000, [310]

(*a*) Ag, $\varepsilon = 20\%$; (*b*) Ag + MgO, $\varepsilon = 18\%$

can also be caused by the difference in the elastic moduli of the adjacent phases.

The appearance of such numerous dislocation sources must not only increase sharply the dislocation density but also activate dislocation slip in many systems even on light deformations. This effect was observed experimentally in Al-Cu system [308]. More easier multiple slip must in turn cause a more uniform distribution of dislocations and a less distinct dislocation texture, produce less favourable conditions for local accumulation of excess dislocations of like sign and, as a result, diminish local misorientation, so that a cellular structure must change to a structure with randomly distributed dislocations.

The barrier effect of particles at the deformation stage acts in the same manner. Collisions of screw dislocations and particles facilitate cross slip and the formation of dislocation jogs and dipoles. Edge dislocations tend to bow around particles and their screw segments which form on bending can move by cross slip, thus leaving jogs and loops in a dislocation line.

In the above discussion we have dealt only with the specific changes of the dislocation structure of the matrix in the course of deformation due to the presence of disperse phase particles. As regards the structure of particles proper, it has not been analysed or considered in the majority of the cited published works. Under certain conditions, however, it is necessary to take into account the structural changes caused by plastic deformation of disperse phase particles.

These changes are associated, in the first place, with the possibility of plastic deformation and disintegration of disperse particles, especially those of a lamellar shape (or in general of not a globular shape). That the possibility of deformation of hard phases (carbides and oxides) exists has been shown convincingly in [304, 312] for lamellar iron carbide (cementite) and complex carbides on its base. The respective effect that this circumstance has on recrystallization will be discussed later in the chapter.

Particles of an isotropic form can also change to a lamellar (flattened) shape after heavy deformations, as, for instance, has been observed in cobalt particles in the Cu-Co system [313]. This must delay recrystallization, especially at a large concentration of particles.

Let us now discuss the effect of particles on the formation and growth of recrystallization nuclei. This effect may be either indirect or direct. The indirect effect is due to the above considered influence of particles on the nature of the dislocation structure that forms during deformation. As should be clear from the foregoing, this effect can be either accelerating or retarding. Particles also produce a direct effect by retarding dislocation slip and boundary migration; this effect can naturally be only retarding.

The presence of a small quantity (volume concentration $f < 3$ to 4%) of large (>0.3-0.4 μm) hard particles increases the local dislocation density and the excess of like-sign dislocations. Large distances between particles form favourable conditions for unobstructed migration of subboundaries through distances which are sufficiently large for the formation of large-angle boundaries. The process of recrystallization then occurs rather more quickly than in a matrix free from excess particles.

With a large concentration ($f > 5\%$ by volume) of very fine particles (<0.05-0.01 μm), the small distances between them (0.10-0.05 μm) favour a still greater increase in the dislocation density. However, the excess of like-sign dislocations is much lower here and the distribution of dislocations is more uniform. All this impedes the formation and especially the growth of subgrains. For subboundaries to transform into large-angle boundaries for subgrains into recrystallization nuclei, boundaries must move along over much larger distances than they do in a material with coarse particles. On the other hand, because of the retarding effect of particles the rate of boundary migration in a fine-grain material is lower than in a material with coarse particles.

As a result, subgrains (blocks) form at the initial stage of annealing, but since there are no favourable conditions for the preferable rapid growth of any of the subgrains, neighbouring subgrains will grow to a comparable size before large-angle boundary centres originate, and therefore the driving force of the growth will diminish appreciably. Thus, further growth of subgrains practically comes to an end and the process is finished, as it were, at the stage of prerecrystallizational polygonization.

After very heavy deformations at which a cellular structure forms, annealing results in the transformation of cells into subgrains. The further transformation of subgrains into recrystallization nuclei depends on the uniformity of a cell size.

Finally, for the case where the size of particles is within 0.3-0.05 μm and the distance between them is within 1.0-0.1 μm, the indirect effect of particles ceases to be decisive. Now it is the direct effect of particles on the movement of dislocations and low- and large-angle boundaries that becomes predominant. Since the distances between particles are sufficiently large for the formation of recrystallization nuclei surrounded by large-angle boundaries, the role of particles essentially reduces to retardation of the growth of recrystallization nuclei. In the case considered, common methods of analysis may fail to detect the beginning of recrystallization if the concentration of particles and the distances between them are such that the nuclei being formed are very small (<1 μm). The beginning of recrystallization can also be masked by stresses in the matrix that arise from the difference in thermal expansion coefficients.

The above discussion will be illustrated by some examples that follow.

Recrystallization of ferrite of steels with different content of carbides. Experiments were carried out on commercial iron containing 0.08% C (by mass), whose initial structure was ferritic; steel Ст 3 with 0.15% C (initial structure being ferrite and pearlite); and steel ШХ15 with 1.5% C (initial structure being granular pearlite). Chromium steel ШХ15, in which the alloyed cementite is more resistant to coagulation, was taken for comparison in order to preclude the effect of dissolution and coagulation of carbides on recrystallization.

The specimens were upsetted to 20, 40, 60 and 80% at room temperature, after which t_r^s in the middle section of the specimens was determined by various methods.

The results are given in Table 32. The temperature of the beginning of recrystallization for Ст 3 (which is low in carbides) turns out to be below that of commercial iron.

Further, experiments have proved that a large concentration of disperse particles (carbides) masks the onset of recrystallization. For instance, a common radiographic technique with steel ШХ15 gives a result that is inexplicable on the face of it: t_r^s increases with the degree of deformation (see Table 32). In specimens deformed 40%, point reflections appear in heating to 550°C, and in specimens deformed 80% only to 625°C.

The results obtained by hardness tests are more explicable even if the temperature of 50-% softening is taken as t_r^s. In this case (see Table 32) t_r^s lowers with increasing deformation.

TABLE 32. **Values of t_r^s for Selected Alloys, as Found by Various Methods**

Method*	Deformation, %				Method	Deformation, %			
	20	40	60	80		20	40	60	80
	Commercial iron					*Steel* ШХ15			
X-R	600	575	575	550	*X-R*	550	550	550	625
H	565	575	565	565	*X-R (m)*	—	—	—	550
	Steel Ст3				*HD*	—	500	500	450
X-R	600	550	525	525	*H*	570	525	515	510
HD	—	550	550	540					
H	585	580	560	550					

* Explication: *X-R* – common radiographic technique with a beam $d = 1$ mm (Cr-K radiation); *X-R (m)* – micro-beam radiography ($d = 0.1$ mm, transmission photography of Mo-K radiation); *HD* – hardness-difference test (see Ch. 15); *H* – hardness test (50-% softening).

The results obtained by some special methods for determining the actual beginning of recrystallization (as described in Ch. 15) differ even more from those obtained by the common radiographic techniques. For instance, the temperature of the beginning of recrystallization in steel ШХ15 deformed 80%, as found by the hardness-difference test, is approximately 450°C, i.e. 60 degrees C below that determined by the temperature of 50-% softening; in steel specimens deformed 60%, t_r^s is around 500°C, etc. In steel specimens deformed 80%, the beginning of recrystallization is detectable by the microbundle method beginning from 550°C, i.e. also earlier than by the common techniques. This is obviously associated with the fact that a heavy deformation changes both the matrix and the hard carbide phase in steel ШХ15.

Plastic deformation of cementite platelets in the pearlite of carbon steel was first noted by B. N. Orlov and B. G. Livshits [312] and was later confirmed and studied in more detail by V. K. Babich [304]. Disintegration of carbides in steel ШХ15 after 80-% deformation was also proved metallographically. Disintegration increases the quantity of disperse particles and diminishes their size, while the volume concentration of particles remains unchanged; this must slow down the growth of recrystallization nuclei and diminish the average size of recrystallized grains.

The presence and disintegration of carbides are responsible for some other specifics of the process. For instance, the hardening effect of deformation is greater when more carbides remain in the original state. The hardness increases after 80-% deformation by 100 HV in commercial iron, 120 HV in steel Ст3, and 150 HV in steel ШХ15.

The reverse is true where alloying elements enter the solid solution; in deformation, the original metal hardens to a greater extent than the alloyed solution.

A specific pattern of hardness variation is also observed in heating high-carbide steels (Fig. 176). In heating commercial iron and steel Ст 3 above t_r^s, the hardness of the most heavily deformed specimens is found to be the same as in lightly deformed ones (Ст 3) or even lower (commercial iron). The pattern is different for steel ШХ15. Up to the end of the primary recrystallization, more heavily deformed specimens remain harder (the hardness difference is quite high, 40 HV). This peculiarity can be explained by disintegration of the cellular structure during deformation and, as a result, by disintegration of recrystallized ferritic grains, whose growth is additionally impeded by particles.

The effect described is of essential importance for developing an appropriate technique of intermediate softening-annealing stages for steels with various concentrations of disperse phases.

This clarifies the results obtained by I. A. Sobolevsky [303] who has found (by common X-ray analysis) that t_r^s of the matrix (α-Fe)

in carbon steel and the activation energy of the process increase with the content of carbon.

The temperature which was taken by Sobolevsky as the temperature of the beginning of recrystallization was actually that of the beginning of intensive growth of recrystallization nuclei, rather than the actual value of t_r^s. As regards the effective activation energy, it only reflects the temperature dependence of the rate of the

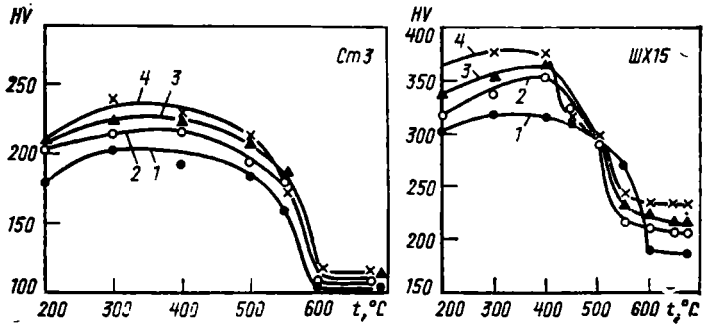

Fig. 176. The hardness of steel after heating to various temperatures and deformation to various degrees

1—ε = 20%; *2*—40%; *3*—60%; *4*—80%

process. It is clear that the temperature dependence of the rate of growth of recrystallization nuclei in a steel is more pronounced at a higher concentration of carbides which retard the growth of nuclei more strongly at low temperatures than at elevated temperatures (owing to their coagulation).

Recrystallization in Al-Al_2O_3 alloy (SAP). Experiments were made initially on an alloy containing 4% aluminium oxide. Specimens were made by hot pressing, which were then cold rolled to 65% without intermediate heating, heated at various temperatures for one hour, and cooled in air.

The orientations (111) [112], (001) [110], (110) [1$\bar{1}$0], (112) [111] and (110) [1$\bar{1}$2] were revealed in the specimens immediately after cold rolling. The large diversity of orientations is obviously associated with the above described effect of hard disperse particles. In heating, two temperature intervals of softening were distinguished clearly (Fig. 177): the first interval (near 200°C) within which hardness diminished only insignificantly

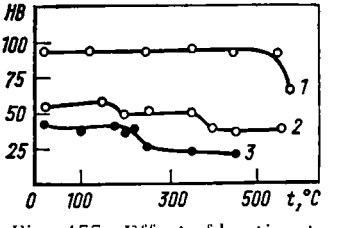

Fig. 177. Effect of heating temperature on hardness of cold-rolled aluminium and SAP

1—SAP (9% Al_2O_3); *2*—SAP (4% Al_2O_3); *3*—aluminium

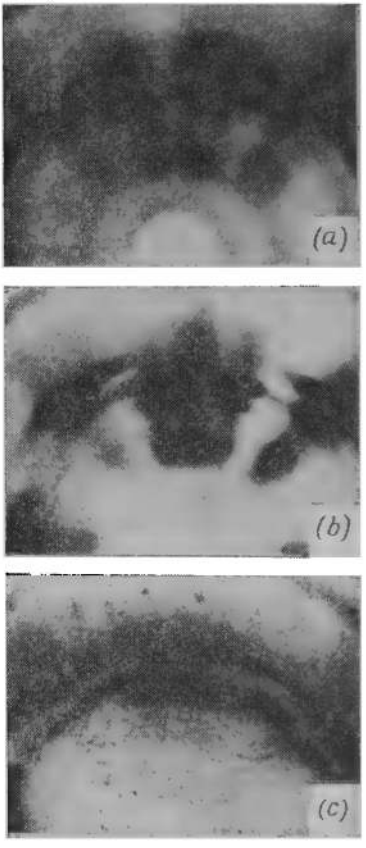

Fig. 178. Radiograms of cold-rolled SAP alloys with 4% Al_2O_3
(*a*) as-deformed; (*b*) deformed and heated at 225°C; (*c*) same at 450°C

and the second interval (near 360-400°C) which gave the main loss of hardness. In the case of pure aluminium, there was only one temperature interval of sharp softening, associated with recrystallization: it was near 225°C, i.e. 10-15°C above the first temperature interval of softening in SAP alloy.

Apart from weak softening, heating of a SAP alloy with 4% Al_2O_3 to 225°C involved a change in the texture (Fig. 178*a* and *b*). The extent of the texture maxima shortened and, what is most important, the type of texture changed to a new one having the orientations (110) $[1\bar{1}2]$, (112) $[\bar{3}51]$ and (112) $[\bar{3}12]$. This result clearly shows that the cold-rolled SAP alloy undergoes primary recrystallization in heating to 225°C, but recrystallization nuclei remain very fine, which is confirmed by the fact that lines on radiograms remain continuous, i.e. the process of recrystallization is localized in microvolumes.

On heating at 350°C for one hour (i.e. at a temperature of 0.7 T_m of aluminium), texture maxima on radiograms became weaker and individual reflections appeared, which were the traces of reflection of X-rays from individual large grains. This effect was still stronger at 400°C. On heating at 450°C (Fig. 178*c*), traces of texture maxima disappeared almost fully and the radiograms looked much like those typical of very coarse-grained specimens in which grain growth was completed.

Thus, the nature of structural changes during deformation and recrystallization in the SAP alloy with 4-5% Al_2O_3 is very similar to that observed in high-carbide steels. The aluminium matrix in the cold-rolled SAP alloy is strain-hardened to a greater degree than similarly deformed pure aluminium. Disintegration of brittle oxide particles also takes place.

These results, like the data obtained for steel IIIX15, show that a disperse phase in a concentration of a few per cent can separate the two elementary processes of recrystallization—nucleation and grain growth—by a wide temperature interval.

As may be seen from the results for the SAP alloy, what is essential is that the formation of recrystallization nuclei causes softening to a lesser extent than the process of growth of these nuclei. For that reason, the process of softening in SAP alloy turns out to be shifted into the region of higher temperatures, approximately by 175-200°C compared to pure aluminium.

In an alloy with 6% Al_2O_3 (by volume), the onset of recrystallization in the aluminium matrix and the softening effect in the alloy can be detected by structural analysis and hardness measurements starting only from 500°C, i.e. at a temperature 175°C above that in pure aluminium.

A qualitatively different result was obtained with the content of Al_2O_3 increased to 9% by volume. Neither hardness measurements nor special structural methods for determining the actual t_r^s could give evidence of the beginning of recrystallization up to a temperature of 550°C, i.e. to a temperature near the melting point of the aluminium matrix. The alloy turned out to be practically unrecrystallizable. It may be supposed that this effect is associated with the fact that the aluminium matrix consists of very small regions which are homogeneous in size and only slightly misoriented relative to one another and are surrounded by barriers of high-disperse Al_2O_3 particles. This stability against recrystallization of alloys with a high concentration of disperse particles should obviously be attributed primarily to the absence of conditions for dislocation redistribution and boundary migration, and therefore for the formation of recrystallization nuclei.

$Ag + MgO$ and $Cu + Al_2O_3$ alloys [310]. The structures of these groups of alloys in deformed state have been discussed earlier. In alloys with disperse particles of this type, the changes in heating are much similar to the changes occurring in the SAP alloy.

In the presence of oxide particles, the process of softening in silver and copper is shifted to a higher temperature. At an MgO content of 0.5% (by mass), recrystallization of silver is fully suppressed up to 840°C, i.e. to 0.9 T_m of silver.

At medium concentrations (0.25% MgO), two temperature intervals are detected within which hardness drops heavily, though the authors of [310] have attached no importance to that fact.

The rate of formation of subgrains at a high temperature (840°C or $0.9T_m$) is relatively high at the beginning of annealing, but then drops markedly. Subgrains grow very slowly, notwithstanding the high temperature.

In contrast to single-phase metals and alloys, no recrystallization by migration of boundaries of the initial grains is observed in alloys high in disperse particles after moderate deformations.

Up to now, in considering the barrier effect of particles, we have assumed that they remain immobile in the matrix during recrystallization, though this is not always so under real conditions.

During prolonged high-temperature annealing or holding, the moving grain boundaries can drag along particles. This results in redistribution of particles and their coagulation and local accumulation.

The interactions of secondary-phase inclusions with moving boundaries have been studied by a number of Soviet [37, 314, 315] and foreign workers [316-318].

A migrating boundary can capture a particle when the driving force of migration, P_{dr}, is smaller than the maximum force of interaction between the boundary and particles, i.e. when the condition $P_{dr} \leqslant n_p P_{br}$ is met, where P_{dr} is the unit driving force of boundary migration, P_{br} is the maximum force of interaction between the boundary and a particle, and n_p is the density of particles in the boundary. Particles will not retard a moving boundary if this condition is not observed.

If a boundary, after covering a distance X (Fig. 179), drags along all the particles in the volume it has passed through, the amount of the secondary phase accumulated in the boundary will be related to X by the relationship $4\pi r^3 n_p/3 = VX$, where V is the volume concentration of the secondary phase in the alloy, and r is the radius of a particle.

A change in the number and size of particles on the moving grain boundary can change the force P_{br} of interaction between the boundary and a particle [316, 317]: $P_{br} = (P_{dr}/n_p) \cdot [1 - n_p \pi (r \cdot \sin \alpha)^2]$, where α is the angle between the boundary direction and a radius drawn to the line of intersection of the boundary and particle.

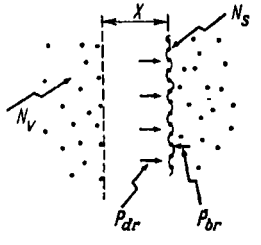

Fig. 179. Concentration of secondary phase particles on a migrating boundary (schematic). N_V and N_S—particle density per unit volume and unit area of boundary; X—path of migration; P_{dr} and P_{br}—driving and braking force of boundary migration [318]

Ashby and Centamore [318] studied the movement of oxides of various structure (liquid—B_2O_3, GeO_2; amorphous—SiO_2, and crystalline—Al_2O_3) together with boundaries of primary recrystallization nuclei in single crystals of copper. The technique used by them consisted in that large-angle boundaries were produced in a copper single crystal with uniformly distributed inclusions (introduced by internal oxidation) by pressing an indentor, after which the specimen was heated. In migrating into the depth of the crystal, bounda-

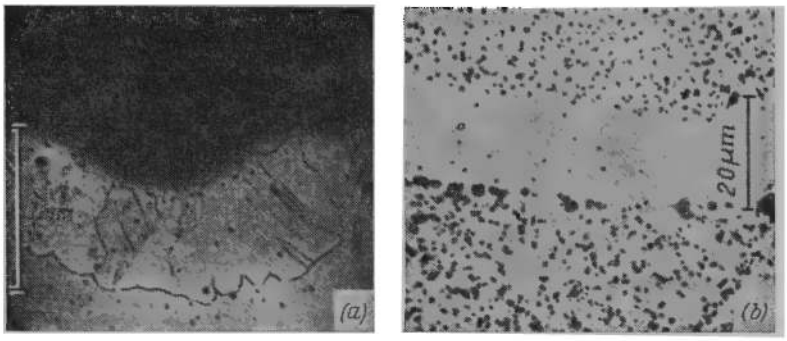

'ig. 180. Section of a copper single crystal with SiO_2 particles after indenting and annealing (1000°C, $\tau = 2$ h) [318]

a) etched to reveal grain boundaries; the recrystallized zone and the recrystallization front re seen clearly; (*b*) enlarged portion of the recrystallization front before etching; the clear region is the particle-free zone behind the front

ies dragged along inclusions and left behind an inclusion-free egion (Fig. 180).

Knowing the effect of the temperature and time of annealing on he width of that region, X, it was possible to obtain data on the rate f migration, activation energy of the process, etc. At the same ime, the microstructure of the alloy and the shape of particles were nalysed. The authors [318] have found that the path particles cover ogether with a boundary increases as the temperature increases and article size diminishes. The rate of boundary migration is limited y the rate of particle motion, which is different for particles of arious nature. In the high-temperature region (above 1000°C), vhere the three oxides—SiO_2, GeO_2 and B_2O_3—are relatively fluid, ll these particles are highly mobile to the same extent.

Within the temperature range of 650-1000°C, the particles that re fluid at these temperatures (B_2O_3, GeO_2) have the highest rate f motion. Amorphous particles are less mobile and crystalline Al_2O_3 articles are practically immobile.

Thus, the mobility of particles definitely depends on their visco- ity (on the rate of self-diffusion and diffusion of copper in particles), .e. on the composition and crystal chemistry of particles.

The fact that all particles moving with boundaries change their hape against that they have had before [318] is good evidence in upport of the assumption that the migration of particles with boun- laries also involves mass exchange in particles proper. For instance, pherical particles become lenticular after being dragged along by . boundary (Fig. 181).

In their analysis of the interactions of particles and boundaries, erebryakov et al. [314, 315] have come to a conclusion that under

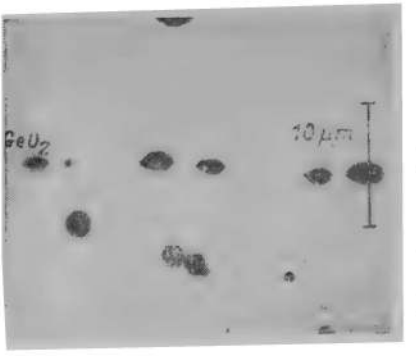

Fig. 181. Lenticular GeO_2 oxide particles in copper, moving together with the boundary [318]

definite conditions the migration of a grain boundary must take place through the accomplishment of a number of successive stages, such as accumulation of particles on a boundary and detachment of the boundary from the accumulated particles. The authors have formulated conditions for conjoint movement of boundaries and particles, accumulation of particles, and detachment of boundaries. They have observed experimentally an interrupted migration of boundaries in a Cu — 0.37% Si alloy (mass percentage) after internal oxidation at 850°C, cold rolling, and annealing at 980°C. The distribution of particles before and after annealing is shown in Fig. 182. As seen, the initially uniform distribution of particles changes upon annealing to a non-uniform one; the position of the clusters of particles is shown at the moment when the boundary is ready to detach from them. Such accumulations of particles can be considered in the general case as a typical feature of the completed recrystallization in an alloy where particles before recrystallization were distributed uniformly throughout the volume.

A special case is recrystallization in heterophase alloys of the type where interlayers of one phase envelop every particle (crystallite) of another phase and thus preclude direct contact between the latter

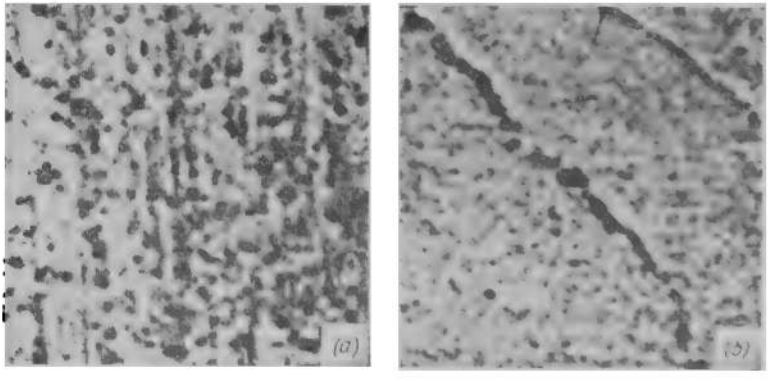

Fig. 182. Distribution of particles before (*a*) and after annealing (*b*) in Cu + + 0.37% Si alloy oxidized internally at 850°C, cold rolled and annealed at 980°C [314]

and the matrix. In such systems, large-angle boundaries are mostly of the inter-phase type.

Many of the materials produced by powder metallurgy belong to the systems of this type. They may be either mixtures of powders of various metals (alloys) or powders of metals whose particles have been oxidized on the surface or subjected to another chemical or thermochemical treatment. A very popular type of material is that in which some additions form a liquid phase at the temperature of sintering and envelop particles of the more hard-melting main substance.

Recrystallization and grain growth in such systems have been studied by Geguzin et al. [365].

An experimentally confirmed calculation has shown that the kinetics of grain growth in such alloys deviates from the law $(D - D_0) \approx \approx \tau$ or $(R - R_0) \approx \tau$, which is true of single-phase systems (see Ch. 3), but is governed by the relationship $(R^3 - R_0^3) \approx \tau$.

Geguzin and Klinchuk [365] have explained this fact as evidence that the rate of grain growth in such systems is controlled by diffusion mass transfer through a secondary-phase interlayer rather than by the processes of atom displacements on a boundary.

If so, the thickness of the interlayer as well as the diffusion properties of that interlayer, must exert a strong influence on the grain growth. Coarsening of grains must proceed more quickly with a smaller thickness of the interlayer, i.e. an appropriate relationship should be of the form $(R^3 - R_0^3) \approx (\tau/H)$, where H is the thickness of the interlayer and τ is the time of annealing.

Chapter 13

Recrystallization in Compounds

Modern technology makes ever increasing use of various compounds and solid solutions on their basis, usually prepared by powder metallurgy methods, such as high-melting compounds, which find wide applications as structural and tool materials, and a large group of compounds with special physical properties. These include ferrites (oxides of the type $MeO \cdot Fe_2O_3$), compounds based on chalcogenides of Group IV and V elements (Bi_2Te_3, Sb_2Te_3, SnTe, PbTe, etc.), which are used in thermoelectric converters, and also piezoelectrics, ferroelectrics, etc.

13.1. High-melting Compounds

The high interest to the temperature level of recrystallization and softening in high-melting compounds is determined by the fact that these materials are widely used in cutting tools for heavy-duty operation and as the base of heat-resisting metal ceramic (cermet) alloys.

The literature data on recrystallization in these compounds are very scarce, which can be explained by a high brittleness of these materials, so that they cannot be deformed by common methods. This difficulty can be overcome partially by using a method in which the surface of specimens is strain-hardened and annealed in vacuum and the processes of recovery and recrystallization occurring in the surface layer during heating are examined by X-ray analysis. The method was employed in [319, 320] for analysis of recrystallization in high-melting carbides and borides.

The reliability of this method has been checked on nickel, iron, and chromium, and the results obtained have shown that the temperatures of the beginning of recrystallization in strain-hardened surface layers coincide with those measured in specimens deformed by common methods to a high degree (60-70%).

Later, G. V. Samsonov [321] has managed to deform high-melting carbides by uniform compression. The temperature of recrystallization after this type of deformation has proved to be practically the same as in a strain-hardened surface layer.

The method of surface strain-hardening was employed for analysis of recrystallization in carbides of the WC-TiC-TaC system and

in WB, MoB, TiB, TiB_2 and ZrB_2 borides. Among them, there were pure compounds, solutions of metals in compounds, and solid solutions of various compounds in one another, such as (Ti, W) C, (Ta, W) C, and (Ti, Ta, W) C, with various proportions of binary compounds, including unsaturated (single-phase) and supersaturated (age-hardening) alloys. The compositions of many alloys were close to or identical with the compositions of commercial alloys. The particular compositions and the methods for preparing specimens are given in [319].

In most of the alloys tested, cobalt powder was the binder. Only in ZrB_2 boride, iron was used instead of cobalt. The use of cobalt (or iron) was dictated by the fact that TiC and TaC carbides and also TiB_2 borides without cobalt (iron) could not be strain-hardened even by emery disc roughing, obviously in view of the extremely low bondage between particles.

The presence of an excess plastic cobalt (or iron) as a binder, in which brittle high-melting particles are embedded, changes radically the conditions of deformation, so that they become much like the conditions of uniform compression in which brittle phases deform more easily. If cobalt (iron) dissolves in a compound, it improves plastic properties obviously because of changes in the interatomic bonds. Further, the addition of cobalt makes the alloys under test more comparable to commercial alloys in composition, which is of much practical significance.

Recrystallization in high-melting compounds obeys the general laws, but has some specific features of its own:

1. The relative temperature of recrystallization in these compounds roughly corresponds to the maximum level for single-phase alloys, i.e. $T_r/T_m = 0.5\text{-}0.6$.

2. The effective activation energy of recrystallization is relatively low (with rare exceptions) and is approximately the same as in solid solutions of the metals having an appreciably lower temperature of recrystallization than high-melting compounds.

For instance, the 'activation energy' of recrystallization in WC (approx. 75 kcal/mole) is even lower than that in aluminium, though the temperature of recrystallization of this carbide is roughly 8-10 times that of aluminium.

3. Soluble minor additions influence the recrystallization in compounds in a different manner than they do in pure metals. For instance, a minor addition of cobalt lowers t_r^s of a compound, the effect being stronger with a higher concentration of dissolved cobalt. An addition of 2% Co to WC, (Ti, W)C, and TiC carbides before sintering lowers the t_r^s of these carbides from 1300° to 1260°C, 1440° to 1360°C, and 1560° to 1460°C, respectively.

Measurements of variations in the lattice spacing have shown that the solubility of cobalt decreases with an increase of the concentra-

tion of WC in a complex carbide. The highest quantity of cobalt that can be dissolved in TiC carbide is more than 1% against 0.1% in WC carbide. The maximum drop of t_r^s has been found in TiC + Co carbide.

4. For complex compounds with varying concentrations of the simple constituents, t_r^s increases linearly with an increase of the molar concentration of a higher-melting constituent. For instance, with a decrease in the molar concentration of WC in the complex (Ti, W)C carbide from 44% to 30% and then to 25%, t_r^s increases respectively from 1400° up to 1450° and 1500°C.

5. If recrystallization is accompanied by the decomposition of a compound, which is a supersaturated solid solution. t_r^s is shifted to higher temperatures, as also is the case with supersaturated solid solutions based on metals. At a higher saturation, the concentration of a disperse phase increases and t_r^s rises more appreciably.

6. With an increase in the excess of binder metal in an alloy, the recrystallization temperature of the compound drops noticeably. For instance, an increase in the concentration of cobalt from 2% to 10% (by volume) lowers t_r^s of titanium boride by 100°C.

It should be emphasized that this relates only to an excess concentration of cobalt, since an increase in the concentration of cobalt within the limits indicated earlier has no effect on its dissolution in a compound. Therefore, the role of excess cobalt obviously reduces to changing the conditions of deformation.

Analysis of broadening of radiographic lines has shown that the deformation of carbide phases involves structure changes typical of brittle materials, i.e. refinement of coherent scatter regions and very low values of microstresses. The ratio of the broadening of lines with large reflection angles to the broadening of those with low angles is always lower than the ratio of the secants of these angles. This means that the microstresses are so low that they do not contribute to broadening. As has been found, mosaic blocks are refined to a size of 150-500 Å.

In all cases, either in compounds or in their supersaturated solid solutions, narrowing of radiographic lines stops fully before the onset of recrystallization.

In an age-hardening complex carbide (Ti, Ta, W)C, the narrowing of radiographic lines, which starts at relatively low temperatures of heating, slows down near 1300°C because of decomposition and the lines remain wider than they are in the original state (before strain-hardening) up to 1450°C. Since the broadening effect, even in as-deformed state, is associated only with dispersity, it is natural to conclude that the narrowing of lines results from the enlargement of coherent scatter regions. As determined by the width of lines, an intensive growth of blocks begins during heating above 900°C in WC carbide and above 1100 C in TiC, TaC and (Ti, Ta, W)C carbides.

In an age-hardening complex carbide, the precipitated disperse phases retard the growth of blocks up to 1450°C.

The mechanism of recrystallization in high-melting compounds seems to be determined largely by the structural changes that take place during deformation. This mechanism is obviously typical for all brittle materials. Recovery and recrystallization in these materials occur mainly as the processes of growth of grains (blocks) and the principal driving force here is the tendency of the system to lower its grain-boundary energy. The role of the volume energy (the energy of dislocations inside blocks that accelerates recrystallization) is very low, especially in more brittle materials. This is probably one of the reasons why brittle compounds have a high temperature level of recrystallization.

Another reason is obviously a higher energy of bonds in high-melting compounds compared to that in pure metals.

It is however impossible to explain the high temperature of recrystallization of interstitial phases only by the high energy of bonds. This becomes clear, for instance, if we compare the results obtained for molybdenum boride, MoB, with those for pure molybdenum. With the time of annealing for 2 h, the temperature of the beginning of recrystallization t_r^s is 1150°C for MoB and 800°C for pure molybdenum. The energy of bonds in MoB, if judged roughly from the melting point, must not differ sharply from that in pure molybdenum (T_m of MoB is even slightly lower than that of molybdenum). Therefore, assuming that the temperature of recrystallization is determined solely by the energy of bonds, t_r^s of MoB should be close to that of molybdenum. As found experimentally, however, it is 350°C higher.

This difference in t_r^s is evidently due to a large difference in the structures of MoB and Mo in as-deformed state. In pure molybdenum, deformation is accompanied by the appearance of rather large stresses and a relatively low dispersion of the structure. The opposite is true in the case of brittle molybdenum boride. For that reason, one of the main stimuli of recrystallization—the elastic volume energy of dislocations—is sharply suppressed in high-melting compounds.

This circumstance obviously accounts for the above-mentioned effect of a decrease of t_r^s in high-melting compounds (TiB and WC) on increasing the excess concentration of a plastic binder-metal. The presence of the binder changes the type of stressed state in deformation and the conditions of deformation, which thus approach the conditions of deformation of plastic metals, and therefore changes the structure in as-deformed state.

In view of the low dislocation density, the stage of nucleation and the associated redistribution of dislocations become inessential, and therefore the role of impurity atoms, which elastically interact with

dislocations, also becomes inessential. In that case, there must be no sharp rise of t_r^s in the range of minor concentrations. The effect of minor additions must show up only through the changes in the strength of interatomic bonds.

Such is obviously the mechanism by which minor quantities of dissolved cobalt can lower the temperature of recrystallization.

The rise of t_r^s in complex carbides (Ti, W)C, (Ti, Ta, W)C with an increase in the concentration of TiC and TaC carbides should also be attributed to the effect they have on bonding forces.

Thus, there are two ways for raising the temperature level of recrystallization in brittle materials, particularly in high-melting compounds: (1) by addition to the solid solution of elements or compounds which can increase the strength of interatomic bonds; and (2) by alloying to obtain a supersaturated solid solution which can decompose in recrystallization annealing and form a heterophase system with a uniformly distributed disperse phase which is stable against coagulation.

Alloying with minor additions, which is very effective for increasing t_r^s in plastic materials, gives no positive result with brittle materials.

This conclusion is partially true also for brittle metals in which, as has been established, microstresses in as-deformed state are low and minor additions can only slightly influence t^s.

The dislocation structure in as-deformed state can evidently be changed effectively by varying the temperature of deformation. In particular, the dislocation structure seems to be dependent appreciably on whether the plastic deformation takes place above or below the ductile-to-brittle transition point. It may be supposed that a material deformed at a temperature slightly above that point will have a lower t_r^s than a material deformed at a temperature below that point.

13.2. Ferrites

The principal magnetic properties of ferrites (see Ch. 1) depend largely on the microstructure parameters: grain size and inequigranularity. In ferrites used for high-power permanent magnets, texture is also essential.

Ferrites are manufactured industrially mainly by the methods of powder metallurgy. The desired structure parameters are ensured by controlling properly the technological conditions of ferritization, grinding, pressing, sintering, and by introducing various additions which can accelerate or retard grain growth. These problems have been discussed in recent years in a number of published works [56, 322, 323, 324]. Some results of these studies are considered below.

During grinding, ferritic particles become finer and strain-hardened. As shown in [325], a particular grinding process sets a definite limit on particle size (i.e. a material cannot be ground to a smaller particle size), but a longer time of grinding after reaching that limit increases the strain-hardening effect in particles. This has been confirmed by progressive broadening of interference lines on radiograms. Broadening effect is due to microstresses, i.e. to an increase of dislocation density in particles. Thus, in powders ground for a longer time, primary recrystallization begins at lower temperatures and occurs more actively, with the formation of a large number of nuclei. Accordingly, a fine-grained structure forms at the end of primary recrystallization.

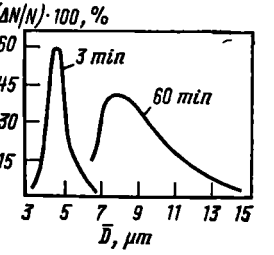

Fig. 183. Grain size distribution in lithium-alloyed ferrite after sintering at 1050°C for 3 min and 60 min [322]

The effect is not limited, however, to the structural changes in powder particles. A higher strain-hardening effect in powder particles has another consequence of practical importance, namely that sintering, i.e. intensive mass exchange between particles, begins at a lower temperature*. In our view, this is due to vacancies formed at the stage of nucleation (see Ch. 4).

This effect is of much practical interest. Firstly, with a lower temperature of sintering, the concentration of bivalent iron ions (Fe^{2+}) in a powder usually decreases, which raises the resistivity and lowers magnetization reversal losses. Secondly, a lower temperature of sintering (and of primary recrystallization) favours the formation of a more homogeneous and fine-grained structure, since the processes of grain growth and secondary recrystallization require a higher temperature. Thirdly, a low temperature of sintering is favourable for obtaining a less porous material [37]. Finally, it is favourable economically.

If a slight increase in the concentration of Fe^{2+} has no essential effect on the properties of a powder, grain refinement can be achieved by a special sintering technique including short-time heating at a high temperature (to form a large number of recrystallization nuclei) and the subsequent long sintering at a lower temperature to diminish porosity. In this process, the time of heating at the high temperature should be short, since otherwise the processes of boundary migration will develop and the structure formed will be inhomogeneous.

Figure 183 shows the grain size distribution curves for lithium ferrite after sintering at 1050°C for 3 min and 60 min. As may be seen, the shorter time of sintering (3 min) results in a fine-grained

* This phenomenon is usually called the increase in the activity of a powder.

and homogeneous structure, whereas a longer time (60 min) causes grain coarsening and sharp inequigranularity. Accordingly, the properties of the material in the second case are appreciably worse.

According to the work [326], annealing in a relatively low vacuum is also favourable for the formation of uniformly fine-grained and compact material. Vacuum accelerates the diffusion of vacancies and thus eliminates pores more intensively.

In most ferrites, inequigranularity is utterly undesirable, though it is promoted in many cases by the specifics of the technological process and by the composition of the materials.

The technology of making ferrites is such that the final product is inevitably porous, which however is typical of all materials prepared by powder metallurgy processes. Like disperse phase particles, pores impede boundary migration. With a non-uniform distribution of pores over the volume, the conditions of migration of various boundaries in contacting particles and between them may be different.

The effect of inequigranularity may be enhanced sharply if a porous ferrite also contains undissolved particles of disperse phases. Examples are alloyed ferrites. Comparative data on the grain growth in nickel-zinc ferrites of the original composition $Ni_{0.5}Zn_{0.5}Fe_2O_4$ and with various alloying additions are given in [322]. An intensive grain growth is observed on alloying such ferrites with tungsten trioxide (the composition $Ni_{0.48}Zn_{0.48}W_{0.04}Fe_2O_4$) and with copper oxide ($Ni_{0.46}Zn_{0.46}Cu_{0.08}Fe_2O_4$).

In order to determine the causes and mechanism of this effect, variations of the microstructures of these three compositions have been analysed in the course of isothermal heating at 1200°C. At this temperature, the process of grain growth develops quickly and becomes completed in a relatively short time (less than 4 h).

Figure 184 shows the grain size distribution curves for the three compositions annealed during various time periods. The typical microstructures obtained are illustrated in Fig. 185. In the original (unalloyed) nickel-zinc material (Fig. 184*a*), the size of grains increases with the time of annealing, but there are no grains which would grow preferably. The growth of grains is uniform, as is typical of the stage of grain growth.

In the presence of alloying additions, grains grow non-uniformly by the kinetics typical of secondary recrystallization (Fig. 184*b*). The inequigranularity that arises in the course of annealing (secondary recrystallization) practically disappears at the end of the process. The structure changes to a relatively uniform coarse-grained one. The final grain size in the material alloyed with tungsten trioxide and in the material alloyed with copper has turned out to be respectively about 10 times and 40 times that in the unalloyed materials.

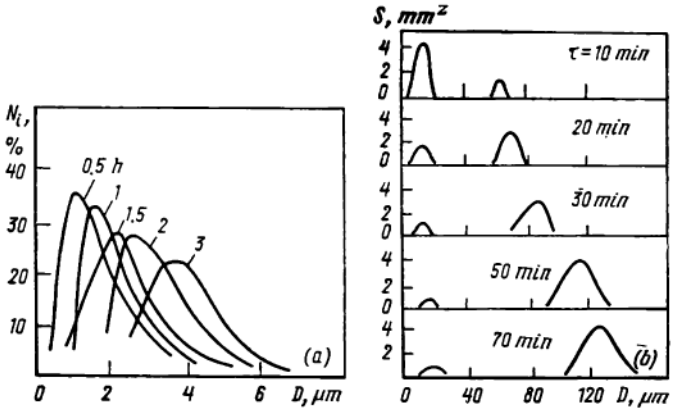

Fig. 184. Grain size distribution depending on the time of isothermal annealing at 1200°C. Ni-Zn ferrite [322]

(a) without addition of CuO; (b) with 4% (mol.) CuO

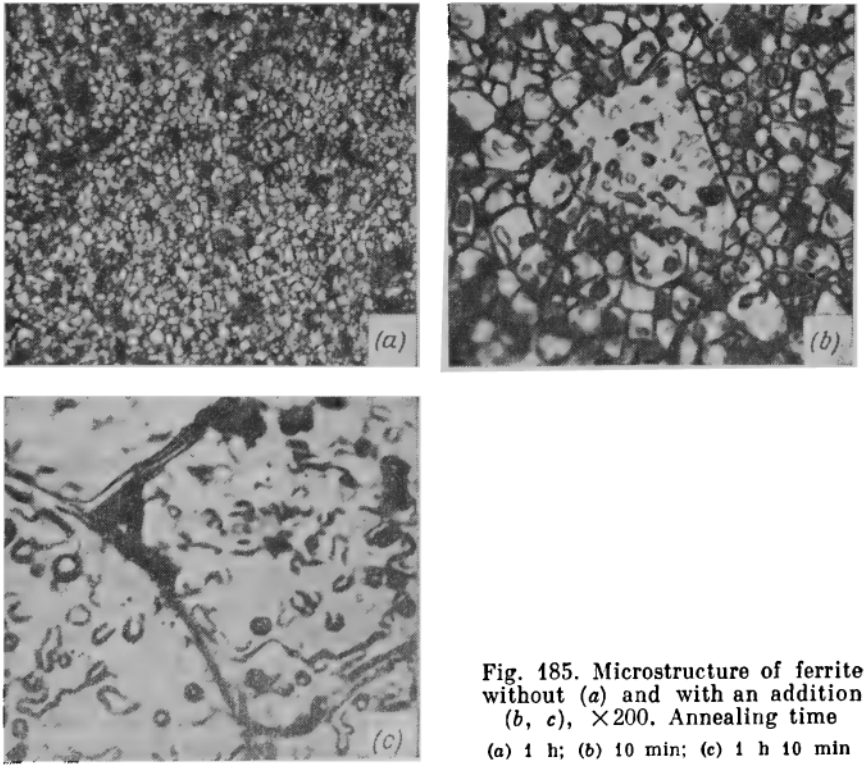

Fig. 185. Microstructure of ferrite without (*a*) and with an addition (*b*, *c*), ×200. Annealing time

(a) 1 h; (b) 10 min; (c) 1 h 10 min

As found by metallographic and X-ray microstructural analyses, the materials alloyed with tungsten and copper contain respectively unevenly distributed undissolved particles of tungstate, the type $Me^{2+}WO_4$ (where Me^{2+} stands for Ni^{2+}, Zn^{2+} or Fe^{2+} ions), and of copper oxides. With coarsening of grains of the matrix and with an increasing difference in the size of larger and finer grains (ΔD), the driving force of the process increases (see Ch. 3) to a level at which it can overcome the barrier effect of undissolved particles.

It can be also supposed, not without reason, that apart from secondary phase particles, an elevated concentration of vacancies in the materials with additions of copper and tungsten can also promote an accelerated growth of grains. The point is that the dissolution of impurities in compound crystals (where ionic chemical bonds are essential) is often realized by the subtraction mechanism. According to [327], a slight addition of copper (copper oxide) results in the formation of anionic vacancies, and an addition of tungsten in the generation of vacancies in the cathionic sublattice. An elevated concentration of vacancies must increase boundary mobility and thus facilitate boundary migration.

One of the most effective methods for microstructure control in ferrites, in particular for prevention of inequigranularity, is obviously fusion with the formation of small regions of the liquid phase (solid-liquid fusion). In [323, 328, 329], this has been convincingly demonstrated for lithium-alloyed rectangular-loop ferrites whose properties are strongly structure-sensitive.

The experiments were carried on ferrites of the compositions $Li_{0.5}Fe_{2.5}O_4 + \gamma$ and $Li_{0.54}Mn_{0.13}Fe_{2.33}O_4 + \gamma$, which after annealing (800°C, 3 h) were alloyed with 0.5 to 3% (by mass) of fusible additions, Bi_2O_3 and V_2O_5. In sintering these formed a liquid phase of the eutectic type with a relatively low melting point (near 600-700°C). The inequigranularity was estimated in terms of the $\sigma^2 D$ ratio, where σ^2 is the mean-square deviation of grain size, and D is the average grain size.

The analysis of the microstructure of these materials after annealing at various temperatures, with or without the additions indicated (Fig. 186), shows that the processes of microstructure formation are noticeably different. The following regularities can be mentioned.

1. Specimens with the fusible additions are pressed more easily and have a higher density.

2. Specimens with fusible additions of Bi_2O_3 and V_2O_5 have a developed microstructure already after annealing at 750-800°C, whereas those without additions show it only after annealing at 1100°C. The process of grain growth in the alloyed specimens may conditionally be divided into two stages: the first is noted for a relatively slow growth and the second for intensive growth. The transfer from the first to the second stage occurs in the range of 1100-1200°C. In

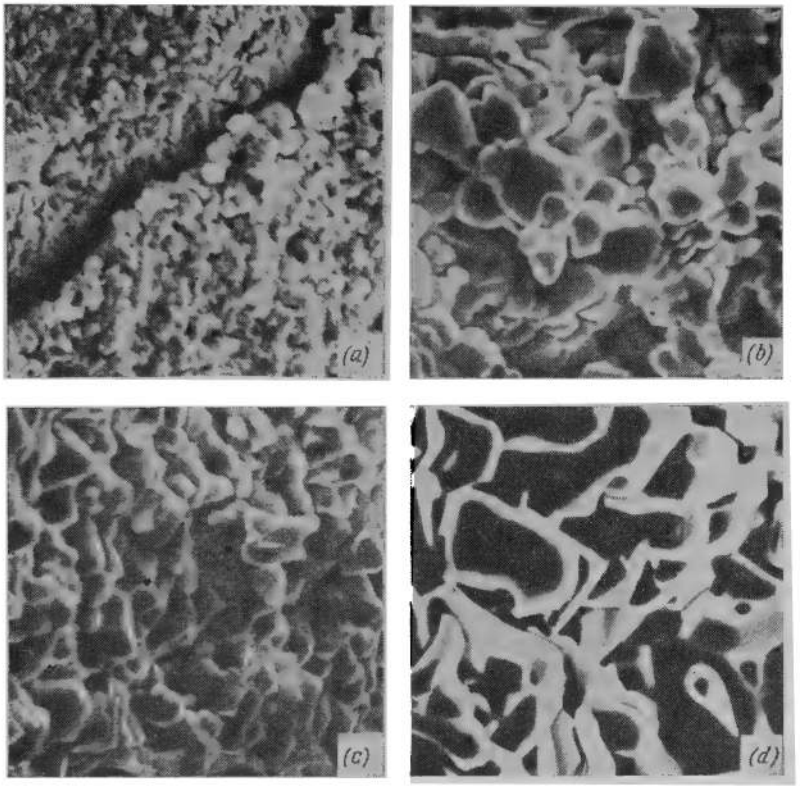

Fig. 186. Effect of Bi_2O_3 additions on microstructure of lithium-alloyed ferrite $Li_{0.5},Fe_{2.5}O_4 + \gamma$. Raster microscopy, ×1000

(*a*, *b*) without Bi_2O_3; (*c*, *d*) with Bi_2O_3 additions; (*a*, *c*) 800°C, 1 h; (*b*, *d*) 1100°C, 1 h

specimens without low-melting additions the stage of slow growth is practically absent and the intensive grain growth starts immediately from 1100°C; the value of $\Delta D/\Delta T$, which characterizes the effect of annealing temperature on grain growth, is higher in specimens with Bi_2O_3 and V_2O_5. At temperatures above 1000-1100°C, $\Delta D/\Delta T$ is higher in ferrites without low-melting additions. At 1250-1300°C, $\Delta D/\Delta T$ is roughly the same in ferrites with and without additions.

3. The maximum inequigranularity of the microstructure in specimens with Bi_2O_3 and V_2O_5 is substantially lower than it is in the specimens without additions.

Noting these circumstances, the process of formation of microstructure in alloyed specimens can be imagined as follows. The liquid phase obviously appears at 650-700°C and is distributed evenly between particles of the original powder. This facilitates the movement

of particles relative to one another. Besides, rough places on the surface (protrusions, steps, etc.) dissolve in the liquid phase and the shape of particles changes from an irregularly angular to a more regular ellipsoidal form. This causes an increase in the packing density of particles and a slight change in their orientations and thus results in intensive compaction and increased density. Sintering begins at a definite degree of contact between particles. With an increase of temperature, the growth of grains occurs by diffusion of individual atoms through the liquid phase, and the common process of grain growth takes place only between crystallites in the volume of individual particles, but not between crystallites belonging to various particles. The latter process is impeded by thin films of melt formed on boundaries of particles. The formation of microstructure by diffusion of individual atoms through the liquid phase is characterized by a slow and uniform growth of crystallites. Liquid phase layers are also favourable for decreasing porosity. Pores disappear and generate vacancies, which migrate into the boundary liquid phase and are then removed from particles by diffusion in that phase.

With liquid interlayers between particles, the disbalance of the grain-boundary energy in grain joints (which is an important stimulating factor for grain growth) disappears. The mechanisms of cooperative movement of atoms are also excluded. With an increase of the temperature of annealing, the liquid phase partially evaporates or flow from the joints between particles; this enables local grain growth which is characterized by a fast and uneven growth of crystallites.

In the absence of liquid phase, when the process of sintering occurs less intensively, the degree of contact of particles required to initiate grain growth is attained at temperatures 250-300 C above that at which grain growth begins in specimens containing the liquid phase in sintering. Since unalloyed specimens have no liquid phase which would impede migration of grains, the growth of crystallites that begins at a higher temperature obviously occurs by the quick process of grain growth between particles, which results in a higher inequigranularity of the microstructure and an appreciable porosity in the volume of individual grains. In that case the stage of slow growth of crystallites is practically absent, so that $\Delta D\ \Delta T$ here exceeds the respective value for alloyed specimens until an annealing temperature of 1100-1200°C is reached. At temperatures above 1250 C, the values of $\Delta D/\Delta T$ are equalized, since sintering occurs in both types of specimen under similar conditions, i.e. in the absence of the liquid phase. Since, however, their microstructure has been formed by different mechanisms, the inequigranularity in the unalloyed specimens remains substantially higher than that in the alloyed ones.

Thus, the difference in the formation of microstructure in specimens with and without the liquid phase is determined, firstly, by the temperature shift of the moment of the beginning of growth and,

secondly, by qualitative differences in the mechanisms of grain growth in various temperatures intervals.

It should be noted that the relative concentration of the liquid phase is also of importance. Its concentration must obviously be high enough to form liquid films envelopping every particle. Yet, an excessive quantity of the liquid phase impairs the magnetic properties of the material. It should also be remembered that evaporation and flow of the liquid phase from joints can occur at elevated temperatures, which may result in local direct contact of solid particles and in worsening of the characteristics of the material.

The effect of recrystallization on the texture and properties of ferrites can be illustrated by the data for permanent magnets on the base of barium ferrite, $BaO \cdot 5.6Fe_2O_3$. The process of making this material includes the stages of ferritization, i.e. synthesis of the compound from a mixture of Fe_2O_3 and $BaCO_3$ powders; grinding, in which particles of the compound are broken into monocrystalline fragments along the basal planes; and pressing in a magnetic field to orientate fragments with their basal planes in the direction of the magnetic field. This ensures favourable properties and texture in the sintered material.

According to the work [330], as the temperature (or time) of ferritization exceeds the optimal values, the processes of sintering and recrystallization between compound particles take place. The result is that polycrystalline, but not monocrystalline, aggregates form in grinding, which impair the texture and properties after pressing in the magnetic field.

Chapter 14

Recrystallization in Thin Films

The progress in novel branches of engineering has stimulated the use of materials in the form of thin (a few thousand angstroms or a few micrometres) and superthin films (tens or hundreds of angstroms). These materials have found the widest application in electronics. Thin films of metals, alloys, semiconductors and dielectrics are used as conductors, magnetic elements of memory devices, resistors, capacitor electrodes, radiation detectors, transistors, and various optical coatings. In space engineering, thin films are employed as temperature-controlling coatings of space vehicles, etc.

Thin films enable us to diminish the dimensions and mass of devices and circuits. In many cases they have the properties not found in massive specimens of the same substance. For instance, because of the high contribution of surface scatter of electrons, the resistivity of thin films is much higher and the temperature coefficient of resistivity lower than those of massive specimens.

Thin-layer structures of the *metal-dielectric-metal* type exhibit what is called the tunneling effect. In films of a thickness less than 2000 Å, the rupture strength increases sharply compared to that in massive specimens. In some cases, thin films may be in specific metastable phase states and structural states not observed in massive specimens. The minimal size of recrystallization nuclei and grains in films may be one-two orders of magnitude smaller than in massive deformed specimens.

Along with metallic films (Al, Cr, Mo, W, Ag, Fe-Ni alloys, etc.), films of elemental semiconducting substances (Ge, Si), semiconducting compounds ($A^{III}B^{V}$-InSb, GaAs; $A^{II}B^{VI}$-CdTe, CdS, CdSe; $A^{IV}B^{VI}$-SnTe, PbTe, etc.) and also insulating dielectric coatings attract ever increasing interest.

The preparation of thin films with specified properties is a very complicated problem [331-346]. The principal methods for making thin films are: deposition on substrates by vaporization in vacuum; cathode sputtering; chemical and electrochemical deposition; formation of films by surface reactions in a vapour or liquid phase. Thin metal foils are also made by rolling. These methods have in turn numerous varieties and features which determine the composition

and structure of films and the density and distribution of defects in them.

The structural changes in polycrystalline films associated more or less with recrystallization* will be discussed below.

The properties of thin films can be made more reproducible and their phase and structural states can be additionally controlled by means of annealing, i.e. by making use of the processes of recovery and recrystallization. In this way, amorphous films can be transformed into polycrystalline or even monocrystalline films. In some cases, recrystallization annealing can alter the orientation of monocrystalline films or transform them into polycrystalline films of a particular texture.

The problems of the analysis and control of polymorphic and structural variations in films are much more complicated than is the case with massive specimens. This is associated with some additional factors which can influence the course of recrystallization in thin films.

The most important ones among them are the nature of the substance of the substrate and the state of its surface; the surface energy and anisotropy of the deposited substance; the type of structural conformity and the differences in thermal coefficients of expansion between the substrate and film; the conditions of film deposition (the temperature of the substrate, the rate of film deposition, the degree of vacuum, etc.). With compound films, of much importance is also the volatility of the individual components of the compound, the differences in their volatilities and points of condensation, and deviations of the film composition from the stoichiometric ratio.

Because of these additional factors, films deposited on a substrate may be in various states before annealing—from amorphous to monocrystalline—and may differ from massive specimens in an appreciably higher concentration of point defects (structural and chemical) and higher microstresses.

The conditions of annealing, i.e. the rate and temperature of heating, intermediate steps of isothermal holding, the heating medium, etc., can influence the structure of films more strongly than that of massive specimens. Stabilization of the structure by thermal etch pits is a common phenomenon in recrystallized films.

The changes in annealed films are examined by the same methods as used for massive specimens, i.e. metallography, radiography and transmission electron microscopy, though a wider use is made of some special methods, such as electronography which gives information on the structure of thin films, and methods of electrophysical measurements, particularly for analysis of resistivity in metallic

* Epitaxial monocrystalline layers, a special and important class of films, whose formation is not associated with recrystallization are not considered here.

films, magnetic properties in magnetic films and the concentration and mobility of carriers in semiconductor films. The particular methods of analysis are selected depending on the application of films. Besides, the analysis of variations in properties gives valuable information on the type and concentration of defects and the contribution they make to the processes of recovery and recrystallization.

Since the size of grains in polycrystalline films obtained by crystallization is usually very small (tens or hundreds of angstroms), the early stages of recrystallization in thin films often show no point reflections on radiograms, nor even on electronograms. In such cases, the onset of recrystallization can be determined by a change in the texture of a film which often accompanies recrystallization.

Before considering the structural changes in thin films during annealing, let us discuss briefly the mechanism of their formation [371], for example, in films obtained by vaporization in vacuum.

When a deposited atom enters a potential pit in the substrate, it stays there for a statistically determinate time which is called the lifetime $\tau = \tau_0 \exp(\varphi/kT)$.

The deposited atom can then either wander on the surface (surface diffusion) until it encounters a new potential pit, or be re-vaporized.

Denoting by N the number of atoms impinging the substrate and by n the number of sublimated (re-vaporized) atoms, we obtain the ratio $(N - n)/N = a$ which is called the accommodation coefficient.

If the temperature of the substrate is substantially below the melting point of the deposited substance, a approaches unity, which implies a high probability for 'adhesion' of vaporized atoms.

Freshly condensated atoms form a two-dimensional surface layer which is characterized by a high surface mobility of atoms and is in many respects similar to the liquid phase. The structure of a film is strongly influenced by the surface migration of atoms and by the formation of nucleation centres in the mobile surface layer, and also by the atomic structure of the surface of the substrate and the presence of deep potential minima in it, which facilitate the process of heterogeneous nucleation. On crystalline substrates under the conditions of a high vacuum, these minima can be associated with a high roughness of the substrate surface and the existence of atomic steps and protrusions in it; under the conditions of a low vacuum, these are associated with atoms of adsorbed gases, islets of oxides, etc. Amorphous substrates also have irregularities on their surface which facilitate nucleation and result in uneven film deposition.

In the course of deposition, the number of recrystallization nuclei increases, and these grow freely until mutual collisions begin. At this stage, nuclei are either spherical (Fig. 187*a*) or of a shape determined by their crystallochemical nature. As nuclei begin to collide, the grain-boundary tension becomes operative and the system tends

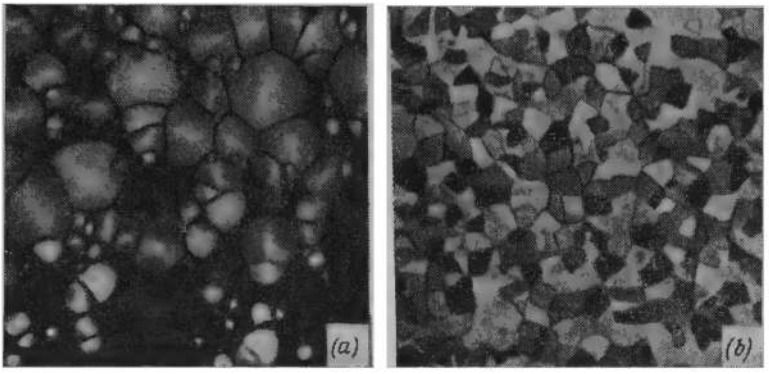

Fig. 187. Crystallites formed in films by collisions of spherical recrystallization nuclei [331]

to balance out the grain-boundary tension in grain joints. Nuclei thus form into polygonal crystallites (Fig. 187*b*). Their size at that stage is usually a few hundredths or at best a few tenths of a micrometre. Large-angle boundaries of these nuclei obviously differ from large-angle boundaries formed at the stage of primary recrystallization in deformed materials by less regular structural units and dislocation structures and by an elevated concentration of point defects and their groups.

With a very high rate of deposition and a low temperature of the substrate, in which case migration of atoms is inhibited, amorphous films can form. The weaker the bond between atoms of a film and substrate, the greater the rate of surface diffusion and the higher the probability for the formation of islets of the deposited substance, which further produce a continuous but easily detachable film. This phenomenon is typical of atoms of noble metals.

If a low-volatile metal is deposited onto another metal with a lower melting point, an alloy is usually formed in the interface [331].

If the energy of interatomic bonds in the film substance is greater than that between atoms of the film and substrate and the surface mobility of film atoms is high, crystallization nuclei in a polycrystalline film will have a preferable crystallographic orientation. If the direction of flow of deposited atoms is normal to the substrate, the film texture will be axial; all crystallites in the film have their definite crystallographic plane parallel to the surface of substrate, more strictly to the external surface of the film, but are oriented randomly around the direction normal to this plane.

Often a plane having the lowest surface energy turns out to be parallel to the substrate surface. The preferable role of the surface

energy of film crystallites is also confirmed by the fact that this type of texture can even form on amorphous substrates.

All factors which facilitate surface diffusion (an increased temperature of substrate and lower rate of deposition), as a rule, promote the formation of a texture with the lowest surface energy. For instance, germanium films deposited onto a substrate at a temperature of 400-450°C had a {100} + {110} texture. At a higher temperature of the substrate, the share of {100} texture decreased and disappeared fully at 700-800°C [343].

A particular texture of a film can be changed to another type if the proportion of the surface energies of the planes with various crystallographic indices is changed by introducing impurities, varying the degree of vacuum or by using other methods. For instance, a polycrystalline film of zinc oxide formed by oxidation of pure zinc is oriented with its $\{10\bar{1}0\}$ plane parallel to the plane of the substrate. If, however, the oxide film is prepared by oxidation of ZnSe compound, it will be oriented with its {0001} plane parallel to the substrate. In the latter case, the film obviously causes partial dissolution of selenium, which changes the proportion of surface energies: the {0001} plane, but not the {1010} plane, will now have the lowest energy.

If the direction of flow of the substance does not coincide with the normal to the substrate, the axis of the texture usually shifts towards the direction of flow [331].

The most important parameters which determine the structure and composition of films are the presence of residual gases (degree of a vacuum), the rate of deposition, and the temperature of the substrate. The presence of adsorbed gases (in a slight vacuum) lowers the surface mobility of atoms and decreases the size of crystallites. If the gases have a close affinity for the substance being deposited, inclusions or islets of compounds can form under certain conditions (temperature and pressure), and these will disturb the uniformity of the film. This effect can be prevented by using a vacuum not less than 10^{-7} mm Hg.

Such a high vacuum is, however, detrimental when preparing films of compounds with volatile components. In that case, in order to obtain compounds approaching the stoichiometric ratio, it is reasonable to raise the partial pressure of corresponding gases up to 10^{-4}-10^{-3} mm Hg.

The surface mobility of atoms is inversely proportional (exponentially) to the temperature of the substrate [331]. At low temperatures of the substrate, the type of structure is mainly determined by the type of chemical bond in the film substance. Simple metals (Cu, Al, Hg, Pb, etc.) can form crystalline films at very low temperatures of the substrate, even at the temperature of liquid helium [344]. Substances with covalent bonds are condensated at low temperatu-

res of the substrate in the form of amorphous films: Bi, Ga, and Sb at a temperature of a few K; CdS, CdSe at room temperature; Ge up to 573 K; Si up to 723 K; and Al_2O_3 and SiO_2 up to 923 K. It has been observed, however, that when an amorphous film grows to a definite thickness, it recrystallizes instantaneously, so that a polycrystalline textured film is formed.

With an increase of the temperature of the substrate, crystalline films form instead of amorphous type. The higher the temperature of substrate, the larger is the size of crystallites and the lower the concentration of defects. This relationship is however far from being monotonic, especially in the presence of residual gases. At definite temperatures, there is observed a maximum of the size of crystallites and of the density and, correspondingly, a minimum of the resistivity. The phenomenon of decreasing size of crystallites at temperatures above the maximum is associated with various factors: with greater oxidation at a rough vacuum or with the presence of a texture, a higher homogeneity of crystallites, etc.

The rate of deposition has a complicated effect on the quality and structure of films. With an insufficiently deep vacuum, the number of gas molecules adsorbed by a film will be higher at a lower deposition rate [337]. On the other hand, with a decrease in the deposition rate, the rate of nucleation also decreases. In that case the time of migration of atoms over the surface (the lifetime) will be sufficiently long to enable the preferable growth of nuclei oriented with their crystallographic planes of the minimum energy parallel to the external surface of the film. In this case, however, the films will be rough and porous. With an increase in the deposition rate, denser and smoother films are formed and the average size of grains diminishes, but the concentration of point defects and defects at grain boundaries increases.

Zonal stresses appearing in films during their preparation influence appreciably the structure of films. These stresses can be quite high in value. They cause bending and plastic deformation of films and substrates and thus influence the subsequent processes of recovery and recrystallization.

The main sources of stresses are as follows: (a) structural non-conformity and the differences in the coefficients of thermal expansion between the film and substrate and also between the oxide phases and other inclusions present in the film; (b) presence of atoms of dissolved impurities and gases distributed unevenly in the film; (c) 'freezing' of structural defects in the film lattice during condensation; (d) surface tension at the boundary between the film and surroundings.

Zonal stresses in films can partially be relieved by subsequent annealing or diminished by raising the temperature of the substrate. It should be noted, however, that a higher temperature of deposition

may increase the stresses due to a difference in the thermal expansion of the substrate and film. There is an optimal temperature of deposition which should be determined experimentally.

It can be supposed that it is the effect of zonal stresses that is responsible for the fact that substrates influence the temperature of recrystallization in films of compounds $A^{II}B^{VI}$(CdS, etc.). For instance, a temperature of around 500°C is needed for recrystallization in argon of CdS films applied on pyrex glass, whereas the same film on a quartz substrate can recrystallize only when heated above 700°C [332]. A probable cause is a difference in strain-hardening associated with a different plastic deformation in films during relaxation of zonal stresses of different magnitude.

The fact that scratching of the substrate before the application of a film causes a preferable nucleation in the film along the scratch (Fig. 188) is also indicative of an appreciable role of plastic deformation.

Let us discuss briefly the probable structural changes in films in annealing.

The effect of contamination of films by molecules of gases, in the first place by oxygen, can be illustrated by the following examples.

Silver films 300 to 500 Å thick were deposited onto mica plates at 10 K in vacuum (10^{-6} to 10^{-10} mm Hg) and subjected to isochronous annealing at different temperatures, after which their resistivity was measured.

The curves of restoration of resistivity for films deposited at $5 \cdot 10^{-8}$ mm Hg and lower showed at 40 K an anomalous 'reverse' restoration, i.e. a slight rise of resistivity. With films deposited at $1 \cdot 10^{-9}$ mm Hg and higher, the resistivity decreased monotonically with increased temperature. The anomalous restoration might be associated with the dissociation of O_2 molecules captured by silver during its deposition in a manner similar to physical adsorption.

According to [336], oxygen captured by a growing film can form an oxide layer and thus accelerate recrystallization. A similar effect was observed [336] in chromium films 200-1000 Å thick obtained on glass by vacuum vaporization at 10^{-5} mm Hg. Condensation was performed at two rates: $\omega_{x_1} = 10$ Å s^{-1} and $\omega_{x_2} = 200$ Å s^{-1}. After deposition, films were kept in the air at room temperature and atmospheric pressure.

In the course of this holding, films obtained at the lower condensation rate (10 Å s^{-1}) were aged and recrystallized partially (after a holding time of $5.7 \cdot 10^7$ s, roughly 0.2 of the volume was recrystallized). A layer of chrome oxides formed on the surface of films. No changes took place during that time in films prepared at the higher condensation rate (200 Å s^{-1}).

As has been noted earlier in this chapter and in [337], the quantity of residual gases captured by a film increases with a decrease in the condensation rate. According to [345], at a rarefaction less than 10^{-6} mm Hg, the content of residual oxygen is sufficient to form a monomolecular oxide layer on chromium. The rate of formation of an oxide film, as calculated in [336], is $1.35 \cdot 10^{-9}$ m/s, i.e. close to the above-mentioned lower rate of condensation.

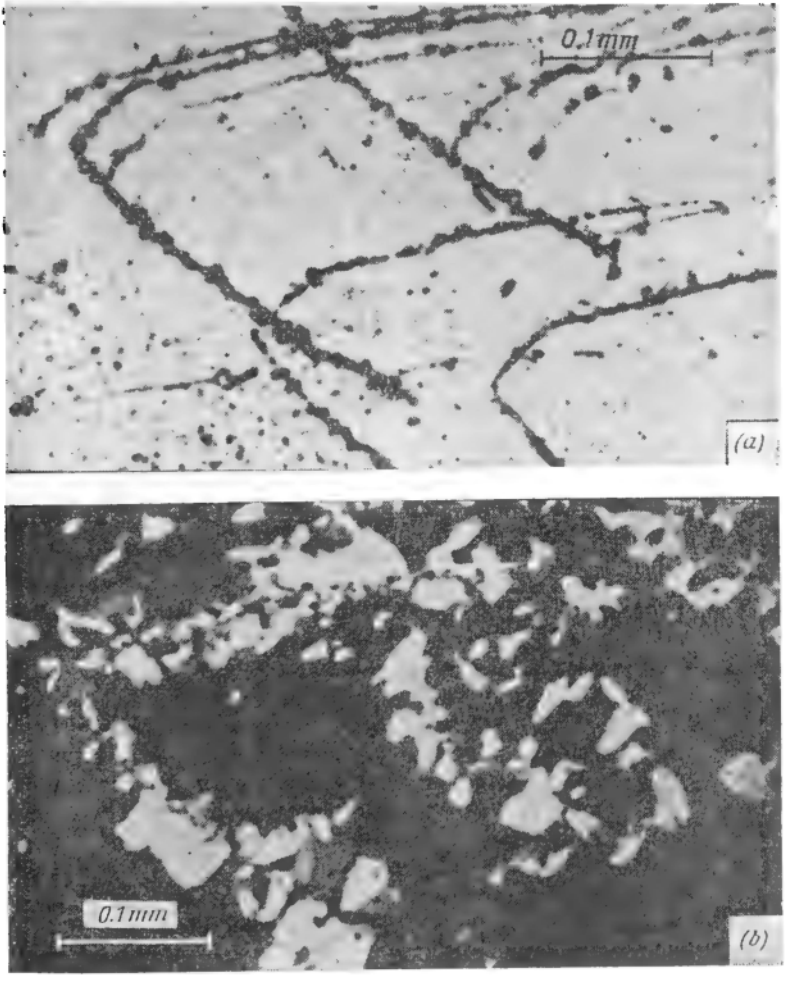

Fig. 188. Recrystallization nuclei formed in CdS film at scratches on the surface of a glass (pyrex) substrate

(*a*) reflected light microscopy [332]; (*b*) polarized light microscopy

An oxide film formed at an early stage of the process grows into the surface. Since chromium and its oxides have different elastic characteristics, elastic stresses appear at the chromium-oxide interface (tensile stresses in chromium and compressive in oxide), which results in the formation of dislocation-free regions in boundary volumes. If these regions are sufficiently large in size (3-4 times the size of the surrounding grains), they can grow by dislocation climb at the expense of the vacancies in the stress field. The authors of [336] do not disclose the causes of the preferable orientation of recrystallized grains. This orientation may be associated with the preferable conditions for the formation of an oxide film on certain, definitely oriented, crystallographic planes. In that case a small number of closely oriented nuclei is operative.

The possibility of forming anomalously large grains in thin films by secondary recrystallization has been proved in [338]. Thin (0.4 to 1.1 μm) films of Al-Mg and Al-Cu alloys with additions of chromium, silver, and manganese were prepared by layerwise vacuum deposition (at $2 \cdot 10^{-7}$ mm Hg) onto a degassed amorphous substrate of SiO_2. Subsequent annealing caused recrystallization and growth of grains. Additions of silver, and chromium in Al-Cu alloy speeded up secondary recrystallization. The grain grew to 1.8 mm in size, i.e. its size was roughly 2000 times the thickness of film (around 1 μm). Manganese additions retarded secondary recrystallization (Table 33).

TABLE 33. Effect of Annealing Temperature on Grain Size in Alloyed Aluminium Films of Various Thickness [381]

Alloying additions, % (by mass)	Annealing temperature, °C	Film thickness, μm	Grain size, μm
2% Cu+0.3% Cr	530	0.40	18
2% Cu+1.0% Ag	530	0.40	15
2% Cu+0.3% Cr	500	0.90	1350
2% Cu+0.3% Cr	530	1.10	1800
4% Cu	480	0.85	60
4% Cu+0.6% Mn	480	0.85	2
6% Mg	340	0.50	100

Thus, chromium and manganese, both being low-soluble in aluminium, produce the same retarding effect in massive specimens, but act differently in thin films.

What draws the attention is that the effect of grain enlargement is definitely associated with film thickness. For the same temperature of annealing and with an addition of 0.3% Cr, the diameter of grains in thicker films (1.1 μm) was 100 times that of the grains in

thinner films (0.4 μm). This difference can be explained by a stronger stabilizing effect of thermal etch pits in thinner films.

According to Gattman [346], the formation of etch pits on subboundaries can raise the temperature of the beginning of recrystallization, as has been observed in thin foils of vanadium and molybdenum. In massive specimens of these metals, recrystallization started respectively at 780° and 900°C; in foils of these metals recrystallization did not occur until after 1200-1300°C. But polygonization developed similarly both in massive specimens and thin foils.

Gattman [346] concludes from this that the surface of a foil cannot inhibit dislocation rearrangement, but retards the movement of subboundaries and stabilizes the structure by etch pits.

Of special interest are cases where the orientation of films changes during annealing. As has been found roughly at the same time by the authors [339] and [340], a monocrystalline {100}-oriented film of gold transforms during recrystallization into a polycrystalline film with the {111} orientation.

In [339], a {100}-oriented gold film was prepared as follows. An epitaxial layer of silver 1 μm thick was deposited by evaporation from the source under the action of an electron beam in vacuum (10^{-7} mm Hg) onto an NaCl substrate heated at 300°C. The temperature of the substrate was then lowered to 80°C and a gold film 800 A thick was applied by a similar method. Further, the layers of NaCl and Ag were removed by dissolution and the gold film, fastened in a holder, was heated to a temperature 400° to 700°C and examined with an electron microscope (or it was heated directly in the microscope column).

Annealing formed polycrystalline {111} films, whose crystallites had only two orientations associated regularly with the original one. Besides, {111} crystallites in the volume were more perfect than the original {100} film.

The fact of transformation of a monocrystalline film into polycrystalline is in itself of high interest, since, on the face of it, it violates the principle of reduction of energy in the system during the spontaneous processes that occur in annealing. It is clear that only the surface energy can be the driving force of that transformation.

As found in [339], $\Delta\sigma/\sigma_{100} = [(\sigma_{111} - \sigma_{100})/\sigma_{100}]\ 100\%$ for f.c.c. metals is approximately 6%, whereas $\Delta\sigma \approx 3\%$ is sufficient for the migration of a boundary in a thin film if this migration is stimulated by a gain in surface energy.

In its magnitude, $\Delta\sigma \approx 6\%$ is equal to approximately 90 erg·cm^{-2} (for comparison, the average value of σ for gold is roughly 1500 erg·cm^{-2}). The gain in the volume energy associated with a higher perfection of crystallites is approximately 15 erg·cm^{-2} by the estimation of the authors cited.

Thus, a gain in the surface energy is the main driving force for a change in orientation.

This is only true, however, if we suppose that regions with the {111} orientation have existed in the original state. Otherwise, their formation must involve an energy gain owing to the formation of boundaries between the {111} nuclei and the {100} matrix. Calculations show that a gain in the surface energy cannot offer a sufficient driving force for this process.

The authors cited could not manage to observe directly the formation of {111} nuclei, but the presence of two distinct orientations made it possible to suppose that these appeared by the mechanism of 'oriented nucleation'.

It is most probable that {111} nuclei are associated with twins detected in the {100} matrix. This is confirmed by the fact that first nuclei of {111} orientations were detected in those regions of the {100} matrix which had a high density of twins. Besides, secondary twins were found in those regions.

The process of twinning in a {100} film can result in that the {111} planes, instead of {100} planes, will come to the surface. The formation of a twin is accompanied by the appearance of stresses, which can be relieved at high temperatures of heating; this disturbs the coherence of twin boundaries and transforms them into mobile boundaries.

Nuclei of the {111} orientation can also form from secondary twins. For this, the lattice of these twins should rotate through 38° about the ⟨111⟩ direction (i.e. the boundaries of these twins become partially conjugate and highly mobile).

In [340], a similar phenomenon was observed in gold films approximately 500 Å thick deposited directly on NaCl plates (without an intermediate silver layer) at 75°C by vaporization in a high (10^{-7} mm Hg) and ultrahigh vacuum (10^{-11} mm Hg) with electron bombardment.

An increase of the temperature of NaCl substrate resulted in a gradual change of the {001} orientation to {111} orientation.

As stated in [340], the most probable cause of the changes in orientation during heating is recrystallization after plastic deformation due to the stresses that form as a result of differences in the coefficients of thermal expansion between gold ($\alpha_{Au} = 14.66 \cdot 10^{-6}\ °C^{-1}$) and NaCl ($\alpha_{NaCl} = 43.2 \cdot 10^{-6}\ °C^{-1}$).

It is still unclear whether the leading part in the case considered is played by deformation twins, i.e. by oriented nucleation, or by oriented grain growth. In the latter case, it is supposed that variously oriented nuclei appear in primary recrystallization, but {111} nuclei grow quicker as they are more favourable from the energy standpoint.

Similar results were obtained from the analysis of recrystallization in a polycrystalline silicon film 200 μm thick applied onto a film of SiO_2 that coated the {111} surface of monocrystalline silicon. Immediately after film application, silicon crystallites had a columnar shape stretched perpendicular to the substrate. The ⟨110⟩ axis was along the direction of grain growth (axial texture). As found by electron microscopy, grains had numerous twins and stacking faults.

During annealing at 1200°C, intensive recrystallization took place, in the course of which the ⟨110⟩ texture changed to ⟨111⟩. The ⟨111⟩ grains were much larger than ⟨110⟩ ones, less anisotropic and practically had neither twins nor stacking faults.

An important example of practical application of recrystallized films is the films of type $A^{II}B^{VI}$ compounds: sulphides, selenides, and tellurides of zinc and cadmium (ZnS, ZnSe, CdS, CdSe, CdTe, etc.).

These compounds are alloyed with various impurities and employed as thin-film transistors (CdS and CdSe), phosphors and photoconductors [332] in cathode-ray and other tubes, scintillation counters and memory devices, as screens of electron microscopes, etc. The compounds mentioned are characterized by a high emissivity and high sensitivity in the red and infrared regions of the spectrum.

The use of these materials in the form of thin films offers a number of advantages over their use in monocrystalline or powdered form. Because of some uncontrollable factors in their manufacture, however, as-deposited films are usually amorphous or are composed of very disperse crystals, have a very high and unpredictable density of defects and, for these reasons, do not possess the required reproducible photoconducting and luminescent properties.

Their properties can be improved and stabilized by recrystallization annealing, which produces large textured crystallites of higher structural perfection. A characteristic feature of this annealing is that its effectiveness can be raised appreciably if a thin layer of an activator metal is applied onto a film just before annealing. The activator metal plays a dual role. On the one hand, it diffuses partially into the depth of the film during annealing and thus acts as an alloying impurity and, on the other, it facilitates recrystallization and the formation of a large-crystalline textured structure.

Thus, the process of manufacture of thin films of the compounds considered includes in the general case the preparation of a film proper, alloying, and recrystallization. The last two procedures are usually combined.

The method of activator-stimulated recrystallization was initially applied by Gilles and Van Gakenberghe [347]. The mechanism of the process was later analysed by A. Vecht [332] and by V. B. Tolutis *et al.* [333, 334].

Many important details of the activator-stimulated recrystallization are still unclear. Besides, since the diffusion of the activator atoms into the film occurs parallel with recrystallization of the film, it is difficult to determine separately the contribution of the impurity atoms and that of recrystallization to the film properties, and what is more, to single out the effect of enlargement of crystallites and that of texture formation.

The examples given below illustrate certain regularities of structure formation in films of cadmium telluride (CdTe) directly during deposition and in subsequent annealing, as established in [332, 333, 334, etc.].

In [333, 334], films were deposited onto glass substrates heated to various temperatures (from 120° to 400°C). A molecular beam was obtained by sublimation of a CdTe batch with various deviations from the stoichiometric composition. The beam consisted of molecular tellurium (Te_2) and atomic cadmium. Since the temperatures of condensation and desorption of tellurium and cadmium are different, as are the rates of their surface diffusion, the composition of the film deviated from that of the original beam; this resulted in the appearance of free tellurium and cadmium in the form of disperse particles of excess phases, especially at relatively low temperatures of the substrate.

Figure 189 shows the curves of the average size of crystallites versus the temperature of substrate, t_s, for a compound of stoichiometric composition (curve *1*) and with an excess of tellurium (curves *2* and *3*). Each of the curves has a maximum. In the presence of disperse particles of excess tellurium (curve *3*), the average size of grains in the film diminishes and the maximum of the curve shifts towards higher values of t_s. Besides, excess tellurium increases the concentration of defects and weakens the texture. Similar changes are observed in a film with an excess of cadmium, but the film has a different phase composition.

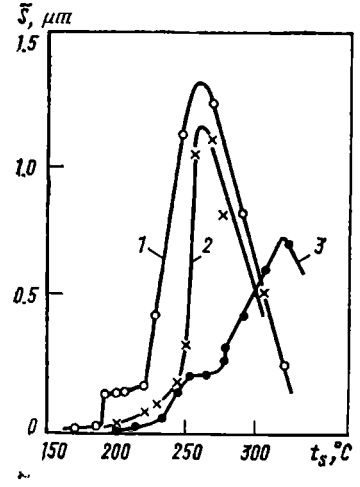

Fig. 189. Dependence of average size of crystallites in CdTe film on substrate temperature t_s [333]

The curve of grain size distribution taken at the maximum of t_s has a shape typical of incomplete secondary recrystallization (there are two grain size maxima).

The temperature of the substrate can also influence the phase composition and texture of films. Massive specimens of CdTe have the cubic lattice of

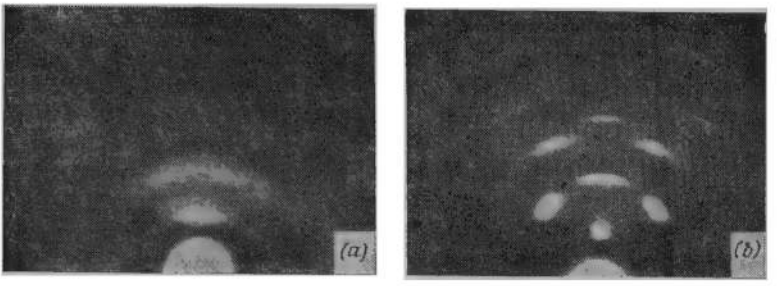

Fig. 190. Electron micrographs of CdTe films of various thickness to illustrate the effect of substrate thickness on the structure perfection and texture of films [333]

(a) 0.03 μm thick; (b) 1.6 μm

sphalerite at temperatures below 300°C and the hexagonal lattice of wurtzite at higher temperatures, whereas CdTe films deposited at $t_s < 270$°C at room temperature show a mixture of two phases—cubic and hexagonal—with a high concentration of stacking faults. Both phases have a regular crystallographic orientation. The closest packed planes of the two phases—respectively {111} and {0001}—are oriented parallel to the substrate surface.

The quantitative proportion of the phases varies with t_s. Above 270°C, the amount of the cubic phase increases sharply and the texture gradually disappears. At the substrate temperature corresponding to the condensation point of the compound (>300°C), the film is practically single-phase and untextured.

It has been found that in addition to the metastable state of the main phase, the film at the substrate temperatures below 230°C contains excess tellurium, whose quantity increases with decreased temperature. Tellurium has also been detected in a film obtained from the source of a stoichiometric composition; its presence is due to the difference in volatilities and condensation points between tellurium and cadmium ($t_{c(Te)} < t_{c(Cd)}$).

For a given temperature of the substrate, the structure of film also depends on film thickness H. With an increase in H, the structure is more perfect and has a more distinct texture (Fig. 190). This means that a film becomes thicker due to the selective growth of crystallites having the least surface energy. This fact agrees well with the existence of two maxima on the grain size distribution curves.

Recrystallization annealing sharply changes the structure and phase composition of films towards equilibrium. Recrystallized films always have only a cubic structure with a texture less scattered than in the original state. So the most perfect and most strictly oriented regions in a film serve as recrystallization nuclei.

The size of recrystallized grains depends, however, on the original (prior to annealing) state of a film, i.e. on the conditions of film preparation. Under certain conditions, recrystallization results in a noticeable (5-7 times as great) enlargement of crystallites (though they remain small in absolute size, around 1 μm, if formed without an activator) and improvement of their structure, whereas in other cases the structure remains very fine-grained.

Figure 191 shows the hatched region of substrate temperatures and temperatures of annealing, which in combination result in enlargement of the size of recrystallized grains.

It follows from the foregoing that the films structure noticeably coarsens in annealing only if it is imperfect and two-phase, has a relatively small proportion of cubic phase and, what is especially important, an excess of tellurium.

Studies into the kinetics of the process by the methods of structural analysis and by the analysis of changes in electrophysical properties, have enabled the authors [333, 334] to ascertain that during annealing first the hexagonal phase transforms into the cubic form and later (probably at the beginning of partial dissolution of tellurium) most perfect crystallites of the cubic phase, which have their {111} planes oriented most strictly parallel to the substrate (more exactly, to the external surface of the film), start to grow. This means that the microstructure of a matrix, which is stabilized by the precipitates of tellurium, coarsens as a result of secondary recrystallization stimulated by the tendency of the system to decrease its surface energy.

The above-described recrystallization process was effected without activators and the resulting grain enlargement was not high. The use of activators makes it possible to obtain a very coarse-grained recrystallized structure with the size of crystallites up to a few millimetres, i.e. with the grain size increased roughly by three orders of magnitude.

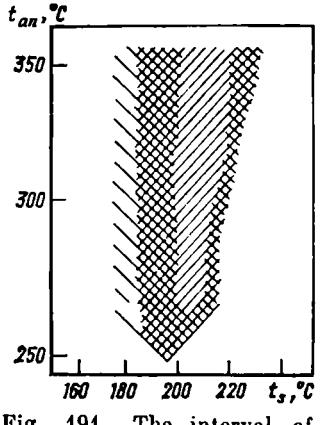

Fig. 191. The interval of substrate temperatures and annealing temperatures in which the size of crystallites in CdTe films increases [333]

The authors [334] used silver and copper as activators for CdTe. A layer of the activator (Ag or Cu) in a concentration of 0.003-0.005% (by mass) was applied onto films 3-4 μm thick.

The difference in the size of grains obtained by recrystallization without and with an activator is seen in Fig. 192*a*. The figure shows a CdTe film whose upper portion is recrystallized in the presence of an activator (Ag) applied after

preliminary recrystallization without an activator (the lower portion in the figure). After activator-stimulated recrystallization, spherulitic aggregates (see Fig. 192*b*) are often found in film structures. The size of spherulites in CdTe films may reach a few millimetres. Spherulites consist of finer crystallites slightly misoriented relative to one another. Crystallites grow in directions lying in the {111} plane, probably under the effect of surface energy.

Interesting results have been obtained from the analysis of the effect of substrate temperature t_s (i.e. the original state of film) and of the type of activator on the rate of growth of crystallites (v_r) and the rate of nucleation (N) [333].

Fig. 193*a* shows the effect of t_s and of the temperature of recrystallization annealing on v_r and N for a given type and invariable con-

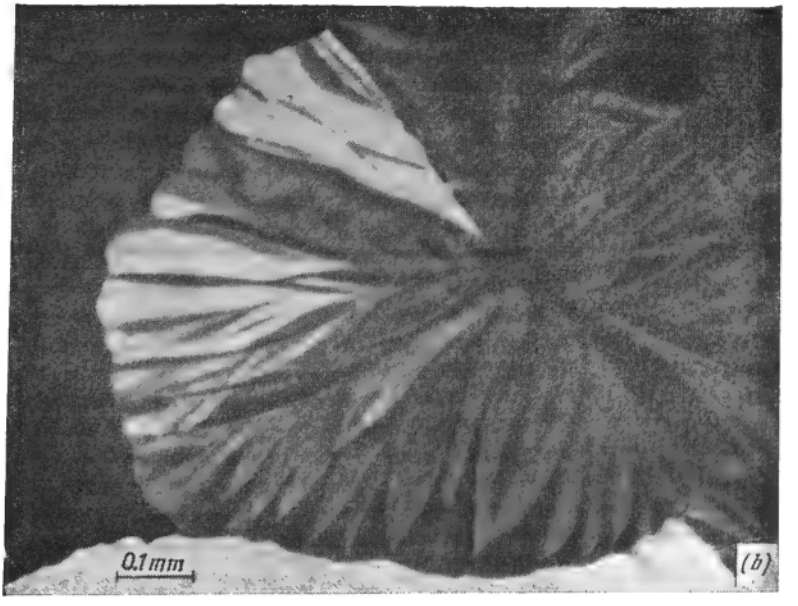

Fig. 192. Effect of activator on the microstructure of recrystallized CdTe film
(*a*) isotropic grains; (*b*) spherulites

centration of activator (Ag). Fig. 193*b* illustrates the effect of the temperature of heating ($1/t$) on v_r for two temperature intervals of substrate heating and for two various activators (*1*—low temperatures corresponding to a high rate of grain growth in recrystallization annealing and *2*—high temperatures corresponding to low rates of grain growth).

As seen, with a decrease of t_s below 200°C, v_r drops sharply and N increases. This interval of temperatures is just below the condensation point of tellurium, i.e. corresponds to a substrate temperature at which the composition of a film differs from the stoichiometric, and therefore disperse particles of excess tellurium appear in the film.

It follows from Fig. 193*b* that, for a given activator, the rates of

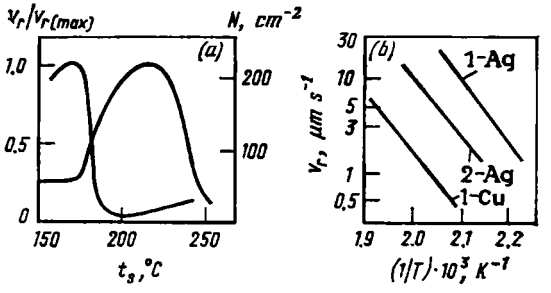

Fig. 193. Dependence of the rate of formation of crystallites (N) and rate of growth (v_r) on the temperature of substrate t_s (*a*) and the type of activator (*b*)

growth of crystallites may differ by a factor of five (lines *1*-Ag and *2*-Ag). Given the same original state of film and various activators, these rates may differ even more, roughly by a factor of 25 (lines *1*-Cu and *1*-Ag in Fig. 193*b*).

It is essential that an activator is effective but not in all possible states of film. At high values of t_s (>250°C), when a film consists of relatively large crystallites of only the cubic phase of stoichiometric composition, an activator has practically no effect on the course of recrystallization.

It is obvious that an activator can initiate intensive growth of grains only under particular conditions required for the stage of grain growth (these are a gradient in the size, certain misorientations or surface energy of crystallites). Activator atoms can evidently enhance this gradient or its role.

It is still difficult to decide definitely on the particular role of activators. As has been given earlier, part of activator atoms moves by diffusion into the depth of a film during recrystallization annealing, while another part remains on grain boundaries as secondary phase particles. Thus, the role of activators can be similar to that of stabilizers (inhibitors) in secondary recrystallization. According to ano-

ther, quite reasonable, supposition, adsorbed activator atoms may influence the surface energy of {111} planes and increase the surface energy gradient between the nuclei oriented with their {111} planes strictly parallel to the film surface and all nuclei of other orientations.

A third mechanism also seems to be probable. It is associated with the effect of dissolved activator atoms on the concentration of vacancies. Silver and copper, which stimulate recrystallization in CdTe and in other $A^{II}B^{VI}$ compounds, behave as acceptors, i.e. promote the formation of sulphur vacancies. On the other hand, an addition of donor impurities: indium, gallium or chlorine, which decrease the concentration of vacancies, inhibits recrystallization.

The supposition that the vacancy mechanism is indeed responsible for the effect of activators has been confirmed by the results of a recent analysis of the relationship between the photosensitivity of polycrystalline CdSe films and their recrystallization in annealing. The beginning of recrystallization in these films is found to be always accompanied by a noticeable increase in luminescence. The activators which increase the concentration of vacancies also facilitate recrystallization and additionally enhance photosensitivity.

Chapter 15

Methods for Studying Recrystallization

Various direct and indirect methods are employed for studying the numerous effects of recrystallization.

When choosing a particular technique, one should consider the properties, state and special characteristics of a given material. An essential characteristic is the structure prior to deformation, i.e. the size of grains, the presence of disperse phase particles, their nature, concentration, dispersity and distribution, the texture, and the conditions of plastic working (the temperature, degree and rate of deformation), which determine the structure in as-deformed state.

Recrystallization is often accompanied by other processes: recovery, decomposition of solid solutions and precipitation of disperse phases, phase transformations, etc. These processes can influence the course of recrystallization and often mask the picture revealed by certain methods of analysis.

Specific difficulties arise in the analysis of recrystallization in fusible metals, whose t_r^s is below the room temperature, in brittle metals and alloys which cannot be deformed by common methods of plastic working, etc.

The mechanism of nucleation can be examined most effectively on the basis of a comprehensive approach, for instance, analysis of thin foils by transmission electron microscopy, X-ray structural analysis of variations in the shape of X-ray lines (with the application of harmonic analysis), analysis of variations in microhardness and resistivity, calorimetric analysis, etc.

The thin-foil technique* enables observing the distribution of dislocations directly in as-deformed state and at various stages of recovery and recrystallization, with the specimen being heated either directly in the microscope column or outside. Direct heating in the microscope, despite its apparent advantages, has not yet found a wide use. Its principal drawback is low contrast of the image because of the incoherent scatter of electrons, which increases sharply with temperature.

Heating thin foils outside the microscope does not always give satisfactory results.

* Naturally, the method is applicable only to materials which can be worked into thin foils.

As has been shown in the previous chapter in discussing recrystallization in thin foils and massive specimens of vanadium and molybdenum [346], thermal etch pits, which form in foils on heating, impede the movement of subboundaries and rearrangement of the subgrain structure and thus inhibit recrystallization. The kinetics and nature of redistribution of dislocations and migration of boundaries can also be affected by contamination of thin foils with, say, carbon, which can occur during heating or in observations. For that reason, the main method one generally resorts to at present is the investigation of thin foils obtained by flattening deformed and annealed massive specimens. This method makes it possible to observe flattening of cell walls and their transformation into subboundaries, the transformation of cells into subgrains, the formation of recrystallization nuclei by boundary migration or by coalescence of subgrains. An important advantage of the method is that it offers the opportunity to determine (by electron microdiffraction) the orientations of microregions 2-3 μm in size (i.e. subgrains, recrystallization nuclei and the surrounding matrix).

The temperatures of the beginning and end of recrystallization, t_r^s and t_r^f, and the course of the process are examined by direct methods (metallography and X-ray structural analysis) and by indirect methods, i.e. by analysing variations in the mechanical and physical properties.

The metallographic method for determining t_r^s is based on detection of the new, visible, recrystallized grains on the background of deformed grains. Its sensitivity depends on many factors. In an optical microscope at a magnification of 1000, new grains can be revealed clearly when their size is 10 to 50 μm. Therefore, if recrystallization is examined after a light (supercritical) or moderate deformation, the method is applicable only if the size of original grains is sufficiently large (index 1 to 4). New grains can then be revealed easily since in hot deformation they form on the boundaries of original large grains, and in heating after cold deformation they appear on the boundaries of original grains and in the bulk of grains on twin boundaries and along slip lines.

If original grains are small in size, a few micrometers (index 7-8 or less), the onset of recrystallization cannot be detected reliably enough by the metallographic technique, and so preference should be given to X-ray structural analysis (see later).

After heavy deformations, when original grains have the form of stretched, easily etchable, fibres, recrystallization nuclei can as a rule be readily detected metallographically since they have a more regular shape and are etched rather less easily.

Recrystallized grains can be identified by using a control method, i.e. by measuring their microhardness.

The end of primary recrystallization (t_r^I) in heavily deformed materials is determined by the disappearance of the deformed structure regions which are etched more easily than recrystallized grains. In materials deformed to light or moderate degrees, the end of primary recrystallization approximately coincides with a minimum on the curve relating the time (temperature) of annealing to average grain size.

Quantitative metallographic analysis [188] can be used to determine the relative area or volume occupied by recrystallized grains. In many practically important cases, as in this problem, for construction of third-order recrystallization diagrams or for optimization of the conditions of hot plastic working, it is essential to find a technique which would distinguish between deformed (unrecrystallized) and recrystallized grains. The use of the difference in etchability of these grains would be a most convenient approach for the purpose. However only in rare cases can one manage to select the appropriate conditions of etching.

A recent work [293] has shown that for selected age-hardening alloys this problem can be solved effectively by making use of the fact that, under proper conditions of cooling, the decomposition of a solid solution and the associated strain-hardening may be different in deformed and recrystallized grains, and therefore these grains will be etched differently.

A typical illustration is a nickel-base ХН65КМВЮБ alloy (12-15% Cr, 5.5% Co, 5.0% W, 4.5-5.0% Al, 1.5% Nb, balance nickel), in which a large quantity of γ'-phase (type Ni_3Al) precipitates at temperatures below 1050°C. In specimens of this alloy cooled from the temperature of hot plastic working at a high rate (quenching), all grains were etched almost similarly, irrespective of the degree of strain-hardening. In specimens cooled at a low rate (in air), i.e. under the conditions in which the solid solution could decompose partially, recrystallized and unrecrystallized grains were etched rather differently by Krupp's reagent and differed in colour. The former were light and the latter dark (Fig. 194*a*). Electron-microscopic analysis showed that the slow cooling caused decomposition of the solid solution and precipitation of the γ'-phase. The concentration of that phase was roughly the same in all grains (either unrecrystallized or recrystallized), but the phase decorated clearly the dislocations in deformed grains and was seen in the latter in the form of regular squares (the upper right corner in Fig. 194*b*). In recrystallized grains, the concentration of particles of that phase was lower and particles had on the average larger size and rounded-off irregular shape, which is typical of the stage of coagulation (the region denoted by *R* in Fig. 194*b*). These results and the results of an additional X-ray examination, which showed a greater distortion in deformed grains, suggested a conclusion that the decomposition in deformed grains

was coherent and caused strong strain-hardening. In recrystallized grains, a higher concentration of vacancies resulted in the conditions favourable for diffusion coagulation of γ'-phase particles; this disturbed the coherence between that phase and the matrix.

Similar results may generally be obtained in all age-hardening alloys with a high concentration of precipitating phase if this phase causes appreciable strain-hardening during coherent decomposition.

In many cases, especially with a small size of original grains, t_r^s can conveniently be determined by the radiographic method which is based on the fact that X-ray reflections produced by recrystallized grains (nuclei) with an undistorted crystal lattice are much more intensive and sharp than those from deformed portions of the metal.

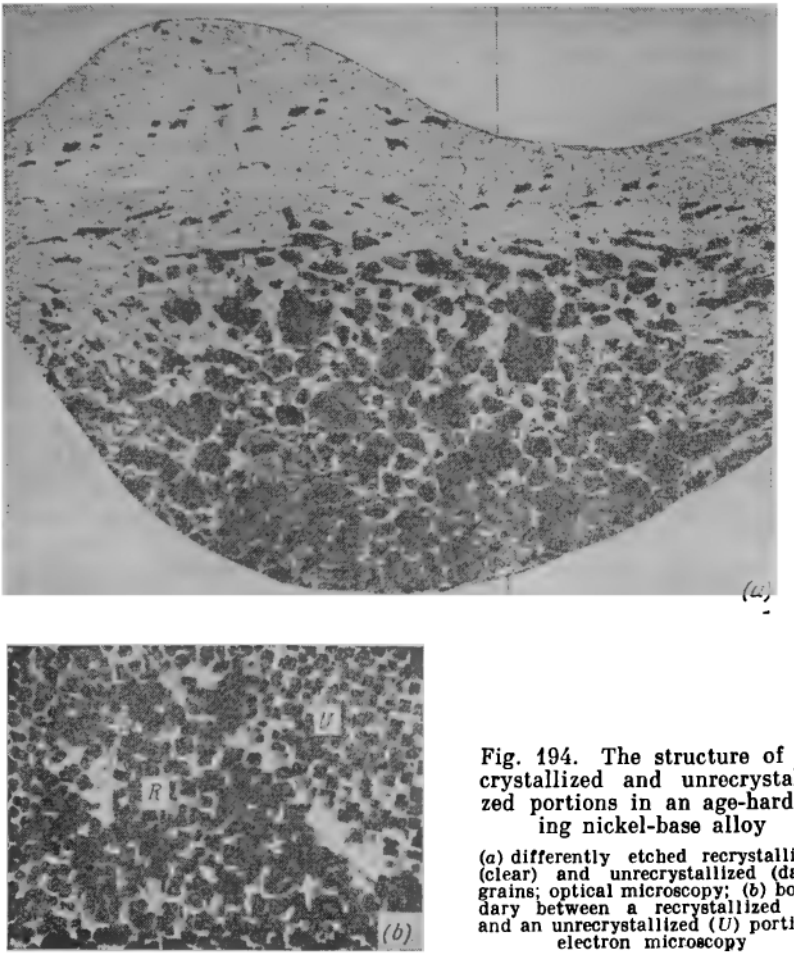

Fig. 194. The structure of recrystallized and unrecrystallized portions in an age-hardening nickel-base alloy

(*a*) differently etched recrystallized (clear) and unrecrystallized (dark) grains; optical microscopy; (*b*) boundary between a recrystallized (*R*) and an unrecrystallized (*U*) portion, electron microscopy

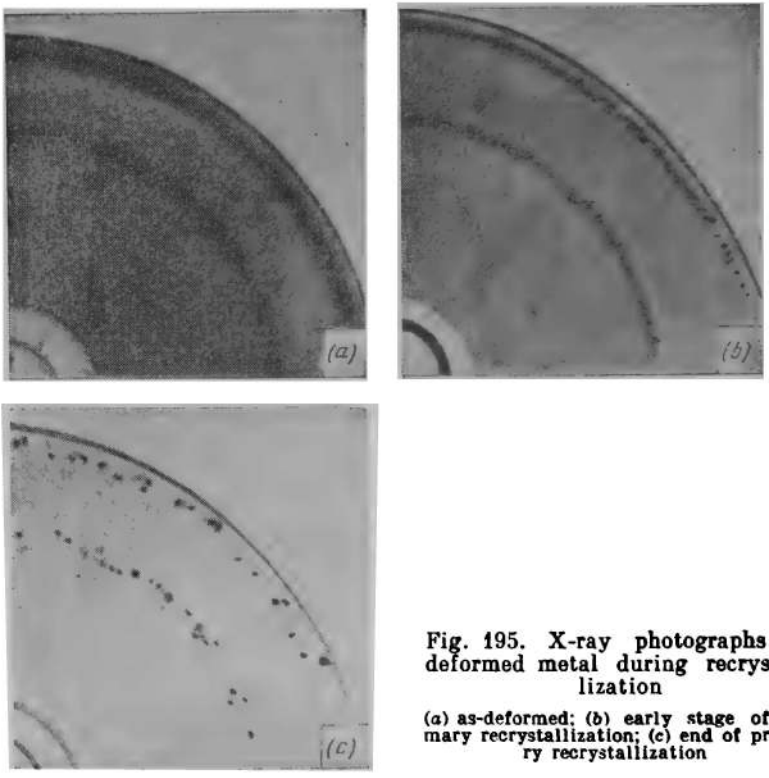

Fig. 195. X-ray photographs of deformed metal during recrystallization

(a) as-deformed; (b) early stage of primary recrystallization; (c) end of primary recrystallization

After moderate or heavy deformations, X-ray interference lines are seen to be strongly blurred. Reflections from individual crystallites merge together and cannot be resolved. Besides, if there is a texture, the intensity of lines along a Debye ring is non-uniform and varies by a periodic law which depends on the type of texture. After light deformations, reflections from individual crystallites are seen separately and have the form of diffuse arcs on the Debye ring.

As soon as first recrystallized grains form in a material, clear reflections appear on the background of a continuous ring in X-ray photographs (Fig. 195*b*). The sensitivity of the method can be improved if a line with a high repetition factor is selected for analysis.

If the number of nuclei formed at the early stage of the process is not very high and there is no risk that their reflections will merge together into a continuous line, it is possible to increase the volume being analysed by using a wide defocussed beam. This method offers certain advantages in operation with textured materials.

Using microfocus X-ray tubes, one can manage to detect the first recrystallized grains (nuclei) at a rather early stage of the process

when their size is only 1-3 μm or even smaller. Since, however, the volume being analysed is here very small and it is less probable that a nucleus will be detected in it, the number of radiographs to be taken should be increased.

X-ray analysis of recrystallization in weakly deformed specimens involves additional difficulties, since it is not always possible to distinguish between clear reflections produced by new grains and blurred reflections from weakly deformed crystallites. For that reason, the radiographic method is in this case less reliable than metallographic or microhardness techniques. Some novel X-ray techniques are devoid of this disadvantage.

An interesting method has been suggested by Masing [348] and employed for analysis of the kinetics of recrystallization in aluminium alloys. It consists in the following. Specimens of a coarse-grained material are prepared in the form of thin plates to enable 'transmission' radiography; therefore, their thickness depends on the X-ray absorption coefficient of the material. Transmission X-ray photographs are taken in polychromatic radiation. A radiograph of a deformed specimen is essentially a Laue photograph of a few large undistorted crystallites with the asterism of spots forming ellipses (Fig. 196*a*). As soon as recrystallization begins, clear reflections appear on radiographs, which have no asterism and are positioned randomly (Fig. 196*b*).

The method is advantageous over the conventional one in that new reflections appear in free portions of a photograph, which are not associated with the position of the zonal ellipses, whereas in the conventional method new reflections appear on the background of Debye rings. This circumstance, coupled with the use of polychromatic radiation (which gives a higher probability that recrystallization nuclei will be taken in reflecting positions), increases the sensitivity of the method.

Whenever it is difficult to prepare thin plates or the materials under test are heavy and strongly absorbing metals, one may employ the 'reflected light' radiography. But since this method uses a smaller volume of the material that participates in the formation of a

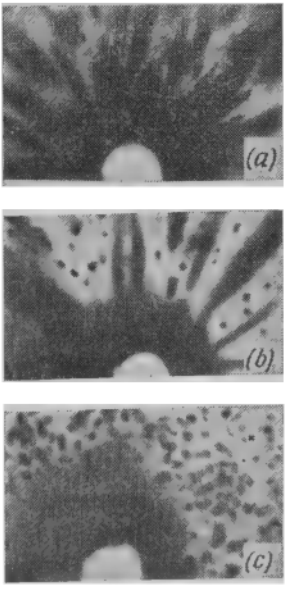

Fig. 196. Polychromatic transmission X-ray photographs of coarse-grained aluminium [348]

(*a*) as-deformed; (*b*) at an intermediate stage of primary recrystallization; (*c*) at the final stage

diffraction pattern than the former method, it is less sensitive.

X-ray photography also enables us to determine to a certain approximation the end of primary recrystallization. In heavily deformed specimens, this moment coincides with the disappearance of continuous Debye rings in the background of radiographs (Fig. 195*c*) and with a maximum on the curve relating the number of reflections to the time (temperature) of annealing. In lightly deformed specimens, the end of recrystallization is determined less reliably; it corresponds to the moment when axially stretched blurred reflections disappear on Debye rings or spots with asterism disappear on Laue photographs.

The scope of application of radiography for studying the kinetics of recrystallization can be greatly widened with the use of the method of recording X-ray interference lines by means of counters, i.e. photographing based on diffractometers.

This method markedly shortens the exposure time and, what is most important, enables us to analyse recrystallization directly during isothermal heating, i.e. at rather low (below room temperatures) or high temperatures, without the need for interrupting the process to take radiograms or prepare specimens. The last aspect is very important since cooling and repeated heating of specimens often tangibly change the kinetics of recrystallization.

The method is essentially as follows [349]. A specimen and the counter are arranged in the diffractometer in a position satisfying the Wulff-Bragg angle θ for a selected intensive line in the material being tested. Then, without changing the position of the counter, the specimen is rotated at a slow speed through a few degrees first in one direction and then in the opposite direction from the angle θ in order to cover the whole angular interval of an interference maximum whose shape is recorded by a recording device. In individual cases, satisfactory results can be obtained with the specimen held stationary or tilted slightly, but this necessitates the use of a wide diverging beam of rays.

For a deformed material, the maximum mentioned has the shape of a relatively smooth line. When recrystallization nuclei grow to a definite size in the course of isothermal heating, some nuclei which come to a reflecting position during the rotation of the specimen produce tooth-shaped peaks on the record (Fig. 197). The apparatus should preliminarily be adjusted so that the peaks associated with background fluctuations be substantially weaker than those which form at the onset of recrystallization. Since the original line must be smooth, this method is only applicable to heavily deformed materials.

If the material being tested recrystallizes below the room temperature, both deformation and recording should be naturally carried out at a temperature below the point of recrystallization and without intermediate heating to room temperature.

If the type of deformation is inessential and it is only important that the material be deformed heavily, this can be done most simply by surface strain-hardening (by emery roughing or local hammering).

With the type of radiation properly selected, when the depth of penetration is small compared with the size of growing grains, the method makes it possible to analyse the rate of growth of nuclei during isothermal heating from variations in the integral intensity of individual peaks. This intensity can be taken to be proportional to

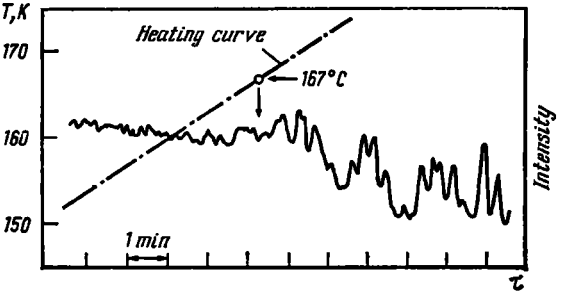

Fig. 197. Variations in the shape of diffractometric interference line of deformed metal at the onset of recrystallization [349]

the area of corresponding grains on the surface of a specimen. This possibility has been utilized in [349] for the analysis of recrystallization in high-purity zone-refined lead.

The success of the diffractometric method depends appreciably on proper selection of the conditions of recording (the size of slits, divergence of the beam, the rate of rotation of specimen, the speed of tape, the type of radiation, etc.). Useful recommendations can be found in [349].

The radiographic method (photographic or ionizational) is obviously suitable for determining the temperature level of recrystallization in brittle materials which cannot be deformed by common methods. In that case, deformation can be made by surface strain-hardening, for instance, by roughing with an emery disc. In order to check that the material has actually been strain-hardened, a radiogram should be taken on a stationary film. If a material is very brittle, then even after surface roughing the radiograms may show, along with diffuse Debye rings, individual sharp reflections from crystallites which have undergone brittle fracture. In that case, a different abrasive material should be taken [319, 320].

The strain-hardened specimens are heated in vacuum or in an inert atmosphere, after which the structural changes that have taken place in the strain-hardened surface layer during heating are analy-

sed radiographically. The moment of the onset of recrystallization is determined by the appearance of point reflections.

Indirect methods for determining t_r^s and analysing the kinetics of recrystallization are based on registering changes in the structure-sensitive properties which react most strongly to the variations in the density and distribution of dislocations that take place during heating. These properties include macro- and microhardness, yield strength, ultimate strength, electric conductivity, internal friction, etc.

Often, t_r^s is taken conditionally as the temperature of 50-% softening, i.e. the point at which the gain in hardness produced by prior strain-hardening diminishes by one-half. Some researchers take t_r^s as the temperature at which the hardness, yield strength or ultimate strength begin to drop sharply.

It should be noted, however, that these indirect methods give only approximate results. The extent to which a particular property is restored at the recovery stage may heavily differ with the type and degree of deformation and the properties and dislocation structure of the material. Lightly deformed metals and alloys regain their properties more easily. These methods, however, have limited possibilities, even for heavily deformed metals noted in Ch. 3, the process of recovery depends on the stacking fault energy of materials. In aluminium, intensive recovery has enough time for its completion even before the onset of recrystallization, which is associated with softening of the structure, narrowing of radiographic lines, etc. In copper no traces of recovery are detected at temperatures up to t_r^s. It is clear that an indirect method for determining t_r^s by, say, a decrease in hardness or by a 50-% softening will give a too low value for aluminium against that for copper.

Mould and Cotterill [350] analysed the sensitivity of various methods when used for detecting various stages of recrystallization in 99.99-% pure aluminium cold-rolled to $\varepsilon = 60\%$. The following methods were tested: the methods for measurement of Vickers macrohardness and of microhardness at a load of 100 gf s with construction of hardness distribution curves, methods of optical metallography in polarized light, and the Laue method.

The structural methods (determination of microstructure by polarized light metallography and Laue method) turned out to be more sensitive at the early stages of recrystallization. At later stages of the process, however, the structural methods failed to detect traces of unrecrystallized grains while these were readily detected by the method of microhardness measurement.

The results of the authors [350] and those of earlier works allow us to affirm that the beginning of recrystallization can be detected to high accuracy by the structural methods, and the moment of completion of recrystallization by constructing microhardness distribution curves.

The sensitivity of the microhardness method to the beginning and end of the process can be raised by applying a lower force to the indentor, i.e. by decreasing the volume being indented.

Valuable information on the kinetics and mechanism of recovery and recrystallization can be obtained by analysing changes in internal friction—a structure-sensitive property that depends on the density, distribution and mobility of defects and vacancies. By analysing a high-temperature low-frequency relaxation spectrum, it is possible to determine quite accurately the temperature intervals and the activation energy of recrystallization.

As the temperature rises to a definite value, the mobility of defects (in particular, dislocations) noticeably increases. This causes redistribution of defects, which leads at first to an increase in the internal friction and then to its decrease as the density of defects diminishes with their annihilation and lacking. Variations of internal friction in specimens heated under non-isothermal conditions cannot be estimated quite accurately. For that reason [351, 102], recrystallization parameters are usually determined not by the level of internal friction, but by the positions of relaxation maxima, i.e. peaks on the temperature curve of internal friction, Q^{-1} (T).

Indirect methods for determining t_r^s become even less reliable if recrystallization is coupled with phase transformations.

In supersaturated solid solutions, if recrystallization is accompanied by ageing, the latter process can mask the onset of recrystallization, cause strain-hardening of new recrystallized grains and retard their growth (see Ch. 12). The loss in hardness due to recrystallization can then be compensated for partially or fully by an increase in hardness due to decomposition of the solid solution. That is why a value of t_r^s determined by the onset of softening may be a few hundred degrees higher than its actual value. Overstated values of t_r^s also result from the use of direct (radiographic and metallographic) methods if t_r^s is taken as the temperature at which intensive growth of recrystallization nuclei begins, but not the temperature of the beginning of their formation.

Incorrect results are obtained in analysing heterophase alloys if the particles of a brittle disperse phase are broken under heavy deformation (see Ch. 12).

In such cases, special direct or indirect methods should be used to determine the actual value of t_r^s. Some of them will be discussed later. None of them can however be regarded as universal and accurate in all cases. For that reason, it is advisable to employ several methods at once in order to check the results.

Texture analysis. In heterophase and age-hardening alloys, a change in the deformation texture or its scatter (after heating, in which case t_r^s is impossible to determine by common methods) may be indicative of primary recrystallization taking place and thus can be

used for estimating the actual t_r^s (at the start of nucleation).

Micro-beam method. With a decrease in the diameter of the primary X-ray beam, the metal volume being irradiated diminishes, the resolution of the method increases and it is more likely that reflections from new grains will not merge together.

In age-hardening alloys, where a large number of nuclei often form at once, and these cannot grow because of the inhibiting effect of the secondary phase, micro-beam technique can reveal recrystallization at an earlier stage. With single-phase alloys, the use of this method gives no essential advantages in determining t_r^s.

Differential-hardness method. After very heavy deformations, the loss in hardness is observed practically at the same time with the onset of recrystallization and the contribution of the softening effect of recovery is very low.

If two specimens are deformed heavily, but to different degrees (for instance, $\varepsilon_1 = 50\%$ and $\varepsilon_2 = 70\%$), the latter will have a higher hardness than the former. In subsequent heating, the hardness of the former will slightly diminish (which is due to recovery) and the difference $\Delta H = H_2 - H_1$ will initially increase (Fig. 198). On reaching t_r^s, however, the hardness of the specimen deformed to ε_2 will decrease more intensively than that of the specimen deformed to ε_1 and the difference ΔH will become smaller (see Fig. 198). The temperature at the intersection of the curves *1* and *2* can be taken approximately as t_r^s for the deformation ε_2. More strictly, t_r^s should be taken as the temperature at the beginning of the bend of the curve $\Delta H = f(t_h)$. It is clear that heavy and essentially different deformations are required to obtain distinguishable values of t_r^s in two specimens.

This method gives quite accurate results for age-hardening and heterophase alloys. On heavy deformations, a difference in the degree of deformation affects to a lesser extent the rate and nature of decomposition than it does the rate and temperature of recrystallization.

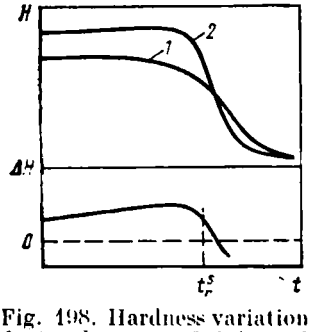

Fig. 198. Hardness variation during heating of deformed specimens (differential hardness method)

$1-\varepsilon_1 = 50\%$; $2-\varepsilon_2 = 70\%$

The effective activation energy of recrystallization, Q_r, which characterizes the effect of temperature on the rate of the process, can be determined from the data on the time of onset of recrystallization, τ_r^s, as determined at various temperatures T. Since the relationship between τ and the absolute temperature T, K, is of the form $\tau = \tau_0 \exp(Q/RT)$, it can be represented graphically in the $1/T$-ln τ coordinates (see Fig. 151). Depending on the temperature interval in

which τ is measured, and also on the alloy composition and some other factors, the experimental points may fall on a single straight line or on a broken line (see Figs. 151 and 152). In the latter case, Q_{ef} can be found for each straight section of the broken line, i.e. for a corresponding narrower temperature interval.

Two points, preferably spaced wide apart, are then taken on the straight line and the values of $\ln \tau_1$, $\ln \tau_2$, $1/T_1$ and $1/T_2$ are found. If τ_0 is independent of temperature in a given temperature interval, $Q_{ef} = R (\ln \tau_1 - \ln \tau_2)/(1/T_1 - 1/T_2)$.

It should be noted again that Q so found characterizes the effect of temperature on the rate of recrystallization in a given temperature interval, but in most cases it is not the actual activation energy of the process. When analysing the values of Q_{ef} and the probable causes responsible for variations in these values, one should consider the numerous factors which can exert an influence on the rate of the process at various temperatures (see Ch. 11) that takes place in a particular material under the given conditions of the experiment.

Of essential interest is the determination of the rate of growth, G, at various stages of recrystallization. This is most often done by resorting to statistical methods. Using the results of metallographic analysis, for instance, the curves of grain size distribution $N_i = f(D)$, the maximum size of grains at the initial moment of annealing, D^s_{max}, is determined. Similarly, the maximum size of grains at the end of the annealing procedure of time length τ is found, D^f_{max}. Assuming that the average rate of growth is the same for all grains, this is found by the formula $G = (D^f_{max} - D^s_{max})/\tau$.

Note that this formula is applicable only when the size of grains corresponds to a linear portion of the curve $\bar{D} = f(\tau)$. If the final size of grains, D^f_{max}, falls on the attenuating portion of the curve (which represents the process stage in which mutual collisions of growing grains become quite noticeable or the angles at grain joints approach their equilibrium values), the calculated values of G will be too low as against the actual rate of growth.

Apart from the statistical-average method, the rate of grain growth can also be determined by observing the growth of individual grains or the migration of grain boundaries. This can be done successfully by using high-temperature metallography [352] or electron emission microscopy [353, 70]. Both methods enable one to follow variations in the microstructure directly during the process of isothermal heating and record these variations photographically without intermediate cooling of the specimen.

High-temperature metallography reveals the structure owing to the preferable evaporation of grain boundaries. The time and temperature required for intensive evaporation are such that the early stages of primary recrystallization cannot be observed by this method.

The method is only applicable for analysis of grain growth and secondary recrystallization. Besides, it cannot detect low-energy boundaries (twins, etc.).

The method of emission microscopy for revealing metal structure is based on the crystallographic anisotropy of thermionic emission. Crystallites in which different crystallographic planes come to the surface of the specimen emit different numbers of electrons and give different brightness on the screen. The temperature of intensive thermionic emission can be lowered by using an appropriate activator [353, 70]. In the work [70], concerned with recrystallization in nichrome (Ni + 13% Cr) the activator was a solution of formic acid, isopropyl alcohol, and barium and cobalt formates taken in relative concentrations 75:25:8:11. This made it possible to observe structural changes at 925-950°C and analyse the earliest stages of recrystallization after the critical or slight supercritical deformation.

It should be noted, however, that the rate of grain growth in the surface of specimens may differ from that in the bulk of the metal owing to the effect of surface tension, etch pits, etc.

The growth of individual grains can be investigated by using polarized-light microscopy. A coat of oxide films (whose thickness depends on the crystallography of individual grains) gives various grains of various colours in polarized light. After annealing and application of a new film, it is possible to reveal both the old and the new boundaries. The method has been worked out thoroughly for aluminium [156, 354]. After electropolishing, specimens are coated by an anode film [354] in an electrolyte of a composition: 49 cm^3 H_2O, 49 cm^3 alcohol, and 2 cm^3 HF, at a voltage of 30 V.

Finally, the common optical microscopy can be used if the corresponding portions of a microsection are marked properly (for instance, by a microhardness indentor).

In the last two methods, however, the process must be interrupted more than once for examination of specimens and the repeated cycles of heating and cooling can influence the rate and nature of migration, which fact must be taken into account.

The rate of nucleation, N, can be found by calculating the number of new grains (nuclei) detected per unit time. For this, an experimental curve is plotted to show how the number of nuclei (new grains) n varies with the time of annealing τ, i.e. $N = \Delta n / \Delta \tau$.

After light and moderate deformations and with large original grains, new grains can be easily revealed in the optical microscope, and the value of n can be readily found by using conventional metallographic techniques.

After heavy deformations, it is possible to find radiographically the number of reflections n_r from new nuclei on the Debye ring. The value of n_r is proportional but not equal to n since reflections are formed only by nuclei which are in reflecting positions. This de-

pends, as noted earlier, on the repetition factor for $\{hkl\}$ planes which produce the given Debye ring on a radiogram. In many cases, the relative rate of nucleation can be judged by the data on $n_r = f(\tau)$ obtained for a few Debye rings.

The mechanism of recrystallization can be understood from the analysis of an expression describing the kinetics of the process in isothermal annealing. Most often, Avrami's equation is used for the purpose [see expression (5) in Ch. 3].

For practical use, the form of expression (5) obtained from two logarithmic operations is more convenient:

$$\log \ln [1/(1 - X_V)] = B + K \log \tau$$

where X_V is the relative recrystallized volume.

With this expression being satisfied, the corresponding relationship is represented in the $\log \ln [1/(1 - X_V)]$ and $\log \tau$ coordinates as a straight line with its tangent equal to K. The point of intersection of this line with the ordinate at $K = 1$ gives B. If the kinetics of the process is different at various stages of the process (for instance, in-situ recrystallization at the initial stage of annealing and normal primary recrystallization afterwards), the above relationship is described by a broken line with different values of K and B. Avrami's relationship is quite simple and for that reason is used most often.

The relative recrystallized volume X_V is usually determined metallographically. The area occupied by recrystallized grains is found by a point counting method, i.e. by counting the number of intersections on the graticule that fall into recrystallized regions. The number of microsection regions by which the calculation is made to provide for the reliability of obtained data depends on magnification.

With pure metals and single-phase alloys in which no decomposition of the solid solution takes place during recrystallization, the relative recrystallized volume X_V can be found from the relationship $X_V = (H_d - H_\tau)/(H_d - H_r)$, where H_d is the hardness (or yield strength) after deformation, H_r is the hardness in fully recrystallized state, and H_τ is the hardness after annealing for a time τ.

Figure 199 shows the typical graphical relationships obtained from the analysis of recovery and recrystallization in aluminium after hot rolling and pressing. As seen, at certain temperatures the process occurs in two stages with different kinetics. For the stage represented by a less inclined line on the diagram, K is less than unity (approximately 0.1-0.2), which, according to Avrami, must not be the case.

Comparison of these data with the results of structural analysis has shown that the softening effect at the stage considered is associated with in-situ recrystallization, whereas the second stage is associated with actual recrystallization.

The effective activation energy Q for these two stages has been found from the expression $\tau = \tau_0 \exp(Q/RT)$, where τ is the time at which a given softening effect is attained. The activation energy of in-situ recrystallization has turned out to be equal to approximately 30 kcal/g-atom, and that of actual recrystallization, 60-70

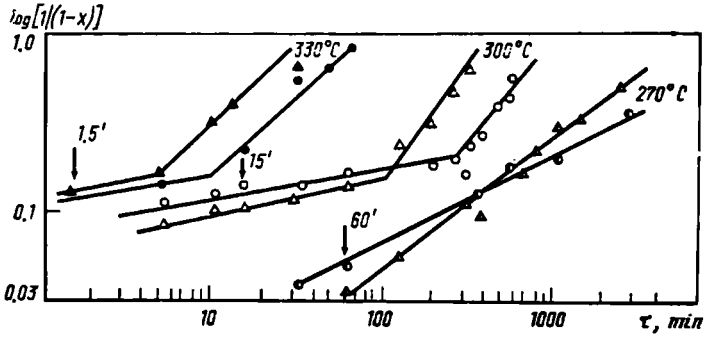

Fig. 199. Avrami analysis of the kinetics of softening during annealing of hot-deformed aluminium

kcal/g-atom. Thus, though in-situ recrystallization does not correspond to the model of nucleation and grain growth described by Avrami's relationship, the latter nonetheless can give useful information.

Recrystallization textures can be examined most reliably by X-ray structural analysis.

If recrystallized grains are fine and produce numerous small reflections in Debye rings, the textures formed are photographed on film by common methods in a texture chamber or in an ionization diffractometer with the use of a texture attachment. With coarse-grained materials, Laue photographs are taken from individual grains and then the orientations of these grains are determined. The results obtained are used for constructing pole figures which give the required data on the type of texture.

The pole figures of a crystal are essentially the stereographic projections of the normals (pole) to definite atomic planes $\{h_i k_i l_i\}$, which are constructed for all crystallites of a polycrystal.

As an example, Fig. 200 shows the pole figure of the {110} plane in cold-rolled iron, which has been constructed by G. V. Kurdyumov and G. Sachs. As is seen from this pole figure, cold-rolled iron has a complicated texture composed of three orientations which can be written briefly as follows: (1) {100} ⟨011⟩; (2) {112} ⟨110⟩; and (3) {111} ⟨112⟩. The index in the braces corresponds to the crystallographic indices of the plane which is parallel to the rolling plane and the index in ⟨ ⟩ brackets, to the indices of direction in crystallites

parallel to the rolling direction.

As follows from this designation, one group of crystallites (the most numerous one) is oriented with {100} planes parallel to the rolling plane and with the ⟨011⟩ directions parallel to the rolling direction. The projections of normals to {110} planes in this group of crystallites are marked by dark squares in the pole figure.

The two other, less numerous, groups of crystallites, as may be judged by the density of their maxima, are oriented with their {112} and {111} planes parallel to the rolling plane and with their respective directions ⟨110⟩ and ⟨112⟩ in the direction of rolling. The projections of normals to {110} planes of these crystallites are marked respectively by crosses and triangles.

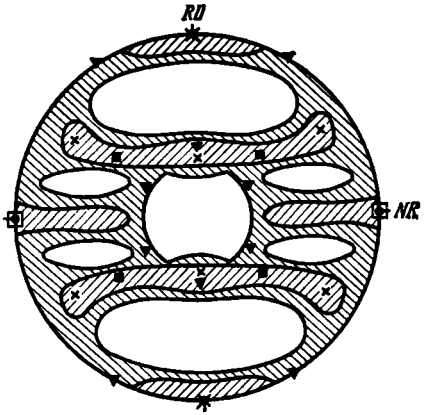

Fig. 200. A {110} pole figure of cold-rolled iron (after G. V. Kurdyumov and G. Sachs)

RD—rolling direction; *NR*—direction normal to rolling

In modern practice, pole figures are constructed most often by the data of X-ray diffractometry [355, 356, 357].

To construct a complete pole figure including the whole range of diffraction angles, the reflected light photography by the method proposed by Schultze [401] should be combined with 'transmission' photography [402].

The practical details of the combined 'transmission' and 'reflected-light' diffractometry for construction of pole figures can be found in [355] and [357]. The pole figures obtained in this way make it possible to determine, with satisfactory accuracy, the relative volume or area of a given orientation in the whole texture of a material. The method is based on an assumption that the 'reflected' light intensity, as fixed on a pole figure, is regarded as the volume above the pole figure plane. This volume consists of the volumes of individual texture maxima. A detailed description of the method, with all corrections to be made in its application, may be found in [357].

In analysis of the mechanism of formation of recrystallization textures and of ways for controlling these textures, valuable information can be obtained by examining the sequence in which recrystallization nuclei of various orientations appear, the rates of their formation and growth (N_{hkl} and G_{hkl}) and variations of these parameters in time. The problem reduces to determining the concentration and size of grains of particular orientations at various stages of annealing.

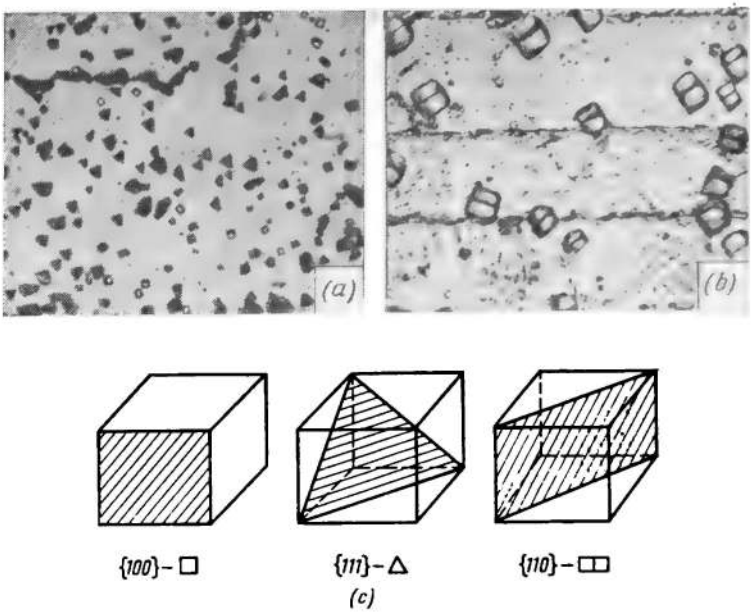

Fig. 201. Typical shapes of etch pits (*a*, *b*) in the principal crystallographic planes of cubic crystals (*c*)

The orientations of individual grains in a polycrystal are determined by etch pits [358-360] or from electronograms obtained by the microdiffraction technique. Figure 201 shows typical shapes of etch pits in the principal planes of a cubic symmetry. But if the size of grains is less than 15-20 μm, it is difficult to obtain clear etch pits. The use of electron microscopy for the purpose in that case is very labour-consuming.

With very large grains (above 0.5 mm), their orientations can be determined on Laue photographs or reflected-light Laue photographs taken from individual large grains [355]. The orientations thus found are marked as dots on a corresponding pole figure. The pattern of distribution of these dots on a pole figure will then characterize the texture. Pole figures characterize the type of texture more reliably with a larger number of Laue photographs taken from various crystallites. This method is however rather labour-consuming.

In that connection, X-ray methods based on measuring the intensities of reflections from individual crystallites are finding ever wider use for analysis of recrystallization.

V. Ya. Goldstein [361] has proposed an improved quantitative method for studying the rate of nucleation and growth of recrystallized grains of various orientations by taking X-ray diffractograms.

The method is similar to the Schultze's method [362] for constructing pole figures, but records not texture maxima, but reflections from individual recrystallized grains as these successively come into reflecting positions with the rotation of a specimen from the initial position.

A specimen and the counter are arranged initially in the positions of Bragg-Brentano focussing. The counter is fixed in the 2θ (hkl) position to record reflections from individual (hkl) planes and the pecimen is then rotated* about the normal to the surface (rotation through angle β) and tilted towards the plane of the primary and teflected beam (rotation through angle α). The number of reflections rrom grains (n) on the Debye ring is direcly proportional to the vofume of metal involved in reflection (V) and inversely proportional to lthe grain size (v_{av}), i. e. $n = 0.5\ Vkp \cos\theta\ \Delta\theta/v_{av}$, where k is the relative recrystallized volume, p is the repetition factor, $0.5 \cos\theta\Delta\theta$ is the probability for a crystal to be in the reflecting position, and $\Delta\theta$ is the divergence angle.

To prevent superposition (merging) of reflections from individual grains, the irradiated area of the specimen should be diminished, especially with finer grains and sharper textures. This is achieved by using narrow horizontal and vertical slits which limit the primary X-ray beam. Scanning is not to be used here.

The integral intensity of a reflection is proportional to the size of crystallite and is determined by the equation

$$E_\omega/I_0 = \int_{t'}^{t''} P(\theta)\, d(\theta) = QVA(\theta)$$

where $p(\theta)$ is the reflectivity of a crystal of volume V in direction θ; t' and t'' is the time of the beginning and end of recording of a peak; Q is reflectivity of the plane, and $A(\theta)$ is the absorption factor.

It then follows that the size of crystallites can be judged of by the intensity of peaks. To do this, a correction should be introduced into the experimental values of intensity. This correction depends on the angle α and is determined experimentally by comparing the intensities of reflection from crystallites in a standard specimen at various angles (this specimen has uniform grains of the thermal orientation). The corrected intensity is then found as

$$(I_\alpha)_{cor} = (I_\alpha)_{obs}\ (I_0/I'_\alpha)$$

where I'_0/I'_α is the ratio of the intensities from crystallites at $0°$ and $\alpha°$ in the standard specimen.

The passage from the corrected intensity of reflections to the actual size of grains in the tested specimen can be effected either

* The angular speed of rotation should be low, not more than 3-6 degrees per minute.

by comparing the results obtained with the intensities of reflection from the crystallites (whose size is known) in the standard specimen or by comparing the size of intensity peaks with the size of grains in the tested specimen (whose size can be determined metallographically). For more details see [361]. The sizes of grains thus found are transferred onto the stereographic projection and their orientations are analysed by means of Sachs' grids.

As an example, Fig. 202 shows the projections of normals to {110} planes of recrystallized grains in coarse-grained steel 08кп (the grain size in the deformed matrix is approximately 0.2-0.3 mm). The diameters of the circles in the projection are proportional to the size of reflecting grains.

To determine $N_{(hkl)}$ and $G_{(hkl)}$ in the course of recrystallization, regions of particular texture components are found on the stereographic projections corresponding to specimens at various stages of annealing, and the number and size of reflections occurring in them are analysed.

After determining the variation in the number and size of reflections that fall into a particular region of the stereographic projection, it is easy to find the rates of nucleation and growth of variously oriented grains and variations of these paramers in the course of annealing:

$$N_{(hkl)} = (n^{\tau_2}_{(hkl)} - n^{\tau_1}_{(hkl)})/(\tau_2 - \tau_1)$$

$$G_{(hkl)} = (D^{\tau_2}_{(hkl)} - D^{\tau_1}_{(hkl)})/(\tau_2 - \tau_1)$$

where $n^{\tau_1}_{(hkl)}$, $n^{\tau_2}_{(hkl)}$ are the number of grains of (hkl) orientation after annealing for a time τ_1 and τ_2, and $D^{\tau_1}_{(hkl)}$ and $D^{\tau_1}_{(hkl)}$ are their size respectively.

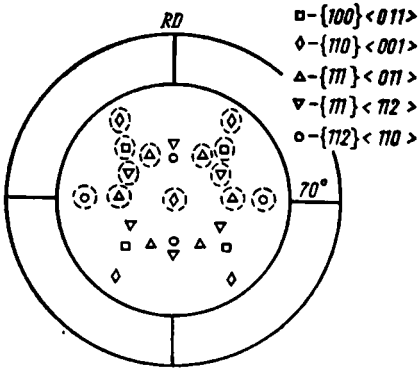

Fig. 202. Stereographic projections of {110} planes of large recrystallized grains in steel 08кп

RD—rolling direction

To analyse the distribution of texture over the depth of a specimen, this is etched layerwise and radiograms (electronograms) are taken each time.

Textures can be analysed to an appreciable depth without layerwise etching by using the method of neutron diffraction, since the the penetrability of neutrons is substantially higher than that of X-rays. The difficulties in the application of this method are mainly associated with the need to get a source of neutrons.

The techniques and apparatus for neutronographic analysis of

textures have been described by H.I. Bunge in a number of publications [363].

In thin films, radiographic and electronographic analyses of variations in recrystallization textures can be used for determining the onset of recrystallization.

Methods of quantitative metallography, which have been discussed thoroughly by S.A. Saltykov in his monograph [188], can give valuable data for estimating the nature of microstructures, their uniformity and stability.

As has been shown in [188], the absolute unit surface area of grain boundaries, ΣS, mm^2/mm^3 (whose square root is inversely proportional to the average linear size of grains), can be found easily by the secant method from the equation $\Sigma S = 2m$ $[mm^{-1}]$, where m is the average number of intersections, which a randomly drawn secant line makes with grain boundaries on a microsection, per millimetre of the line length.

This equality holds true for any system of planes in space irrespective of the shape and position of these planes. A secant line can also be of an arbitrary form, not necessarily a straight line, though a straight line is more convenient.

It is essential to determine the relative error ε_{re} in the value of unit surface area ΣS thus found.

The required number of intersections Z that gives a certain relative error P with predetermined reliability can be found by the formula $Z = 10^4 K^2 t^2 / \varepsilon_{re}^2$, where K is a coefficient depending on the non-uniformity of distribution of intersection points along the secant line. This non-uniformity is determined by the specific features of a given structure. K may vary within 0.7 to 1.2. Lower values correspond to a uniform distribution of intersection points. On the average, $K = 1$. In the formula above, t is the standard deviation which is associated with the probability of obtaining the specified error by the relationship

$$P = \sqrt{2/\pi} \int_0^t \exp(-0.5t)^2 \, dt$$

Values of P for various values of t are as follows:

t	0.10	0.5	1.0	1.5	2.0	2.5	3.0	4.0
P	0.0796	0.3830	0.6826	0.8664	0.9544	0.9870	0.9973	0.999936

For instance, to ensure that $P = 0.9$ and $\varepsilon_{re} = 5\%$ at $K = 1$, the required number of intersections is 1082. This means that 90% of determinations (with 1082 points in each) will have an error of less than 5%. All this is only true of isotropic structures.

Special techniques for determining these parameters for anisotropic structures are given in [188].

In practice, the average size of grains is determined by using standard grain size scales. The indices in which the size of grains is found on standard photo-scales (State Standard GOST 5639-65, see Table 34) correspond to the size of grains ($\bar{S}_{av}$ is the average area of grains, mm^2, and $\bar{d}_{con}$ is the average conditional diameter, mm).

TABLE 34. Grain Size Indices According to GOST 5639-65

Index	$\bar{S}_{av}$	$\bar{d}_{con}$, mm	Index	$\bar{S}_{av}$	$\bar{d}_{con}$, mm	Index	$\bar{S}_{av}$	$\bar{d}_{con}$, mm
—3	1.024	0.875	3	0.016	0.0111	9	$2.5 \cdot 10^{-4}$	0.0138
—2	0.512	0.650	4	0.008	0.0788	10	$1.25 \cdot 10^{-4}$	0.0099
—1	0.256	0.444	5	0.004	0.0553	11	$6.2 \cdot 10^{-5}$	0.0070
0	0.128	0.313	6	0.002	0.0391	12	$3.1 \cdot 10^{-5}$	0.0049
1	0.064	0.222	7	0.001	0.0267	13	$1.6 \cdot 10^{-5}$	0.0032
2	0.032	0.167	8	$5 \cdot 10^{-4}$	0.0196	14	$8 \cdot 10^{-6}$	0.0023

Saltykov [188] also gives methods for constructing various grain size distribution curves. Among the valuable information which can be obtained from them, the following cases should be emphasized.

1. Curves of grain size distribution by linear dimensions, $N_i = f(D_i)$. With homogeneous structures, they have the form of normal distribution curves only when plotted in semilogarithmic coordinates, $N_i = f(\ln D_i)$. In common (rectangular) coordinates, these curves are asymmetric, with $D_{max} D_{av} = 2.5$-3 (see Fig. 123). With inequigranular structures, this ratio may be appreciably higher, up to 8-10.

2. Curves of distribution of the area occupied by grains of a given size, $S_i = f(D_i)$. These curves are useful for analysis of inequigranular structures and secondary recrystallization. Inequigranularity is determined by the appearance of a second maximum on a curve of this type (see Fig. 38).

3. Curves of grain distribution by the number of edges, $N = f(p)$. With stable structures, a maximum of such a curve corresponds to $p = 5.75$-6. Any deviation of the maximum from this value is indicative of an unstable structure.

4. Curves of distribution of angles in grain joints, $N = f(0)$. With stable structures, in which grain-boundary tension can be taken to be isotropic, the maximum of a curve should correspond to approximately 120°. Deviations from this value point to instability of the structure.

References

1. Горелик С. С., Рекристаллизация металлов и сплавов. Москва, «Металлургия», 1967.
2. Honeycomb R. W. K., The Plastic Deformation of Metals. London, Arnold, 1968.
3. Recrystallization of Metallic Materials. Ed. by F. Haessner. Stuttgart, University a. Max-Planck Inst. für Metallforschung, 1971.
4. Recrystallization, Grain Growth and Textures. New York, ASM, 1966.
5. Новиков В. Ю., «Итоги науки и техники. Металловедение и термическая обработка». Москва, ВИНИТИ, 1969.
6. Горелик С. С., «Итоги науки и техники. Металловедение и термическая обработка». Москва, ВИНИТИ, 1972.
7. Рогельберг И. А., Шпиченецкий Е. С., Диаграммы рекристаллизации металлов и сплавов. Москва, Металлургиздат, 1950.
8. Houdremont E., Handbuch der Sonderstahlkunde. 3. Aufl. Berlin, Springer-Verlag, 1956.
9. Бережковский Д. И., «Металловедение и термическая обработка металлов», 1962, № 9; «Заводская лаборатория», 1964, № 12.
10. Масленников Б. Ф., Горелик С. С., «Физика металлов и металловедение», 1972, т. 34, вып. 2.
11. Молотилов Б. В., Афанасьев С. В., Барсуков В. Н. и др., «Прецизионные сплавы». Сб. № 2. Москва, «Металлургия», 1975.
12. Вайнблат Ю. М., Ланцман П. Ш., «Технология легких сплавов», 1974, № 3.
13. Бочвар А. А., ЖПФ, 1927, № 4.
14. Иверонова В. И., в книге: Применение рентгеновских лучей к исследованию материалов. Ленинград, 1949.
15. Савицкий Е. М., Терехова В. Ф., Холопов А. В., ДАН СССР, 1956, т. 109, № 4; 1959, т. 125, № 4.
16. Ларшков Л. Н. в книге: Физические основы прочности и пластичности металлов. Москва, Металлургиздат, 1963.
17. Корнеев Н. И., Скугарев И. Г., Основы физико-химической теории обработки металлов давлением. Москва, Машгиз, 1960.
18. Елагин В. И., Легирование деформируемых алюминиевых сплавов переходными металлами. Москва, «Металлургия», 1975.
19. Маевский И. Л., Обработка давлением жаропрочных сплавов. Москва, «Машиностроение», 1964.
20. Smart J. S., Smith A. A., *Trans. AIME*, 1943, v. 152, 1946, v. 166.
21. Phillips V. A., Phillips A. J., *J. Metals*, 1952-53, v. 26, No. 4.
22. Lücke K., *Z. Metallkunde*, 1961, Bd. 52.
23. Кудрявцев И. П., Текстуры в металлах и сплавах. Москва, «Металлургия», 1965.
24. Wassermann G., Grewen J., Texturen metallischer Werkstoffe. 2. Aufl. Berlin, Springer, 1962.
25. Горбачев В. Н., Молотилов Б. В., Соснин В. В., «Физика металлов и металловедение», 1970, т. 29, вып. 5.

26. Goss N. P., *Trans. ASM*, 1935, v. 23.
27. Beck P. A., Hu H. In: Recrystallization, Grain Growth and Textures, New York, ASM, 1966.
28. Walter J. L., Hibbard W. R., Fiedler H. C., *J. Appl. Phys.*, 1958, v. 29, No. 3.
29. Cahn R. W., *Proc. Phys. Soc.*, 1950, A63.
30. Лозинский М. Г., Бернштейн М. Л., Верчинская Т. В., «Металловедение и термическая обработка металлов», 1962, № 1.
31. Бернштейн М. Л., Штремель М. А., «Физика металлов и металловедение», 1963, т. 15, № 1.
32. Приданцев М. В., Жаропрочные стареющие сплавы. Москва, «Металлургия», 1973.
33. Химушин Ф. Ф., Жаропрочные стали и сплавы. Москва, «Металлургия», 1964.
34. Бернштейн М. Л., Термомеханическая обработка металлов и сплавов. т. 1-2. Москва, «Металлургия», 1968.
35. Соколков Е. Н., Садовский В. Д., «Физика металлов и металловедение», 1965, т. 19, № 2.
36. Бернштейн М. Л., Прочность стали. Москва, «Металлургия», 1974.
37. Гегузин Я. Е., Физика спекания. Москва, «Наука», 1967.
38. Ивенсен В. А., Кинетика уплотнения металлических порошков при спекании. Москва, «Металлургия», 1971.
39. Скороход В. В., «Порошковая металлургия», 1961, № 2.
40. Садовский В. Д., Структурная наследственность в стали. Москва, «Металлургия», 1973.
41. Гуляев А. П., Лешинская Р. П., «Металловедение и термическая обработка металлов», 1963, № 9.
42. Липчин Н. Н., «Металловедение и термическая обработка металлов», 1974, № 8.
43. Буйнов Н. Н., Захарова Р. Р., Распад металлических пересыщенных твердых растворов. Москва, «Металлургия», 1964.
44. Hornbogen E., Praktische Metallographie, 1970, No. 9.
45. McLean D., Grain Boundaries in Metals. London, Oxford Univ. Press, 1957.
46. Grabski M. W., Struktura granic ziarn w metalach. Katowice, «Śląsk», 1969.
47. Gleiter H., Chalmers B., High-angle Boundaries. Oxford, Pergamon Press, 1972.
48. Burke J. E., Turnbull D. In: Progress in Metal Physics. Vol. 4. Ed. by B. Chalmers. Oxford, Pergamon Press, 1953.
49. Бернштейн М. Л., Займовский В. А., Структура и механические свойства металлов. Москва, «Металлургия», 1970.
50. Morrison W. B., *Trans. ASM*, 1966, v. 59.
51. Codd R. M., Petch N. I., *Phyl. Mag.*, 1960, No. 5.
52. Белолипецкий Ю. П., Эндзелин М. А. и др. в книге: Структура и свойства жаропрочных металлических материалов. Москва, «Наука», 1967.
53. Копецкий Ч. В., Кулеско Г. И., «Физика металлов и металловедение», 1970, т. 30, вып. 1.
54. Дружинин В. В., Прасова Т. И., и др. «Изв. АН СССР. Физика». 1970, т. 34, № 2.
55. Зельбет Б. М., Безлепкина Л. Г., «Труды института ВНИИПП», вып. 1 (49), 1967.
56. Летюк Л. М., Нифонтов В. А., «Электронная техника, серия 6. Материалы», 1975, вып. 4.
57. Зайдман И. Д., «Информация института Черметинформация», сер. 12, 1967, № 1.

58. Holden A. N., Physical Metallurgy of Uranium. Reading, Addison-Wesley Publ. Co., 1959.
59. Дробинский М. М., Новиков В. Ю., Шарипов Э. И., «Изв. вузов. Черная металлургия», 1973, № 5.
60. Seeger A., Dislocations and the Mechanical Properties of Crystals. New York, Wiley, 1957.
61. Berner R., Kronmüller H., Plastische Verformung von Einkristallen. Berlin, Springer-Verlag, 1965.
62. Шмид Э., Боас В. Пластичность кристаллов, в особенности металлических. С нем. Москва, ОНТИ, 1938.
63. Новиков Г. И., Тираспольский В. И., «Физика металлов и металловедение», 1970, т. 29, вып. 4.
64. Physical Metallurgy. Ed. by R. W. Cahn. Amsterdam, North-Holland, 1965.
65. Steeds I. W., *Proc. Roy. Soc.*, 1966, A292.
66. Kuhlmann-Wilsdorf D., *Trans. AIME*, 1962, v. 224.
67. Andrade E. N., Da C., Aboav D. A., *Proc. Phys. Soc.*, 1957, A240.
68. Вишняков Я. Д., Современные методы исследования структуры деформированных кристаллов. Москва, «Металлургия», 1975.
69. Blewitt T. H., Coltman R. R., Redman I. K. In: Dislocation and Mechanical Properties of Crystals. New York, Wiley, 1967.
70. Горелик С. С., Розенфельд А. М., Скаков Ю. А., Спиридонов В. В., «Изв. вузов. Черная металлургия», 1960, № 2.
71. Лившиц Б. Г., Новиков В. Ю., Рощина Л. В., «Физика металлов и металловедение», 1972, т. 34, вып. 4.
72. Урусовская А. А. в книге: Итоги науки. Физико-математические науки. Вып. 3. Некоторые вопросы физики пластичности кристаллов. Москва, Изд. АН СССР, 1960.
73. Равич И. Г., Розенберг В. М., Козаковцева В. А., «Изв. АН СССР. Металлы», 1973 № 5.
74. Recovery and Recrystallization of Metals. Ed. by L. Himmel. New York, Interscience Publ., 1963.
75. Горелик С. С., Гольдштейн В. Я., «Физика металлов и металловедение», 1968, т. 26, вып. 1.
76. Инденбом В. Л. в книге: Итоги науки. Физико-математические науки. Вып. 3. Некоторые вопросы физики пластичности кристаллов. Москва, Изд. АН СССР, 1960.
77. Clark R., Chalmers B., *Acta Metal.*, 1954, No. 2.
78. Усиков М. П., Утевский Л. М., «Физика металлов и металловедение», 1961, т. 11, № 6.
79. Boas W., Ogilvie G. J., *Acta Metal.*, 1954, No. 2.
80. Горелик С. С., Барабанов С. П., Белолипецкий Ю. П. и др., «Физика металлов и металловедение», 1974, т. 37, вып. 5.
81. Jaoul B., *J. Mech. Phys. Solids*, 1957, No. 5.
82. Brandon D. G., Nutting I. I., *Iron a. Steel Inst.*, 1960, v. 196, No. 2.
83. Messager C., Morgan P., *C. R. Acad. Sci.*, 1960, v. 251, No. 23.
84. Weissmann S., Imura T., Hosokawa N. in: Recovery and Recrystallization of Metals. Ed. by L. Himmel. New York, 1963.
85. Усиков М. П., Утевский Л. М., «Проблемы металловедения и физики металлов», 1964, вып. 8.
86. Кидин И. Н., Штремель М. А., «Кристаллография», 1962, т. 7, № 6.
87. Barrett C. S., Structure of Metals. New York, McGraw-Hill, 1943.
88. Hu H., Grevdman S. R., *Trans. AIME*, 1963, v. 227.
89. Dillamore I. L., Roberts W. T., *Acta Metallurg.*, 1964, v. 12, No. 3.
90. Горелик С. С., Гольдштейн В. Я., Вербовецкая Д. Я., «Изв. вузов. Черная металлургия», 1968, № 5.

91. Ashby M. F., *Z. Metallkunde*, 1964, Bd. 55.
92. Balluffi R. W., Koehler G. S., Simmons R. O. In: Recovery and Recrystallization of Metals. Ed. by L. Himmel. New York, Interscience Publ., 1963.
93. Mott N. F., Dislocations and Mechanical Properties of Crystals. New York, Wiley, 1956.
94. Titchener A. L., Bever M. B. In: Progress in Metal Physics. London, the Institute of Metals Monograph and Report Series No. 23, 1958.
95. McQueen H. J., Jonas J. J. In: Treatise on Materials Science and Technology. V. 6. Plastic Deformation of Materials. Ed. R. J. Arsenault. New York, Academic Press, 1975.
96. Копецкий Ч. В., «Физика металлов и металловедение», 1973, т. 35, вып. 3.
97. Van Bueren H. G., Imperfections in Crystals. Amsterdam, North-Holland, 1960.
98. Бублик В. Т., Горелик С. С., «Физика металлов и металловедение» 1964, т. 18, № 1.
99. Kuhlmann-Wilsdorf D., Sizaki K., Proc. Intern. Conf. on Crystal Lattice Defects, 1962, Tokyo-Kyoto. *J. Phys.* Japan, Suppl. No. 3.
100. Горелик С. С., Ковалева Л. А., Блантер М. С., «Физика металлов и металловедение», 1972, т. 33, вып. 3.
101. Robinson P. M., Richards P. N., *Phil. Mag.*, 1965, v. 11, No. 110.
102. Горелик С. С., Беликов А. М., Юрьев В. А., Жигунов В. В., «Физика металлов и металловедение», 1972, т. 34, вып. 4.
103. Molenaar J., Aarts W. H., *Nature*, 1950, v. 166.
104. Goedeme G., Stals L., Nikoul I., *Scripta Metallurg.*, 1970, v. 4, No. 6.
105. Kankom M., Okumura N., Sugeno T., *Scripta Metallurg.*, 1969, v. 3, No. 11.
106. Clarebrough L. M., Hargreaves M. E., Loretto M. H., West G. W., *Acta Metal.*, 1960, No. 8.
107. Bell F., Kusement O., *Acta Metal.*, 1962, No. 10.
108. Stals L., Nikoul I. I., *Physica*, 1969, v. 42, No. 2.
109. Lihl P., Ebel H., Lugscheider W., Karczatk P., *Acta Phys. Austr.*, 1969, v. 30, No. 4.
110. Gobercht I., *Scripta Metallurg.*, 1969, v. 3, No. 8.
111. Hibbard W. R., Dunn C. G. In: Creep and Recovery. Ohio, ASM, 1957.
112. Cahn R. W., *J. Inst. Metals*, 1949, v. 76.
113. Cahn R. W., *Progr. in Metal Physics*, 1950, No. 2.
114. Mott N. F., *Proc. Phys. Soc.*, 1951, v. 64, part 9, No. 381B.
115. Cottrell A. H., Dislocations and Plastic Flow in Crystals. Oxford, Clarendon Press, 1953.
116. Amelinckx S., *Acta Metal.*, 1954, v. 2, No. 6.
117. Dunn C. G., Hibbard W. R., *Acta Metal.*, 1955, No. 4.
118. Вайнблат Ю. М., Горелик С. С., Саралова Т. Б., «Физика металлов и металловедение», 1971, т. 32, вып. 4.
119. Talbot J. in: Nouvelles propriétés physiques et chimiques des metaux de trés haute pureté. Paris, CNRS, 1960.
120. Rachinger W. A., Wood W. A., *J. Inst. Metals*, 1949, v. 76.
121. Broom T., Ham R. K. In: Vacancies and Other Point Defects in Metals and Alloys. A symposium organized by the Institute of Metals and held at the Atomic Energy Research Establishment, Harwell, 10 December 1962.
122. Gilman J. J., *Acta Metal.*, 1955, v. 3, No. 2.
123. Crussard C., *Revue Metallurg.*, 1944, v. 41, No. 1.
124. Montuelle J. In: Nouvelles propriétés physiques et chimiques des metaux de trés haute pureté. Paris, CNRS, 1960.
125. Горелик С. С., Спектор Э. Н., «Физика металлов и металловедение», 1963, т. 16, вып. 6.

126. Миркин И. Л., «Проблемы теоретического металловедения». Москва, Оборонгиз, 1938.
127. Avrami M., *Chem. Phys.*, 1939, v. 7, No. 8.
128. Deeker B. F., Harker D. J., *Appl. Phys.*, 1951, v. 22, No. 8.
129. Schweizer M., Form W., *J. Inst. Metals*, 1973, v. 101.
130. Semell I. W., Machlin E. S., *Acta Metal.*, 1957, No. 5.
131. Рафалович Ч. Н.,« Физика металлов и металловедение»,1956, т.2, № 2.
132. Иванов В. И., Осипов К. А., Возврат и рекристаллизация в металлах при быстром нагреве. Москва, «Наука», 1964.
133. Dimitrov M. O., C. R. Acad. Science, 1958, v. 247, No. 25.
134. Задумкин С. Н., Дигилев Р. М. в книге: Поверхностные явления в расплавах и возникающих в них твердых фазах. Кишинев, «Штиинца», 1974.
135. Лариков Л. Н., Засимчук Е. Э., «Укр. физич. журнал», 1962, т. 7.
136. Fullman I., *Trans. AIME*, 1953, v. 197.
137. Beck P., *Z. Metallkunde*, 1961, v. 52, No. 1.
138. Beck P., Kremer I. C., *Trans. AIME*, 1948, v. 175.
139. Mullins W. W., *Acta Metal.*, 1958, v. 6, No. 6.
140. Walter J. L., Dunn C. G., *Trans. AIME*, 1959, v. 215.
141. Coulomb P., Lacombe P., *C. R. Acad. Science*, 1959, No. 248.
142. Сато С. в книге: Рекристаллизация металлов. Москва, ОНТИ НКТП, 1933.
143. Захарова М. И., Кузнецов Г. Ф., «Изв. вузов. Физика», 1968, № 3.
144. Doherty R. D., Cahn R. W., *Less-common Metals*, 1972, v. 28, No. 2.
145. Пинес Б. Я., «Успехи физ. наук», 1954, т. 54, вып. 4.
146. Пинес Б. Я., Чайковский Э. Ф., Калужникова Н. В., «Физика твердого тела», 1959, № 2.
147. Dehlinger U., Theoretische Metallkunde. Berlin, Springer-Verlag, 1955.
148. Beck P., *J. Appl. Phys.*, 1949, v. 20, No. 6.
149. Burgers W. G., *Z. Metallkunde*, 1961, Bd. 52, No. 1.
150. Bollman W., *J. Inst. Metals*, 1959, v. 87, No. 12.
151. Fujita H., *Phys. Soc. Japan*, 1961, No. 16.
152. Weissmann S., *Trans. ASM*, 1961, v. 53.
153. Li J. C. M., *J. Appl. Phys.*, 1962, v. 33, No. 10.
154. Cahn R. W. In: Impurities and Imperfections. Cleveland, ASM, 1958.
155. Воронов С. М., Елагин В. И., О структуре и свойствах прессованных и штампованных изделий из алюминиевых сплавов. Москва, Оборонгиз, 1958.
156. Beck P., Sperry E. R., *J. Appl. Phys.*, 1950, v. 21, No. 5.
157. Bailey J. E., Electron Microscopy and Strength of Crystals. New York, Interscience Publ., 1963.
158. Ryum N., *Acta Metal.*, 1969, v. 17, No. 7.
159. Michels L. C., Richettes B. G., *Trans. AIME*, 1967, v. 239, No. 11.
160. Hamasi M. *et al.*, *J. Jap. Inst. Metals*, 1970, v. 34, No. 6.
161. Дубовицкая Н. В., Лариков Л. Н., «Металлофизика», вып. 31. Киев, «Наукова думка», 1970.
162. Fujita Hirochi, *J. Phys. Soc. Japan*, 1969, v. 26, No. 6.
163. Засимчук Е. Э., Максименко Е. А., «Металлофизика», вып. 31. Киев, «Наукова думка», 1970.
164. Ястребков А. А., Оплеснин Б. А. и др., «Физика металлов и металловедение», 1971, т. 31, вып. 4.
165. Guttmann V., *Metal.*, 1969, v. 23, No. 12.
166. Trueb L. F., *J. Appl. Phys.*, 1969, v. 40, No. 7.
167. Balluffi R. W., Woolhouse G. R., Komen Y., Nature and Behavior of Grain Boundaries. New York, Plenum Press, Symposium TMS-AIME, Detroit, Michigan, 1972.

168. Bay B., *Scripta met.*, 1970, v. 4, No. 6.
169. Бокштейн С. З. и др., «ДАН СССР», 1958, т. 121, № 6.
170. Жуховицкий А. А., «Успехи физики», 1955, т. 24, № 5.
171. Горелик С. С., Производство и обработка стали и сплавов. Москва, Металлургиздат, 1960.
172. Сиренко А. Ф. и др., «Физика металлов и металловедение», 1973, т. 35, вып. 4.
173. Розенберг В. М., Ползучесть металлов. Москва, «Металлургия», 1967.
174. Бабич В. К., Дроздов Б. Я., Пирогов В. А., Термическое упрочнение проката. Москва, «Металлургия», 1970.
175. Smith C. H., *Trans. AIME*, 1948, v. 175.
176. Read W. T., Shockley W., *Phys. Rev.*, 1950, v. 78.
177. Lacombe P., Berghesan A., *Metaux Corrosion*, 1949. No. 25.
178. Швиндлерман Л. С. и др., «Физика металлов и металловедение», 1973, т. 35, вып. 4.
179. Kronberg M. L., Wilson F. H., *Trans. AIME*, 1949, v. 185.
180. Архаров В. И., «Физика металлов и металловедение», 1961, т. 12, вып. 2.
181. McLean D., *J. Mater. Science*, 1973, No. 8.
182. Aust K. T., Rutter J. W., *Trans. AIME*, 1959, v. 215.
183. Gleiter H., *Phys. Stat. Solid.* (b), 1971, v. 45, No. 1.
184. Bishop J. F. W., Chalmers B., *Scripta Met.*, 1968, v. 2.
185. Rosi F. D., Alexander B. H., *Trans. AIME*, 1960, v. 188, No. 1.
186. Cole D. G., *Proc. Phys. Soc.*, 1954, No. 67, part 2.
187. Gleiter H., Lissowski A., *Z. Metallkunde*, 1971, Bd. 62, No. 2.
188. Салтыков С. А., Стереометрическая металлография. Москва, Металлургиздат, 1958.
189. Кунин Л. Л., Поверхностные явления в металлах. Москва, Металлургиздат, 1955.
190. Feltham P., *Acta Metal.*, 1957, v. 5, No. 2.
191. Бай А. С. и др., «Физика металлов и металловедение», 1972, т. 33, вып. 1.
192. Hu H., Smith C. S., *Acta Metal.*, 1956, v. 4, No. 4.
193. Криштал М. А., Давыдов Ю. П., Лернер М. И. и кн. Взаимодействие между дислокациями и атомами примеси. Тула, Тульский политехнический институт, 1969.
194. Жак К. М., Погребной Э. П., «Металловедение и термическая обработка металлов», 1974, № 4.
195. Виноград М. П. и др., «Металловедение и термическая обработка металлов», 1975, № 1.
196. Smith J. E., Dillamore I. S., *Metal Science*, 1970, v. 4.
197. Mecking H., Kirch F. In: Recrystallization of Metallic Materials. Ed. F. Haessner. Stuttgart, 1971.
198. Jonas J. J., Sellars C. M., *et al.*, *Metallurg. Rev.*, 1969, v. 14, No. 130.
199. Honeycomb R. W. K., Pethan R. W., *Less-common Metals*, 1972, v. 28.
200. Вайнблат Ю. М., Родина П. П., «Физика металлов и металловедение», 1973, т. 35, № 4.
201. McQueen H. J., Jones J. J., *J. Phys.*, 1967, v. 45, No. 2.
202. McQueen H. J., *J. Metals*, 1968, v. 20, No. 4.
203. Richardson G. J., Schnoble E., Stüwe H. P., *Metall*, 1969, Bd. 23, No. 11.
204. Rossard C., Blain P., *Rev. Met.*, 1958, v. 55, No. 6; 1959, v. 56, No. 4; 1960, v. 57, No. 3.
205. Luton M. J., Sellars C. M., *Acta Metal.*, 1969, v. 17.
206. Вайнблат Ю. М., Хаюров С. С., «Физика и химия обработки материалов», 1973, № 1.

207. Синельников М. И. и др., «Физика металлов и металловедение», 1973, т. 36, вып. 2.
208. Вайнблат Ю. М., Сагалова Т. Б., «Физика металлов и металловедение», 1970, т. 30, вып. 6.
209. Вайнблат Ю. М., Родина И. Б., «Технология легких сплавов», Вып. 5, 1969.
210. Лозинский М. Г., Соколов Е. Н., Строение и свойства металлов и сплавов при высоких температурах. Москва, «Металлургия», 1968.
211. Долженков И. Е., Вербоглаз В. Д., «Термическая обработка металлов», вып. 1, 1972.
212. Горелик С. С. и др., «Металловедение и термическая обработка металлов», 1971, № 7.
213. Горелик С. С., «Металловедение и термическая обработка металлов», 1961, № 3.
214. Раузин Я. Р., «Металловедение и термическая обработка металлов», 1959, № 9.
215. Равич И. Г. и др., «Металловедение и термическая обработка металлов», 1973, № 3.
216. Burke J. E., Shiau V. J., *Trans. AIME*, 1948, v. 175.
217. Горелик С. С., Спектор Э. Н., «Физика металлов и металловедение», 1963, т. 16, вып. 6.
218. Горелик С. С., Граник Г. И., «Физика металлов и металловедение», 1959, т. 7, вып. 3.
219. Инденбаум Г. В. и др., «Физика металлов и металловедение», 1964, т. 17, вып. 5.
220. Aust K. T. In: The Art and Science of Growing Crystals. New York, Wiley, 1963.
221. Edwards C. A., Pfeil L. B., *J. Iron and Steel Inst.*, 1924, v. 109.
222. Gensamer M., Mehl R., *Trans. AIME*, 1938, v. 131.
223. Dunn C. G., Wouker G. C., *Met. Progress*, 1955, v. 67.
224. Fisknoff K., Lücke K., *Z. Metallkunde*, 1952, Bd. 43, No. 4.
225. Гольдштейн В. Я., Савинская А. Л., «Физика металлов и металловедение», 1973, т. 36, вып. 3.
226. Спектор А. Г., «Заводская лаборатория», 1955, № 2.
227. Добаткин В. И., «Легкие сплавы», Сборник № 1. Изд. АН СССР, 1958.
228. Горелик С. С., Сафонов Ю. С., Козловская В. П., «Физика металлов и металловедение», 1969, т. 28, вып. 5.
229. Добаткин В. И., Бухов С. К., Селицкий П. И. в книге: Исследование деформируемости сплавов. Москва, Оборонгиз, 1955.
230. Меськин В. С., Основы легирования стали. Москва, «Металлургия», 1964.
231. Eyre T. S., *Metal Treatment and Drop Forging*, 1964, v. 31, No. 228.
232. Мороховец Г. М., Каплин Ю. И., Гайдебуров А. А. в книге: Исследование деформируемости сплавов. Москва, Оборонгиз, 1955.
233. Горелик С. С. и др., «Металловедение и термическая обработка металлов», 1960, № 9.
234. Горелик С. С., Спектор Э. Н., «Исследования по жаропрочным сплавам», т. 10, Изд. АН СССР, 1962.
235. Савицкий Е. М. и др., ДАН СССР, 1956, т. 109, № 4.
236. Савицкий Е. М. и др., ДАН СССР, 1959, т. 126, № 4.
237. Савицкий Е. М. и др., ДАН СССР, 1958, т. 118, № 4.
238. Савицкий Е. М., Терехова В. Ф., ДАН СССР, 1957, т. 112, № 2.
239. Тылкина М. А., Кириленко Р. В., Савицкий Е. М., ДАН СССР, 1959, т. 127, № 2.
240. English A. T., Backofen W. A., *Trans. AIME*, 1964, v. 230.

241. Гладков А. С. и др., Металлы и сплавы для электровакуумных приборов. Москва, «Энергия», 1969.
242. Иверонова В. И., Жданов Г. С. в книге: Рентгенография в применении к исследованию материалов. Москва, ОНТИ, 1936.
243. Лайнер Д. И., Крупникова-Перлина Е. И., «Физика металлов и металловедение», 1960, т. 9, № 4.
244. Green R. F. *et al.*, *Trans. AIME*, 1950, v. 215.
245. Burgers W. G., *Acta Metal.*, 1953, v. 1, No. 2.
246. Burgers W. G., Verbraak C. A., *Acta Metal.*, 1957, v. 5, No. 12.
247. Beck P. A., *Acta Metal.*, 1953, v. 1, No. 2.
248. Избранов П. Д. и др., «Физика металлов и металловедение», 1965, т. 8, вып. 3.
249. Wiener G., Carcoran R., *Trans. AIME*, 1956, v. 206.
250. Каверина С. Н., Котко В. А., Перлович Ю. А., «Металлофизика», вып. 50. Киев, «Наукова думка», 1974.
251. Akisne Osawu *et al.*, *Jap. Inst. Metals*, 1972, v. 36, No. 11.
252. Cook M., Richards T. L., *J. Inst. Met.*, 1941, v. 67; 1947, v. 73.
253. Merlini A., Beck P. A., *Trans. AIME*, 1955, v. 203.
254. Goodman S. R., Hu H., *Trans. AIME*, 1966, v. 236.
255. Афанасьев С. В. и др., «Физика металлов и металловедение». 1971, т. 31, № 2.
256. Новиков В. Ю., Семеновская И. В., «Изв. вузов. Черная металлургия», 1973, № 7.
257. Дубров Н. Ф., Лапкин Н. И., Электротехнические стали. Москва, Металлургиздат, 1963.
258. Кокшарова И. К. и др., «Физика металлов и металловедение», 1962, т. 14, вып. 3.
259. Молотилов Б. В. и др., «Металловедение и термическая обработка металлов», 1967, № 4.
260. Молотилов Б. В. и др., Прецизионные сплавы. Сборник № 2. Москва, «Металлургия», 1973.
261. Шестаков И. А. и др., «Изв. АН СССР. Металлы», 1974, № 1.
262. Молотилов Б. В., Иванова И. М., «Изв. АН СССР. Металлы», 1972, № 3.
263. Иванова И. М., Молотилов Б. В., «Изв. АН СССР. Металлы», 1973, № 4.
264. Иванова И. М., Молотилов Б. В., Самарина Н. М., «Изв. вузов. Черная металлургия», 1974, № 1.
265. Миронов Л. В. в книге: Проблемы производства и применение электротехнических сталей. Свердловск, 1960.
266. Dunn C. G., Koch P. K., *Acta Metal.*, 1957, v. 5, No. 10.
267. Лившиц Б. Г., Новиков В. Ю., «Физика металлов и металловедение», 1963, т. 16, вып. 6.
268. Новиков В. Ю., ДАН СССР, 1973, т. 42, № 3.
269. Титоров Д. Б., «Физика металлов и металловедение», 1973, т. 36, вып. 1; 1974, т. 37, вып. 6.
270. Горелик С. С., Гольдштейн В. Я., «Физика металлов и металловедение», 1967, т. 23, вып. 4.
271. Авраамов Ю. С., «Физика металлов и металловедение», 1968, т. 26, вып. 3.
272. Брюхатов Н. Л., Лагидзе Р. М., «Физика металлов и металловедение», 1968. т. 26, вып. 4.
273. Соснин В. В., Ястребов Т. Я., «Металловедение и термическая обработка металлов», 1974, № 7.
274. Воробьев Г. М. и др., «Изв. АН СССР. Металлы», 1969, № 5.
275. Петров А. К. и др., «Физика металлов и металловедение», 1969, т. 28, вып. 3.

276. Wiener G. J., *Appl. Phys.*, 1964, v. 35.
277. Молотилов Б. В., Червоненков В. А., «Изв. АН СССР. Металлы», 1969, № 4.
278. Walter J. L., Dunn C. G., *Trans. AIME*, 1960, v. 218.
279. Gilman J., *J. Metals*, 1954, No. 5.
280. Mölins H. E., Pawlek F., *Arch. Eisenhüttenw.*, 1958, No. 7.
281. Расторгуев А. А. и др., «Сталь», 1958, № 11.
282. Dahl W., Geisler J., *Z. Metallkunde*, 1960, Bd. 51, No. 7.
283. Ван Лимпт Дж. в книге: Рекристаллизация металлов. Москва, ОНТИ, 1933.
284. Грузин П. Л., Тютюник А. Д., «Физика металлов и металловедение», 1961, т. 11, вып. 1.
285. Смит М. К., Основы физики металлов. Москва, Металлургиздат. 1959.
286. Antonione C., Gatta G. D., *et al.*, *Acta Metal.*, 1970, v. 18, No. 11.
287. Засимчук Е. Э., Максименко Е. А. в книге: Монокристаллы тугоплавких и редких металлов. Москва, «Наука», 1970.
288. Runalls O. J., Biucher R. R., *Less-common Metals*, 1967, v. 13, No. 4.
289. Герцрикен С. Д., Дехтяр И. Е., Диффузия в металлах и сплавах в твердой фазе. Москва, Физматгиз, 1960.
290. Olsen K. M., *Trans. ASM*, 1960, v. 52.
291. Rolling G. F., Winegard W. C., *Acta Metal.*, 1950, v. 6, No. 4.
292. Harrington R. H., *Trans. ASM*, 1949, v. 41.
293. Барабанов С. П., Горелик С. С., Сагалова Т. Б., Сафонов Ю. С., «Металлофизика», вып. 61. Киев, «Наукова думка», 1975.
294. Millner T., Bartha L., Prohaszka J., *Z. Metallkunde*, 1960, Bd. 51, No. 11.
295. Бокштейн С. З., Кишкин С. Т., Мороз Л. М. в книге: Процессы диффузии. Структура и свойства металлов. Москва, «Машиностроение», 1964.
296. Архаров В. И., «Физика металлов и металловедение», 1955, т. 1, вып. 2.
297. Seeman Z., *Z. Metallkunde*, 1958, Bd. 49.
298. Бочвар А. А., Металловедение. Москва, Металлургиздат, 1956.
299. Полеся А. Ф., Пасальский В. М., «Физика металлов и металловедение», 1969, т. 28, вып. 4.
300. Hornbogen E., *Prakt. Metal.*, 1970, Bd. 7, No. 7.
301. Kreyer H., Hornbogen E., *Phys. Stat. Solid.* (a), 1970, v. 1, No. 1.
302. Smalin R. A., Geisler A. K., *J. Inst. Metals*, 1957, v. 86, No. 3.
303. Соболевский И. А., «Научные труды Днепропетровского металлургического института». Сб. № 33. Киев, 1955.
304. Бабич В. К., Пирогов В. А. в книге: Взаимодействие между дислокациями и атомами примесей в металлах и сплавах. Тула, Тульский политехн. институт, 1969.
305. Donerty R. D., Martin J. W., *J. Metals*, 1963, v. 91, No. 10.
306. Rollason T. C., Martin J. W., *J. Mater. Science*, 1970, v. 5, No. 2.
307. Вайнблат Ю. М., Горелик С. С., Сагалова Т. Б., «Физика металлов и металловедение», 1971, т. 31, вып. 1.
308. Köster U. In: Recrystallization of Metallic Materials. Ed. F. Haessner. Stuttgart, 1971.
309. Ahlborn H., Hornbogen E., Köster U., *J. Mater. Science*, 1969, v. 4, No. 11.
310. Brimha J. L., Huggins R. A., *Trans. AIME*, 1965, v. 233.
311. Структура и свойства металлов и сплавов. Деформация, последеформационный нагрев. Москва, «Металлургия», 1970.
312. Лившиц Б. Г., Орлов Б. Н., ДАН СССР, 1950, т. 70, № 2.
313. Phillips V. A., *Trans. AIME*, 1965, v. 236.

314. Serebryakov A. V., Redkova T. M., *Phys. Sta. Solid.* (a), 1971, v. 5, No. 2.
315. Serebryakov A. V. *et al.*, *Phys. Stat. Solid.* (a). 1972, v. 14, No. 1.
316. Speight M. V., Greenwood G. V., *Phil. Mag.*, 1964, No. 2.
317. Shewmon P. G., *Trans. AIME*, 1964, v. 230.
318. Ashby M. F., Centamore R. M., *Acta Metal.*, 1968. v. 15.
319. Горелик С. С. и др., «Изв. вузов. Цветная металлургия», 1960, № 5; 1962, № 4.
320. Кушталова И. П., Рекристаллизация и дисперсионное упрочнение металлов и сплавов. Киев, «Наукова думка», 1969.
321. Самсонов Г. В., Божко Г. А., «Изв. вузов. Цветная металлургия», 1972, № 2.
322. Горелик С. С. и др., «Изв. вузов. Черная металлургия», 1970, № 1.
323. Летюк Л. М., Горелик С. С., Бабич Э. Л., Нифонтов В. А., «Неорганические материалы», 1976, № 11.
324. Дугар-Жабон К. Д., Щербакова А. Н., Хуторская Н. Н., в книге: Ферриты. Минск, «Наука и техника», 1968.
325. Горелик С. С. и др., Структура и свойства ферритов. Минск, «Наука и техника», 1974.
326. Горелик С. С. и др. в книге: Методы получения и анализа ферритовых материалов и сырья для них. Донецк, 1975.
327. Blacman L., *J. Appl. Phys.*, 1957, v. 28, No. 12.
328. Глотов В. Г., «Неорганические материалы», 1970, т. 6, № 8.
329. Технология электрокерамики. Москва, «Энергия», 1974.
330. Гладков А. С., Горелик С. С., Лемешко О. В., Дьячков В. М., «Электронная техника, Материалы», 1974, вып. 7.
331. Thun R. In: Physics of Thin Films. Vol. 1. New York. Academic Press, 1963.
332. Vecht A. In: Physics of Thin Films. Vol. 1. New York, Academic Press, 1963.
333. Толутис В. Б., Ясутис В. В. в книге: Тонкие пленки соединений теллура с металлами подгрупп цинка и кадмия. Вильнюс, 1970.
334. Сертулис К. П., Станневичюс М. В., Толутис В. Б. в книге: Тонкие пленки соединений теллура с металлами подгрупп цинка и кадмия. Вильнюс 1970.
335. Захаров В. П., Чугаев В. Н., «Физика и химия обработки материалов», 1968, № 4.
336. Александров Я. Н. и др., «Изв. вузов. Физика», 1973, № 3.
337. Данилин Б. С., Вакуумное нанесение тонких пленок. Москва, «Энергия», 1967.
338. Gangulee A., D'Heurle F. M., *Thin Solid Films*, 1973, v. 16, No. 2.
339. Matter S., Feder R., Chandhare P., *Thin Solid Films*, 1972, v. 14, No. 1.
340. Quintame M. C., Sacedon I. L., *Thin Solid Films*, 1972, v. 14, No. 2.
341. Трусов Л. И., Холмянский В. А., Островковые металлические пленки. Москва, «Металлургия», 1973.
342. Палатник Л. С., Фукс М. Я., Косевич В. М., Механизм образования и субструктура конденсированных пленок. Москва, «Наука».
343. Via G. G., Thun R. E. in: Vacuum Symposia. Vol. 8. New York, Pergamon Press, 1968.
344. Buckel W. In: Structure and Properties of Thin Films. New York, Wiley, 1959.
345. Kubaschewski O., Hopkins B. E., Oxidation of Metals and Alloys. London, Butterworths, 1962.
346. Gattman V., *Z. Metall.*, 1972, Bd. 63, No. 2.
347. Gilles J. M., Van Gakenberghe Y., *Nature*, 1958, v. 182, No. 4639.
348. Masing C *et al.*, *Z. Metallkunde*, 1956, Bd. 47, No. 2.

349. Barrett C. S. In: Direct Observation of Imperfections in Crystals. Ed. by J. B. Newkirk and J. H. Wernick. New York, Interscience Publ., 1962.
350. Mould P. R., Cotterill P., *Metallurgia*, 1965, v. 71, No. 425.
351. Александров Я. Н., Морфюк В. С. в книге: Свойства и применение жаропрочных сплавов. Москва, «Наука», 1966.
352. Лозинский М. Г., Высокотемпературная металлография. Москва, Машгиз, 1956.
353. Grube W. I., Rouze S. R. In: Tools and Techniques in Physical Metallurgy. In two volumes. Ed. by F. Weinberg. New York, 1970.
354. Горелик С. С., Кальянова С. И., Розенберг В. М., «Физика металлов и металловедение», 1960, т. 10, вып. 2.
355. Горелик С. С. и др., Рентгенографический и электронномикроскопический анализ. Москва, «Металлургия», 1970.
356. Горелик С. С. и др., «Физика металлов и металловедение», 1967, т. 24, вып. 1.
357. Лайнер Д. И., Радишевский А. И., Металловедение медных деформируемых сплавов. Москва, «Металлургия», 1973.
358. Пшеничнов Ю. П., Выявление тонкой структуры кристаллов. Москва, «Металлургия», 1974.
359. Tacker G. E., Murphy Q. C., *J. Metals*, 1952-53, v. 8.
360. Barber D. J., *Phys. Mag.*, 1962, No. 11.
361. Гольдштейн В. Я., «Заводская лаборатория», 1973, № 6.
362. Schulz L. G., *J. Appl. Phys.*, 1949, v. 20, No. 11.
363. Bunge H. I., *Hutnické listy*, 1973, v. 28, No. 2.
364. Lucci A., Riontino G., Venturello G., Colloques intern. du CNRS, *Thermochimie*. Paris, 1972.
365. Гегузин Я. Е., Клинчук Ю. И., «Физика металлов и металловедение», 1974, т. 37, вып. 5.
366. Гуляев А. П., Металловедение. Москва, «Металлургия», 1977.
367. Бодяко М. Н., Астапчик С. А., Ярошевич Б. Б., Термокинетика рекристаллизации. Минск, «Наука и техника», 1968.
368. Meyzaud J., Parniese P., Memoires scientifiques. *Rev. metallurgie*, 1971.
369. Duggan B. J., Roberts W. T., *Metal Sci.*, 1975, v. 9.

Index

Aarts W. H. 72
Activator-stimulated recrystallization 438
Alloy texture 59
Alloying, effect on recrystallization 339
Alterthum H. 129
Aluminium alloys 276
Anderson W. A. 131
Annealing twins 38, 174, 193
Arkharov V. I. 170, 348, 369
Arrhenius equation 98
Ashby M. F. 63, 399, 410
Asterism streaks 77
Aust K. T. 172, 365
Average grain size 15
Avraamov M. 14, 96, 183, 192, 457
Axial deformation texture 57

Babich V. K. 163, 398, 401, 406
Bailey J. E. 119, 149
Bakhmetyev E. F. 133
Barrett C. S. 45, 102, 316
Barrier effect of disperse particles 196
Basal slip 21
Beaujard L. 146
Beck P. A. 110, 112, 133, 148, 241, 308, 311, 316
Berezhkovsky D. I. 294
Bernstein M. L. 162
Bishop J. F. W. 174
Blain P. 209
Blocks 81
Boas W. 51
Bochvar A. A. 133, 345, 346, 363, 372
Bockstein S. Z. 367
Bollman W. 134
Boundary mobility 179
Brass texture, 59
  formation of 317
Brendon's model 173
Bryukhatov N. L. 332
Burgers W. G. 131, 134, 193, 234, 307, 308, 315, 379
Burke J. E. 234

Cahn R. 53, 77, 78, 81, 129, 133, 134, 253, 254, 366, 367
Carpenter H. C. H. 253, 254
Cells 81
Cell boundaries 81
Cell walls 81
Centamore R. M. 410
Chalmers B. 50, 174
Clarebrough L. M. 118, 119
Clark R. 50
Coalescence of grains 195
Coalescence of subgrains 155
Coarse structures 258
Coherent boundary 174
Coincidence boundaries 171
Coincidence-site lattice 171
Coincidence-site model 174
Compounds, recrystallization in 414
Cook M. 96
Copper texture 59
Cotterill P. 452
Cottrell A. H. 78, 134, 359
Cottrell atmospheres 89
Coulomb P. 116
Critical deformation of metals 229
Critical shear stress 23
Cross slip 36
Crussard C. 88
Cube texture, 306
  in transformer steel 335

Dahl W. 343
Dangled boundaries 195
Deeker B. F. 96
Deformation, by irregular
  rotation of lattice 44
  in polycrystals 49
  by twinning 38
Deformation textures 56
Deformation twins 38
Dehlinger U. 131
Diffusion of point defects 70
Dislocation density 149
Dislocation dipoles 33
Dislocation forest 85, 207
Dislocation mechanism of polygonization 78
Dislocation pile-up 33
Dislocation regrouping 133
Dislocation slip 19
Dislocation tangles 32
Disperse inclusions 109
Disperse phases in iron and nickel alloys 264
Dobatkin V. I. 261
Donerty R. D. 398
Donor impurities 443
Dorn J. E. 131
Dubrov N. F. 337
Dunn C. G. 76, 87, 116, 120, 256, 257, 330, 331
Dynamic recrystallization 203
Dynamo steel, low-textured 338

Elagin V. I. 363
Elam C. F. 253, 254
Electric steel, texture formation in 322
Extrusion effect 147
Eyre T. S. 263

Feltham P. 193, 194, 200
Ferrites 418
First-order recrystallization diagrams 292
First-order stress 62
Fluctuation theory of nucleation 129
Frank-Read dislocation sources 33, 34
Friction forces, effect on inhomogeneity 61
Fujita H. 135, 142

Gaideburov A. A. 263
Gartman Yu. M. 337
Gattman V. 435
Geguzin Ya. E. 413
Geisler J. 343
Geodakyan V. A. 158
Gilles J. M. 437
Gilman J. J. 86
Gleiter H. 173, 174, 175, 177, 181
Gnomonic projection 25
Goedeme G. 75
Goldstein V. Ya. 51, 153, 321, 460
Gorelik S. S. 51, 234, 235, 236
Grain boundaries, structure of 165
Grain-boundary dislocations 174, 178
Grain-boundary tension 183
Grain coarsening 258
Grain growth 90, 105
Granik G. I. 236
Green R. F. 306
Gruzin P. L. 349
Gulyaev A. P. 234, 262
Guttmann V. 155

Hall-Petch relationship 15
Hardening curves 28
Harker D. J. 96
Harrington R. H. 365
Heterophase alloys, recrystallization in 397
Hibbard W. R. 76, 87, 120
High-melting compounds 414
Hirsch P. B. 34, 119, 149
Homologous temperatures 205
Honeycombe R. W. K. 212, 218
Hornbogen E. 384, 385, 400
Hu H. 46, 117, 136, 155, 194

Impurity atmospheres 359
Incoherent boundary 174
Incubation period of nucleation 142
Indenbaum G. V. 248, 253, 254
Indenbom V. L. 46, 48
Inequigranular structures 258
Inequigranularity 16, 258
Inhibitors 329
In-situ recrystallization 88, 314
Interstitial atoms 64
Islet inequigranularity 258
Iveronova V. I. 303, 352, 379, 381
Izbranov P. D. 311

Jaffrey D. 234
Jaoul B. 54
Jogs on dislocations 34
Johnson W. A. 95
Jonas J. J. 67, 122, 173, 207, 213

Kaplin Yu. I. 263
Karnop R. 190
Kaverina S. N. 313
Khayurov S. S. 211
Khimushin F. F. 263
Kidin I. N. 128
Kink bands 31, 44
Kirch F. 205
Kishkin S. T. 367
Kitaigorodsky A. I. 397
Klinchuk Yu. I. 413
Koch P. K. 330, 331
Koksharova I. K. 326
Kolmogorov A. N. 94, 95
Konobeevsky S. T. 77
Kornfeld M. O. 132, 191
Kossel's method 128
Krishtal M. A. 262
Kronberg M. L. 170, 172
Krupnikova-Perlina E. I. 311
Krupp's reagent 446
Kudryavtsev I. P. 62
Kuhlmann-Wilsdorf D. 34, 76
Kurdyumov G. V. 458
Kuznetsov G. F. 128

Lacombe P. 116, 146
Lainer D. I. 311
Larikov L. N. 103, 132
Lerinman R. M. 389
Li J. C. M. 136
Lihl P. 75
Lineage structure 16
Livshits B. G. 330, 406
Lomer-Cottrell locks 35, 207
Lomer-Cottrell sessile dislocations 33
Low-textured dynamo steel 338
Lozinsky M. G. 217
Lücke K. 103, 131, 160, 182, 344, 366, 367
Luton M. J. 210

Maevsky I. L. 249, 263
Malyshev K. A. 262
Martin J. W. 398, 399
Masing G. 233, 449
Matrix restabilization 273
McLean D. 131, 171, 183, 247, 262
McQueen H. J. 67, 122, 173, 207
Mecking H. 205
Mehl R. F. 14, 95, 131, 183, 191, 192
Merkuryev N. E. 363
Mes'kin V. S. 262
Metadynamic recrystallization 213
Metal structure 59
Microbands 46, 142
Microinequigranularity 258
Mirer I. I. 77
Mirkin I. L. 94
Molenaar J. 72
Mölins H. E. 337
Molotilov B. V. 60, 303 320, 328, 329
Montuelle J. 89, 134, 146
Morokhovets G. M. 263
Mott N. F. 34, 65, 78, 85, 131
Mott's islet model 173
Mould P. R. 452
Mullins W. W. 139, 337
Multiple slip 50

Neumann bands 43, 52
Novikov I. I. 31
Novikov V. Yu. 46, 320, 330
Nucleation rate 94

Ogilvie G. J. 51
Oriented growth 308, 315
Oriented nucleation 307, 315
Orlov B. N. 406
Orowan E. 44, 77

Pavlov I. M. 296, 297
Pavlov V. A. 191
Pawlek F. 337
Peierls-Nabarro forces 32
Peierls-Nabarro locks 207
Pethan R. W. 218
Phase transformation 9
Pines B. Ya. 131, 136, 157, 163, 186, 342, 374
Plastic anisotropy index 17
Pogrebnoy E. N. 262
Point defects 64
Point-defect annihilation 71
Polar mechanism of twinning 41
Pole figures 312
Polycrystals, deformation in 49
Polygons 81
Polygonization 77
Polymorphous transformation 9
Post-dynamic recrystallization 213
Prerecrystallizational polygonization 84
Primary recrystallization 18, 90, 92
Primary slip system 23
Prismatic slip 21

Rafalovich Ts. N. 311
Rate of boundary migration 178
Rate of nucleation 94
Rauzin Ya. R. 234
Ravich I. G. 302, 317, 398
Read W. T. 168
Recovery 71
Recrystallization, 90
  in compounds 414
  in hot deformation 203
  in thin films 426
  on critical deformation 227, 233
Recrystallization diagrams 289
Recrystallization embrittlement 162
Recrystallization nuclei, formation mechanism 127
Recrystallization textures 304
Redistribution of dislocations 70
Relay-race transmission of strain 50
Repetition segment model 174
Repolygonization 212
Reticular density 19
Rib texture in transformer steel 323
Richards T. L. 96
Richardson G. J. 208
Rimming in aluminium alloys 283
Rodina I. G. 216
Rollability index 17
Rolling G. F. 365
Rosenberg V. M. 302, 317
Roshchina L. V. 46
Rossard C. 209
Rovinsky B. M. 235
Rowland's transformation 308
Rutter J. W. 172, 365
Ryum N. 150

Sachs G. 190, 458
Sadovsky V. D. 217
Safonov Yu. S. 287
Sagalova T. B. 153, 216
Saltykov S. A. 463, 464
Samsonov G. V. 414
SAP alloy 407
Sato S. 118, 136
Savitsky E. M. 234, 269
Schmid E. 311
Schmid law 22
Schultz G. 459, 461
Schultz's method 196
Schwindlerman L. S. 169
Secondary recrystallization 90, 113
Secondary slip systems 33
Second-order recrystallization diagrams 292
Seeger A. 21, 29, 33, 35
Seidman I. D. 313, 326, 328
Sellars C. M. 210
Semenchenko V. K. 347, 348
Semenovskaya I. V. 320
Serebryakov A. V. 411
Shear deformation 23
Shestakov I. A. 328
Shiau V. J. 234
Shockley W. 168
Shtremel M. A. 128
Single crystals, deformation in 19
Slip bands 32
  in iron 21
Slip deformation, in crystals 19
Slip systems 19, 22
Smart J. S. 362, 363
Smith A. A. 362, 363
Smith C. H. 175, 183
Smith M. 233, 349
Sobolevsky I. A. 398, 406
Softening 203
Sokolkov E. N. 217
Solute impurities 102, 109
Sosnin V. V. 333, 337
Spektor A. G. 259
Spektor Ya. I. 212, 235
Sperry P. R. 148, 241, 311
Spherulites in films 441
Stabilizing phases 329
Stabilizing polygonization 84
Stacking fault energy 35
Stanley J. K. 95, 191
Static recrystallization 203
Stenberg S. S. 233
Stereographic projections of lattices 23
Stored energy of cold work 66
Strain-anneal process for growing single crystals 253
Strain hardening 203
Strain-induced migration 148, 230, 243
Stress-strain curves 28
Structural changes in hardening 28
Structural diagrams 225
Structural unit model 174
Structure of grain boundaries 165
Stüwe R. 367
Subboundaries 81
Subgrains 81
Superlattice 171
Supersaturated solid solutions, recrystallization in 378
Superthin films 426
Suzuki atmospheres 89, 365

Talbot J. 83, 89, 121, 134, 146
Temperature level of recrystallization 345
Temperature of beginning of recrystallization 339
Ternary recrystallization 116
Texture analysis 453

Texture of transformer steel 320
Texture weakening in recrystallization 321
Thin films, recrystallization in 426
Thin-foil technique 444
Third-order recrystallization diagrams 293
Tikhy N. V. 212, 215, 218
Tilt boundary 167
Tiraspol'sky V. I. 31
Titorov D. B. 331
Tkachenko F. K. 196
Tolutis V. B. 437
Tongues 148, 243
Transformer steel, with cube texture 335
  with rib texture 323
Turchinskaya M. I 389
Twin boundaries 174
Twin habit planes 38
Twinning 38
Twinning dislocations 174
Twist boundary 168
Tyutyunnik A. D. 349

Umansky Ya. S. 133
Urusovskaya A. A. 44
Usikov M. P. 50, 63
Utevsky L. M. 50, 63

Vacancies 64
Van Bueren H. G. 73
Van Gakenbergbe Y. 437
Van Liempt J. A. M. 347, 348
Vecht A. 437
Verbraak C. A. 308, 315
Vinograd M. I. 196
Vorobyev G. M. 330

Walter J. L. 116
Wassermann G. 311
Weinblat Yu. M. 211, 216, 222, 224, 288, 303
Weissmann S. 55, 135, 142, 157
Wiener G. J. 335, 337
Wilson F. H. 170, 172
Winegard W. C. 365
Work-hardening coefficient 30
Wulff-Bragg angle 450

X-ray structural analysis 444

Yastrebov T. Ya. 333, 337
Yatsenko R. V. 212

Zakharova M. I. 128
Zener C. 110, 111
Zhak K. M. 199, 262
Zhdanov G. S. 133, 303
Zhukhovitsky A. A. 158
Zonal inequigranularity 260, 276
Zonal stresses, 62
  in films 431

TO THE READER

Mir Publishers welcome your comments on the content, translation, and design of the book.

We would also be pleased to receive any suggestions you care to make about our future publications.

Our address is:

USSR, 129820, Moscow, I-110, GSP, Pervy Rizhsky Pereulok, 2, Mir Publishers.

Printed in the Union of Soviet Socialist Republics